Litho-chemo-stratigraphic, structural and mineral prospectivity aspects of the Rosebery Group, an enigmatic Cambrian volcano-sedimentary succession in western Tasmania

By
Eyob Fisseha Andemeskel

B.Sc. (University of Asmara)

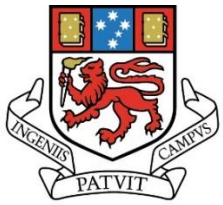

UNIVERSITY
OF TASMANIA

Submitted in fulfilment of the requirements for the

Degree of Master of Science in Earth Sciences

November, 2018

CODES

ARC Centre for Ore Deposits and Earth Sciences

Declaration

This thesis contains no material which has been accepted for the award of any other degree or diploma in any tertiary institution, and to the best of my knowledge and belief, contains no material previously published or written by another person, except where due reference is made in the text of the thesis.

Date 20th Nov, 2018

Signa

Authority of access

This thesis may be made available for loan and limited copying in accordance with the Copyright Act 1968.

Abstract

The Middle to Late Cambrian Rosebery Group is a 2-5 km wide, continuous belt of highly deformed, marine siliciclastic and volcaniclastic strata, situated on the western flank of the Mt Read Volcanics (MRV), in western Tasmania. It occupies a transitional position between volcanogenic sequences to the east, known for their world class volcanic hosted massive sulphide deposits (VHMS), and broadly coeval sediment-dominated packages to the west. The transitional character is manifested by rapid lateral facies and provenance changes, which have historically led to confusing and contradictory stratigraphic relationships. Also contributing to the complexity is an unusual structural style characterised by abrupt change in younging direction across anastomosing faults zones, in some cases containing slivers of basement strata, and disappearance and reappearance of units along strike. This study examines these problems through a combination of litho- and chemo-stratigraphic and structural techniques.

The belt is bounded to the west by a N-S trending domain of basement inliers that define a major sub-basin boundary. To the east is the Rosebery Fault, a moderately E-dipping thrust born during the principal phase of basin inversion in the mid-Devonian. The Rosebery VHMS deposit (28.3 Mt at 14.3% Zn, 4.5% Pb, 0.6% Cu, 145 g/t Ag and 2.4 g/t Au) occurs within the hangingwall block of the Rosebery Fault, hosted largely by a narrow interval of siltstone and sandstone. The host interval records a brief episode of relative volcanic quiescence that separates an older feldspar-phyric dacitic phase of magmatism (Hercules Pumice Formation), from a younger heterogeneous magmatic phase comprising quartz + feldspar-phyric rhyodacite and basaltic-andesite components (White Spur Formation).

In the eastern part of the Rosebery Group, within the immediate footwall of the Rosebery Fault, VHMS style mineralization occurs in strongly sericite altered, quartz-phyric volcaniclastic sandstone. The mineralisation is characterised by banded and disseminated concentrations of mainly sphalerite, galena and pyrite, and includes a drill hole interval of 9.8 m at 8.3% Zn, 4.5% Pb,

0.4% Cu, 514 g/t Ag and 5.5 g/t Au. The host package is dominated by volcanogenic facies that have affinities with the Rosebery ore body hangingwall sequence. Defined herein as the Marianoak Formation, the package is considered chrono-stratigraphically equivalent to western intervals dominated by siltstone, sandstone, and conglomerate, but containing a distinctive pumice breccia unit known as the Natone Volcanics.

Lower levels of the Marianoak Formation (MRF 1) comprise subaqueously erupted and deposited, juvenile fragment-rich, quartz-feldspar-phyric pumice breccia, and volumetrically minor peperitic rhyolite intrusions and mudstone interbeds. VHMS-style occurrences are towards the top of this interval. The pumice breccia shows minor cross-strata mineralogical variation, mainly in the abundances of quartz and feldspar crystal components. MRF 1 is overlain by a pumice-poor sequence of feldspathic volcaniclastic breccia and volcaniclastic sandstone, rich in intermediate volcanic fragments, interpreted to represent minor epiclastic reworking (VBX I/VSST, MRF 2). Narrow intervals of rhyolite pumice breccia and monomict, jigsaw fit breccia facies (VBX II/VSST, MRF 2) punctuate the facies association, recording episodic felsic explosive and less significant effusive volcanism that typified MRF 1. The rhyolite monomict, jigsaw fit breccias and peperite, suggests a local rhyolitic source for the deposit rather than input from adjacent sub-basins.

The fundamental two-fold lithostratigraphic framework of the volcanogenic Marianoak Formation corresponds with marked differences in whole rock geochemical signatures, which in turn reflect changes in magma composition. MRF 1 pumice breccia facies are characterised by incompatible element-rich signatures indicative of rhyodacitic magmatism. Parts of the sequence possess remarkably coherent chemical signatures, with notably elevated Th/Sc and Th/Ti values, indicating derivation from a homogenous magmatic source, most likely from a single volcanic centre. MRF 2 is characterised by a more heterogeneous signature, with an abrupt increase in Ti and Sc abundances relative to various incompatible elements at its base. Although episodic rhyodacitic input persists throughout the unit, the dominance of more mafic compositions records a progressive shut-down of explosive felsic volcanism.

Chemical analysis of the White Spur Formation reveals a very similar upsection profile to that of the Marianoak Formation, providing the basis of a robust chemo-stratigraphic correlation of packages across the surface of the Rosebery Fault. The Hercules Pumice Formation, or stratigraphic footwall to the Rosebery orebody, has a distinct chemistry, with no known equivalents in the Marianoak Formation (although equivalents at depth, beyond the present limits of drilling and sampling remain possible). The VHMS-style occurrences within MRF 1 of the Marianoak Formation are stratigraphically positioned above the Rosebery ore body host, and that the latter is yet to be penetrated by drilling within the Rosebery Fault footwall block.

Pumice breccias of the Natone Volcanics (i.e. western Rosebery Group) are shown to be direct chemo-stratigraphic equivalents of MRF 1 of the Marianoak Formation and lower levels of the White Spur Formation. In this case, however, the pumice breccias are entirely enclosed within basement-derived non-volcanogenic strata. The facies relationships are interpreted to indicate deposition in a basin marginal position, distal to major volcanic centres, with volcanic input only from the most violent and volumetrically significant eruptive events. Situated at the equivalent stratigraphic position of the Hercules Pumice Formation is the basement-clast-rich Salisbury Conglomerate. It is likely that the tectonic phase heralded by the influx of coarse basement-sourced debris at the basin margin is linked to the coeval change in magmatic composition and deposition of epiclastic sediments of the Rosebery Host Rock Member towards the basin's interior.

Lateral facies variants of the Rosebery Group accumulated in a series of broadly N-S trending sub-basin compartments. Devonian inversion of these sub-basins led to a domainal structural style characterised by dismembered upright folds. Sheared out fold hinges and consequential facing flips correspond locally with fault-bounded basement inliers that were emplaced along short-cuts transecting the footwall blocks of inverted grabens. The eastern sub-basin is considered to remain prospective for VHMS-style mineralisation as it is yet untested and is inferred to be a stratigraphic

equivalent of the Rosebery orebody. However, cross section construction indicates that this level is relatively deep (> 500 m below surface), at least in the vicinity of the Rosebery Mine.

Acknowledgement

First and foremost, I would like to thank my supervisors, Dr. David Selley and Dr. Rebecca Carey, for their brilliant critique and relentless guidance, without which this work would have been impossible. The amount of time and energy dedicated by both supervisors for this work, from inception of the project to the write-up of thesis, cannot be paid back.

Special appreciation goes to Prof. Bruce Gemmell for his encouragement and assistance in partly securing my living scholarships from the University of Tasmania. I would like to extend my deepest gratitude to all of the Earth Sciences academic staff, and in particular to Dr. Ron Berry and Dr. Rob Scott, for their valuable discussions, insights and assistance. Special thanks go to Prof. Jocelyn McPhie for her continuous support in reviewing most of the chapters. I would like also to thank all the colleagues from the University of Tasmania for their emotional and intellectual support throughout the project.

I am also highly indebted to the geologists and staff from Mineral Resources of Tasmania for their unreserved support in providing me access to the historical drill holes. Assoc. Prof. Andrew McNeill is greatly thanked for his support and discussions.

Additionally, I would like to acknowledge MMG Ltd (Minerals and Metals Group) for their initial funding and continuous support in providing access to drill cores and geochemical data. To mention some names, Kim Denwer, Michael Thomson, Troy Lowien, Kate Lester (GIS Manager), Craig Archer and others are greatly appreciated for their support.

Last but not least, I am indebted to my family for their moral support and love throughout the study period.

Contents

Appendices

List of Figures:

Chapter 1

Chapter 2

Chapter 3

Chapter 4

Chapter 5

List of Tables:

Chapter 1: Introduction

The Rosebery Group comprises a narrow N-S trending belt of late Middle to Late Cambrian marine siliciclastic and volcaniclastic strata, situated on the western flank of the Mount Read Volcanics (MRV) (Fig. 1.1). Compared to other parts of the MRV, including both the volcanogenic succession to the east (Corbett et al., 2014), rich in base metal ores, and the sedimentary-dominated basin marginal packages to the west (Selley, 1997), the Rosebery Group remains poorly understood in terms of its stratigraphy and mineral potential. Contributing factors are poor surface exposure, a general paucity of clear litho-stratigraphic markers, rapid lateral facies changes, and an enigmatic structural style. The latter is characterised by non-cylindrical macroscopic folds, with sheared out or intensely attenuated limbs, causing disappearance and reappearance of units along strike (Green, 1983; Selley, 1997). Presently juxtaposed domains of opposing facing and distinct lithostratigraphic character are often separated by shear zones, in places characterised by broken formations, or discontinuous fault-bounded 'basement' inliers. The package thus appears, not as a uniformly deformed sequence, but rather as an amalgam of initially distinct sub-basin compartments.

A renewed interest in the stratigraphic framework of the Rosebery Group was triggered by discovery of volcanic hosted massive sulphide (VHMS) style mineralisation in its eastern part in 2010 (MMG, 2014). The host of this mineralisation appears spatially, stratigraphically, and compositionally distinct from that of the classical MRV VHMS ores, and thus raises the potential for alternative styles and positions of mineralisation throughout the belt.

The western and central part of the Rosebery Group is sediment-dominated, a package of basement-derived siltstone, mudstone and dolomitic sandstone overlain by polymictic conglomerate (Loftus-Hills et al., 1967; Green, 1983). The conglomerate is, in turn, overlain by a ~120 m thick quartz-feldspar-phyric pumice breccia interval, the Natone Volcanics (NV). Compositionally similar pumice breccia, intercalated with feldspathic volcanogenic sandstone, accounts for much of the

eastern succession, defined in this study as the Marianoak Formation (MRF), positioned in the immediate footwall of the Rosebery Fault. A return to basement-sourced sedimentation, and accompanying cessation of explosive volcanism, is recorded by the overlying Stitt Quartzite, the uppermost stratigraphic unit of the Rosebery Group.

The volcano-sedimentary sequence was mainly regionally deformed and altered during the Devonian Tabberrabberan Orogeny, and metamorphosed under greenschist facies conditions. A more cryptic Late Cambrian phase of mild basin inversion is recorded locally. Macroscopic upright folds and moderate- to steeply-dipping faults developed in response to broadly ENE-WSW Devonian shortening. Inheritance of Cambrian structural elements is evidenced in part by the non-cylindrical form, and cleavage transection, of many large-scale folds (Berry, 1995; Selley, 1997).

The principal aim of this research is to improve understanding of the Rosebery Group geology by employing lithologic and structural mapping, and rigorous lithofacies/lithogeochemical analyses of the volcaniclastics that host the VHMS style of mineralization. Geochemical and lithologic features will be compared to the classical MRV stratigraphy that encloses the neighbouring Rosebery VHMS ore horizon (i.e. its footwall, host rock, and hangingwall), to understand the Rosebery Group's stratigraphic framework in a more regional context.

1.1. Access and exposure

The study area is covered by dense vegetation, rugged mountains with narrow rivers, creeks and water falls. Fresh outcrop is mainly limited to creeks, whereas tracks and road cuttings are affected, to various degrees, by weathering and moss or lichen overgrowths. Unusually good road-side exposures occur in the region of the Rosebery Mine: i.e. the so-called Flume Road, and parts of the Rosebery township road network (Fig. 1.2). Central and western areas were accessed along Natone Creek, where exposure is very good in parts, and old exploration tracks with intensely weathered track-floor exposure that lead westward onto Westcott Hill (Fig. 1.2).

The southern part of the study area was mainly accessed along the historic NE Dundas Tramway between Williamsford and Montezuma Falls, a track that follows the Ring River (Fig. 1.2). Tributaries of the Ring River, Conliffe and Bather creeks, provided access to the southern most part of the mapping area, albeit limited by several water falls and dense vegetation.

The Rosebery Mine drill holes were logged in the Tullah exploration camp during the course of four expeditions. Most of the drill cores are held in Tullah but some were transported from the Bobadil and Rosebery Mine repositories. In addition to the Rosebery Mine drill holes, four holes from the Natone Creek were accessed from the Mineral Resources Tasmania drill core library in Hobart.

1.2. Aims and significance of the project

The aims of this study are to:

1) understand the volcano-sedimentological evolution of the Rosebery Group during Middle Cambrian to Late Cambrian basin development, using lithofacies and lithogeochemical analyses,
2) stratigraphically and structurally characterize the volcaniclastic units of MRF (host to VHMS style of mineralization in the Rosebery Fault footwall),
3) determine whether stratigraphic equivalents of the MRF occur elsewhere in the Rosebery Group, and if so, assess their mineral prospectivity,
4) establish the position of the MRF within the context of the classical MRV stratigraphy to the east, in particular, the broader host succession to the Rosebery VHMS deposit,
5) determine which structural features, if any, are directly inherited from initial extensional sub-basin architecture.

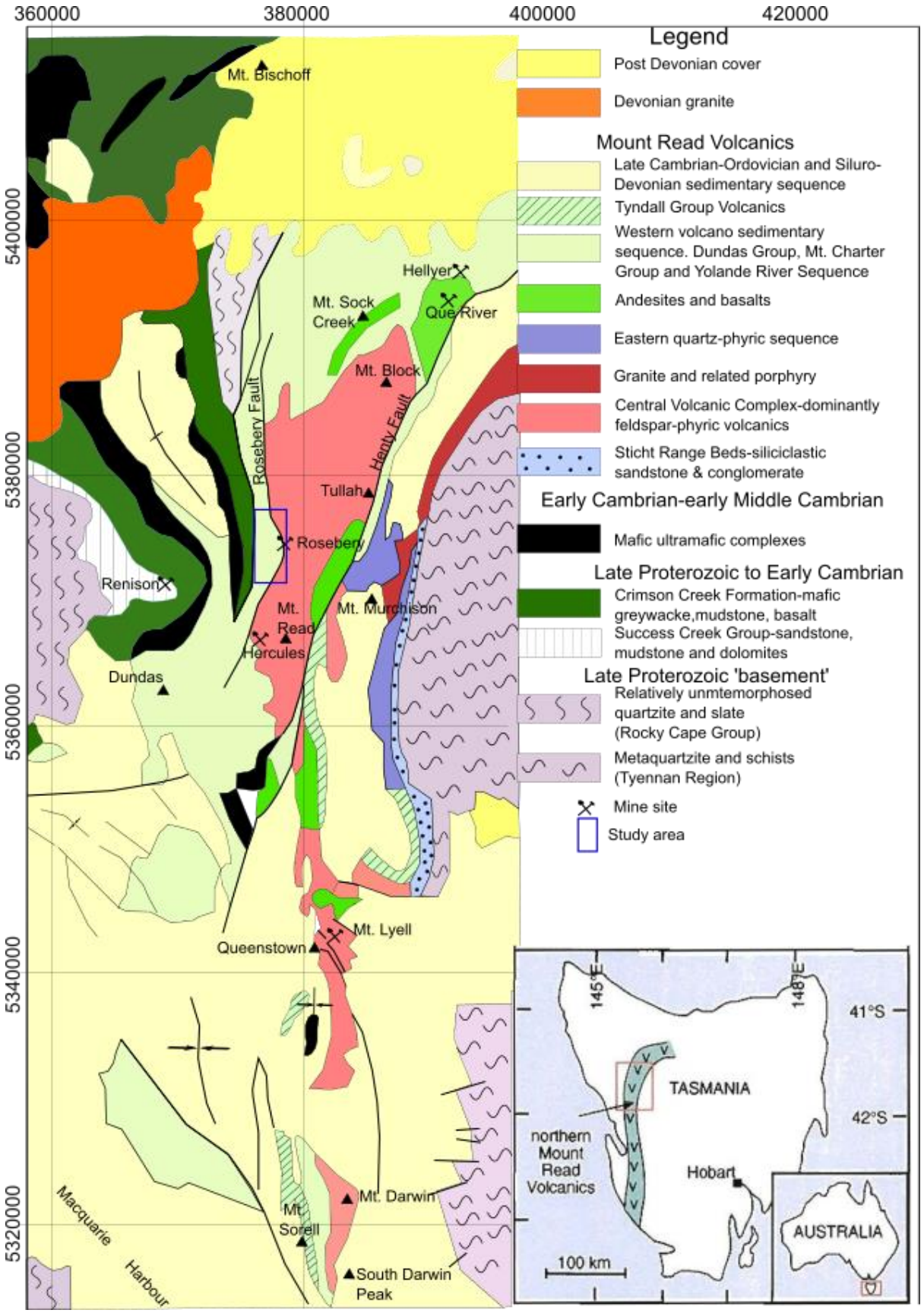

Figure 1.1. Geologic map of the economically significant central MRV (modified from Corbett, 1992). The study area is highlighted in blue.

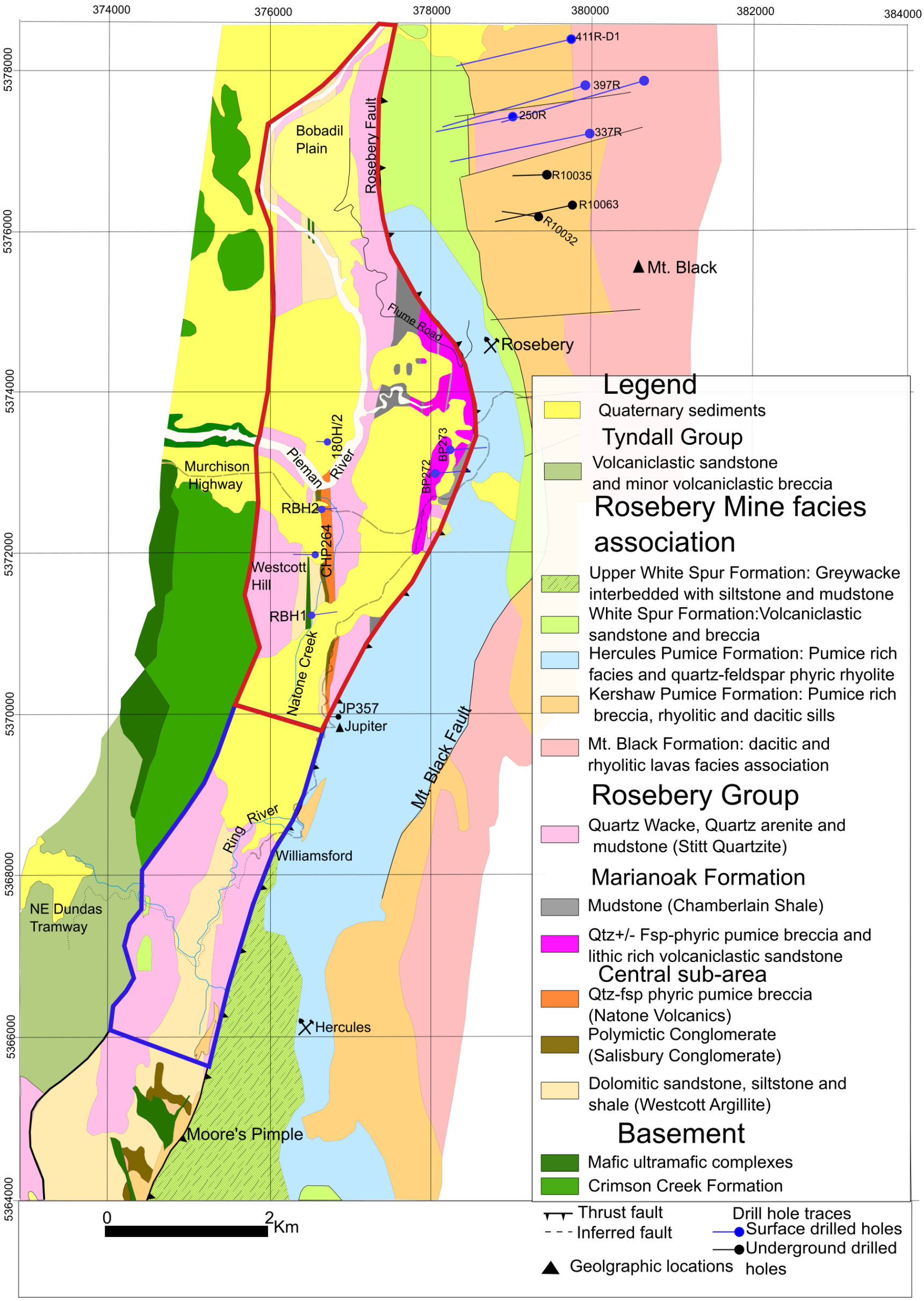

Figure 1.2. Geological map of the Rosebery district, showing the limits of the study area: subdivided into the northern zone (red polygon) and southern zone (blue polygon). Surface projected traces of drill holes used in this study are indicated in black (underground) and blue (Surface) drilled holes. The map is a compilation of data collected during this study, and previous works of Green (1983), EZ, MRT mapping division, and Gifkins (2001).

1.3 Thesis structure

The thesis is organized in six chapters and the details of each chapter are presented below.

Chapter 1 introduces the aims, location, accessibility, thesis structure and previous work. An overview of VHMS style mineralisation is presented.

Chapter 2 reviews the regional geological setting of the Rosebery Group. A tectono-stratigraphic evolution of western Tasmania is summarised from the Neoproterozoic Era to the Devonian Period. Elements of bio-, litho-, and chrono-stratigraphy and basin evolution that are considered salient to the Rosebery Group's history are emphasised.

Chapter 3 analyses lithofacies associations based on drill core logging, surface mapping, and petrographic analysis. Interpretations of the mode of eruption, emplacement, and depositional environment are made. The facies associations underpin a newly devised lithostratigraphic framework for the Rosebery Group.

Chapter 4 characterises the lithogeochemistry of volcanogenic facies. High density geochemical data, principally in the vicinity of the Rosebery mine (including the eastern Rosebery Group), provides the basis of chemostratigraphic correlations both within the Rosebery Group itself, and with neighbouring sequences.

Chapter 5 presents the structural relationships of the Rosebery Group via classical domain analysis.

Chapter 6 summarizes each chapter and synthesises the main research outcomes.

1.4 Previous Work

The Rosebery Group has seen a number of studies by university scholars, minerals exploration groups, and government survey geologists. From the earliest investigations, particular emphasis was placed on understanding the stratigraphic and structural relationships with ore-bearing strata to the east. While controversy existed as to the relative timing of mineralisation and host deposition,

accounts as far back as Montgomery (1895) and Hills (1915) recognised that the principal mineral occurrences of the Rosebery district were broadly stratabound: careful analysis of fold patterns, and identification of structurally repeated marker horizons, could therefore aid in the discovery of favourable horizons. However, despite numerous mapping campaigns, expansion of exposures with mine infrastructure development, and drilling, reports on stratigraphic relationships, structural coherency of the sequence, and fundamental facing directions from these early publications through until the 1970's are inconsistent (Finucane, 1932; Taylor, 1954; Campana and King, 1963; Loftus-Hills, 1964; Loftus-Hills et al., 1967; Brathwaite, 1970). Much of the contention is borne from the facts that strata are unfossiliferous (or at least robust biostratigraphic constraints are yet to be determined), and ore-bearing intervals are strongly affected by hydrothermal alteration, which in turn, has led to anomalously intense foliation development. Primary textures, composition, and protolith identification is, at least locally, significantly hampered.

With the exception of Brathwaite (1970), the main point of agreement between the early authors outlined above, was that the sedimentary rock-dominated parts of the Rosebery Group are older than underlying ore-bearing volcanogenic strata of the central MRV. This tenet was overturned in 1980's with the discovery of a major moderately E-dipping thrust, the Rosebery Fault (Figs. 1.1 and 1.2), which separates Rosebery Group strata lying within its footwall, from structurally overlying volcanogenic units, the latter hosting the Rosebery VHMS orebody (Green et al., 1981; Green, 1983; Corbett and Lees, 1987b). This period of research also heralded a number of significant advances in the understanding of deposit- to regional-scale lithostratigraphic relationships of the MRV(Corbett and McNeill, 1986; Allen, 1991). These advances were directly linked to a systematic large scale government survey mapping program, and rapidly developing research into volcanic facies analysis. The latter was strongly influenced by work on the Tertiary Kuroko VHMS deposits of Japan, and allowed geologists to 'see through' the intense alteration and strains affecting parts of the succession. Through application of these techniques, Corbett and Lees (1987), Allen (1991), and Gifkins (2000) demonstrated that the Rosebery district as a whole comprises a series of fault-

bounded volcanogenic and sedimentary packages that are in part chronostratigraphic equivalents (but with significant lateral variation in lithofacies associations), but in a gross sense progressively young towards the west.

In the early to mid-1990's, there were significant advances in the understanding of the regional tectonic evolution of western Tasmania (Berry and Crawford, 1988; Crawford and Berry, 1992), and more specifically, structural development of the MRV, the latter presented in a series of reports linked to the AMIRA P.291 project (Berry and Keele, 1993; Berry et al., 1997). It was becoming apparent that the MRV formed during the later stages of an arc-continent collisional event, with volcano-sedimentary sequences accumulating in a series of post-collisional extensional sub-basins. The interpreted compartmentalised character of the MRV went a long way in explaining a number of structural and stratigraphic irregularities. For example, Green (1983), Corbett and Lees (1987), and Selley (1997) highlighted the fact that the Rosebery Group was not a simple uniformly facing package of rocks as previously described, but rather a series of fault slices, with stratigraphic repeats, and zones of unusually high degrees of strata disruption and dismemberment. Green (1983) described these high strain zones as 'tectonic slides', whereas Corbett and Lees (1987) drew analogies in terms of texture and geometry with accretionary prism-related melange, and took the rather extreme view that the Rosebery Group immediately overlay a Cambrian subduction zone. Selley (1997), by contrast, argued that the structural style was a product of facies type and obliquity between stress field imposed during Devonian orogenesis and pre-existing sub-basin architecture. The specifics of the controversy aside, the strain patterns of the Rosebery Group are agreed to be unusual compared to the relatively simple Devonian fold and thrust geometries seen in other parts of the belt.

Chemostratigraphic techniques have been applied increasingly in the Rosebery district over the past 25 years, taking advantage of the progressively expanding brownfields multielement geochemical dataset (Parfrey, 1993; Winter, 2012; Baker, 2013). The studies have been focussed on

volcanogenic units, and have established, to various degrees of success, correlation both within the Rosebery Group, and between the latter and units located within the hangingwall of the Rosebery Fault. Recent high precision U-Pb zircon dating has gone further in solidifying these relationships (Baker, 2013; Mortensen et al., 2015).

The present study employs, for the first time, each of the techniques outlined above (geochronology excepted), and importantly expands the dataset to examine complete sequences positioned in the respective foot- and hanging-walls of the Rosebery Fault.

1.5 Overview of VHMS deposits

VHMS deposits are strata-bound massive to semi-massive sulphide lenses that are formed on or near the seafloor through the focussed discharge of hot, metal rich hydrothermal fluid in an extensional tectonic setting. It is now well understood that VHMS deposits form syngentically as a product of seafloor hydrothermal systems that formed in spatial and temporal and genetic association with contemporaneous volcanism (Franklin et al., 1981; Large, 1992; Large et al., 2001b; Franklin, 2005; Galley et al., 2007). The formation of VHMS deposits as discussed herein is largely based on the deposit model presented by Franklin (2005). The model in Figure 1.3 illustrates the six main elements that are considered to be essential to the formation of VHMS deposits. These are:

1. Subvolcanic intrusions that act as a heat source to drive the hydrothermal convective system along with some metal contribution.

2. A high temperature reaction zone that acts as a reservoir from which some metals are leached from the volcano-sedimentary strata through interaction with evolved seawater.

3. Footwall and less commonly, hanging-wall alteration zones produced by high-temperature fluid-rock reaction involving mixtures of ascending hydrothermal fluid and locally heated ambient seawater.

4. Synvolcanic growth faults that permit focussed discharge of hydrothermal fluid.

5. The massive sulphide formed at or near the sea floor.

6. Distal products that represent a hydrothermal contribution to background sedimentation.

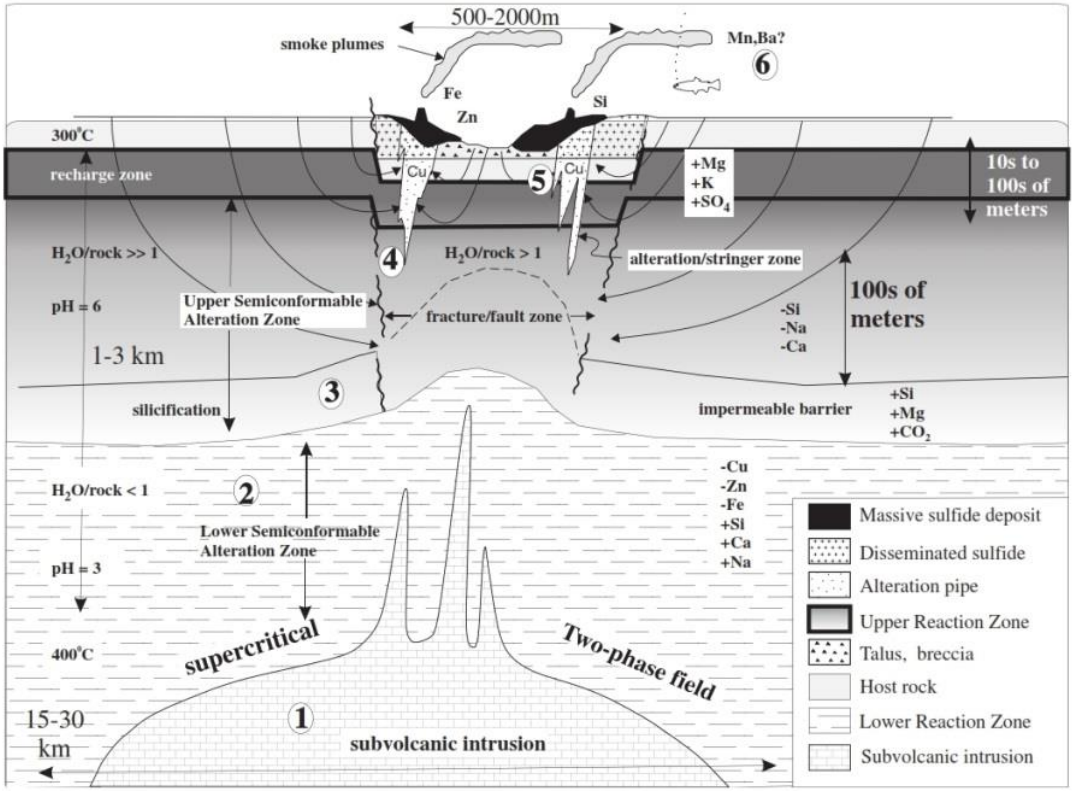

Figure 1.3 General model for the formation of VHMS deposts, illustrating the basic components of high - temperature VHMS hydrothermal systems (after, Galley, 1993; Franklin, 1995 and 2005). Note variable horizontal and vertical scales.

1. A heat source that derives the hydrothermal system

Subvolcanic intrusives are considered to be the heat source that initiate and sustain sub-seafloor convective hydrothermal cells, and in some instances contribute metal (Franklin, 2005; Gibson et al., 2007). In order to act as a heat engine, an intrusive complex has to be a long lived, with sustained temperatures of 300-400°C to drive hydrothermal convection (Large, 1992; Large et al., 1996). A possible example of a sub-volcanic intrusive body within the Mount Read Volcanics is the Cambrian

Granite suite (i.e., Murchison and Darwin granitoids). Evidence of magmatic contribution to the western Tasmanian VHMS ores is reported at the Mt. Lyell deposit (Fig. 1.1, Large et al. 1996).

2. High temperature convection zone and sources of the ore fluid

A high temperature convection zone contains modified seawater and acts as a reservoir for metals leached principally from volcanic and sedimentary strata (Figure 1.3). Both chlorine (i.e., principal metal complexing agent) and sulphur are derived partly from seawater, and interact with strata in the high temperature convective zone and/or magmatic-hydrothermal zones. Previous research has shown that the salinity of VHMS fluids is elevated relative to the seawater (Huston et al., 2006), implying that unmodified seawater is not the sole source of chlorine. Two additional sources appear likely: 1) incorporation of high salinity magmatic-hydrothermal fluid into the seawater dominated ore fluid (Huston et al., 2006) or 2) phase separation of NaCl within the high temperation reaction zone relative to the seawater (Lécuyer et al., 1999; Huston et al., 2006). As discussed above within the high temperature reaction zone, large quantities of fluid reacts with the rocks and the reaction zone approaches equilibrium. However, further beyond a certain pressure-temperature condition a supercritical phase separation of NaCl-H_2O results in condensation of high salinity brines (Lécuyer et al., 1999; Huston et al., 2006). This is an important mechanism that causes variability in the salinity of VHMS deposits (Huston et al., 2006). The δ^{34}S values of sulphide minerals of Phanerozoic VHMS deposits are generally between those of coeval seawater and magmatic sulphur, indicating a mixing between the two (Huston et al., 2006).

3. Semi-conformable alteration zone

The semi-conformable alteration zone occurs due to high temperature water-rock interaction which results in regionally extensive areas of alteration (Figure 1.3). The zone may extend for hundreds of kilometres along strike and down to and below the subvolcanic intrusive and upward to the paleo sea floor. The alteration zone shares mineralogical compositions similar to greenschist facies and is difficult to recognize as hydrothermal alteration in low grade metamorphic terrains (Franklin, 2005).

Upper and lower semi-comformable alteration zones can be separated by an impermeable barrier or aquiclude, each of which consist of convective cells (Fig 1.3). The upper semi-comformable alteration zone is generated through continuous circulation and recharge of large volume of seawater above the impermeable barrier. The lower semi-comformable alteration zone consists of highly evolved seawater circulating below the capped zone in an insulated system at high temperature, leaching metals from the volcanic rocks generating the main mineralizing hydrothermal fluid (Franklin, 2005). Episodic rapturing of the impermeable barrier by extentional tectonics results in focussed upflow of the mineralized fluid onto or just below the seafloor. This focussed flow of the hydrothermal fluid into the upper levels of the volcanic stratigraphy generates the footwall alteration pipe immediately below the massive sulphide (Franklin et al., 1981; Franklin, 2005). If the hydrothermal activity continues after the deposition of the massive sulphide, the alteration may extend into the hangingwall strata (Franklin, 2005).

4. Synvolcanic growth faults that focus the hydrothermal fluid

The hydrothermal fluid carrying the leached metals is focused along a zone of high permeability, such as growth faults, fracture zones and volcanic vents as shown in Figure 1.3 (Franklin et al., 1981; Large, 1992). In the Mount Read Volcanics, the major VHMS deposits of Rosebery, Hercules, and Mount Lyell (Fig 1.1) are located along regionally extensive longitudinal structures that are interpreted to be major rift faults associated with the development of the volcanic arc (Large, 1990).

The upward focussing of the hydrothermal fluid carrying metals along the synvolcanic faults has the potential to form VHMS deposits, however is affected by the nature of the footwall volcano-sedimentary facies association. For example, if the fluid is focussed along the faults within impermeable footwall volcanic sequences, such as lavas and domes, it can lead to the formation of exhalative mound-style deposits (e.g., Hellyer, (Large, 1992). In the cases of more permeable host strata, such as epiclastic mass-flow breccias, the hydrothermal fluids have the potential to infiltrate the pore spaces of unconsolidated volcanogenic sediments, resulting in replacement sheet- and lens-

style deposits with extensive alteration zones (e.g., Rosbery; Allen, 1991; Franklin, 2005). The latter scenario is thought responsible for the formation of large deposits, wherein fluids are largely trapped, whereas in the former, exhalative scenario, a large amount of the sulphide is dispersed into the sea (Large, 1992; Franklin, 2005).

5. Massive sulphide formed at or near the seafloor

As discussed above, the hydrothermal fluid is fed along growth faults or fractures to near surface strata either to be deposited as replacement- or exhalative-type deposits (Figure 1.3). Most of the deposits consist of two components (Fig. 1.4): 1) a concordant, mound shaped to tabular stratabound massive sulphide (>40% sulphide minerals), associated with quartz and subordinate phylosilicates and iron-oxides (Galley et al., 2007), and 2) an underlying discordant zone of stock-work veins and disseminated sulphide mineralization (Large, 1992; Franklin, 2005; Galley et al., 2007; Gibson et al., 2007). The deposition of massive sulphide may involve a history of "zone of refining", in which progressively hotter fluids replace the base of the sulphide body with high temperature mineral assemblages (Large, 1992; Huston et al., 2006). In such cases, Zn-rich ore produced at low temperature is progressively replaced by Cu-rich and then pyritic ores (Fig. 1.4). As a result, the massive sulphide body possesses a vertical and lateral zonation from a core dominated by pyrite → Cu → Zn – Pb ± Ba (Large, 1992; Huston et al., 2006). The underlying stock-work vein also shows lateral zonation from a chlorite ± silica rich core to sericite rich alteration envelope with corresponding sulphide minerals of chalcopyrite stringer and galena-sphalerite, respectively (Fig. 1.4, Large et al. 1992; Galley et al., 2007).

6. Distal products of the hydrothermal fluid

The distal products of hydrothermal discharge are thin and extensive units composed of exhalites, with terriginous or tuffaceous components (Franklin, 2005). The occurrence of distal products could be due to very extensive, diffuse, low-temperature and unfocussed hydrothermal venting that can be deposited pre-, synchronous with, or post ore formation (Large, 1992; Franklin, 2005; Huston et

al., 2006). In the Rosebery ore deposit, the distal products of such processes are interpreted to include lenses of massive and bedded carbonates, with varying amounts of barite, sulphide, and chlorite, reflecting cooling of dispersed exhalative fluids (Large, 1992). Distal alteration products was coincident with abrupt changes in volcanic-sedimentary architecture, and can be used to vector towards mineralisation (Franklin, 2005).

Forms and shape of the VHMS deposits

The classical mound shaped VHMS deposits show a stratiform zinc rich massive sulphide top that overly a cross-cutting Cu-rich massive sulphide and stock-work or stringer zone (Fig. 1.4). However, most VHMS deposits have a wide range of morphologies from mound, lens, sheet, to pipe or stringer types. The VMS deposits of the Mount Read Volcanics exhibit considerable variation in form, but can be broadly grouped into three classes (Large, 1992).

1) **Mound type** deposits have high aspect ratio of >10 (lateral extent: thickness ratio), comprising narrow and elongate massive sulphide bodies underlain by discordant to semi-concordant stock-work veins and disseminated sulphides (e.g., the Zn-Pb-Cu Hellyer depost; Large, 1992; Galley et al., 2007). These types of deposits are considered to form along a synvolcanic faults cutting through impermeable strata (lava flows or domes) restricting the ascending hydrothermal fluid along the structure (Large, 1992). Alteration halos are consequently vertically extensive but laterally restricted, with ore chemistry zonation from chlorite-silica rich core to sericite-rich envelope, and Fe→Cu→Zn, Pb→high grade Zn-Pb-Ag-Au→Ba, respectively (Large, 1992).

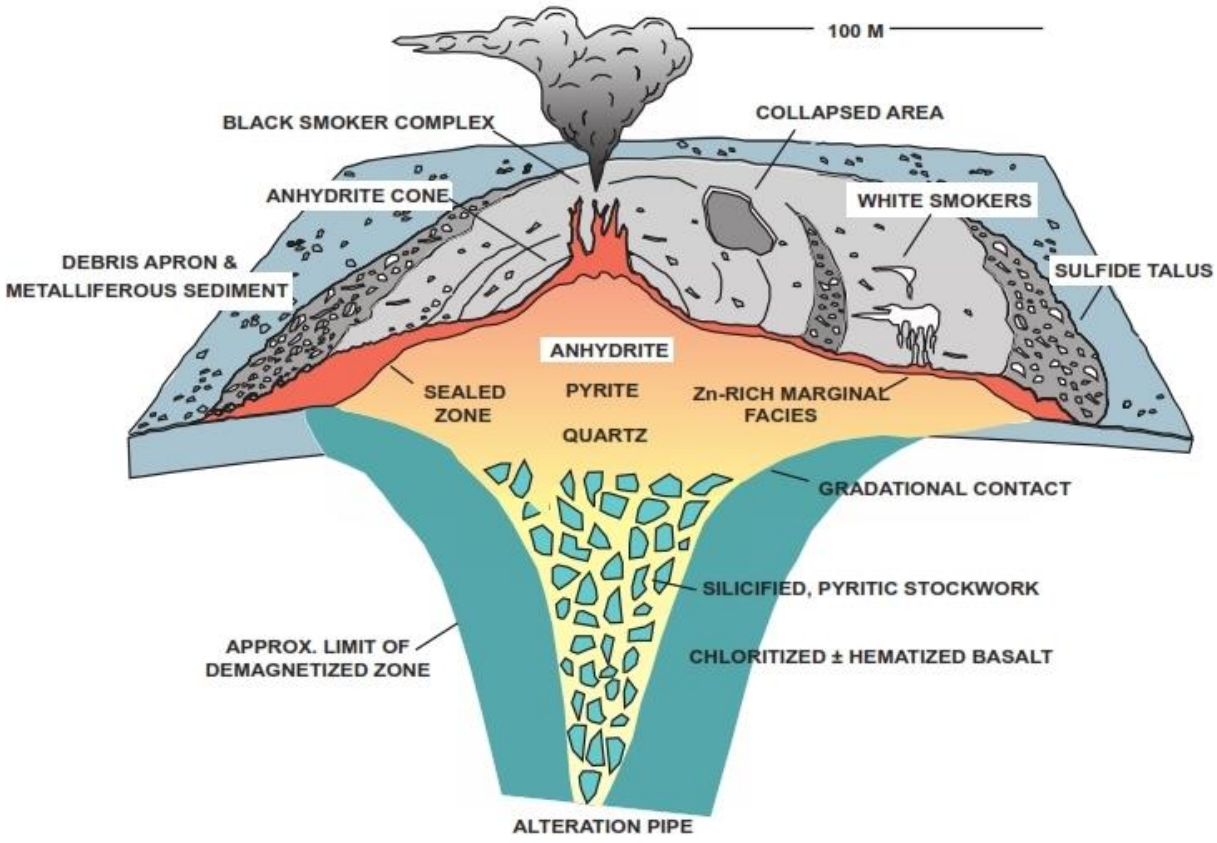

Figure 1.4 Schematic diagram of a classical cross-section of a modern TAG sulphide deposit on the Mid-Atlantic ridge. The diagram shows a classical VMS deposit with concordant semi-massive sulphide lense underlain by a discordant stock-work vein system and associated alteration halo (pipe). From Hannington et al. (1988) and (Galley et al., 2007)

2) **Lens and sheet** type deposits have low aspect ratio and are dominantly composed of Zn-rich massive sulphide lenses and subordinate stringer zones (Lydon, 1988; Large et al. 1999; e.g., Rosebery, Fig. 1). Generally, these deposit types are of Zn-Pb-Cu and Zn-Cu types with thin and extensive sheets without stringer zones (Large, 1992).

3) Massive sulphide pipe style deposits are similar to the stock-work and stringer zones that underlie the mound type deposits, and are formed by replacement of volcanics below the seafloor. The sulphide pipe develops from hot and highly focused hydrothermal fluid ascending through a major structure replacing the adjacent volcanics (Large, 1992). Unlike the mound and sheet like morphologies which are dominated by banding, the pipe style is manifested by sulphide breccia

textures and is composed of pyrite-chalcopyrite stringer zones with minor Zn-rich stratiform zones (e.g. Prince Lyell, Lyell Blow, Large, 1992).

In summary, volcanogenic massive sulphide deposits are formed at or near the seafloor from hot metal rich hydrothermal fluid initiated by subvolcanic intrusives in an extensional tectonic setting. The convection zone initiated by the intrusive bodies modifies the descending seawater leaching metals from the volcano-sedimentary sequence. During the process sulphur and chlorine sourced from both seawater and magmatic-hydrothermal phases, along with leached metals, are focussed along growth faults, fracture zones and volcanic vents. The focussed ore fluid can be formed either at or below the seafloor depending on the permeability and porosity of the host rock succession (Large, 1992; Franklin, 2005). The shape and morphology of the VHMS deposits is also controlled by the porosity and permeability of the host rock.

Chapter 2: Regional geological setting of the Rosebery Group

2.1 Introduction

The Rosebery Group is situated close to the western flank of the MRV within a large Middle- to Late Cambrian domain referred to as the Dundas-Fossey Trough. Dominantly Precambrian basement rocks of the Tyennan Block and Rocky Cape Block occur to the east and west of the trough, respectively (Fig. 2.1). The overall framework is considered below in terms of four main successions: 1) metamorphosed and folded rocks of Proterozoic age >540 Ma; 2) parautochthonous and allochthonous Neoproterozoic to Early Cambrian passive margin sequences (>520 Ma) 3) Early Cambrian (~520 Ma) allochthonous ophiolitic strata that record a Cambrian obduction event referred to as the Tyennan Orogeny; 4) the Middle-Late Cambrian MRV, recording initial post-collisional extension-related magmatism and ultimate basin inversion. The Devonian Tabberraberan Orogeny (445-360 Ma) subsequently affected all the older rocks of Tasmania, and account for the principal structural elements in Middle Cambrian and younger strata.

2.2 Neoproterozoic basement rocks

The Neoproterozoic basement rocks of the Tyennan and Rocky Cape Blocks have broad lithological affinities (Fig. 2.1). The Rocky Cape Block is dominated by shallow marine quartz siltstone, shale, cross-bedded quartz arenite and minor carbonates that are metamorphosed from sub-greenschist facies to greenschist facies (Green, 1983; Corbett and Lees, 1987b; Black et al., 2004; Corbett et al., 2014). The Tyennan Block comprises quartzite, quartz-mica schist, phyllite and minor eclogite that are more deformed and of higher metamorphic grade (garnet-amphibolite grade) than the Rocky Cape Block (Corbett and Lees, 1987a; Black et al., 2004; Corbett et al., 2014).

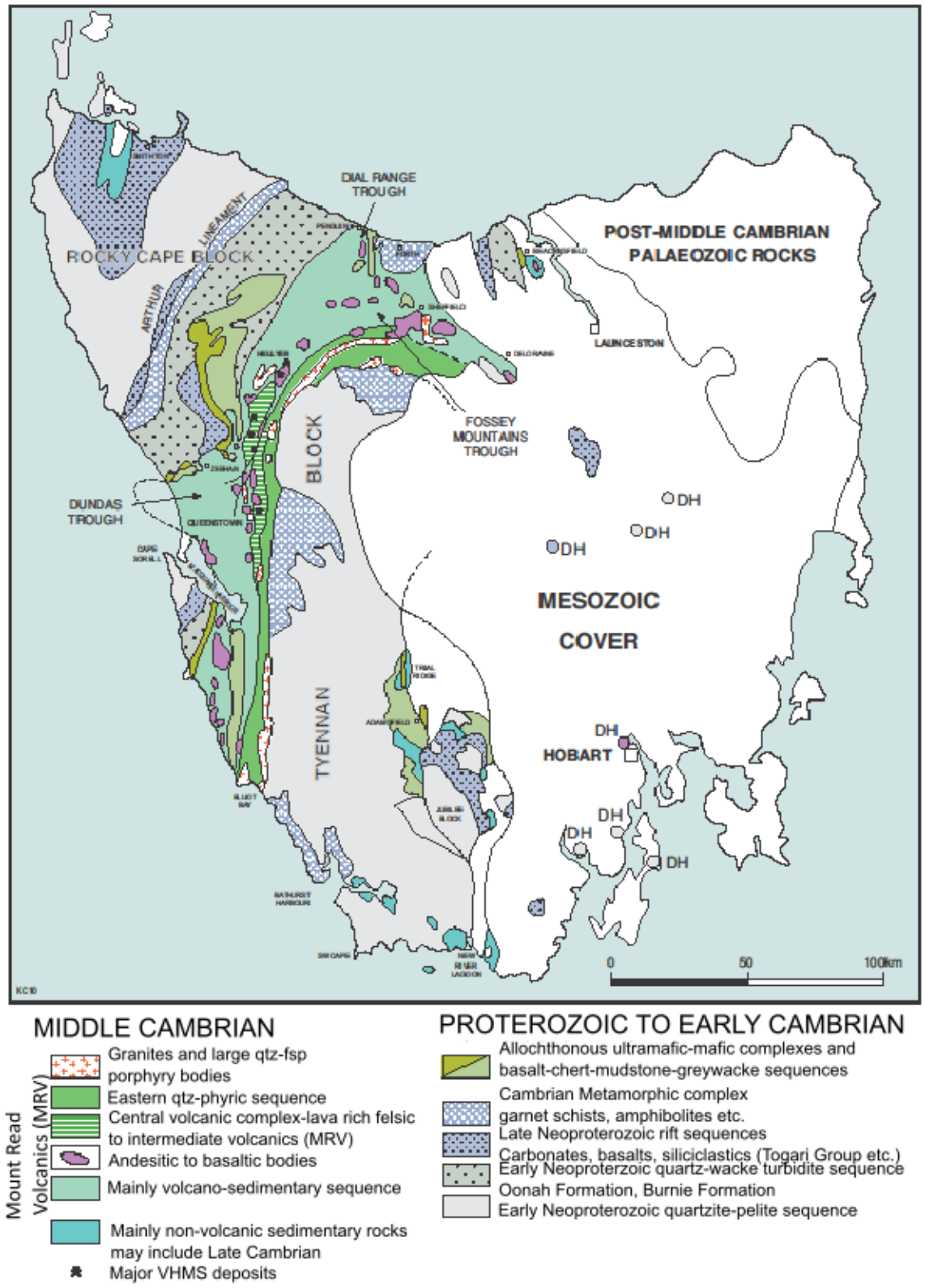

Figure 2.1. Geological map of western Tasmania showing Neoproterozoic to Early Cambrian 'basement' and Middle Cambrian volcano-sedimentary units of the MRV. From Corbett et al, (2014).

2.3 Neoproterozoic to Early Cambrian

Rocks of the Rocky Cape Block are unconformably overlain by the Togari Group, a latest Neoproterozoic to Early Cambrian volcano-sedimentary succession (Fig. 2.1). It is conventionally separated into two lithostratigraphic packages: the Success Creek Group and the Crimson Creek Formation. The former is a shallow marine shelf sedimentary sequence composed of sandstone, mudstone and dolomites that conformably overly rocks of the Rocky Cape Block (Fig. 1.1 & 2.1; Brown, 1980; Corbett and Lees, 1987b, Corbett et al., 2014). The Crimson Creek Formation records a period of mafic rift-related magmatism, and includes subaqueously deposited volcaniclastic lithicwacke, subordinate siltstone and mudstone, and minor tholeiitic basalts. Turbiditic volcaniclastics are composed of immature mafic-volcanic fragments, including reworked hyaloclastite detritus, and minor non-volcanic components of quartz, quartzite, chert, detrital carbonate and mudstone (Brown, 1980; Corbett et al., 2014).

2.4 Late Early Cambrian-Early Middle Cambrian mafic and ultramafic complexes

Mafic and ultramafic complexes (MUC) and various other allochthonous and para-autochthonous blocks of mainly sedimentary formations, were tectonically emplaced on the Crimson Creek Formation and other lower-plate successions during Early or Middle Cambrian (510-515 Ma) arc-continent collision (Tyennan Orogeny; Crawford and Berry, 1992; Corbett et al., 2014). In the Serpentine Hill (west of the study area), the MUC consists of a complex multiphase succession, faulted against the Crimson Creek Formation (Fig. 1.1 & Fig. 2.1). Lithologic components include high Mg and low Ti basalts, peridotites, and serpentinised layered cumulate assemblages (Crawford and Berry, 1992).

2.5 Middle to Late Cambrian volcanism and sedimentation

The Early Cambrian or early Middle Cambrian collision-obduction event was immediately followed by extensional basin development and the accumulation of the MRV (Figs. 1.1 & Fig. 2.1). Depositional cycles involved competing basement-derived sedimentation, principally around the fringes of the basin system (but likely occurring ubiquitously at earliest basin stages), and volcanism with calc-alkaline post-collisional geochemical affinities (Crawford and Berry, 1992; Corbett et al., 2014). Sedimentation and volcanism occurred almost exclusively within a marine environment during Middle Cambrian basin growth. Later stages of basin development during the Late Cambrian saw re-emergence of Precambrian basement terrains, and largely non-volcanogenic sedimentation in initially submarine, but ultimately subaerial depositional environments (Berry and Crawford, 1988; Corbett et al., 2014).

The interplay of sedimentary, volcanic, and tectonic processes during the evolution of the MRV manifest in a complex facies architecture, which in turn has led to the erection of localised and often confusing stratigraphic frameworks. The complex, contradictory, and continually evolving stratigraphic nomenclature related to the Rosebery Group is a classic example (e.g. Finucane, 1932

Taylor, 1954; Campana and King, 1963; Green, 1983; Parfrey, 1993). At the regional scale, attempts have been made to simplify the stratigraphic framework on biostratigraphic, geochemical, lithostratigraphic, and chronostratigraphic grounds (Crawford et al., 1992; Berry et al., 1997; Corbett et al., 2014; Mortensen et al., 2015). Each of these methods have had some success, and collectively lead to a better understanding of the tectono-stratigraphic evolution of the MRV but are limited in part by continuity of data: for example, fossil control, while abundant and robust in marine sedimentary sequences, is somewhat lacking in volcanogenic packages, whereas the opposite is the case for dating of magmatism by U-Pb geochronometers.

The approach used to provide regional stratigraphic context for the Rosebery Group in this thesis is to initially summarise a 3-fold biostratigraphic framework, and then to examine litho- and chrono-stratigraphic variations within each of these subdivisions.

2.5.1 Regional bio-, litho-, and chrono-stratigraphic elements of the MRV

Berry et al. (1997) proposed what they considered to be a regionally applicable biostratigraphically-constrained framework for the MRV. This framework, modified in Corbett et al. (2014), is shown in Figure 2.2, comprising from base to top, 'pre-Tyndall sequences' or 'Yolande Cycle' (Templetonian-Undillan), the Tyndall Group (Boomerangian-lower Mindyallan), and the Owen Group (mid-Mindyallan-Payntonian). The most complete fossil-constrained MRV profile occurs in the westernmost depocenters of the Dundas region, where dominantly basement-derived coarse-grained turbidites and subordinate volcanogenic deposits accumulated in a series of fault-bounded sub-basins (Elliston, 1954; Brown, 1986; Selley, 1997). Here, 'Yolande Cycle' sedimentation included input mainly from proximal MUC sources, with basin starvation associated with the deposition of fossiliferous mudstones (i.e. Hodge Slate) towards the top. Tyndall Group sedimentation recorded an increase in seismic activity and basin growth, a switch to western Crimson Creek Formation source terrains, with coeval felsic to intermediate explosive volcanic products increasing in volume to the east. A tholeiitic geochemical signature in magnetite-bearing volcaniclastic mass-flows in the eastern Dundas region heralds maximum crustal attenuation (Selley, 1997). The younger Owen Group equivalents were interpreted to record progressive sedimentation starvation, submergence of local sources, and ultimate molasse-type deposition due to uplift of the Tyennan region during a mild phase of basin inversion (Selley, 1997). It can be seen in Figure 2.2 that the rocks in the adjacent Rosebery area are poorly constrained biostratigraphically (the single fossil locality for the Stitt Quartzite occurring some 20 km south of the Rosebery Group type section) but are considered to contain elements from all three levels.

'Yolande Cycle'

'Yolande Cycle' deposits in the central and eastern MRV are conventionally separated into three partly interfingering, and geographically overlapping packages: Eastern Quartz Phyric Sequence (EQPS), Central Volcanic Complex (CVC), and the Western Volcano-sedimentary Sequence (WVSS; Figs. 2.1 and 2.3; Corbett et al., 2014).

The EQPS unconformably overlies the Tyennan Block and overlies a sequence of interbedded quartzite-clast, pebble-cobble conglomerate, siliceous sandstone and micaceous grey siltstone, assigned to the Stitch Range Beds (Corbett and Lees, 1987a; Corbett et al., 2014).The EQPS comprises quartz-feldspar-phyric rhyolitic and dacitic lavas, breccias and volcaniclastic rock, and intrusive bodies (Corbett, 1992; Corbett et al., 2014). The sequence is intruded by small and large granitic bodies, such as the Murchison Granite in the Murchison area (Corbett, 1992).

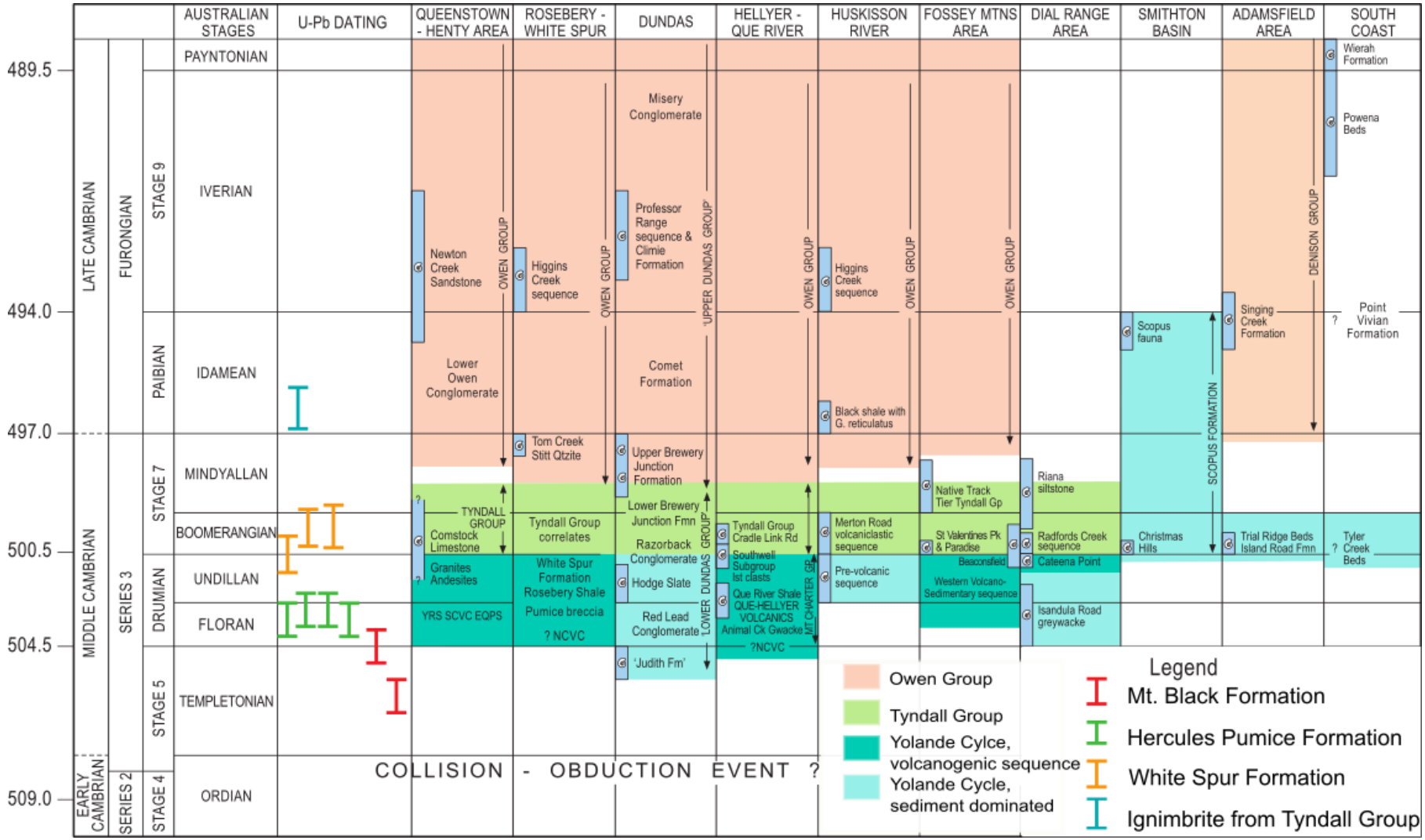

Figure 2.2. Biostratigraphic correlation chart for the Middle Cambrian and some Late Cambrian rocks in Tasmania (based on Berry et al., 1997). Blue bars with fossil symbols indicate age range of fossil fauna (Corbett et al., 2014). High precision U-Pb zircon crystallisation ages from the northern MRV (Mortensen et al., 2015).

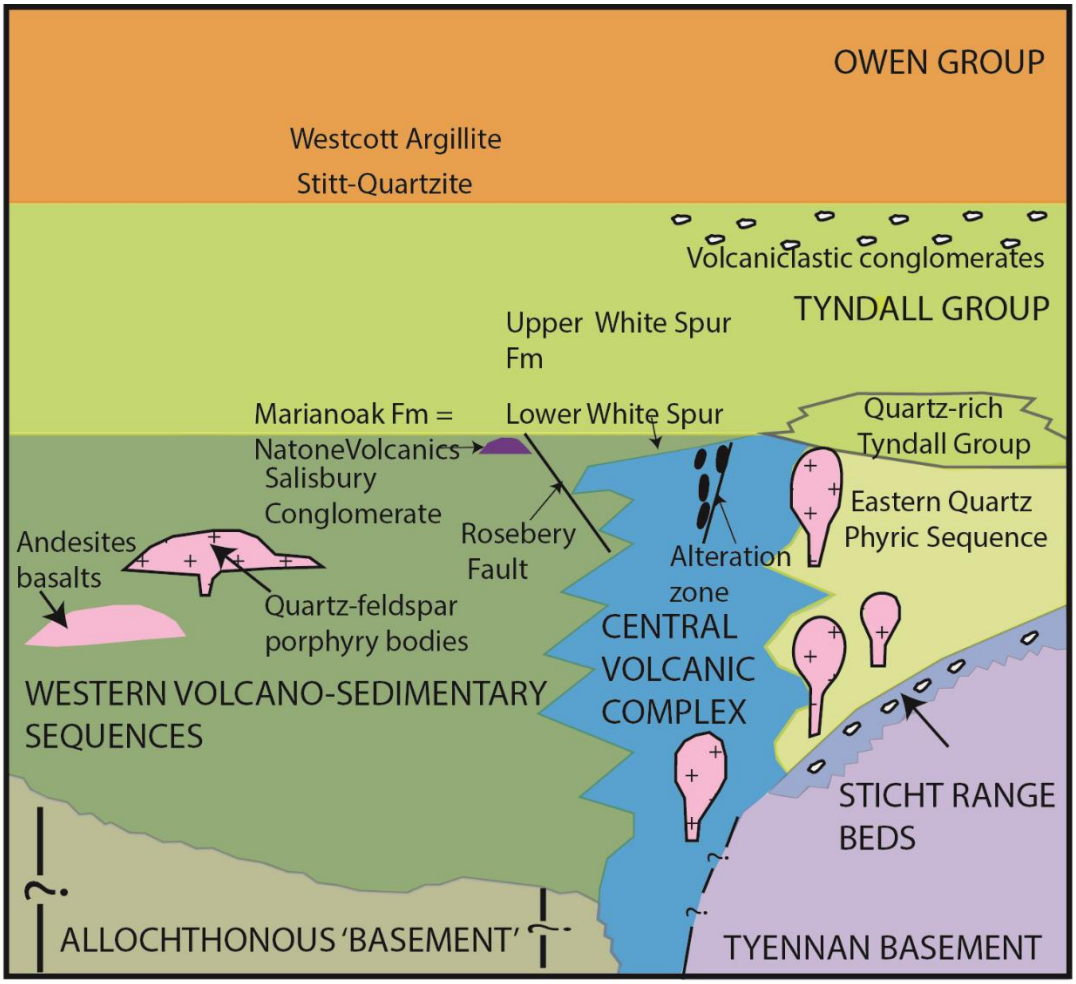

Figure 2.3. Schematic showing the arrangements and correlations of the major Middle and Late Cambrian lithostratigraphic units in western Tasmania (from Corbett et al., 2014). The figure shows relative spatial and temporal stratigraphic positions of the units/successions within the basin.

Rocks of the CVC define a ~10 km wide volcanogenic 'core' to the MRV and are predominantly composed of feldspar-phyric rhyolite and dacite lavas, syn-volcanic intrusions and extrusive domes of feldspar-phyric dacite, and quartz-feldspar-phyric rhyolite sills, with minor intercalated andesites and basalts (Corbett and Lees, 1987a; Corbett, 1992; Gifkins and Allen, 2001). It is further divided into northern and southern facies associations, separated by a sub-basin bounding structure, the Henty Fault (Fig. 1.1). The Southern Central Volcanic Complex (SCVC) comprises feldspar-phyric rhyolite to dacite lavas, syn-volcanic intrusions and volcaniclastic rocks, with minor non-volcanic sandstone and shales (Corbett, 1992; Corbett et al., 2014). It interfingers

with the EQPS on its eastern side and to the west with the WVSS (Fig. 2.3: Corbett et al., 2014). The Northern Central Volcanic Complex (NCVC), extends from Mount Read in the south to Mount Block (Figs. 1.1 and 2.1), and is predominantly composed of feldspar-phyric rhyolitic and dacitic lavas, syn-volcanic intrusions and syn-eruptive pumice breccias (Corbett and Lees, 1987b; Gifkins, 2001). It is bounded by the east dipping Rosebery Fault and west dipping Henty Fault to the west and east, respectively (Gifkins, 2001; Corbett et al., 2014).

In the region of Rosebery, detailed lithofacies and structural analysis provide the basis for a 3-fold litho-stratigraphic subdivision of the NCVC: from base to top, the Sterling Valley Volcanics, Mt Black Formation, and Hercules Pumice Formation (Fig. 2.4). The Sterling Valley Volcanics are composed of tholeiitic basaltic andesite rocks of polymictic mafic breccia, mafic sandstone and siltstone, and dacitic and basaltic lavas and sills. The overlying Mount Black Formation marks a change to felsic magmatism, its component feldspar ± quartz ± hornblende-phyric rhyolitic and dacitic lavas, cryptodomes and sills, minor pumice breccias, sandstones and shard-rich siltstones, defining a particularly complex facies architecture in a vent proximal submarine environment (Gifkins, 2001; Corbett et al., 2014). High resolution U-Pb zircon dating reveals an age range of ~507-504 Ma for this phase of magmatism (Fig.2.2; Mortensen et al., 2015).

The uppermost Hercules Pumice Formation is, for the most part, a regionally mappable sequence of feldspar-phyric pumice breccia, with bodies of syn-volcanic quartz-feldspar (-biotite) porphyry, and less common feldspar-quartz-phyric rhyolite and feldspar-phyric dacite intrusions (Allen, 1991; Gifkins, 2001; Corbett et al., 2014). The pumice breccia comprises massive to graded depositional units, 150-300 m thick, composed of feldspar-phyric tube pumice fragments with lesser shards, crystal fragments, chlorite or sericite fiamme and rare (3-5 cm, < 1%) lithic fragments. It records a major explosive felsic eruption episode prior to a conspicuous period of relative volcanic quiescence that coincides with the VHMS emplacement (Allen, 1991; Gifkins, 2001).

The Rosebery Mine Host succession is a discontinuous layer of variably stratified epiclastic sandstone interbedded with siltstone (5-60 m thick), that directly overlies the pumice breccia sequence. Although unconstrained biostratigraphically, the break in magmatism recorded at the top of the NCVC is conventionally interpreted to equate with the upsection transition from non-volcanogenic MUC-derived sedimentation to basin starvation in 'Yolande Cycle' deposits of the Dundas region to the west (Fig. 2.2). Comparison of high resolution U-Pb (zircon) geochronological data from the Hercules Pumice Formation (~504-502 Ma; Mortensen et al., 2015) with biostratigraphic control on the Hodge Slate (~502 Ma) supports this interpretation (Fig. 2.2). The regional shift in basin conditions at this level suggests a fundamental tectonic control on VHMS deposition (Berry et al., 1997).

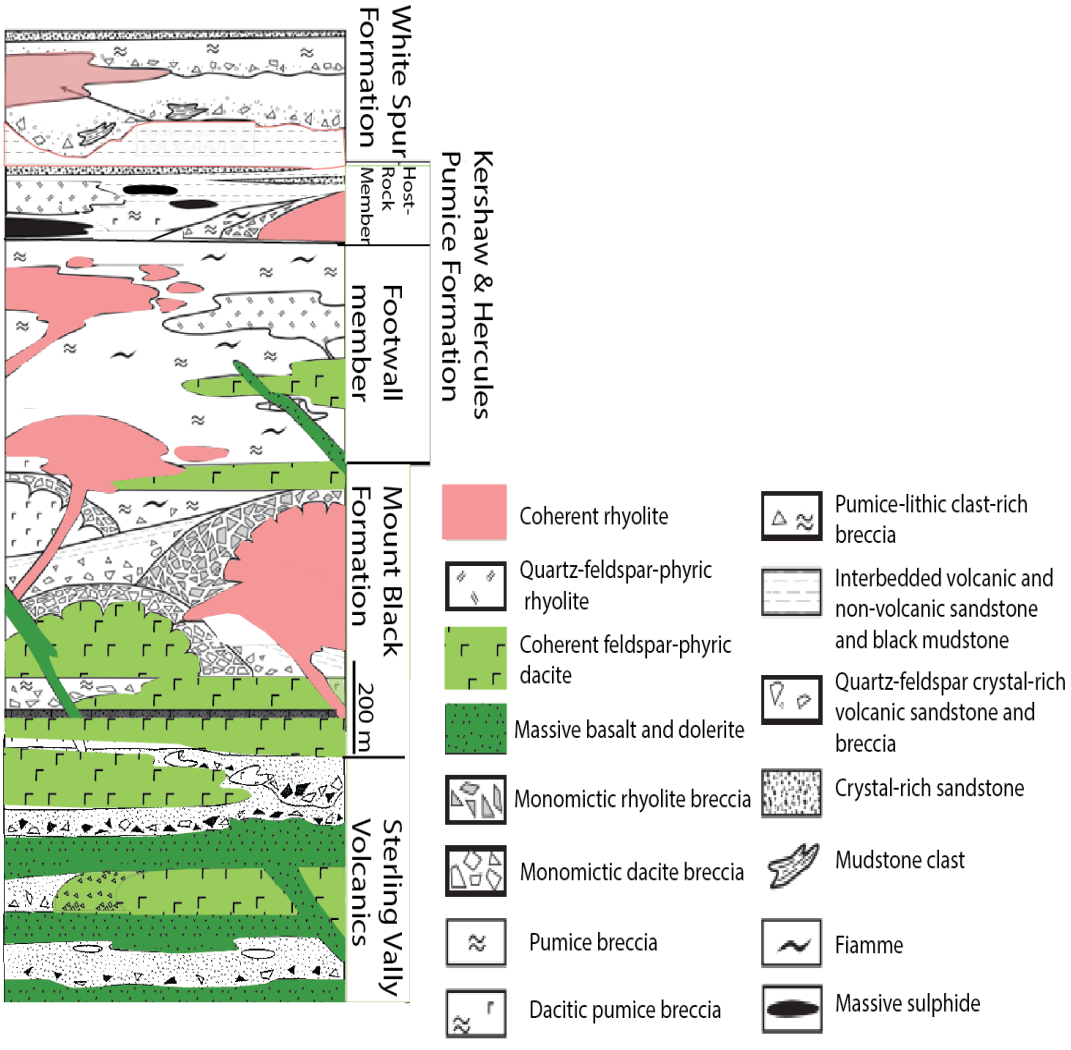

Figure 2.4. Stratigraphic and facies architecture of the NCVC (Gifkins, 2001).

The WVSS is a term that historically was used to classify all sediment-bearing sequences to the west and north of the CVC (e.g. Figs. 2.1 & 2.3). It encompassed a series of fault-bounded stratigraphic elements, including amongst others, the Dundas and Rosebery groups in their entirety, but in Figure 2.3 is used to describe only their 'Yolande Cycle' components. The basal part of the sequence is typically but not exclusively non-volcanogenic, and either lies outboard of coeval CVC strata (e.g. Dundas region), or more commonly interfingers with the upper parts of, or overlies, the latter. Facies types are diverse and includes turbiditic shale, siltstone, sandstone and conglomerate, andesitic to basaltic lavas and breccias, and volumetric felsic mass flow deposits, the widespread products of explosive felsic magmatism (Corbett et al., 2014). There is considerable lateral facies variation along the length of the belt, relating in part to localisation of volcanic centres, but also sub-basin compartmentalisation. Some of the mafic facies (e.g. Hellyer Basalt, positioned immediately above VHMS ore) possess a distinctive, primitive, high-K shoshonitic signature that records reworking of subduction-related metasomatised lithospheric mantle (Crawford et al., 1992). The signature is considered a key piece of evidence for the post-collisional setting of the MRV, the primitive character of the parent melts again suggesting a link between crustal-scale tectonic processes (i.e. attenuation) and VHMS emplacement.

In the Rosebery region, the WVSS is represented by the White Spur Formation, a succession of volcaniclastic breccia, sandstone, and siltstone (Figs. 2.3 and 2.4; Allen, 1991; Gifkins, 2001; Jago, 2005; Corbett et al., 2014). Pumice breccia deposits that overly the Rosebery mine host sequence, and are distinguished petrographically from the footwall Hercules Pumice Formation by conspicous quartz (Allen, 1991). Quartz-feldspar ± biotite sills and dykes, emplaced within the upper part of the Hercules Pumice Formation (in cases closely spatially associated with VHMS mineralisation) and lower White Spur Formation, commonly possess peperitic margins, and are interpreted to form part of the White Spur Formation magmatic phase (Corbett et al. 2014). Geochronological constraints on the intrusions suggest a narrow, post-Hodge Slate equivalent age range of ~500-499 Ma (Mortensen et al., 2015), but reveal a mismatch with the biostratigraphic framework (Fig. 2.2): the age range

overlaps biostratigraphic stages corresponding to fossil occurrences at the base of the Tyndall Group. Although the Tyndall Group fossil control is not ubiquitously robust, the relationship indicates that there is room for improvement in linking bio- and chrono-stratigraphic frameworks. In the Dundas region, the Hodge Slate is overlain by a 'Tyndall Group' package containing felsic shard-rich volcaniclastic mass-flows (Brown and Jenner, 1989; Selley, 1997) which bear superficial lithologic affinites with the lower White Spur Formation. Thus, stratigraphic problems aside, the general pattern of basin-starvation, followed by explosive felsic magmatism appears recognisable throughout the western part of the basin at least.

Tyndall Group

The Tyndall Group records the final phase of magmatism in the MRV. It occurs in its most characteristic form to the south and east of the Henty Fault as a thick, rapidly deposited submarine succession of crystal-rich feldspar, quartz and magnetite-bearing sandstone, with epiclastic conglomerate appearing towards the top of the cycle (Figs. 1.1, 2.2 & 2.3: White and McPhie, 1996). Rare occurrences of welded ignimbrite blocks within the basal mass-flow deposits indicate that for the first time, at least some of the volcanic centres were subaerial. A change in tectonic configuration during this phase of magmatism is also indicated by exhumation and reworking of high level Cambrian granites (Corbett et al., 2014).

Northward of the Henty Fault, correlation of units with the Tyndall Group in a litho-stratigraphic context is based principally on the occurrence of magnetic crystal rich sandstones. These occur sporadically in the southern and eastern Dundas areas (Selley, 1997; Van Einjndthoven, 2006) where they are interbedded with principally basement-derived turbiditic siliciclastic deposits. Along the trace of the Henty Fault itself, a bimodal package of intrusive and extrusive tholeiitic basaltic ± andesitic rocks and pumice-bearing felsic volcanic rocks are also tentatively attributed to the Tyndall Group (Corbett et al., 2014).

Mortensen et al. (2015) report a single crystallisation age for an ignimbrite block of 496.0 ± 0.9 Ma from the northern part of the Tyndall Group. Statistically younger than the White Spur Formation ages (Fig. 2.2), the age again raises the disparity between chrono- and biostratigraphic frameworks, which in this case, falls within Owen Group biostratigraphic stage-ranges.

Owen Group

Latest Middle to Late Cambrian Owen Group strata possesses both conformable and unconformable contacts with other (partly) volcanogenic sequences (Fig. 2.2 & 2.3). They are described as quartz-rich conglomeratic and sandy siliciclastics deposited in fluvial to shallow marine settings during inversion-related emergence of Tyennan basement sources (e.g. Corbett et al. 2014). In western areas, however, Selley (1997) argued that lower Owen Group submarine strata recorded continued extension-related input from western Crimson Creek Formation sources, with episodic, typically fine to medium grained basin-axial input from 'cleaner' quartz-bearing sources. The upsection transition from marine to subaerial deposition conditions was likely diachronous from east to west across the basin.

Complex structural and stratigraphic relationships occurs in the eastern part of the MRV in relationship to a number of prominent structures, including the Henty and Great Lyell faults (Berry, 1989a; Corbett et al., 2014), for which a syn-Owen Group inversion history is permissible, but tenuous. More convincing is the accumulation of Owen Group strata within the cores of N-S trending synformal depocentres formed by Late Cambrian basin inversion (Berry, 1995).

2.5.2 Litho- and chronostratigraphic aspects of the Rosebery Group

Putting aside the complexities and controversy surrounding the internal stratigraphic relationships of the Rosebery Group, and its position relative to neighbouring packages, the lithologic components are relatively well understood. Five lithologic packages are distinguished, corresponding to a stratigraphic nomenclature formalised by Brathwaite (1970), and largely adopted by subsequent

workers: these are, in no specific stratigraphic order, Chamberlain Shale, Stitt Quartzite, Westcott Argillite, Salisbury Conglomerate, and Natone Volcanics.

Westernmost strata are exposed in a structural window below the east dipping Rosebery Fault in the region of the Rosebery Mine (Fig. 2.5). They are conventionally ascribed to the ~500 m thick Chamberlain Shale (e.g. Green, 1983), but include not only fine grained mud and silt rocks, but also quartz-feldspar phyric volcaniclastic sandstone and breccia intervals with decimetre-scale thickness. Given the diversity of lithotypes, and the inappropriateness of the existing name, the package is referred to in this thesis as the Marianoak Formation (Fig. 2.5). Several workers have considered that the quartz-phyric character of the volcaniclastic deposits provides the basis for correlation with basal units of the White Spur Formation (i.e. Rosebery Fault hangingwall: Green, 1983; Corbett and Lees, 1987; Allen, 1991; Parfrey, 1993). Applying the biostratigraphic framework of Berry et al. (1997), this correlation would place the Marianoak Formation within the upper part of the 'Yolande Cycle' (c.f. Fig. 2.2). As noted above, however, this is at odds with the 'higher' stratigraphic position implied by the ~500-499 Ma geochronological constraints for the White Spur Formation.

Occurrences of massive sulphide within the Marianoak Formation were reported as early as Montgomery (1895). However, it was not until recently that an economically significant example was intersected in deep drilling. A narrow interval of massive, banded and disseminated sulphide lens of sphalerite, galena and pyrite is hosted in the strongly sericite altered, stratified top of quartz-phyric pumice breccia containing 8.3 % Zn, 4.5 % Pb, 0.4 % Cu, 514 g/t Ag and 5.5 g/t Au over 9.8 m interval (MMG, 2014). However, the high grade mineralization was not intercepted within adjacent drill holes but low grade mineralization was evident over a wider area along the stratigraphy (MMG, 2014).

The Marianoak Formation passes upsection to the west with apparent structural conformity to the Stitt Quartzite, a relatively resistant package of texturally-mature quartz-wacke, siltstone, and

mudstone, originally well exposed along the now flooded banks of the Pieman River (Fig. 2.5: Green, 1983). The ~350 m thick package contains well-developed Bouma sequences and records 'basement'-derived sediment input via a submarine fan system (Green, 1983; Selley, 1997). Similar facies occur on the western side of the belt, extending southward from Westcott Hill through the Ring River, and represent a probable structural repeat. Compositionally similar fossiliferous units (although considerably coarser grained) occur 10 km to the south of Dundas (Fig. 2.1), where an upper Mindyallan stage, or lower Tyndall Group biostratigraphic position, is indicated (Tom Creek fossil locality, Fig. 2.2: Van Eijndthoven, 2006).

Structural and stratigraphic continuity within the central part of the Rosebery Group is less obvious, with emplacement of thin fault-bounded slivers of likely MUC-derived mafic and ultramafic plutonic rocks along broadly meridional trends (adjacent to Westcott Hill and Moores Pimple in Figure 2.5). In this domain, one of the most complete and intact sequences occurs in the region of Natone Creek, where correlates of the Westcott Argillite pass upsection (eastward) to the Salisbury Conglomerate, and ultimately the Natone Volcanics (Fig. 2.5). The Westcott Argillite is a siltstone-dominated package at least 200 m in thickness, with typically low volumes of fine grained sandstone (Green, 1983). The latter has turbiditic textures and geometries and differs from those of the Stitt Quartzite principally by an additional component of carbonate. In southern regions, tholeiitic basaltic detritus is a major component, interpreted by Selley (1997) to indicate an extrabasinal Crimson Creek Formation provenance. Mafic and ultramafic detritus remain conspicuous components in the Salisbury Conglomerate, a closed framework fuchsite-bearing polymictic facies with a thickness in the order of ~100 m (Loftus Hills, 1964; Green, 1983). Compositionally and texturally similar units occur in the Moores Pimple area, where there is again a close spatial association with MUC inliers, raising the potential for local sourcing (Fig. 2.5: von Eijndthoven, 2006).

The Natone Volcanics is a ~120 m thick sequence of poorly structured quartz-phyric vitric tuff and breccia (Loftus Hills, 1964; Green, 1983; Parfrey, 1993; Baker, 2013). Each of these workers

considered a striking similarity with volcanogenic units of the Marianoak Formation, but only Parfrey (1993) was confident of the correlation. A high precision U-Pb zircon age from the Natone Volcanics of 498.6± 0.80 Ma, reported in Baker (2013), provides a crucial chronostratigraphic link across the basin, lying within error of White Spur Formation volcanism (~500-499 Ma: Mortensen et al., 2015). Given that the latter occurs within ~50-100 m stratigraphic distance from a world class VHMS orebody, the potential correlation westward into the Rosebery Group has great exploration significance.

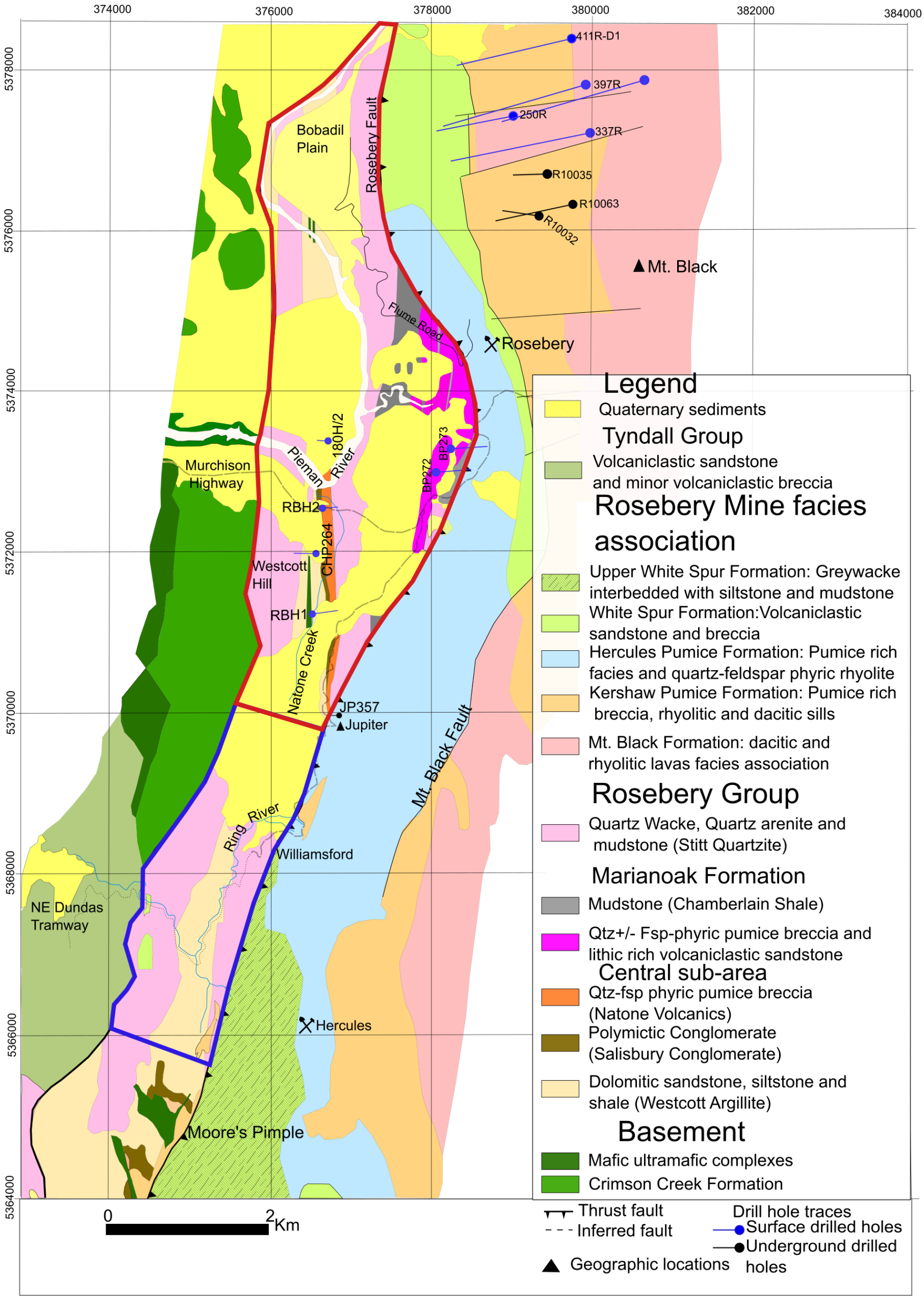

Figure 2.5. Regional geological map of the study area modified from Mineral Resources of Tasmania 1:25000 maps. The eastern part of the Central Volcanic Complex is modified from Gifkins (2001).

2.6 Palaeozoic tectonic history of western Tasmania

The structural configuration of western Tasmania is principally related to two orogenic phases, the Cambrian Tyennan and Devonian Tabberabberan orogenies (Corbett et al., 2014). The 3-stage Tyennan Orogeny is broadly equivalent to the Delamerian Orogeny in South Australia and the Ross Orogeny in Antarctica (Berry and Crawford, 1988; Turner, 1989; Crawford and Berry, 1992; Seymour and Calver, 1995; Corbett et al., 2014). The effects of Precambrian deformation events are now considered very localised and poorly constrained and will not be considered here.

2.6.1 Tyennan Orogeny Stage 1: Early Middle Cambrian collision and allochthon emplacement

The first stage of Tyennan Orogeny resulted in the assembly of several exotic and parautochthonous blocks in what is presently the western half of Tasmania. A key advance in the understanding of the tectonic development came from the recognition that MUC complexes were allochthonous and emplaced westward along one or a series of basal mylonitic shear zones (Berry, 1989b). Berry and Crawford (1988) drew analogies between the structural morphology and that of the Oman Ophiolite, while Crawford and Berry (1992) demonstrated that the components of the MUC allochthon were geochemically and petrologically compatible with an intra-oceanic forearc origin. A model was presented that involved ophiolite emplacement onto a previously attenuated passive margin sequence defined by rocks of the Success Creek and Crimson Creek Formation (Fig. 2.6a-c).

More recent tectonic models demonstrate that a number of other high strain high- to low-grade metamorphic complexes, such as the Arthur Lineament (Fig. 2.1), also form part of the Stage 1 tectonic assembly (e.g. Turner, 1989; Meffre et al., 2000; Holm and Berry, 2002). These relationships indicate that parts of the passive margin sequence were rapidly buried and subsequently exhumed during the collisional process. Dating of metamorphic phases (i.e. monazite, hornblende, zircon, muscovite, and biotite) from several parts of the complexes provide an age range of 523-500 Ma, with a main cluster around ~510 ± 3-5 Ma (Turner, 1993; Turner et al., 1998; Berry et al., 2007).

These ages, considered indicative of obduction/collision, appear permissible given a 516 ± 0.9 Ma for plutonic MUC components (Mortensen et al., 2015). The presence of MUC-derived detritus in basal MRV strata, including mylonitic fragments from the Dundas area (Selley, 1997), provides a minimum age of allochthon emplacement of ~505 Ma on biostratigraphic grounds. Corbett et al. (2014) estimated that the entire obduction process occurred over less than 10 Ma.

2.6.2 Tyennan Orogeny Stage 2: Middle Cambrian orogenic collapse

Rapid decompression during the final stages of the obduction event, potentially linked to slab break-off, is interpreted to record exhumation of the orogen, influx of asthenospheric mantle, and the onset of post-collisional magmatism within an extensional basin setting (Fig. 2.6 c-d: Corbett et al., 2014). As noted above, the oldest high precision MRV U-Pb zircon age is 506.8 ± 1.0 Ma (Mt Black Formation; Mortensen et al., 2015), while the oldest biostratigraphic age of sedimentary strata from the Dundas region is ~505 Ma.

While much of the basin's history appears to have involved below wave-based subaqueous sedimentation, igneous geochemical data indicate a likely extension maximum either associated with emplacement of primitive shoshonitic magmas at or immediately above the VHMS ore position within the 'Yolande Cycle', or tholeiitic mafic magmatism at the onset of the Tyndall Group cycle.

Facies types indicative of proximity to active growth faults such as talus and amalgamated coarse-grained turbidite fan deposits are relatively common, particularly on the western margin of the basin (e.g. Selley, 1997), yet clear definition of controlling structures is surprisingly difficult. As noted above, however, a fault-controlled compartmentalisation of the basin is likely to account for much of the complex lateral litho-stratigraphic variation.

Berry and Keele (1997) proposed a simple N-S trending graben geometry, transected by oblique transfers, the intersection of which was conducive to both volcano and VHMS localisation. Supported in part by facies architecture, the general N-S orientation of depocentres is in accordance

with regional fold-Devonian foliation relationships: typically, macroscopic folds are transected in an anticlockwise fashion by the regionally NW- to NNW-oriented Devonian foliation, suggesting nucleation of folds on some form of N-S oriented structural feature (e.g. Selley, 1997).

Parts of the Henty Fault appear to have an extensional Cambrian history, most convincingly about its southern end where it is spatially associated with tholeiitic mafic dyke swarms (Corbett et al., 2014). By contrast, the Rosebery Fault, another of the major faults paralleling the trace of the MRV, appears to be entirely related to Devonian basin inversion (Berry, 1993).

2.6.3 Tyennan Orogeny Stage 3: Late Cambrian basin inversion

In the Late Cambrian, MRV volcanism waned and the uplifted Proterozoic basement rocks ultimately became the dominant source of sediments (Corbett et al., 2014). Widespread unconformities at the top of the Owen Group, and a fundamental shift from compartmentalised sub-basin form to extensive layer-cake shelf-type sedimentation associated younger Ordovician and Silurian strata, mark a major change in tectonic conditions.

As is the case for Middle Cambrian extensional faults, unequivocal definition of specific Late Cambrian compressional structures is generally lacking. Inversion of Henty Fault prior to Devonian folding is proposed by Berry et al. (1989b), and some evidence exists for reverse movement on the Great Lyell Fault near Queenstown in the central MRV, during Owen Group sedimentation (Corbett 2001). Intra-Owen Group angular unconformities on the flanks of N-S trending synforms were identified by Berry (1994) and interpreted to indicate syn-depositional amplification of open folds. While Selley (1997) favoured an inherited an extensional sub-basin geometry to account for the anticlockwise cleavage transection of regional folds, others have suggested that it reflects tightening of N-S trending folds nucleated during Late Cambrian E-W compression (Berry and Keele, 1993).

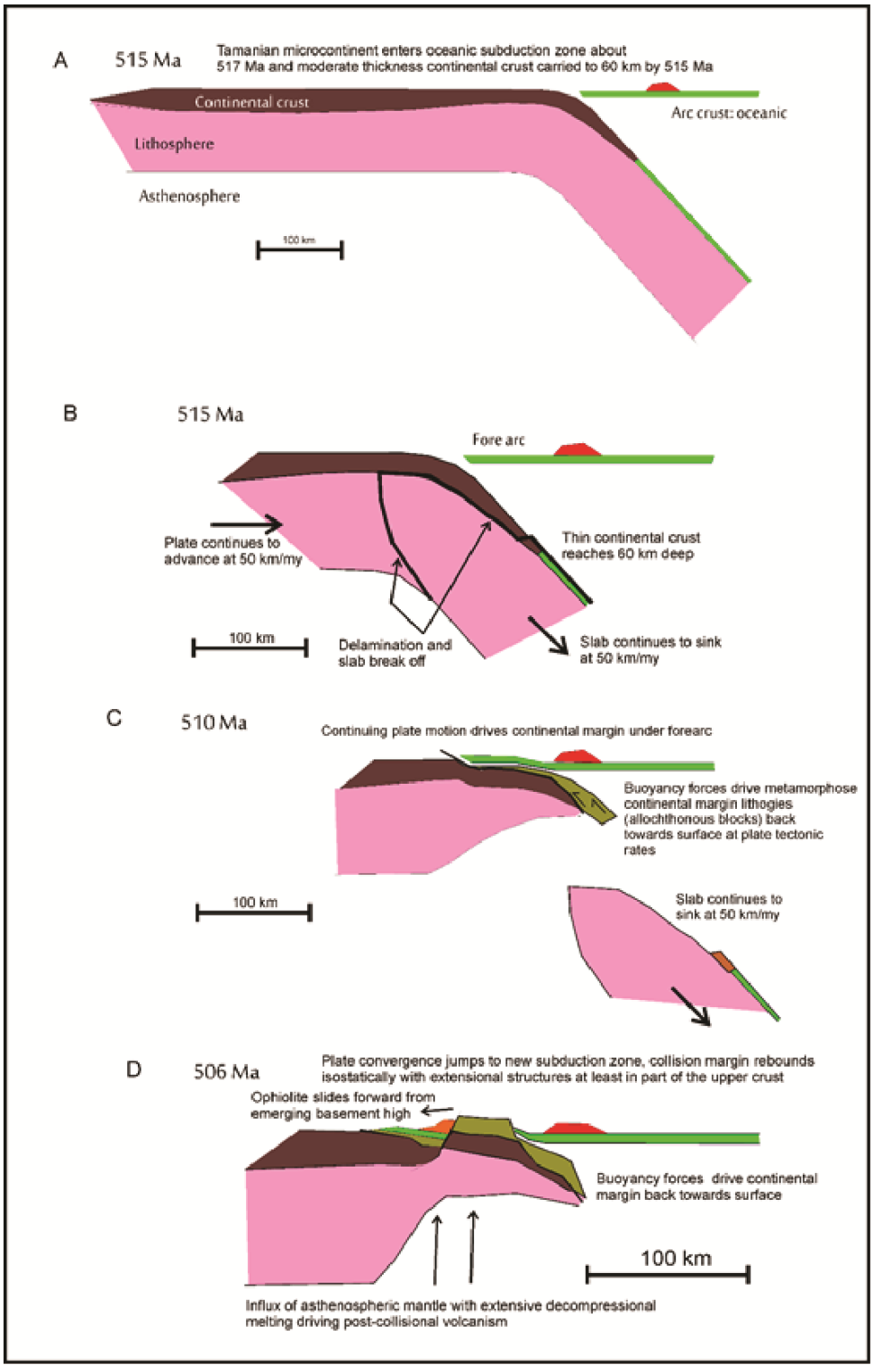

Figure 2.6. Tectonic model for the Cambrian collision and ophiolite emplacement of western Tasmania, from Corbett (2014)

2.7 Devonian Tabberabberan Orogeny

The Cambrian volcano-sedimentary sequence of Western Tasmania was metamorphosed to greenschist facies, folded and cleaved during a Late Early to Early Middle Devonian phase of orogenesis, correlated with the Tabberabberan Orogeny of Eastern Australia (Williams, 1978; Selley, 1997; Corbett et al., 2014). Folds are typically upright, with kilometre scale wavelength, and in lower Palaeozoic strata, variable in trend from E-W, NW, N-S, and NE. Early research concluded that the various trends resulted from systematic rotations of the principal stress field (Seymour, 1980), however, more recent work has argued for inheritance of Cambrian structures, both extensional and compressional, under a relatively stable Devonian ENE-WSW stress field (Selley, 1997; Selley and Meffre, 1997; Stacey and Berry, 2004). Supporting this interpretation is a relatively simple fold configuration in Ordovician and Silurian strata, with axial planar NNW-striking foliation.

Inversion of MRV depocentres led to the emplacement of elongate fault-bounded inliers of Proterozoic to Early Cambrian 'basement' rocks into the Middle-Late Cambrian succession. These are particularly well developed to the west of the Rosebery Fault (Fig. 2.5), and thought to represent either directly inverted sub-basin boundaries, or short-cut thrusts that propagated through sub-basin footwall fault blocks (Berry, 1993; Selley, 1997). As noted above, Berry (1993) interpreted the Rosebery Fault to have nucleated during Devonian orogenesis as a (sub-basin) hangingwall bypass thrust, largely accommodating ~50% shortening and ~3 km of W-directed throw.

Granite bodies were emplaced during the waning stages of the Tabberabberan Orogeny, their sub-surface geometries deduced from gravity modelling (Leaman and Richardson, 2003). The latter is particularly important in exploration for granite-related skarns(Kitto, 1994) demonstrating that the world class Renison Sn deposit is located in an extensional fault array, produced adjacent to a sub-surface 'shelf' on a granite's outer shell, by forceful upward intrusion. Granite classifications conform to both I- and S-types, and are interpreted to record involvement of mantle derived mafic, lower crustal, and supracrustal Proterozoic components (Corbett et al., 2014).

2.8 Summary

The Rosebery Group comprises marine volcano-sedimentary succession that was deposited within a sub-basin that transitions from a volcanic dominated depocentre in the east to a turbidite sediment dominated basin margin in the west. Deposition occurred in a series of sub-basin compartments, with significant lithofacies variation.

The central part of the Rosebery Group records an early phase of basin starvation, during which fine grained mudstone, siltstone and minor dolomitic sandstone were deposited, derived mainly from extra-basinal sources. Localised and abrupt coarsening of the stratigraphy is marked by the deposition of polymictic conglomerate that can best be explained by increased tectonic activity along the basin margin. The basin suddenly transitioned from basement dominated sediments to quartz-feldspar phyric-pumice breccia (Natone Volcanics). The pumice breccia has been correlated on geochemical grounds with the White Spur Formation. This correlation was further strengthened through U-Pb dating that constrained its age to be 498.6 ± 0.8 Ma, an age that falls within the error limits of the White Spur Formation (~500-499 Ma; Baker, 2013; Mortensen et al., 2015). The U-Pb dating obtained corresponds to the Pre-Tyndall Group stage of volcanism in MRV, but it largely falls within the biostratigraphic age range of Tyndall Group, highlighting the disparity between correlation methods, and the need for further refinement. Generally, the geochemical and geochronological correlations record a transition from basement derived sediments to felsic volcanics within the Rosebery Group that parallels the transition from epiclastic deposition of the Rosebery-Hercules host rock to felsic volcanism at the base of White Spur Formation. The correlation can be extended further to the south in the Dundas Group that has biostratigraphy control on the Hodge Slate (~502 Ma) that equates to the geochronological limits of the Hercules Pumice Formation (~504-502 Ma, Mortensen et al., 2015) where it shows a transition from non-volcanogenic MUC derived sedimentation to basin starvation and mudstone deposition (Fig. 2.2).

On the eastern side of Rosebery Group that transitions towards the basin centre, the Marianoak Formation is composed of quartz-feldspar-phyric pumice breccia, lithic rich volcaniclastic breccia interbedded with volcaniclastic sandstone and siltstone. It is overlain by thick (~300 m) mudstone of Chamberlain Shale that suggests a prolonged period of basin 'starvation'. The prolonged quiescence was followed by the deposition of compositionally mature sediments of Stitt Quartzite that was sourced from the uplifted Precambrian basement during the early Late Cambrian, lower Owen Group depositional cycle (Corbett et al., 2014). The western part of the belt that flanks the 'basement' inlier of Crimson Creek Formation is composed of similar facies association with the Stitt Quartzite.

Chapter 3: Facies Analysis

3.1 Introduction

Facies analysis of volcano-sedimentary successions using detailed geological mapping, logging and petrographic study is a very important tool in understanding volcanic and sedimentary processes. In turn, facies analysis may underpin volcanic reconstruction and correlation, which are critical for the identification of favourable hosts of volcanogenic massive sulphide deposits.

In this study, facies analysis of the Rosebery Group volcano-sedimentary sequence is conducted. The sequence was long perceived to be non-prospective for VHMS mineralization due to the dominance of siliciclastic sediments, and distance from MRV volcanic centres. Nevertheless, lenses of VHMS style of mineralization were discovered in 2010 in the eastern part of the Rosebery Group, an interval positioned immediately below the Rosebery Fault, referred to in this study as the Marianoak Formation. While previous workers have drawn comparisons between the Marianoak Formation and the White Spur Formation (e.g. Corbett and Lees, 1987), lithofacies associations and the precise stratigraphic position of the mineralised intervals relative to those of the Rosebery mine host sequence remain only partly constrained.

The principal aims of this study is to characterize the lithofacies associations of the Rosebery Group and build a robust lithostratigraphic framework based on drill hole and surface mapping. Secondly, to examine and compare the lithofacies associations of the Rosebery Group and the VHMS-bearing Rosebery Mine stratigraphy, positioned in the hangingwall of the Rosebery Fault.

The study area extends for ~15 km strike length and ~2-5 km width. The volcano-sedimentary sequence is diverse with complex stratigraphic correlation from north to south. For ease of understanding it is divided into two zones, the northern zone and southern zone.

- The northern zone encompasses the Marianoak Formation where it is partly exposed in the Rosebery Township, and extends from the northern part of Rosebery Mine to Jupiter (Fig. 1 'map pocket'). The sequence passes westward through the Natone Volcanics (NV), exposed along Natone Creek in the central part of the study area, onto the flanks of Westcott Hill.
- The southern zone includes outcrops along the Ring River and its tributaries, and the NE Dundas tramway (Fig. 1 'map pocket')

3.1.1 Methods

Geological mapping

Geological mapping was conducted in one summer season with four expeditions. All field maps at 1:2000 scale (Appendix 1) were compiled with existing maps that will be used in the subsequent chapters. Moreover, 140 representative hand specimens were collected for mineral identification and facies analysis (Appendix 5). Eighteen thin-sections were prepared for petrographic observation. The final product also incorporated data from previous mapping expeditions in the areas that today are not accessible; in particular, those of Green (1983), Electrolytic Zinc Company of Australasia Ltd, regional geological maps compiled by the Mineral Resources Tasmania, and Gifkins (2001).

Drill hole logging

The study involved detailed geological logging of 13 drill holes at 1:200 scales and summarized at 1:1000 scale (Appendix 2). Of these, nine drill holes were collared along the eastern part of the belt, from the Rosebery Mine southward to the Jupiter prospect, each of which intersected the Rosebery Mine stratigraphy and Marianoak Formation strata (Fig. 3.1). Three of the nine drill holes (R10032, R10063 and R10035) were drilled from underground. The remaining four drill holes are collared in the region of Natone Creek (Fig. 1 'map pocket'). Logs of the complete dataset are included in Appendix 2. Observations and data collected include grain size, bedding, contact relationships, bed geometry, primary and secondary structures, and alteration type. Sixty-four representative samples were chosen and prepared for petrographic analysis from a total of 210 drill core slabs.

3.2 Facies analysis of the Marianoak Formation

The Marianoak Formation comprises three mappable volcano-sedimentary facies associations (Fig. 3.1). The oldest facies association is a rhyolite breccia with volcanogenic mudstone and siltstone matrix (peperite), quartz-phyric and quartz-feldspar-phyric pumice breccia, which is interbedded with mudstone (MRF 1). There are two facies associations within MRF 2: (1) a basaltic andesite volcaniclastic breccia (VBX I) interbedded with volcaniclastic sandstone and siltstone (VSST), and intervals of black mudstone, and (2) rhyolite volcaniclastic breccia (VBX II) interbedded with volcaniclastic sandstone and siltstone (VSST).

3.2.1 MRF 1: Rhyolite breccia (peperite), quartz-phyric pumice breccia and quartz-feldspar-phyric pumice breccia with mudstone

MRF 1 facies association comprises four facies types, distinguished on the bases of texture and composition. Volcanogenic facies types appear stratigraphically distinct, and in ascending stratigraphic order include rhyolite breccia (peperite), quartz-phyric pumice breccia and quartz-feldspar-phyric pumice breccia. Thick (10-70 m) black mudstone facies occurs below the quartz-feldspar-phyric pumice breccia in holes 250R and JP357 and volumetrically minor (1-3 m) that separates the pumice breccia facies (Figs. 3.1-3.2). A type section is intersected in drill hole R10063 (Fig. 3.1) but can be correlated with various degrees of completeness from the northern part of the Rosebery Mine to Jupiter in the south (Fig. 3.2).

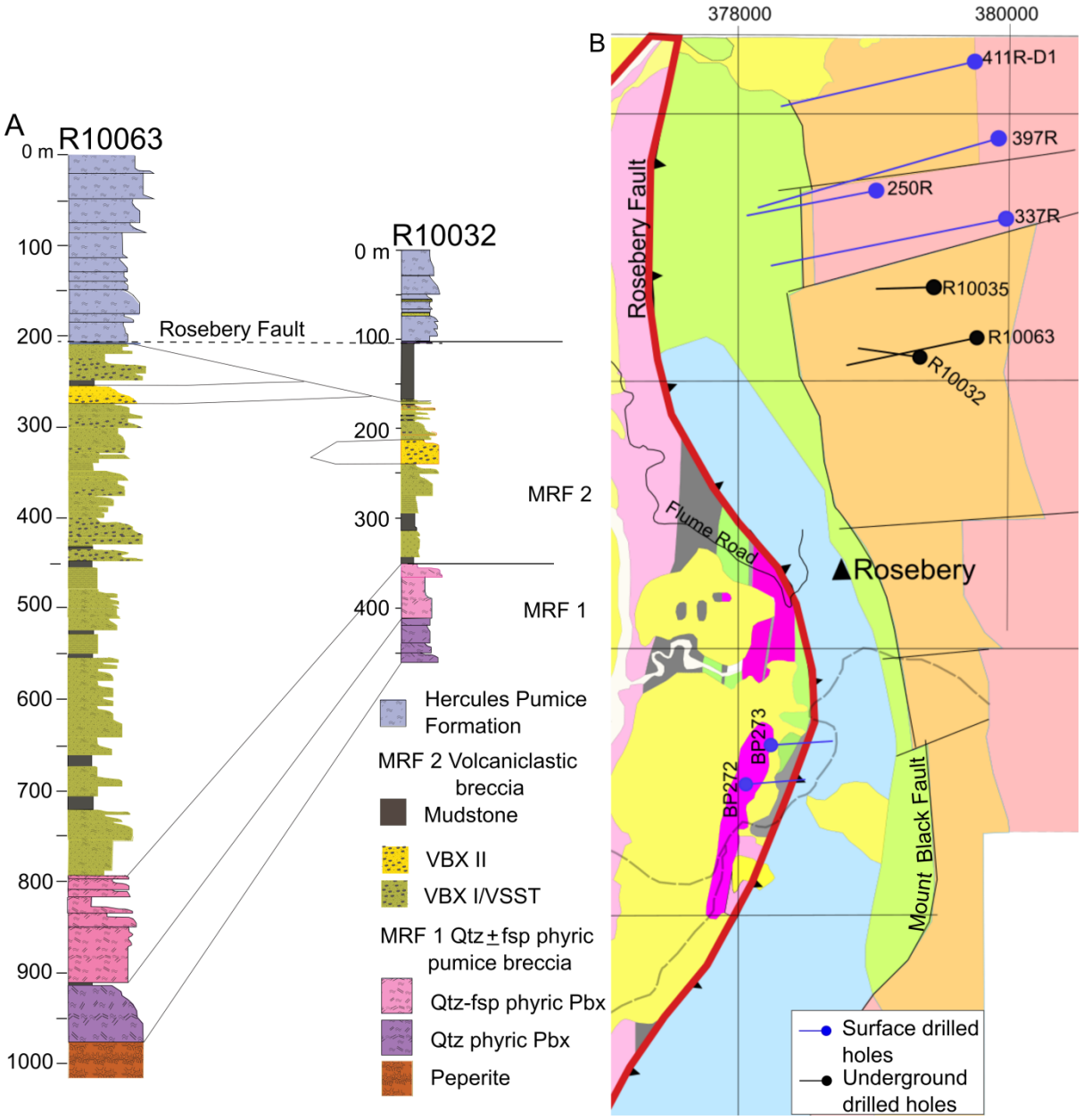

Figure 3.1. A) Lithostratigraphic profiles of the Marianoak Formation. The lowest facies association consists of rhyolitic breccia (peperite), quartz ± feldspar-phyric pumice breccias, interbedded with black mudstone (MRF 1). Stratigraphically above is MRF 2 with two facies associations of i) basaltic andesite volcaniclastic breccia and volcaniclastic sandstone (VBXI/VSST), which is interbedded with black mudstone, and ii) rhyolitic volcaniclastic breccia/volcaniclastic sandstone (VBXII/VSST). (B) Geological map showing drill hole collars and traces (refer to Fig. 1. in the 'map pocket' for the legend).

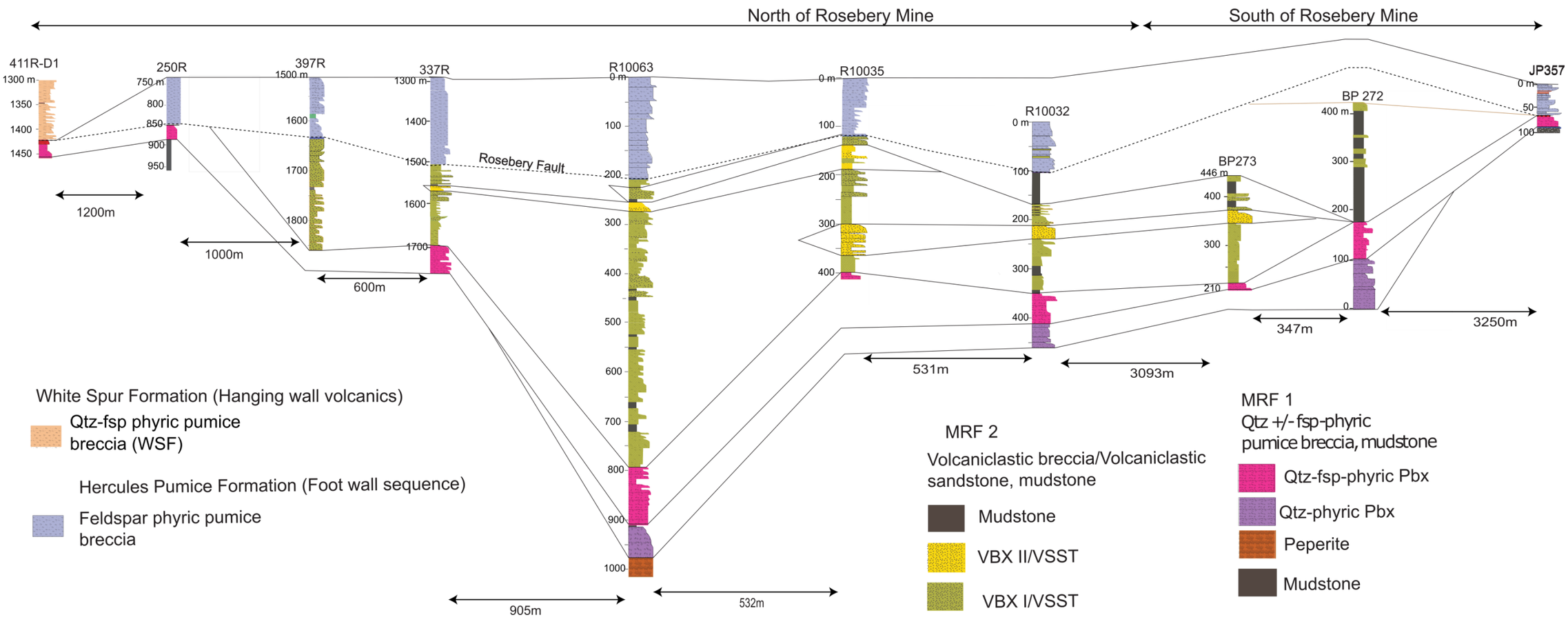

Figure 3.2. Lithostratigraphic correlation of the volcano-sedimentary sequence of Marianoak Formation from the Northern part of the Rosebery Mine, below the Rosebery Fault, to the south in Jupiter

Facies 1: Rhyolite breccia (peperite)

The rhyolite breccia facies comprises a monomictic jigsaw fit arrangement of poorly sorted, grey to brown colour, angular to sub-rounded, fine grained rhyolitic clasts (1-10 cm, 40-70%) with planar to curviplanar margins set in a volcanogenic siltstone and mudstone matrix (Fig. 3.3).

It is ~60 m thick and was intercepted only in R10063 (Fig. 3.2). In thin section, the matrix of the breccia possesses a very fine grained and silty texture with floating quartz crystal fragments (50-100 µm, 10-15%) and minor former glass shards (Fig. 3.4).

Figure 3.3. Photograph of rhyolitic breccia with angular, curviplanar clasts, jigsaw fit texture and siltstone-mudstone matrix. R10063: 1115.30 m. Pencil length shown is 10 cm.

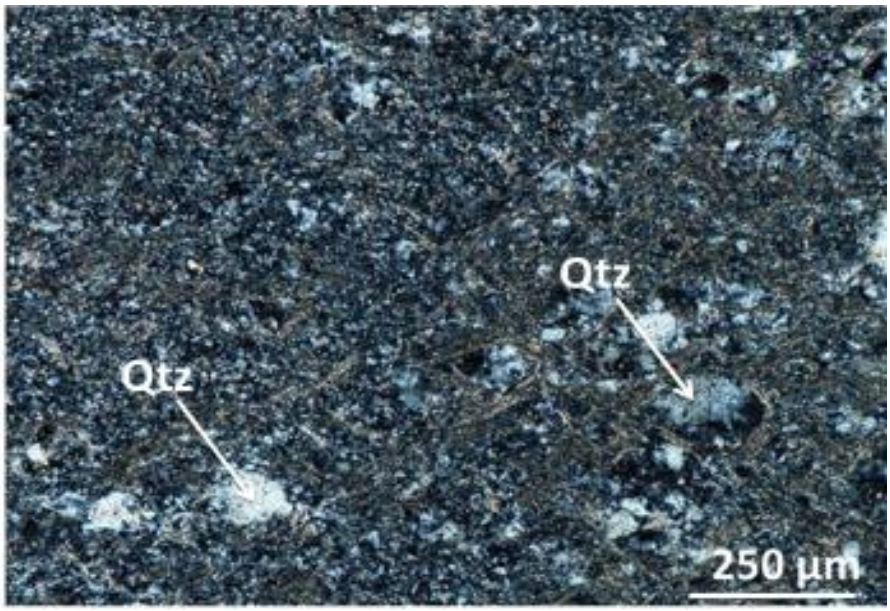

Figure 3.4. Photomicrograph of the volcanogenic silt to mudstone matrix of rhyolitic breccia with fine grained quartz crystal fragments. R10063: 1115.30 m. Image taken under cross polarized light (XPL).

Facies 2: Quartz-phyric pumice breccia

Quartz-phyric pumice breccia overlies the rhyolitic breccia, varying in thickness from 40 to 100 m across the northern zone (Fig. 3.2). It consists of amalgamated beds of 15-20 m thickness. All beds are normally graded, with a 1-3 m basal interval that is mainly composed of poorly to moderately sorted, very coarse quartz-phyric pumice fiamme, with minor 2-5 cm mudstone rip up clasts. The very coarse bases grade upward through a volcaniclastic sandstone to a stratified siltstone top, with minor black mudstone facies (Fig. 3.5).

The quartz-phyric pumice breccia is mainly composed of pumice fiamme clasts (1-5 cm, 50-60%) that sit within a matrix of mainly angular to sub-rounded, medium to coarse grained, frequently embayed quartz crystal fragments (0.25-2mm, 1-2%), very fine quartz (<0.25 mm, 10%), minor euhedral feldspar crystals (1-2%, 0.25-1 mm), and former glass shards (5-10%: Figs. 3.7-3.8). Weak to moderate sericitisation affects both clasts and matrix. A defining characteristic of this facies is the high quartz to feldspar ratio of 95: 05.

Facies 3: Quartz-feldspar-phyric pumice breccia

The quartz-feldspar-phyric pumice breccia stratigraphically overlies the quartz-phyric pumice breccia and has a highly variable thickness from 34 m to a maximum of 110 m in drill hole R10063 (Fig. 3.1). Individual beds are massive to subtly normally graded, and 10-20 m in thickness. The bases are 1-2 m thick and composed of coarse 1-5 cm highly flattened and ellipsoidal quartz-phyric pumice fiamme and minor mudstone lithic clasts (Figs. 3.8 & 3.9). Generally, upper parts of beds are stratified, consisting of volcaniclastic sandstone and siltstone. In the northern part of the study area (drill hole 411R-D1: Figs. 1 & Fig. 3.2) a relatively fine-grained breccia top hosts a high grade massive sulphide lens.

The facies type is intensely sericite and moderately silica-altered, and massive to weakly cleaved. It is composed of 1-5 cm pumice fiamme (50-60%) and minor 1-3 cm mudstone lithic clasts (1-2%), set in a matrix of fine and medium-grained angular to sub-rounded quartz crystal fragments

(15% <0.5 mm and 5%, 0.5-2 mm), euhedral feldspar crystal fragments (5%, 0.5-2 mm), and former glass shards (Fig. 3.8-3.9). The quartz to feldspar ratio is slightly lower than that of Facies 2 at 80:20.

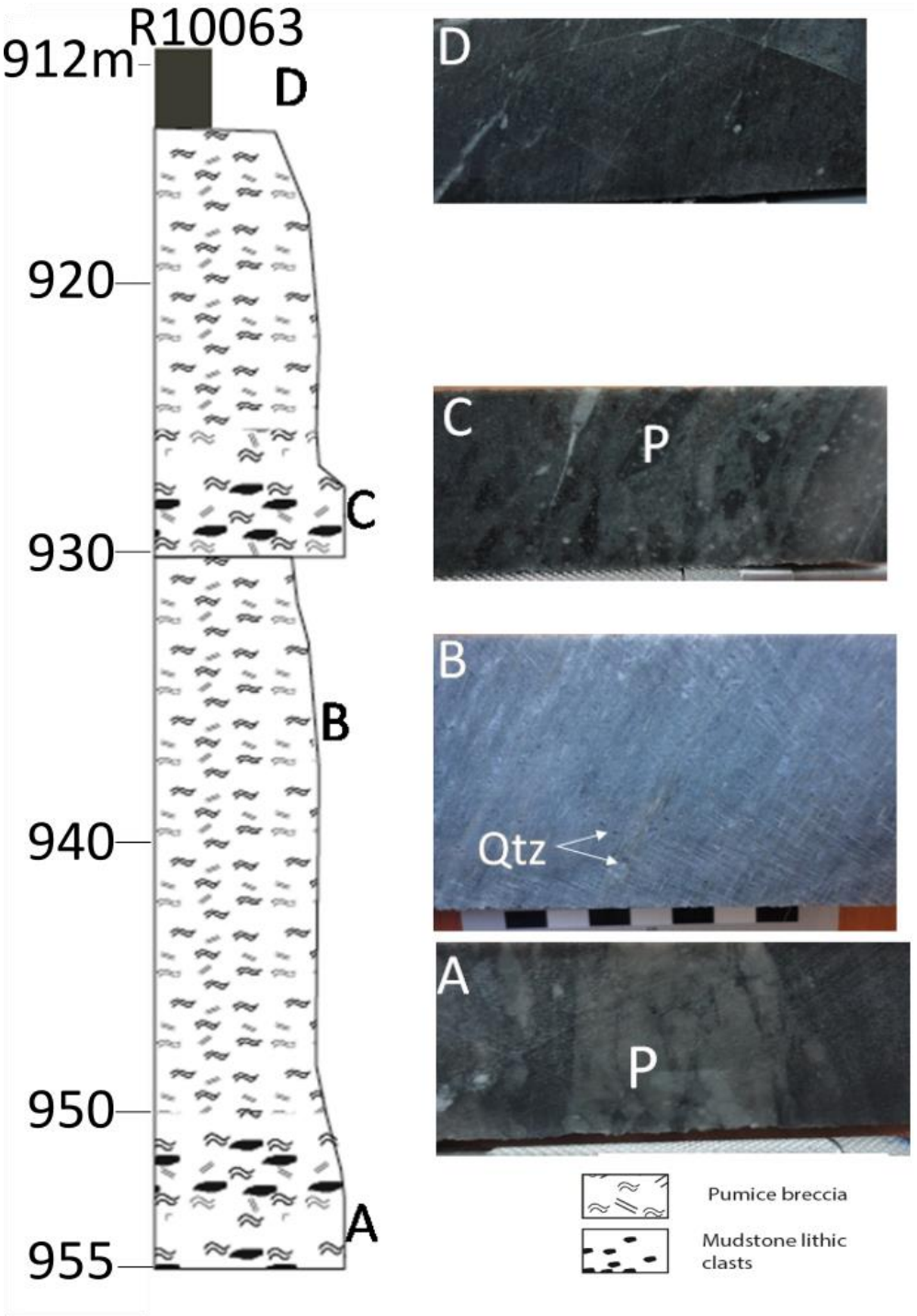

Figure 3.5. Geometry and texture of the quartz-phyric pumice breccia facies, MRF 1, R10063. Amalgamated beds grading upward from coarse pumice and mudstone-lithic bearing bases (A and C), to quartz-phyric volcaniclastic sandstone (B). Dark grey mudstone facies occurs at the top of the interval (D). P = pumice.

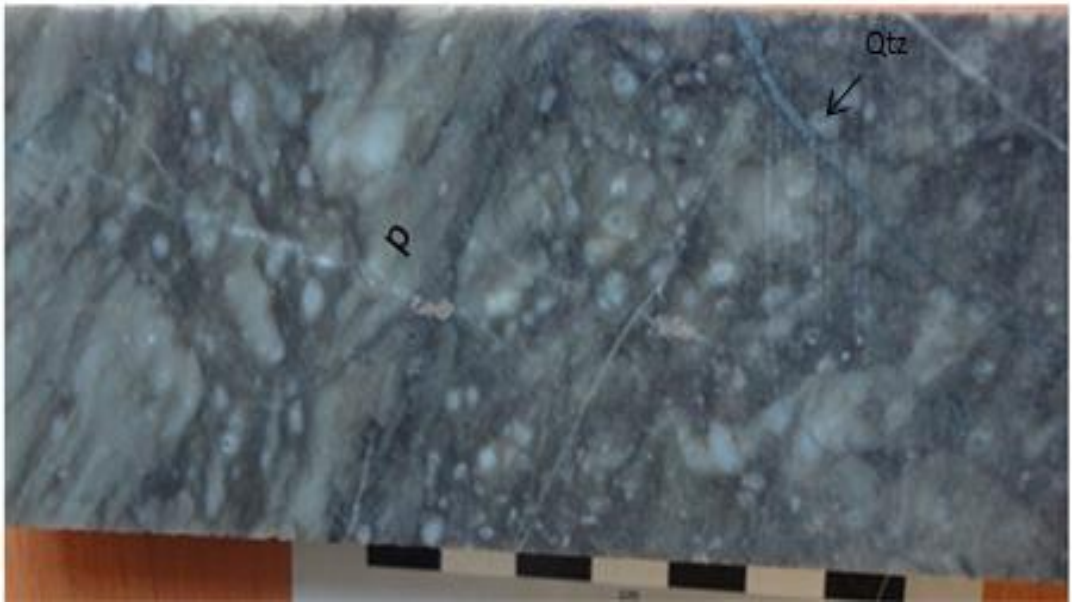

Figure 3.6. Photograph of quartz-phyric pumice breccia showing the pumice clasts (p) and coarse white clots of quartz crystal fragments (Qtz). R10032: 438.10 m. Scale shown is in centimetre.

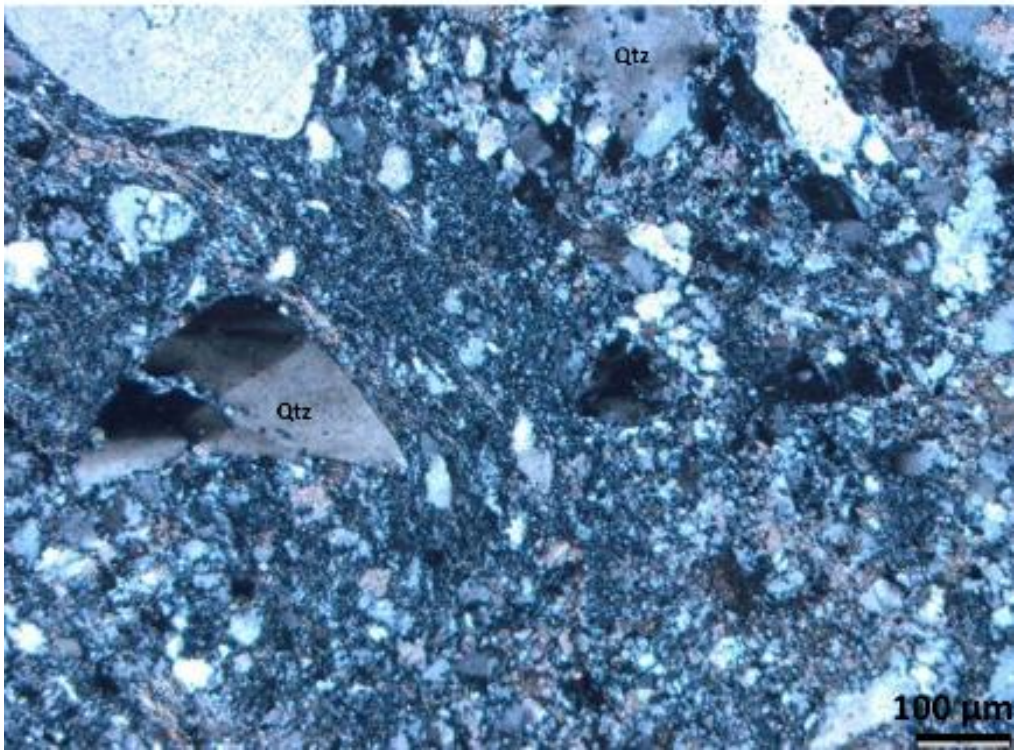

Figure 3.7. Photomicrograph of quartz-phyric pumice breccia showing dominantly angular quartz (Qtz) crystal fragments in moderately sericite altered matrix. R10063: 933.20 m. XPL

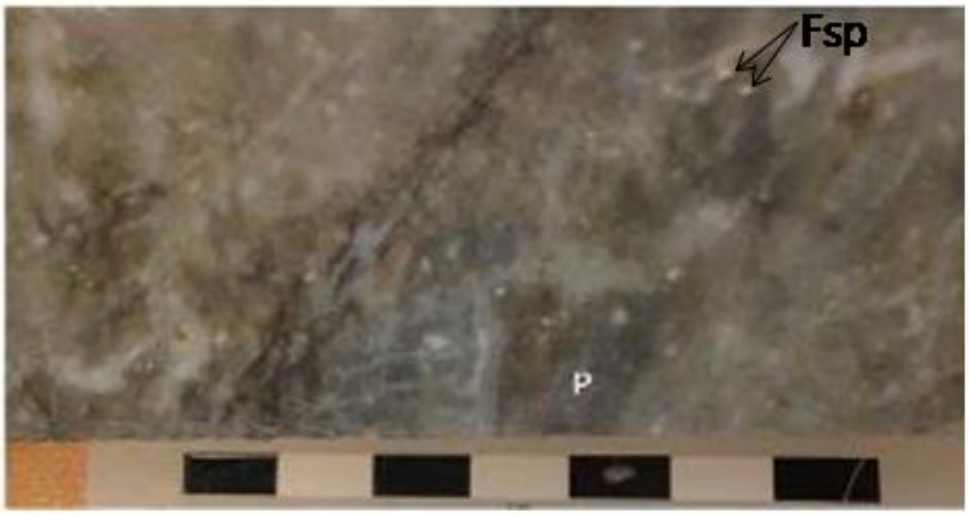

Figure 3.8. Quartz-feldspar-phyric pumice (P) breccia with white clots of feldspar crystal fragments. R10032:403.40m. Scale shown is in centimetres.

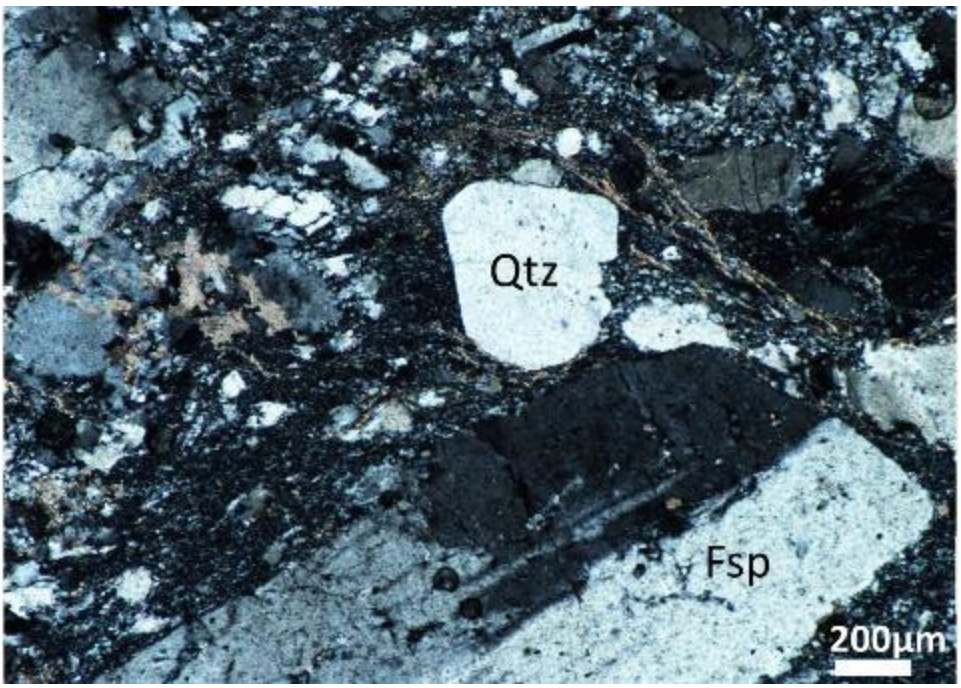

Figure 3.9. Photomicrograph of framework and matrix components of the quartz-feldspar-phyric pumice breccia facies. R10063: 909.00 m. XPL

Facies 4: Black mudstone

The black mudstone facies within MRF 1 is quartz-carbonate altered, strongly cleaved and partly pyritic. It occurs in two stratigraphic levels: below the quartz-feldspar phyric pumice breccia in holes 250R and JP357, with about 70 m and 10 m thickness respectively; and as thin 1-3 m beds that separate the volcanogenic mass-flow beds of Facies 2 and Facies 3 in holes R10063 and BP272 (Fig. 3.2).

Interpretation

The rhyolite breccia has a monomictic coherent clast type with curviplanar margins, and jigsaw fit clast texture. These features, coupled with a highly invasive volcanogenic mudstone and siltstone matrix, suggests the facies is a peperite. Peperites are formed by the deposition of lava onto, or intrusion of magma into, water-saturated unconsolidated sediments. The curviplanar margins are consistent with quench fragmentation (McPhie et al., 1993).

The quartz ± feldspar-phyric pumice breccia facies are generally normally graded, containing dominantly altered pumice fiamme, broken quartz ± feldspar crystals. This assemblage suggests that they were generated from explosive felsic eruptions(Yamagishi, 1987; Gifkins, 2001). The combined ~200 m thickness and ~9 km extent of these lithofacies suggest very large volume pyroclastic eruptions and extensive dispersal.

Massive pumice breccia beds with normal grading, lithic–rich bases and stratified tops suggests their deposition from water-supported gravity flows, most probably from high concentration density currents or debris flows (Cas and Wright, 1991). Thickly bedded and weakly developed grading is interpreted to be as a result of rapid and voluminous deposition from concentrated mass-flows immediately after eruption(Gifkins, 2001). The mudstone lithic clasts are interpreted to be eroded from unconsolidated mud substrates that were incorporated into the base of the mass flow and demonstrate a submarine environment of eruption, transport and deposition. The pumice-rich sandstone and siltstone ash top is interpreted to be from water settled fallout

suspension sourced either directly from the eruption plumes or from the trailing an ash cloud associated with the high concentration flows (Gifkins and Allen, 2001).

The mudstone beds record prolonged periods of volcanic quiescence with pelagic sedimentation. 10-70 m-thick mudstone beds beneath the pumice breccias in holes JP357 and 250R respectively record a long period of volcanic quiescence prior to a voluminous felsic eruption with extensive dispersal. The thin mudstone beds between the pumice breccias demonstrate that they are not derived from the same eruptive event, and that there was an extended period of quiescence between them. The change in relative crystal abundances from Facies 2 to 3 (i.e. reduction in quartz: feldspar value) is best explained by a change in parental magma composition, also consistent with a volcanic hiatus.

3.2.2 MRF 2: Volcaniclastic breccia, volcaniclastic sandstone and siltstone, and massive mudstone

MRF 2 comprises two facies associations; 1) intercalated basaltic andesite volcaniclastic breccia, volcanogenic sandstone and siltstone (VBX I/VSST), interbedded with black mudstone, and 2) rhyolite volcaniclastic breccia in volcaniclastic sandstone (VBX II/VSST).

In general, the VBX I/VSST facies type coarsens upsection, with coarse-grained breccia dominating the upper parts of stratigraphic profiles (e.g. Fig. 3.2). Throughout, basaltic andesite clasts are the main components. Intervals of the quartz-bearing and relatively pumice-poor VBX II/VSST facies association occur at a number of intervals in the upper Marianoak Formation, but most commonly towards its top.

Facies Association VBX I/VSST: basaltic andesite volcaniclastic breccia/volcaniclastic sandstone

The VBX I/VSST facies association overlies MRF 1 stratigraphy and laterally has a highly variable thickness that ranges from ~130 m in hole R10032 to a maximum of 600 m in hole R10063 (Figs. 3.1 and 3.2).

Facies 5: Volcaniclastic sandstone and siltstone.

This facies comprises graded beds of 1-15 m thickness. Beds generally have poorly sorted polymictic bases of medium to coarse grained volcaniclastic sandstone with light grey to dark grey, angular to sub-rounded clasts (0.5-1.0 mm, 5%) and minor quartz crystal fragments in a sericite-altered matrix that grades into volcaniclastic siltstone (Fig. 3.10). Beds within this sequence can be separated by ~1-20 m thick, dark grey and pyritic mudstone beds (Figs. 3.1 and 3.2).

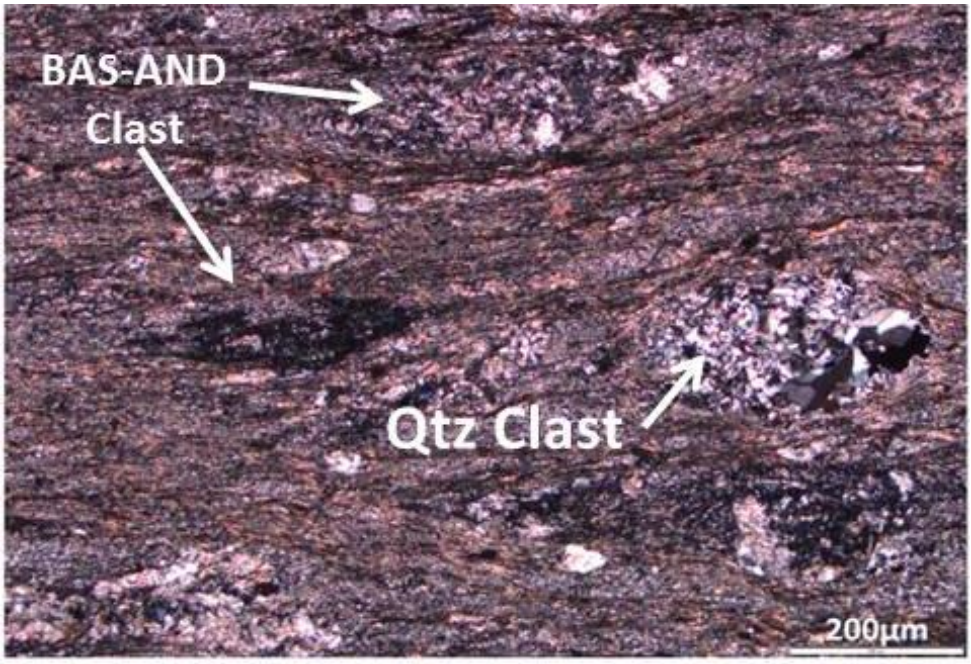

Figure 3.10. Poorly sorted polymictic volcaniclastic sandstone containing fine grained basaltic andesite clasts and less abundant quartz clast, set in a sericite-altered fine grained matrix. R10063: 610 m. XPL

Facies 6: Polymictic basaltic andesite breccia

This facies comprises ~15-20 m thick graded beds with polymictic bases of very coarse grained volcaniclastic breccia dominated by dark green basaltic andesite clasts (1 mm-5 cm, 10-15%), minor light grey angular to sub-rounded aphanitic clasts and mudstone lithic clasts (3-4 cm, 1-2%) that grades to stratified volcaniclastic sandstone and siltstone top (Fig. 3.11).

These framework components are set in a volcaniclastic sandstone matrix with minor angular to sub-rounded and fractured volcanic quartz (0.5-1 mm, 1-2%) and minor euhedral feldspar crystals (1-2%) that grades to volcaniclastic sandstone (Figs. 3.12 A & B). The facies is interbedded with quartz-carbonate altered black mudstone beds of ~1-8 m that are in turn interbedded with volcaniclastic siltstone.

Facies 7: Dark grey mudstone

At the top of MRF 2 in holes R10032 and BP 272, mudstone with bed thicknesses of 160-220 m is interbedded with minor volcanogenic sandstone and siltstone of VBXI/VSST (Fig. 3.1 & 3.2). It is generally massive to weakly cleaved, dark grey in colour, with intense quartz-carbonate veining and fine, locally pyritic, lamination. A very thick interval crops out to the west of Rosebery Township, forming the principal lithofacies in what is conventionally referred to as the Chamberlain Shale (Brathwaite, 1970; Green, 1983; Parfrey, 1993).

Interpretation

Although VBX I/VSST is strictly polymictic, the predominance of basaltic andesite clasts throughout the facies association indicates derivation from a relatively uniform volcanic source. The general upsection increase in grain size suggests progradation of the sediment input system with time.

The clast textures and shape (i.e. angular to sub-rounded) along with a lack of pumice fiamme suggests that original clasts were dense and therefore are possibly derived from an effusive eruption, with variable reworking from the source. Thick beds of 15-20 m with normally graded and stratified tops suggests their deposition from water supported gravity flows, most probably high concentration density mass-flow currents or debris flows (Cas and Wright, 1991). The increased abundance of large volcanic clasts with minor mudstone lithic-clasts towards the base of beds implies density sorting, and the mudstone rip up lithic clasts at the base of the beds are interpreted

to be scoured and eroded from unconsolidated mud substrate during the lateral transport of mass flows (Allen, 1991; McPhie et al., 1993).

Mudstone beds preserved between the mass-flow deposits record below wave base pelagic sedimentation. They represent periods of basin starvation and probable volcanic inactivity, the great thickness of some the intervals reflecting particularly prolonged hiatuses.

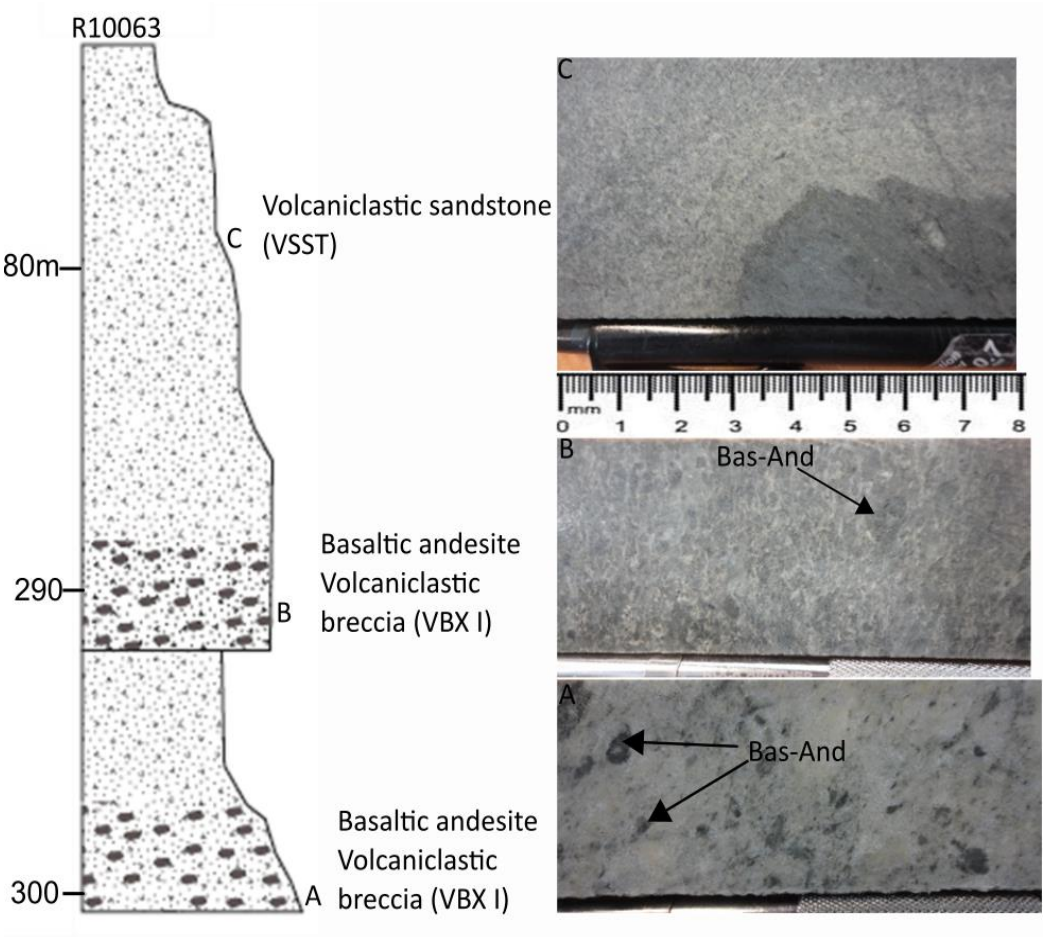

Figure 3.11. VBX I geometry and textures in R10063. In A) & B) Basaltic andesite (Bas-And) clasts dominated breccias grading to volcaniclastic sandstone (e.g., C).

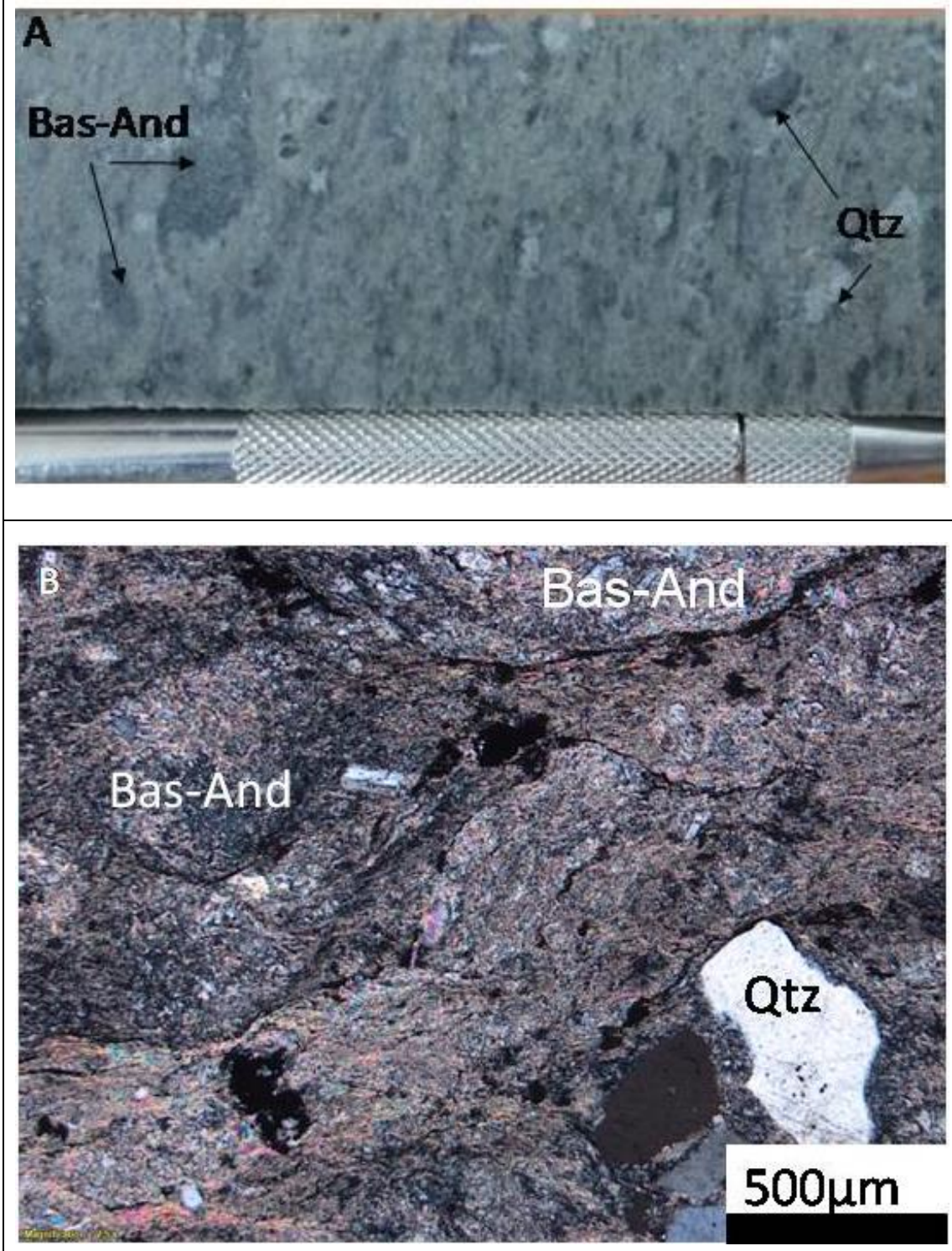

Figure 3.12 (A). Polymictic volcaniclastic breccia dominated by basaltic andesite (Bas-And) clasts set in quartz-phyric volcaniclastic sandstone matrix and (B). Photomicrograph of polymictic volcaniclastic breccia with angular to sub-rounded basaltic andesite (Bas-And) clasts and quartz crystal fragments. R10063: 416.40 m. XPL.

Facies 8: Rhyolitic volcaniclastic breccia with volcaniclastic sandstone and siltstone

The rhyolitic volcaniclastic breccia interbedded with volcaniclastic sandstone and siltstone VBX II/VSST intercalates with VBX I/VSST mainly, but not exclusively, within the upper parts of coarse sequence of MRF 1 except in hole 397R (Figs. 3.1 & 3.2). Individual bed thicknesses are about 2-17 m with very coarse bases grading to stratified siltstone top beds ~ 1m except in hole R10035 where a 60 m thickness is attained (Fig. 3.2).

It is composed of coarse and poorly sorted 1-6 cm quartz-phyric, monomictic, rhyolitic clasts and minor 1-6 cm feldspar-phyric pumice fiamme that grade into volcaniclastic sandstone and stratified siltstone (Fig. 3.2). It also comprises angular to sub-rounded quartz crystal fragments (2-3 mm, 7-10 %), euhedral feldspar crystals (0.25-0.5 mm, 1-2%), and former glass shards in a strongly sericite altered matrix (Fig. 3.13). Unlike the well graded beds in most of the holes (R10035, BP 273 & R10063) locally jigsaw fit texture of quartz phyric rhyolite clasts with planar and curviplanar margins in intensely silicified matrix is observed in hole R10032.

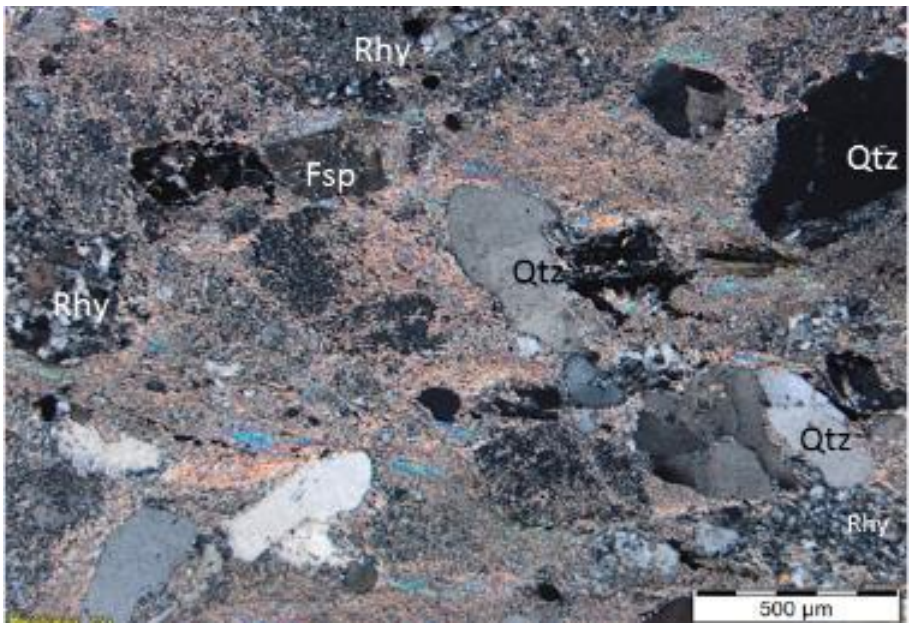

Figure 3.13. Photomicrograph of rhyolitic volcaniclastic breccia, VBX II/VSST, showing quartz (Qtz), feldspar (Fsp) crystal fragments and rhyolitic clasts (Rhy) from hole R10032 at 226 m. XPL

Interpretation

The VBXII/VSST facies association is composed of dominantly monomictic quartz-phyric rhyolite clasts that are poorly sorted, normally graded with stratified tops indicative of its deposition from water supported gravity flows, possibly high concentration density currents soon or after eruption (Gifkins, 2001). The paucity of pumice clasts and dominance of monomictic rhyolitic clasts indicates explosive eruption is unlikely and it is possibly sourced from reworking of effusive volcanism of rhyolitic composition. The local jigsaw fit textures with minor curviplanar clast morphology of monomictic quartz-phyric rhyolitic clasts at the base of hole R10032 is consistent with quench fragmentation in a subaqueous environment (McPhie et al., 1993; Cas and Wright, 2012).

3.3 Facies 9: Quartz-wacke interbedded with black mudstone (Stitt Quartzite)

The Stitt Quartzite, in its type section, overlies the thick massive mudstone interval at the top of the Marianoak Formation, and is well exposed along the Flume Road ('map pocket' Fig. 1). Its western contact can be traced along Natone Creek in the central part of the northern zone. The package uniformly faces west, and has a thickness of ~400 m. A similar package of rocks consisting of micaceous quartz-wacke with intensely cleaved shales crops out on the western part of the study area (Westcott Hill). Likely correlatives also occur in the southern zone at Williamsford and along the Ring River (Fig. 1).

The lower part of the Stitt Quartzite comprises 10-30 cm thick, fine to medium grained normally graded beds of quartz-wacke, interbedded with 5-10 cm beds of intensely cleaved, laminated, black mudstone. Metre- to decimetre-scale upward-coarsening and thickening cycles are exhibited in some good exposures (Fig. 3.14). This package passes upsection to massive or crudely bedded, 1–2 m thick micaceous quartz-wacke beds, interbedded with less than 50 cm-thick intervals of black mudstone. The petrography of the quartz-wacke from these localities invariably shows well

sorted, sub-rounded to angular polycrystalline or undulose quartz (80-90%), coarse detrital mica (2-5%), and 5% lithic clasts (Fig. 3.15).

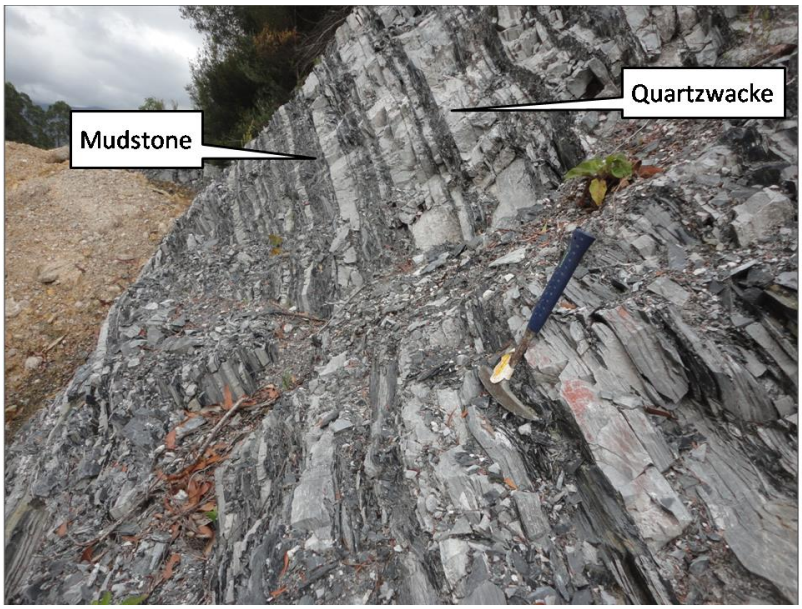

Figure 3.14. Stitt Quartzite: quartz-wacke interbedded with mudstone, with upward (to right) coarsening and thickening. Strata are moderately dipping 52 degrees to the west. Photo taken looking south; Flume roadcutting 377448E/5374975N.

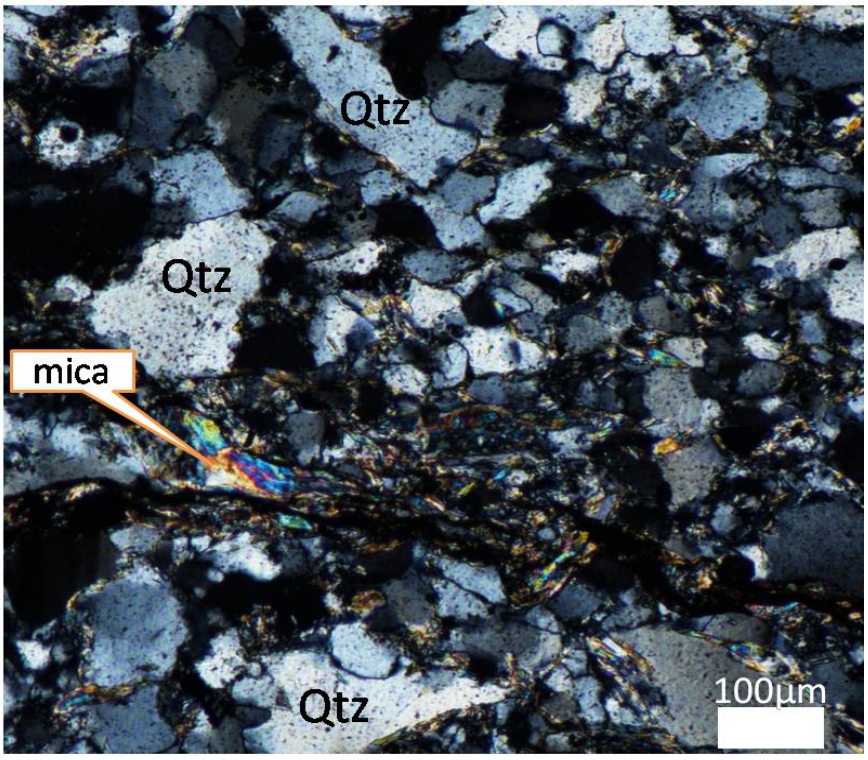

Figure 3.15. Cross-polarized photomicrograph of Stitt Quartzite showing fine to medium grained, moderately sorted, angular to sub-rounded metamorphic quartz (Qtz) and mica.

Interpretation

The normally graded structure of sandstone layers is consistent with deposition from medium- to low-energy turbidity currents (Lowe, 1982). Mudstone interbeds likely record waning low density currents or hemipelagic fallout. The lack of features indicative of reworking by traction currents suggest a below wave-base depositional setting.

Upward coarsening and thickening cycles, evident both at metre scales and from base to top of the sequence are interpreted to record progradation of the fan system. The compositionally mature character of the quartz-wacke, including quartz and mica of probable metamorphic origin, indicates limited input from volcanic centres (i.e. distal or inactive volcanism) and dominant contribution from siliciclastic Precambrian basement sources.

3.4 Geology of the northern-central area (Natone Creek)

The northern-central part of the study area comprises a lithologically-diverse sequence 350-400 m in thickness. In ascending stratigraphic order, it includes; 1) very fine to medium grained siltstone, mudstone and dolomitic sandstone (Westcott Argillite), 2) very coarse grained polymictic conglomerate (Salisbury Conglomerate), and 3) quartz-feldspar-phyric pumice breccia and minor volcaniclastic sandstone (Natone Volcanics) (Fig. 1 & 3.16). Bedding dips are generally to the west, but easterly younging sedimentary directions were recorded by Green (1983) and corroborated in this study. The eastern contact with the west facing Stitt Quartzite block is thus inferred to be a fault (Fig. 1). The present study involved logging of four drill holes (RBH1, RBH2, CHP264 and 180H2: Fig. 3.16) and detailed mapping (Appendix 1B) along Natone Creek. Detailed description of the lithofacies from west to east is given below.

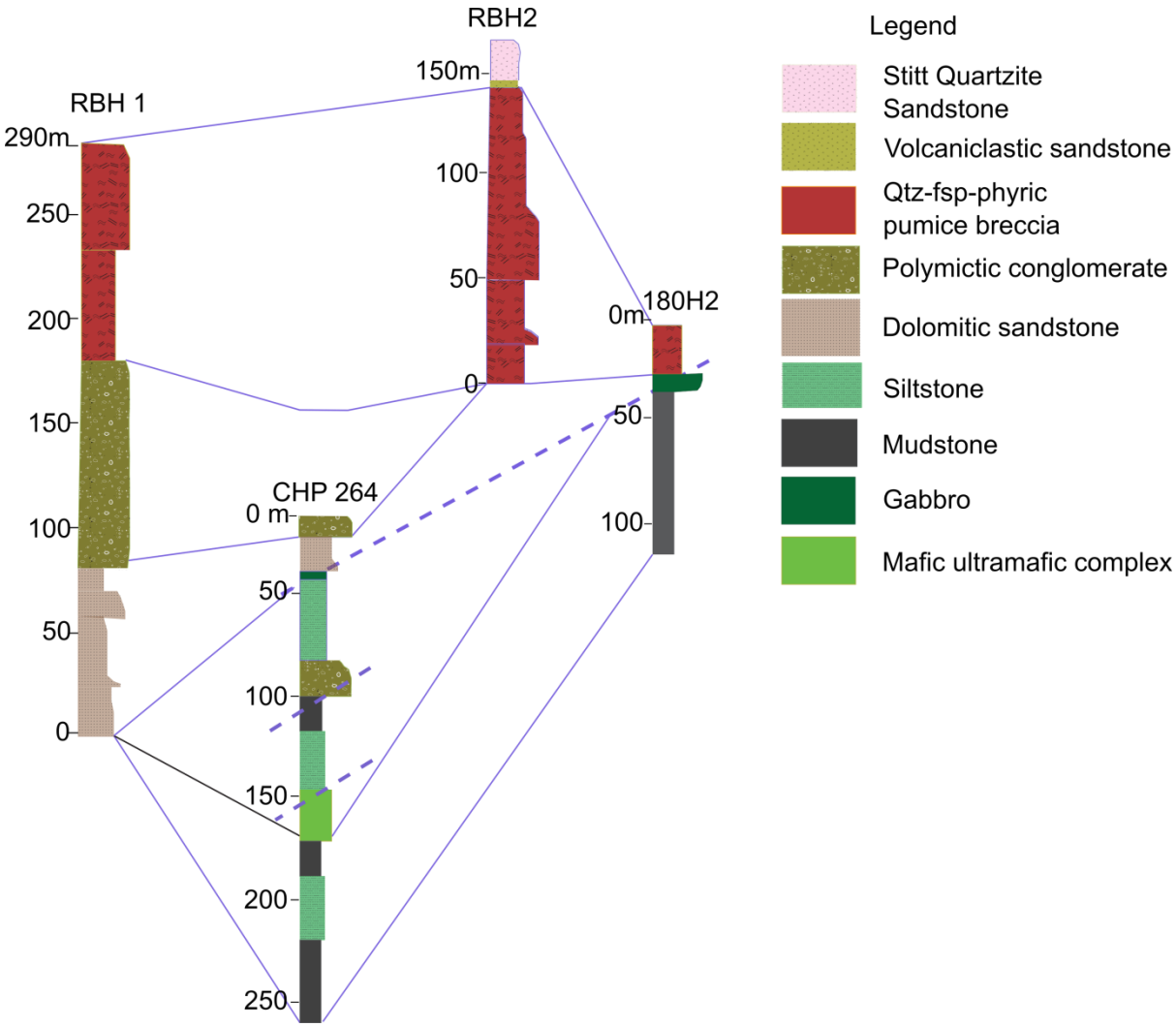

Figure 3.16. Lithostratigraphy of the central part of the study area (Natone Creek) showing lower sequence of mudstone interbedded with siltstone, dolomitic sandstone and polymictic conglomerate overlain by quartz-feldspar-phyric pumice breccia and volcaniclastic sandstone of Natone Volcanics and top most part of Stitt Quartzite.

3.4.1 Facies 10: Mudstone interbedded with siltstone

The lowest stratigraphic level within the northern-central part of the study area comprises mudstone interbedded with siltstone that has a total thickness of 200-250 m. Generally, the mudstone is dark grey to black, finely laminated, partly silty, in places pyritic and carbonaceous (Fig. 3.17). The interbedded non-volcanogenic siltstone is very fine grained, olive green and thinly

laminated (Fig. 3.18). Higher in the stratigraphy, the sequence is more abundantly interbedded with medium grained basement derived sandstone and thin beds of polymictic conglomerate.

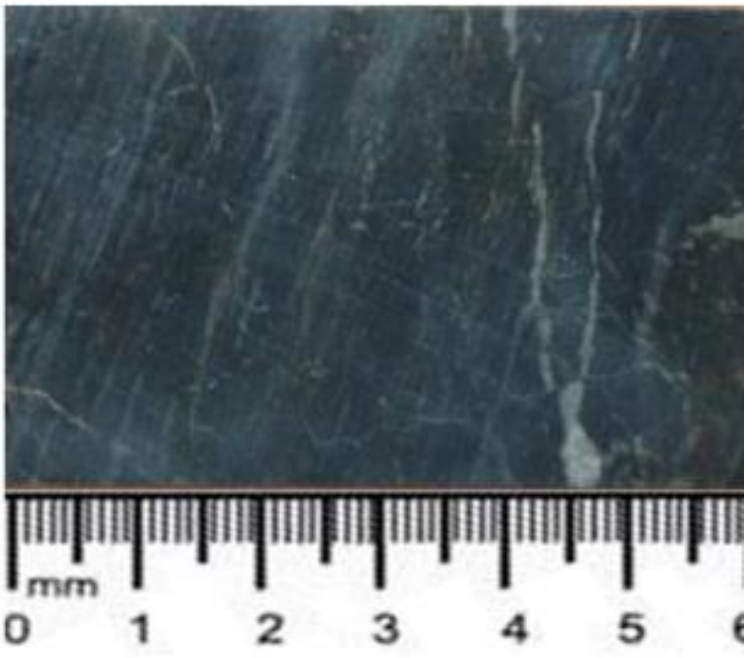

Figure 3.17. Photograph of dark grey to black shale from Hole CHP264 at 221.15m.

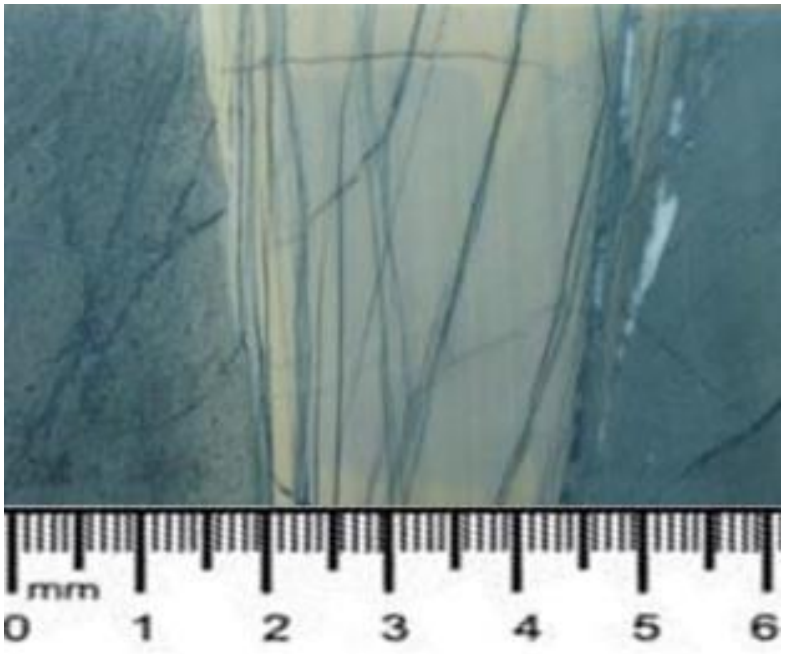

Figure 3.18. Photograph of grey to creamy, thinly laminated siltstone from hole CHP264 at 199.25m.

3.4.2 Facies 11: Dolomitic sandstone and conglomerate

The dolomitic sandstone-conglomerate facies overlies the fine-grained sequence of mudstone interbedded with siltstone. A maximum thickness of ~ 80 m thickness occurs to the south, decreasing towards north along strike (Fig. 3.16). Individual sandstone-conglomerate intervals range up to 3-8 m in thickness, and likely represent amalgamated beds. Some show normal grading, with basal 1-2 m-thick polymictic conglomerate layers. The latter are clast supported and poorly sorted, containing rounded to sub-angular polymictic clasts of maroon to brown chert, mudstone, lithic-wacke. Finer dolomitic sandstone is mainly composed of sub-rounded to angular metamorphic quartz (0.2-0.3 mm, 10-20%), mafic lithic clasts (0.3-0.5 mm, 10-15%) and minor mica grains in dolomitic groundmass (1-2%: Fig. 3.19).

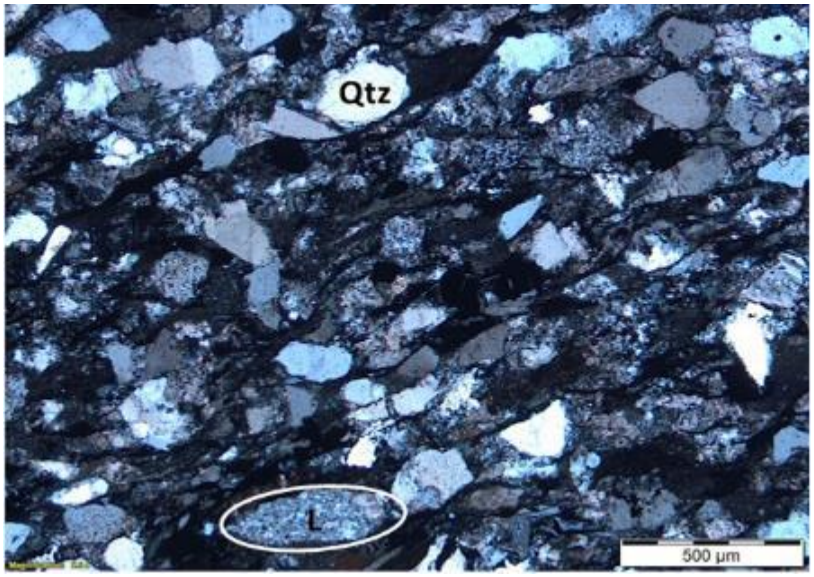

Figure 3.19. Photomicrograph showing very fine grained angular to sub-rounded quartz grains and minor mafic lithic clasts (L) within the dolomitic sandstone from drill hole RBH01 at 52.00m. XPL

Interpretation

Facies 11 mudstone interbedded with siltstone is interpreted to have been deposited from pelagic suspension in a deep-sea environment. Its significant thickness of 200-250 m suggests low detrital input into the basin for a prolonged period. However, higher in the stratigraphy the appearance of

thick normally graded dolomitic sandstone-conglomerate (Facies 12) suggests a resurgence of sediment supply via moderate to high energy turbidity currents (Shanmugam, 1997). The paucity of fine-grained facies within this upper interval suggests sediment accumulation within a proximal lobe or principal feeder channel in a submarine fan system.

The non-volcanic character of the detrital quartz is consistent with input from basin marginal sources. It cannot be discounted that the mafic volcanic clast component is intrabasinally derived, but given the association of metamorphic quartz, 'basement' sources of the Crimson Creek Formation or MUC are considered likely.

3.4.3 Facies 12: Polymictic Conglomerate (Salisbury Conglomerate)

The Salisbury Conglomerate stratigraphically overlies Facies 11. It crops out as a single band extending from Jupiter in the south to the Pieman River in the north of Natone Creek (Fig. 1). The descriptions given here come mainly from good exposures in Natone Creek, and drill hole RBH1 where the unit has a thickness of ~90 m (Figs. 1 & 3.16).

The conglomerate is polymictic, with a clast assemblage of poorly sorted maroon- to white-coloured chert, quartz, sandstone, with minor mudstone, mafic lithics and fuchsitic clasts (Fig. 3.20 & 3.21). It is clast supported at the base with sub-rounded clasts, and grades into dolomitic sandstone matrix supported top. Clasts are imbricated along the cleavage plane with long axis reaching to about 10 cm in diameter (Fig. 3.20-3.21).

Interpretation

The very coarse grained, clast supported and poorly sorted organization of the Salisbury Conglomerate indicates deposition from high energy currents that are characteristic of basin marginal environments (Cook et al., 1983). An up section increase in mass flow density is recorded from the underlying sandstone-conglomerate facies, a feature that could indicate major basin reorganisation and source area uplift. Detrital components remain consistent with a dominant

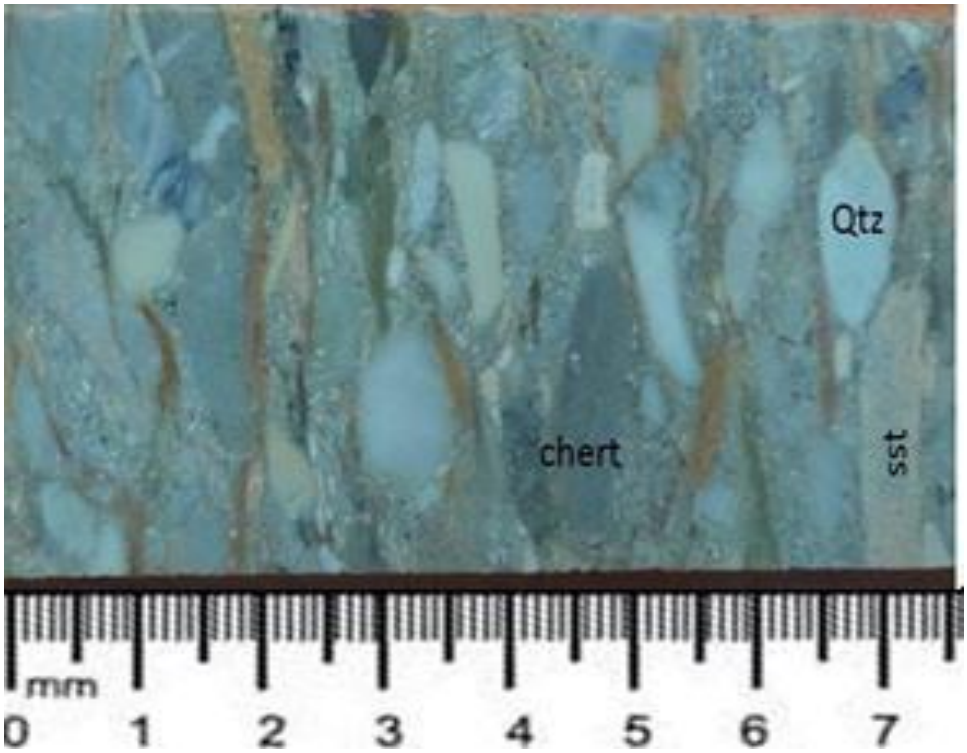

Figure 3.20. Photograph of a polymictic conglomerate with poorly sorted clasts of quartz (Qtz), chert and sandstone (sst),

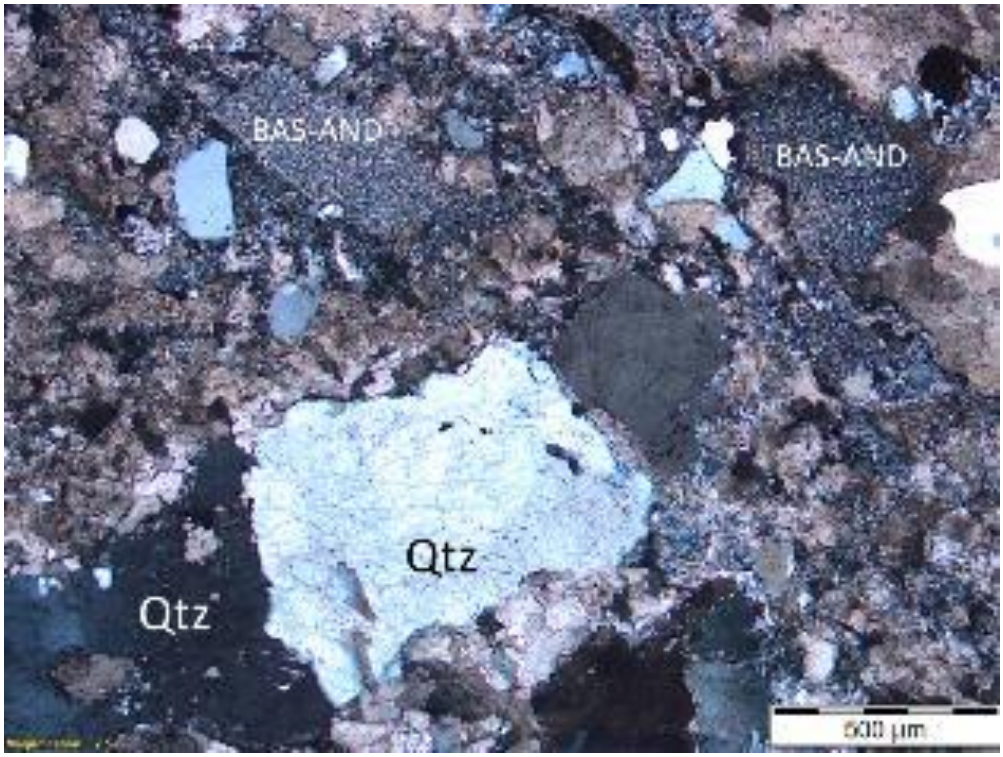

Figure 3.21. Photomicrograph showing poorly sorted, angular to sub-rounded mafic (BAS-AND) clasts and quartz (Qtz). XPL

'basement' provenance, the distinctive fuchsite (Cr-mica) rich clasts best explained by derivation from the MUC, which are known to be anomalously Cr-rich (e.g. Crawford and Berry, 1992).

3.4.4 Facies 13: Quartz-feldspar-phyric pumice breccia (Natone Volcanics)

The quartz-feldspar phyric pumice breccia of Natone Volcanics crops out along Natone Creek, extending over 3 km from Jupiter in the south to Pieman River (Fig. 1). Stratigraphically, it overlies the Salisbury Conglomerate and has a thickness of ~118 m (Fig. 3.16). The quartz-feldspar-phyric pumice breccia facies shows normal grading, consistent with eastward facing. Individual bed thicknesses are ~10 m, and normally graded from a 2-3 m thick coarse base to a stratified siltstone top.

The facies is light grey, massive to weakly cleaved and is composed of quartz-feldspar-phyric pumice-fiamme (1-4 cm, 40-60%), sparsely disseminated often embayed quartz (0.2-1 mm, 1-2%), altered feldspar crystal fragments (1-2 mm, 1%), former glass shards and sparse mudstone lithic clasts (1%), set in a moderately sericite altered matrix (Figs. 3.22 & 3.23).

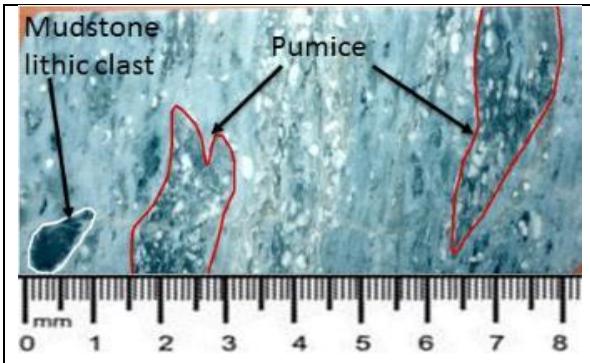

Figure 3.22. Photograph of a slab showing quartz and feldspar crystal phyric pumice clast and mudstone lithic clasts from hole RBH2 at 85.35 m.

Figure 3.23. Photomicrograph of Qtz-fsp-phyric pumice breccia from hole RBH02 at 34.6 m. XPL

3.4.5 Facies 14: Crystal-rich basaltic andesite volcaniclastic sandstone

Facies 14 is a fine to medium grained, crystal-rich basaltic andesite volcaniclastic sandstone of about 2 m in thickness that overlies the quartz-feldspar-phyric pumice breccia of Facies 13 (Fig. 3.16). Unlike Facies 13, it lacks pumice clasts. Its petrography in Figure 3.24 shows mainly euhedral feldspar crystals (0.5-1 mm, 15-20%), angular to sub-rounded basaltic andesite clasts (0.5-1 mm, 10%) and minor angular to sub-rounded quartz (0.25-0.5 mm, 2-3%). It has quartz to feldspar ratio of 05:95.

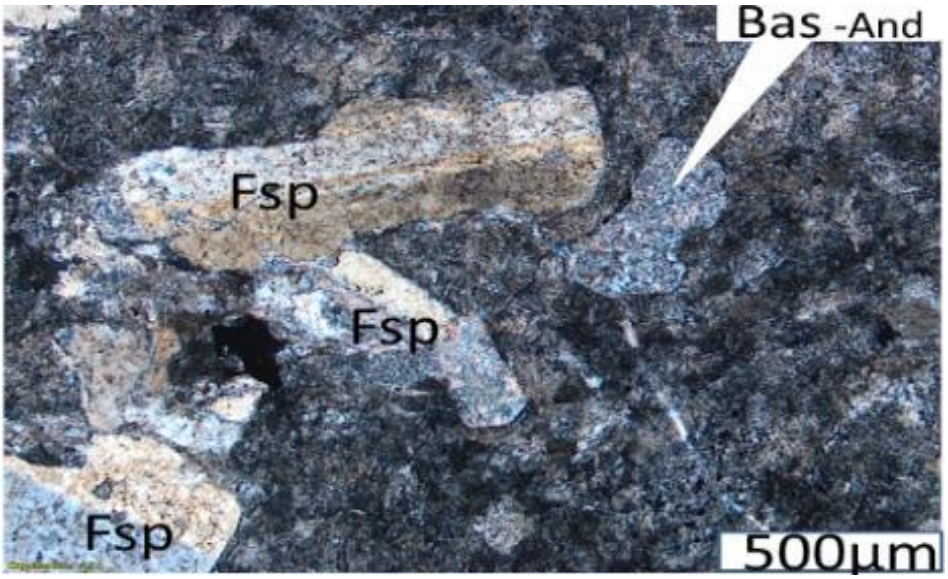

Figure 3.24. Crystal-rich volcaniclastic sandstone showing euhedral feldspar (Fsp) crystals and basaltic andesite (Bas-And) clasts. RBH2: 147.00 m.

Interpretation

The quartz-feldspar-phyric pumice breccia facies of the Natone Volcanics is composed of pumice fiamme and shards, angular to sub-rounded volcanic quartz and feldspar crystal fragments. The dominance of the pumice fiamme component and broken nature of the crystals suggests an explosive eruption process.

Massive normally graded pumice breccia beds with minor mudstone lithic clasts and stratified tops suggests a transport process that includes density sorting and basal erosion of the substrate, likely from water-supported gravity flows. Thick and massive normally graded beds

coupled with pumice fiamme as the overwhelmingly dominant component suggests transport via high concentration density currents (Gifkins, 2001).The volcaniclastic sandstone and siltstone tops of the pumice breccia beds are possibly due to water-settled fallout from suspension, or turbidites sourced either directly from the eruption or from secondary remobilization and transport processes (Gifkins, 2001).

The central part of the northern zone is enclosed by extra-basinal sediments mainly derived from the Precambrian basement, Crimson Creek Formation and mafic-ultra-mafic complexes. The deposition of the quartz-feldspar phyric pumice breccia is interpreted to be sourced from felsic explosive eruption outside the immediate sub-basin related to the Mount Read Volcanic centres to the east.

Facies 14 volcaniclastic is composed of a compositionally distinct assemblage of basaltic andesite clasts, and feldspar crystals, that lacks a voluminous pumice component. Derivation from explosive felsic volcanism would seem unlikely, its fine to medium grain size indicates its deposition from low to moderate turbidity currents (Lowe, 1982; Gifkins, 2001). The sub-angular to sub-rounded clast and euhedral feldspar crystal shape indicates minimal reworking and proximal derivation. The very low quartz: feldspar crystal ratio, coupled with basaltic andesite clast component suggests a mafic to intermediate volcanic source. The texturally immature character of the lithic volcanic components, their rather monomictic compositions, and the overall paucity of metamorphic quartz, are collectively interpreted to indicate an intrabasinal MRV volcanic source.

3.5 Geology of the southern part of the study area

The geology of the southern part of the study area around Williamsford, Ring River and its tributaries is dominated by mudstone interbedded with siltstone (Westcott Argillite) and quartz-wacke interbedded with mudstone (Stitt Quartzite), greywacke (Facies 15) and massive crystal-rich volcaniclastic breccia of Facies 16 (Fig. 1). The correlates to the Westcott Argillite and Stitt-Quartzite are discussed in section 3.4.1 and 3.3 respectively and will not be discussed here. However, both facies 15 and 16 will be discussed based on detailed mapping and petrographic observations.

3.5.1 Facies 15: Greywacke

Facies 15 comprises euhedral feldspar crystal fragments (0.5-1 mm, 20-30%), with minor basaltic andesite lithic clasts (0.5-1 mm, 3-5%), set in a clay matrix (Fig. 3.25). Similar outcrops are mapped along the Ring River and its tributaries to the east and further to the south (Fig. 1). Its thickness is generally 20-25 m but a very thick portion is mapped on the southern part of the study area by previous workers (E.Z.Report, 1986). Individual bed thicknesses range from 0.5-1 m. Beds are graded from medium to fine grained stratified siltstone interbedded with mudstone at the top.

Interpretation

The facies is dominated by fine grained euhedral feldspar crystals suggesting a crystal-rich volcanic provenance. Crystal-rich deposits are generated either through primary eruption processes, quench fragmentation, or secondary processes such as weathering and erosion (Gifkins and Allen, 2001; Cas and Wright, 2012). The feldspar crystal fragments are possibly sourced from unconsolidated crystal-rich sandstone through weathering and the sub-rounded basaltic andesite lithic clasts suggest significant reworking from a distal source. Thin beds (~0.50-1 m) with stratified tops suggest deposition from low concentration gravity currents (Lowe, 1982).

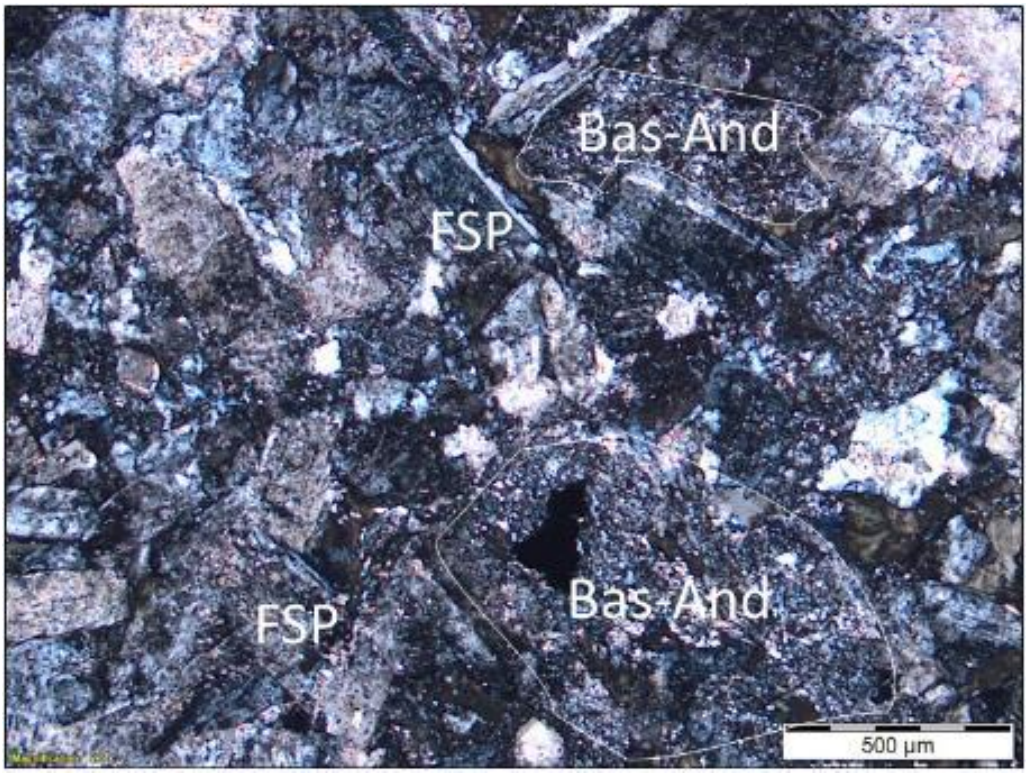

Figure 3.25. Photomicrograph showing fine grained, feldspar (Fsp) and basaltic andesite (Bas-And) lithic clasts of greywacke from Conliffe River (Sample RG002 at 375133E /5366679N)

3.5.2 Facies 16: Crystal-rich volcaniclastic breccia

Facies 16 outcrops on the western edge of the study area along Ring River and has an exposed thickness of about 30 m (Fig. 1). It has a faulted contact relationship to the west and east with a sub-horizontal siltstone and mudstone beds. It is generally massive to weakly bedded and predominantly consists of euhedral and broken feldspar crystals (1-2 mm, 10-15%), angular to sub-rounded andesite clasts (5-10%), angular to sub-rounded, fractured and often embayed quartz crystal fragments (1-2 mm, 2-3%), and minor opaque minerals (magnetite) in chlorite altered matrix (Figs. 3.26 & 3.27).

During this study, only a small portion of this facies was mapped. A full description and interpretation of the facies is given by Selley (1997). The base of the facies is a moderately to poorly sorted polymictic crystal-rich volcaniclastic breccia with intraclasts of 0.5-5 m long contorted

mudstone rip up clasts eroded from an unconsolidated substrate and andesite clasts. The breccia base passes into massive, homogeneous, crystal-rich sandstone that comprises the bulk of the facies. The volcaniclastic sandstone transitions into a thinly stratified mudstone top (Selley, 1997).

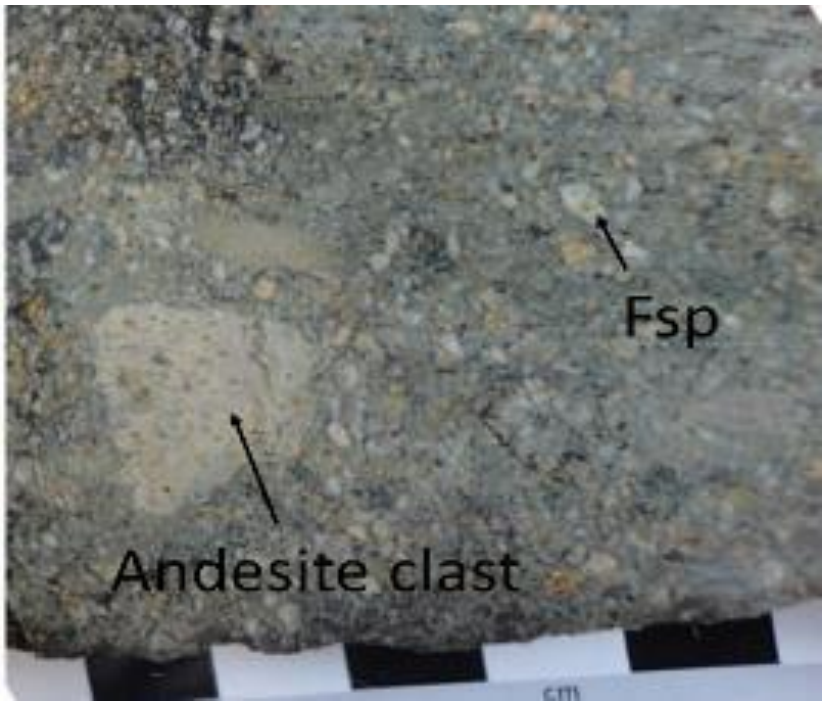

Figure 3.26. Massive, feldspar crystal fragment rich with andesitic volcaniclastic breccia from the south-western side of the study area along the Ring River at 374451E/5367696N.

Figure 3.27. Photomicrograph of massive, crystal-rich feldspathic volcaniclastic breccia showing dominantly broken feldspar (Fsp) crystals with some fractured quartz and lithic clasts from the south-western part of the study area in the Ring River)

Interpretation

The coarse polymictic base with rip-up clasts and relatively homogenous composition of the massive volcaniclastic breccia indicates deposition from a single lateral depositional event of high energy currents (Lowe, 1982; Selley, 1997). The massive, homogenous composition of the breccia with insignificant non-volcanic components likely indicates an explosive eruption source and primary processes of transport and deposition soon after eruption (Selley, 1997; Cas and Wright, 2012). The primary transport process is likely high energy and high particle concentration density currents. The thinly stratified siltstone and mudstone top is interpreted to be deposited from settling of unsteady low-density turbidity currents after the deposition of the volcaniclastic sandstone (Selley, 1997; Gifkins, 2001; Cas and Wright, 2012).

3.6 The Rosebery Mine host stratigraphy

The lithostratigraphy of Rosebery Mine stratigraphy comprises the Hercules Pumice Formation (footwall sequence) of dominantly dacitic, feldspar-phyric pumice breccia; Rosebery Host Rock Member of volcaniclastic sandstone and siltstone, black mudstone, and the White Spur Formation (hanging wall sequence) as shown in Figure 3.28. The lithostratigraphy of each sequence will be discussed based on logging of four drill holes. Three drill holes are logged in detail in this study (337R, 397R, 411R-D1) and one more drill hole (250R) lithology and detailed mineralogy and textural description is interpreted from the MMG exploration geologists' database (Fig. 3.35). In addition, a feldspar-quartz-phyric intrusion of the host rock sequence in hole 250R will be discussed separately based on MMG's data and petrographic observations of Martin (2004: Fig. 3.35). The detailed logging is supplemented with petrographic analysis to discern subtle differences between the rock units.

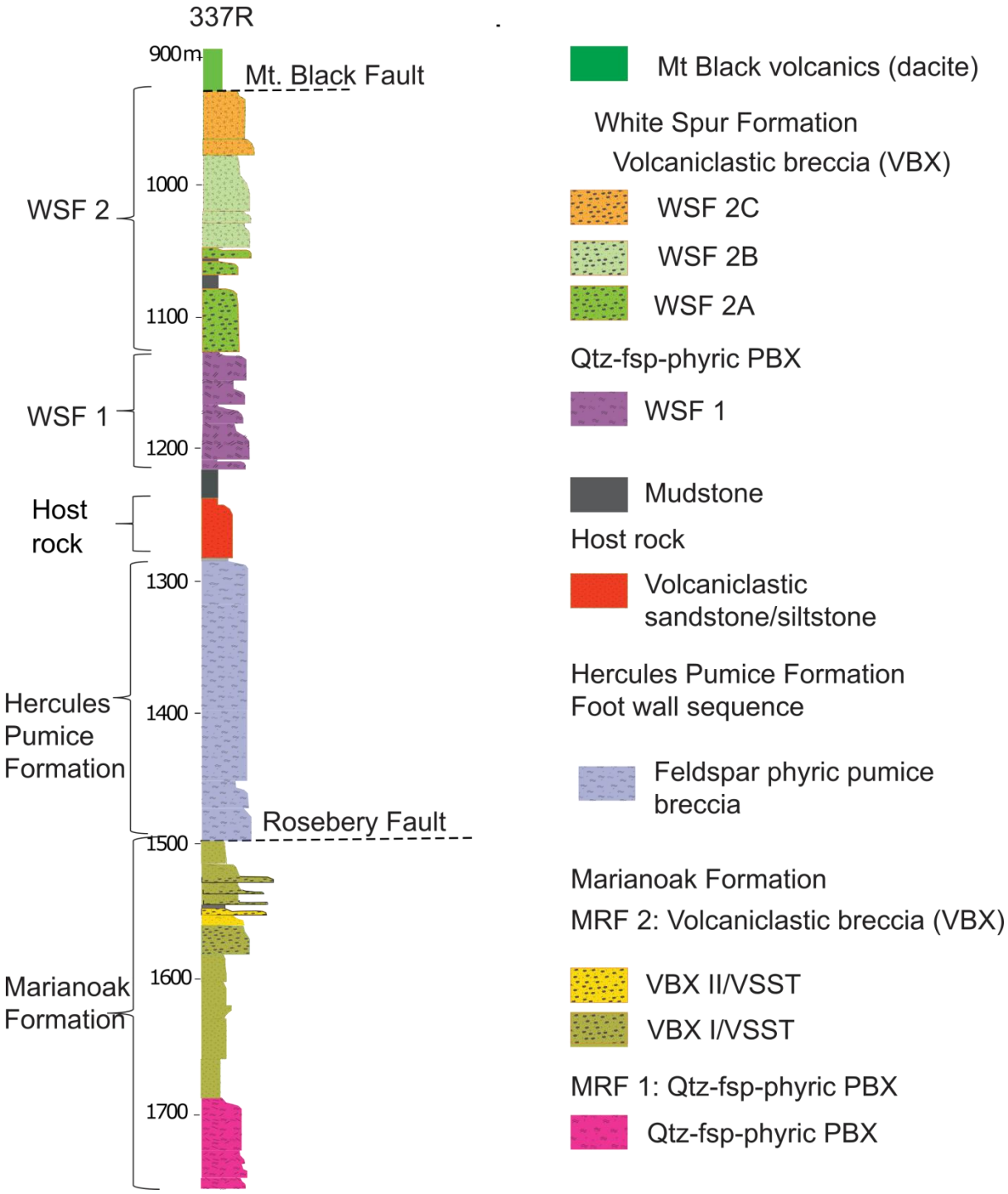

Figure 3.28. Lithostratigraphy of volcanogenic facies in the immediate footwall position of the Rosebery Fault: drill hole 337R. The Marianoak Formation occupies a footwall position, and has been discussed in detail above. The overlying Rosebery Mine sequence consists of the Hercules Pumice Formation, Host Rock Member, Black Mudstone and the White Spur Formation

3.6.1 Hercules Pumice Formation (footwall sequence)

The Hercules Pumice Formation is a poorly stratified succession of dacitic, feldspar-phyric pumice breccias intruded by quartz-feldspar-phyric rhyolite sills (McPhie et al., 1993; Gifkins and Allen, 2001) (Fig. 3.28). The succession has a regionally mappable thickness of about 500 m, but it is only ~200 m thickness within the studied holes (Fig. 3.42). The succession is overlain by the Rosebery-Hercules Host Member and its lower boundary is in fault contact with the Rosebery Group volcano-sedimentary sequence along the Rosebery Fault (Fig. 3.28).

Individual beds of the Hercules Pumice Formation within the studied holes are 2-20 m in thickness. Each bed grades from a 10-15 m thick polymictic very coarse base comprising of pumice fiamme and lithic clasts, to a variably crystal- and pumice fiamme-rich stratified volcaniclastic sandstone and siltstone top (Fig. 3.28). All beds are dominantly composed of pumice fiamme (60-80%, <6 cm), former glass shards (10-15%), euhedral feldspar crystal fragments (0.5-1mm, 5%), quartz crystal-fragments (1%) and minor mud lithic clasts (Fig. 3.29-3.30).

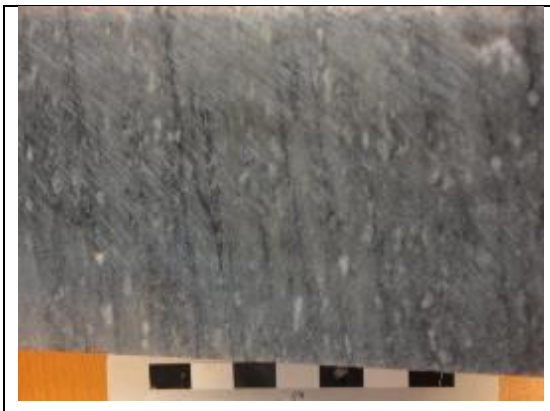

Figure 3.29. Photograph of crystal-rich and feldspar-phyric pumice breccia from hole 337R at 1461.90 m. Scale is in centimetres.

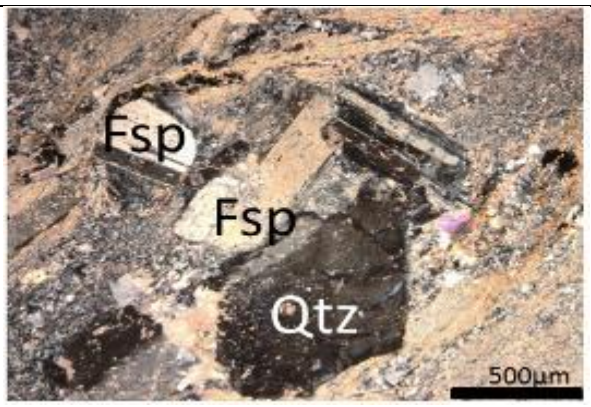

Figure 3.30. Photomicrograph of feldspar-quartz phyric pumice breccia from hole 337R at 1461.90 m. Scale shown is 500 µm taken in XPL

3.6.2 Rosebery Host Rock Member

The Rosebery host rock succession is a discontinuous 5-60 m thick sequence above the feldspar-phyric pumice breccia of the Hercules Pumice Formation in hole 337R (Fig. 3.28) (Allen, 1991; Gifkins and Allen, 2001). It comprises two intervals of crudely graded volcaniclastic sandstone interbedded with volcaniclastic siltstone, distinguished on compositional grounds. The lower interval is 30 m thick in hole 337R composed of mainly euhedral feldspar crystals (0.50-1.0 mm, 30-40%), pumice fiamme, minor mafic lithic clasts (2-3%) and quartz crystals set within a calcite altered matrix (Fig. 3.31 & 3.32).

The upper part of the Host Rock Member is about 18 m thickness in hole 337R and consists of a quartz-rich volcaniclastic sandstone interbedded with volcaniclastic siltstone (Figs. 3.33-3.34). Its petrography shows angular to sub-rounded quartz crystal fragments (10-15%), euhedral feldspar (0.50-0.75 mm, 5%), lithic clasts (0.5-1.0 mm, 1-2%) and secondary calcite.

Figure 3.31. Photograph a slab of feldspar-phyric pumice fiamme volcaniclastic sandstone host rock from hole 337R at 1271.2 m. Scale is in centimetres.

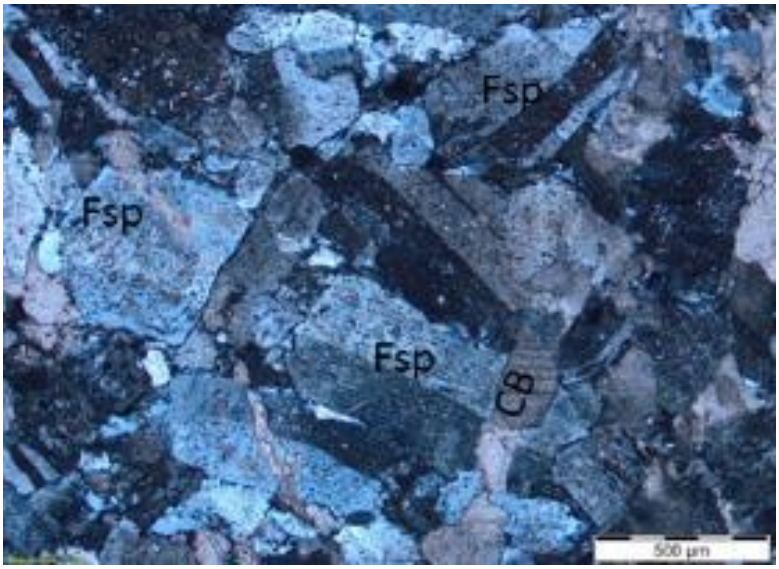

Figure 3.32. Photomicrograph of feldspar (Fsp) phyric volcaniclastic sandstone (host rock) with minor secondary calcite (CB) from hole 337R at 1271.20. Image taken under XPL

Figure 3.33. Photograph of a slab of quartz phyric volcaniclastic sandstone Host Rock Member from drill hole 337R at 1251.50 m. Scale is in centimetres.

Figure 3.34. Photomicrograph of quartz (Qtz)-feldspar (Fsp) rich volcaniclastic sandstone from drill hole 337R at 1251.50 m. Scale shown is 500 µm and image is taken in XPL.

3.6.3 Feldspar-quartz porphyritic sill

A feldspar-quartz porphyritic sill of about 50 m thickness intrudes the host rock member in hole 250R (Fig. 3.35: Martin, 2004). Other sills of similar composition are common in the vicinity of Rosebery ore Mine and their petrography was described in detail by Martin (2004) in addition to MMG's database (Martin, 2004). It has distinctive embayed quartz (2-4 mm) and euhedral feldspar phenocrysts (1-2 mm) in a fine-grained groundmass (Martin, 2004). The intrusion varies laterally

from a thick coherent body with peperitic margins to a coarse hyaloclastite with occasional jigsaw fit texture is often mineralized (Martin, 2004).

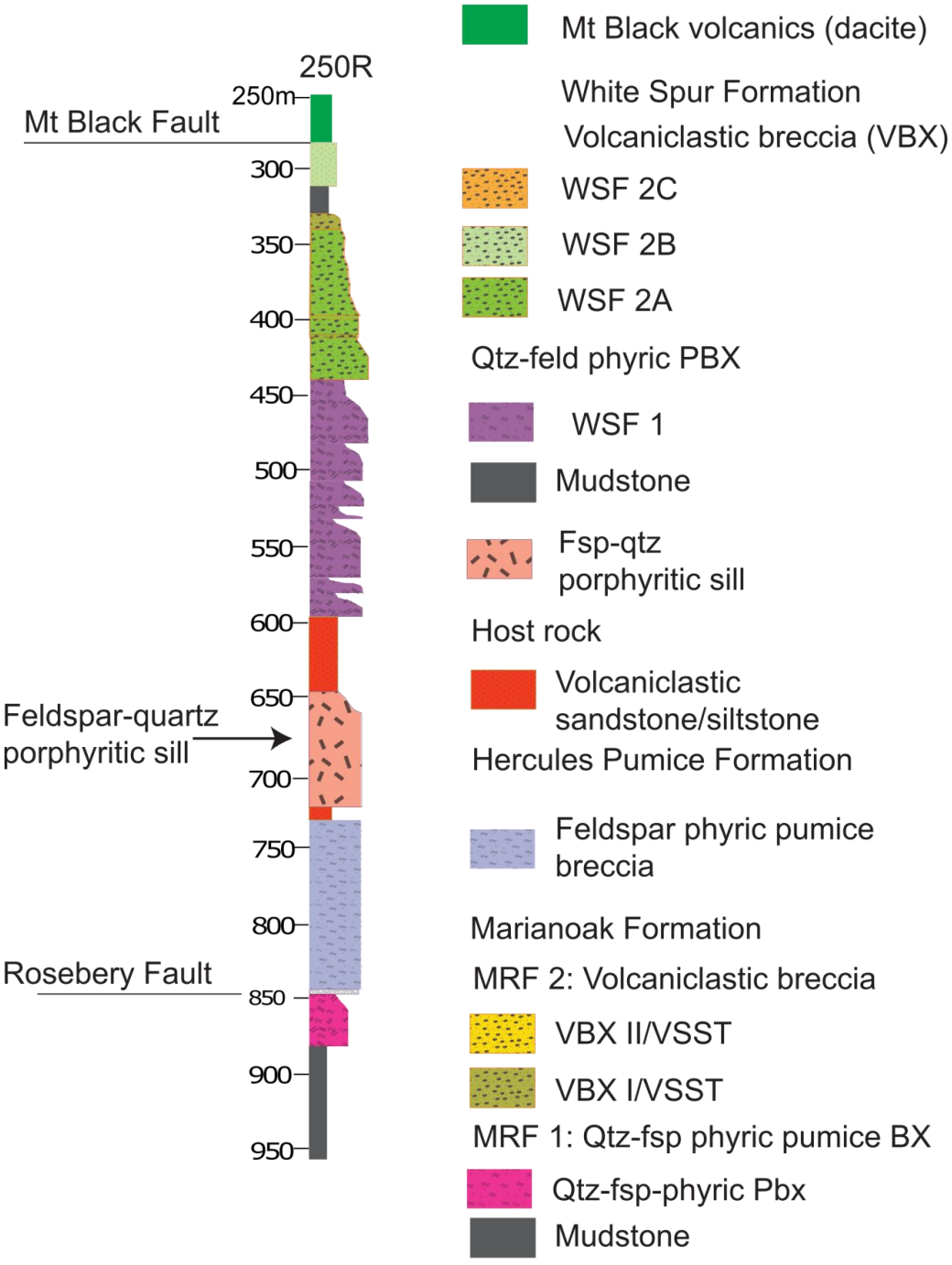

Figure 3.35. Lithostratigraphy of hole 250R showing feldspar-quartz-porphyry sill that intrudes the Host Rock Member.

3.6.4 Massive mudstone

The host rock is overlain by lenses of massive, black mudstone of 5-20 m thickness in Rosebery, Hercules and South Hercules mine areas (Fig. 3.28) (Allen, 1991; Gifkins and Allen, 2001). Stratigraphically it is considered as the base of the White Spur Formation. The massive mudstone lenses contain biogenic pyrite, and are interbedded with quartz-feldspar-phyric siltstone and sandstone composed of Precambrian quartzite and quartz-mica schist (Corbett and Solomon, 1989; Corbett et al., 2014).

3.6.5 White Spur Formation (hanging wall sequence)

The massive mudstone and host rock of the Rosebery Mine are overlain by the White Spur Formation (Fig. 3.28: Corbett and Lees, 1987; Allen, 1991; Gifkins and Allen, 2001; Corbett et al., 2014. The White Spur Formation consists of quartz-feldspar-phyric pumice breccias with minor beds of black mudstone (WSF 1), and facies association (WSF 2) comprising of three facies: basaltic andesite volcaniclastic breccia interbedded with minor 5-10m black mudstone (WSF 2A), polymictic volcaniclastic breccia (WSF 2B) and rhyolitic breccia (WSF 2C: Fig. 3.28). Detailed descriptions of the facies are given below.

Facies WSF 1: Quartz-feldspar-phyric pumice breccia

WSF 1 overlies the thick mudstone which in turn overlies the host rock (Fig. 3.36). It is 100-120 m in thickness and consists of multiple weakly normally graded beds of 5-20 m. Beds are composed largely of pumice-fiamme fragments, with medium to coarse grained quartz and euhedral feldspar crystal fragments and subordinate volcaniclastic siltstone and mudstone lithic clasts at the base (Fig. 3.36 A-D). Interbeds of black mudstone and volcaniclastic siltstone, 1-4 m in thickness, are common. Siltstone layers may contain outsized feldspar-phyric-fiamme in their upper parts.

As the pumice breccia facies was very texturally homogeneous in hand specimen, two samples were taken from the quartz-feldspar-phyric pumice breccia at 1211 m and at 1135 m of drill hole 337R (Fig. 3.36). The sample taken from the lower part of the stratigraphy at 1211 m is

dominantly composed of pumice-fiamme clasts (1-5 cm, 60-70 %), angular quartz crystal fragments (0.25-0.50 mm, 15-20 %), euhedral feldspar crystal fragments (0.25-0.50 mm, 2-3%), glass shards (2-3%), and mudstone lithic clasts (1-2%) in sericite altered matrix (Fig. 3.36 A-B). The quartz: feldspar ratio is estimated to be 90:10. The upper part of the stratigraphy at 1135 m is also dominantly composed of pumice-fiamme clasts (1-5 cm, 60-80%), angular quartz crystal fragments, often fractured and embayed (0.5 mm, 5-10%), euhedral feldspar crystals (10-15%) and mudstone lithic clasts (1-2%) in sericite altered matrix (Fig. 3.37 C-D). The estimated quartz: feldspar proportion is 40:60.

Interpretation

The quartz-feldspar-phyric pumice breccia is primarily composed of juvenile pumice clasts, former glass shards and angular crystal fragments that were produced by explosive felsic eruptions (Dimroth and Yamagishi, 1987; Branney and Kokelaar, 1992; Gifkins, 2001). The thick 10-20 m scale bedding, grading from coarse pumice and other lithic clasts at the base to variably crystal-rich pumiceous sandstone is consistent with density sorting. This interpretation combined with the dominant pumice component suggests deposition from high concentration density currents during or soon after eruption (Fig.3.36 A-D: Branney and Kokelaar, 1992; Gifkins, 2001)

The mudstone and siltstone intraclasts at the base of the beds are interpreted to be eroded from the underlying unconsolidated mudstone substrate suggesting that the density currents were highly erosive and its transport in a submarine setting. The pumice-rich sandstone and siltstone ash tops are interpreted to be from water settled fallout suspension sourced either directly from the eruption plumes or from the trailing of ash cloud associated with the high concentration flows (Gifkins and Allen, 2001). The outsized pumice fiamme within the stratified volcanogenic siltstone and mudstone tops of most of the beds are interpreted to represent pumice clasts that were initially buoyant but became water logged and settled from suspension in the water column (Gifkins,

2001). The deposition of the narrow intervals of black mudstones suggests periods of volcanic quiescence in between the eruption pulses.

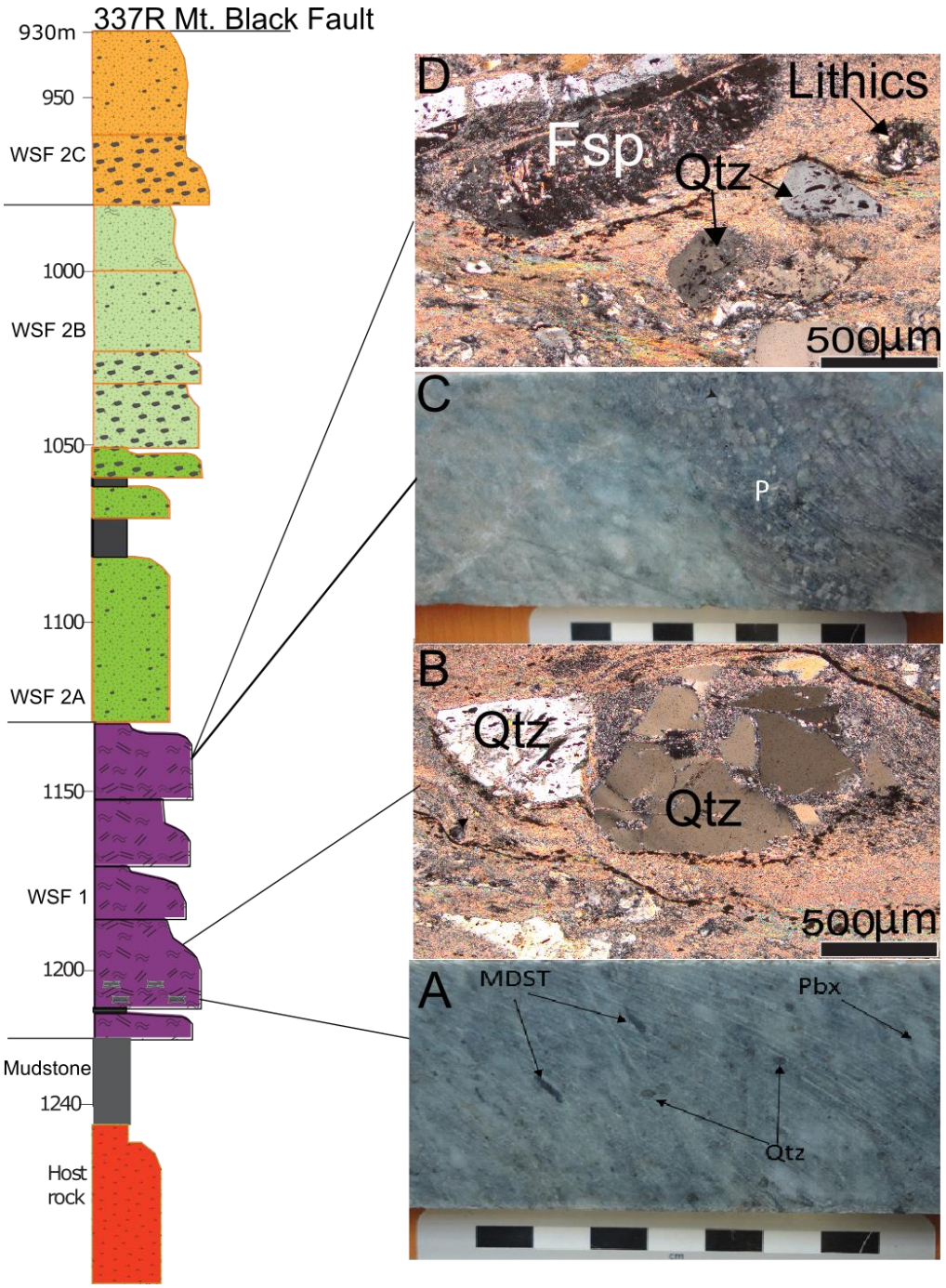

Figure 3.36. Stratigraphy of the White Spur Formation showing (A) photograph of a quartz-feldspar phyric pumice breccia (Pbx) with mudstone (MDST) lithic clasts. (B) Photomicrograph of qtz-fsp-phyric pumice breccia. (C) Photograph of qtz-fsp-phyric pumice (P) breccia. (D) Photomicrograph showing fractured quartz (Qtz) and feldspar (Fsp) from the upper part of the pumice breccia (cross-polarized light).

Facies WSF 2A: Basaltic andesite volcaniclastic breccia

The basaltic andesite volcaniclastic breccia overlies the quartz-phyric pumice breccia of WSF 1. It is about 50-70 m in thickness in total with 10-40 m thick beds that grade from very coarse breccia bases to volcaniclastic sandstone tops, in places separated by 3-10 m thick black and pyritic mudstone beds (Fig. 3.36).

It is mainly composed of angular to sub-rounded, feldspar-phyric basaltic andesite clasts (~10 cm diameter, 40-70%), euhedral feldspar crystal fragments (0.5-1.0 mm, 15%) and minor quartz (0.25 mm, 1-2%) in volcaniclastic sandstone matrix that lack pumice clasts (Figs. 3.37, 3.38). The matrix of WSF2A has quartz to feldspar proportion of 90:10, which distinguishes it from other facies.

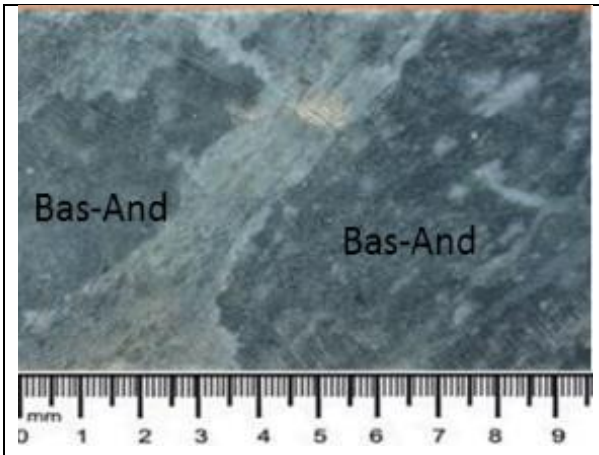

Figure 3.37. Photograph of a slab of WSF 2A showing clasts of feldspar-phyric basaltic andesite of about 10 cm diameter. Drill hole 397R: 1356.80 m.

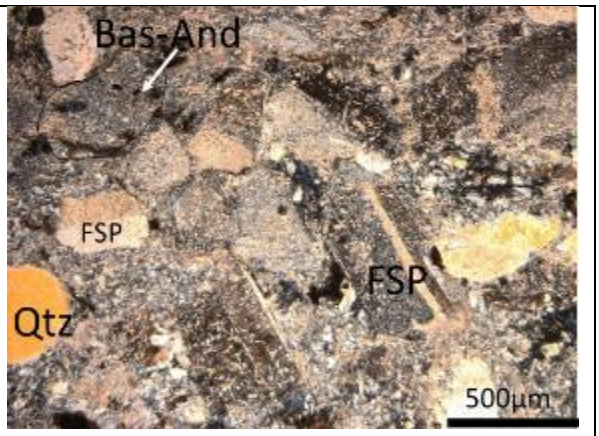

Figure 3.38. Photomicrograph of crystal-rich volcaniclastic breccia of WSF 2A showing feldspar (Fsp)–phyric basaltic andesite (Bas-And) clasts and minor quartz (Qtz). Drill hole 337R: 1106.3 m. Image taken under XPL

Interpretation of basaltic andesite volcaniclastic breccia (WSF 2A)

The thick (10-40 m) graded beds of facies 2A suggest rapid deposition from high concentration mass-flow current. The normally grading from very coarse grained base of basaltic andesite clasts and mudstone lithic clasts that fines to volcaniclastic sandstone is consistent with density sorting (Gifkins, 2001). The presence of mudstone lithic clasts indicates that the mass-flow currents were

erosive. The angular to sub-rounded clast morphology indicates minimal reworking and the dominance of basaltic andesite clasts indicates an intermediate source. The facies is characterized by dense clasts that lack pumice suggesting it was a product of effusive volcanism.

The thinly stratified pyritic, black mudstones and siltstone beds interbedded with the graded pumice-rich beds suggests below wave base sedimentation either from water-settled fallout or secondary turbidite currents.

Facies WSF 2B: Polymictic volcaniclastic breccia

WSF 2B overlies WSF 2A and varies between 40-80 m in thickness laterally across the observed drill holes (Fig. 3.42). It is pale grey to greenish, massive to weakly foliated, and individual bed thicknesses range from 10 m in hole 250R to a maximum of 20 m in hole 337R and is absent in hole 411R-D1 (Fig. 3.42). Individual beds generally grade from very coarse clast-rich base to a ~1 m volcaniclastic sandstone top.

It is composed of sub-rounded to angular clasts with the following components: feldspar-phyric and aphanitic basaltic andesite, minor amygdaloidal basalt (2.0-2.5 mm, 5-7%), aphanitic and quartz-phyric rhyolite (1-2 mm, 1-2%), in addition to euhedral feldspar (3-5 %), angular quartz crystal fragments (0.5 mm, 3-5%) in a sericite altered matrix (Fig. 3.39-3.40).

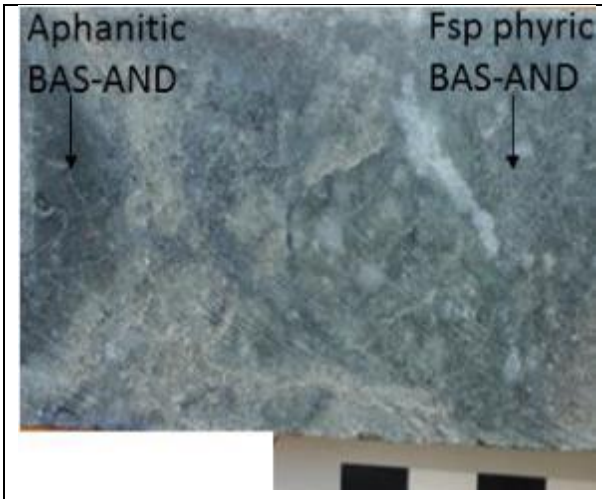

Figure 3.39. Photograph of WSF 2B showing Fsp-phyric and aphanitic basaltic andesite clasts from hole 337R at 1013 m. Scale shown is in centimetres.

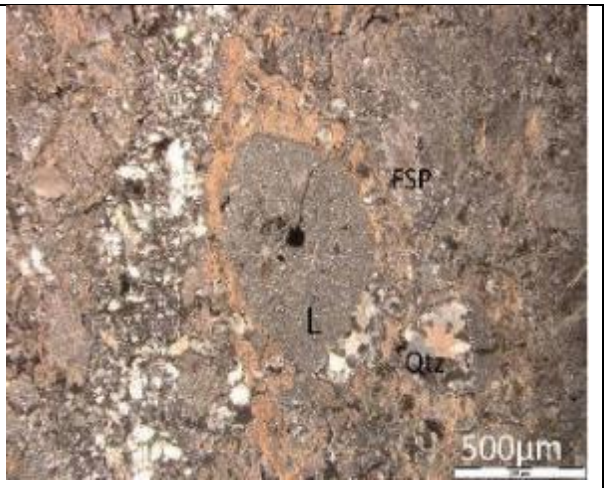

Figure 3.40. Photomicrograph of WSF 2B showing quartz (Qtz), feldspar (Fsp) crystals and basaltic andesite (L) rich volcaniclastic breccia from hole 337R at 1013 m. Image taken under XPL

Interpretation of polymictic volcaniclastic breccia (WSF 2B)

WSF 2B has thick 10-20 m beds that are graded with ~ 1m thick volcaniclastic sandstone tops suggesting transport by gravity currents. The polymictic mixed clast composition of both felsic and mafic clasts indicates erosion and incorporation of multiple volcanic products into the gravity currents. The sub-rounded to angular clast morphology indicates moderate reworking from the source area. Black mudstone beds are absent in this facies suggesting there was a continuous supply of detritus into the basin.

WSF 2C: Rhyolitic volcaniclastic breccia

WSF 2C overlies WSF 2B and is generally about 40-50 m in thickness with a maximum of ~200 m in drill hole 411R-D1 (Fig. 3.42). Individual bed thicknesses range from 10-40 m and grade from a coarse base dominated by sub-rounded to sub-angular 1-3 cm diameter clasts of grey, aphanitic (40-60%) and (2-5 cm, 5%) quartz-phyric clasts set in volcaniclastic sandstone. The matrix is dominated by angular quartz crystal fragments (0.25-0.5 mm, 10-15%), euhedral feldspars (<0.25 mm, 1-2%) and minor quartz-phyric clasts (0.5 mm, 2%: Figs. 3.41). The facies is distinguished from the

underlying facies as it lacks basaltic andesite clasts and the matrix has an estimated quartz to feldspar proportion of 85:15.

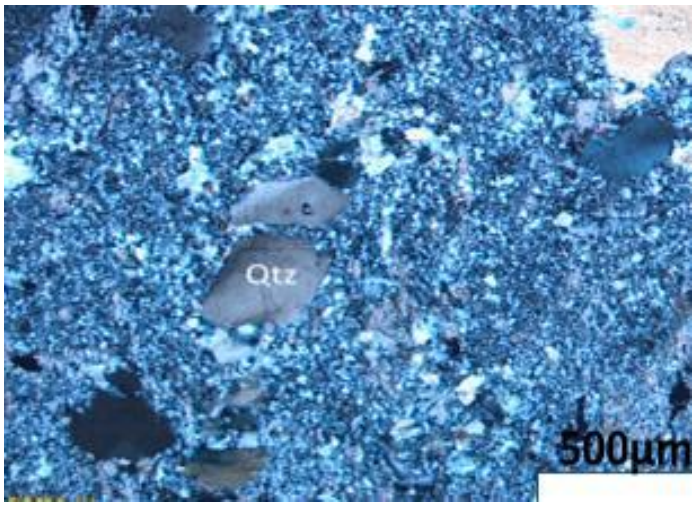

Figure 3.41. Photomicrograph of quartz crystal fragment-rich volcaniclastic breccia from hole 397R at 1298.60 m. Image taken under XPL

Interpretation of rhyolitic volcaniclastic breccia (WSF 2C)

The WSF 2C is comprised of thick 10-40 m beds that are poorly to moderately sorted, that grade to siltstone suggesting a possible transport from high concentration density currents or gravity currents. The clast composition is dominated by aphanitic and quartz-phyric clasts and quartz crystal fragments that indicate a felsic to intermediate dominated provenance. The angular, fractured and embayed quartz crystal morphology indicates minimal reworking derived from a proximal unconsolidated crystal rich rhyolitic source.

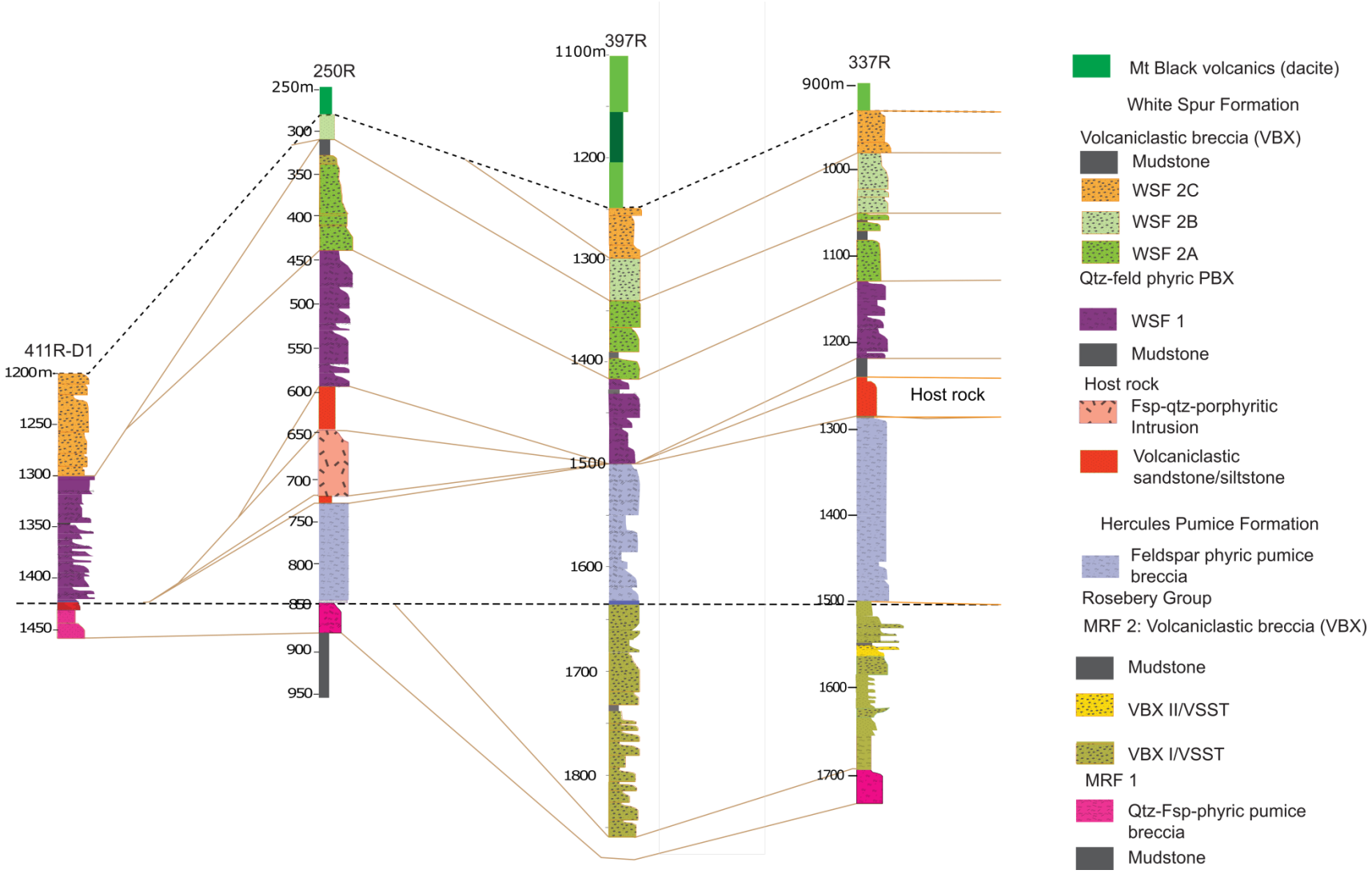

Figure 3.42. Lithostratigraphic correlation of the Marianoak Formation and the Rosebery mine, footwall, host rock and White Spur Formation.

3.7 Lithostratigraphic correlation

The facies analysis presented above places constraints on the modes of eruption, transportation and deposition, as well as the source of particles, and in turn provides a basis for lithostratigraphic correlation both within the Rosebery Group and neighbouring sequences. A correlative framework, summarised from five representative drill holes, is shown in Figure 3.43.

The lowest stratigraphic interval of the Marianoak Formation records a distinctive phase of felsic magmatism, and includes shallow level intrusive products, peperitic breccia, and thick intervals of quartz and quartz-feldspar-phyric pumice breccias that were produced from voluminous explosive volcanic eruptions and emplaced via high concentration mass flows. The pumice breccia deposits possess subtle upsection variation in crystal composition and are separated by narrow intervals of non-volcanogenic mudstone interpreted to record eruptive hiatuses. The package as a whole may represent progressive compositional evolution of a single magma chamber, or eruption from genetically and spatially disparate volcanic centres.

The eruption and deposition of felsic volcanic products was followed by the deposition of more mafic volcanic products that are interpreted as the distal products of secondary transport and reworking (MRF 2: Fig. 3.43). The absence of pumice clasts in the mafic-intermediate VBXI/VSST facies, and sub-rounded to angular clast shapes, are consistent with their origin as a reworked product of effusive volcanism. The mafic-intermediate breccias are punctuated by narrow zones of graded monomictic rhyolitic breccias and sandstones (VBX II/VSST), demonstrating multiple volcanic sources into the basin. Non-volcanogenic mudstones punctuate the succession, indicating that volcanism was not continuous in the uppermost levels of the Marianoak Formation. A prolonged period of volcanic quiescence and basin starvation is implied.

Renewed sediment input is recorded by the arenaceous components of Stitt Quartzite. Broadly upward coarsening and thickening cycles, evident from the metre-scale (i.e. para-sequences)

to the scale of the package as a whole, are interpreted to record progradation of submarine turbiditic fans from the basin margin, most likely in response to increased tectonic activity. Sandstone provenance appears almost exclusively 'basement'-derived, indicating that either volcanism had shut down completely, or that basin reorganisation had effectively barred coeval volcanogenic input from the depocentre.

Facies associations within the central and southern parts of the Rosebery Group are more diverse but dominated by fine- to medium-grained turbiditic sediments of the Westcott Argillite (Fig. 3.43). Initially accumulating mudstone and siltstone facies, deposited from low energy currents, are overlain by progressively coarsening carbonate cemented sandstones, and ultimately polymictic conglomerate (Salisbury Conglomerate). This upward coarsening cycle is dominated by input from 'basement' sources, a likely combination of Neoproterozoic metamorphic siliciclastic strata and mafic to ultramafic rocks, is again interpreted to record progressively increasing tectonic activity and activation of sub-basin bounding fault zones (e.g. Cook et al., 1983).

The inferred peak of tectonic activity coincides with an apparently brief, but voluminous input of quartz-feldspar-phyric pumice breccia: Facies 13 of the Natone Volcanics (Fig. 3.43). The textural and compositional characteristics of Facies 13 are comparable with those of MRF 1, raising the possibility that they are products of the same eruptive phase(s). Further support for this correlation will be presented in Chapter 4 on the basis of geochemical affinities. However, the paucity of peperitic intrusive facies in the Natone Volcanics would imply that if directly a correlate of MRF 1, they were deposited more distal to volcanic centres.

The uppermost preserved part of the central Rosebery Group, albeit thin and fault-truncated, also bears similarities to the Marianoak Formation. The abrupt compositional switch from felsic to mafic-intermediate volcanism recorded by the transition from Facies 13 to 14, is interpreted to correlate with the boundary of MRF 1 and MRF 2 facies associations (Fig. 3.43). Volcaniclastic

sandstone (Facies 14) of basaltic andesite composition has similar mineralogy, texture and mode of emplacement VBX I/VSST of MRF 2.

Volcaniclastic facies of the southern Rosebery Group, Facies 15 and 16, also appear to record input from mafic-intermediate volcanic sources. In the case of Facies 16 crystal-rich volcaniclastic breccia, the monogenetic and texturally immature character of the framework components indicates short-lived transport and deposition from a coeval volcanic phase. Facies 15 greywacke is compositionally similar, but more texturally mature, raising the possibility of epiclastic reworking of Facies 16-type products. Both facies are tentatively correlated with the mafic-intermediate volcanic phase recorded by Facies 14 of the Natone Volcanics and VBX I/VSST of MRF 2.

Facies associations within the hangingwall block of the Rosebery Fault, the Rosebery Mine sequence, record a protracted history of dominantly syn-eruptive volcanic input. The lowest interval, feldspar-phyric juvenile clast-rich breccias of the Hercules Pumice Formation, has no equivalent facies in the Rosebery Group. Although feldspar-rich facies types include VBX I/VSST and Facies 16, the presence of mafic-intermediate lithic components in these Rosebery Group strata is at odds with the overall dacitic composition of the Hercules Pumice Formation. Similarly, the paucity of crystal fragments of quartz in the latter demonstrates a fundamentally distinct parental magma composition from felsic eruptive products of the Marianoak Formation and Natone Volcanics. Volcanic quartz first appears as a conspicuous component in the Rosebery Host Rock Member, which along with greater structuring of bedded facies, overall grain size reduction, minor abrasion of framework components, and polymictic detritus, indicates epiclastic reworking of a variety of volcanic sources. The upsection transition from feldspar- to quartz-dominant crystal components at this level may record decreasing contribution from the underlying Hercules Pumice Formation, and greater input from distal quartz-phyric sources. Alternatively, the transition may track a change in the magma composition of a single volcanic source. Given the paucity of juvenile volcanic products within the upper part of the Rosebery Host Rock Member in particular, and the continuing upsection

trend to deposition of non-volcanogenic mudstone, the second scenario appears less likely. The progressive starvation of the basin recorded by the upward fining trend thus is interpreted to record shut down of active volcanism, submergence of basin marginal source areas and/or trapping of basin margin-derived detritus in peripheral sub-basins.

Resurgence of explosive volcanic activity, manifest in the deposition of quartz-feldspar-phyric pumice breccias at the base of the White Spur Formation (WSF 1), is interpreted to relate to MRF 1 and Facies 13 of quartz-feldspar-phyric pumice breccia of the Natone Volcanics (Fig. 3.43). The breccia facies from the three different localities are of broadly equivalent thickness, have mineralogical, textural, and geometric affinities, permitting the interpretation of deposition from a single extensive felsic volcanic phase (Fig. 3.43).

The upsection transition to WSF 2A is considered to record the similar appearance of mafic-intermediate volcanic source material in MRF 2 and Facies 14 of the Natone Volcanics (Fig. 3.43). WSF 2A association of thickly bedded, normally graded basaltic andesite clast-bearing breccias and sandstone, is directly comparable to the VBX I/VSST facies association of MRF 2. Furthermore, additional contribution from felsic volcanic sources recorded by VXB II/VSST of MRF 2 is mirrored by the appearance of rhyolitic volcanic products in the upper levels of the White Spur Formation (i.e. WSF 2C). However, while the felsic volcanogenic input appears episodic in MRF 2 with, VBX II/VSST punctuating VBX I/VSST accumulation at various levels of the profile, the contribution in the upper White Spur Formation is more transitional.

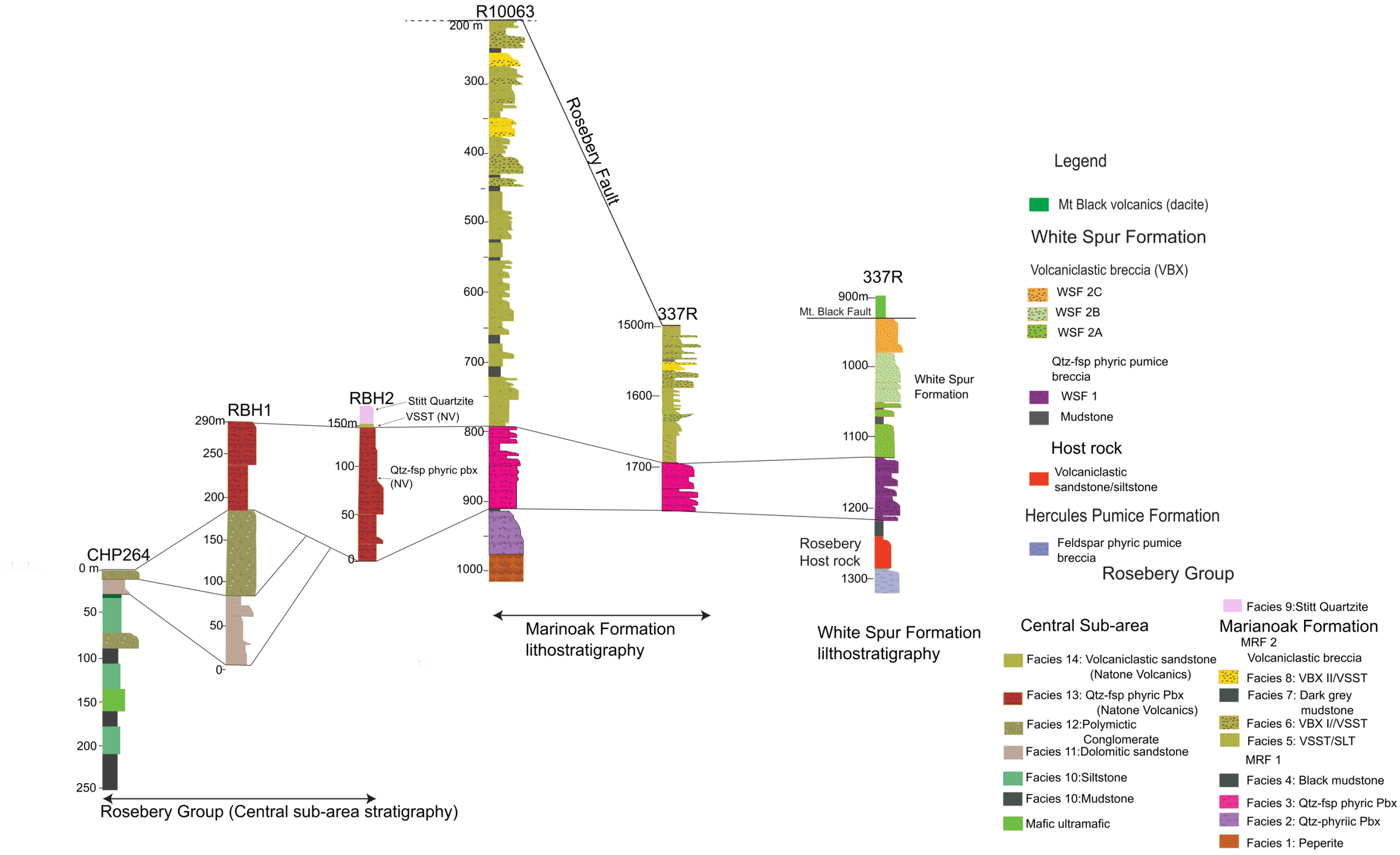

Figure 3.43. Lithostratigraphic correlations of the Marianoak Formation, Natone Volcanics and White Spur Formation. It has to be noted that the three volcano-sedimentary sequences stratigraphically overlie the Rosebery host stratigraphy

3.8 Conclusion

A lithostratigraphic framework is proposed which links spatially and structural disparate domains of the broader Rosebery region. Underpinning this framework is the detailed examination of lithofacies associations related to an apparently unique phase of submarine explosive felsic volcanism, recorded by quartz ± feldspar-phyric pumice breccias of the White Spur Formation, Marianoak Formation, and Natone Volcanics. The work broadly confirms aspects of previous studies (e.g. Green, 1983; Corbett and Lees, 1987; Allen, 1991; Parfrey, 1993; Winter, 2012; and Baker, 2013), but reinforces the correlation through the recognition of a regionally mappable upper component of the eruptive phase characterised by variably reworked mafic-intermediate volcanic material.

Although correlation of the quartz ± feldspar phyric pumice breccia 'marker horizon' is considered robust, its enclosing lithofacies associations show considerable lateral variation. This is most clearly demonstrated in the contrasting lithofacies associations that underlie the White Spur Formation to the east, and the Natone Volcanics to the west: i.e. volumetric feldspar-phyric pumice breccia of the Hercules Pumice Formation, and the upward coarsening Westcott Argillite-Salisbury Conglomerate cycle, respectively. The lateral variation is interpreted to reflect 1) relative proximity to basin marginal sediment input and intrabasinal volcanic centres, and 2) sub-basin reorganisation roughly at the level of the Rosebery host rock. These concepts will be examined further in subsequent chapters. Chapter 4 will also test the robustness of stratigraphic correlation through the use of lithogeochemistry.

Chapter 4: Lithogeochemistry

4.1 Introduction

In intensely hydrothermally altered, highly strained and metamorphosed environments, mineralogical and textural modification hampers correct identification of lithofacies and establishment of a robust litho-stratigraphic framework (MacLean and Barrett, 1993; Barrett and MacLean, 1994; Piercey, 2008). To overcome these problems, a number of researchers have successfully employed a complementary chemo-stratigraphic approach, whereby immobile element concentrations provide constraints on primary lithofacies classification. Barrett and MacLean (1993, 1994), Herrmann (1998), and Rollinson (2014) have shown that Al, Ti, Zr, Nb, Y, heavy REE, Hf, Ta, Th and to some extent Sc, V and Cr, remain immobile throughout most VHMS alteration processes, even along feeder pipe systems that are characterised by high water rock interaction. The water-rock interaction can result in net mass gains or losses of mobile components that can affect the concentration of immobile elements but the inter element ratios remain mostly constant (Herrmann, 1998).

Use of these immobile elements and their ratios leads to improved chemostratigraphic correlation and identification of altered rock precursors (MacLean and Barrett, 1993). This method works best for coherent igneous rocks or relatively massive, juvenile volcaniclastics, such as pumice breccia facies, where the rock's composition effectively mimics that of its parental magma (Herrmann, 1998). However, in highly reworked volcaniclastics, immobile elements are potentially enriched or depleted by sedimentary fractionation processes, such that compositions deviate from those of their magmatic sources. For example, Zr can be fractionated by sedimentary processes as zircon, a mineral resistant to mechanical and chemical abrasion, leading to 'overrepresentation' in particular epiclastic facies. Thus, chemo-stratigraphic analysis of complex volcano-sedimentary environments requires care, consideration of facies type, and an appreciation of processes that have the potential to disturb chemical signatures.

In this study, three stratigraphic associations are considered, initially individually, and subsequently through comparison: 1) the Marianoak Formation, or massive sulphide-bearing volcanogenic-dominant interval of the Rosebery Group positioned in the immediate footwall of the Rosebery Fault (Fig. 1); 2) the Natone Volcanics, positioned within the sediment-dominant central part of the Rosebery Group, and 3) the classical Rosebery Mine host stratigraphy, located in the structural hangingwall of the Rosebery Fault. Voluminous volcanic (-lastic) facies that are relatively homogenous are the particular focus of the study. The principal aims of the analysis are to erect a robust chemo-stratigraphy for the massive-sulphide bearing intervals of the Rosebery Group, to constrain their regional stratigraphic position, in particular, relative to other 'favourable' intervals of the Mt Read Volcanics.

4.1.1 Previous chemo-stratigraphic correlations of the Rosebery Group

In addition to 'in-house' chemical analysis of the Rosebery Group by MMG, three undergraduate level research projects have been undertaken prior to this study (Parfrey, 1993; Winter, 2012; Baker, 2013). Each study considered mainly juvenile volcaniclastic strata, which occur in two spatially-distinct intervals of the Rosebery Group: 1) quartz-feldspar-phyric pumice breccias of the Natone Volcanics, located within the central part of the belt, and 2) a mixed quartz and feldspar-phyric volcaniclastic succession in the immediate footwall of the Rosebery Fault (Marianoak Formation), traceable from the northern part of the Rosebery Mine, southward to the Jupiter prospect (Fig. 1). As discussed in Chapter 3, the broader lithostratigraphic associations of each package have certain similarities and differences. The volcaniclastics of the Marianoak Formation comprise a heterogenous succession of pumice breccias, shallow-level intrusions with peperitic margins, and volcaniclastic breccia interbedded with volcaniclastic sandstone (Fig. 4.2). These facies occur intercalated with mudstone and volumetrically subordinate sandstone and siltstone. The Natone Volcanics, by contrast, consists mostly of homogenous quartz-feldspar-phyric pumice breccia, and

occurs enclosed with basement-derived polymictic conglomerate and structural slices of mafic-ultramafic complex material (the latter likely basement-derived).

The volcaniclastics of Marianoak Formation were previously studied by Parfrey (1993) through mapping and logging of three drill holes. He broadly compared the lithogeochemistry of these units to the Natone Volcanics, as well as the stratigraphic hanging- and footwalls of the Rosebery Mine host sequence, noting that bivariate plots of Zr vs SiO_2 and Zr vs Al_2O_3 were the best chemical discriminants. His conclusion was that the Natone Volcanics and the Marianoak Formation have geochemical affinities, with typically low Zr (<180 ppm) values, whereas the Rosebery Mine footwall and hangingwall sequences have characteristically higher Zr (>180 ppm). It should be noted, however, that Parfrey's study was fairly cursory, with little attempt to link lithogeochemical and lithofacies variations. Rather, each package was considered as a single lithogeochemically-homogenous interval, and as such potentially useful chemical signatures were obscured. For example, Parfrey (1993) failed to distinguish the petrographically distinct hangingwall and footwall components of Rosebery Mine host sequence: i.e. the quartz-phyric White Spur Formation and feldspar-phyric footwall sequence (Hercules Pumice Formation), respectively.

A greater interest in the stratigraphic position of Rosebery Group strata occurred after the 2010 discovery of high grade massive sulphide lenses within the Marianoak Formation. Accordingly, MMG conducted systematic multi-element whole rock geochemical analyses of the formation, involving sampling at 10 m intervals in drill cores that extend between 350 m and 1 km below the position of the Rosebery Fault.

The studies revealed that the host rock to the massive sulphide lenses, a quartz-feldspar-phyric pumice breccia, was characterized by unusually high Th abundances (22.20-51.00 ppm), this feature providing the basis for chemo-stratigraphic correlation throughout the Rosebery Mine-Jupiter area (MMG, 2014). Nevertheless, its position within the regional stratigraphic context of the Mount Read Volcanics was not established.

Complementary research by Geology Honours students at the University of Tasmania revisited the chemical relationships between the Marianoak Formation, White Spur Formation (hangingwall) interval at the Rosebery Mine, and the Natone Volcanics, albeit with a limited number of samples (Winter, 2012; Baker, 2013). Only two samples from the lower Marianoak Formation quartz-feldspar-phyric pumice breccia were considered and compared with the White Spur Formation and Natone Volcanics on the basis of Ti/Zr, SiO_2 and P_2O_5 contents (Fig. 4.1). Analyses showed that the Marianoak Formation pumice breccia yielded very low Ti/Zr (1.98) and P_2O_5 (<0.01 wt. %) values, distinct from Natone Volcanics and White Spur Formation (Fig. 4.1). The White Spur Formation samples obtained from Parfrey (1993) possess a narrow range of Ti/Zr (2.5-7.5) consistent with rhyolite to rhyodacite compositions, whereas those obtained from MMG (Large et al., 2001a) showed a wide range of Ti/Zr values (7.0-20), consistent with rhyolite to andesite compositions (Baker, 2013). Natone Volcanics samples obtained both from Parfrey (1993) and Baker (2013) possessed a narrower range of Ti/Zr values (7-10) except one sample from the volcaniclastic sandstone top of sequence with higher Ti/Zr (16.29), but consistently higher than those of the two Marianoak Formation samples (Fig. 4.1). As a result, a conclusion was reached that the Marianoak Formation, with very low Ti/Zr, was distinct. However, the Natone Volcanics samples overlapped with a wide range of White Spur Formation lithogeochemistry and a crude correlation was established, although the latter bears significant lithofacies variation.

Baker (2013) reinforced the correlation of the Natone Volcanics and the White Spur Formation chronostratigraphically. High precision TIMS dating of zircon from the quartz-feldspar phyric pumice breccia revealed well-constrained, overlapping ages of 498.26 ± 0.78 Ma and 499.60 ± 0.8 Ma for the respective units (Baker, 2013; Mortensen et al., 2015).

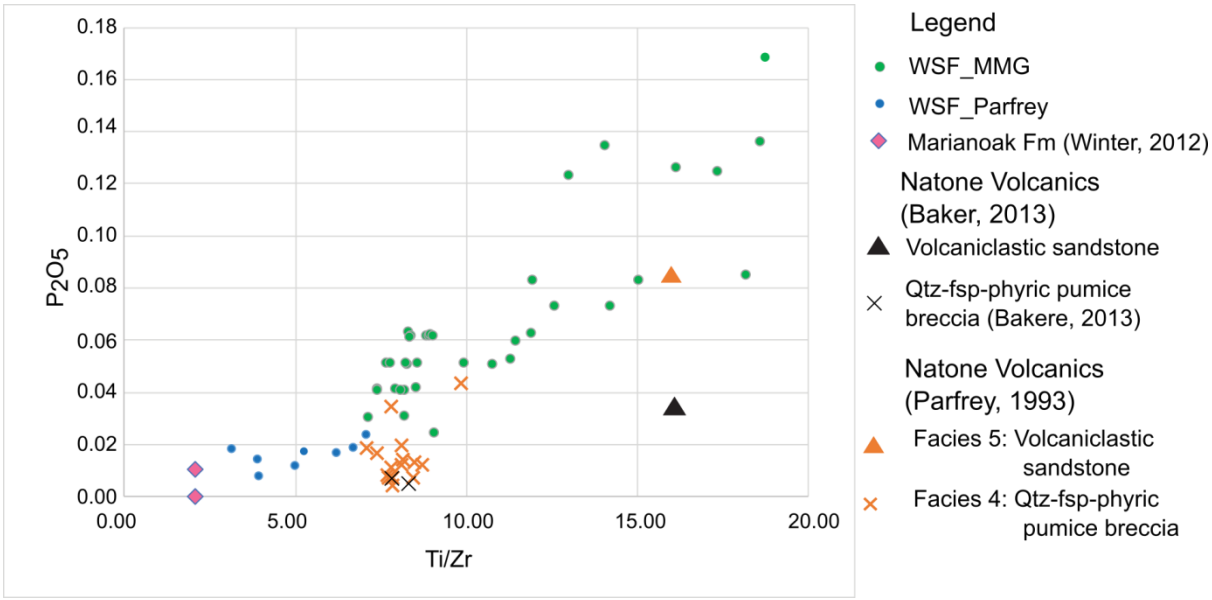

Figure 4.1. Ti/Zr vs P_2O_5 plot of Natone Volcanics (Parfrey, 1993; Baker, 2013), Marianoak Formation (Winter, 2012), and White Spur Formation samples (Parfrey, 1993; Large et al, (2001). See text for discussion.

4.1.2 Methodology

Drill hole logging

A total of 11 drill holes bearing chemical analyses were used in this study, their surface-projected collar positions shown in Figure 1. Most of these drill holes intersected the Marianoak Formation in the vicinity of the Rosebery Mine, 9 of which were logged in detail and analysed petrographically (see also Chapter 3) and Appendix 2. An additional Marianoak Formation drill hole (250R) was collared sufficiently high in the structural complex to include an interval of the Rosebery Mine host stratigraphy, including a section of the White Spur Formation. This drill hole was not logged directly but interpreted upon the basis of MMG's detailed petrographic and lithofacies descriptions. A single drill hole from the Natone Creek area (RBH02) has geochemical analyses. This was logged in detail for the chemo-stratigraphic analysis and is compared to neighbouring drill holes on lithological grounds in Chapter 3.

Lithogeochemical sampling and database management

Lithogeochemical sampling of the Rosebery Mine host sequence and the Marianoak Formation was conducted by MMG. Ten cm long samples were collected every 10 m down hole and a total of 475 analyses from the 10 drill holes were used in this study. The location of each geochemical sample was noted during the logging process, with particular care taken to observe the associated lithofacies. All samples were prepared and analysed using ICP-MS in an ALS laboratory using a four-acid digest for 48 major and trace elements (Appendix 4A). The major elements that were reported as a single element were converted into their oxide forms by multiplying with a factor as follows: Al x 1.889, Ca x 1.399, Fe x 1.43, K x 1.205, Mg x 1.658, Mn x 1.291, Na x 1.348, P x 2.291, Si x 2.139, Ti x 1.668. The detection limit of the elements as reported by ALS are as follows: Al (0.01 %), Ca (0.01 %), Cr (0.3 ppm), Fe (0.002 %), Ga (0.05 ppm), Ge (0.05 ppm), Hf (0.004 ppm), K (0.01 %), La (0.005 ppm), Mg (0.01 %), Mn (0.2 ppm), Na (0.001 %), P (0.001 %), Sc (0.01 ppm), Th (0.004 ppm), Ti (0.001), U (0.01 ppm), V (0.1 ppm), W (0.008 ppm), Y (0.01 ppm) and Zr (0.1 ppm)

The Natone Volcanics drill hole (RBH02) has 15 samples analysed (Parfrey, 1993) for major and selected trace elements (Appendix 4B). Fifty centimetre long samples were collected every 5-15 m from split NQ drill core. Major elements, Nb, V, Zr, Sr and Ba were determined by glass fusion and pressed powder X-ray fluorescence, and rare earth elements by Neutron Activation. From the same drill hole, Baker (2013) collected 3 lithogeochemical samples that include Sc and Th analyses, these elements lacking in the Parfrey (1993) dataset, but important in chemical discrimination.

The geochemical database was firstly examined within the context of the lithostratigraphic framework presented in Chapter 3. Basic lithogeochemical classification was undertaken for the volcanics in accordance with that of Pearce (1996). More rigorous classification and establishment of lithogeochemical discriminators was then achieved using immobile major and trace element ratios (e.g. Zr/Al_2O_3, Zr/TiO_2, Al_2O_3/TiO_2). Data were examined both in bivariate and downhole plots, the

latter revealing distinctive chemo-stratigraphic patterns and trends, which underpin correlations within and between the various litho-structural domains.

4.2 Geochemical classification of the Marianoak Formation

A basic 2-fold lithostratigraphic subdivision of the Marianoak Formation has been presented in Chapter 3 and summarised in Figure 4.2. The lower interval, MRF 1, consists predominantly of quartz ± feldspar phyric pumice breccia. A basal rhyolitic breccia, interpreted as a peperitic sub-volcanic intrusion, is intersected in one drill hole (R10063). Mudstone, volcanogenic sandstone, and massive sulphide horizons represent volumetrically minor facies within MRF 1. MRF 2 comprises a more heterogenous succession of conspicuously pumice-poor volcaniclastics that range in grain size from siltstone, sandstone to breccia. It will become apparent that the geochemical features of MRF 2 record contribution from two 'end-member' volcanic sources: a felsic source, not dissimilar to that recorded by the quartz-phyric MRF 1 strata, and a more basic source. These end-member compositions are recognisable independently of grain size.

As discussed in the introduction to this chapter, the study focusses on coarser-grained lithofacies that contain either demonstratively juvenile clastic material, such as pumice, or texturally-immature monomictic detritus, that indicate derivation from single eruptive events. It is anticipated that voluminous and widespread eruptive products are in cases chemically distinct, providing markers that can be used to test the robustness of correlations between the three packages. The mudstone facies, while locally volumetrically significant, is interpreted to have been deposited during periods of volcanic quiescence, with probable intrabasinal and extrabasinal detrital input.

For the purpose of general volcanic rock classification, 200 samples from ten drill holes of MRF 1 and MRF 2 were plotted on Pearce discrimination diagrams of Figures 4.3 and 4.4 respectively. MRF 1 strata possess highly evolved rhyodacite to alkali-rhyolite compositions, whereas the volcaniclastic breccias, and volcaniclastic sandstone and siltstone of MRF 2 are more

intermediate in composition but show an appreciable range from andesite and basaltic-andesite to rhyodacite.

Further subdivision is achieved by examining coupled variations of Th, Zr, Ti, Sc, and Al (Figs. 4.5A-D), revealing five distinct geochemical populations of data ranging from felsic to intermediate end members. The majority of these chemical groups correspond to unique lithofacies, however, overlap exists for some, highlighting the importance of combined petrographic-lithologic and chemical features in stratigraphic analysis. While the chemical distinction between the evolved rhyolitic units (MRF 1) and VBX I/VSST of basaltic andesite composition in Figure 4.5 is profound because of its large chemical variation, the distinction within the MRF 1 subunits is subtle. The weaker discrimination within the MRF 1 is possibly explained due to very low concentration of the compatible elements (Ti and Sc) in the highly evolved felsic volcanics and minor chemical variation within the subunits.

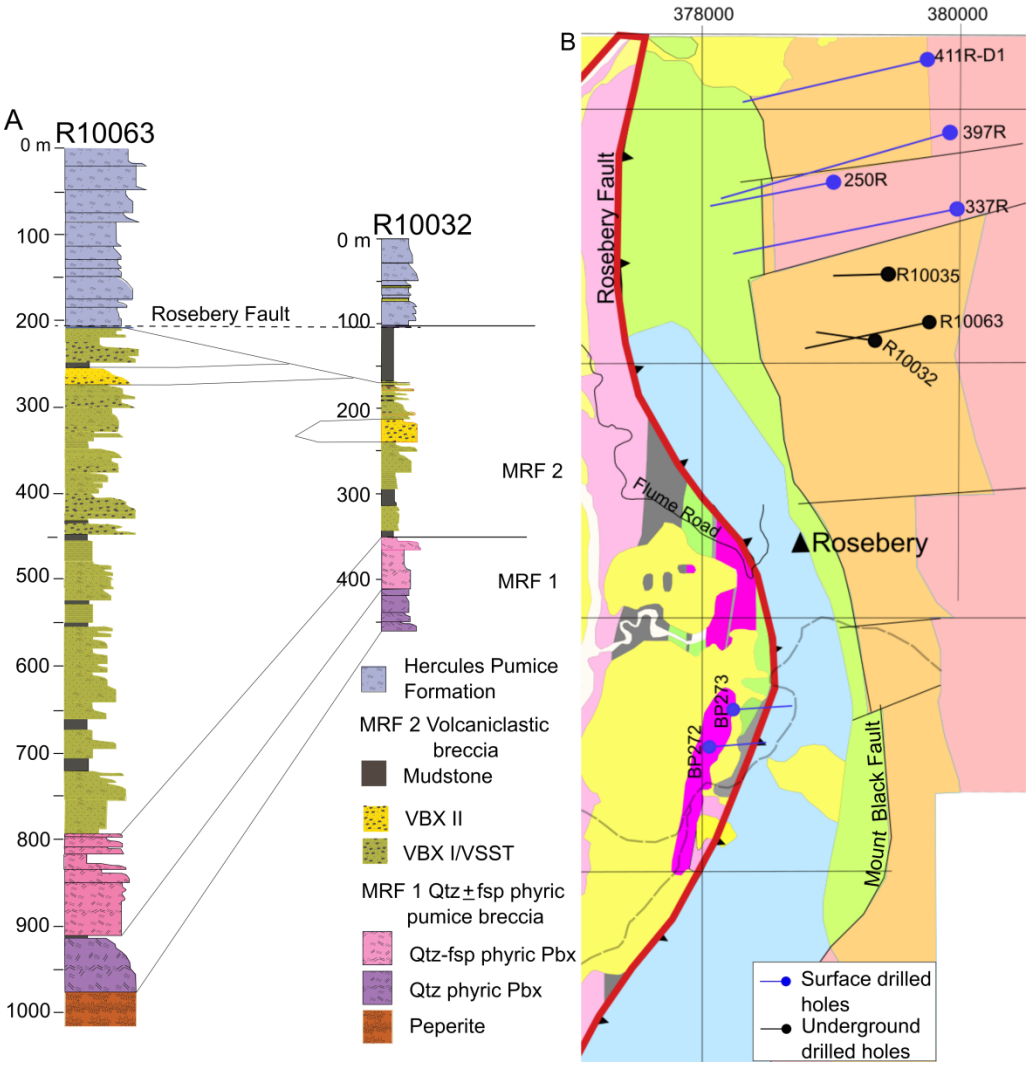

Figure 4.2. Lithostratigraphic framework of the Marianoak Formation, as summarized in two adjacent underground drill holes, and geological map showing surface projected collar locations. Refer to Figure 1 on the "map pocket' for map legend.

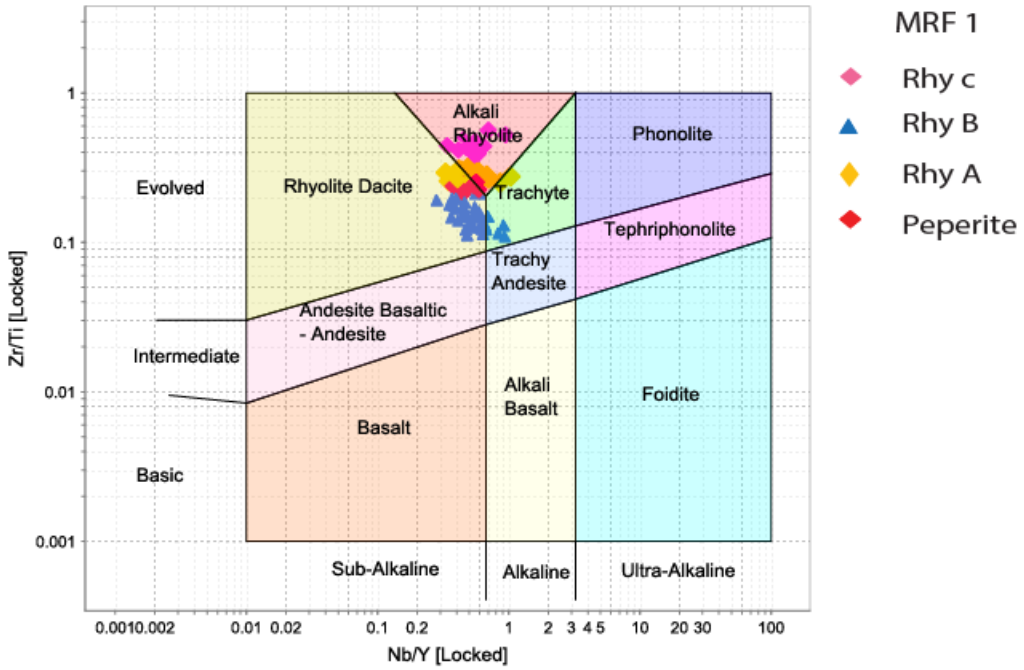

Figure 4.3. Zr/Ti and Nb/Y plot of Pearce (1996), comparing MRF 1 volcanogenic facies. A revised facies classification is shown in the legend, based on a combination of lithologic and chemical characteristics: refer to Figure 4.6 for relative stratigraphic positions.

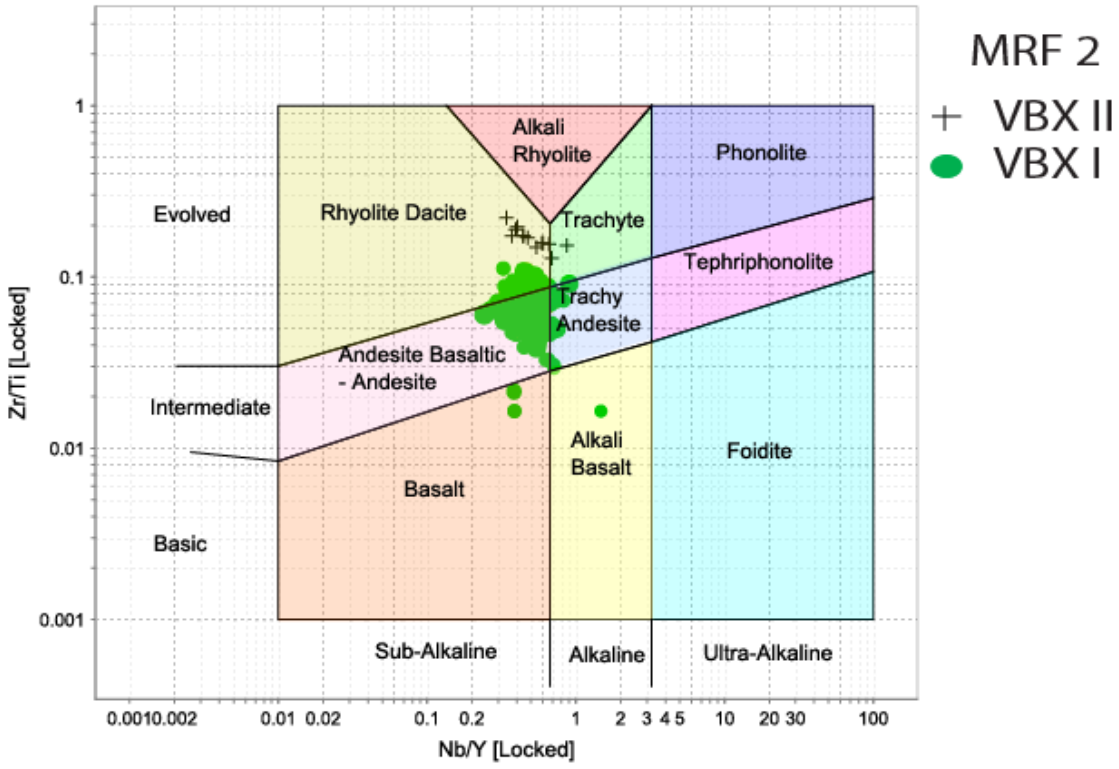

Figure 4.4. Zr/Ti and Nb/Y plot of Pearce (1996), comparing MRF 2 volcanogenic facies. Compositions conform largely to basaltic andesite and rhyodacite.

4.2.1 MRF 1 facies association

MRF 1 comprises three principal volcanogenic lithofacies: from base to top these include rhyolitic breccia (peperite), quartz-phyric, and quartz-feldspar phyric pumice breccia (Figs. 4.2). A down hole plot of selected chemical discriminators (Fig. 4.6) in R10063 (the thickest and most complete MRF 1 intersection) shows distinct and abrupt compositional shifts across each of the sub-facies boundaries, with further subdivision of the upper quartz-feldspar-phyric pumice breccia. The 4-fold chemo-stratigraphic nomenclature employed throughout this work includes, in ascending order, Peperite, Rhy A, Rhy B and Rhy C. While the facies name 'Peperite' is retained, the quartz-phyric pumice breccia is replaced with Rhy A, whereas the quartz-feldspar-phyric pumice breccia is divided into two chemical subunits, Rhy B and Rhy C. Less complete profiles, coupled with lateral facies variation in neighbouring drill holes, lead to complexities that will be discussed further below.

Rhyolitic breccia (Peperite)

The lower Peperite is intersected only in hole R10063, with a true thickness of ~60 m (Fig. 4.6). It comprises a jigsaw fit arrangement of monomictic, quartz-phyric rhyolitic volcanic fragments set in a siltstone- to mudstone-sized matrix.

Geochemically, it is classified as evolved rhyolite to rhyodacite according to the Pearce plot (Fig. 4.3). It has a very low average Ti/Zr value of 4.16 and a characteristically high average Th value of 33.54 ppm (Table 4.1). A combination of Al_2O_3/TiO_2, Th/Sc, and Ti/Zr values allow the facies to be distinguished from other levels in MRF 1 (Figs. 4.5 A-D and 4.6). Generally, it has significantly elevated incompatible element (Th) abundances and very low compatible element (Ti, Sc) concentrations (Fig. 4.5B-D), characteristic features of products of evolved, felsic magmatism.

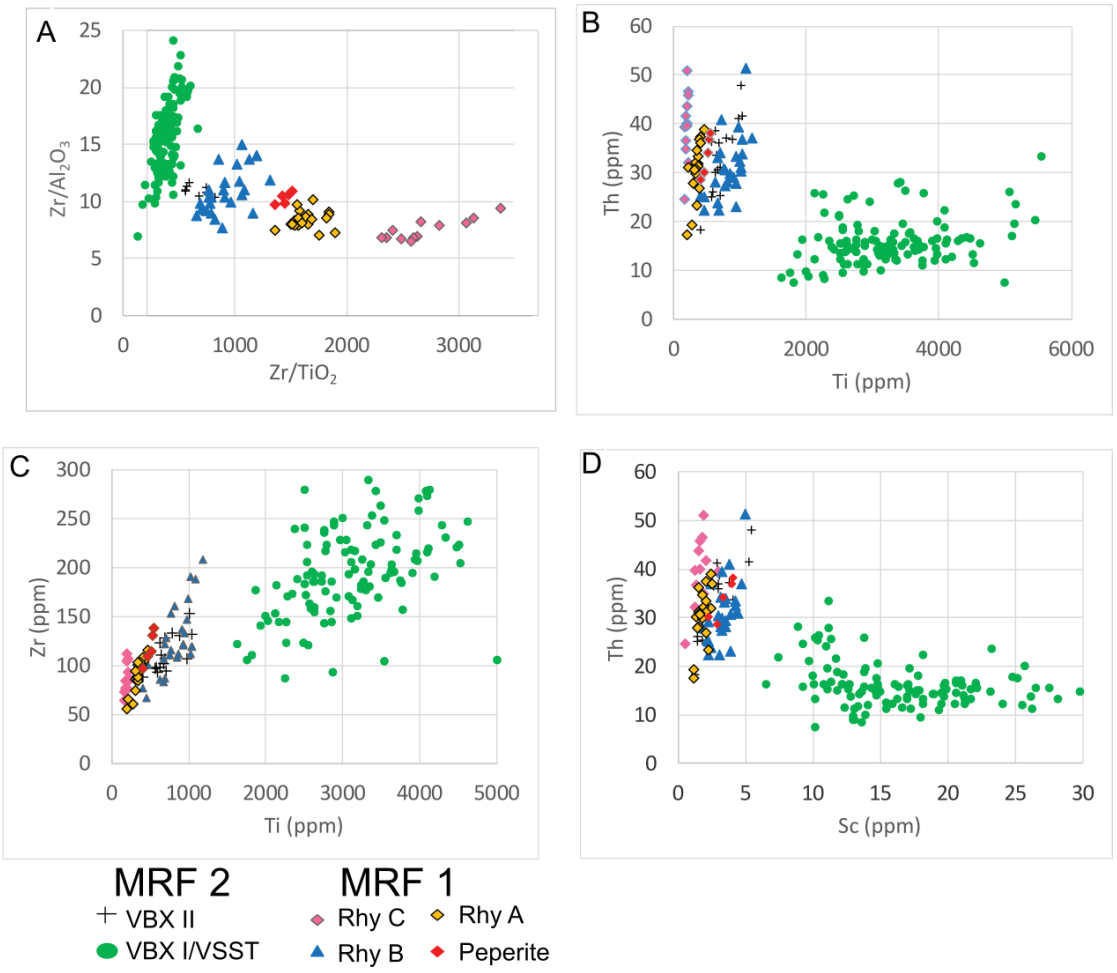

Figure 4.5. Immobile elements plots of Marianoak Formation volcaniclastic strata. A) Zr/TiO_2 vs Zr/Al_2O_3 effectively discriminates most units, and provides the basis of a 6-fold chemostratigraphic classification: refer to Figure 4.6 for relative stratigraphic positions. B-D) Immobile element bivariate plots, showing clear discrimination of VBX I/VSST, with its distinctive 'basic' composition. More felsic facies show partial overlap, and in several facies types clear linear trends.

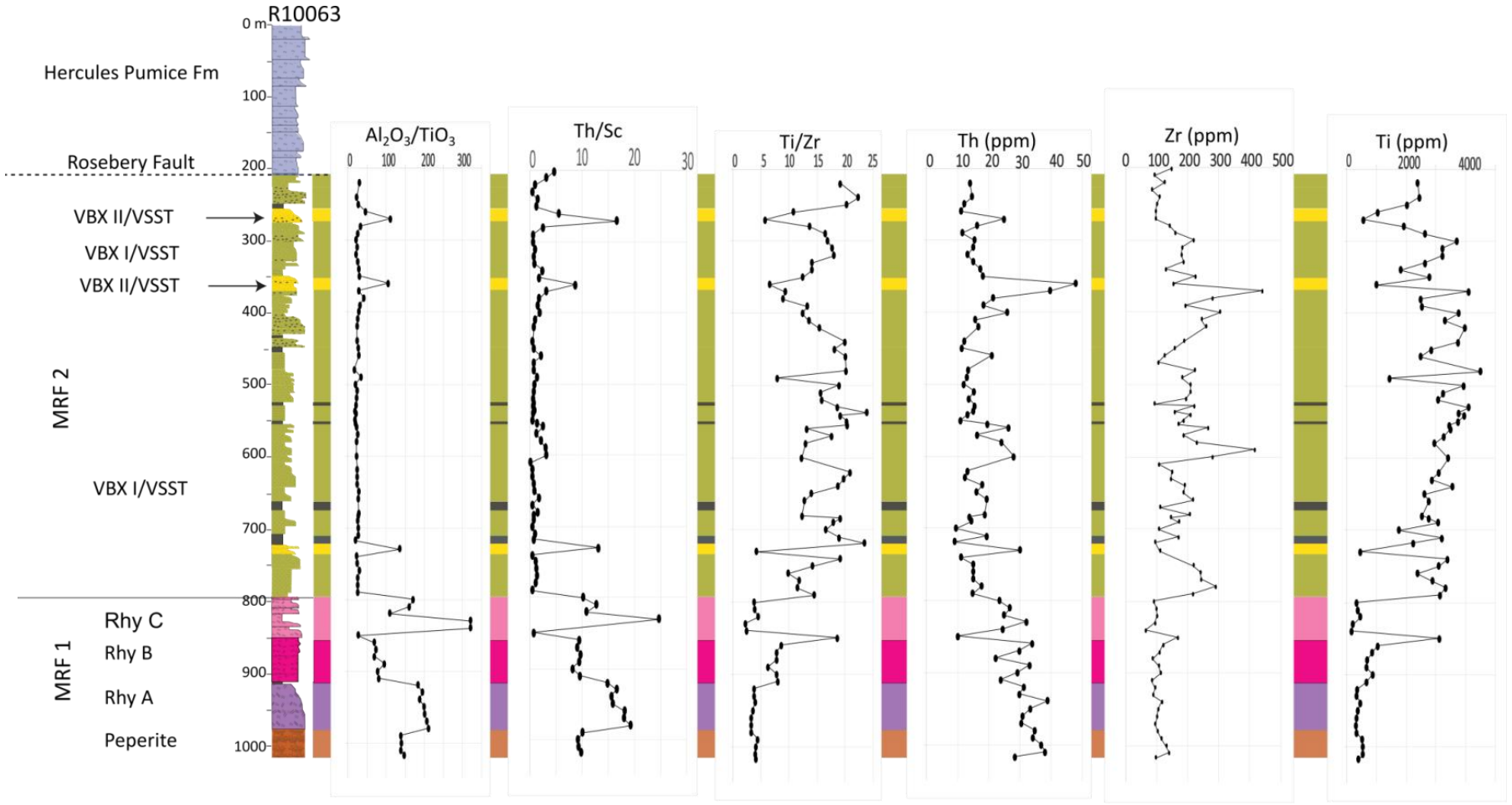

Figure 4.6. Down-hole plot of immobile elements and their ratios for Marianoak Formation strata in hole R10063. Abrupt cross-stratal compositional shifts are revealed at a number of levels in the stratigraphy. These boundaries, and the contrastingly homogenous chemical signatures within individual units (MRF 1 facies types in particular), form the basis for the chemostratigraphic subdivision shown on the left. Note the close correspondence of chemo-stratigraphic boundaries and lithofacies types.

Table 4.1. Immobile element abundances and their ratios that characterize the six distinct geochemical subunits of MRF 1 and MRF 2. Note there exists chemical overlaps in VBX II/VSST and Rhy B.

Lithofacies	Chemo-units		Ti/Zr	Al2O3/TiO2	Th/Sc	Th	Zr	Ti
Volcaniclastic breccia	VBX I/VSST	min	8.93	17.77	0.17	7.40	87.40	1630.00
		max	47.39	42.38	3.15	33.40	489.00	5550.00
		average	16.52	24.69	1.06	15.77	203.66	3236.95
		STD	4.81	4.93	0.62	4.71	58.70	838.39
Volcaniclastic breccia	VBX II/ VSST	min	4.52	71.25	7.83	18.30	88.50	400.00
		max	9.02	113.05	18.29	47.90	154.00	1030.00
		average	6.33	97.77	13.38	33.48	112.72	715.00
		STD	1.08	11.53	3.46	7.51	18.83	176.67
Qtz-Fsp phyric Pbx	Rhy C	min	1.78	321.95	13.10	24.50	64.20	160.00
		max	2.60	390.71	40.83	50.90	112.50	220.00
		average	2.25	358.17	25.31	39.62	86.61	191.67
		STD	0.26	23.03	6.80	7.08	14.99	18.01
Qtz-Fsp phyric Pbx	Rhy B	min	4.55	61.81	5.92	22.20	66.80	400.00
		max	9.11	128.54	15.50	51.30	208.00	1180.00
		average	6.69	85.27	9.52	30.97	125.57	822.96
		STD	1.25	1.25	2.32	6.39	35.06	201.30
Qtz-phyric Pbx	Rhy A	min	3.17	160.64	10.17	17.40	55.60	190.00
		max	4.41	258.86	22.63	38.90	115.50	460.00
		average	3.70	194.97	16.66	30.49	91.00	336.36
		STD	0.29	0.29	2.91	5.35	15.34	60.75
Peperite	Peperite	min	3.96	135.65	9.20	28.50	96.70	400.00
		max	4.43	146.94	13.09	38.20	139.00	550.00
		average	4.16	139.94	10.29	33.54	118.14	490.00
		STD	0.18	4.20	1.60	4.18	4.18	60.42

Rhy A

Rhy A is characterized by a high abundance of angular to sub-rounded, in places embayed, quartz crystal fragments, minor euhedral feldspars, glass-shards and pumice clasts set in a sericite altered groundmass. Petrographically, the subunit is defined by high proportion of quartz to feldspar (95:05). Although not all drill holes penetrate this deep stratigraphic level, Rhy A is mappable as a petrographically and chemically distinct, 70-100 m thick subunit, between the northern part of the Rosebery Mine and Jupiter in the south (Fig. 4.7).

Rhy A plots within the alkali rhyolite to rhyodacite field in the Pearce volcanic rock classification plot of Figure 4.3, partly overlapping Peperite data. It is best discriminated using the Zr/

Al_2O_3 vs Zr/TiO_2 plot (Fig. 4.5A). On average, it has slightly lower values of Ti/Zr (3.70) and Th (30.49 ppm) compared to the underlying Peperite facies (Fig. 4.6, Table 4.1). Distinct linear trends are revealed in Ti vs Th, Ti vs Zr, and Sc vs Th plots (Figs. 4.5B-D), the spread of data likely reflecting mechanical fraction via eruptive and/or depositional processes (e.g. separation of glass and crystal, in particular quartz, components). Downhole geochemical plots provide further clear evidence of compositional differences from enclosing MRF 1 chemical subunits of peperite, Rhy B most notably its very high Th/Sc (av. 16.66) and Al_2O_3/TiO_2 (av. 194) values (e.g. Fig. 4.6; Table 4.1).

Rhy B

Rhy B represents the lower part of the quartz-feldspar phyric pumice breccia. It has a thickness of about ~60 m in the northern part of the Rosebery Mine, but becomes highly variable, and locally absent, to the south (Fig. 4.7). Beds are 10-20 m in thickness and normally graded from very coarse pumice- and mudstone-clast bearing bases, and better stratified quartz-phyric volcaniclastic sandstone and siltstone tops. The stratified top part of Rhy B hosts a high-grade sphalerite and galena bearing massive sulphide lens in drill hole 411-R1 (Fig. 4.7).

The breccia is composed of pumice clasts (1-5 cm, 60%), medium and fine grained angular to sub-rounded quartz crystal fragments (0.5-2 mm, 2 % and <0.5, 15%) and euhedral feldspar crystal fragments (0.5-2 mm, 5%), glass shards and mud lithics. Its quartz to feldspar ratio is estimated to be 80:20, lower than that of Rhy A.

Unlike the other chemo-stratigraphic subunits that transition from alkali rhyolite to rhyodacite, Rhy B completely falls in the rhyodacite field of the Pearce volcanic rock classification plot (Fig. 4.3). Further discrimination from the other subunits of MRF 1 is possible using Zr/Al_2O_3 vs Zr/TiO_2 (Fig. 4.5A), although there is partial overlap with the MRF 2 volcaniclastic breccia, VBX II/VSST, which has similar geochemical character (Fig. 4.5A-D). Discrimination of the Rhy B and VBX II requires additional textural and petrographic information (see below).

On average, Rhy B has slightly higher values of Ti/Zr (av. 6.69; range 4.55-9.11) than both underlying subunits (Rhy A and Peperite), with average Ti values of 822.96 ppm and a range of 400-1180 ppm (Table 4.1). Thorium abundances average 30.97 ppm and range 22.20-51.30 ppm, overlapping the ranges for underlying subunits (Table 4.1), however, Th/Sc values are consistently lower than enclosing strata (Fig. 4.5). The progressive upsection transition to towards relatively lower incompatible element concentrations (note also the distinctive upsection increasing Ti/Zr in Figure 4.6 is indicative of a less felsic composition compared to Rhy A. The appearance of feldspar as a volumetric crystal component accords with this trend and may indicate a subtle change in parental magma composition. Alternatively, dilution of the magmatic component by mudstone, which is a conspicuous detrital component, could also contribute to the chemical signature.

Rhy C

The upper part of the quartz-feldspar phyric pumice breccia, Rhy C, is recognised only in the southern part of section (Fig. 4.7). Where present, it has a maximum thickness of ~50 m, with relatively minor lateral variation. Pumiceous intervals are composed mainly of quartz crystal fragments, euhedral to subhedral feldspar, former glass shards and pumice clasts set in a sericite-altered, groundmass. The quartz: feldspar ratio is slightly higher than that of Rhy B (90:10).

On the Pearce volcanic rock classification plot, Rhy C falls entirely within the alkali rhyolite field (Fig. 4.3) and is apparently derived from a more evolved magma than all other MRF 1 facies association. It has the lowest average Ti/Zr value (2.4), and a very high average Th abundance of 39.62 ppm, with a range of 24.50-50.90 ppm (Table 4.1, Fig. 4.6). The very abrupt increase in Th/Sc value from underlying units (Figs. 4.6 and 4.7) makes the basal contact, and the subunit as a whole, highly distinct. As is the case with Rhy A, the subunit forms definite ‘fractionation trends’, with high correlation coefficients, in compatible-incompatible trace element plots (Figs. 4.5B-D), revealing a remarkably homogenous magmatic source.

4.2.2 MRF 2 facies association

MRF 2 comprises two volcanogenic facies associations: basaltic-andesite volcaniclastic breccia interbedded with volcaniclastic sandstone, siltstone and black mudstone (VBX I/VSST) and rhyolitic volcaniclastic breccia in volcaniclastic sandstone (VBX II/VSST: Figs. 4.2 and 4.7). The volcaniclastic breccia VBX I/VSST is distinguished from VBX II/VSST by its dominant clast component of basaltic andesite. The groundmass contains euhedral feldspar and minor quartz crystal fragments (quartz: feldspar = 05:95). By contrast, VBX II/VSST contains quartz-phyric clasts with considerably higher quartz: feldspar ratio (75:25). The quartz-feldspar phyric breccia is pumice-poor and thus readily distinguished from MRF 1 facies association at the hand specimen scale.

Basaltic-andesite volcaniclastic breccia and sandstone (VBX I/VSST)

VBX I/VSST overlies MRF 1 and has significant and rapid lateral thickness variation from ~130 to 600 m (Fig. 4.7). Overall, stratigraphic profiles reveal an upward coarsening and thickening patterns. Normally graded coarse to medium grained sandstones and siltstones, punctuated locally by 1-20 m mudstones, occur towards the base, whereas stacked upward-fining breccias dominate upper levels (Fig. 4.7). The lower facies association is dominated by angular to sub-rounded basaltic-andesite (0.5-1mm) and minor quartz crystals interpreted to be sourced from a distal volcanic eruption. However, the upper mass-flows contain angular to sub-rounded basaltic-andesite clasts (1-5cm), and euhedral feldspar crystals, suggesting limited transport from a more proximal source soon after eruption. The monogenetic and texturally-immature characters of the clasts and crystal assemblages that lack a voluminous pumice fraction suggest non-explosive eruptive products that are reworked from effusive volcanism.

All facies variants have relatively high Ti (av. 3236 ppm) and Zr (av. 203.66 ppm) contents that readily distinguish the population from MRF 1 and VBX II/VSST (Table 4.1). In a similar fashion to Ti/Zr, Th-Ti-Sc systematics show a high concentration of compatible elements relative to incompatible elements (Figs. 4.5B-D). Such relationships demonstrate that these volcaniclastics are

products of the most basic phase of magmatism that contributed to the Marianoak Formation, a feature consistent with andesite to basaltic-andesite chemical classification (Fig. 4.4), the presence of andesitic clasts, and relative paucity of quartz and rhyolite clasts.

Rhyolitic volcaniclastic breccia (VBX II/VSST)

VBX II/VSST breccia occurs principally as 20-120 m intercalations within the upper coarse-grained part of MRF 2, and less commonly as 10-20 m thick interbeds within the lower sandstone dominated intervals (Fig. 4.7). Breccia facies are generally medium to very coarse grained, comprising a texturally heterogenous, but felsic-volcanic dominated clast assemblage, set in a strongly sericite-altered groundmass: poorly sorted, angular to sub-rounded juvenile rhyolitic clasts of 1-5 cm, quartz crystals fragments, euhedral feldspar crystals, glass shards, minor feldspar-phyric pumice fragments and lesser mud lithics. The breccias locally fine upward into siltstones that are distinguishable from similar VBX I/VSST facies only on a chemical basis. The abundance of rhyolitic clasts and higher quartz to feldspar crystal proportions of 75:25 distinguishes the subfacies from the predominantly andesitic VBX I/VSST.

The VBX II/VSST marker horizons have rhyodacite to rhyolite compositions (Fig. 4.4), with a very low average Ti/Zr value of 6.33 and a range of 4.52-9.02 (Table 4.1). It is characterized by a high average Th value of 33.48 ppm, low average Zr and Ti values of 112.72 and 715.00 ppm, respectively, features that readily distinguish it from other MRF 2 facies (Table 4.1; Figs. 4.5A-D and 4.6). However, also shown in Figures 4.5A-D, is an indistinguishable chemical signature from the quartz-feldspar phyric pumice breccia facies (Rhy B) of MRF 1, with some additional overlap with subunits Rhy A and Peperite in terms of Th/Sc. Generally, it is enriched in the highly incompatible elements (Th) and depleted in Ti and Sc, indicating a highly evolved magmatic composition.

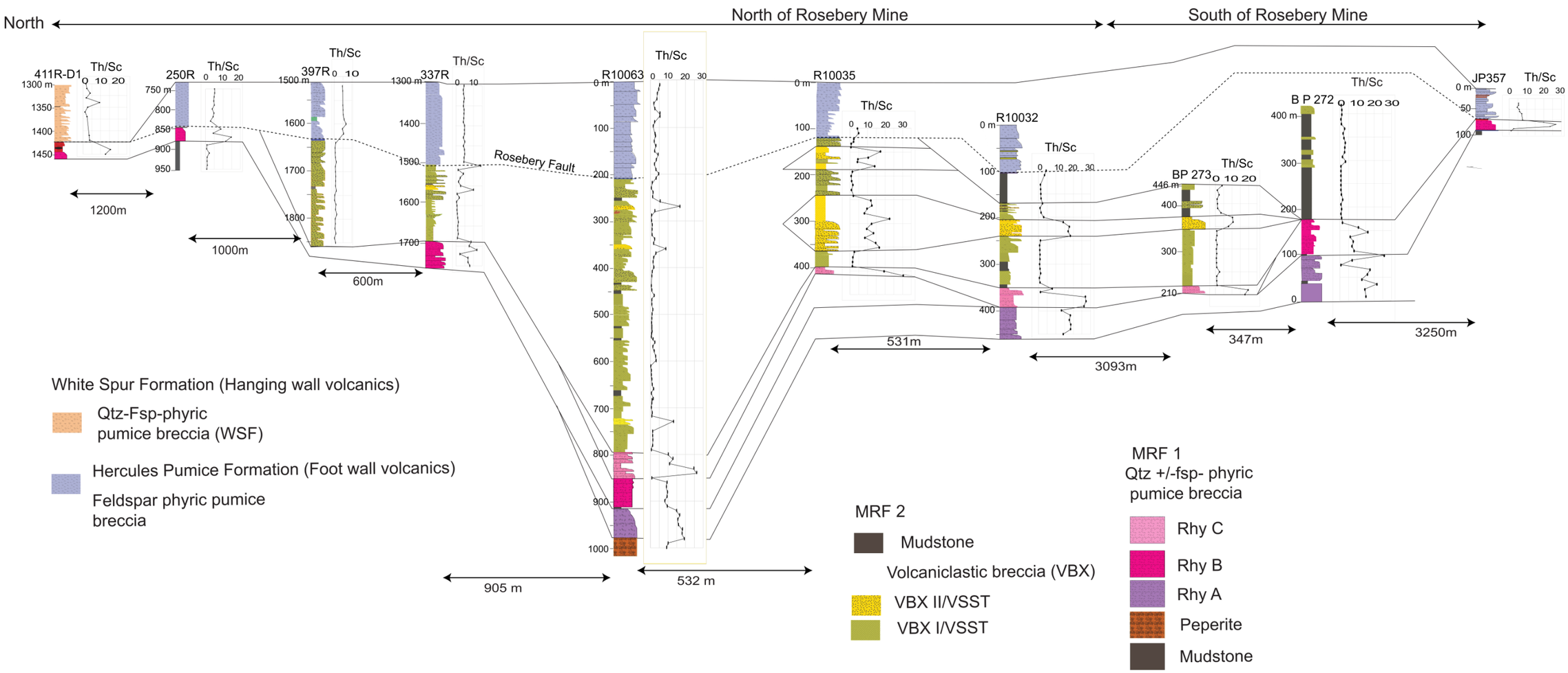

Figure 4.7. Chemostratigraphic framework of the Marianoak Formation, shown in down-hole plots of Th/Sc from the northern part of Rosebery Mine to the southern part of the belt at Jupiter (collar locations are shown in Figure 1.1). See text for discussion.

4.3 Lithogeochemistry of the Natone Volcanics

The Natone Volcanics comprises quartz-feldspar-phyric pumice breccia that crops out in the central part of the study area, where it occurs enclosed within a package of fine to very coarse-grained non-volcanogenic turbiditic deposits (Figs. 1, see also section 3.4 of Chapter 3). At the base of the sequence is a fine-grained interval of siltstone, mudstone, and dolomitic sandstone, passing upward to the Salisbury Conglomerate, the latter characterised by extrabasinal input of basement-derived mafic-ultramafic and quartzitic detritus (Van Einjndthoven, 2006; Baker, 2013; Corbett et al., 2014). To the east the Natone Volcanics is flanked to the Stitt Quartzite, a package of relatively mature, largely basement-derived quartzwackes and interbedded mudstones along an inferred N-S trending fault (Figs. 1 & 4.8: Green, 1983).

The pumice breccia has a thickness of approximately 118 m thickness and comprises several normally graded beds with fine stratified sandstone and siltstone ash tops (Fig. 4.8). Framework components include sparsely disseminated, medium grained, angular to sub-rounded, occasionally embayed, quartz (0.2-1 mm, 1-2 %), euhedral and subhedral altered feldspar crystal fragments (1-2 mm, 1-3 %), glass shards, pumice clasts (1-5 cm, 40-60 %) and sparse mudstone lithics.

Overall, the package fines upward, with a narrow interval of volcaniclastic sandstone separating the upper ashy levels of the pumice breccia interval from the quartzwackes of the Stitt Quartzite (Fig. 4.8). The volcaniclastic sandstone at the top of the succession in hole RBH02 consists of angular to sub-rounded basaltic-andesite clasts (0.5-1 mm, 20%), euhedral and fractured feldspar crystals (0.5-1 mm, 10-15 %), and minor quartz (0.25-0.5, 1-2%). It is thus petrographically distinct from the underlying pumice breccia unit, recording input from a more basic volcanic source.

Pearce volcanic rock classification of the Natone Volcanics shows that the quartz-feldspar phyric pumice breccia has a rhyodacitic composition, whereas the upper volcaniclastic sandstone has a basaltic-andesite composition (Fig. 4.9A). The former is characterized by low average Ti/Zr (8.06), Th/Sc (7.88), and elevated Th (30.34 ppm), as shown in Table 4.2 and Figures 4.8 & 4.9. The

bivariate plots show enrichment in the highly incompatible element, Th, and depletion in the most compatible elements (Ti) signifying its evolved rhyodacitic magma source. The upper volcaniclastic sandstone has higher Ti/Zr (16.29), lower Th/Sc (5.13) and Th (16.42 ppm) than the pumice breccia, again indicative of an intermediate to mafic magma composition (Table 4.2 and Fig. 4.9B-C).

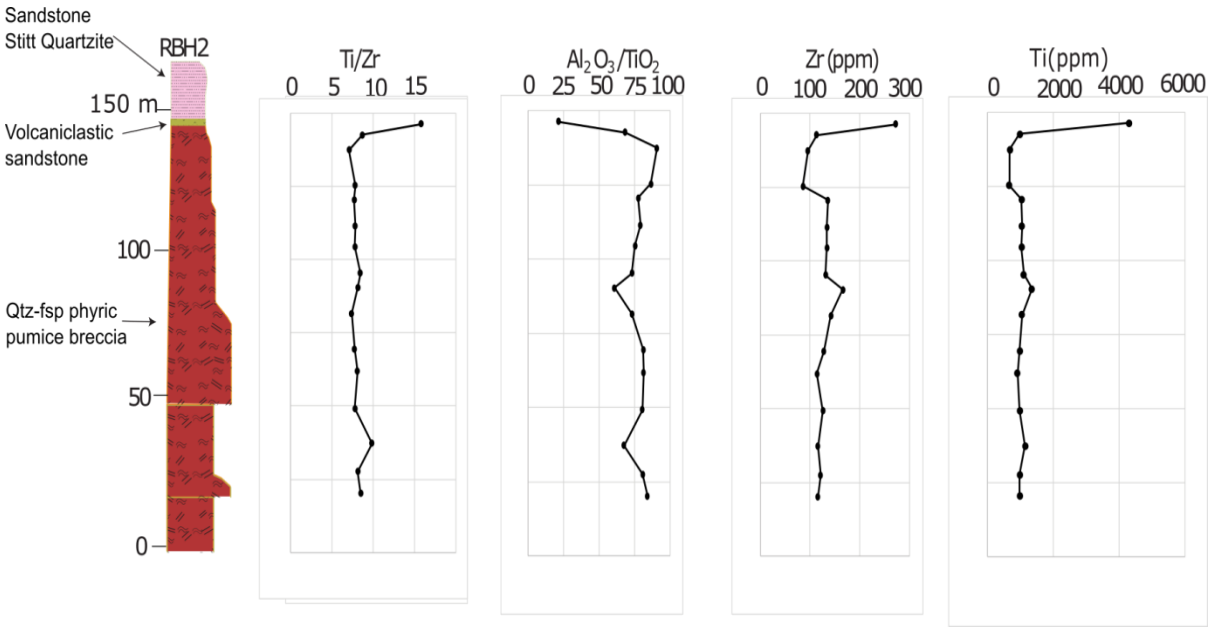

Figure 4.8. Down-hole plots of immobile trace element abundances and their ratios in the Natone Volcanics, from drill hole RBH2. The plot shows a thick and homogenous quartz-feldspar-phyric pumice breccia overlain by a thin volcaniclastic sandstone interval at 146-148.00 m. The volcaniclastic sandstone is overlain by mature sandstone of Stitt Quartzite.

Table 4.2. Geochemistry of Natone Volcanics

Lithofacies		Ti/Zr	Al_2O_3/TiO_2	Th/Sc	Th (ppm)	Zr (ppm)	Ti (ppm)
Qtz-Fsp-phyric Pumice breccia	min	7.09	60.91	7.09	26.95	86.00	673.84
	max	17.92	91.00	8.67	30.34	166.00	1349.34
	average	8.06	77.49	7.88	28.65	123.93	998.46
	STD	0.65	7.83	1.12	2.40	19.06	164.36
Volcaniclastic sandstone	Values	16.29	21.86	5.13	16.42	272.00	4431.66

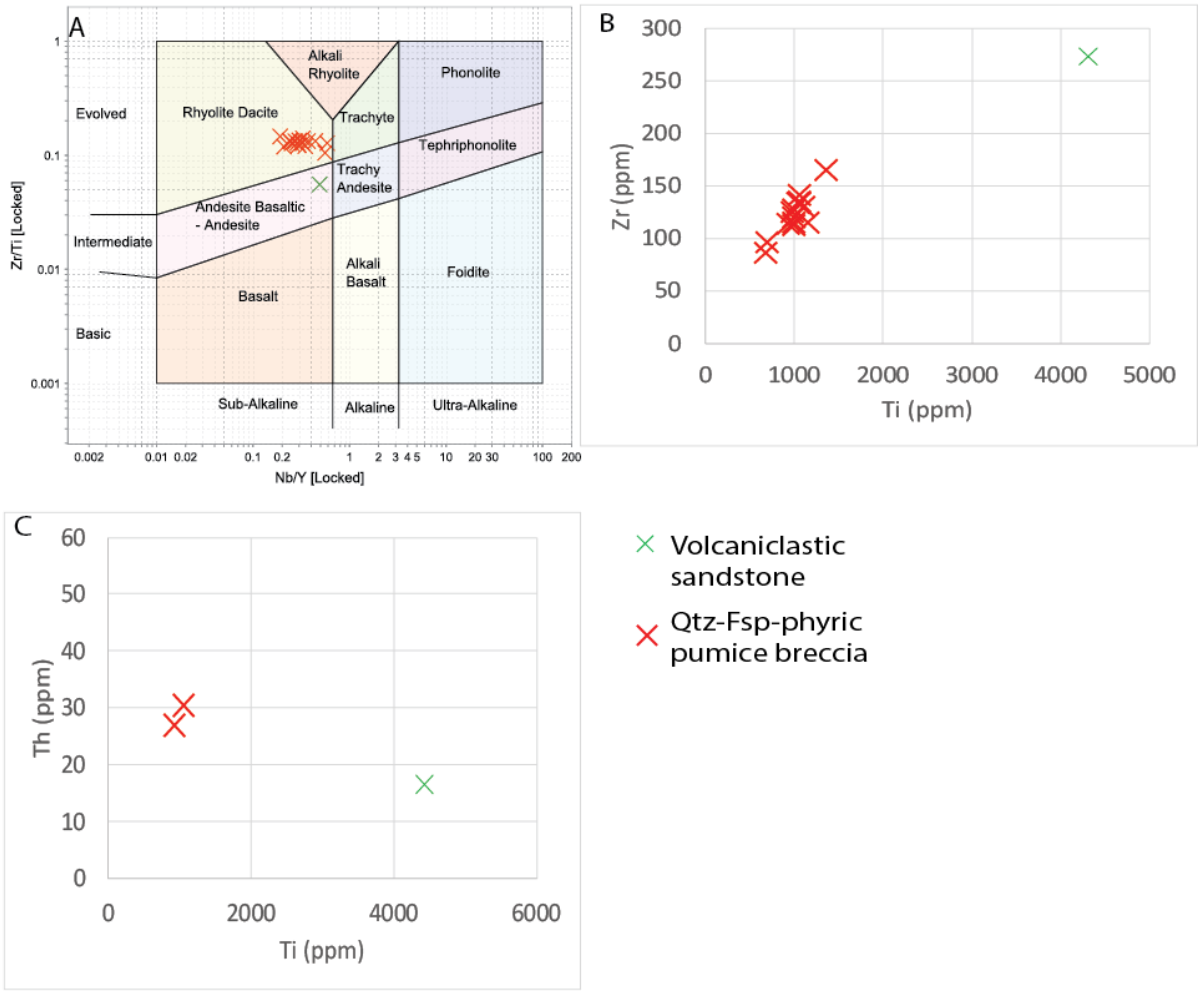

Figure 4.9. Immobile element plots of Natone Volcanics samples: A) Pearce volcanic rock classification plot effectively discriminates pumiceous and volcaniclastic sandstone facies types. B-C) Relatively low Ti abundances characterise the pumice breccia facies.

4.4 Lithogeochemistry of the Rosebery Mine stratigraphy

The lithogeochemistry of the Rosebery Mine stratigraphy is considered in terms of the three sequences that enclose and host the ore body (Fig. 4.10): 1) Hercules Pumice Formation (footwall sequence), a package of dominantly dacitic feldspar-phyric pumice breccia; 2) the Host Rock Member, a sequence of volcaniclastic sandstone and siltstone, and 3) the White Spur Formation (hangingwall sequence), a heterogenous association of quartz-feldspar-phyric pumice breccia and volcaniclastic breccia facies. In addition, a feldspar-quartz porphyritic sill, with peperitic margins,

locally intrudes the sequence at the level of the host rock: an example is examined from drill hole 250R.

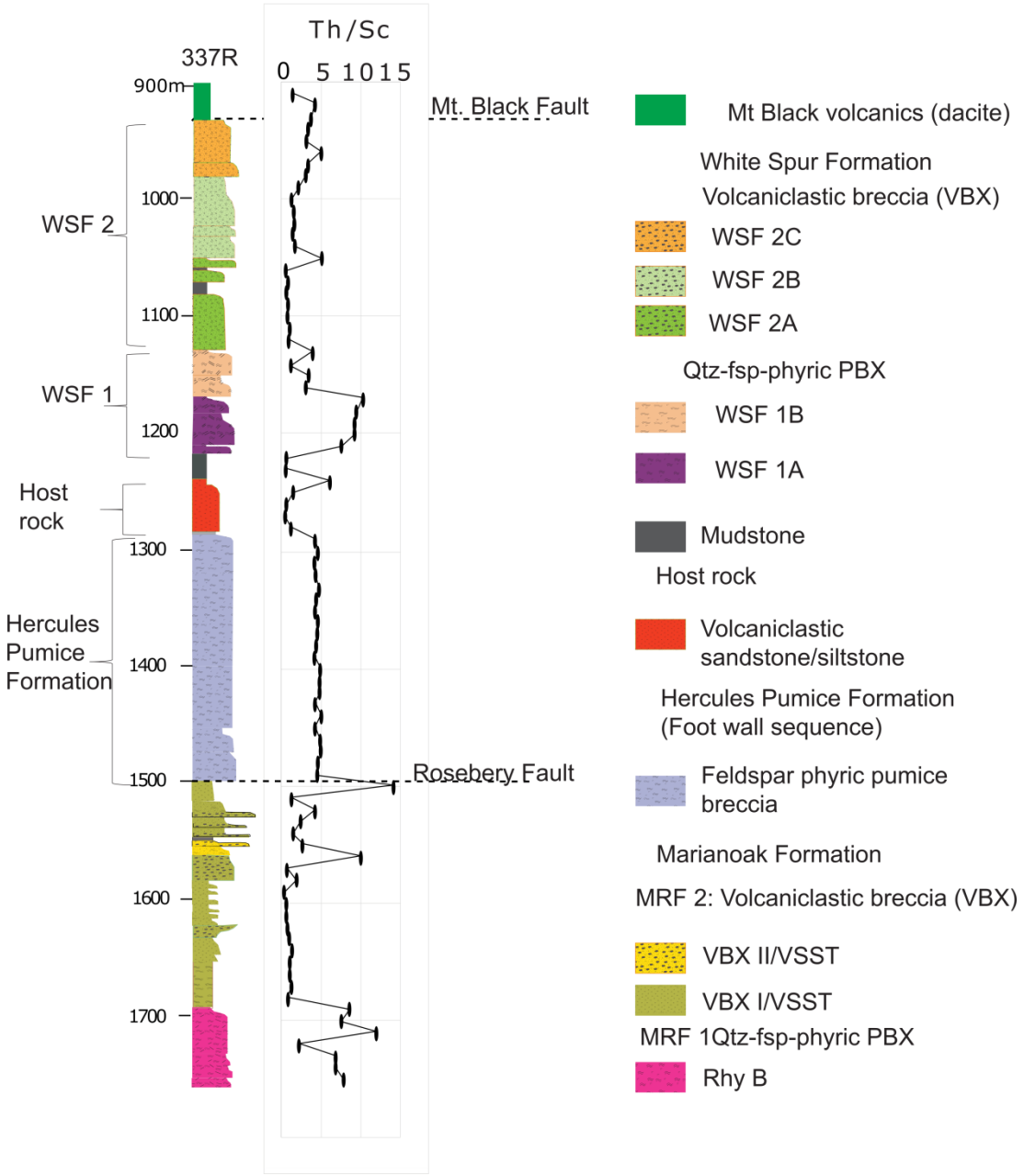

Figure 4.10. Lithochemical profile through the Rosebery Mine stratigraphy in drill hole 337R. Data are also included for Marianoak Formation strata (below the Rosebery Fault) for comparison. The Rosebery Mine stratigraphy involves 3 basic components: Hercules Pumice Formation (orebody footwall), Host Rock Member, and the lithologically diverse White Spur Formation (hangingwall).

4.4.1 Lithogeochemistry of the Hercules Pumice Formation (footwall sequence)

The Hercules Pumice Formation consists of a series of graded to poorly stratified, syn-eruptive mass-flow deposits of dacitic, feldspar phyric pumice breccia, intruded by quartz-feldspar phyric rhyolite sills and felsic lava flows (McPhie et al., 1993; Gifkins, 2001; Corbett et al., 2014). The pumice breccia facies is interpreted to be the product of large explosive felsic eruption in a submarine environment. The base of the sequence is ubiquitously defined by the Rosebery Fault (Marianoak Formation strata positioned in its structural footwall), and a maximum of ~200 m is preserved in Rosebery Mine area (Fig. 4.10).

Pumice breccia beds grade from massive, coarse grained, variably crystal rich bases, to stratified sandstone and siltstone ash tops. They are composed of juvenile pumice clasts (60-80%, < 6cm), euhedral feldspar crystal fragments (0.5-1 mm, 5%), quartz crystal-fragments (1-2%), glass shards (10-15%) and minor mud lithics.

A rhyodacite to dacite composition is indicated using the Pearce volcanic rock classification (Fig. 4.11A). Generally, the pumice breccia is characterized by moderate average Ti/Zr (11.12), Th/Sc (4.64), Th (19.55 ppm) and Ti (1719 ppm) values (Table 4.3, Figs. 4.10 & 4.11). The downhole plot in Figure 4.10 clearly demonstrates the distinct geochemistry of Hercules Pumice Formation from both White Spur and Marianoak Formation strata. Plots of Ti vs (Th & Zr) and Sc vs Th in Figures 4.11B-D show low to moderate concentrations of the compatible (Ti & Sc) and incompatible elements (Th, Zr), consistent with its dacite to rhyodacite composition.

Table 4.3. Summary of geochemical data from the Rosebery Mine sequence.

Litho-units	Chemo-units		Ti/Zr	Al2O3/TiO2	Th/Sc	Th	Zr	Ti
Rhyolitic volcaniclastic breccia	WSF 2C	min	6.62	38.43	1.90	11.40	91.00	1140.00
		max	15.49	63.83	5.66	27.50	260.00	1720.00
		average	9.78	47.68	3.14	18.55	157.93	1479.09
		STD	2.16	6.35	0.75	3.00	37.75	148.96
Polymictic volcaniclastic breccia	WSF 2B	min	11.40	29.56	1.11	8.90	74.00	1630.00
		max	22.70	44.43	3.03	21.80	179.00	2450.00
		average	16.24	37.89	1.73	14.65	128.11	2008.40
		STD	3.00	4.28	0.46	3.00	28.88	230.79
Basaltic-andesite volcaniclastic breccia	WSF 2A	min	17.30	19.34	0.54	9.40	102.00	2370.00
		max	28.65	28.31	1.52	20.20	180.00	3970.00
		average	22.43	24.92	0.98	12.82	136.63	3027.39
		STD	3.14	2.38	0.29	2.58	21.46	411.70
Qtz-feldspar-phyric pumice breccia	WSF 1B	min	7.12	91.43	1.71	9.90	67.60	680.00
		max	15.91	65.31	8.86	32.70	208.00	1640.00
		average	9.98	53.27	4.70	18.52	137.75	1272.31
		STD	2.90	5.66	2.50	6.42	49.65	286.16
Qtz-feldspar-phyric pumice breccia	WSF 1A	min	7.27	66.48	7.57	24.60	81.10	710.00
		max	10.44	87.00	13.81	40.60	148.00	1230.00
		average	8.62	77.15	11.10	33.13	114.73	983.33
		STD	0.82	6.88	2.18	5.17	19.96	158.76
Fsp-Qtz porphyritic sill	Fsp-Qtz porphyritic sill	min	12.45	43.83	1.61	9.90	72.90	1030.00
		max	16.87	65.31	2.43	11.60	105.50	1780.00
		average	15.39	51.42	1.82	10.88	89.12	1380.00
		STD	1.70	8.71	0.34	0.63	15.35	334.14
interbedded sandstone	upper host rock	value	8.59	58.53	6.10	25.60	138.50	1190.00
interbedded sandstone siltstone	Lower host rock	min	12.40	26.69	0.51	6.60	87.90	2840.00
		max	32.42	36.89	1.45	15.80	250.00	3110.00
		average	19.03	30.97	0.94	11.90	179.48	2975.00
		STD	9.06	4.27	0.44	4.60	67.36	150.22
Feldspar phyric pumice breccia	Hercules Pumice Formation	Min	7.65	34.86	2.81	12.50	92.60	1120.00
		max	16.67	64.70	7.22	27.00	230.00	2460.00
		average	11.12	43.85	4.64	19.55	156.44	1719.00
		STD	1.89	4.65	0.77	2.90	25.48	297.20

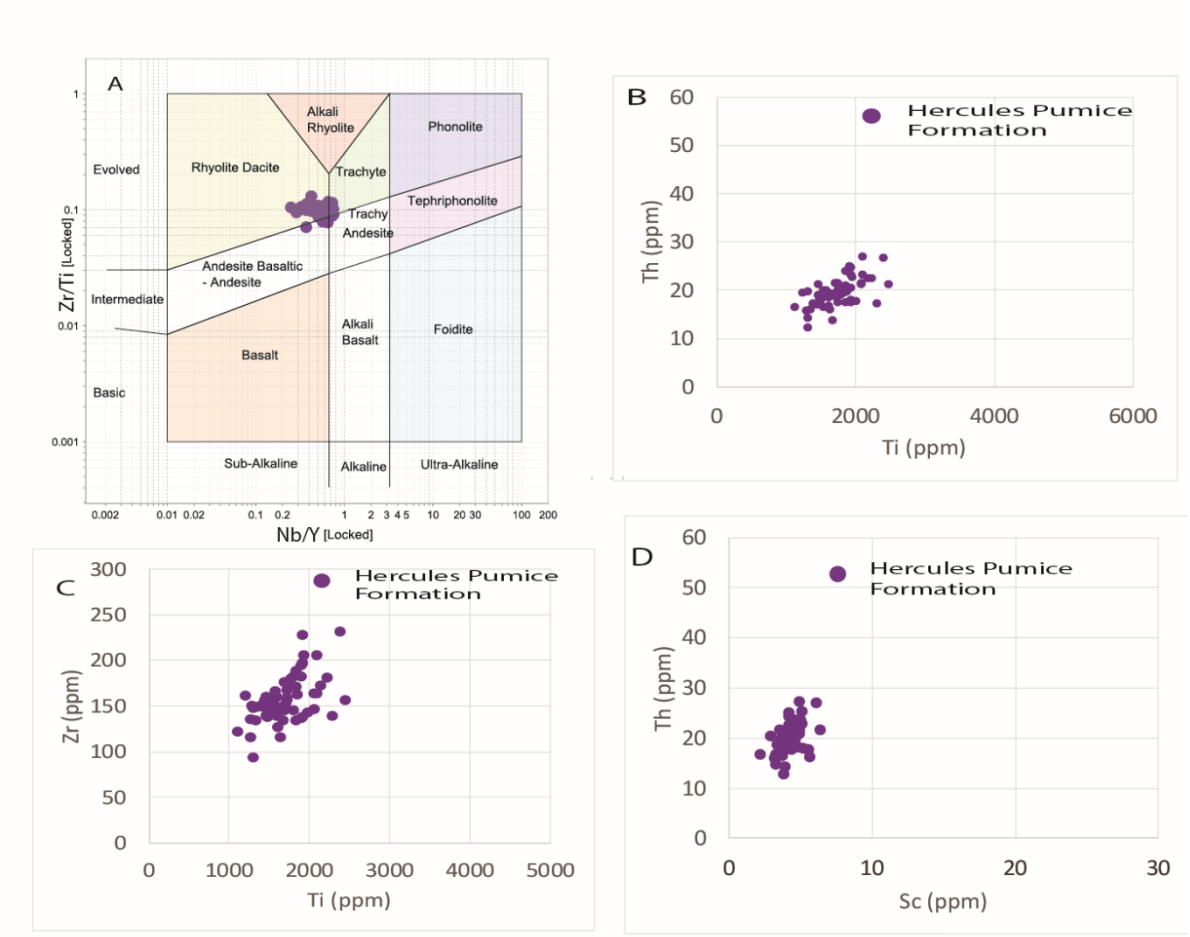

Figure 4.11. Immobile elements plot of Hercules Pumice Formation. A) Pearce volcanic rock classification shows most of the samples fall within the rhyodacite field B-D) Bivariate immobile element plots.

4.4.2 Lithogeochemistry of the Rosebery Host Rock Member

The Rosebery Host Rock Member is a discontinuous, 5-60 m thick, interval of volcaniclastic sandstone and interbedded siltstone (Fig. 4.10: Allen, 1991; Gifkins and Allen, 2001; Corbett et al., 2014). In drill hole 337R, the interval totals 48 m in thickness and comprises two compositionally-distinct subfacies. The lower 30 m is composed of massive, pumiceous, feldspar-quartz-phyric volcaniclastic sandstone (feldspar >> quartz). The upper 18 m of the volcaniclastic sandstone is quartz-phyric with closer compositional affinities to the overlying White Spur Formation.

The geochemistry of the lower part of the host rock has average Ti/Zr (19.30), Th (11.90 ppm) and Ti (2975.00 ppm) values, whereas the quartz-phyric upper sequence has average Ti/Zr

(8.59), Th (25.60 ppm) and Ti (1190.00 ppm) values (Table 4.3). The Th/Sc downhole plot in Figure 4.10 clearly distinguishes the two subfacies, with an intermediate to mafic composition indicated for the lower interval and more felsic composition of the upper interval. This is further substantiated by the bivariate plot Ti vs Th (Fig. 4.12), in which the lower host facies has higher Ti and low Th, and upper facies has low Ti and high Th, indicative of intermediate to mafic and felsic compositions, respectively.

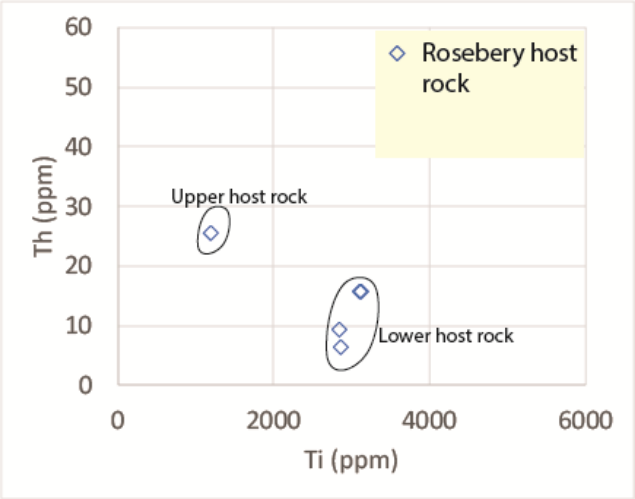

Figure 4.12. Ti vs Th plot for the Rosebery Host Rock Member, clearly distinguishing upper and lower components.

Feldspar-quartz-porphyritic sill

A feldspar-quartz porphyritic semi-coherent unit of about 50 m thickness intrudes the host rock member in hole 250R (Fig. 4.13). It has distinctive embayed quartz (~2-4 mm) and euhedral feldspar phenocrysts (~1-2mm: Martine, 2004) The intrusion varies laterally from a thick coherent body with peperitic margins to a coarse hyaloclastite with occasional jigsaw fit texture (Martin, 2004). The peperitic margins are often overprinted with sulphide mineralization indicating intrusion of the sill into unconsolidated sediments prior to hydrothermal alteration (Martin, 2004).

The geochemical profile of the sill shows slight chemical variation between its core and upper and lower margins (Fig. 4.13). The subtle decrease in Th/Sc values toward the margins is likely explained by ingestion of more basic country rock (i.e. unconsolidated sediments) during the peperitic process. Generally, it has low average value of Ti/Zr (12.45), Th/Sc (1.82), Th (9.90 ppm) and Ti (1030 ppm) indicative of its intermediate dacitic composition (Table 4.3).

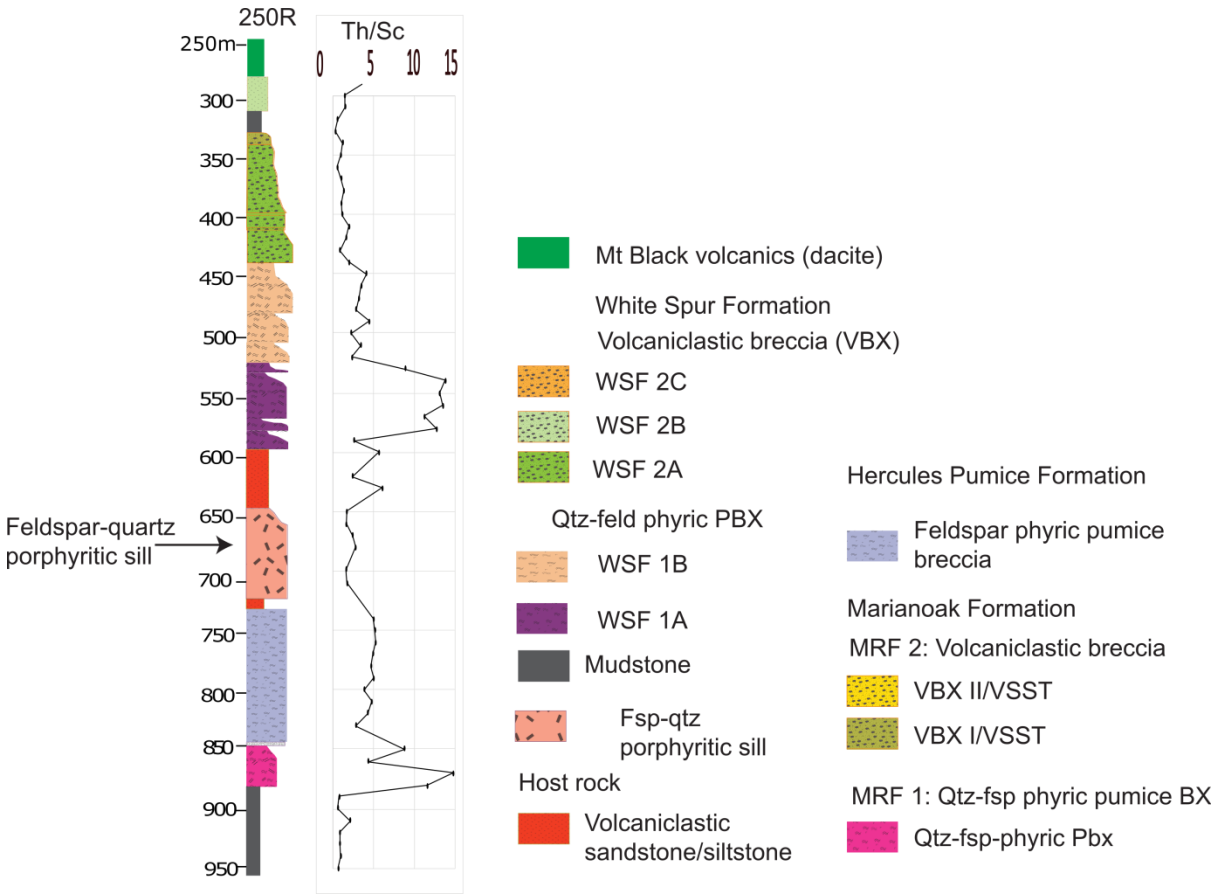

Figure 4.13. Chemostratigraphic profile of drill hole 250R, showing the position of a feldspar-quartz-porphyritic sill at the level of the Rosebery Host Rock Member. Note the broadly symmetrical Th/Sc profile through the sill, transitioning to lower values (overall more basic composition) at upper and lower contacts.

4.4.3 Lithogeochemistry of the White Spur Formation

The Rosebery Mine host rock is overlain by lenses of massive black mudstone of 0.5-30 m which are interpreted as the base of the White Spur Formation (Fig. 4.10: Allen, 1991; Gifkins, 2001; Corbett et al., 2014). The mudstone in turn is overlain by a thick package of massive to normally graded mass-flow deposits of quartz-feldspar-phyric pumice breccia and volcaniclastic breccia. For the purpose of this stratigraphic analysis, geochemical data are initially separated according to a basic 2-fold lithofacies subdivision, WSF 1, a lower quartz-feldspar phyric pumice breccia, and WSF 2, an overlying volcaniclastic breccia (Fig. 4.10). The latter is further divided into three subunits on the basis of petrographic and textural evidence (see also Chapter 3). Further subdivision of WSF 1 into two subunits is achieved on examination of geochemical data.

Pearce volcanic rock classification plots indicate that WSF 1 is of rhyodacite composition, except for a few andesitic samples (Fig. 4.14), whereas WSF 2 has a wide range of compositions from rhyodacite, trachyte and andesite-basaltic andesite (Fig. 4.15). Data are further classified, using a combination of bivariate immobile element plots and petrographic features, into five laterally-mappable subunits: WSF 1A, WSF 1B, WSF 2A, WSF 2B and WSF 2C (Fig. 4.16).

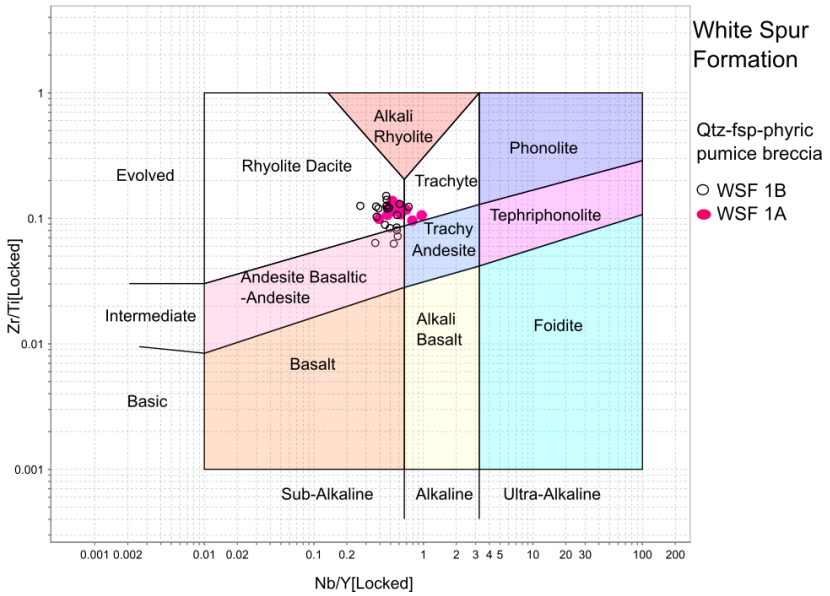

Figure 4.14. Volcanic rock classification of the lower White Spur Formation quartz-feldspar phyric pumice breccia dominated facies association: WSF 1. The two subfacies (WSF 1A and 1B), distinguishable in the discrimination plots shown in Figure 4.16, fall largely within the rhyolite-dacite field.

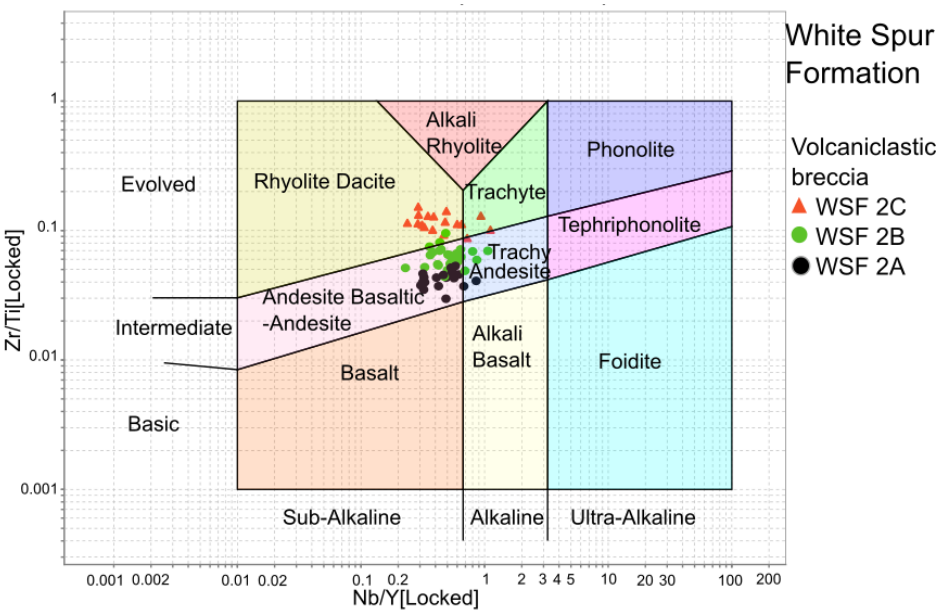

Figure 4.15. Volcanic rock classification of the upper White Spur Formation (WSF 2), showing a diversity of compositions. The package can be further subdivided into 3 subfacies, based on a combination of lithologic and chemical criteria. The relative stratigraphic positions of the subfacies are shown in Figure 4.17

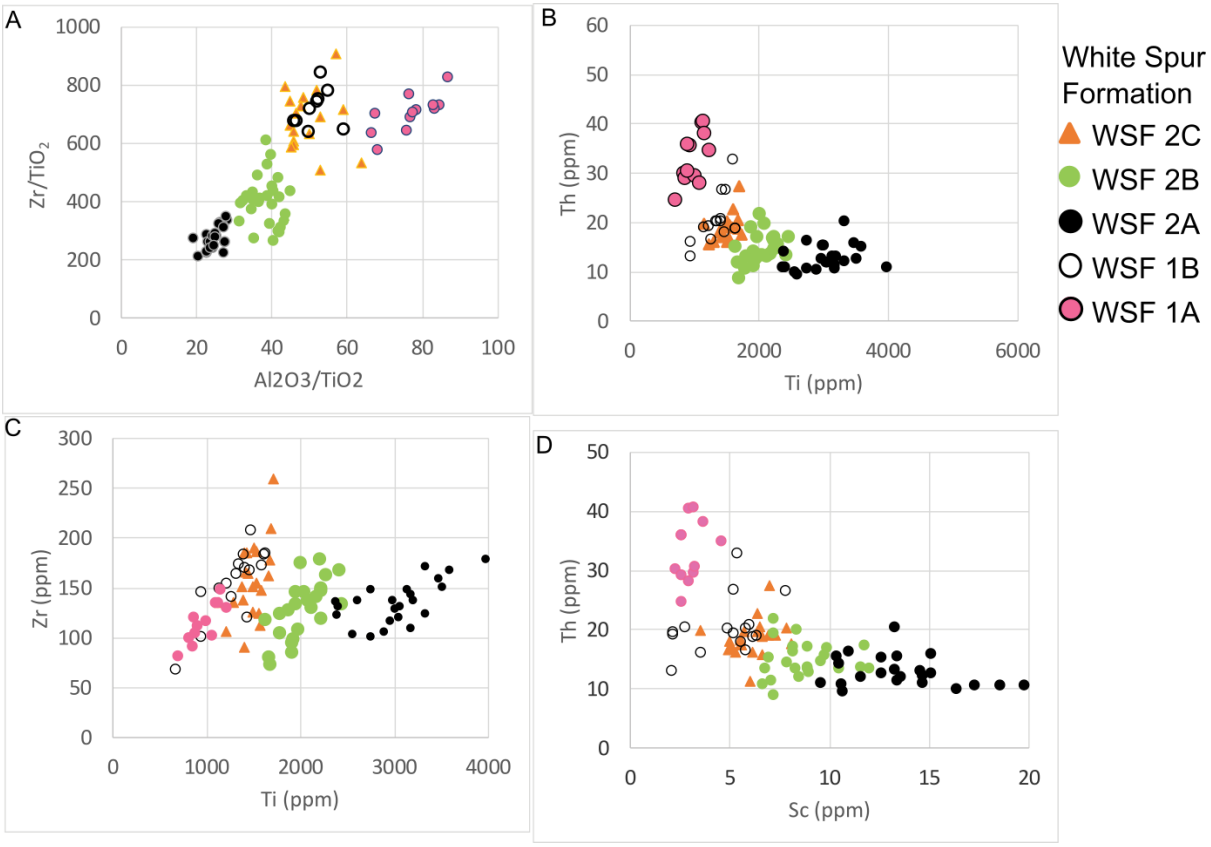

Figure 4.16. Immobile element plots of the White Spur Formation. Separation of most facies types is achievable in the various discrimination plots, with the exception of WSF 1B and 2C, where there is partial overlap. WSF 2B displays and intermediate composition between WSF 2A and WSF 1A (± WSF 2C/WSF 1B) end members, and may reflect a mixing trend.

WSF 1A: Quartz-feldspar-phyric pumice breccia

The basal White Spur Formation subunit, WSF 1A (Fig. 4.18), is a 50 m thick series of upward fining pumice breccia beds, consisting of quartz (0.25-0.50 mm, 15-20%), feldspar (0.25-0.50 mm, 2-3%), glass shards (2-3%), and juvenile pumice clasts (60-70%). It has an estimated quartz to feldspar crystal ratio of 90:10.

Geochemically, WSF 1A is characterized by a high average Th concentration of 33.30 ppm (range 24.60-40.60), and a low average Ti/Zr ratio of 8.62 (ranging 7.27-10.44: Table 4.3). These features, coupled with high Th/Ti and Th/Sc values (Fig. 4.16B, 4.16D, 4.17 & 4.18), attest to the unit's felsic composition and make it readily distinguishable from other levels of the White Spur Formation. It is noteworthy, however, that the conventional use of Ti/Zr fails to discriminate WSF 1A from WSF 1B (Figs. 4.16C & 4.17).

WSF 1B: Quartz-feldspar-phyric pumice breccia

WSF 1B is a 50 m thick pumice breccia subunit composed of angular and often embayed quartz crystal fragments (0.5 mm, 10-15%), euhedral feldspar (2-3%), quartz-phyric rhyolitic lithics (1-2%) and pumice clasts (1-5 cm, 70-80%). It has lower quartz: feldspar ratio than the underlying WSF 1A (i.e. 40:60).

Although the mineralogic and textural character of the subunits is comparable with that of WSF 1A, a geochemical distinction is profound. As shown in Figure 4.17, from the base of WSF 1B, there is an abrupt upsection reduction in the relative concentration of incompatible elements (with the exception of Zr). Thorium (av. 18.50 ppm) in particular is considerably diminished, whereas compatible elements Ti and Sc are slightly elevated (Table 4.3, Figs. 4.16 & 4.17). Similar patterns have been shown for the transition of Rhy A to Rhy B in the Marianoak Formation, where ingestion of mud was postulated as a driver towards more basic compositions. In this case, however, there is

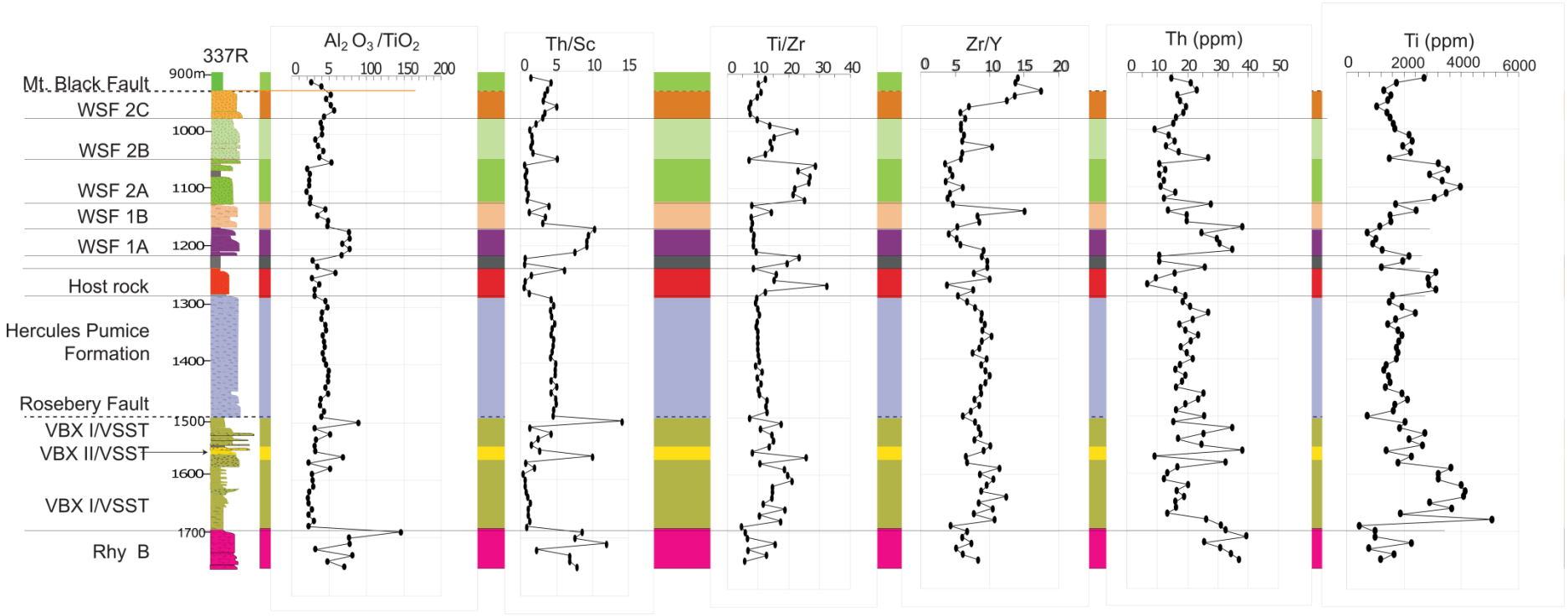

Figure 4.17. Down hole plot of immobile element abundances and selected ratios of the Rosebery Mine sequence in drill hole 337R. Data from the Marianoak Formation positioned below the Rosebery fault are included for comparison.

little evidence of a mudstone-sourced component, and as such, the compositional variation manifested by the increase in feldspar possibly a function of differing parental magmas.

WSF 2A: Basaltic andesite volcaniclastic breccia

WSF 2A has a thickness range of 50-70 m in most drill holes but is absent in 411R-D1 (Fig. 4.18). It contains dark green, angular to sub rounded feldspar-phyric basaltic andesite clasts (1-6 cm, 70%), euhedral feldspars (0.5-1 mm, 10%), and angular to sub-rounded, often embayed quartz (1-2%, 0.5 mm). Its petrography shows very low abundance of quartz: feldspar proportion (10:90). The rock is texturally-immature, largely composed of monomictic basaltic andesite breccia, and while lacking pumice, is considered to have undergone little reworking following eruption.

Pearce volcanic rock classification indicates of a basaltic andesite composition (Fig. 4.15), the most basic composition of the White Spur Formation. The abrupt upsection switch to very high Ti/Zr (Figs. 4.17 & 4.18) indicates a change in the magma composition from more felsic magma of the lower units (WSF 1A & WSF 1B) towards more basic composition. It is generally enriched in the most compatible elements, Ti (av. 3027 ppm) and Sc, that classify the unit as high Ti basaltic andesite (Table 4.3: Fig. 4.16A-D). The homogeneous composition of the subunit is well demonstrated by flat patterns of immobile elements and their ratios in the down hole profiles plot of the immobile elements and their ratios Ti/Zr, Al_2O_3, Th/Sc, Zr/Y and Th with minor variation in Ti (Fig. 4.17).

WSF 2B: Polymictic volcaniclastic breccia

The volcaniclastic breccia of WSF 2B has lateral thickness variation of 20-80 m (Fig. 4.18). The subunit has a polymictic composition of feldspar-phyric and aphanitic basaltic andesite, minor amygdaloidal basalt (2.0-2.50 mm, 5-7%), and minor pale grey angular to sub-rounded quartz-phyric rhyolitic clasts. The crystal component consists of roughly equal proportions of feldspar (1-2%) and angular quartz (1-2%), lesser magnetite (1%), set within a sericite altered matrix.

WSF 2B data fall largely within the basaltic andesite to trachy-andesite fields on Pearce rock classification (Fig. 4.15), with slightly evolved compositions compared to those of WSP 2A. Titanium concentrations progressively diminish upsection (Fig. 4.17, Table 4.3), coupled with slightly elevated Th/Sc (av. 1.73), and lower Ti/Zr (av. 16.24) values, indicating greater felsic input (Figs. 4.16B-D, Table 4.3). A broader scatter of incompatible/compatible trace element ratios and an increasing range in Zr values (e.g. Fig. 4.17, Table 4.3), reveals a heterogeneous provenance of felsic and mafic sources with moderate reworking.

WSF 2C: Rhyolitic volcaniclastic breccia

WSF 2C has a gradational contact with the lower subunit, a typical thickness range of 40-50 m, with a significant increase to 200 m in hole 411R-D1 (Fig. 4.18). The upsection transition to more felsic provenance continues in subunit WSF 2C with a clast assemblage dominated by aphanitic to quartz-phyric rhyolite as opposed to the basaltic andesite clast-dominated underlying subunits.

It is composed of quartz crystal fragments of (0.25-0.5 mm, 10-15%), feldspar (<0.25 mm, 1-2%), quartz-phyric clasts of (2-5 cm, 5%), lithics (0.5 mm, 2%) and angular to sub-rounded aphanitic clasts (50-60%). The crystal component involves a considerably higher quartz: feldspar value of 85:15 as compared to WSF 2B.

Geochemically, WSF 2C samples mainly fall within the rhyodacite and trachyte field on the Pearce rock classification plot (Fig. 4.15). It has slightly higher Th/Sc (av. of 3.25), Th (av. 18.55 ppm) and lower Ti/Zr (av. 9.78) values, revealing a more evolved felsic composition than the underlying WSF 2B (Table 4.3, Fig. 4.16B-D, 4.17 & 4.18). However, it has similar geochemical character to WSF 1B, despite its textural differences (Fig. 4.16B-D). Its variable Zr concentration from 91.00-260 ppm (Table 4.3, Fig. 4.16B-D) indicates a mixed provenance of felsic and mafic composition with significant felsic components.

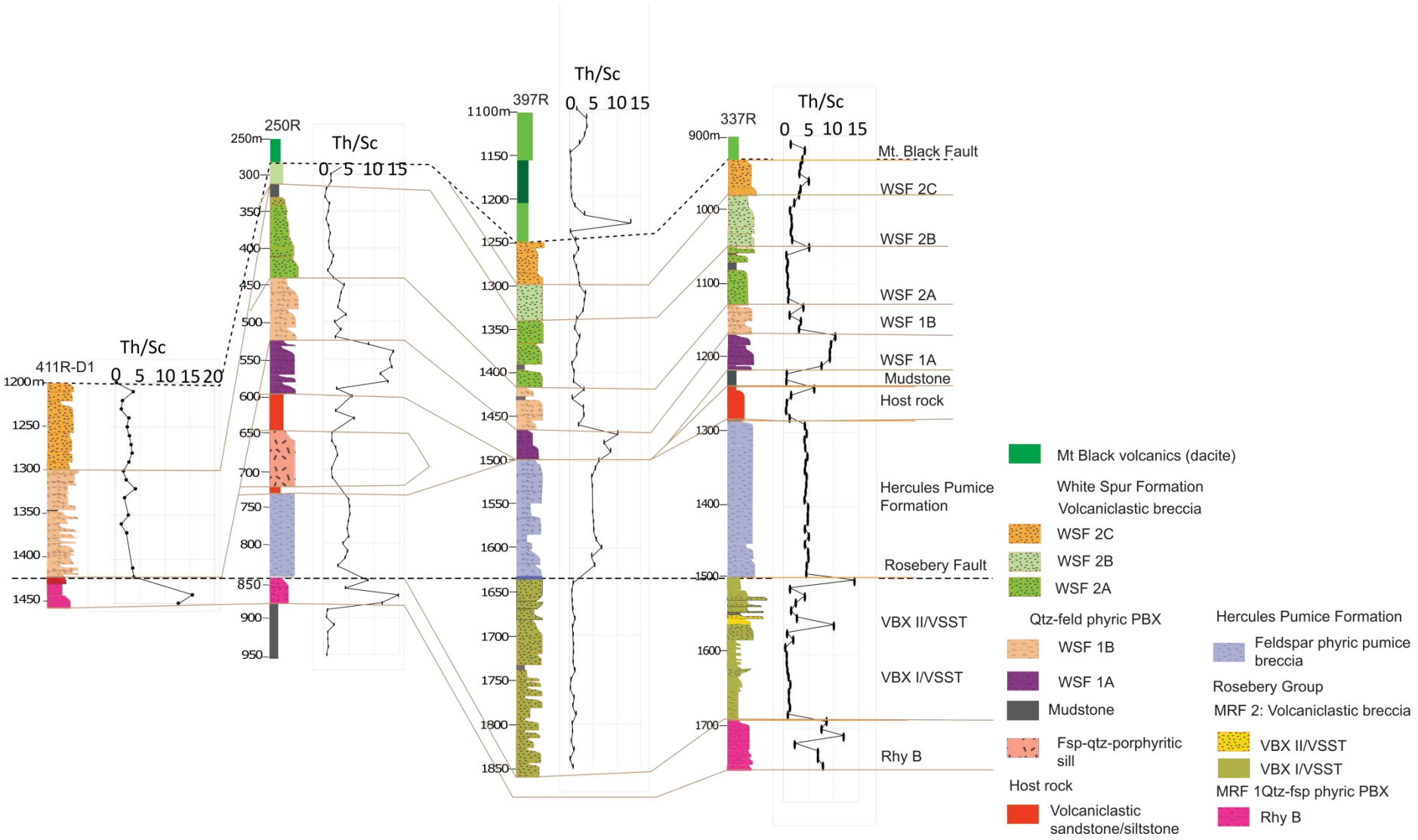

Figure 4.18. Lateral litho- and chemo-stratigraphic correlation within the Rosebery Mine sequence. Data from the Marianoak Formation shown for comparison.

4.5 Chemo-stratigraphic correlation

Systematic lithogeochemical analysis underpinned by lithofacies association and petrographic observations has effectively discriminated the lithofacies into chemical subunits within the Marianoak Formation and revealed a number of fundamental similarities in neighbouring packages. Below, a synthesis of the chemo-stratigraphic evolution of the Marianoak Formation is proposed. Chemical data from all packages are then compared in terms of Ti and Th systematics, and a subset of drill holes are correlated chemo-stratigraphically on the basis of their Al_2O_3/TiO_2 profiles (Figs. 4.19 and 4.20).

As presented, the lower levels of the Marianoak Formation are interpreted to have been accumulated mainly as juvenile pumice-dominated syn-eruptive mass flows. Although a highly evolved felsic magma signature is recorded throughout MRF 1, parental compositions appear to have varied throughout the eruptive history, as recorded by the unusually Ti-poor and Th-rich pumice breccia Rhy C at the top of the interval (Fig. 4.19). A trend to slightly more basic compositions in Rhy B complicates the profile, a feature best explained by ingestion of 'background', or 'inter-eruptive' sediments, by the mass flow. Intervals of more intermediate composition bear strong chemical affinity to volcaniclastic facies higher in the package. At these upper levels (MRF 2), sedimentation was dominated by input from a basaltic andesite volcanic source, the upward coarsening and thickening profile indicating progradation of mass-flow deposits, a feature most likely explained by the progressive amplification (and mass wasting) of a volcanic edifice. The coarsest, most proximally-derived material towards the top of the profile record a subtle decrease in relative Ti abundance (Fig. 4.19), a feature interpreted to record mixing with a more felsic volcanic source. Intercalation of the dominantly basaltic andesite-derived beds with rhyodacitic mass flow facies, VBX II/VSST, suggests the overall upsection trend to more felsic composition records competing input from coeval, but compositionally-distinct, volcanic centres. Although the upper felsic volcaniclastics are difficult to distinguish from those of MRF 1 on the basis of chemistry alone,

the paucity of pumice is distinctive, and considered indicative of a less volatile-rich parental magma, and less explosive eruption style (see Chapter 3).

Very similar vertical profiles are shown through both the White Spur Formation and Natone Volcanics, although the latter is somewhat truncated in terms of its upsection extent (Fig. 4.19). The thickness of the Natone Volcanics is broadly comparable with that of the MRF 1 of the Marianoak Formation, and while its' Al_2O_3/TiO_2 values are lower on average, there remains a subtle upsection decrease in relative Ti abundance. The basal pumice breccia in the White Spur Formation, WSF 1A is also chemically comparable with both the Natone Volcanics and, in particular, Rhy B of the Marianoak Formation, with its upsection increase in Ti content (Fig. 4.19). This trend continues upward into WSF 1B, however, the process of contamination from ingested 'background' sediments argued for Rhy B does not appear applicable in this case. A fundamental change in parental magma composition, possibly involving mixing of a more basic component, seems more likely. The complete overlap of Ti vs Th data from the Natone Volcanics, MRF 1 of the Marianoak Formation, and WSF 1A (Fig. 4.20A), strongly supports the argument that all three facies were sourced from a common parental magma.

An abrupt transition to basaltic andesite-derived volcaniclastic deposits above the dominantly felsic pumice breccias is evident in all three packages (Fig. 4.19). In the case of the Natone Volcanics, this interval the upper basaltic andesite volcaniclastic sandstone is possibly truncated by a N-S trending inferred fault from the adjacent non-volcanogenic siliciclastic strata of the Stitt-Quartzite. The vertical profile through the various subunits of WSF 2 compares favourably with that of MRF 2 of the Marianoak Formation (Fig. 4.19). A subtle upward coarsening trend is most obvious in 337R (although less evident in other holes: cf. Fig. 4.18), with an accompanying progressive increase in Al_2O_3/TiO_2 values from WSF 2A to WSF 2C. Although there are no discrete mass flow units that form direct analogues of VBX II/VSST of the Marianoak Formation, the

appearance of angular to sub-rounded quartz-phyric clasts and quartz crystal components in WSF 2C means that contribution from a similar, if not the same, volcanic source is permissible.

Figure 4.20A demonstrates overlap between most chemical facies in the upper parts of each of the three packages: VBX I/VSST, volcaniclastic sandstone of the Natone Volcanics, and WSF 2. Only the uppermost WSF 2C is problematic, plotting in an intermediate position between the felsic units lower in the various profiles (but also WSF 1), and higher level basaltic andesite sourced strata. Data do, however, correspond closely with those of WSF 1B. Two alternative explanations are considered possible: 1) WSP 2C records a return to the magmatic composition of WSF 1B, or 2) WSF 2C records an epiclastic mixing trend between the more basic end-member of WSF 2A and felsic facies. Given that petrographic information fails to indicate discrete components of both basaltic andesite and rhyodacitic material, the second of these alternatives would appear less likely. On the other hand, the lack of volumetric pumiceous material in WSF 2C, means that it cannot be a direct analogue of WSF 1B. The most plausible scenario then, is a mixing and homogenisation of coeval rhyodacitic and basaltic andesite components in the parental magma chamber. Accepting this interpretation, the upper level of the White Spur Formation can be argued to correspond with that of the Marianoak Formation, where evidence exists for coeval volcanism with end-member compositions. Further consideration of overall distribution of White Spur Formation data in Figure 4.20B supports this interpretation, with the various chemical facies defining a tight mixing trend between WSF 2A and VBX II/VSST, the upper felsic member of the Marianoak Formation.

The Rosebery Host Rock Member that comprises feldspar-dominated lower, and quartz-dominated upper sequences, is characterized by basaltic andesite and rhyodacitic composition respectively (Fig. 20C). The lower sequence was interpreted on the basis of petrography (Chapter 3) as having been largely derived from reworking of the underlying Hercules Pumice Formation. This is at odds with the distinct geochemical signatures of each unit, the lower Rosebery Host Rock Member having higher Ti abundances and low Th/Sc values (Figs. 4.17 and 4.20C). Despite the

elevated Ti abundances, Al_2O_3/TiO_2 values are diminished relative the Hercules Pumice Formation (Fig. 4.17), a relationship that is potentially explained by an additional argillaceous detrital component in the Rosebery Host Rock Member. It is likely then, that the latter records dilution of a Hercules Pumice Formation geochemical signature by incorporation of 'background' sediments of more mafic composition. This interpretation highlights to potential difficulties when working with epiclastic strata as opposed to volcaniclastics rich in juvenile material. The overlying quartz-phyric interval has a composition which lies on the fringes of the compositional ranges of the MRF 1 and WSF 1 (Figs. 4.20 A and C). Although dealing only with a single sample, it may be argued that a basal White Spur Formation-type magmatic source (likely distal) was also slightly modified by incorporation of 'background' sediments of more mafic composition.

The core of the quartz-feldspar rhyolite sill (i.e. that part least affected by contamination along its peperitic margins) emplaced at the level of Rosebery Host Rock Member does not correspond directly with any of the volcaniclastic facies, but in terms of Ti/Th values at least, lies closest to WSP 1B (compare Figs. 4.20 A and C). A reasonable fit also exists with the Hercules Pumice Formation (Fig. 4.20C), however a common magmatic parentage would seem impossible given the quartz-phyric character of the sill.

The Hercules Pumice Formation can be ruled out as a direct lithostratigraphic equivalent of any other units as its exclusively feldspar-phyric pumice component is unique. Figure 4.20C shows the unit is chemically distinct from other pumiceous facies of the Marionoak Formation and Natone Volcanics. However, chemical distinction from the pumice-bearing units of the White Spur Formation is less clear-cut. Whereas WSF 1A is clearly derived from a different magmatic source, WSF 1B overlaps in part with Hercules Pumice Formation data possibly explained due to subtle contamination from background sediments in WSF 1B that returned to a similar composition to the Hercules Pumice Formation (Fig. 4.20A & C). It has to be recalled from the discussion in chapter 3 both WSF 1A and WSF 1B are quartz-phyric, the latter with slightly lower quartz: feldspar proportion;

this important compositional trait distinguishes the facies from the quartz-poor Hercules Pumice Formation. The failure to clearly discriminate the two units geochemically highlights the importance of combining chemical, petrographic and textural criteria in stratigraphic analysis.

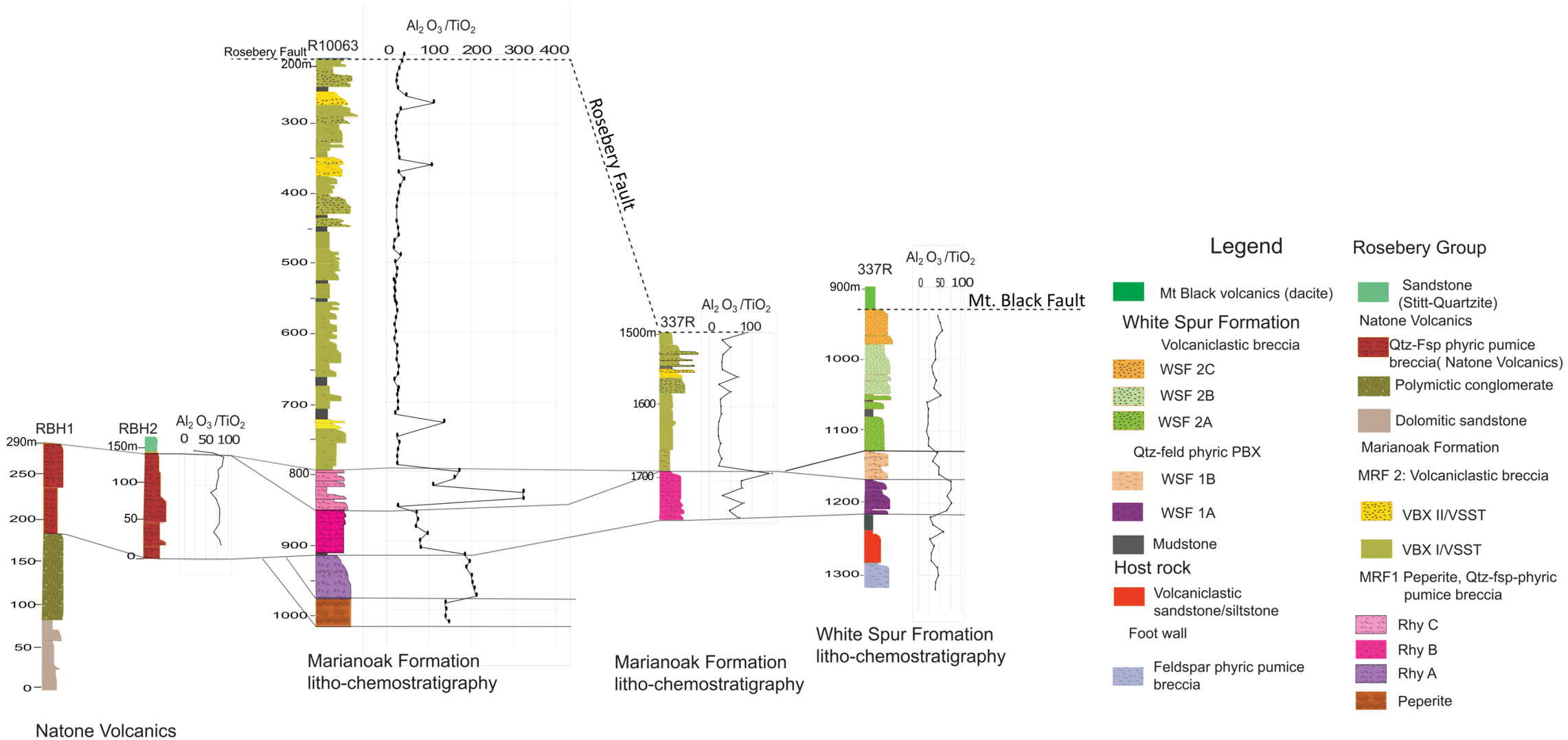

Figure 4.19 Litho- and chemo-stratigraphic correlation of the White Spur Formation, Marianoak Formation and Natone Volcanics.

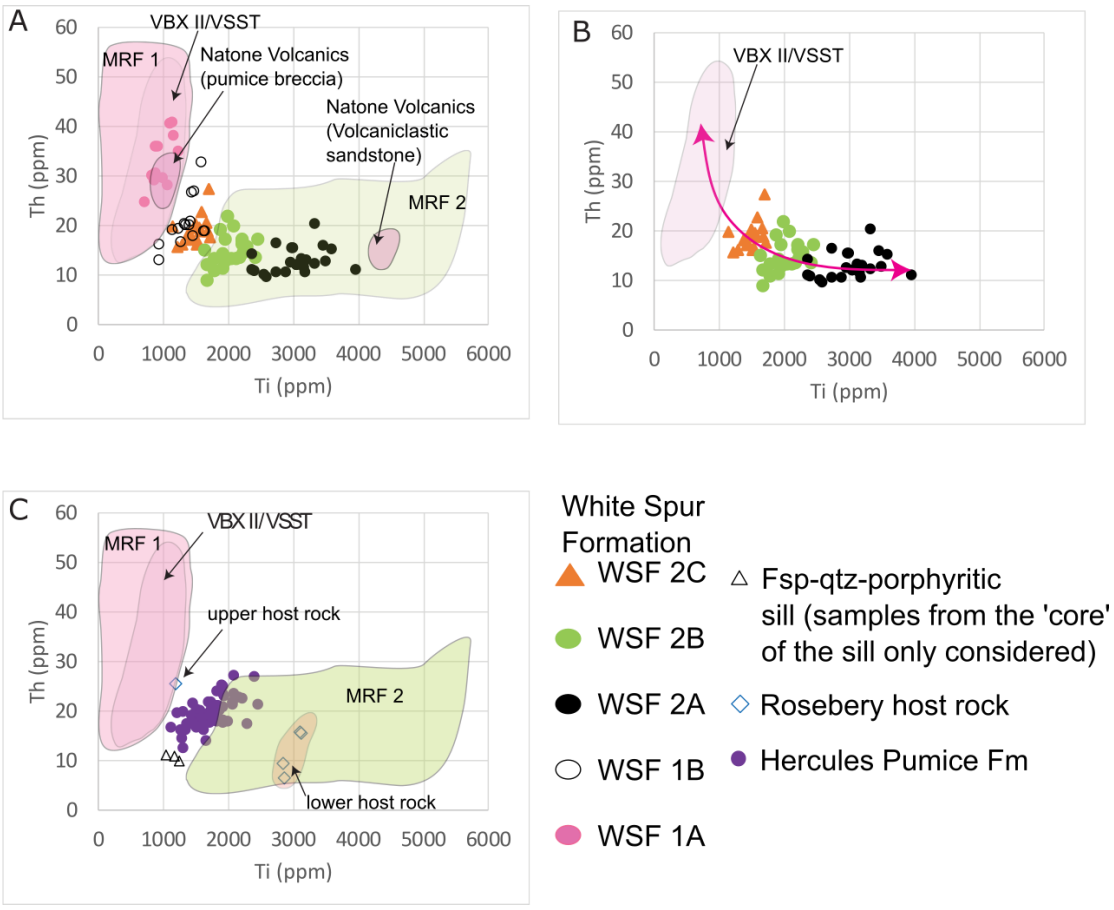

Figure 4.20. Ti vs Th discrimination plots. (A) Comparison of Marianoak Formation, Natone Volcanics and the White Spur Formation data. (B) Mixing trend between VBX II/VSST-type rhyolitic breccia and the WSF 2A end-member compositions. (C) Comparison of Marianoak Formation (MRF) with the Hercules Pumice Formation and Rosebery Host Rock Member.

4.6 Conclusion

Profiles of the Marianoak Formation, White Spur Formation, and Natone Volcanics demonstrate a common two-fold chemo-stratigraphy, involving a lower rhyolitic to rhyodacitic phase of explosive volcanism, and an upper basaltic andesite-dominated eruptive phase. In the cases of the Marianoak and White Spur formations, evidence exists for a component of felsic magmatism that is coeval with the upper basaltic andesite phase. The mass flow deposits that occur throughout these upper levels lack a volumetric pumiceous fraction, and as such are considered to represent proximally reworked products of a more effusive style of volcanism.

The notion that the Natone Volcanics is a vent-distal package is supported by the fact that it is enclosed within non-volcanogenic strata, which bear little resemblance to those in the east. The footwall sequence of Natone Volcanics, in particular, comprises coarse-grained conglomerate reworked from extrabasinal basement sources: i.e. the package occurs in a basin-marginal position (Fig. 4.19). The upward coarsening profile to the level of the conglomerate likely heralds an increase in extensional tectonic activity, with progradation of mass flow deposits across active faults on the basin's edge. Accepting the chemo-stratigraphic framework proposed, this event immediately prior to the onset of felsic explosive volcanism, would equate to the magmatic transition at the top of the Hercules Pumice Formation, and the deposition of the Rosebery Host Rock Member.

Chapter 5: Structural Relationships of the Rosebery Group

5.1 Introduction

The Rosebery Group has a relatively complex structural geometry involving dismembered upright macroscopic folds, leading to facing flips across mainly N-S trending faults, domains of high strain and foliation transposition, and disappearance of units along strike (Fig. 5.1: Green, 1983; Corbett and Lees, 1987; Corbett, 1988; Selley, 1997). The fault zones locally enclose narrow slivers of basement, apparently vertically emplaced into the mid-late Cambrian sequence. Moreover, broadly coeval litho- and chemo-facies associations vary significantly across strike, in part in conjunction with fault zones, with basement-sourced associations dominating to the west, and volcanogenic facies in the east (see Chapters 3 & 4). These unusual structural and stratigraphic relationships have led to long standing debates surrounding the 'transition' between the eastern VHMS-bearing volcanogenic basin(s) and the western sediment-dominated Dundas Group compartments (Campana and King, 1963; Loftus-Hills et al., 1967; Brathwaite, 1970; Green, 1983; Corbett and Lees, 1987a; Selley, 1997; Corbett, 2002). They are, however, compatible with geometries developed during Devonian inversion of sub-basins (Selley, 1997), a model that is tested herein using classical structural domain analytical techniques.

5.1.1 Methodology

High density structural data were collected from surface mapping along selected rivers, creeks, road cuttings and tracks at 1:2000 scale, and presented at 1:6000 scale in Appendices 1A-C. In addition to the surface mapping, structural data collected from oriented drill cores R10032 and R10063 were used for interpretation of levels below the Rosebery Fault. Previously reported mesoscopic structural data (Green, 1983; Mineral Resources Tasmania 1: 25,000 map compilations, 2002) were included in the analysis, and distinguished from data collected in this study in relevant maps and

stereograms. Cross sections were constructed for northern and southern domains, with data projected onto section along trajectories parallel to calculated regional fold axes.

5.2 Domain Analysis

The study area is subdivided into two structurally and geographically distinct domains, a northern domain located westward of the Rosebery Mine, and a southern domain that incorporates data gathered mainly along the course of the Ring River (Fig. 5.1). The northern domain is further separated into three broadly N-S trending litho-structural subdomains (i.e. subdomains N1-3), each bounded by major fault zones, and apparently containing distinct facies associations (Figs. 5.2 & 5.3). Analysis of the northern domain includes data collected from surface exposures and drill core as part of this study, but also historical data from the now flooded Pieman River (Green, 1983; Mineral Resources Tasmania 1: 25,000 map compilations, 2002). The southern area is treated as one domain.

5.2.1 Northern Domain

Subdomain N1

Subdomain N1 is bounded to the east by the Rosebery Fault, which juxtaposes moderately E-dipping Hercules Pumice and White Spur formations strata in its hangingwall with steeply-E to subvertically-dipping chronostratigraphic footwall equivalents (i.e. Marianoak Formation: Figs. 5.2 & 5.3). At surface, the latter passes upsection, with apparent structural conformity, through a thick W-facing succession of Chamberlain Shale and Stitt Quartzite strata. An abrupt flip to E-facing, demonstrable over a 7 km strike length, defines the western boundary of the domain. The change in facing occurs either with Stitt Quartzite persisting to the west, or a lateral change to stratigraphically lower levels of the Natone Volcanics, MRF 2 equivalents of the Marianoak Formation, or the Westcott Argillite. Although an exposed contact was not observed in this study, the facing and across-strike stratigraphic changes are interpreted to indicate the position of a N-S striking fault zone.

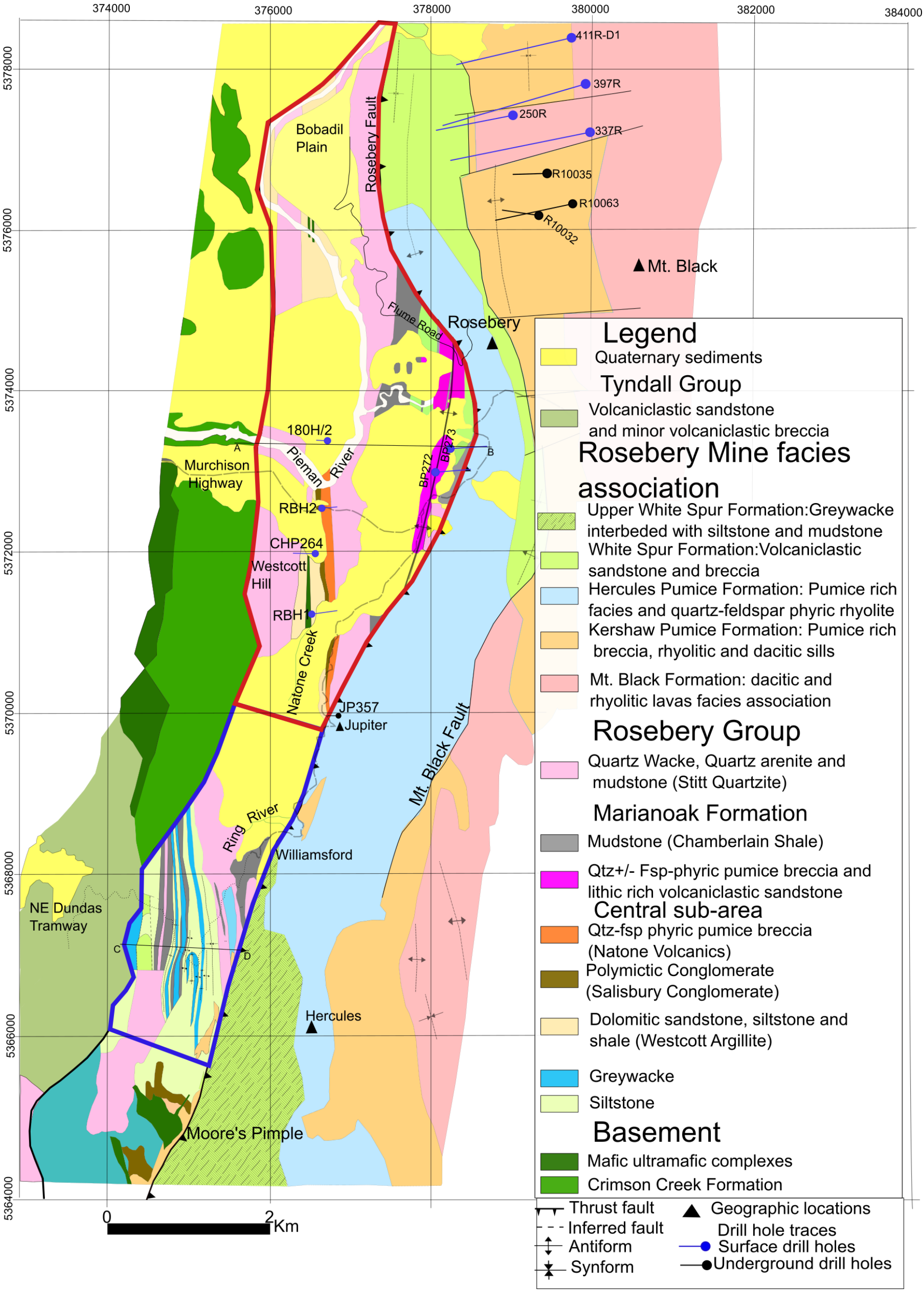

Figure 5.1. Geological map of the study area showing the northern domain in red polygon and the southern domain in blue polygon

The internal structure of the subdomain is relatively simple, involving a macroscopic upright, tight, antiformal closure to the east (Figs. 5.2 & 5.3). The fold axial trace is truncated along trend to the north and south by the Rosebery Fault, indicating that amplification and tightening was effectively complete prior to propagation of the moderately E-dipping thrust. This temporal relationship is illustrated in cross-section, with the relatively planar form of the Rosebery Fault unaffected by folding in its footwall (Fig. 5.4). The section also shows that the central anticline is interpreted to be flanked by two upright synclines, the axial traces of which do not project to surface but are deemed necessary in order produce geometrically viable boundaries with neighbouring subdomains (see below).

Poles to bedding data, collected both at surface and from drill core, reveal a relatively cylindrical morphology, with a fold axis plunging 10° towards 001 (Fig. 5.3). The single penetrative foliation, S_1, appears axial planar when all available data are considered (mean $89^o/268^o$), with associated shallowly N-plunging L_{10} data oriented sub-parallel to both the calculated fold axis and minor F_1 hinge lines. These relationships are unusual for the region, as macroscopic hinge lines are typically transected in an anticlockwise fashion by the S_1 foliation (e.g. Selley, 1997).

Subdomain N2

Subdomain N2 involves a central N-S trending fault-bounded sliver exposing an east facing succession of Westcott Argillite, Salisbury Conglomerate, and Natone Volcanics in the south, and dominantly Westcott Argillite in northern courses of the Pieman River (Figs. 5.2 and 5.3). Its western boundary is defined in part by a narrow zone of gabbroic rocks (exposed at surface and in drill core over a strike length of ~5 km), interpreted to be derived from the mafic-ultramafic basement complex, but also a flip to W-facing Stitt Quartzite strata recorded on the Bobadil Plain to the north (Fig. 5.2). A separate gabbroic sliver is intersected in drill hole 180H/2, and interpreted to correspond with a NNE-striking fault which effectively marks the northernmost projection of Salisbury Conglomerate and Natone Volcanics at surface (Fig. 5.2).

Mesoscopic structural data from the southern part of the subdomain (i.e. in the vicinity of Natone Creek; Fig. 5.2) show tight clustering and parallelism of both S_0 and S_1, with steep dips to the west (Fig. 5.3). In consideration of the consistent E-facing, these data indicate positioning of strata on the overturned limb of a slightly easterly-inclined, very tight dismembered anticline. The subdomain-bounding faults in this area are interpreted to similarly dip steeply to the west (Fig. 5.4). Historical data from the northern Westcott Argillite-dominated part of the subdomain show greater obliquity between dominantly E-dipping S_0 and S_1 (MRT data in Figure 5.3), suggestive of a slightly less tight and more upright axial surface.

Subdomain N3

At surface, subdomain N3 is composed of mainly Stitt Quartzite correlate quartz-wacke interbedded with mudstone. It is bounded by a faulted inlier of Crimson Creek Formation strata to the west, and the gabbroic corridor flanking subdomain N2 to the east (Figs. 5.2 and 5.3). No convincing stratigraphic facing indicators were observed in the poorly exposed southern area about Westcott Hill, however, the significant width of Stitt Quartzite band (>500 m), coupled with sub-vertical bedding dips, raise the possibility of repetition via folding or thrusting. To the north, the width of the Stitt Quartzite band diminishes to ~300 m, and historical data reveal consistent W-facing (Fig. 5.2), suggesting a more simple geometry where the faulted boundary between subdomains 2 and 3 broadly corresponds with the surface trace of a dismembered anticline.

Mesoscopic structural data show patterns very similar to subdomain N2. Bedding in the south lies parallel to steeply WSW-dipping S_1, whereas a single L_{10} measurement is consistent with shallowly S-plunging hinge lines (Fig. 5.3).

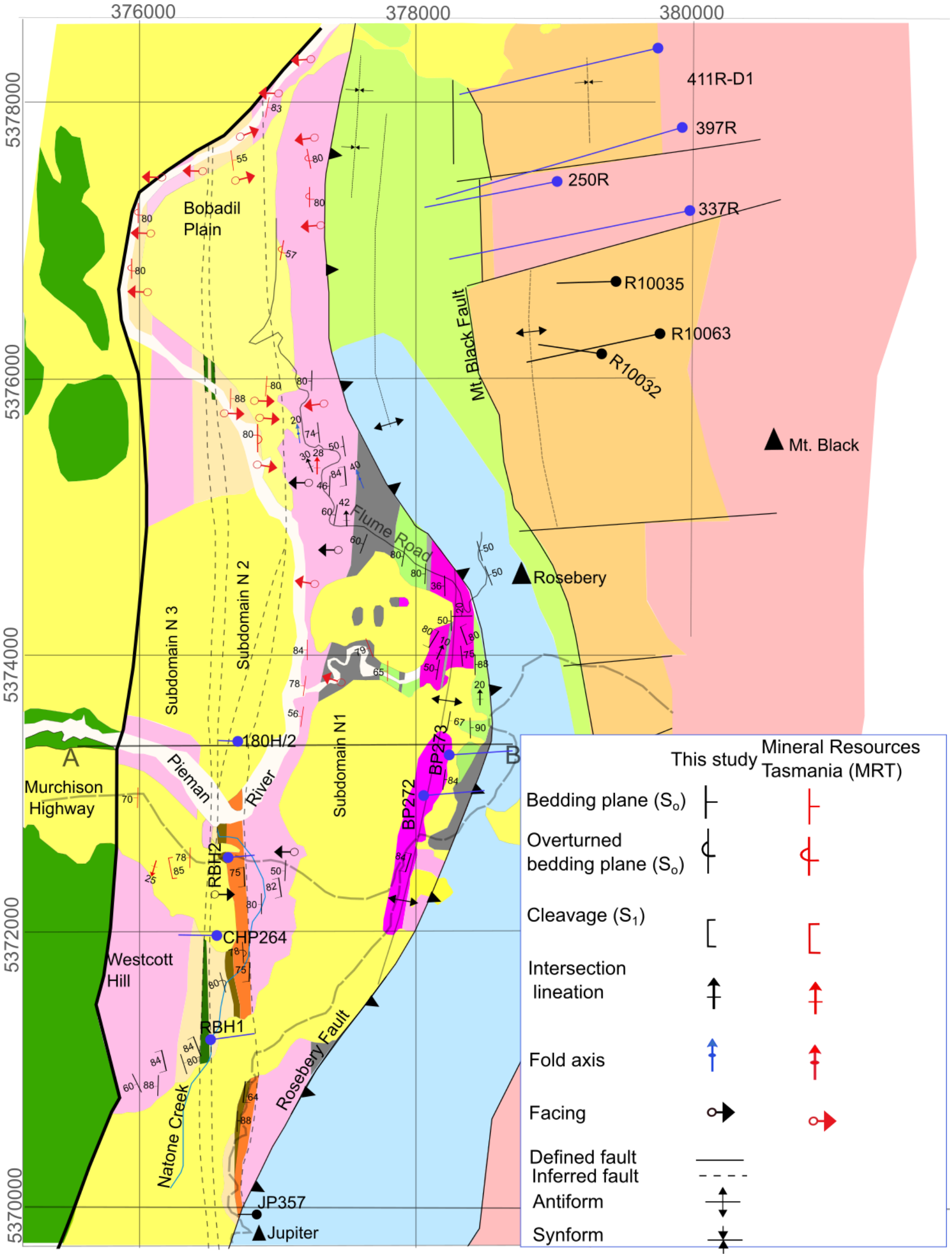

Figure 5.2. Geological map of the northern domain showing classification into three subdomains from east to west, N1-3 (Refer to Figure 5.1 for lithological legend)

A cross section through subdomain N3 shows a series of steeply W-dipping fold axial surfaces, interpreted principally to account for the apparently structurally thickened Stitt Quartzite sequence exposed at surface (Fig. 5.4). The neighbouring inlier of Crimson Creek Formation strata is interpreted to have been emplaced eastward along a thrust surface that parallels the fold axial surfaces in its footwall.

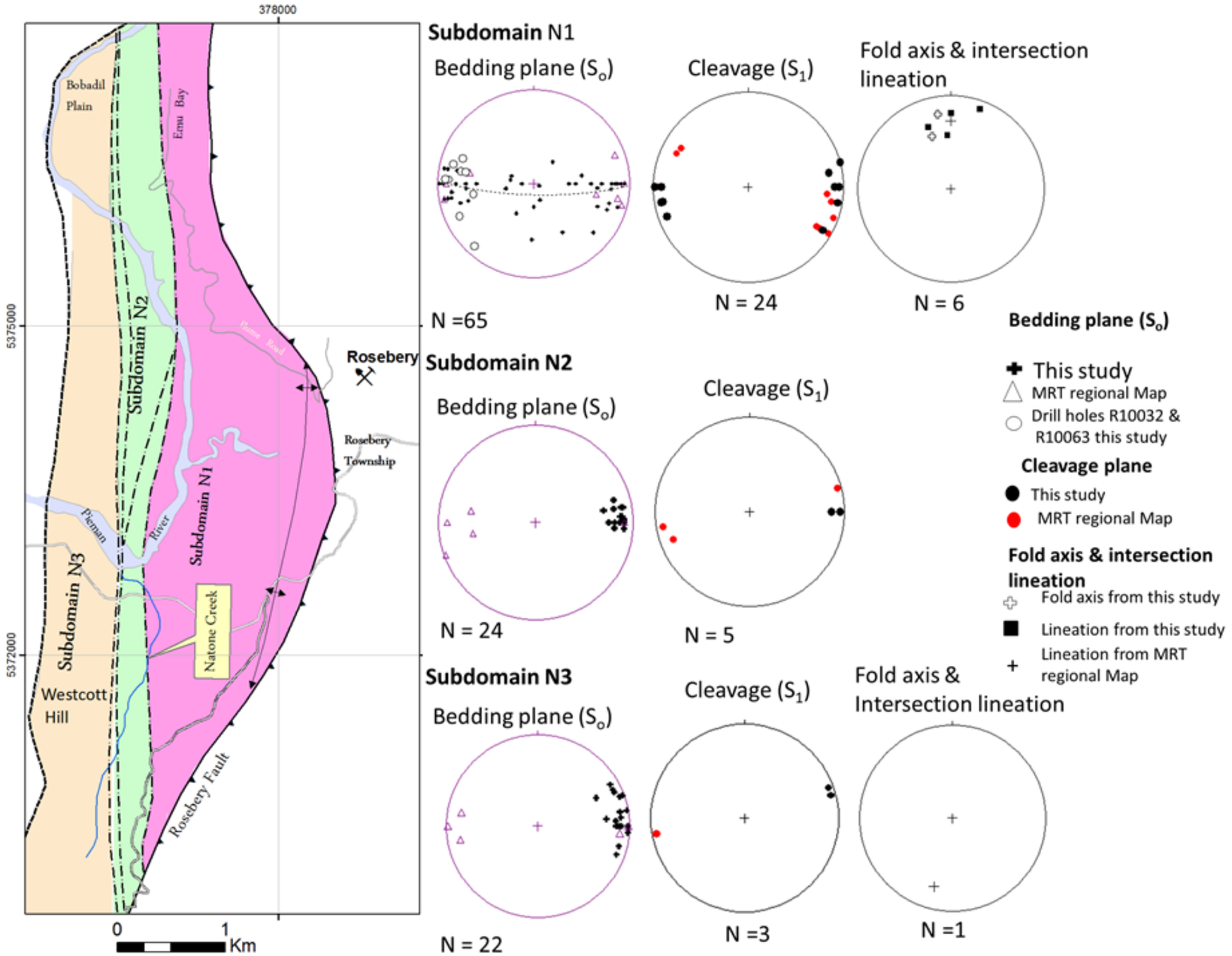

Figure 5.3. Structural subdomains of the northern zone. Subdomain N1 lies within the footwall of the Rosebery Fault, involving an upright, shallowly N-plunging antiform. Subdomain N2 involves a narrow N-S trending belt, bounded and dissected by anastomosing faults. Sub-parallel bedding and foliation data dip steeply west. Strata are interpreted to occupy the E-facing limb of a dismembered antiform (see Figs. 5.2 and 5.4). Subdomain N3 data show similar patterns to N2, but are interpreted to reflect tight folds inclined to the east (see Fig. 5.4).

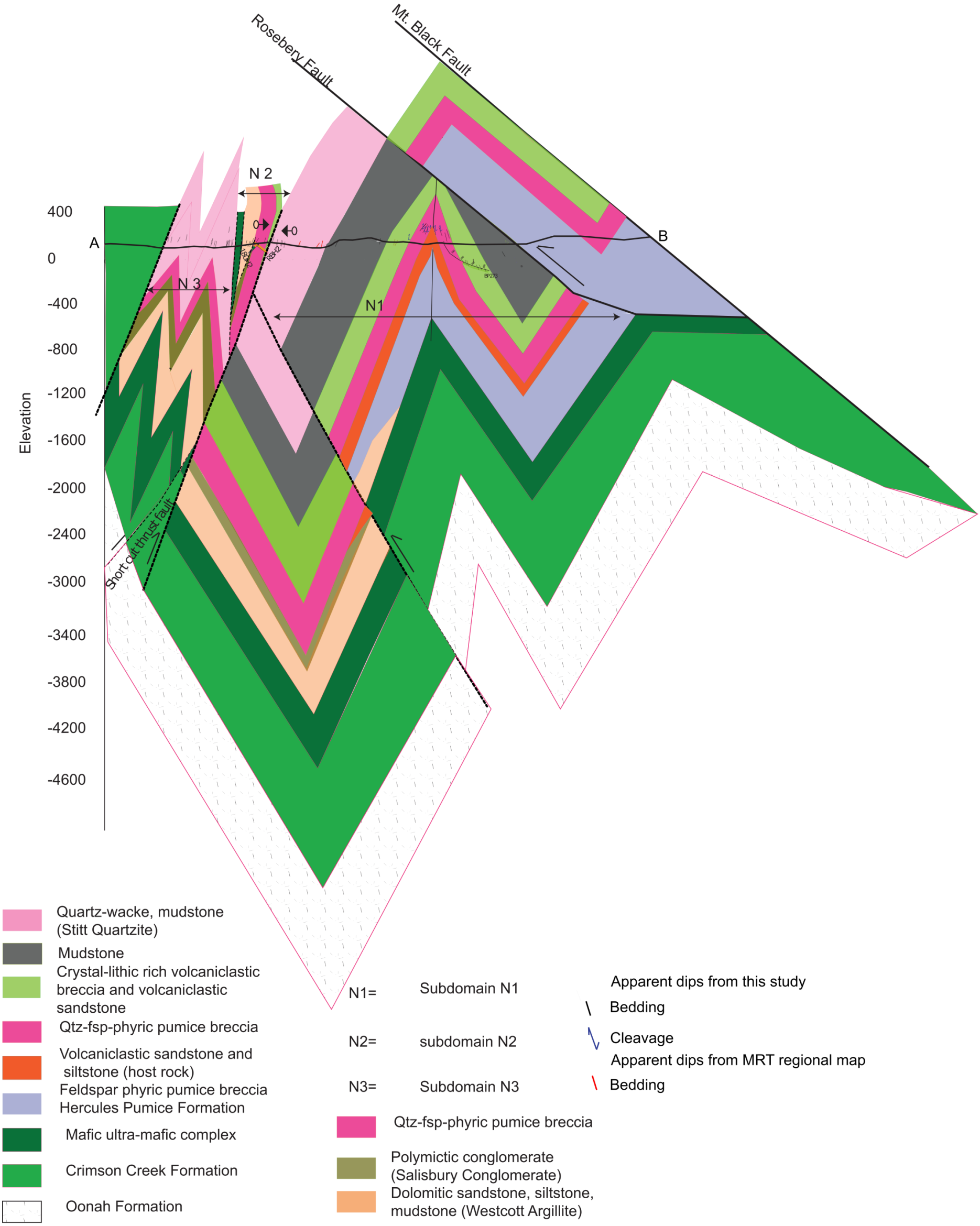

Figure 5.4. East-west cross-section of the northern zone. The Rosebery Group is represented by a wedge-shaped fault-bounded domain, over thrust by the Rosebery Fault to the east and an inlier of Crimson Creek Formation strata to the west. No vertical exaggeration.

5.2.2 Southern Domain

The southern domain is dominantly composed of a lower sequence of siltstone interbedded with mudstone (Westcott Argillite correlates), greywacke (correlate of MRF 2), and Stitt Quartzite quartzwacke and mudstone (Fig. 5.5). An additional crystal-lithic rich feldspathic volcaniclastic facies, also interpreted as a MRF 2 equivalent, crops out as a fault-bounded slice to the west (Fig. 5.5). Bounded obliquely to the northwest by the Crimson Creek Formation inlier, and to the southeast by the Rosebery Fault, the domain is considered a southern extension of subdomain N3 (Fig. 5.1).

The internal structural geometry of the southern domain is characterized by a series of synforms and antiforms, with downward fanning axial surfaces, and an average plunge of 29° to the north (Figs. 5.6 & 5.7). The fold geometry transitions from tight profiles in the east to more dismembered profiles to the west, where the hinge of at least one relatively open synform is preserved (Fig. 5.7). The mean S_1 orientation, 89°/086, strikes a few degrees clockwise of the regional fold axis, as calculated from bedding data (29° to 359: Fig. 5.6). However, cleavage transection would appear unlikely given the consistent N-plunge of both L_{10} and mesoscopic F_1 data (Fig. 5.6).

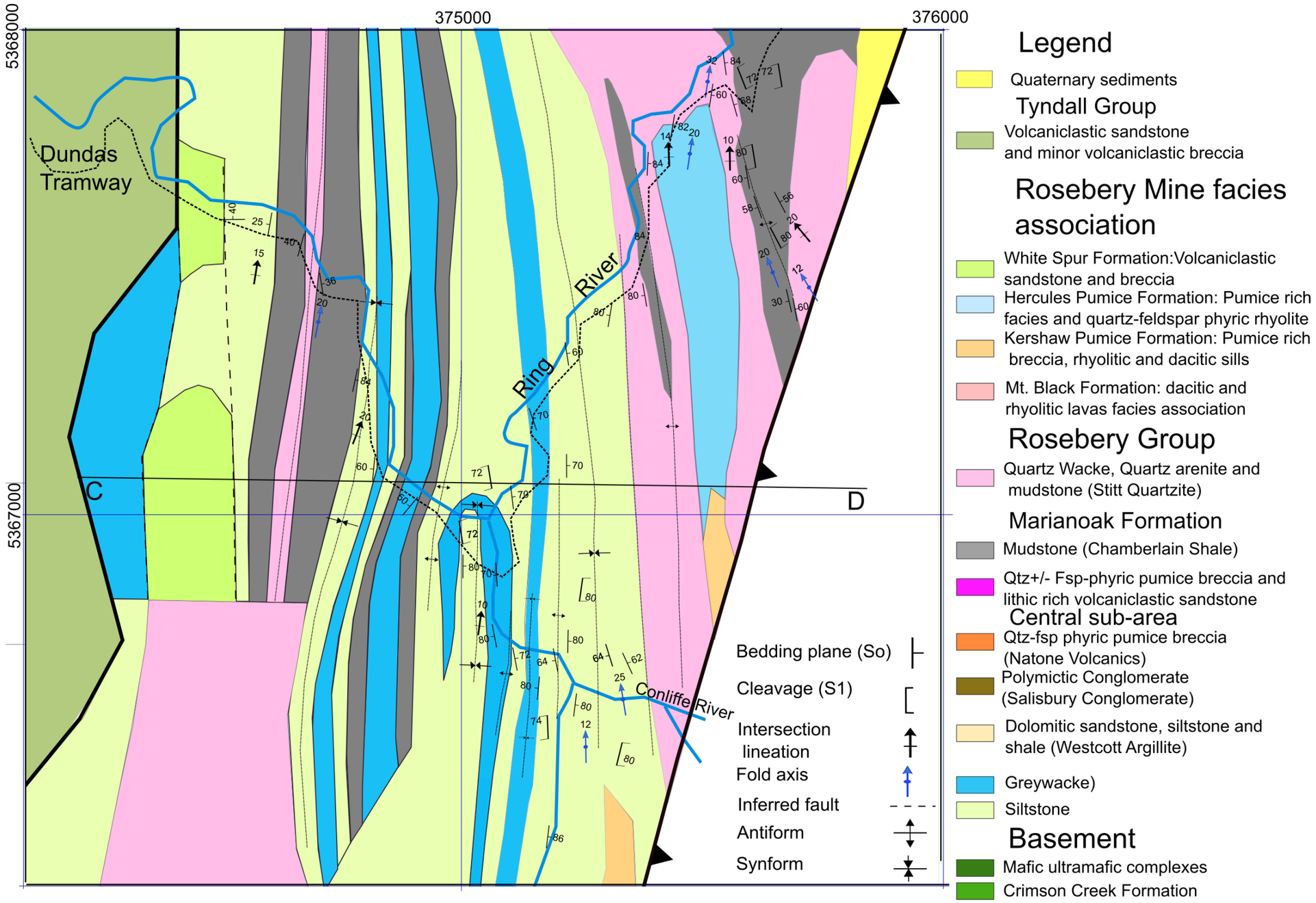

Figure 5.5. Geological map of the southern domain

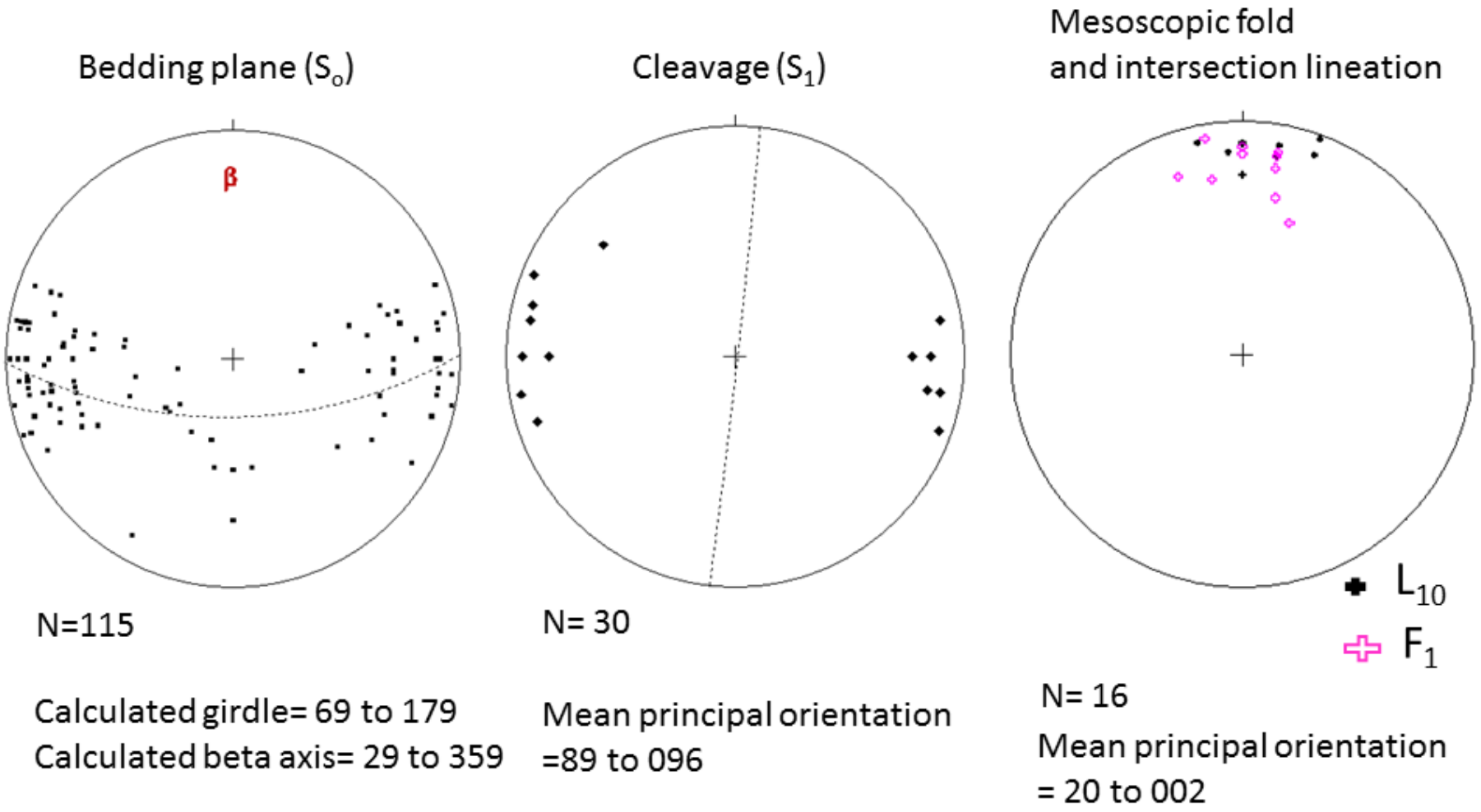

Figure 5.6. Stereograms of mesoscopic structural data from the southern domain.

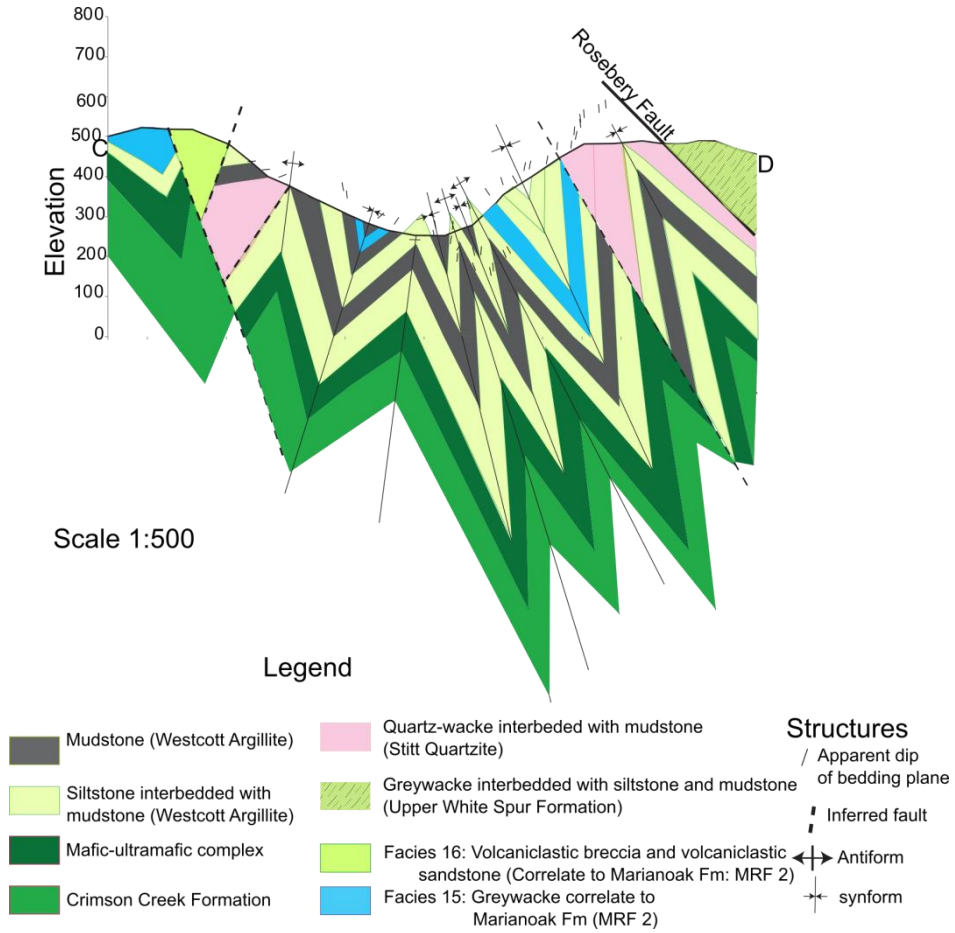

Figure 5.7. East-west cross-section of the southern domain showing mainly tight fold profiles and downward fanning fold axial traces. No vertical exaggeration.

5.3 Discussion

The overall geometry of the northern domain involves an array of upward converging bounding thrust faults: the apparently late-stage moderately E-dipping Rosebery and Mt. Black faults to the east, and the more steeply W-dipping boundary of the 'basement' inlier to the west (Fig. 5.4). Internally, the principal structure is an upright antiform, cored at surface, and to the limits of drilling, by mineralised Marianoak Formation strata (i.e. centre of subdomain N1). Accepting the litho- and chemo-stratigraphic correlations of the Marianoak Formation with the White Spur Formation and Natone Volcanics, deeper levels of the antiformal core are expected to be represented by equivalents of the Rosebery Host Rock Member/Hercules Pumice Formation, or the Salisbury Conglomerate. Either scenario is permissible, yet the former is favoured in the interpretative section (Fig. 5.4). The western contact of the Hercules Pumice Formation with the Westcott Argillite-Salisbury Conglomerate succession is shown to be transitional (i.e. without any demonstrable structural control) on the western flank of the antiform.

Subdomain N2, comprising both lower stratigraphic levels of the Rosebery Group and slivers of 'basement', has apparently been exhumed from a deep structural position, where equivalent strata in neighbouring subdomains N1 and N3 converge at depths of ~2000-3000 m (Fig. 5.4). The significant vertical apparent displacement of subdomain N2 (~ 2 km) is accounted for by a 'pop-up' structural configuration, a fault wedge bounded by downward-converging W- and subvertically-dipping fault zones (the latter possibly originally E-dipping). The apparently anastomosing character of domain-bounding faults in plan view, considered to account for the disappearance of Salisbury Conglomerate and Natone Volcanics levels along strike to the north of subdomain N2 (Figs. 5.2 and 5.3), may indicate an additional component of sub-horizontal stretch associated with the exhumation process. This interpretation is in accordance with the localised development of distinctive 'block-in-matrix' fabrics along major fault zones seen elsewhere in the Rosebery Group,

and considered by Selley (1997) to record intense flattening strains involving components of both vertical and horizontal ductile flow during the Devonian basin inversion phase.

Overall, there appears a tightening of fold profiles towards the west, an interpretation based in part on the near parallelism of S_0 and S_1 in subdomain N3, and the macroscopic geometries shown in the southern domain. Here the package is dominated by fine- to medium-grained equivalents of the Westcott Argillite and Stitt Quartzite, with only a relatively thin intervening interval of upper Marianoak Formation correlates.

An attempt to restore the belt to its Middle-Late Cambrian extensional configuration is shown in Figure 5.8. A series of sub-basins are interpreted, with the Rosebery Group occupying a central position between a volcanogenic depocentre to the east and a deeply subsident Dundas Group depocentre to the west. Inversion of the latter ultimately led to the emplacement of the Crimson Creek Formation-cored inlier on the western flank of the belt. The original westerly dip of the growth faults is interpreted largely on the basis of the dominant steep westerly dips of S_1 in subdomains N2 and N3, and the easterly facing of strata in N2 (i.e. E-verging folds linked to W-dipping thrust faults). Moreover, the apparent lack of lower Marianoak Formation pumice breccia facies in western and southern subdomains may be explained by limited accommodation development, a feature consistent with westward tapering of strata onto a relatively elevated footwall block.

The subdomain N2 'pop-up' is interpreted to represent an inverted narrow graben that formed the locus of coarse-grained detrital input (Fig. 5.8). Maximum growth is considered to be recorded by the upward coarsening cycle to the base of the Salisbury Conglomerate, the absence of which in western and southern domains again supports the notion that accommodation was relatively limited in these regions. Emplacement of MUC inliers within and at the fringe of subdomain N2 were potentially derived via complete inversion of the interpreted sub-basin (i.e.

exhumation of the sub-basin 'floor'), or plucking of basement slivers from the bounding footwall blocks (i.e. short-cut thrusting).

As noted above, a structural control on the westward termination of Hercules Pumice Formation and Mt Black Volcanics strata is less obvious. The westerly-dipping growth fault shown on the right hand side of the restored profile (Fig. 5.8) is speculative, but potentially controlled the nucleation of the upright antiform in the centre of subdomain N1 (Fig. 5.4): the antiform forming as a fault-propagation fold at its tip. Other than the subtle draping of Hercules Pumice Formation and Mt Black Volcanics strata above the tip of the interpreted growth fault, the volcanogenic depocentre is shown to simply thicken across an eastward-dipping ramp. The latter was potentially controlled by a major basin-bounding structure some distance to the east, such as the Henty Fault.

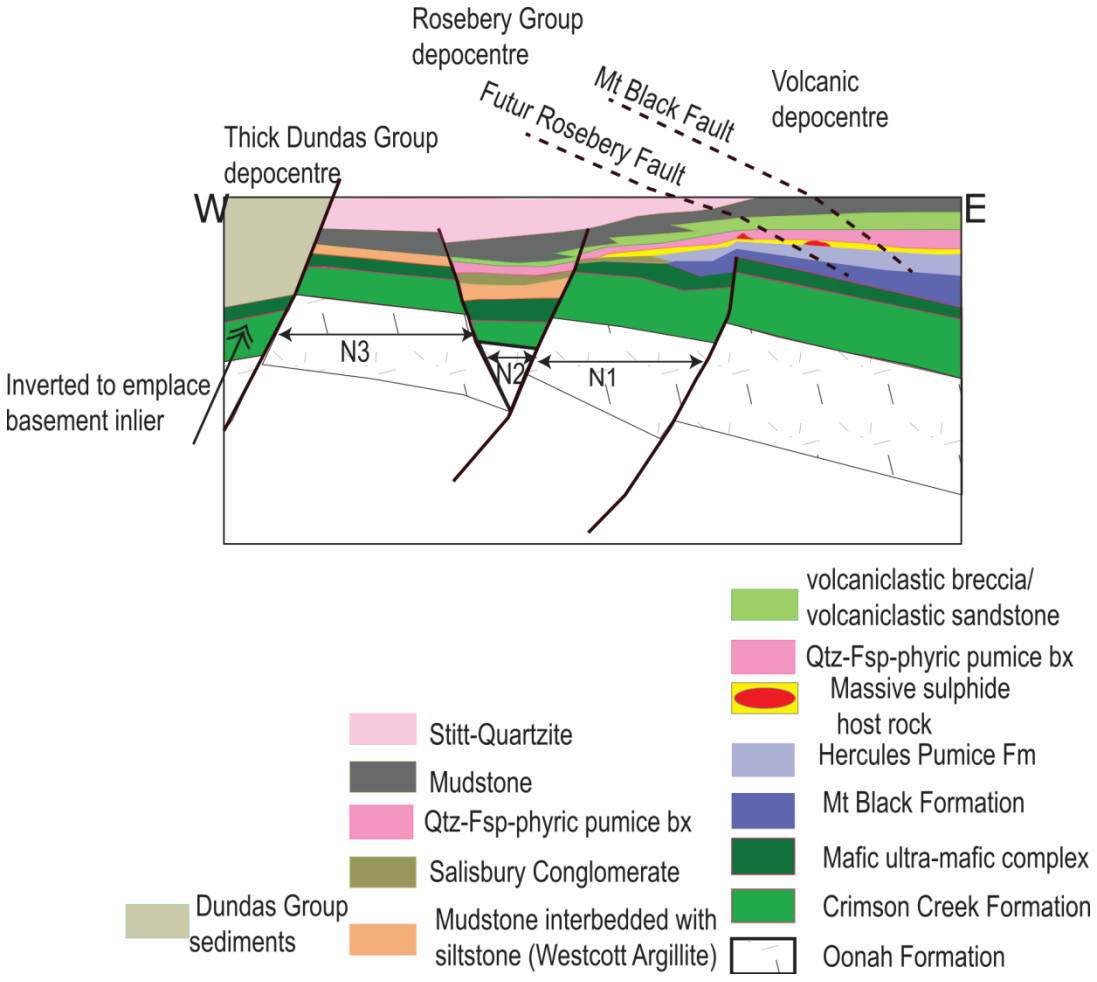

Figure 5.8. Schematic profile showing original Middle-Late Cambrian extensional configuration of the Rosebery Group.

5.4 Conclusion

The unusual structural geometry of the Rosebery Group, involving dismembered folds, emplacement of narrow basement inliers, and loci of high strain, coupled with significant lateral facies variation, is interpreted to relate to Devonian inversion of a compartmentalised basin form. Sediment-dominated western parts of the Rosebery Group are considered to have accumulated on the relatively condensed edge of an eastward thickening ramp. The tapering edge of the ramp corresponds to the footwall block of a major sediment-filled depocentre to the west, presently inverted to exhume a Crimson Creek Formation-cored inlier. The ramp was punctuated near its centre by a narrow graben, presently significantly inverted such that lowermost Rosebery Group strata and 'basement' slivers are re-emplaced at high structural levels. The western margin of this depocentre maximum corresponds with the westernmost limit of White Spur Formation-equivalent pumice breccia deposits.

Direct evidence for a structural control on the lateral transition from the eastern volcanogenic depocentre to western sedimentary depocentres is lacking. It is speculated that a high amplitude antiform containing Marianoak Formation-hosted VHMS-style mineralisation in its core, nucleated above an inverted growth fault tip at depth. Deeper stratigraphic levels within the core of this structure are interpreted to include lateral equivalents of the Rosebery Host Rock Member and are as yet unexplored.

Based on the litho- and chemo-stratigraphic frameworks presented in Chapters 3 and 4, rift climax is likely to correspond with deposition of the Salisbury Conglomerate to west, and coevally to the east with the combined basin-starvation and change in magma composition recorded at the level of the Rosebery Host Rock Member.

The moderately E-dipping Rosebery Fault (± Mt Black Fault) is interpreted to sole into the base of the MRV stratigraphy. It is unaffected by the high amplitude upright folding that

characterises the footwall Rosebery Group rocks, and thus interpreted to have nucleated late in the inversion history.

Chapter 6: Summary and Conclusions

The current study has significantly contributed to the understanding of the Rosebery Group and its setting, using detailed lithofacies, litho-geochemical and structural analyses. Observations of facies geometry, association, texture and composition have underpinned interpretations of mode of eruption, emplacement and deposition of the volcano-sedimentary succession. Petrographic examination, coupled with whole rock geochemical analysis, has proven to be a very effective correlation tool within sequences characterised by complex stratigraphic architecture. A basin model has been presented on the basis of stratigraphic and structural domain analysis, which provides explanations for the westward transition from volcanic- to non-volcanic sediment-dominated facies associations, and the context of VHMS-type mineral occurrences.

Considerable attention has been paid to the VHMS-bearing strata positioned in the footwall of the Rosebery Fault, here named the Marianoak Formation. In this eastern part of the Rosebery Group, the lowest facies association (MRF 1) is dominated by quartz ± feldspar phyric pumice breccia, which records regionally mappable products of explosive felsic volcanic eruptions. Massive sulphide occurrences are restricted to the fine-grained tops of thick normally graded mass flow deposits in MRF 1. More localised facies types at this level include subvolcanic rhyolitic intrusions with peperitic margins. Geochemical characteristics of these facies types include unusually high abundances of Th relative to those of Ti and Sc, consistent with derivation from a highly evolved felsic magmatic source. Pumice breccia units show subtle upsection variations in the relative proportions of feldspar and quartz, which allow the definition of a laterally mappable lithostratigraphic subdivision. Coupled variations are revealed in geochemical data, attributable in part to changes in magma composition throughout the eruptive cycle, but also contamination from 'background' sediments ingested during mass flow emplacement.

An abrupt upsection transition to Ti-rich volcaniclastic breccia, volcaniclastic sandstone and siltstone (MRF 2), dominated by texturally immature angular to sub-rounded basaltic andesite clasts

(VBX I/VSST), records reworking of products from effusive, intermediate to mafic volcanic centres. Intervals of rhyolitic volcaniclastic breccia interbedded with felsic volcaniclastic sandstone and siltstone (VBX II/VSST) indicate a contribution from broadly coeval felsic volcanic sources. The felsic facies are chemically similar to parts of the underlying MRF 1 facies association, and discrimination is based mainly on petrographic grounds, in particular the lack of pumice. Volcanism was episodic and punctuated by periods of basin starvation as indicated by upsection-thickening intervals of black mudstone. An overlying non-volcanogenic sequence of compositionally mature turbiditic sandstone and siltstone, the Stitt Quartzite, records basement uplift and sediment supply from basin-marginal sources.

The central part of Rosebery Group comprises equally diverse facies associations. Lower most strata in these areas include thick sequences of mudstone interbedded with siltstone (Westcott Argillite), deposited during a period of limited sediment supply to the basin. An overlying upward coarsening and thickening cycle, consisting of carbonate-cemented sandstone and ultimately extrabasinally-derived polymictic conglomerate (Salisbury Conglomerate), is interpreted to record a fundamental change in sub-basin configuration, which subsequently allowed input from volcanic sources to the east. The deposition of voluminous quartz-feldspar-phyric pumice breccia of the Natone Volcanics, and its upsection transition to intermediate volcaniclastic sandstone, represents a litho- and chemo-stratigraphic marker, allowing correlation with eastern volcanogenic successions.

Western and southern parts of the Rosebery Group include lithostratigraphic correlates of the Westcott Argillite and Stitt Quartzite, but appear to lack the texturally and compositionally distinctive, correlative felsic volcanic products of the Natone Volcanics and MRF 1. A western barrier to volcanogenic input is implied. However, less well stratigraphically constrained facies associations of basaltic andesite detritus-bearing greywacke (Facies 15) and feldspar crystal-rich volcaniclastic breccia/sandstone (Facies 16) bear some compositional affinities to the upper parts of the

Marianoak Formation and Natone Volcanics. Further work is required to resolve their stratigraphic relationships, both locally and regionally, but on the basis of present data, it is conceivable that the basin progressively opened westward throughout the Marianoak Formation/Natone Volcanics depositional cycle.

The Marianoak Formation and Natone Volcanics are correlated on litho- and chemostratigraphic grounds with the White Spur Formation in the Rosebery Fault hangingwall. This correlation is in accordance with previous interpretations, based on limited data, of Green (1983), Corbett and Lees (1987), Parfrey (1993), and Baker (2013). The recognition of a common fundamental two-fold stratigraphic architecture that comprises a lower Th-rich, quartz-bearing pumiceous interval, and an upper Ti-rich basaltic-andesite detritus-bearing volcaniclastic interval, is crucial to the interpretation.

There are no demonstrable litho-/chemo-stratigraphic equivalents of the Hercules Pumice Formation or Rosebery Host Rock Member in the Rosebery Group. Although there is partial overlap of certain facies in terms of their geochemical characteristics, the feldspar-phyric pumiceous composition of the Hercules Pumice Formation in particular appears unique. Based on the correlation of the MRF 1 with the basal White Spur Formation, it is permissible that the Rosebery Host Rock Member, or a chronostratigraphic equivalent, occurs below the current limit of drilling in the immediate footwall of the Rosebery Fault. It is estimated that a further ~50 m of the Marianoak Formation stratigraphic profile needs to be penetrated to test this hypothesis (i.e. accounting for the ≤20 m thickness of the black shale facies that separates the Rosebery Host Rock Member and White Spur Formation pumice breccia). Nonetheless, the massive sulphide occurrences in MRF 1 cannot be directly equated to the Rosebery ore body, at least in terms of their stratigraphic position.

The chrono-stratigraphically equivalent position of the Rosebery Host Rock Member in the central part of the Rosebery Group is considered to be the boundary of the Salisbury Conglomerate and overlying Natone Volcanics. Until this depositional period was reached, therefore, western and eastern depocentres are interpreted to have evolved independently, at least in terms of sedimentary

and/or eruptive dispersal patterns: restricted basement-derived sedimentation, and dominantly explosive volcanogenic input, respectively.

The concept of an evolving sub-basin configuration throughout Rosebery Group deposition is considered to account for some of the package's unusual structural characteristics, such as the disappearance and reappearance of units along strike, facing flips across high strain zones which entrain basement strata, and dismembered folds. The central fault-bounded domain, comprising a near vertically oriented interval of Westcott Argillite-Natone Volcanics strata, and including mafic ultra-mafic complex slivers, is interpreted as an exhumed graben, now occupying a considerably higher structural position than equivalent strata in neighbouring fault blocks. The graben is interpreted to form one of a series of sub-basins controlled principally by west-dipping growth faults. A major sub-basin boundary is defined by the basement inlier that separates the Rosebery Group from Dundas Group strata to the west.

Despite the distinct lithostratigraphic profiles of the lower Rosebery Group and the eastern volcanogenic sequences (i.e. to the level of the Salisbury Conglomerate and Rosebery Host Rock Member, at least), there is no clear geometric evidence of a discrete sub-basin bounding structure. It is postulated that the lateral changes in detrital input may relate principally to differing positions on a broadly E-dipping ramp. A high amplitude anticline in the eastern part of the Rosebery Group, within which the Marianoak Formation occupies the core, potentially marks the position of an inverted sub-basin margin. However, considering the broadly equivalent thicknesses of Marianoak and White Spur Formation strata in the vicinity of this structure, any displacement on the inferred structure, during this phase of deposition at least, would have been minimal. Further work focussed on alteration geometry associated with the massive sulphide occurrences could aid in determining whether such a structure exists and its possible control on hydrothermal activity.

In conclusion, this work has shown that the Rosebery Group in the immediate position of the Rosebery Fault is yet to be adequately tested for VHMS-style mineralisation. Current drilling has

demonstrated that an equivalent stratigraphic position to the Rosebery ore body hangingwall extends ~9 km N-S in the footwall of the fault, but has failed to intersect chronostratigraphic equivalents of the host rock. This position is exposed to the west, however, at the top of the Salisbury Conglomerate. Although the overlying Natone Volcanics strata indicate that the basin was magmatically active at the time, and thus a driver for hydrothermal flow may have existed, the pumice breccias were potentially deposited a great distance from their eruptive source. Supporting this conclusion is the apparent lack of semi-coherent subvolcanic facies, distinctive features in both the Marianoak and White Spur Formations equivalents to the east. Thus, the prospectivity of the Rosebery Group is considered to diminish significantly in central and western parts.

Globally, many VHMS deposits and their hosts are followed by abrupt changes in the composition and intensity of volcanism; e.g., a pause in felsic volcanism and deposition of mudstone, and in some cases emplacement of basalts (e.g., MRV, Silurian SE Australia, Skellefte, Green Tuff belt, Abitibi, Bathurst and Bergslagen; Allen and Weihed, 2002). The level of ore in these systems, and indeed prospective strata basin-wide, are thus expected to be readily identifiable in chemo-stratigraphic profiles. Hence, the key to a successful discovery of VHMS style of mineralization is the understanding of chemo-stratigraphy, facies architecture and regional deformational evolution of the area.

Massive sulphide within the Marianaok Formation of the Rosebery Group and generally MRV was formed through hydrothermal fluid venting generated pre- and -syn-deposition of the rhyodacitic lava flows, intrusives and pyroclastics of the footwall sequence. The deposition of the massive sulphide lenses that lasted for a short period of time occurred at the end of the explosive eruptive phase mainly through replacement of unconsolidated, pumiceous and epiclastic mass-flow breccias and partly through venting on the seafloor or a combination of these processes (Allen, 1991; Mortensen et al., 2015). The deposition of the massive sulphide lenses was followed by a significant pause in volcanism and deposition of thick mudstone sequence which is the marker

horizon throughout Rosebery and Hercules deposits. The stratigraphic horizon between the top of the footwall volcanics and the mudstone sequence is the main mineralization event identified as “holy host” throughout the MRV (Mortensen et al., 2015). The current chemostratraphic and structural analysis has demonstrated that the stratigraphic repeat of this host horizon occurs on the eastern part of the Rosebery Group as discussed on the earlier part of this chapter; however, the footwall sequence of the basin marginal central and western part of the Rosebery Group characterized by basement derived epiclastics is interpreted to be far from the mineralizing hydrothermal vent.

Reference List

Allen, R. L., 1991, Structure, stratigrphy and volcanology of the Rosebery-Hercules Zn-Pb-Cu-Au massive sulphhide district, Tasmania: unpub Report.

Baker, W., 2013, Correlations and Exploration Signifcance of the Natone Volcanis, Rosebery Group, Western-Tasmania.: Un pub. Graduate Diploma Science thesis, University of Tasmania.

Barrett, T. J., and MacLean, W. H., 1994, Chemostratigraphy and hydrothermal alteration in exploration for VHMS deposits in greenstones and younger volcanic rocks: Alteration and alteration processes associated with ore-forming systems: Geological Association of Canada, Short Course Notes, v. 11, p. 433-467.

Berry, R., 1989a, The history of movement on the Henty Fault Zone, western Tasmania: An analysis of fault striations: Australian Journal of Earth Sciences, v. 36, p. 189-205.

Berry, R., 1989b, Microstructural evidence for a westward transport direction during middle Cambrian obduction in Tasmania: Geological Society of Australia Abstracts, 1989b.

Berry, R., 1993, Rosebery Section: STRUCTURE AND MINERALISATION OF WESTERN TASMANIA, p. 3.

Berry, R., 1995, Tectonics of western Tasmania: Late Precambrian-Devonian: Geological Society of Australia Abstracts, 1995, p. 6-8.

Berry, R., Chmielowski, R., Steele, D., and Meffre, S., 2007, Chemical U–Th–Pb monazite dating of the Cambrian Tyennan Orogeny, Tasmania: Australian Journal of Earth Sciences, v. 54, p. 757-771.

Berry, R., and Keele, R., 1993, Cambrian structure in western Tasmania: STRUCTURE AND MINERALISATION OF WESTERN TASMANIA, p. 55.

Berry, R., Meffre, S., Jenner, G., Fulton, R., Selley, D., White, M., Corbett, K., Bull, S., Davidson, G., and Kitto, P., 1997, Structure and mineralisation of western Tasmania. CODES/AMIRA Project P. 291A Final report, March 1997.

Berry, R. F., and Crawford, A. J., 1988, The tectonic significance of Cambrian allochthonous mafic-ultramafic complexes in Tasmania: Australian Journal of Earth Sciences, v. 35, p. 523-533.

Branney, M. J., and Kokelaar, P., 1992, A reappraisal of ignimbrite emplacement: progressive aggradation and changes from particulate to non-particulate flow during emplacement of high-grade ignimbrite: Bulletin of Volcanology, v. 54, p. 504-520.

Brathwaite, R., 1970, The geology of the Rosebery ore deposit: Unpub, Ph. D. thesis, Univ. Tasmania.

Brown, A., 1980, Early deposits in a Lower Palaeozoic trough of western Tasmania: Prog. & abstracts, 4th Aust. Geol. Conv. Hobart, v. 23.

Brown, A., and Jenner, G., 1989, Geological setting, petrology and chemistry of Cambrian boninite and low-Ti tholeiite lavas in western Tasmania: Boninites and Related Rocks. Unwin Hyman, London, p. 232-263.

Brown, A. V., 1986, Geology of the Dundas-Mt Lindsay-Mt Youngbuck region, Department of Mines.

Campana, B., and King, D., 1963, Palaeozoic tectonism, sedimentation and mineralization in west Tasmania: Journal of the Geological Society of Australia, v. 10, p. 1-53.

Cas, R., and Wright, J. V., 2012, Volcanic successions modern and ancient: A geological approach to processes, products and successions, Springer Science & Business Media.

Cook, H. E., Hine, A. C., and Mullins, H. T., 1983, Platform margin and deep water carbonates, Citeseer.

Corbett, K., and Lees, T., 1987a, Stratigraphic and structural relationships and evidence for Cambrian deformation at the western margin of the Mt Read Volcanics, Tasmania: Australian Journal of Earth Sciences, v. 34, p. 45-67.

Corbett, K., and McNeill, M., 1986, Geology of Rosebery–Mt Block Area. Mount Read Volcanics Project Map 2: Mineral Resources Tasmania, Hobart.

Corbett, K., and Solomon, M., 1989, Cambrian Mt Read Volcanics and associated mineral deposits: Geology and mineral resources of Tasmania, v. 15, p. 84-153.

Corbett, K. D., 1992, Stratigraphic-Volcanic Setting of Massive Sulfide Deposits in the Cambrian Mount Read Volcanics, Tasmania: Economic Geology and the Bulletin of the Society of Economic Geologists, v. 87, p. 564-586.

Corbett, K. D., 2002, Western Tasmanian regional minerals program Mount Read Volcanis compilation: Department of Infrastructure, Energy and Resources, v. Record 2002/19.

Corbett, K. D., and Lees, T. C., 1987b, Reply to discussion; Stratigraphic and structural relationships and evidence for Cambrian deformation at the western margin of the Mt. Read Volcanics, Tasmania: Australian Journal of Earth Sciences, v. 34, p. 533-534.

Corbett, K. D., Quilty, P., Calver, C. R., and Pongratz, J., 2014, Geological evolution of Tasmania.

Crawford, A., Corbett, K., and Everard, J., 1992, Geochemistry of the Cambrian volcanic-hosted massive sulfide-rich Mount Read Volcanics, Tasmania, and some tectonic implications: Economic Geology, v. 87, p. 597-619.

Crawford, A. J., and Berry, R. F., 1992, Tectonic implications of Late Proterozoic-Early Palaeozoic igneous rock associations in western Tasmania: Tectonophysics, v. 214, p. 37-56.

Dimroth, E., and Yamagishi, H., 1987, Criteria for the recognition of ancient subaqueous pyroclastic rocks: Rep. Geol. Surv. Hokkaido, v. 58, p. 55-88.

E.Z.Report, 1986, Annual Report on exploratioin activities in the Colebrook area for 1986: A report submitted to the Department of Mines Tasmania, v. EZ Report No T222.

Elliston, J., 1954, The geology of the Dundas district, Tasmania: Papers and Proceedings of the Royal Society of Tasmania, 1954, p. 161-184.

Finucane, K. J., 1932, The Geology and Ore Deposits of the Rosebery District. Unpublished report 1932. Tasmania Department of Mines, University of Western Australia.

Franklin, J. M., Gibson, H.L., Jonasson, I.R., and Galley, A.G., 2005, Volcanogenic Massive Sulphide Deposits, in Hedenquist, J.W., Thompson, J.F.H., Goldfarb, R.J., and Richards, J.P., eds, 2005, Volcanogenic Massive Sulphide Deposits:: Economic Geology, v. 100th Anniversary, p. 523-560.

Franklin, J. M., Lydon, J., and Sangster, D. F., 1981, Volcanic-associated massive sulfide deposits: Economic Geology, v. 75, p. 485-627.

Galley, A. G., Hannington, M., and Jonasson, I., 2007, Volcanogenic massive sulphide deposits.

Gibson, H., Allen, R., Riverin, G., and Lane, T., 2007, The VMS model: Advances and application to exploration targeting: Proceedings of Exploration, 2007, p. 717-730.

Gifkins, C. C., 2001, Submarine volcanism and alteration in the Cambrian, northern Central Volcanic Complex, western Tasmania, University of Tasmania.

Gifkins, C. C., and Allen, R. L., 2001, Textural and chemical characteristics of diagenetic and hydrothermal alteration in glassy volcanic rocks: examples from the Mount Read Volcanics, Tasmania: Economic Geology, v. 96, p. 973-1002.

Green, G., Solomon, M., and Walshe, J., 1981, The formation of the volcanic-hosted massive sulfide ore deposit at Rosebery, Tasmania: Economic Geology, v. 76, p. 304-338.

Green, G. R., 1983, The geological setting and formation of the Rosebery volcanic hosted massive sulphide ore body, Tasmania. , PhD Thesis,Department of Geology,University of Tasmania.

Herrmann, W., 1998, Use of immobile elements and chemostratigraphy to determine precursor volcanics: Studies of VHMS-related alteration: geochemical and mineralogical vectors to ore. Regional Studies and Volcanic Facies Controls. AMIR/ARC Project P, v. 439, p. 1-12.

Huston, D. L., Stevens, B., Southgate, P. N., Muhling, P., and Wyborn, L., 2006, Australian Zn-Pb-Ag ore-forming systems: a review and analysis: Economic Geology, v. 101, p. 1117-1157.

Kitto, P. A., 1994, Structural and geochemical controls on mineralisation at Renison, Tasmania, University of Tasmania.

Large, R., 1990, The gold-rich seafloor massive sulphide deposits of Tasmania: Geologische Rundschau, v. 79, p. 265-278.

Large, R., Doyle, M., Raymond, O., Cooke, D., Jones, A., and Heasman, L., 1996, Evaluation of the role of Cambrian granites in the genesis of world class VHMS deposits in Tasmania: Ore Geology Reviews, v. 10, p. 215-230.

Large, R. R., 1992, Australian volcanic-hosted massive sulfide deposits; features, styles, and genetic models: Economic Geology, v. 87, p. 471-510.

Large, R. R., Gemmell, J. B., Paulick, H., and Huston, D. L., 2001a, The alteration box plot: A simple approach to understanding the relationship between alteration mineralogy and lithogeochemistry associated with volcanic-hosted massive sulfide deposits: Economic geology, v. 96, p. 957-971.

Large, R. R., McPhie, J., Gemmell, J. B., Herrmann, W., and Davidson, G. J., 2001b, The spectrum of ore deposit types, volcanic environments, alteration halos, and related exploration vectors in submarine volcanic successions: some examples from Australia: Economic Geology, v. 96, p. 913-938.

Leaman, D., and Richardson, R., 2003, A geophysical model of the major Tasmanian granitoids: Tasmanian Geological Survey Record, v. 11, p. 2003.

Lécuyer, C., Dubois, M., Marignac, C., Gruau, G., Fouquet, Y., and Ramboz, C., 1999, Phase separation and fluid mixing in subseafloor back arc hydrothermal systems: A microthermometric and oxygen isotope study of fluid inclusions in the barite-sulfide chimneys of the Lau Basin: Journal of Geophysical Research: Solid Earth, v. 104, p. 17911-17927.

Loftus-Hills, G., 1964, The geology of the Dundas-Pieman River area, University of Tasmania.

Loftus-Hills, G., Solomon, M., and Hall, R. J., 1967, The structure of the bedded rocks west of Rosebery, Tasmania: Journal of the Geological Society of Australia, v. 14, Part 2, p. 333-337.

Lowe, D. R., 1982, Sediment gravity flows: II Depositional models with special reference to the deposits of high-density turbidity currents: Journal of Sedimentary Research, v. 52.

MacLean, W., and Barrett, T., 1993, Lithogeochemical techniques using immobile elements: Journal of geochemical exploration, v. 48, p. 109-133.

Martin, N. K., 2004, Genesis of the Rosebery massive sulphide deposit, western Tasmania, Australia: Un pub. Ph.D. thesis. University of Tasmania, p. 273 pp.

McPhie, J., Doyle, M., and Allen, R., 1993, Volcanic Texture: Centre for Ore Deposit and Exploration Studies, University of Tasmania, Hobart, 196h.

MMG, R.-M. Z. u., 2014, Rosebery Mine Zone update.

Mortensen, J. K., Gemmell, J. B., McNeill, A. W., and Friedman, R. M., 2015, High-precision U-Pb zircon chronostratigraphy of the Mount Read Volcanic belt in Western Tasmania, Australia: Implications for VHMS deposit formation: Economic Geology, v. 110, p. 445-468.

Parfrey, O., 1993, Mesoscopic and microscopic structural evolution in the Dundas Group at Rosebery, Western Tasmania. : Un pub. B.Sc. with Honours Degree thesis. University of Tasmania, v. 4-64.

Piercey, S. J., 2008, Lithogeochemistry of volcanic rocks associated with volcanogenic massive sulphide deposits and applications to exploration: Submarine volcanism and mineralization: modern through ancient. Edited by B. Cousens and SJ Piercey. Geological Association of Canada, Short Course, p. 29-30.

Selley, D., 1997, Structure and sedimentology of the Dundas Group, Western Tasmania: Un pub. PhD thesis. University of Tasmania.

Selley, D., and Meffre, S., 1997, Structure and sedimentology of Middle and Upper Cambrian Strata adjacent to the Firewood Siding Fault: CODES Key Center, Geology Department, University of Tasmania, Hobart.

Seymour, D., and Calver, C., 1995, Explanatory notes for the time-space diagram and stratotectonic elements map of Tasmania: Tasmanian Geological Survey Record, v. 1.

Seymour, D. B., 1980, The Tabberabberan Orogeny in northwest Tasmania, University of Tasmania.

Shanmugam, G., 1997, The Bouma sequence and the turbidite mind set: Earth-Science Reviews, v. 42, p. 201-229.
Stacey, A., and Berry, R., 2004, The structural history of Tasmania: a review for petroleum explorers.
Taylor, B. L., 1954, Progress report on the North Pieman mineral area: Tasmania Dept. Mines Unpub. Report for 1954: 159-199.
Turner, N., 1989, Precambrian: Geology and Mineral Resources of Tasmania, v. 15, p. 5-46.
Turner, N., 1993, K–Ar geochronology in the Arthur Metamorphic Complex, Ahrberg Group and Oonah Formation, Corinna district: Mineral Resources Tasmania Report, v. 12.
Turner, N., Black, L., and Kamperman, M., 1998, Dating of Neoproterozoic and Cambrian orogenies in Tasmania: Australian Journal of Earth Sciences, v. 45, p. 789-806.
Van Einjndthoven, W. T., 2006, Structural and Stratigraphy of the Mount Dundas District.: Un pub. B.Sc. with Honours Degree thesis. University of Tasmania.
Williams, E., 1978, The phanerozoic structure of Australia and variations in tectonic style Tasman Fold Belt System in Tasmania: Tectonophysics, v. 48, p. 159-205.
Winter, C., 2012, Stratigraphy, Structure and Correlations of the Rosebery Hanging wall sequence, Western Tasmania: Unpub. Unpublished B.SC (Honours) thesis thesis, University of Tasmania.
Yamagishi, H., 1987, Studies on the Neogene subaqueous lavas and hyaloclastites in southwest Hokkaido: Report of the Geological Survey of Hokkaido, v. 59, p. 55-117.

377000
377500
378000
378500
5376000
5375500
5375000
5374500
5374000

Flume Road detailed mapping

Quartz wacke and quartz arenite (Stitt Quartzite)

Siltstone

Mudstone

Volcaniclastic breccia

Qtz-fsp-phyric pumice breccia

Bedding plane (So)

Cleavage (S1)

Intersection lineation

Fold axis

Roseberry Fault

Pieman River

80
20
74
74
84
30
50
64
80
46
40
40
42
60
50
70
70
60
60
84
36
54
50
50
80
70
50
80
75
88
20
70

Natone Creek and Westcott Hill detailed mapping

376000 376500 377000

5372500 5372000 5371500 5371000 5370500

Legend

- Quartz-wacke, quartz arenite (Stitt Quartzite)
- Qtz-fsp-phyric pumice breccia (Natone Volcanics)
- Polymictic Conglomerate (Salisbury Conglomerate)
- Dolomitic sandstone
- Siltstone
- Mudstone
- Bedding plane (So)
- Overturned bedding plane (So)
- Cleavage (S1)
- Intersection lineation
- Fold axis

Murchison Highway

Natone Creek

Wstcott Hill

374500

375000

375500

5368000

5367500

5367000

Ring River

Baker Creek

Conliffe Creek

Bather Creek

Legend

- Quartz wacke and quartz arenite (Stitt Quartzite)
- Volcaniclastic breccia
- Greywacke
- Siltstone
- Mudstone
- Bedding plane (So)
- Cleavage (S1)
- Intersection lineation
- Fold axis

Fig. 1

374000 376000 378000 380000 382000 384000

5378000 5376000 5374000 5372000 5370000 5368000 5366000 5364000

411R-D1
397R
250R
337R
R10035
R10063
R10032
Mt. Black
Bobadil Plain
Rosebery Fault
Flume Road
Rosebery
180H/2
Pieman River
Murchison Highway
BP273
BP272
RBH2
CHP264
Westcott Hill
RBH1
Natone Creek
JP357
Jupiter
Mt. Black Fault
Ring River
Williamsford
NE Dundas Tramway
Hercules
Moore's Pimple

0 2 Km

Legend

Quaternary sediments

Tyndall Group

Volcaniclastic sandstone and minor volcaniclastic breccia

Rosebery Mine facies association

Upper White Spur Formation:Greywacke interbeded with siltstone and mudstone

White Spur Formation:Volcaniclastic sandstone and breccia

Hercules Pumice Formation: Pumice rich facies and quartz-feldspar phyric rhyolite

Kershaw Pumice Formation: Pumice rich breccia, rhyolitic and dacitic sills

Mt. Black Formation: dacitic and rhyolitic lavas facies association

Rosebery Group

Quartz Wacke, Quartz arenite and mudstone (Stitt Quartzite)

Marianoak Formation

Mudstone (Chamberlain Shale)

Qtz+/- Fsp-phyric pumice breccia and lithic rich volcaniclastic sandstone

Central sub-area

Qtz-fsp phyric pumice breccia (Natone Volcanics)

Polymictic Conglomerate (Salisbury Conglomerate)

Dolomitic sandstone, siltstone and shale (Westcott Argillite)

Greywacke

Siltstone

Basement

Mafic ultramafic complexes

Crimson Creek Formation

Thrust fault
Inferred fault
Antiform
Synform

Geolgraphic locations

Drill hole traces
Surface drilled
Underground drilled

Appendix 2

The graphic logs of 13 drill holes logged in this study are included at 1:200 and 1:1000 scales. The drill holes are arranged in sequence from 337R, 397R, 411R-D1, BP272, BP273, JP357, R10032, R10035, R10063, RBH1, RBH2, CHP264 and180H2.

EXPLORATION SKILLS MAPPING CAMP

GRAPHIC LOG

Project Rosebery
Location 379003E | 5377423N
Drill hole No. 250R
Location No.

Coords: 379003E | 5377423N | RL: 351.302 | Scale: 1:1000 | Page 1 of 3

Azim: 68.7 | Incl: -87 | Diam: | Logged by: Interpreted mm G data | Date 7/10/2016

Log with grainsize (mud, 1/8, 1/2, 2, 8, 32, max mm)

m	Structure	Samples / TS results / Chemistry	Rock / facies description	Alteration
250		Andesite	254.9-283.5 Andesite Grey, f.g, siliceous rock,	
60				
70				
80	MBF			
			283.5-288.6 mudstone/siltstone with cataclasted vein qtz clasts in silica-clay-matrix	
90		Fault	- sheared mudstone	
300			- Mount black fault	
10		VSST	288.60-312.8 VSST	
20				
		MDST/SLT	312.8-328 mudstone/shale interbedded with epiclastic SST	
30				
40			328.00-339.3 feldspar qtz-phyric VSST	
350		VSST/brx	339.3-409.1 Pale brown grey hard, siliceous & massive volcaniclastic SST, medium to coarse grained	
			- qtz-crystal(lithic) SST	
			- Scattered qtz lithics ≈ 1cm	
			passes to underlying lithic breccia	
400				
10			409.1-437.8 Pale brown siliceous lithic breccia	
20			angular clasts of siliceous rhyolite clasts in m.g-c.g qtz rich matrix	
30				
40				
			437.8-482.5 tuffaceous crystal + lithic rich pumice breccia (qtz> feld)	
450				
60				
70				
80			482.50-505.30 lithic ric vpumice breccia fining to qtz-rich volcaniclastic Sandstone	
90				
500				

EXPLORATION SKILLS MAPPING CAMP

GRAPHIC LOG

Project Rosebery | Drill hole No. 250R
Location | Location No.

Coords: 379000.3 | 5377423N | RL: | Scale: 1:1000 | Page 2 of 3

Azim: | Incl: | Diam: | Logged by: | Date 7/10/2016

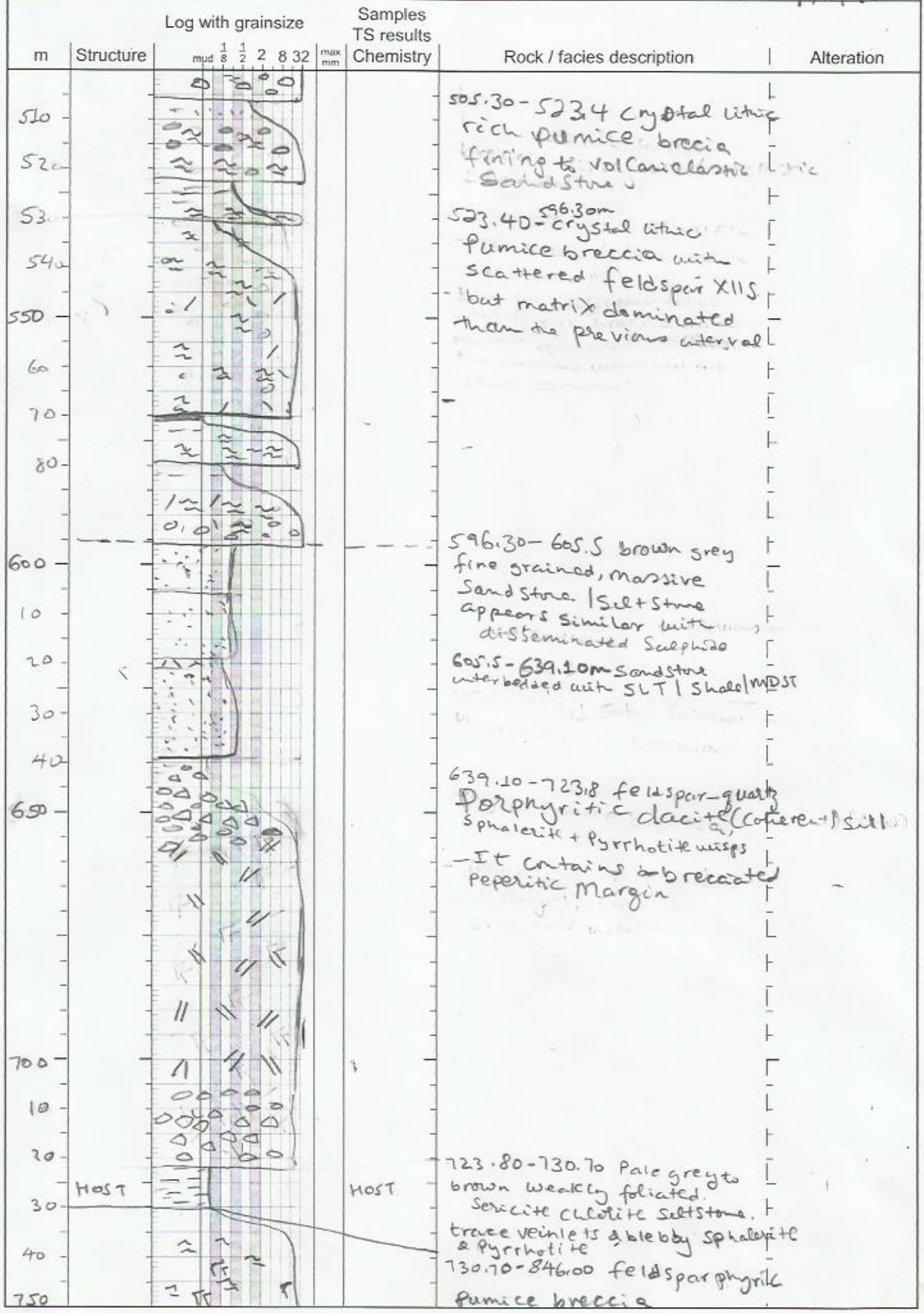

EXPLORATION SKILLS MAPPING CAMP

GRAPHIC LOG

Project Rosebery Location		Drill hole No. 250R Location No.	
Coords:	RL:	Scale: 1:1000	Page 3 of 3
Azim:	Incl:	Diam:	Logged by:	Date 07 | 10 | 2016

Log with grainsize (mud, 1/8, 1/2, 2, 8, 32, max mm) | Samples, TS results, Chemistry

m	Structure	Rock / facies description	Alteration
760		feldspar phyric pumice breccia	
770			
780			
790			
800			
10			
20			
30			
40	Rosebery Fault		
850		846.8 – 881.90 siliceous altered Vol Caniclastic Sandstone	
60			
70			
80		881.90 – 955.5 strongly foliated Shale interbedded with Siltstone & Sandstone	
90			
900			
10			
20			
30			
40			
950			

EXPLORATION SKILLS MAPPING CAMP

GRAPHIC LOG

Project Rosebery | Drill hole No. 337R

Location | Location No.

Coords: 379967.5E / 5377212N | RL: 475.1 | Scale: 1:200 | Page 1 of 10

Azim: 258.98 | Incl: -83.13 | Diam: | Logged by: CYOB | Date 5/12/2016

m	Structure	Log with grainsize (mud, 1/8, 1/2, 2, 8, 32, max mm)	Samples / TS results / Chemistry	Rock / facies description	Alteration
900				900-931.10 Palegreen, grey, massive to weakly cleaved, chlorite altered, dacite (Mt. Black Volcanics)	chlor
910					
920					
930			MBF	931.10 - 980.00 Green, grey, massive - weakly foliated, Qtz-phyric volcaniclastic breccia with scattered Qtz-phyric & aphanitic clasts set in sandstone matrix. The base is v. c g, Qtz-phyric & aphanitic, glassy, grey to white altered clasts 1-3cm	
940					
950					

EXPLORATION SKILLS MAPPING CAMP

GRAPHIC LOG

Project Rosebery
Location

Drill hole No. 337R
Location No.

Coords: 379967.5E/5377212N | RL: 475.1 | Scale: 1:200 | Page 2 of 10

Azim: 258.98 | Incl: -83.33 | Diam: | Logged by: EYOB | Date 5/12/2016

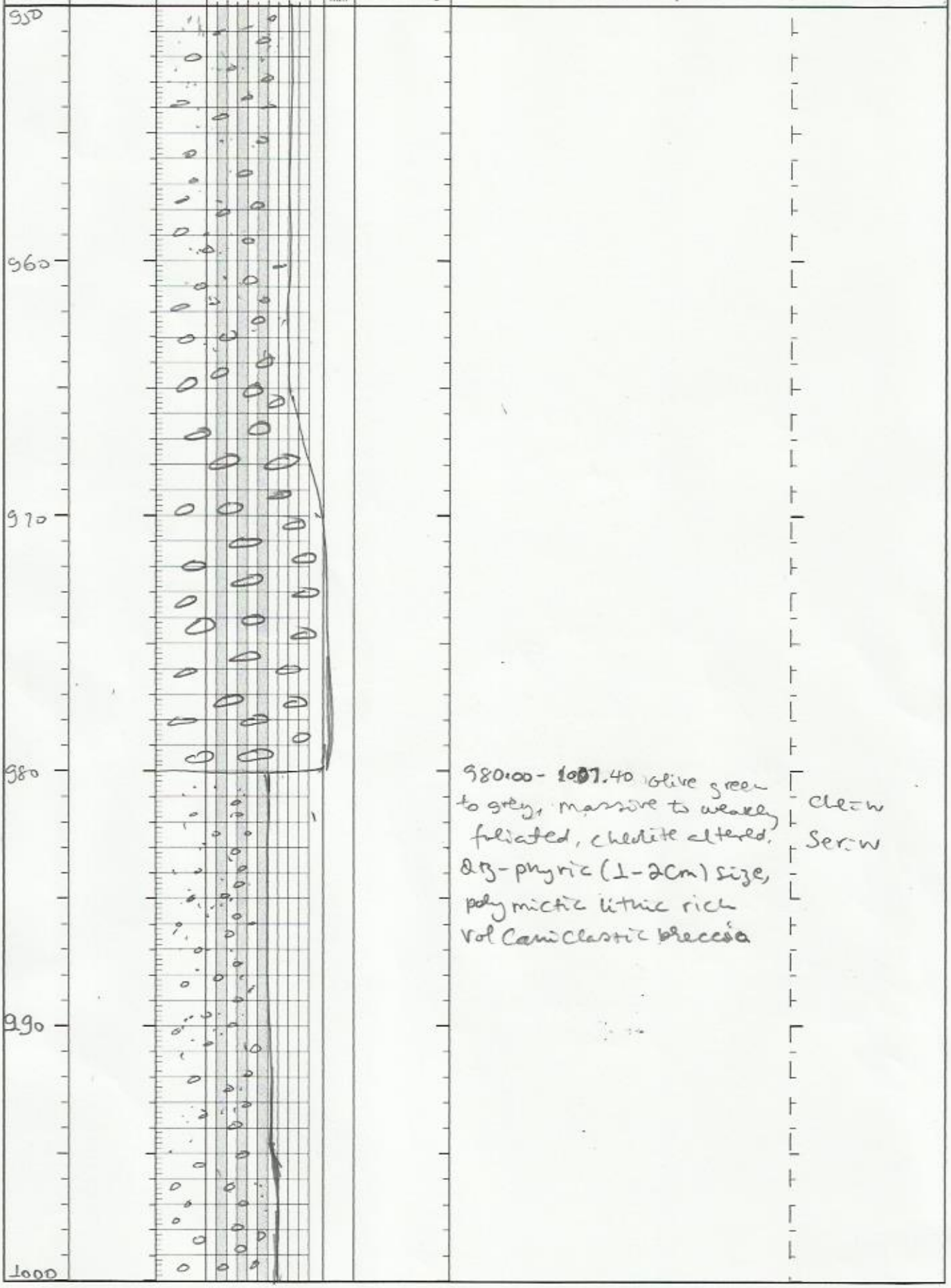

EXPLORATION SKILLS MAPPING CAMP

GRAPHIC LOG

Project Location

Drill hole No. 337R

Location No.

Coords: | RL: | Scale: 1:200 | Page 3 of 10

Azim: | Incl: | Diam: | Logged by: EYOB Andemeskel | Date 5/12/2016

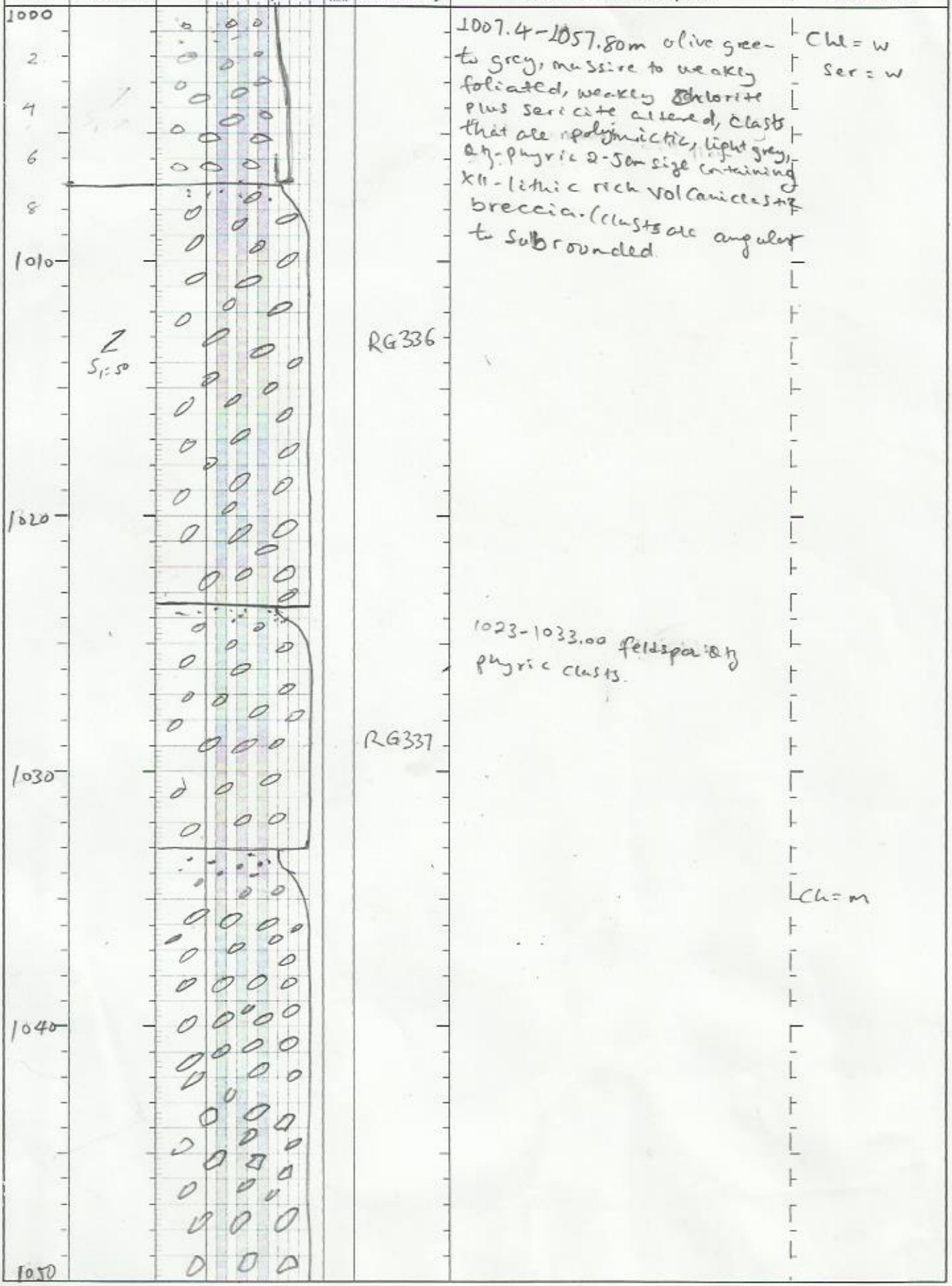

EXPLORATION SKILLS MAPPING CAMP

GRAPHIC LOG

Project Location

Drill hole No. 337R
Location No.

Coords: | RL: | Scale: 1:200 | Page 4 of 10

Azim: | Incl: | Diam: | Logged by: EYOB | Date 5/12/2016

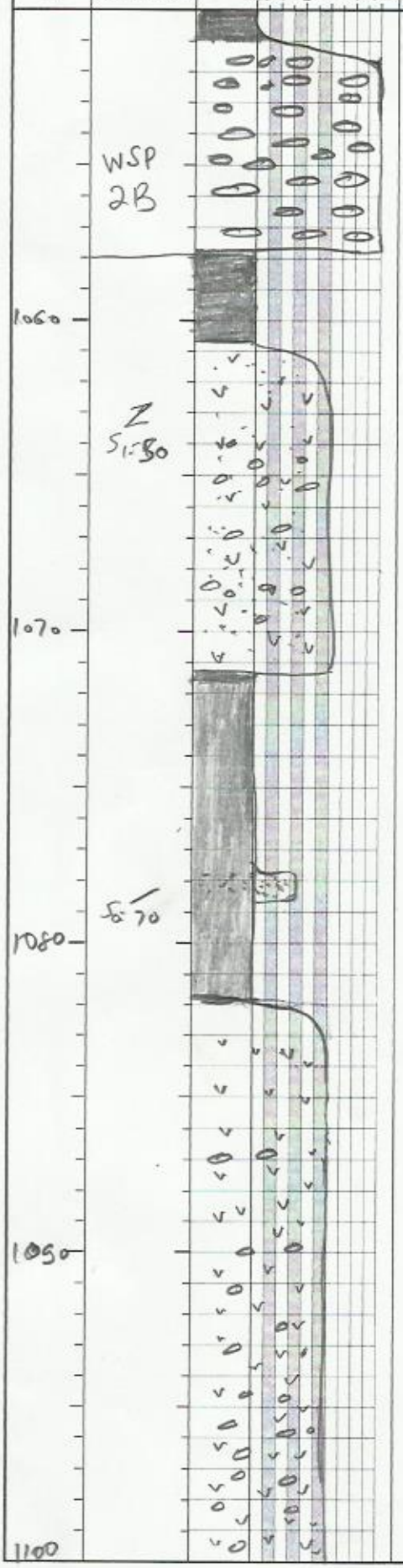

Samples
TS results
Chemistry

RG338

Rock / facies description

1050.10 - 1057.80 relatively finer Xtyl stal- lithic rich vol caniclastic breccia set in a Sandstone matrix. Clasts are highly flattened & subrounded grading to Siltstone / mudstone bedding-top

1057.80 - 1060.60 dark black v. f. g, blackshale / mudstone - Qtz & Carbonate veined.

1060.60 - 1071.30m grey to olive green, massive to weakly foliated, Sericite - chlorite altered, crystal poor with rare Qtz & fld, lithic rich vol caniclastic Sandstone groundmass with Scattered vol Caniclastic breccia

1071.30 - 1081.70m dark grey, v. f. g blackshale interbedded with Qtz-phyric vol caniclastic Sandstone.

1081.70 - 1128.60 grey colored massive to weakly foliated XII poor with Sparse Qtz XIIs, weakly Sericite + chlorite altered lithic-rich volcaniclastic breccia with Scattered clasts set in Sandstone groundmass

1099.00 - 1128.60m moderately

Alteration

Chl = m

EXPLORATION SKILLS MAPPING CAMP

GRAPHIC LOG

Project Location

Drill hole No. 337R
Location No.

Coords: | RL: | Scale: 1:200 | Page 5 of 10

Azim: | Incl: | Diam: | Logged by: EYOB | Date 5/12/2016

Log with grainsize | Samples TS results Chemistry | Rock / facies description | Alteration

m | Structure | mud 1/8 1/2 2 8 32 max mm

1100

S1:70

RG339

Xll rich mainly feldspars & basaltic sparse clasts 3-5cm containing Volcani clastic Sandstone groundmass, VBX

It has a sharp bedding contact with lower unit

Chl = M

1120

WSP2A

1120

CTc (bedding)

S:60

1128.6–1150.30 dark grey, V.f. & Volcaniclastic Siltstone to mudstone with out sized feldspar xlls containing Pumice breccia ash tuff of grey, massive to weakly foliated, weakly sericite altered, Qtz-fld phyric pumice breccia

RG340

1130

1140

1150

EXPLORATION SKILLS MAPPING CAMP

GRAPHIC LOG

Project Roseberry | Drill hole No. 337R
Location | Location No.

Coords: | RL: | Scale: 1:100 | Page 6 of 10

Azim: | Incl: | Diam: | Logged by: EYDB | Date 5/12/2016

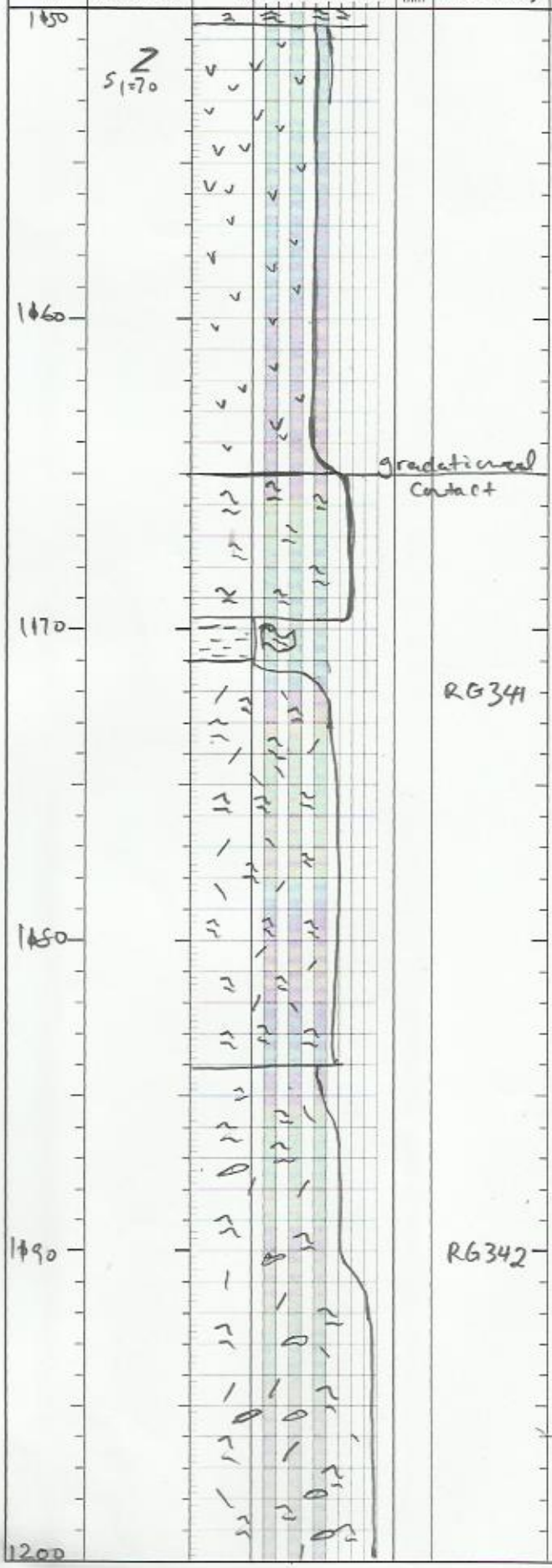

Rock / facies description

1150.30–1165.00 grey, m.g to f massive to weakly cleaved, Volcaniclastic Sandstone top part of the Lower Unit.

1165.00–1169.20m grey, massive to weakly foliated, crystal rich, Qtz-fld phyric pumice breccia

1169.20–1184.10m grey, massive to weakly cleaved, Qtz-phyric pumice breccia fining to Pumiceous Siltstone ash top of the flow

1184.10–1207.50 grey, m.g to c.g, massive to weakly cleaved, Sparse Silty clasts 35% containing, crystal rich, Qtz-phyric pumice breccia

The Silty clasts contain Sp&Py veinlets.

Alteration

SE: W

SE: M

SI: M

SE: M

EXPLORATION SKILLS MAPPING CAMP

GRAPHIC LOG

Project Raseberry
Location

Drill hole No. 337R
Location No.

Coords:

RL:

Scale: 1:200

Page 7 of 18

Azim:

Incl:

Diam:

Logged by: EYOB

Date 5/12/2016

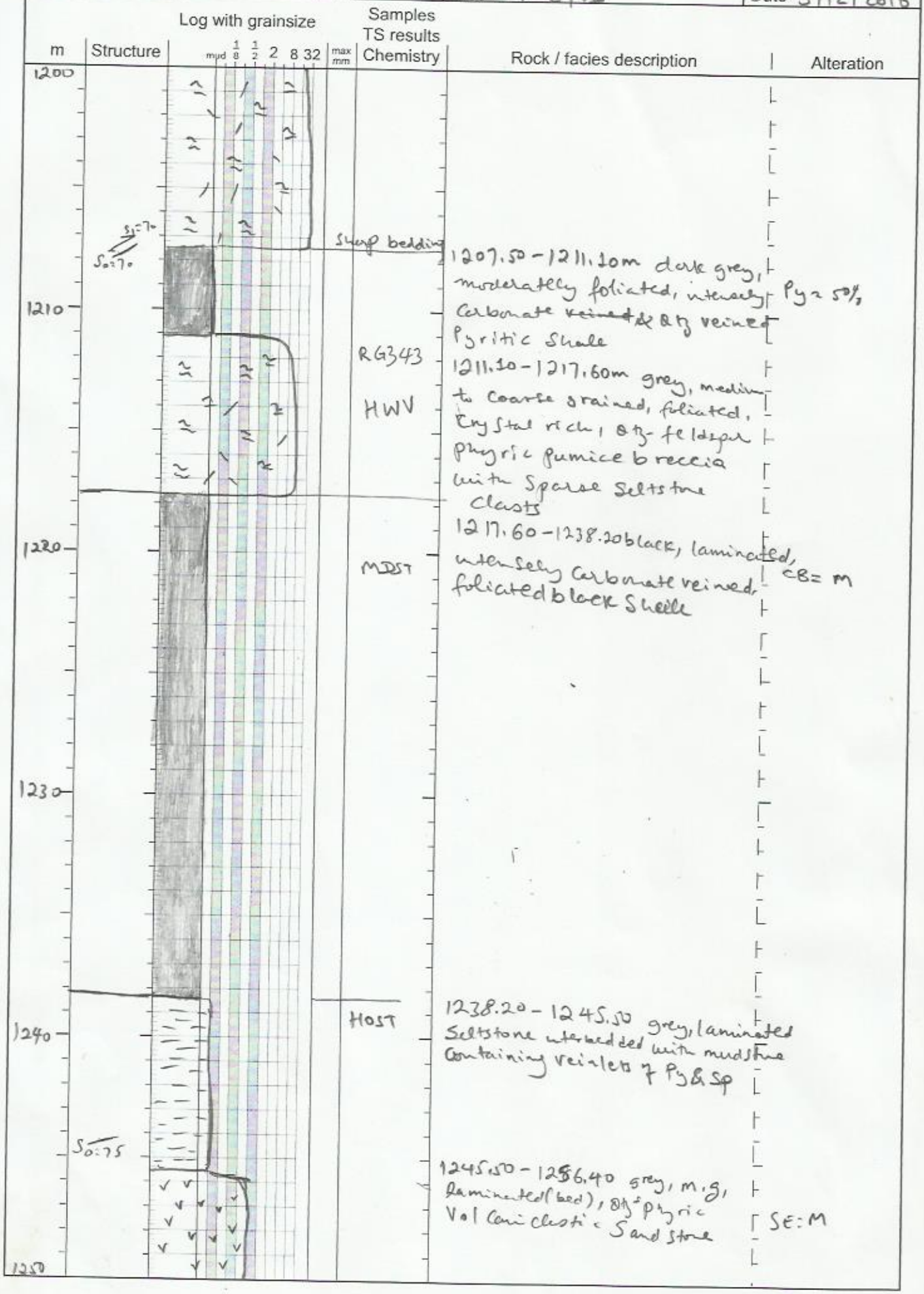

EXPLORATION SKILLS MAPPING CAMP

GRAPHIC LOG

Project / Location		Drill hole No.	337R
		Location No.	
Coords:	RL:	Scale: 1:200	Page 8 of 10
Azim:	Incl: / Diam:	Logged by:	Date 05/12/1993

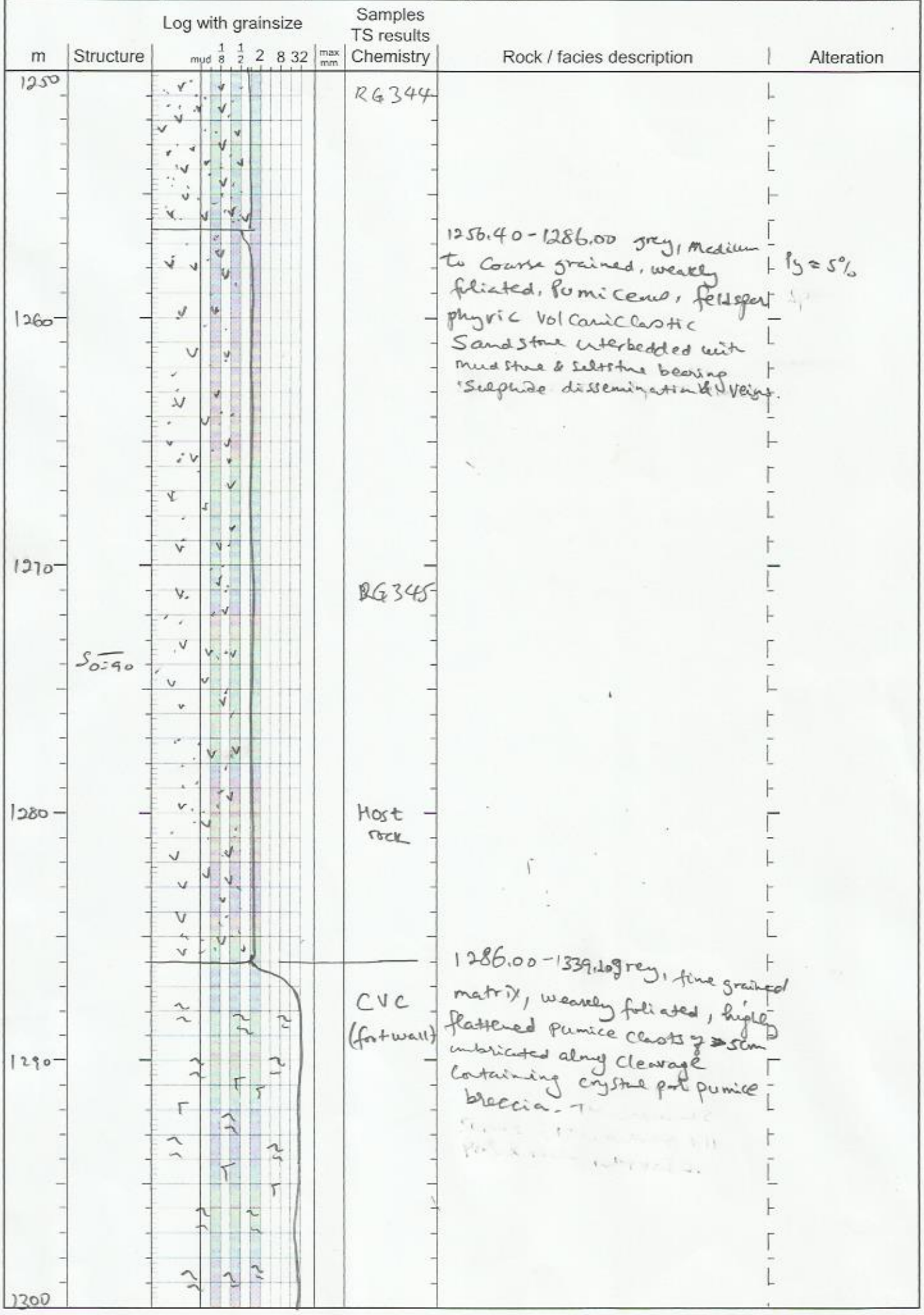

EXPLORATION SKILLS MAPPING CAMP

GRAPHIC LOG

Project Location: Rosebery		Drill hole No.: 337R	
Coords:	RL:	Scale: 1:200	Page 9 of 10
Azim:	Incl: / Diam:	Logged by: EYOB	Date 05/12/1973

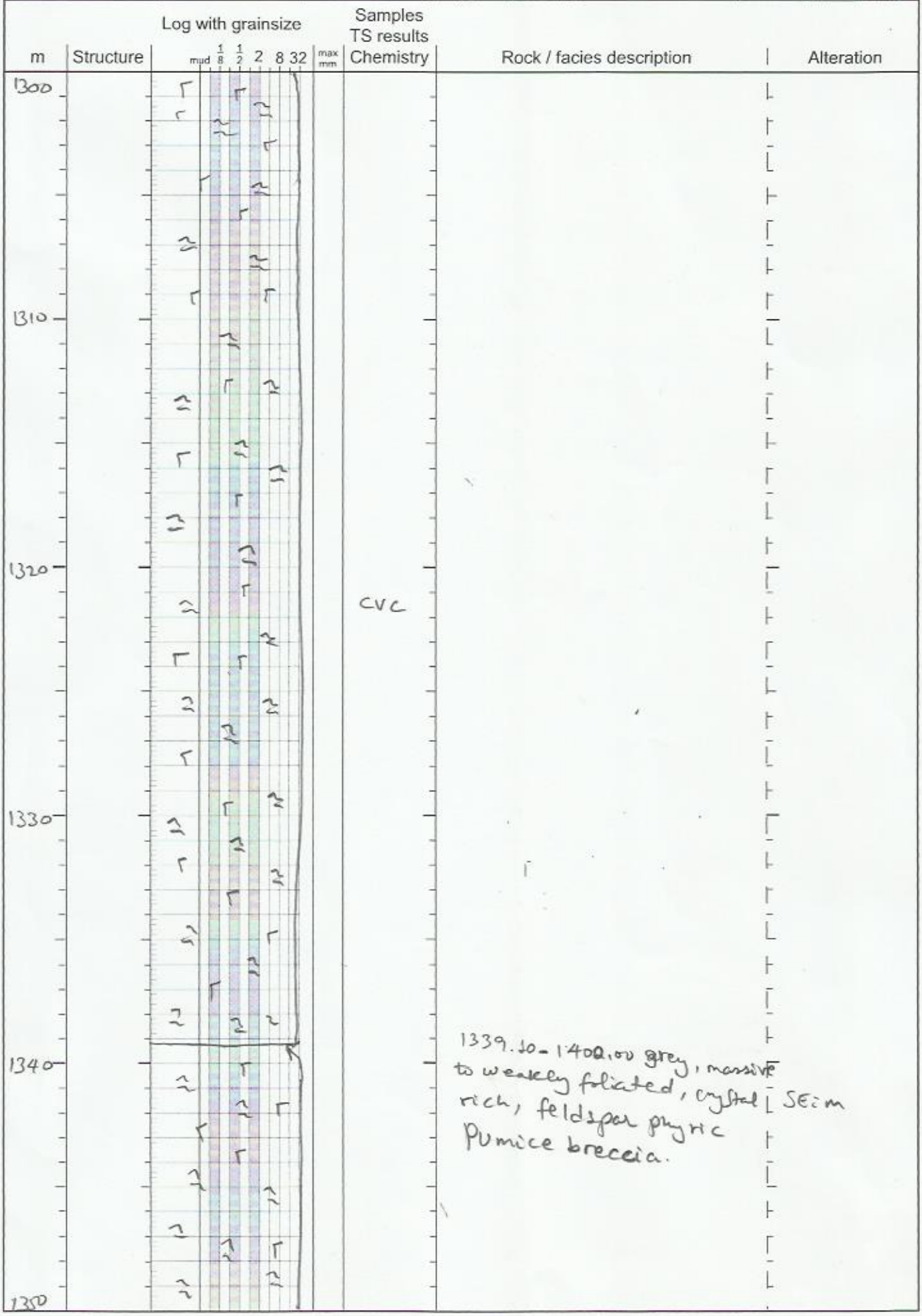

EXPLORATION SKILLS MAPPING CAMP

GRAPHIC LOG

Project Location: Rosebery		Drill hole No.: 337R	
Coords:	RL:	Scale: 1:200	Page 10 of 10
Azim:	Incl: / Diam:	Logged by: EYOB	Date 05/12/16

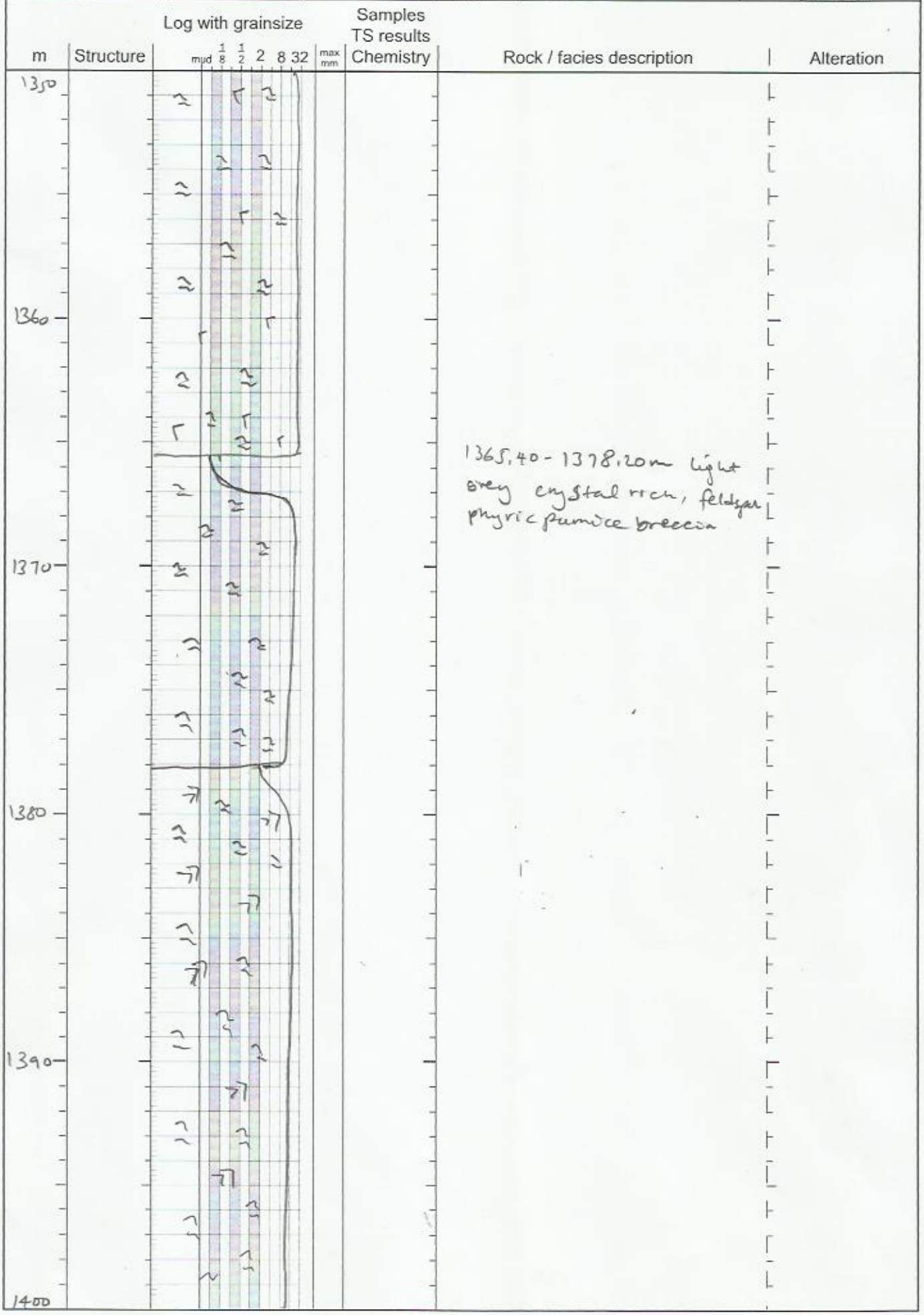

EXPLORATION SKILLS MAPPING CAMP

GRAPHIC LOG

Project Location	Rosebery	Drill hole No. Location No.	RK337-R
Coords: 379967.5E/5377212N	RL: 475.51	Scale: 1:200	Page 1 of 8
Azim: 258.98 / Incl: -83.13	Diam:	Logged by: EYOB ANDEMESKEL	Date 20/04/16

Log with grainsize (mud, 1/8, 1/2, 2, 8, 32, max mm) | Samples / TS results / Chemistry | Structure | m | Rock / facies description | Alteration

1400

1410

1420

1430

1440

1450

1439.00 – 1495.00m dark grey to greenish, massive to weakly cleaved, variably feldspar phyric with XII rich zones, & pumice breccia. The pumice breccia is weakly CL+SE altered & intensely flattened The pumice bx are >5cm long axis thickness

1439.00 – 1448.40 XII rich zone
1448.40 – 1495.60 XII poor zone.

CL=W
Se

EXPLORATION SKILLS MAPPING CAMP

GRAPHIC LOG

Project Rosebery | Drill hole No. 337R
Location | Location No.

Coords: 379967.5E / 6377212N | RL: 475.51 | Scale: 1:200 | Page 2 of 8

Azim: 258.98 | Incl: -83.13 | Diam: | Logged by: EYOB ANDEMESKEL | Date 20/04/16

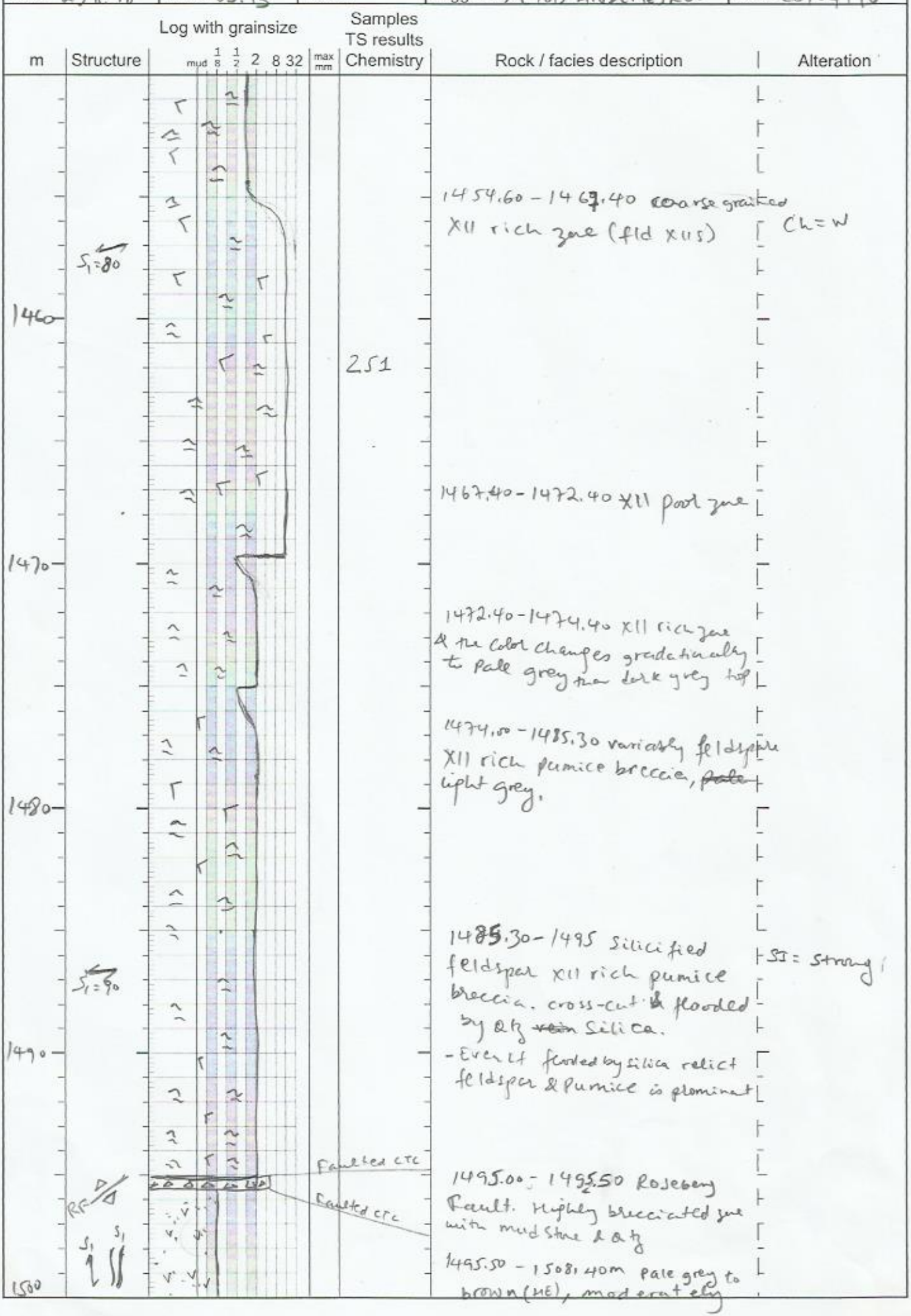

EXPLORATION SKILLS MAPPING CAMP

GRAPHIC LOG

Project Location		Drill hole No. * 337-R Location No.	
Coords:	RL:	Scale: 1:200	Page 3 of 8
Azim:	Incl:	Diam:	Logged by: EYOR / Date 2021/04/16

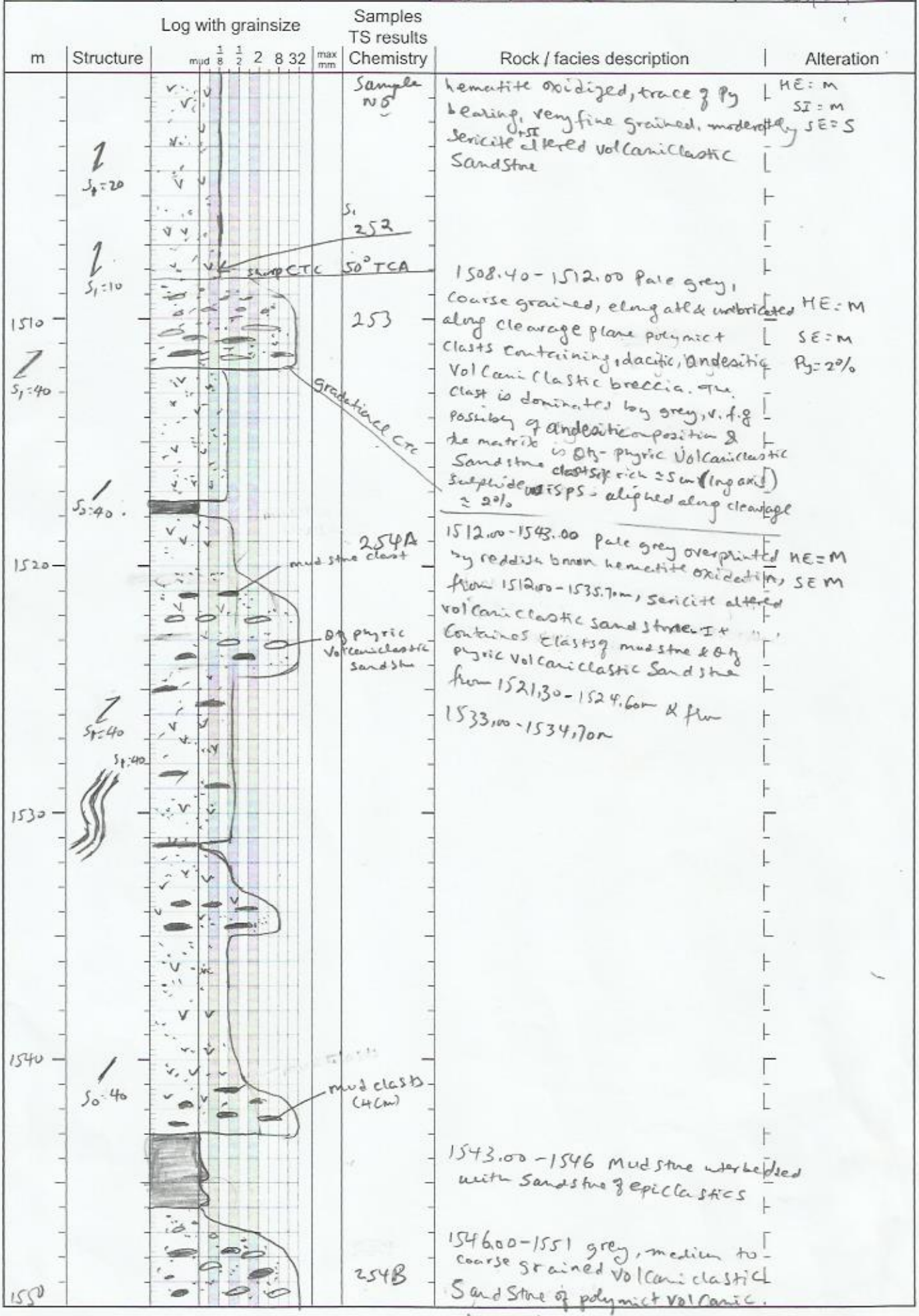

EXPLORATION SKILLS MAPPING CAMP

GRAPHIC LOG

Project / Location		Drill hole No. / Location No.	337R
Coords:	RL:	Scale: 1:200	Page 4 of 8
Azim:	Incl:	Diam:	Logged by: Date 20/04/16

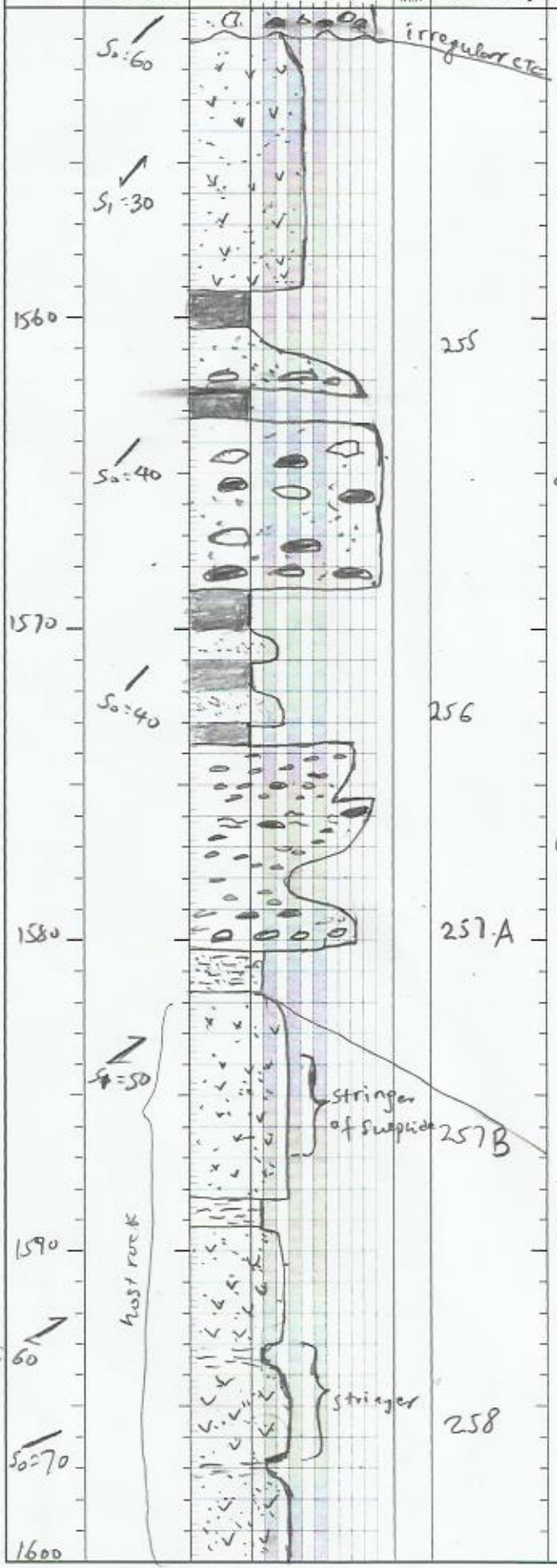

clasts are q&f-phyric (rhyolitic), mudstone, grey glassy felsic volcanic, 73cm

1551–1559 Pale grey, medium grained, speckled blebs of pyrite containing, moderately sericite altered volcaniclastic Sandstone — SE=m, Py=1-2%

1559–1560.30 dark grey, v.f.g mudstone

1560.30–1568.80 very coarse grained, polymictic volcaniclastic breccia. clast size is >6cm

clasts are f – rhyolitic
= dacite, andesite,
– mud ditricss

angular to sub-angular, poorly sorted.

It is interbedded with mudstone from 1562.30–1563.30m

1568.80–1573.70m mudstone interbeded with epiclastic Sandstone of possibly mixed provenance.

1573.70–1580.30m grey, very coarse grained, poorly sorted polymictic clasts of varying size containing volcaniclastic breccia.

clasts of dacite, andesite clasts, breccia >4cm & other silicious (glassy) clasts

1580.30–1581.60m grey, v.f.g Siltstone/mudstone. It is qtz veined from 1581–181.6m

1581.60–1600.90m grey, medium to coarse grained, top 2m prominently q&f phyric, stringer of pyrite bearing, volcaniclastic Sandstone interbedded with siltstone

1593.60–1596.8 stringer to semi & massive sulphide with about 20% Py+Sp — Py + Sp (20%)

EXPLORATION SKILLS MAPPING CAMP

GRAPHIC LOG

Project Rosebery		Drill hole No. 337R	
Location		Location No.	
Coords:	RL:	Scale: 1:200	Page 5 of 8
Azim:	Incl:	Diam:	Logged by: CTOB
			Date 2004 16

Log with grainsize (mud, 1/8, 1/2, 2, 8, 32, max mm) | Samples TS results Chemistry | Rock / facies description | Alteration

m | Structure

1600.90 – 1605.30m grey, V. f. g laminated Siltstone interbedded with minor fine grained Sandstone Contains stringer to semi-massive Sulphide lenses upto 15% (Py+Po+Sp)

15% sulphide — 259

gradational CTC

1605.30 – 1608 grey, fine grained Qtz-phyric Volcaniclastic Sandstone

260

gradational CTC

1608 – 1619.80 grey, f-g, well Cleaved, Sericite altered, trace of Pyrite dissemination & Veinlets Containing Siltstone interbedded with mudstone & minor sandstone of a mixed provenance

1611.50 – 1614.25 f-g, Volcaniclastic Sandstone interbedded with Siltstone/mudstone

15-20% Py — 261

1617.9 – 1619.60m stringer of sulphide with 15-20% Pyrite in qtz-phyric VSST

1619.80 – 1628.50m grey, well cleaved, moderately Sericite altered, Poorly Sorted, elongated & Subrounded Polymictic Volcaniclastic breccia set in very fine grained Sandstone. It grades down hole. Clast sized reaches >3 cm & is dominated by grey glassy, dacite, and dacite breccia

262

1628.50 – 1661.00m grey, v.f.g weakly cleaved, trace of Pyrite bearing v.f.g. Volcaniclastic Sandstone grading to Volcaniclastic Siltstone.

263

264

1648.30 – 1650.30 disseminated Pyrite 5-10%

Py = 5-10%

Alteration: 1600.9 – 1602.6 15% (Py + Po + Sp)

Py < 1% SE = M

Py < 1% SE = M

15-20% Py

1610 1620 1630 1640 1650

S0: 85 S1: 50 S0: 85 S1: 75 S1: 72

EXPLORATION SKILLS MAPPING CAMP

GRAPHIC LOG

Project Rosebery | Drill hole No. 337R

Location | Location No.

Coords: | RL: | Scale: 1:200 | Page 6 of 8

Azim: | Incl: | Diam: | Logged by: | Date 23/04/16

m	Structure	Log with grainsize (mud, 1/8, 1/2, 2, 8, 32, max mm)	Samples / TS results / Chemistry	Rock / facies description	Alteration
				1649.60–1650 Stringer of Sulphide with Pyrite 20–25% is noted	Py = 20–25% Sp = ~3%
	S1=70		265		
1660	S1=60				
				1661.00–1679.70 grey, V.f.g, massive to weakly cleaved, laminated trace of disseminated Pyrite bearing siltstone.	
	S1=60 S0=60				
1670					
	S1=70		266		
1680				1679.70–1681.20m dark grey, massive mudstone (Gross) cut by Qtz vein	
	S1=60	Gwk	267	1681.20–1688.75 dark grey, massive to weakly cleaved, greywacke grading down hole to mudstone → (Volcaniclastic) sandstone	
1690			~~268~~	1688.75–1726.60 Pale grey, fine grained groundmass, massive to weakly cleaved, Sericite + Silica altered, Very coarse quartz phyric 'pumice' breccia (Typical of WSF)	
	S1=60				
1700			268		

EXPLORATION SKILLS MAPPING CAMP

GRAPHIC LOG

Project
Location

Drill hole No. 337R
Location No.

Coords: | RL: | Scale: 1:200 | Page 7 of 8

Azim: | Incl: | Diam: | Logged by: | Date 23/04/16

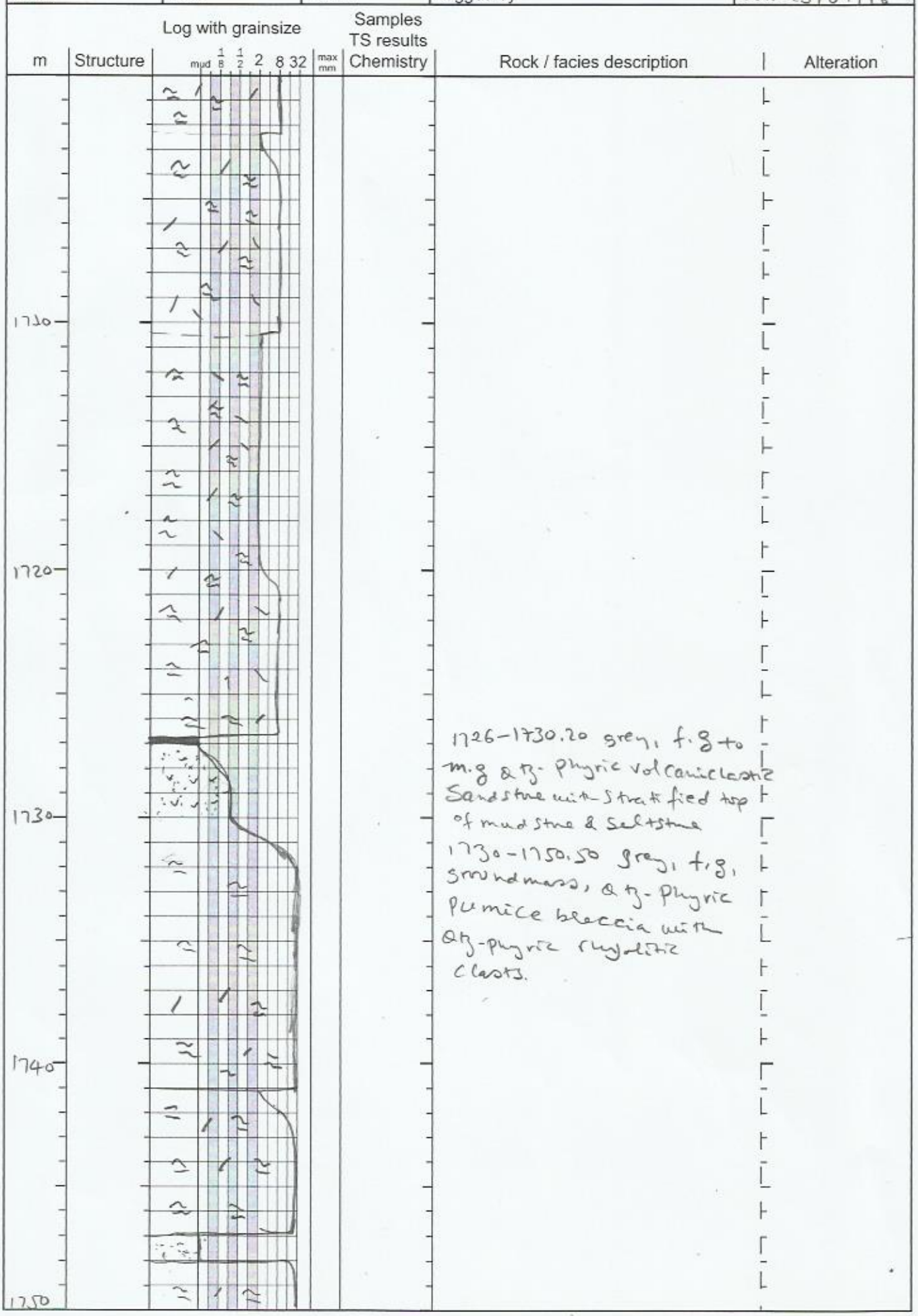

EXPLORATION SKILLS MAPPING CAMP

GRAPHIC LOG

Project Location	Rosebery	Drill hole No. Location No.	337R
Coords:		RL:	Scale: 1:200
Page 8 of 8			
Azim:	Incl:	Diam:	Logged by: EYOB
Date 23/04/16			

Log with grainsize

Samples
TS results
Chemistry

m	Structure	Log with grainsize (mud, 1/8, 1/2, 2, 8, 32, max mm)	Samples / TS results / Chemistry	Rock / facies description	Alteration
1760	J1=50		Sheared CTC	1750.50 - 1758.30 grey, fine grained matrix, massive to weakly cleaved, Qtz-fsp phyric pumice breccia of	Cl = m
			272		
				1755.20 - 1755.50 m Qtz vein	
			273		
	S1=70				
				EOH. 1758.30	

Rosebery mine Stratigraphy

EXPLORATION SKILLS MAPPING CAMP **GRAPHIC LOG**	Project Rosebery Location		Drill hole No. 397R Location No.	
Coords: 379927E 5377808N		RL: 438.4	Scale: 1:1000	Page 1 of 3
Azim: 258.98	Incl: -83.13	Diam:	Logged by: EYOB	Date 9/12/11

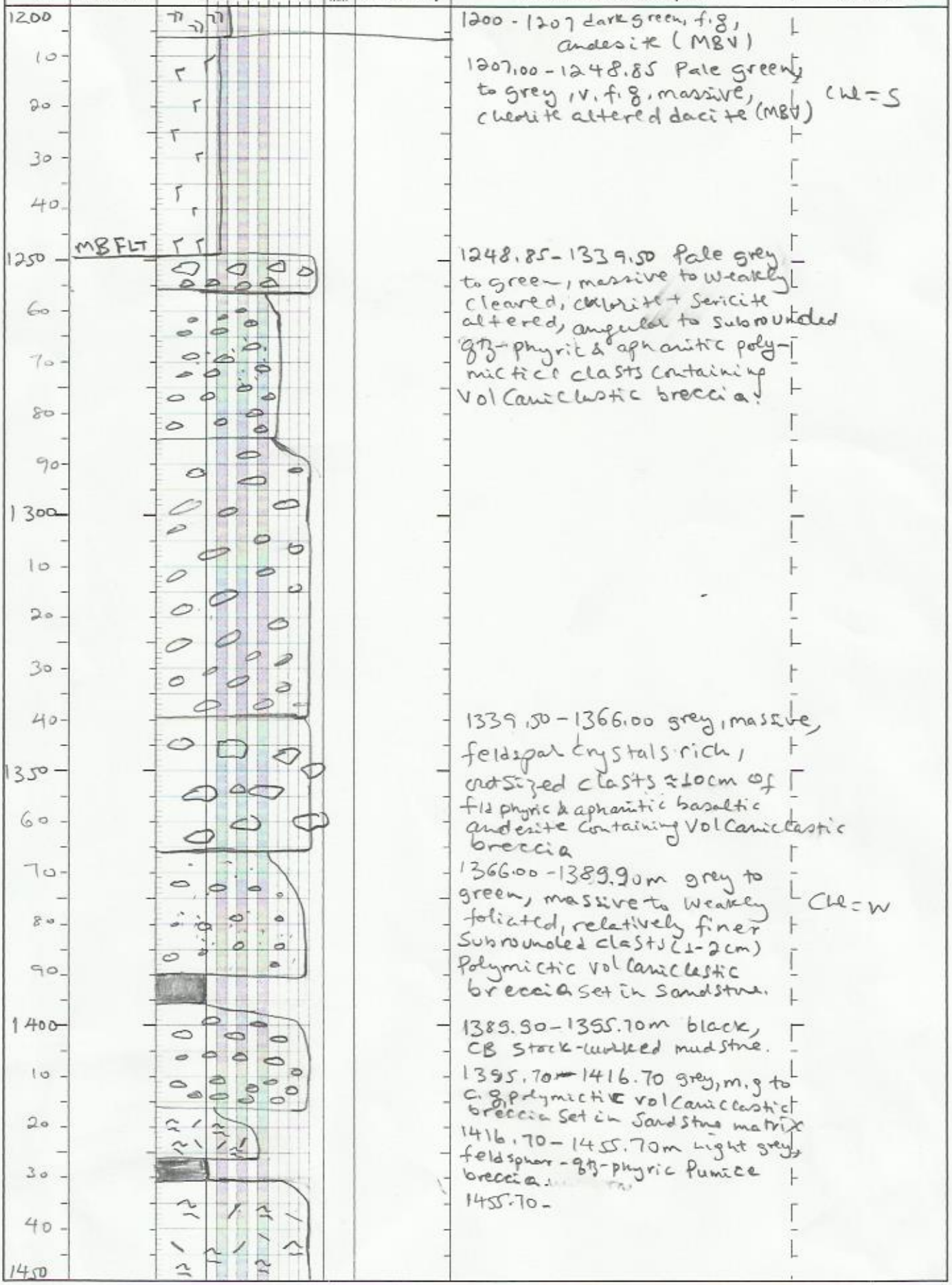

1200 - 1207 dark green, f.g, andesite (MBV)

1207.00 - 1248.85 Pale green to grey, v. f.g, massive, chloritic altered dacite (MBV) Chl=S

1248.85 - 1339.50 Pale grey to green, massive to weakly cleaved, chlorite + sericite altered, angular to subrounded qtz-phyric & aphanitic polymictic clasts containing volcaniclastic breccia.

1339.50 - 1366.00 grey, massive, feldspar crystals rich, coarsed clasts ≈10cm of fld phyric & aphanitic basaltic andesite containing volcaniclastic breccia

1366.00 - 1389.90m grey to green, massive to weakly foliated, relatively finer subrounded clasts (1-2cm) polymictic volcaniclastic breccia set in sandstone. Chl=W

1389.90 - 1355.70m black, CB stock-worked mudstone.

1395.70 - 1416.70 grey, m.g to c.g polymictic volcaniclastic breccia set in sandstone matrix

1416.70 - 1455.70m light grey, feldspar-qtz-phyric pumice breccia.

1455.70 -

EXPLORATION SKILLS MAPPING CAMP

GRAPHIC LOG

Project Rosebery | Drill hole No. 391R
Location | Location No.

Coords: | RL: | Scale: 1:1000 | Page 2 of 3

Azim: | Incl: | Diam: | Logged by: EYOB | Date 9/12/16

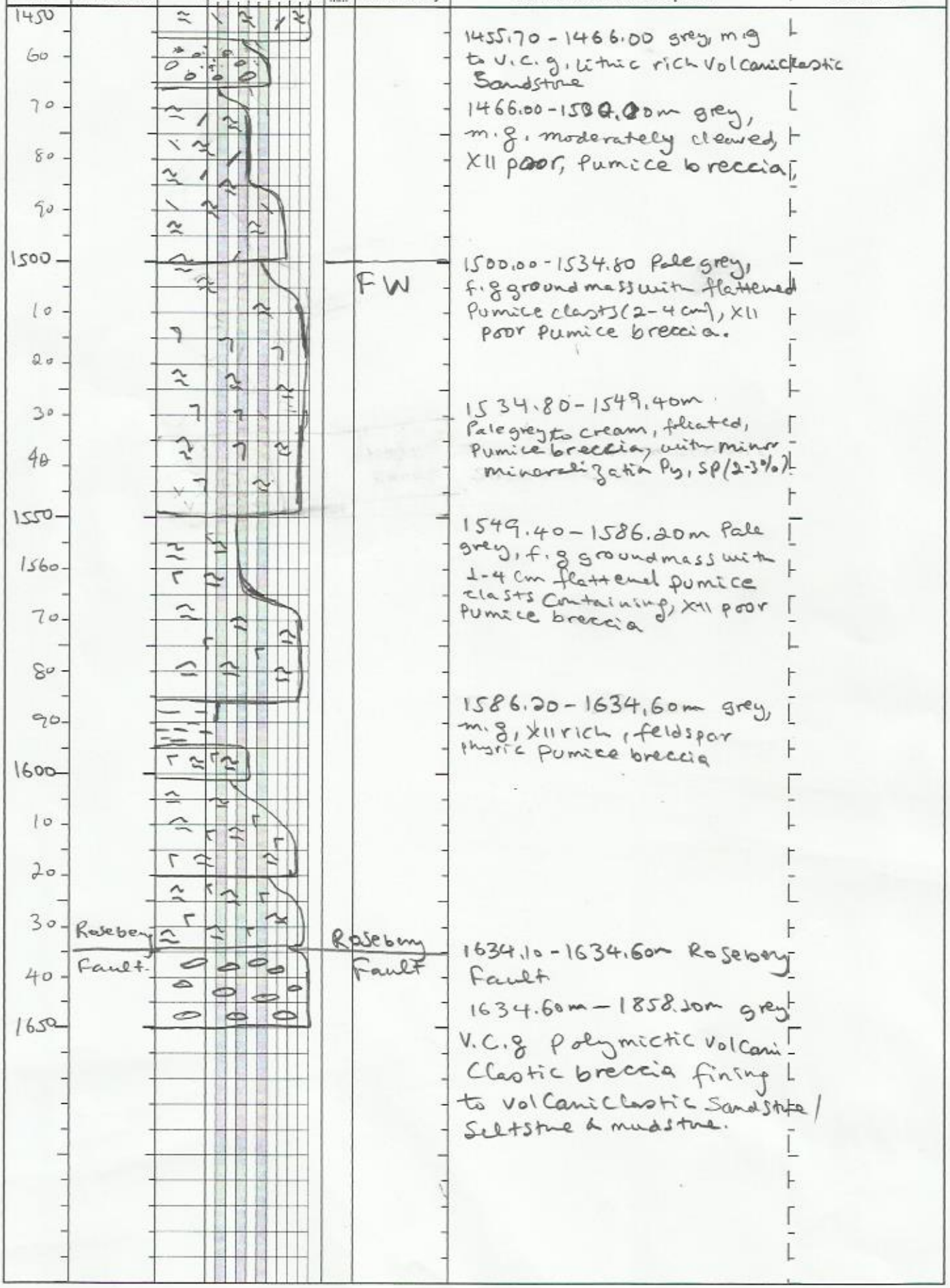

EXPLORATION SKILLS MAPPING CAMP

GRAPHIC LOG

Project Rosebery
Location

Drill hole No. 397R
Location No.

Coords: | RL: | Scale: 1:1000 | Page 3 of 3

Azim: | Incl: | Diam: | Logged by: EYOB ANDEMESKEL | Date 14/07/16

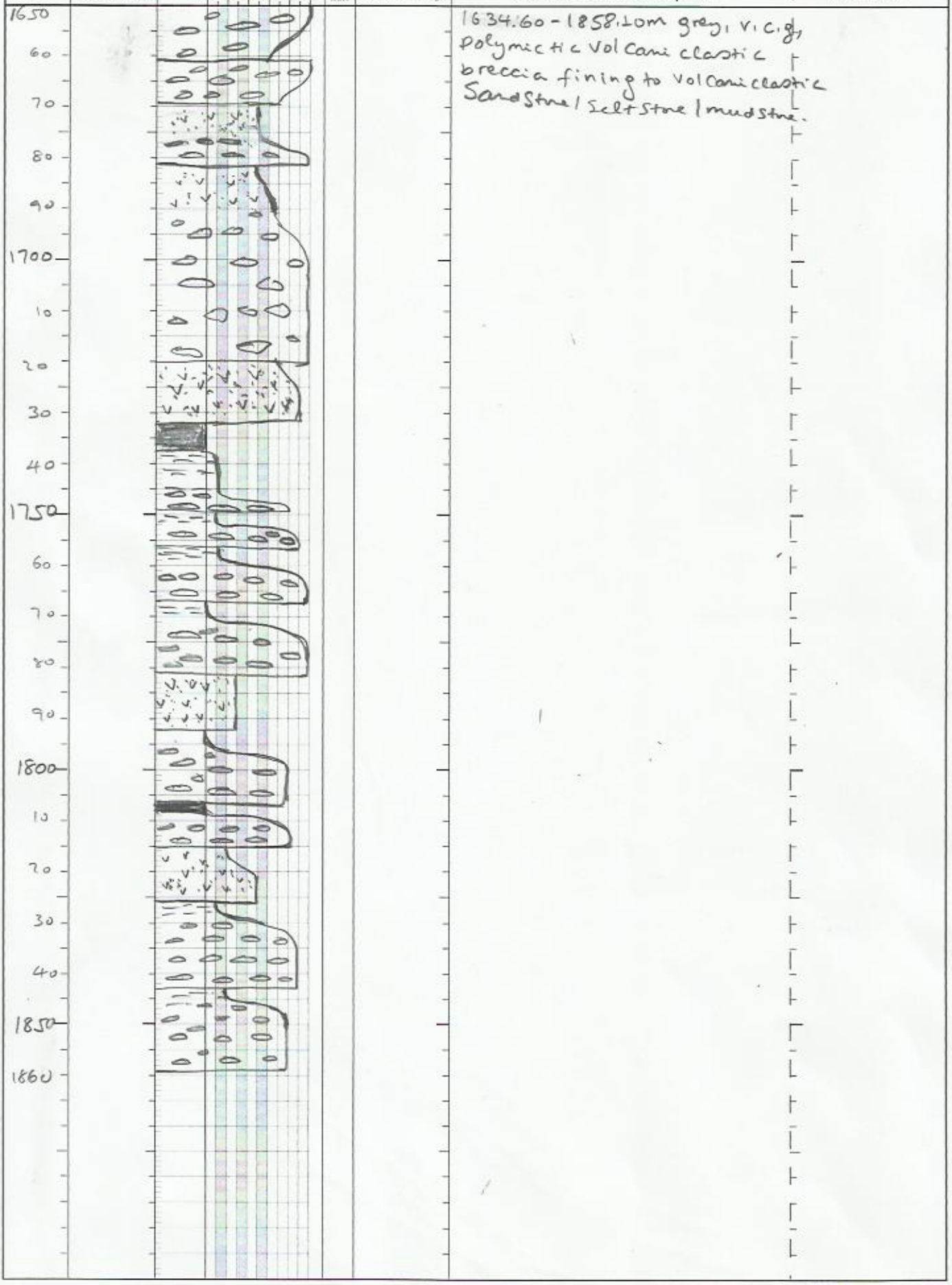

EXPLORATION SKILLS MAPPING CAMP

GRAPHIC LOG

Project Rosebery | Drill hole No. 397R
Location | Location No.

Coords: 379927E/5377808N | RL: 438.4 | Scale: 1:200 | Page 1 of 14

Azim: 258.98 | Incl: -83.13 | Diam: | Logged by: EYOB | Date 06/12/2016

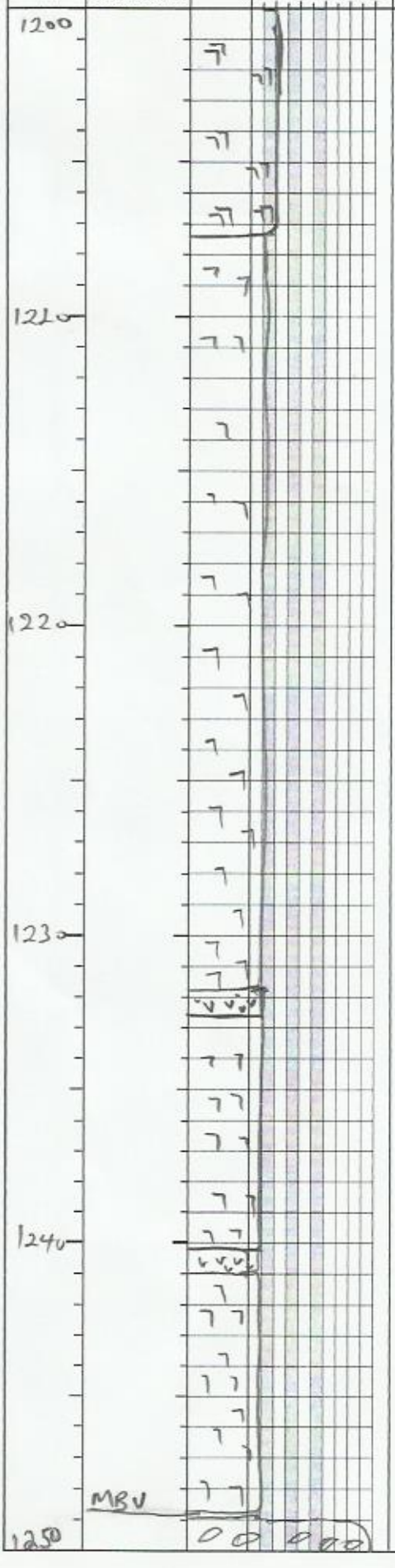

Rock / facies description

1200-1207.40m dark green f.g, massive to weakly cleaved, Qtz-CB veined Chloritic andesite (Mount black Vol Canics)

1207.40-1231.80m Pale green to grey, V.f.g, massive chlorite altered dacite (MBV)

1231.80-1232.4 dark green, massive to weakly cleaved, Patchy & disseminated Pyrite & Sphalerite bearing mafic dike.

1232.40-1240.10 Pale grey, v.f.g, massive, weakly Chlorite altered dacite

1240.10-1241.00 dark green v.f.g, mafic dike with Py & CPy

1241.00-1248.70 Pale grey to olive green, v.f.g, massive dacite (MBV)

1248.70-1248.85 Mount black fault position, the facies transition from coherent to vol Caniclastics

Alteration

Ch = S

Chl = M

Py = 3%
Sp = 2%

Chl = W

Py = 1%
CPy = 1%

EXPLORATION SKILLS MAPPING CAMP **GRAPHIC LOG**	Project Location Rosebery		Drill hole No. 397R Location No.	
Coords:		RL:	Scale: 1:200	Page 2 of #4
Azim:	Incl:	Diam:	Logged by: EYOB	Date 06/12/2016

m	Structure	Log with grainsize (mud, 1/8, 1/2, 2, 8, 32, max mm)	Samples / TS results / Chemistry	Rock / facies description	Alteration
1250			RG346	1248.85 – 1256.30m Pale grey to greenish, massive to weakly foliated, chloritic + Ser altered, angular to subrounded, quartz-phyric and aphanitic; polymictic clasts containing volcaniclastic breccia (clast size 2-5cm)	Chl = W Ser = W
1260				1256.30 – 1285.20m grey to slightly greenish, massive, well sorted, crystal-lithic rich volcaniclastic Sandstone top part of the volcaniclastic breccia - crystals are of feldspar from 1256.30 – 1276.10m & Qtz XLS from 1276.10 – 1285.00	
1270					
1280				1285.00 – 1339.50 light grey to greenish, foliated, chlorite + Sericite altered, crystal-lithic rich volcaniclastic breccia. crystals are dominantly qtz & clasts of aphanitic, glassy grey to white colored & mainly Sub-rounded of 1-3 cm - rarely feldspar porphyritic basaltic altered clasts are noted.	Cla = M Ser = M
1290			WSF 2C		
1300			RG347		

EXPLORATION SKILLS MAPPING CAMP

GRAPHIC LOG

Project
Location

Drill hole No. 347R
Location No.

Coords:

RL:

Scale: 1:200

Page 3 of 8

Azim:

Incl:

Diam:

Logged by: EYOR

Date 06/12/2016

m	Structure	Log with grainsize (mud, 1/8, 1/2, 2, 8, 32, max mm)	Samples / TS results / Chemistry	Rock / facies description	Alteration
1300					Chl = W SE = W
1310					
1320			RG348		
	S1:45				
1330			WSF 2B		CHL = W
	S1:45				
1340				1339.50 - 1366.00 grey, massive feldspar XTLS rich, outsized clasts ± 10cm of feldspar phyric & aphanitic of basalt? containing Volcaniclastic breccia	
			RG349		
1350					

EXPLORATION SKILLS MAPPING CAMP

GRAPHIC LOG

Project Location		Drill hole No. 397R Location No.	
Coords:	RL:	Scale: 1:200	Page 4 of 8
Azim:	Incl: Diam:	Logged by:	Date 06/12/2016

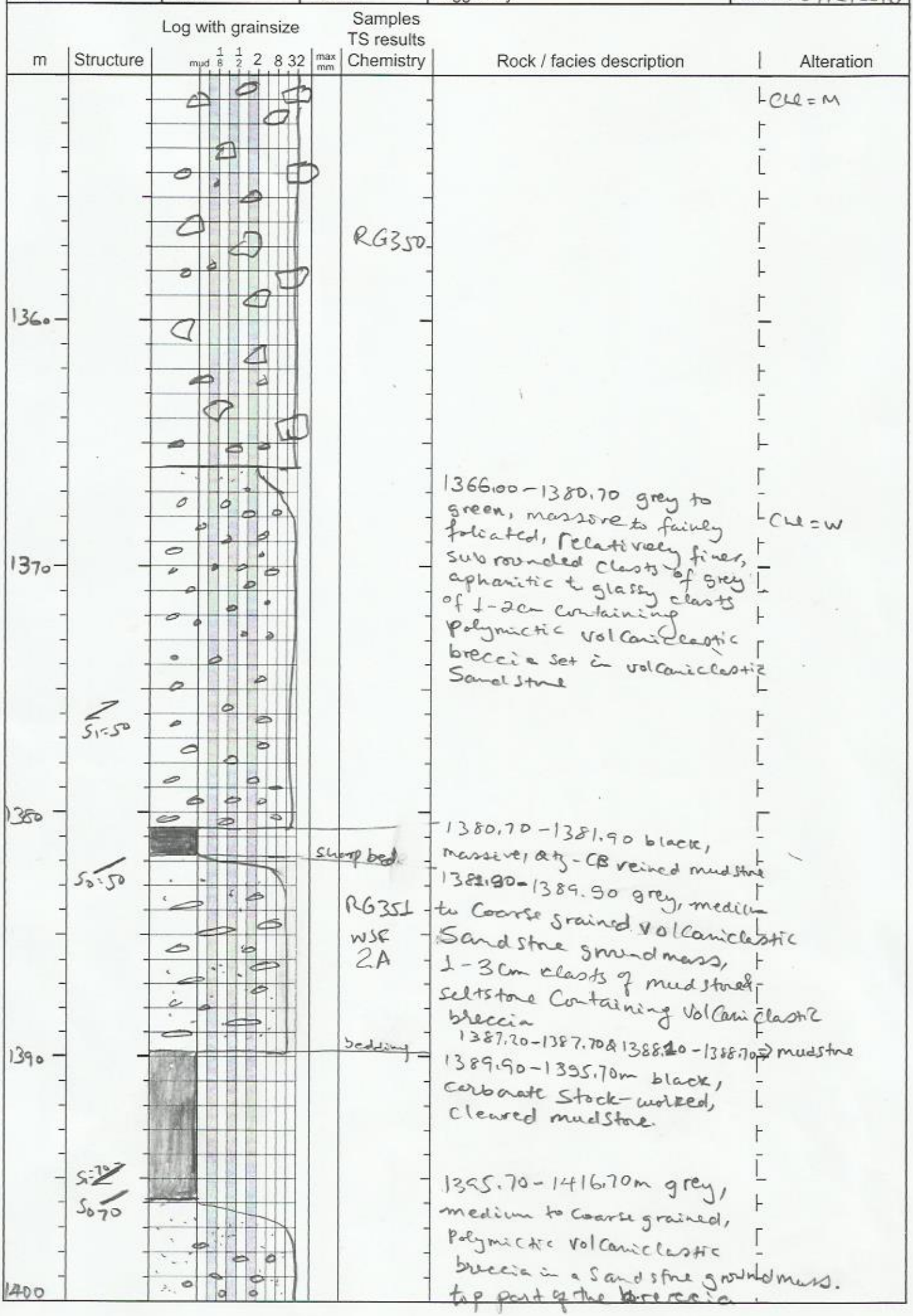

EXPLORATION SKILLS MAPPING CAMP

GRAPHIC LOG

Project
Location

Drill hole No. 397R
Location No.

Coords: | RL: | Scale: 1:200 | Page 5 of 8

Azim: | Incl: | Diam: | Logged by: | Date 06/12/2016

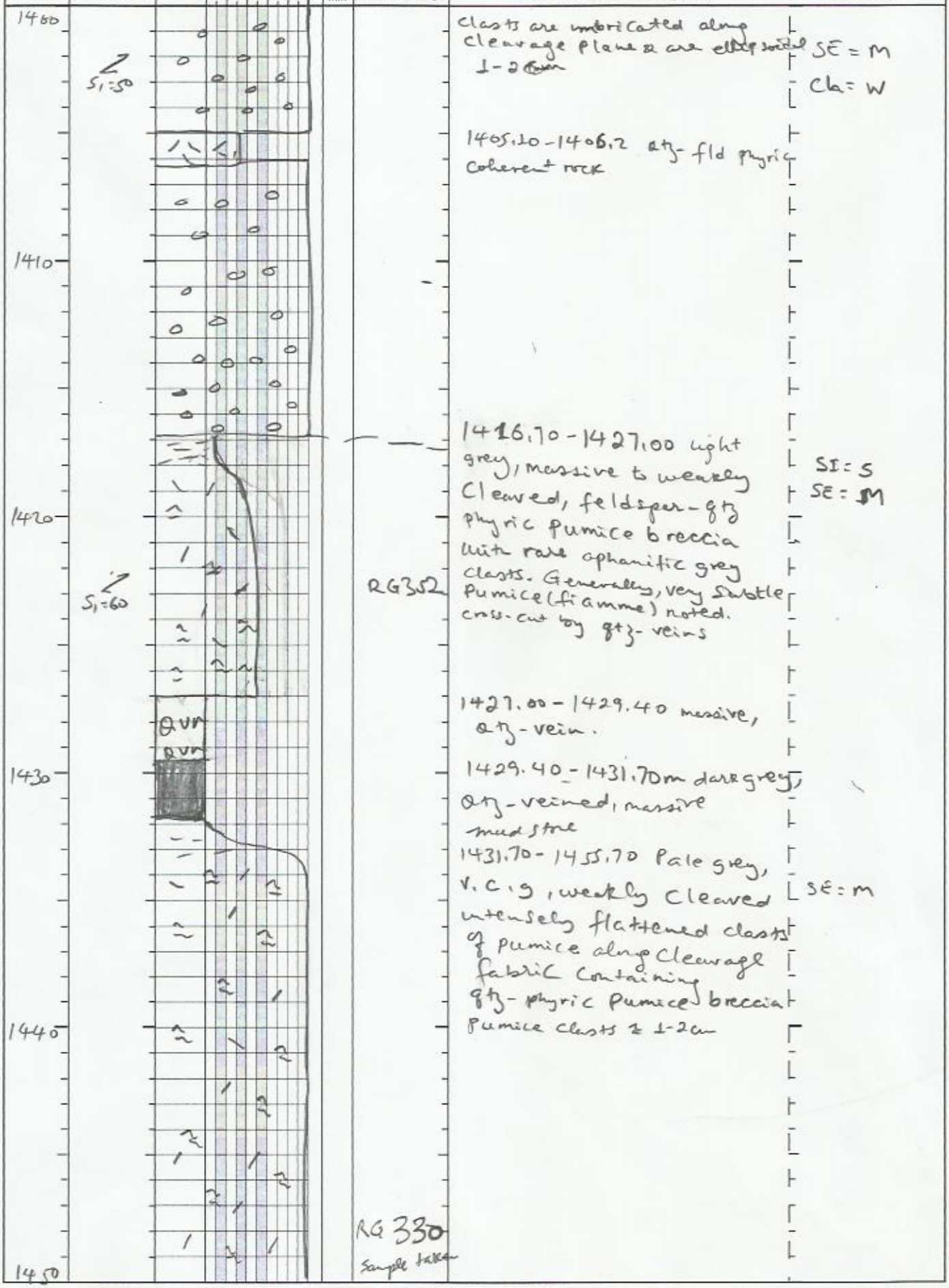

EXPLORATION SKILLS MAPPING CAMP

GRAPHIC LOG

Project
Location

Drill hole No. 397R
Location No.

Coords:

RL:

Scale: 1:200

Page 6 of 8

Azim:

Incl:

Diam:

Logged by:

Date 06/12/2016

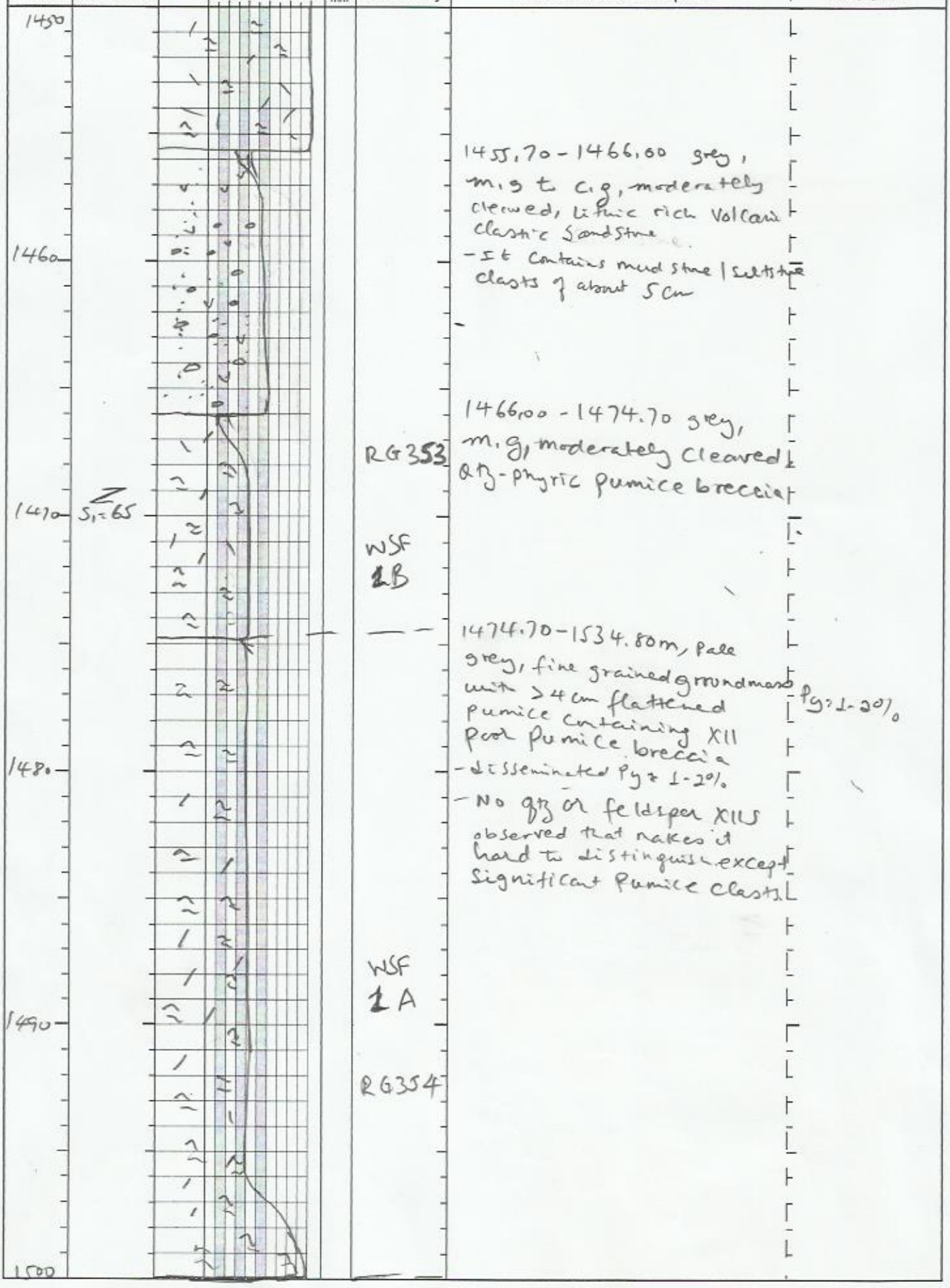

EXPLORATION SKILLS MAPPING CAMP

GRAPHIC LOG

Project / Location		Drill hole No. 397R / Location No.	
Coords:	RL:	Scale: 1:200	Page 7 of 8
Azim:	Incl:	Diam:	Logged by: / Date 07/02/16

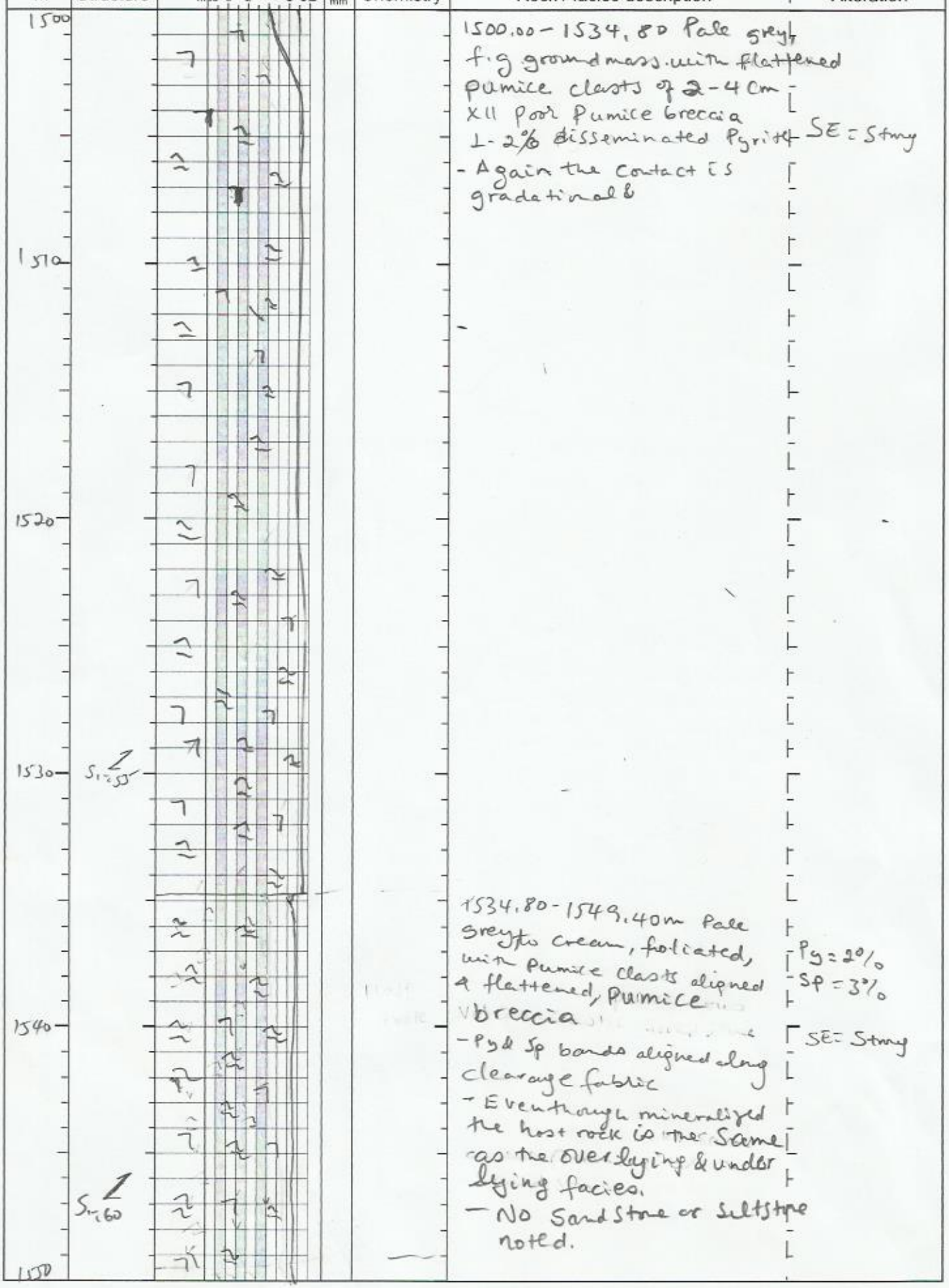

1500.00 – 1534.80 Pale grey, f.g groundmass with flattened pumice clasts of 2-4 cm XII poor Pumice breccia
1-2% disseminated Pyrite
- Again the contact is gradational &

SE = Stmy

1534.80 – 1549.40m Pale grey to cream, foliated, with Pumice clasts aligned & flattened, Pumice breccia
- Py & Sp bands aligned along cleavage fabric
- Even though mineralized the host rock is the same as the overlying & underlying facies.
- No Sandstone or Siltstone noted.

Py = 2%
Sp = 3%

SE = Stmy

EXPLORATION SKILLS MAPPING CAMP

GRAPHIC LOG

Project
Location

Drill hole No. 397R
Location No.

Coords:

RL:

Scale: 1:200

Page 8 of 8

Azim:

Incl:

Diam:

Logged by:

Date 07/12/16

m	Structure	Log with grainsize (mud, 1/8, 1/2, 2, 8, 32, max mm)	Samples / TS results / Chemistry	Rock / facies description	Alteration
1550				1549.40 - 1586.20m Pale grey, f.g ground mass with 1-4 cm flattened Pumice clasts containing, XII poor Pumice breccia. There is no qtz or feldspar to distinguish except it lies below the mineralization	
1560					
1570					
1580					
1590				1586.20 - 1594.20m grey, f.g, cleaved & laminated volcaniclastic Sandstone interbedded with volcaniclastic Siltstone.	
1600				1594.20 - 1634.10 grey, m.g, XII rich, feldspar phyric Pumice breccia	

EXPLORATION SKILLS MAPPING CAMP

GRAPHIC LOG

Project / Location		Drill hole No. 347R / Location No.	
Coords:	RL:	Scale: 1:200	Page 9 of 10
Azim:	Incl:	Diam:	Logged by: / Date 14/07/16

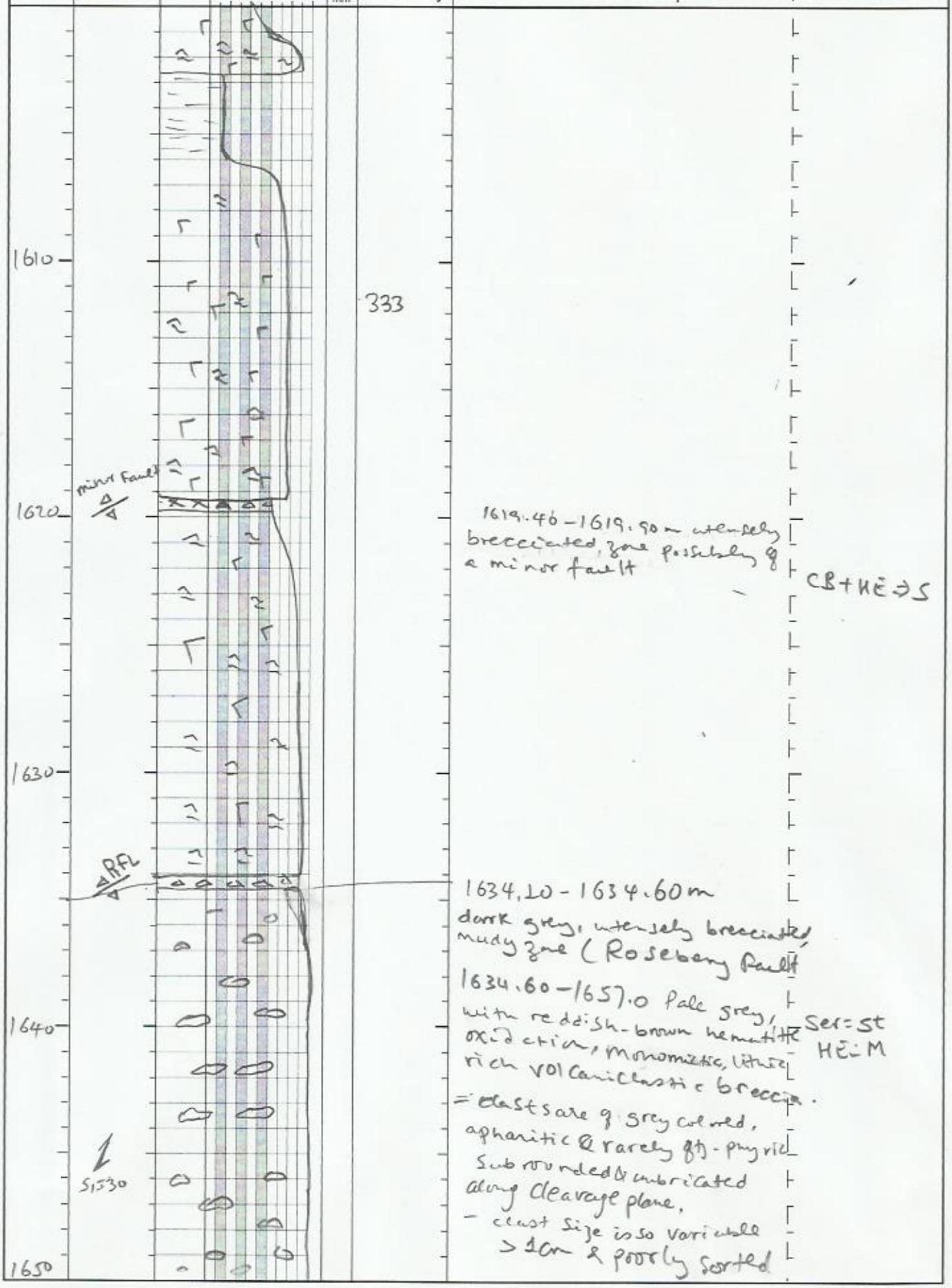

EXPLORATION SKILLS MAPPING CAMP

GRAPHIC LOG

Project
Location

Drill hole No. 397R
Location No.

Coords: | RL: | Scale: | Page 10 of 10

Azim: | Incl: | Diam: | Logged by: | Date 14/07/16

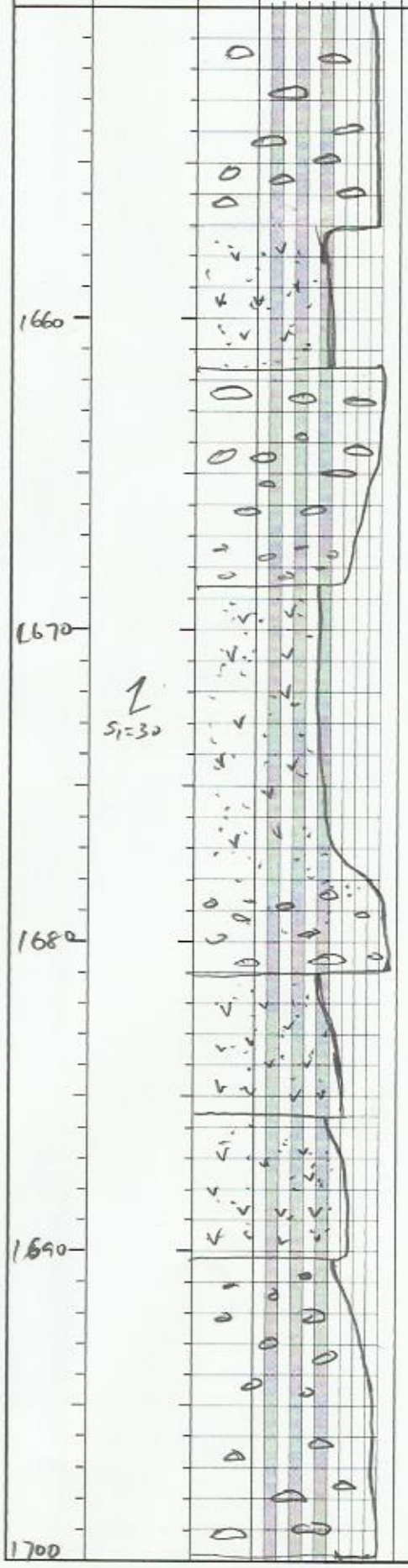

Samples
TS results
Chemistry

334

Rock / facies description

The matrix is mainly Qtz-pyric Volcaniclastic Sandstone

1657.00 - 1681.60 Pale grey with brown hematite oxidation coarse base with polymict volcanic breccia fining to Volcaniclastic Sandstone.

1661.60 - 1668.60 Pale grey, Coarse grained, cleaved, grading downhill, Subrounded glassy, grey, clasts 1-2cm containing polymict volcaniclastic breccia.

1668.60 - 1690.10 Pale grey, m.g, cleaved at low angle to CA, lithic ric Volcaniclastic Sandstone with a v.c.g breccia base.

1690.10 - 1723.20 grey, v.c.g, moderately cleaved, Subrounded clasts, imbricated along cleavage, polymict volcaniclastic breccia. clasts are mainly aphanitic glassy grey colored with minor ~~extra~~ outsized mudstone clasts

Alteration

SE:S
Clim

EXPLORATION SKILLS MAPPING CAMP

GRAPHIC LOG

Project
Location

Drill hole No. 397R
Location No.

Coords: | RL: | Scale: 1:200 | Page 11 of 14

Azim: | Incl: | Diam: | Logged by: | Date 14/05/16

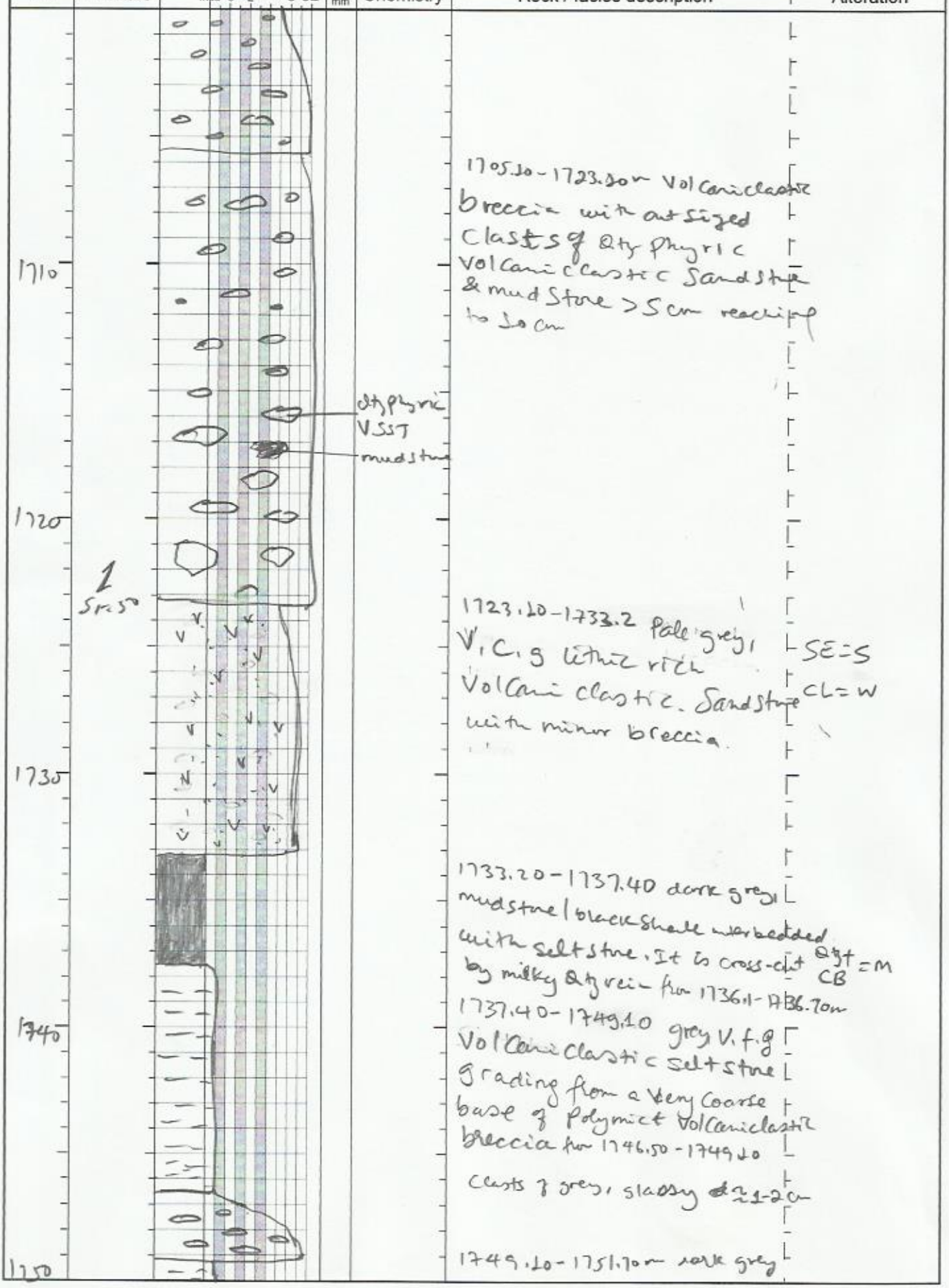

EXPLORATION SKILLS MAPPING CAMP

GRAPHIC LOG

Project Location: Rosebery

Drill hole No. 397R

Location No.

Coords:

RL:

Scale: 1:200

Page 12 of 14

Azim:

Incl:

Diam:

Logged by: EYOB

Date 14/07/16

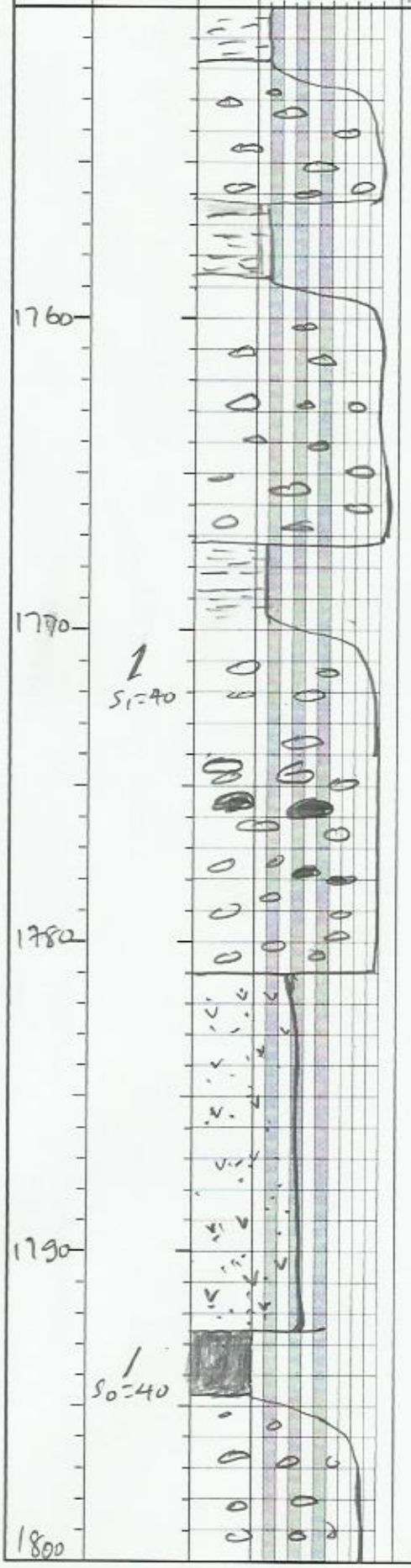

Rock / facies description

Alteration

Siltstone/mudstone. It Contains Stringers of Pyrite & looks Same host rock to R10032 — Py ≈ 10%

1751.70 – 1756.20m grey to light green, weakly cleaved, Polymictic Volcaniclastic breccia. It grades to the top Siltstone part of one flow

1758.20 – 1758.40m dark grey Siltstone/mudstone. massive to weakly cleaved with carbonate alteration — CB=m

1758.40 – 1767.20m. Grey, V.C.g polymictic volcaniclastic breccia. It is partly silted with Subrounded grey, glassy clasts ≈ 2cm — SE=s, CB=m

1767.20 – 1781.00 grey, V.C.g weakly cleaved, polymictic Volcaniclastic breccia. It Contains outsized mudstone clasts 4–7cm

1781.00 – 1792.40 grey, m.g weakly cleaved, Volcaniclastic Sandstone

1792.40 – 1794.60m dark grey, laminated & weakly cleaved mudstone

1794.60 – 1806.70m grey, polymictic C.g Volcaniclastic breccia with mudstone ~~extra~~ clasts.

EXPLORATION SKILLS MAPPING CAMP

GRAPHIC LOG

Project Location: Rosebery

Drill hole No. 397R

Location No.

Coords:

RL:

Scale: 1:200

Page 13 of 14

Azim:

Incl:

Diam:

Logged by: EYOB

Date

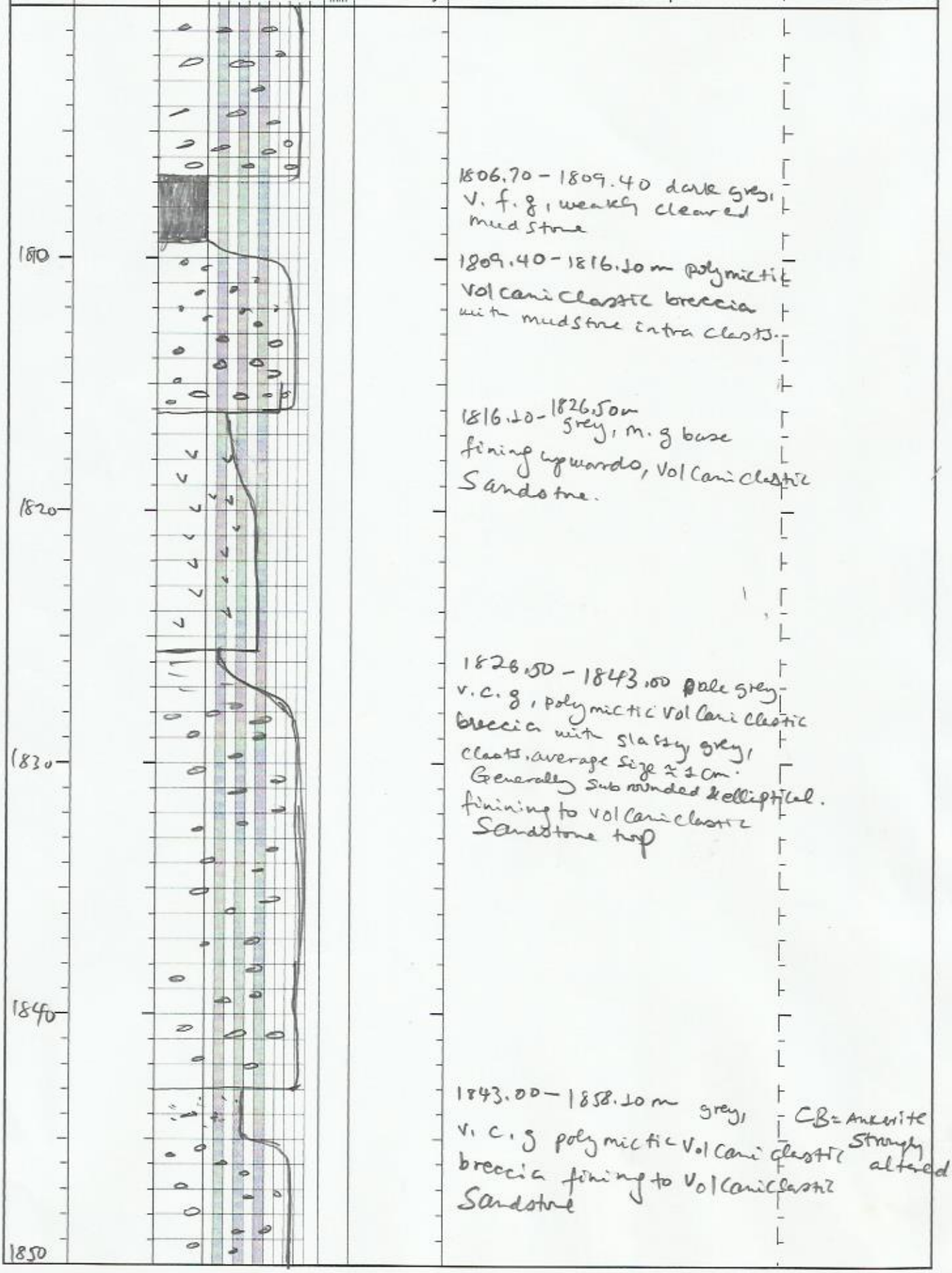

EXPLORATION SKILLS MAPPING CAMP

GRAPHIC LOG

Project / Location: Rosebery		Drill hole No. / Location No.: 397R	
Coords:	RL:	Scale: 1:200	Page 14 of 14
Azim:	Incl:	Diam:	Logged by: EOB / Date: 14/07/16

Log with grainsize (mud, 1/8, 1/2, 2, 8, 32, max mm) | Samples / TS results / Chemistry | Rock / facies description | Alteration

m

1860

Alteration: Ank = S

EXPLORATION SKILLS MAPPING CAMP

GRAPHIC LOG

Project Rosebery		Drill hole No. 4HR-D1	
Location		Location No.	
Coords:	RL:	Scale: 1:1000	Page 1 of 2
Azim:	Incl:	Diam:	Logged by: EYOB / Date 16/06/16

Log with grainsize | Samples TS results | Chemistry

m	Structure	mud 1/8 1/2 2 8 32 mm	Rock / facies description	Alteration
1200			1200 - 1202.2 Qtz-CB altered mud stone	
			1202.2 - 1222.90 Pale grey weakly cleaved, intensely flattened clasts at the base containing, Qtz-phyric polymictic volcaniclastic breccia with minor Pumice	
			1222.90 - 1257.10 massive to weakly cleaved, Pumice containing polymictic volcaniclastic breccia, clasts are glassy, angular, (grey) poorly sorted	
1250			1257.10 - 1300.00 Pale grey m.g, lithic rich volcaniclastic breccia with minor Pumice	
1300				

Summary Log

EXPLORATION SKILLS MAPPING CAMP
GRAPHIC LOG

Project Location

Drill hole No. 411R-D1
Location No.

Coords: 37g 741.8E 1537839N | RL: | Scale: 1:1000 | Page 2 of 2

Azim: 66 | Incl: -86 | Diam: | Logged by: E40R F. ANDEMESKEL | Date

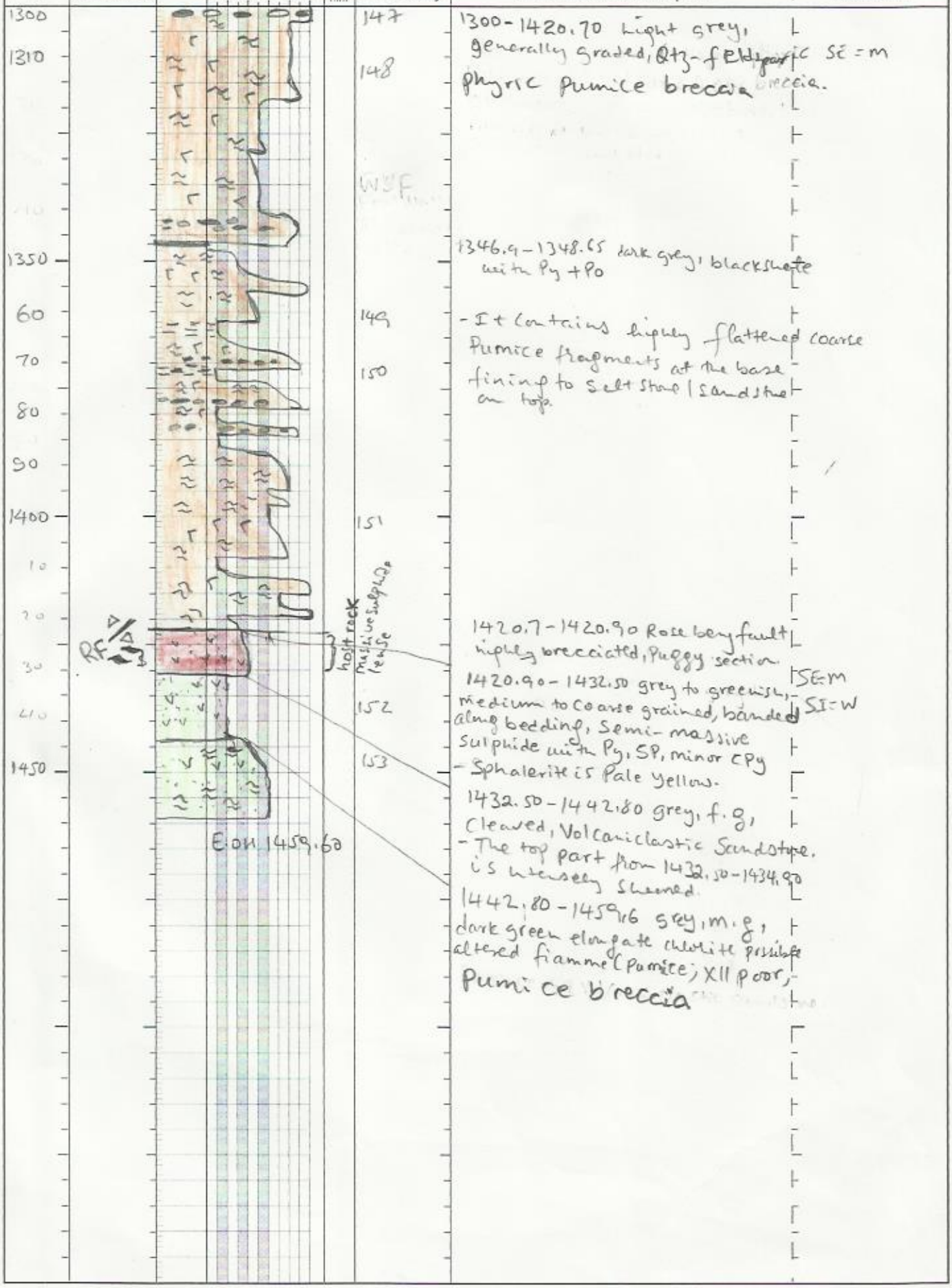

$ massive to semi-massive sulphide lense

1200 - 1300

EXPLORATION SKILLS MAPPING CAMP

GRAPHIC LOG

Project Location: Rosebery

Drill hole No.: 411R-D1

Location No.:

Coords: 379741.8E / 5378393N

RL: 380A

Scale: 1:200

Azim: 66

Incl: -86

Diam:

Logged by: EYOB

Date: 16/06/16

Log with grainsize (mud | 1/8 | 1/2 | 2 | 8 | 32 | max mm)

Samples
TS results
Chemistry

m	Structure	Chemistry	Rock / facies description	Alteration
1200			MRBFLT	
			1202-1222.90 Pale grey, weakly cleaved, intensely flattened lenticular clasts at the base containing qtz-phyric polymictic Vol Caniclastic breccia with minor pumice	
1210		395112		
1220		395113		
			1222.90 - 1257.10 grey, massive to weakly cleaved qtz-feldphyric, pumice containing polymictic Vol caniclastic breccia. The clasts are subang & angular, grey colored & are poorly sorted.	
		328		
1230		395114		
1340		395115		
1250		395116		

Sample

EXPLORATION SKILLS MAPPING CAMP

GRAPHIC LOG

Project Rosebery
Location

Drill hole No. 41R-D1
Location No.

Coords:

RL:

Scale: 1:200

Page 2 of 6

Azim:

Incl:

Diam:

Logged by: EYDS

Date 16/06/14

Log with grainsize

Samples
TS results
Chemistry

m	Structure	mud 1/8 1/2 2 8 32 max mm	Chemistry	Rock / facies description	Alteration
1260			1355117	1257.10 – 1308.20m Pale grey, medium grained, crystal-phyric pumice (fiamme) containing lithic rich volcaniclastic breccia	
1270			1355118		
1280			1355119		
1290			1355120		
1300			1355121		

EXPLORATION SKILLS MAPPING CAMP

GRAPHIC LOG

Project
Location

Drill hole No. 411R-D1
Location No.

Coords: 379741.8E / 5378353N | RL: | Scale: 1:200 | Page 3 of 6

Azim: 66 | Incl: -86 | Diam: | Logged by: E4DB F. ANDEMESKEL | Date 26/02/16

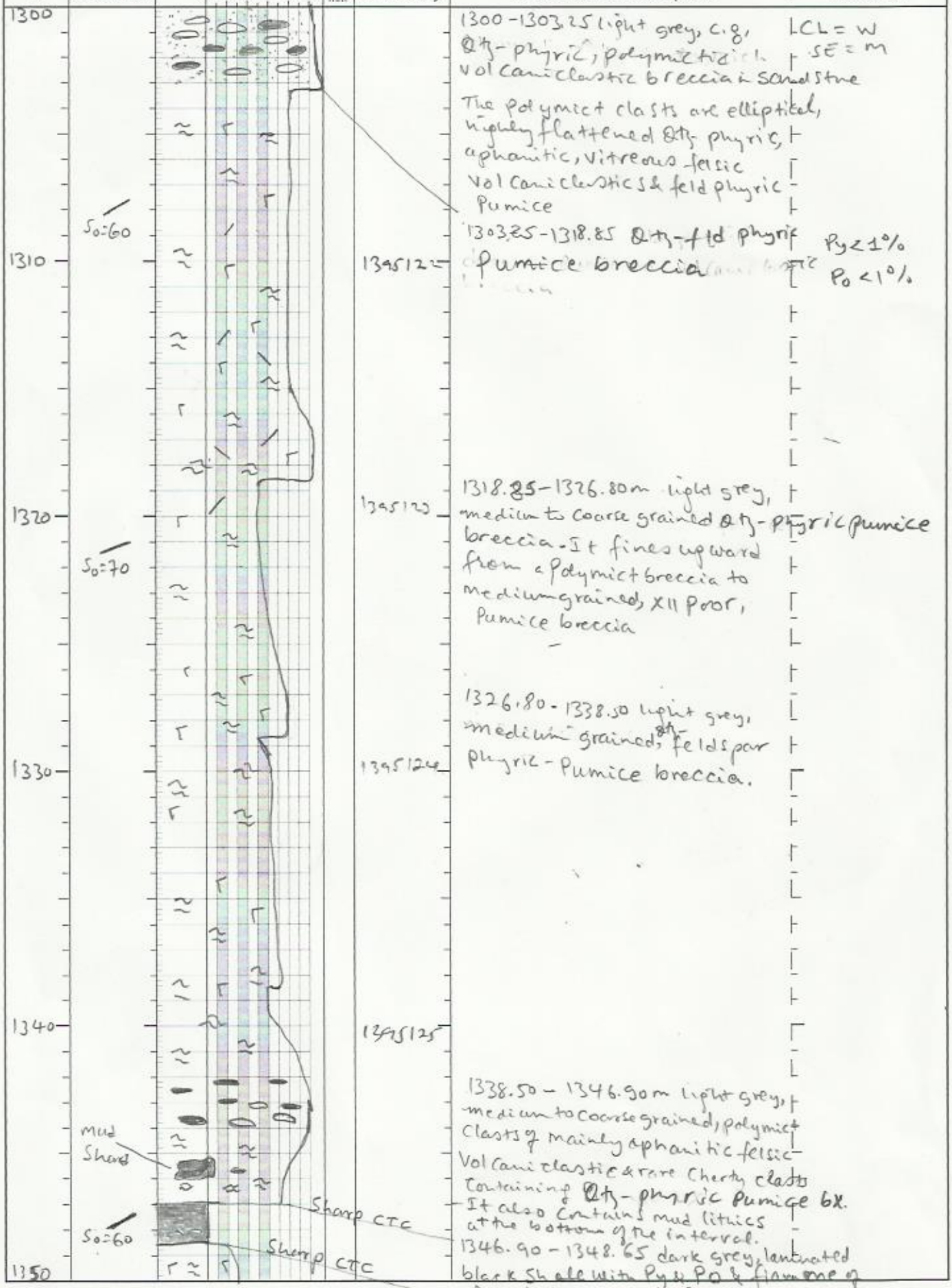

EXPLORATION SKILLS MAPPING CAMP

GRAPHIC LOG

Project / Location		Drill hole No. / Location No.	411R-D1
Coords:	RL:	Scale: 1:200	Page 4 of 6
Azim:	Incl:	Diam:	Logged by: EYOB Andemeskeel / Date 26/02/16

Log with grainsize (mud, 1/8, 1/2, 2, 8, 32, max mm) | Samples TS results Chemistry

m | Structure | Rock / facies description | Alteration

1348.65–1363.30m light grey, m-c g, weakly SE+ch altered, rare fiame containing, Qtz–fld phyric pumiscle breccia.

- Stks mainly feld XII rich from 1353.50 – 1359.00

- Volcaniclastic Bx with flattened Qtz-feld porphyritic clasts from 1355.9 – 1356.80m

TS 412

1360 — 1395127

Sharp bed

S_o=80

1363.30–1372.2 light grey, fine grained top 8m, feldspar phyric pumice breccia Volcaniclastic Breccia – The clasts are quartz-feldspar porphyritic & the pumice raft is feldspar phyric clast size ranges from 1cm – 5cm are ellipsoidal & flattened — Si = W

60/ S_o

1370 — 1395128

Sharp CTC

1372.2–1374.20m, grey, v.f.g planar laminated, volcaniclastic siltstone to interbedded with volcaniclastic Sandstone.

Sharp CTC

1374.20–1378.10m grey, graded upward from very coarse grained Qtz-phyric clastic to siltstone/mudstone Pumice breccia with pumice Bx. The clasts are all flattened.

1380 — 1395129

1378.10–1384.00 light grey, weakly foliated, Volcaniclastic Sandstone – graded fine to m.g with V.C.g clastic Bx bottom — Si = W

1384.20–1407.65m, grey, medium to coarse grained Qtz-phyric pumice breccia

CL = strong

1390 — 1395130

1384.20–1385.50 i+ is V.f.g siltstone interbedded with v.f.g SST

c.g ≥ 2mm

Clasts of Qtz-phyric reach upto 3.5cm on the bottom of the faces & are elongated & flattened

XIIs of Pyrrhotite, Py & cPy as veins & Patches are noted from 1397.80–1398.00m — Pyrr, Py, cPy } < 1%

1399.50–1407.65m the unit is XII rich Coars grained

1400 — 1395131

EXPLORATION SKILLS MAPPING CAMP

GRAPHIC LOG

Project Location

Drill hole No. 411R-D1
Location No.

Coords: | RL: | Scale: 1:200 | Page 5 of 6

Azim: | Incl: | Diam: | Logged by: EYOB ANDEMESKEL | Date 26/02/16

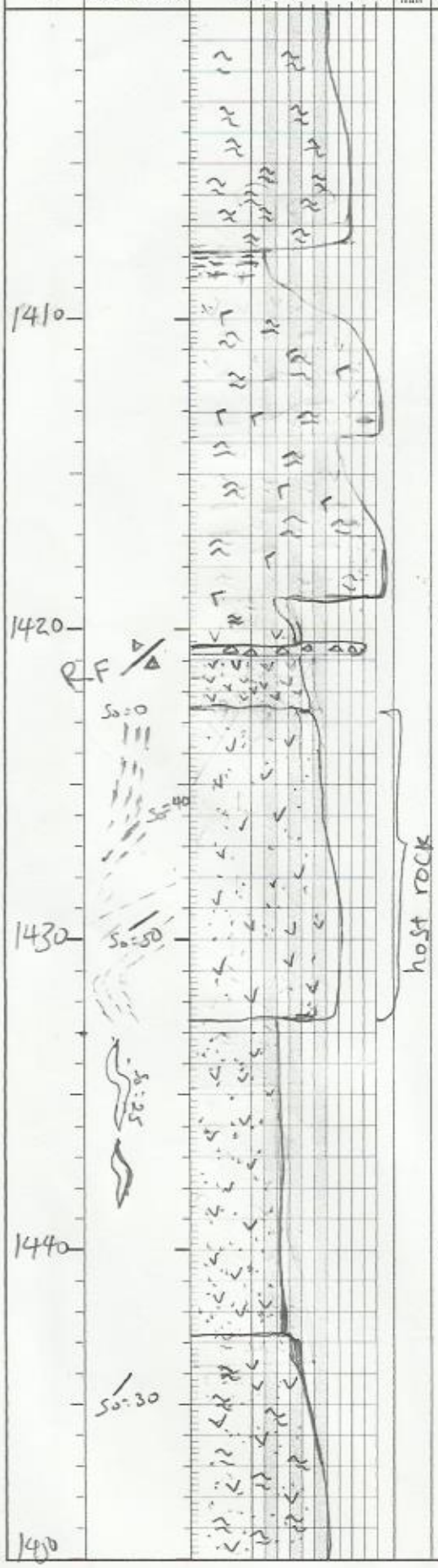

Samples
TS results
Chemistry

1395132
1395133
1395134
1395135

1407.65-1413.90m Light grey, graded, Qtz phyric Pumiceous Volcaniclastic Breccia with lappilli of feldspar phyric clasts (1-2cm)

1413.90-1419 Pale grey, Qtz-phyric pumice breccia

1419.00-1420.70 Light grey, f.gr, fld phyric Volcaniclastic Pumice Lx

1420.7-1420.90 Rosebery fault, grey, strongly brecciated, crumbly Partly pumiceous, coarse sand & angular clasts.

1420.90-1422.40 Pale grey to greenish, fine grained, weakly SE+SI altered, Qtz-phyric Volcaniclastic sandstone containing stringers of Pyrite, Sphalerite

1422.40-1432.50 grey to greenish fine to medium grained, banded along bedding semi-massive Sulphide with Py, SP, rare CPy - Sphalerite is Pale yellow

1432.50-1442.80m grey, pumiceous fine grained, cleaved, Volcaniclastic Sandstone. The top part from 1432.50-1434.90m is intensely sheared & contains Sulphide stringers of <5% Py

1442.80-1459.60 grey, medium grained, dark green elongated Chlorite altered fiamme (Pumice) Containing 1 XII poor, Pumiceous Brecciated Sandstone
- It is moderately cleaved

Alteration

SE=M
Py=10%
SP=3%
Py=2S
SP=20%
CPy=3%
Py<5%
SE:M
SI:W
SE:M
CL:WW

EXPLORATION SKILLS MAPPING CAMP

GRAPHIC LOG

Project
Location

Drill hole No. 411R-D1
Location No.

Page 6 of 6

Coords:

RL:

Scale: 1:200

Azim:

Incl:

Diam:

Logged by: EYOB ANDEMESKE

Date 26/02/16

m	Structure	Log with grainsize (mud, 1/8, 1/2, 2, 8, 32, max mm)	Samples / TS results / Chemistry	Rock / facies description	Alteration
1450				1434.90 – 1442.8m it is very fine grained, X11 poor Pumiceous breccia	
	S:30			1442.8 – 1459.60m the unit medium to coarse grained Pumice breccia	
1460		E.O.H 1459.60			

Summary log

EXPLORATION SKILLS MAPPING CAMP
GRAPHIC LOG

Project Rosebery
Location

Drill hole No. BP272
Location No.

Coords:
RL:
Scale: 1:1000
Page 2 of 2

Azim:
Incl:
Diam:
Logged by: EYOB
Date 22/06/16

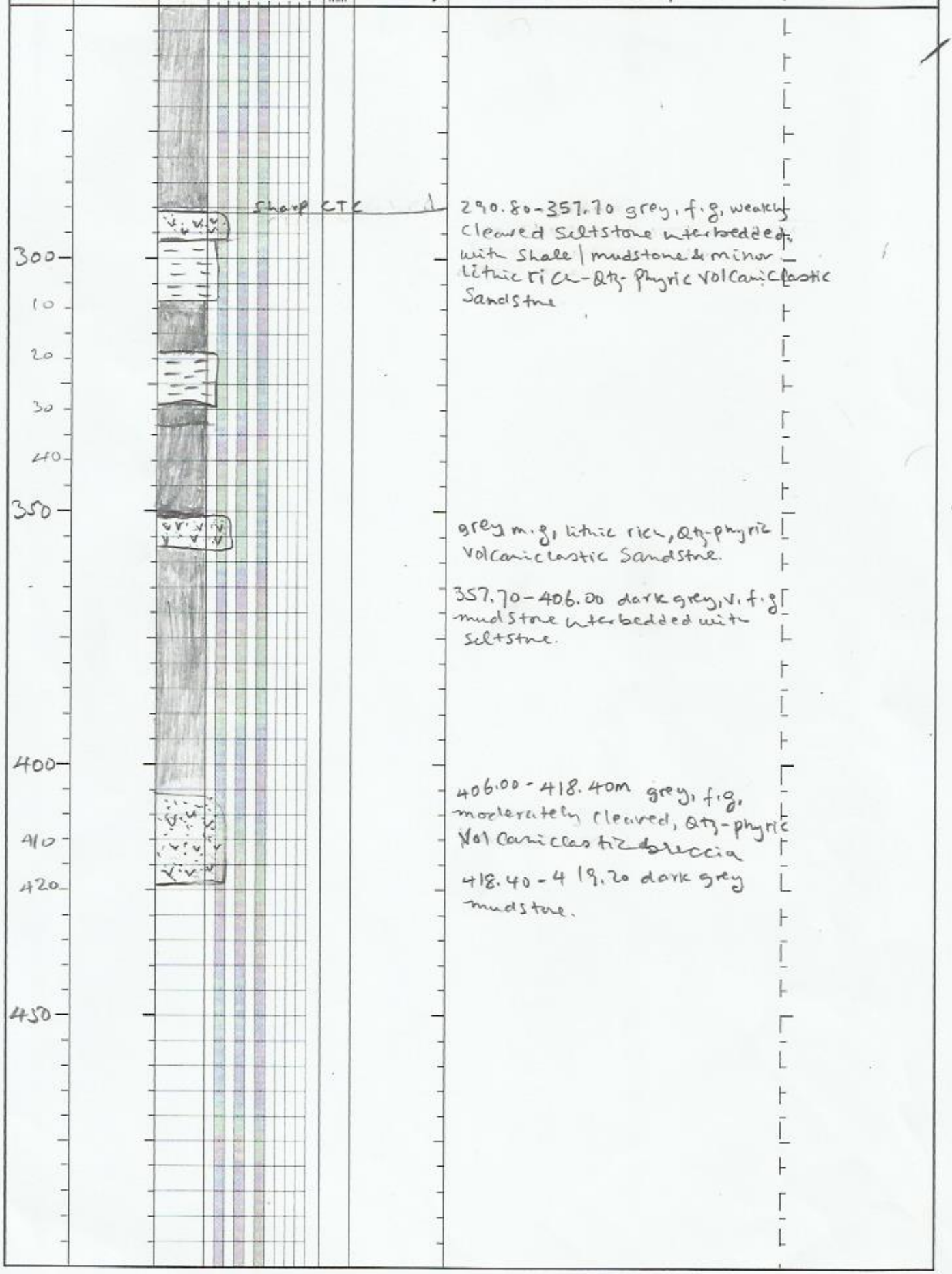

EXPLORATION SKILLS MAPPING CAMP

GRAPHIC LOG

Project CHAMBERLAIN
Location E.O.H 419.20

Drill hole No. BP272
Location No.

Coords: 378059.3E/5372988N | RL: 169.197 | Scale: 1:200 | Page 1 of 9

Azim: -70 | Incl: -84.5 | Diam: | Logged by: EYOB ANDEMESKEL | Date 2016/04/16

Log with grainsize (mud, 1/8, 1/2, 2, 8, 32, max mm)

m	Structure	Samples / TS results / Chemistry	Rock / facies description	Alteration
			0.00-41.70m Pale grey, medium grained, massive to weakly cleaved, weakly sercit altered- dominantly Qtz-phyric pumice breccia	SE = W
		274		
			- Core is highly broken & partly strongly oxidized due to surface exposure giving the ore dark brown color	
10				
20				
			28.00-30.00m strong silica alteration plus fuchsite(?)	ST = Strng
30		275		
40			41.70-46.40 Intensely cleaved mudstone Parallel to bedding	
	So:30	276		
			46.40-62.40m grey, medium grained, Qtz-Phyric Volcaniclastic Sandstone. It is Qtz-feld phyric from 46.40-53.00m	
50				

EXPLORATION SKILLS MAPPING CAMP

GRAPHIC LOG

Project / Location		Drill hole No. / Location No.	BP272
Coords:	RL:	Scale: 1:200	Page 2 of 9
Azim:	Incl: / Diam:	Logged by:	Date 21/04/16

m	Structure	Log with grainsize (mud, 1/8, 1/2, 2, 8, 32, max mm)	Samples / TS results / Chemistry	Rock / facies description	Alteration
60	Qvn 70			62.40 – 73.60m grey, v.f.g intensely Qtz veined (silica) alteration, fractured, Qtz-phyric Pumice breccia	SI = strong
			277		
70	Qvn			73.60 – 78.00 dark grey, V.f.g intensely cleaved, Pyritic black shale	
	S_f = 30			78.00 – 86.50m dark brown, oxidized, Qtz phyric Pumice breccia	oxi = Strong CB = M
80	S_o = 60			86.50 – 89.40 Pale grey with brown oxidation veining, intensely silica altered, Volcaniclastic Sandstone	SI = Strong Hi = W CB = W
90			278	89.40 – 98.30 Pale grey, m.g, Qtz-fsd-phyric Pumice breccia	
				98.30 – 103.80m grey, fine grained [illegible]	
100					

EXPLORATION SKILLS MAPPING CAMP

GRAPHIC LOG

Project Chamberlain Location		Drill hole No. BP 272 Location No.	
Coords:	RL:	Scale: 1:200	Page 3 of 9
Azim:	Incl:	Diam:	Logged by: / Date

Log with grainsize (mud, 1/8, 1/2, 2, 8, 32 mm)

m	Structure	Samples TS results Chemistry	Rock / facies description	Alteration
			Siltstone interbeddings.	SE: W
			103.80-121.80m grey, v.f.g, strongly silicified volcaniclastic Sandstone. The lower part is moderately cleared	SI: S CL: W SE: W
		279	107.10-108.80m, 109.30-109.70 113.80-114.50m milky, barren Qtz vein.	
110				
	So / S1:40			
120	S1			
	S1:30		Faulted CTC	
			121.80-123.90 intensely brecciated volcaniclastic Sandstone suspiciously a fault zone. Centimetre scale displacement is shown in core except 122.90-122.40m not brecciated	
	S1:40	280	123.90-129.70 grey, f-g, cleared weakly chlorite & sericite altered Qtz-phyric volcaniclastic breccia	
130			129.70-132.70m grey to dark brown due to hematite oxidation, massive to weakly cleared volcaniclastic Sandstone	HE = Strong CB: M SE: Strong
		281	132.70-146.50m grey, f-g, massive to weakly cleared Qtz-f-phyric Pumice breccia It is moderately hematite oxidized from 139.40-146.50m	139.40-146.50 HE = M SE = M
140	S1:40			
	VQ 290		146.50-151.00 grey, v.f.g, volcaniclastic Sandstone/ Siltstone interbedded with mud Stone. It is cut by Qtz vein ⊥ to CTA	
150	So: 40			

EXPLORATION SKILLS MAPPING CAMP

GRAPHIC LOG

Project Location: Chamberlain		Drill hole No.: BP272	Location No.:
Coords:	RL:	Scale: 1:200	Page 4 of 9
Azim:	Incl:	Diam:	Logged by: Date: 21/04/16

Log with grainsize (mud, 1/8, 1/2, 2, 8, 32, max mm) | Samples / TS results | Chemistry

m	Structure	Rock / facies description	Alteration
		151.00 – 162.80 grey, fine grained, weakly cleaved, intensely Qtz-veined & silica flooded, Volcaniclastic Sandstone/ Qtz-fld phyric Pumice bx. It is reddish brown due to hematite oxidation from 155.00 - 162.80m	SI = S SE = M HE = M
160		gradational ctc	
	1 S1:40	162.80 – 167.00 grey, medium grained, Qtz-phyric (rounded) epiclastic Sandstone of a mixed provenance (basement dominated). It is cleaved.	
170	1 S0:40 S1:40	167.00 – 179.00 grey, v.f.g., Qtz-phyric Pumice breccia with stratified Silt Stone/ mudstone top.	
		282	
180	1 S1:40	179.00 – 282.30m dark grey intensely Cleaved, in places pyritic black Shale & massive mudstone. It is oxidized from 179.00-193.80m. The core is intensely broken from 187.00 - 189.00 that could be a fault zone (??)	
		- Qtz veined from 193.00 - 194.50	
190		Core is very massive to weakly Cleaved mudstone.	
200			

EXPLORATION SKILLS MAPPING CAMP

GRAPHIC LOG

Project Location: Chamberlain		Drill hole No. / Location No.: BP272	
Coords:	RL:	Scale: 1:200	Page 5 of 9
Azim:	Incl:	Diam:	Logged by: / Date

Log with grainsize (mud | 1/8 | 1/2 | 2 | 8 | 32 | max mm) | Samples / TS results / Chemistry | Rock / facies description | Alteration

m

Structure

1

f: 30

60

Py-Qz

Py-Qz

So

210

2

30

220

Qz-Py-Gn

220.00 - 228.60 intensely Qtz - veined & Py + Gn mineralisation associated in ~~the~~.

Py + Gn ≈ 1%

Qz-Py-Gn

Qz-Py-Gn

230

240

So: 40

250

201.80 - 209.4

Py: 5%

EXPLORATION SKILLS MAPPING CAMP

GRAPHIC LOG

Project Location: Chamberlain		Drill hole No.: BP 272	
Coords:	RL:	Scale: 1:200	Page 6 of 9
Azim:	Incl:	Diam:	Logged by:	Date 21/04/16

m	Structure	Log with grainsize (mud, 1/8, 1/2, 2, 8, 32, max mm)	Samples / TS results / Chemistry	Rock / facies description	Alteration
260	S_0=50				
270	S_1=50, S_0=50				
280			283	282.30 - 285.80 grey, v.f.g, Weakly pyritic, cleaved, qtz-phyric Volcaniclastic Sandstone of a mixed provenance(?)	
				285.80 - 290.80 dark grey Pyritic, cleaved black Shale	
290	S_0=70				
	CTS S_0=85	Sharp CTC (bed)		290.80 - 296.80 grey, f.g, weakly cleaved, epiclastic Sandstone of a mixed provenance.	
				296.80 - 308.00 grey, v.f.g Siltstone interbedded with Shale	
300	S_0=50				

EXPLORATION SKILLS MAPPING CAMP

GRAPHIC LOG

Project Location: Chamberlain		Drill hole No.: BP272	Location No.:
Coords:	RL:	Scale: 1:200	Page 7 of 9
Azim:	Incl:	Diam:	Logged by: / Date

Log with grainsize: mud, 1/8, 1/2, 2, 8, 32 (max mm)

m	Structure	Samples TS results Chemistry	Rock / facies description	Alteration
	S_0=35	284	308.00 - 319.15 dark grey, v.f.g black shale (mudstone) interbedded with siltstone	
310		285		
320	S_0=60	286A	319.15 - 329.20 grey, v.f.g Siltstone / mudstone interbedded	
330	S_0=60		329.20 - 333.10 dark grey, cleaved black shale	
	S_0=60		333.10 - 336.00 grey, v.f.g. Cleaved, Siltstone / mudstone	
340			336.00 - 351.00 grey, v.f.g mudstone interbedded with siltstone	
350			343.00 - 350.00 grey, f.g. siltstone to v.f.g sandstone	

EXPLORATION SKILLS MAPPING CAMP

GRAPHIC LOG

Project Chamberlain
Location

Drill hole No. BP272
Location No.

Coords: | RL: | Scale: 1:200 | Page 8 of 9

Azim: | Incl: | Diam: | Logged by: | Date

m	Structure	Log with grainsize (mud, 1/8, 1/4, 2, 8, 32 mm)	Samples / TS results / Chemistry	Rock / facies description	Alteration
				352.90 - 357.70 grey, m to g, lithic rich quartz-phyric volcaniclastic Sandstone	
			286B		
			*	357.70 - 397.80m dark grey v. f. g, mudstone interbedded with Siltstone	
360					
	S: 65		*		
370					
			*		
380					
			*		
390					
	S: 15°		* 287	397.80 - 401.80 grey to green m v. f. g, Siltstone interbedded with mudstone with ithics	
400					

EXPLORATION SKILLS MAPPING CAMP

GRAPHIC LOG

Project / Location: Chamberlain		Drill hole No.: BP 272	Location No.:
Coords:	RL:	Scale: 1:200	Page 3 of 9
Azim:	Incl:	Diam:	Logged by: EYOS	Date: 21/04/16

Log with grainsize (mud, 1/8, 1/2, 2, 8, 32 mm)

m	Structure	Samples / TS results / Chemistry	Rock / facies description	Alteration
			401.20–406.20m dark grey, cleaved, mudstone	
			406.00–418.40m grey, f.g., moderately cleaved, Volcanic clastic sandstone with intense chlorite alteration	CL = W SE = W
410				
	S1=55	288		
			418.40 – 419.20 dark grey, mudstone	
420				

EXPLORATION SKILLS MAPPING CAMP

GRAPHIC LOG

Project Roseberry
Location Chamberlain

Drill hole No. BP273
Location No.

Coords: 378236.7E / 5373287N | RL: 147.47 | Scale: 1:1000 | Page 1 of 1

Azim: 86 | Incl: -60 | Diam: | Logged by: EYOB F. ANDEMESKEL | Date 22/06/16

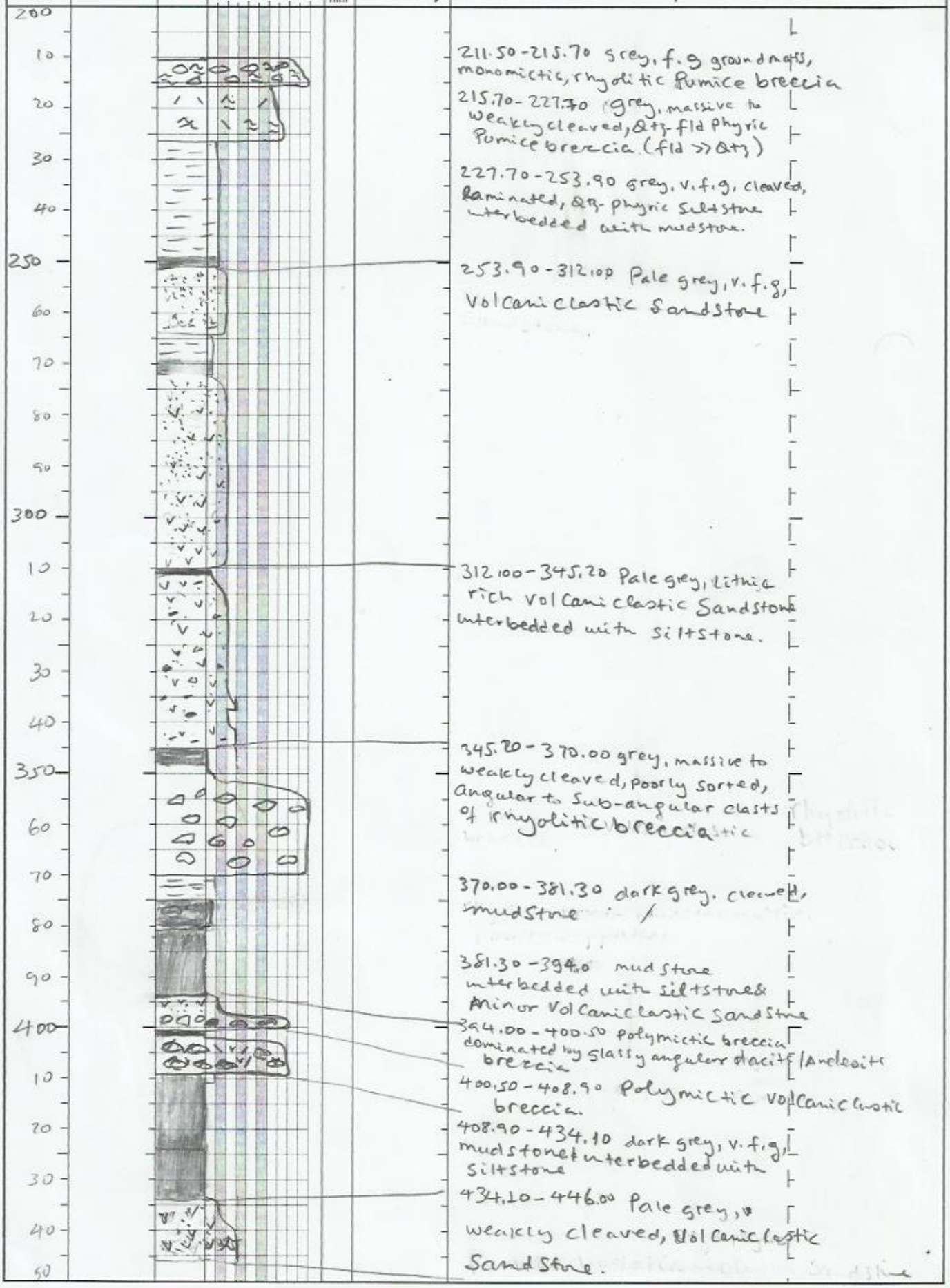

EXPLORATION SKILLS MAPPING CAMP

GRAPHIC LOG

Project CHAMBERLAIN
Location

Drill hole No. BP 273
Location No.

Coords: 378236.7E/5373287N | RL: 147.47 | Scale: 1:200 | Page 1 of 5

Azim: 86 | Incl: -60 | Diam: | Logged by: EYOB ANDEMESKEL | Date 23/04/16

m	Structure	Log with grainsize (mud, 1/8, 1/2, 2, 8, 32, max mm)	Samples / TS results / Chemistry	Rock / facies description	Alteration
210				211.50 – 215.70m grey, fine grained groundmass, monomictic angular to subangular quartz phyric rhyolitic clasts containing pumice breccia	SE=M
			289		
	S_0=60			215.70 – 227.70 m grey, fine grained matrix, massive to weakly Cleaved, qtz–feldspar phyric Pumice breccia – fld >> Qtz The Pumice clasts are dark green & chloritic	CL=W
220			290		
				227.70 – 235.00 grey, v.f.g qtz-phyric Cleaved & laminated Siltstone interbedded with mudstone	SE=M
230	S_0=85			235.00 – 237.70 dark grey, Cleaved mudstone	
				237.70 – 250.40 Pale grey to greenish, v.f.g, Cleaved & laminated siltstone.	SE=M
240	S_0=80				
			291		
250					

EXPLORATION SKILLS MAPPING CAMP

GRAPHIC LOG

Project Location: Chamberlain Rosebery		Drill hole No.: BP 273	
Coords:	RL:	Scale: 1:200	Page 2 of 5
Azim:	Incl:	Diam:	Logged by: EYOB	Date 23/04/16

m	Structure	Log with grainsize (mud, 1/8, 1/2, 2, 8, 32; max mm)	Samples / TS results / Chemistry	Rock / facies description	Alteration
				250.40 – 253.90 dark grey, v.f.g cleaved mudstone/siltstone	SE=M
			292	253.90 – 264.60m pale grey, v.f.g, Vol Caniclastic Sandstone (arg & mixed provenance)	Same as R10063 Siltstone Sandstone same facies. BP273 (406-418)
260	S_1=80				
				264.60 – 268.10m grey, v.f.g cleaved, siltstone (& mixed provenance)	
270	S_0=75			268.10 – 272.30m dark grey, v.f.g, Cleaved mudstone to Shally.	
				272.30-309.90m Pale grey, v.f.g, cleaved. wispy clasts & possibly Pumice Containing Vol Caniclastic Sandstone	
			293		
280					
			294		
290					
300					

EXPLORATION SKILLS MAPPING CAMP

GRAPHIC LOG

Project Chamberlain
Location Rosebery

Drill hole No. BP 273
Location No.

Coords:

RL:

Scale: 1:200

Page 3 of 5

Azim:

Incl:

Diam:

Logged by: EJOB

Date 23/04/16

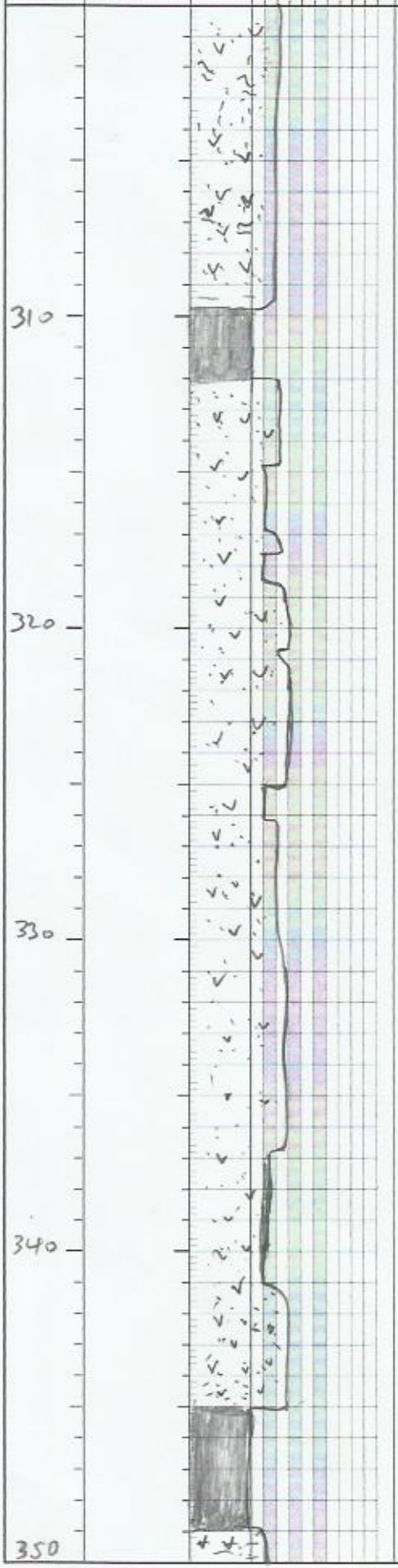

309.90 - 312.00 grey, laminated Siltstone interbedded with mudstone

312.00 - 345.20m pale grey, v.f.g, cleaved, volcaniclastic (lithic rich) Sandstone interbedded with Siltstone. (Generally looks of a mixed provenance)

345.20 - 349.00 dark grey mudstone

349.00 - 370.00m grey massive to weakly cleaved,

EXPLORATION SKILLS MAPPING CAMP

GRAPHIC LOG

Project Location: Chamberlain, Rosebery

Drill hole No. BP273

Location No.

Coords:

RL:

Scale: 1:200

Page 4 of 5

Azim:

Incl:

Diam:

Logged by: EYOB

Date 23/04/16

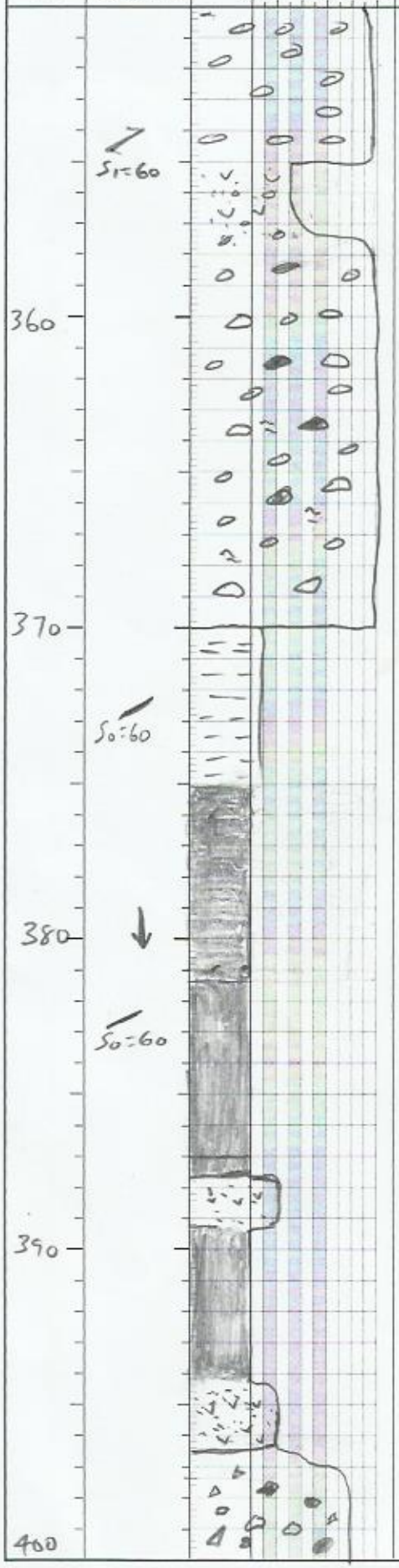

Rock / facies description

Poorly Sorted, angular to Sub-angular clasts of polymictic Volcaniclastic breccia. Clast size ranges from mm to > 30cm & is dominated by grey, glassy rhyolitic breccia & it generally fines up hole to Sandstone & Siltstone. The clasts show agreement jigsaw fit texture set in Volcaniclastic Sandstone

370 - 375.00 Pale grey, ± greenish v.f.g bedded, weakly Cleaved, Siltstone

375.00 - 381.30 dark grey, Cleaved & laminated, mudstone with minor Siltstone.

381.30 - 396.50m dark grey, v.f.g mudstone interbedded with Siltstone & minor Volcaniclastic(epiclastic) Sandstone

396.50 - 400.50 grey, v.c.g moderately cleaved, polymictic breccia dominated by grey glassy angular to Subrounded rhyolitic clast.

Alteration

Sem

Sf = W

Pyr 1%

EXPLORATION SKILLS MAPPING CAMP

GRAPHIC LOG

Project Chamberlain
Location Rosebery

Drill hole No. BP273
Location No.

Coords: | RL: | Scale: 1:200 | Page 5 of 5

Azim: | Incl: | Diam: | Logged by: EJOB | Date 24/04/16

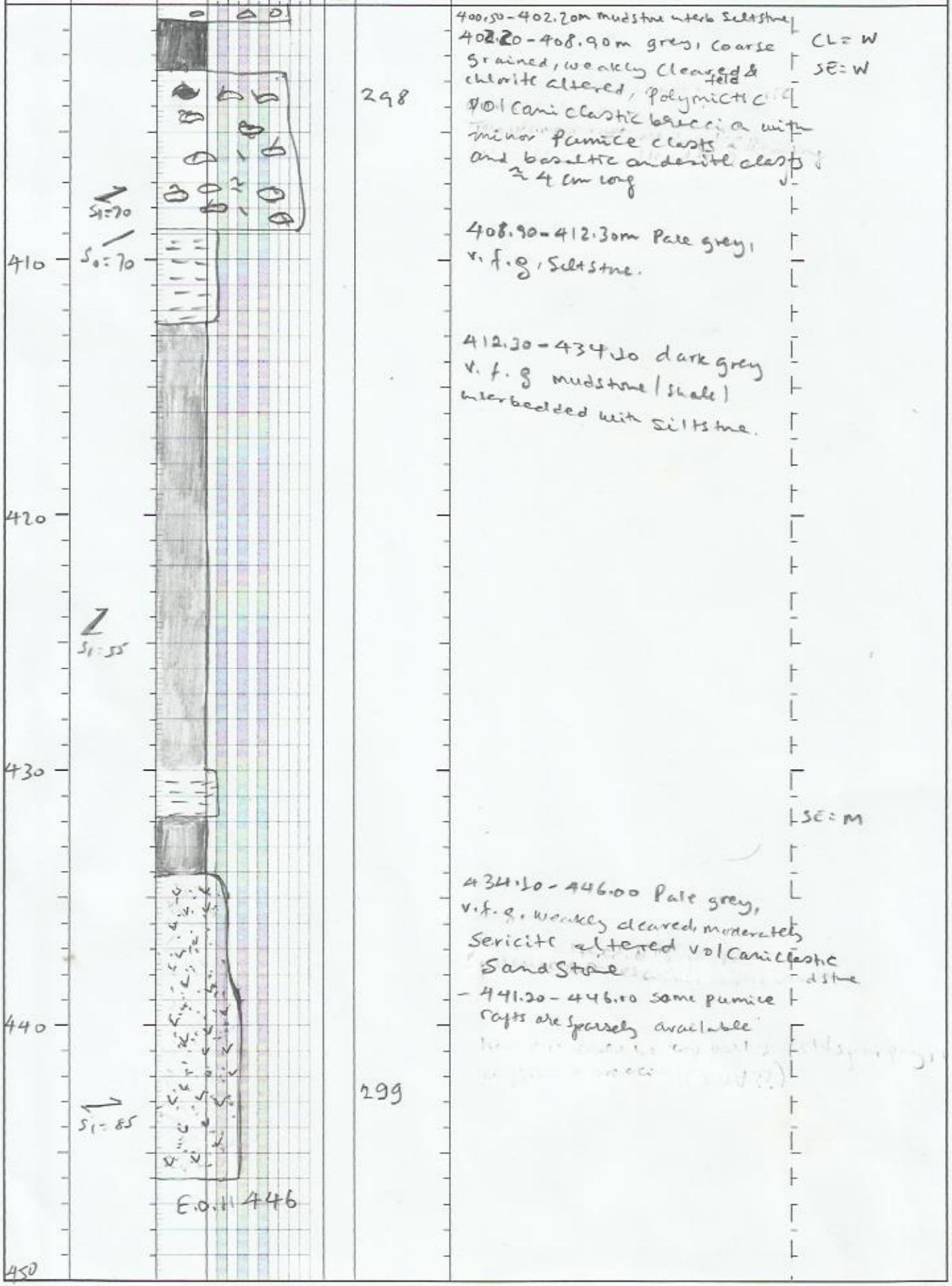

Summary Log

EXPLORATION SKILLS MAPPING CAMP

GRAPHIC LOG

Project Jupitor		Drill hole No. JP357	
Location Total depth 104.5		Location No.	
Coords: 3768474E/5369974N	RL: 370.7	Scale: 1:1000	Page 1 of
Azim: 270	Incl: -57.30	Diam:	Logged by: EYOB ANDEMESKEL	Date 21/03/16

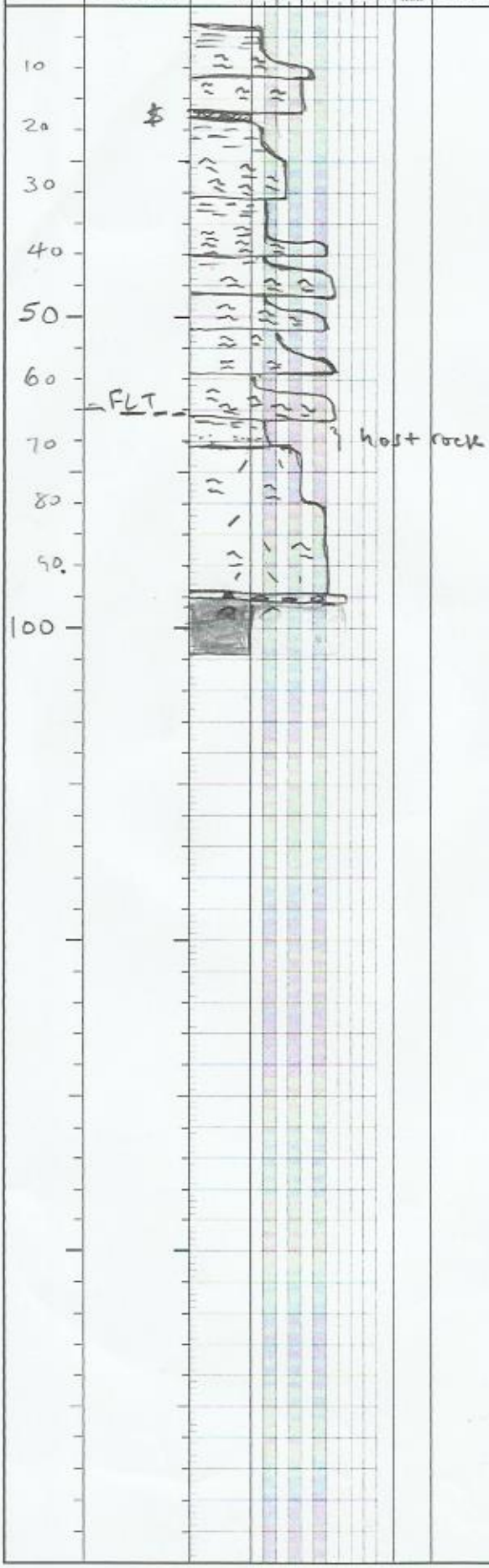

Rock / facies description

0.00 - 2.00 core loss

2.00 - 70.20 m light grey, leached top coarse breccia base fining to volcaniclastic sandstone from fld phyric pumice breccia

17.00 - 20.00 strongly bleached, v.f.g semi-massive sulphide

70.20 - 53.80 m Pale grey, m.g, 8+3-fld phyric Pumice breccia. the Pumice brx ≃ 6cm but Sparse

the top Part 70.20 - 72.20 m is volcaniclastic Sandstone with Stringer of Sulphide.

93.80 - 94.80 Rosebery fault

94.80 - 104.40 dark grey, moderately bleached pyritic Mudstone.

Alteration

Acid = S

SE = S

Py = 25 %

sp = 2-3 %

EXPLORATION SKILLS MAPPING CAMP

GRAPHIC LOG

Project JUPITER
Location Total depth 104.5

Drill hole No. JP357
Location No.

Coords: 376847 4E / 5369974N | RL: 370.7 | Scale: 1:200 | Page 1 of 3

Azim: -57.30 | Incl: 270 | Diam: | Logged by: EYOB ANDEMESKEL | Date 21/03/16

Log with grainsize (mud, 1/8, 1/2, 2, 8, 32, max mm) | Samples | TS results | Chemistry

m	Structure	Rock / facies description	Alteration
0		0.00 - 2.00 loss	
2			
4	S_0 - 70	2.00 - 5.50m light grey to whitish intensely cleaved (schistos), bleached, v.f.g, volcaniclastic Sandstone - core is crumbly & fissile	- Acid = S - SE = S
6			
8		5.50 - 20.00 grey, m.g, generally graded - younging downhole, at 11.00 breccia base of bed, feldspar phyric pumice breccia No qg observed	
10	gb	rhyolitic clast	
		rhyolitic clast ≥ 1cm	
		acid	
		17.00 - 20.00 it is strongly bleached zone with v.f.g semi-massive Sulphide from 17.70 - 18.20m (Sooty Pyrite with minor Sp & Gn)	17.70-18.20 Py 10-15%
			Py = 25%
			- Sp = 2-3%
20	sample → ¼ core	20.00 - 20.70m dark grey, f.g massive Sulphide with Sp, Gn & Py It has dark Sooty with Sp banding (yellow)	Sp = 40 - Gn = 30 - Py = 30
	Sp 85		SI = M - SE = S Acid = M
		20.70 - 25.35m Pale grey, v.f.g intensely bleached Siltstone with stringer of Sulphide (Sp+Gn+Py)	3-5% Sp+Gn 2% Py
	S_0 70	25.35 - 31.00 m grey, f.S Volcaniclastic Pumiceous SST (Cataclasite), moderately bleached, contains bands of Sp+Gn+Py as semi-massive to massive from 28.40 - 29.6m	Acid = S SE = S 20-50% Sp+Gn+Py
30		31.00 - 35.30m Pale grey, v.f.g, strongly silica altered (cherty) banded Sp+Gn+Py containing Vitric Volcaniclastic Siltstone	SI = S It contains Sulphide bands as Stringer to Semi-massive
	200		
	S_1 70 / 20		
	201		
40		35.30 - 74.70 Pale grey, medium grained base to fine grained (Silty) top, brownish due to Fe-Ox alteration, XII Poor Pumice breccia grading to Siltstone down hole.	
	Sample		
50			

OC16901357

EXPLORATION SKILLS MAPPING CAMP **GRAPHIC LOG**	Project Location: Jupiter	Drill hole No.: JP 357
Coords:	RL:	Scale: 1:200
Azim: / Incl: / Diam:	Logged by:	Date: 22/02/16

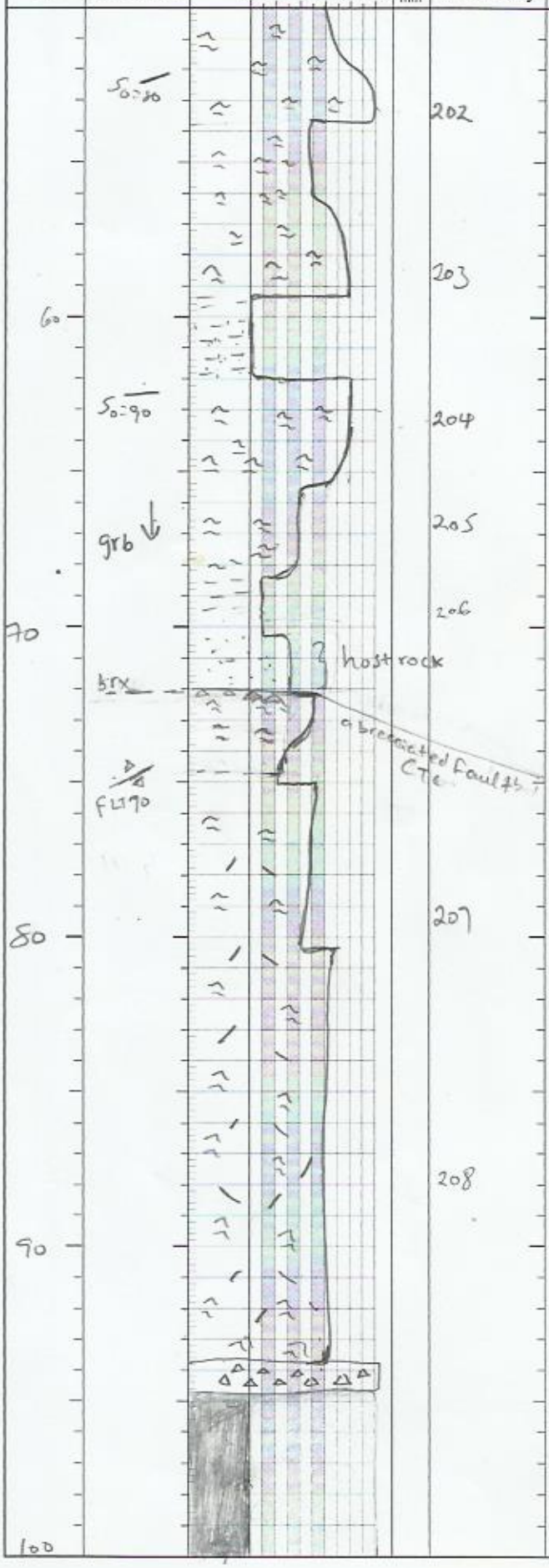

Rock / facies description

Pale grey to white, sericite altered, moderately Sericite altered, Sparse feldspar bearing Pumice breccia
at 53.30m Pumice clasts reach upto 3cm

59.20 - 61.80m Pale grey to white, v.f.g, intensely sericite altered Siltstone top part of the Pumice breccia

61.80 - 65.30m c.g with subrounded clasts(??), very soft possibly barite

65.30 - 70.20m Pumice breccia m. grained Pumice ash SST grading downwards to Siltstone

70.20m - 72.20m grey to brownish due to alteration, stringer of Sulphide (Sp+gn+Py) bearing Volcaniclastic Sandstone interbedded with Siltstone grading downward. It also Contain minor Cpy

72.20 - 93.80m Pale grey m.g Qtz-feldspar phyric pumice breccia. It Contains Qtz-feldspar porphyritic pumice breccia 3 x 6cm but are Sparse

93.80 - 94.80m grey, v.c.g breccia of Qtz feld phyric tuff + Qtz in a puggy mud matrix represents Rosebery fault. Complex

94.80 - 104.40 dark grey, moderately Cleaved, Pyritic mud Stone

Alteration

SE = M

SE = S
SST

EXPLORATION SKILLS MAPPING CAMP

GRAPHIC LOG

Project Jupiter Location		Drill hole No. JP 357 Location No.	
Coords:	RL:	Scale: 1:200	Page 3 of 3
Azim:	Incl:	Diam:	Logged by: Date 22/03/16

Log with grainsize

Samples
TS results

m	Structure	Log with grainsize (mud, 1/8, 1/2, 2, 8, 32; max mm)	Chemistry	Rock / facies description	Alteration
		EOH 104.40			
116					

Summary log

EXPLORATION SKILLS MAPPING CAMP

GRAPHIC LOG

Project Rosebery North

Location Total depth 460m

Drill hole No. R10032

Location No.

Coords: 379331.7E | 5376180N | RL: -660.49 | Scale: 1:1,000 | Page 1 of 1

Azim: 278.7 | Incl: -40 | Diam: | Logged by: EYOB ANDEMESKEL | Date 03/03/16

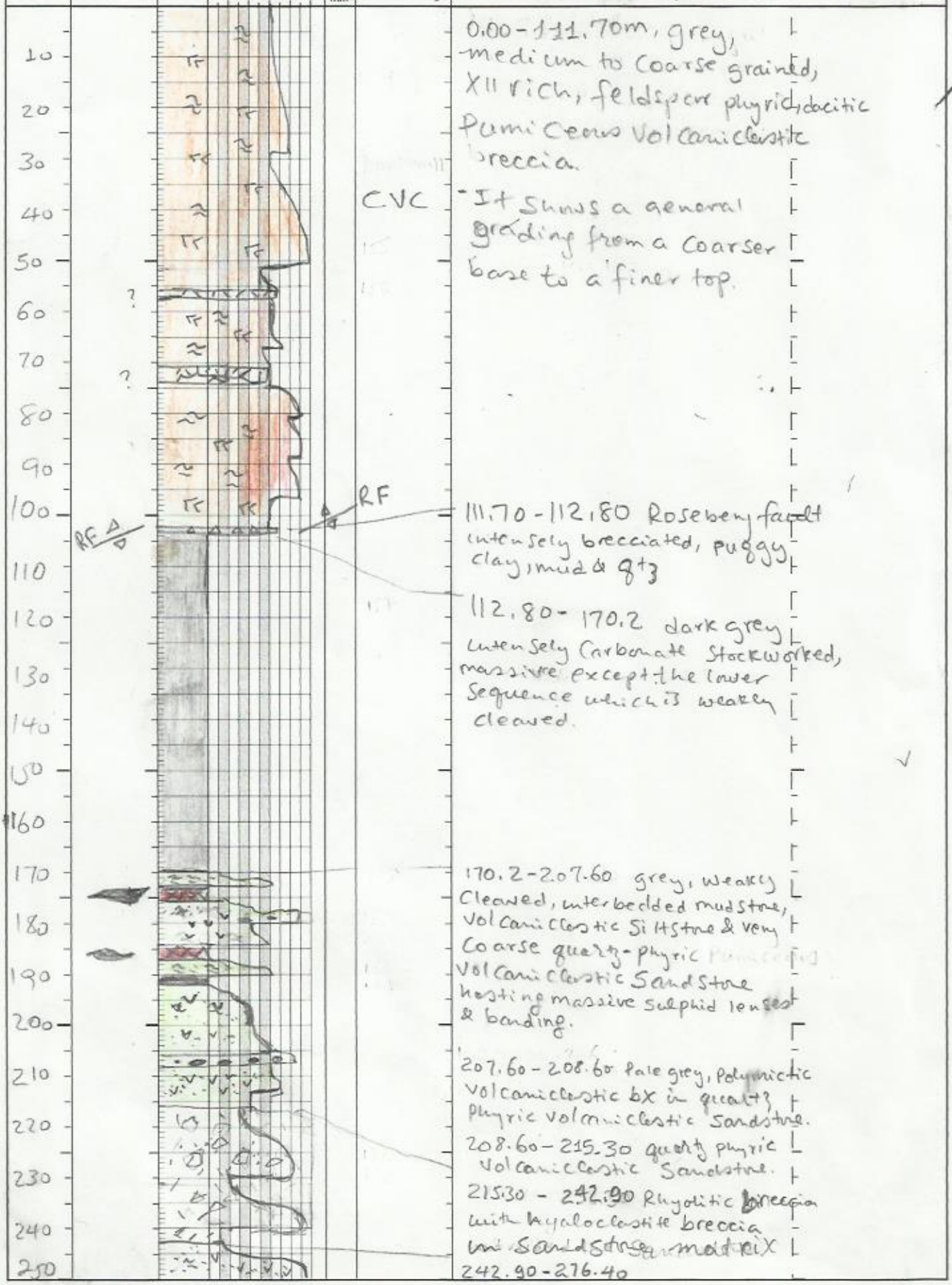

0.00 - 111.70m, grey, medium to coarse grained, XII rich, feldspar phyric, dacitic Pumiceous Volcaniclastic breccia.

- It shows a general grading from a coarser base to a finer top.

111.70 - 112.80 Rosebery fault intensely brecciated, puggy clay, mud & qtz

112.80 - 170.2 dark grey intensely Carbonate Stockworked, massive except the lower sequence which is weakly cleaved.

170.2 - 207.60 grey, weakly cleaved, interbedded mudstone, Volcaniclastic Siltstone & very Coarse quartz-phyric Volcaniclastic Sandstone hosting massive sulphid lenses & banding.

207.60 - 208.60 Pale grey, Polymictic Volcaniclastic bx in qtz phyric volcaniclastic Sandstone.

208.60 - 215.30 quartz phyric Volcaniclastic Sandstone.

215.30 - 242.90 Rhyolitic breccia with hyaloclastite breccia and Sandstone matrix

242.90 - 276.40

$ massive to Semi massive Sulphide lenses

Summary log

EXPLORATION SKILLS MAPPING CAMP	Project Location: Rosebery North	Drill hole No. R10032
GRAPHIC LOG		Location No.
Coords:	RL:	Scale: 1:1000
Azim:	Incl:	Diam:
Logged by: EYOB ANDEMESKEL		Page 2 of 2
		Date 18/05/16

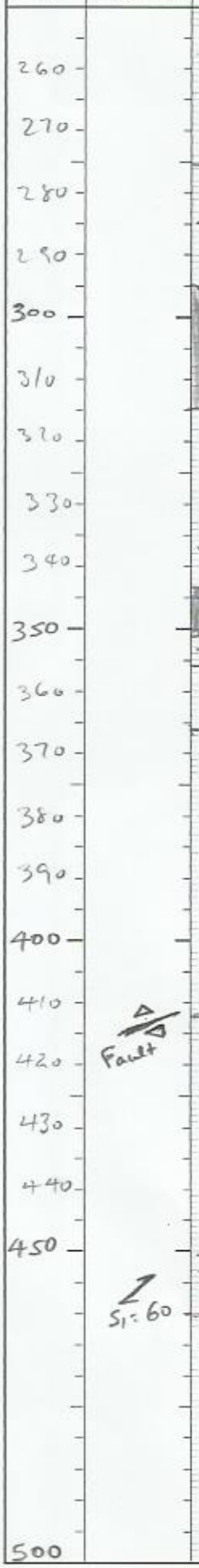

Rock / facies description

242.90 - 276.40 grey, medium to coarse grained lithic rich graded, youngingupwhole, quartz - phyric volcaniclastic Sand Stone.

276.40 - 356.30m Pale grey, v.f.g Silt Stone interbeded with mud stone & v.f.g volcaniclastic Sand Stone.

356.30 - 367.80m Grey, weakly cleaved, Qtz-phyric pumice breccia.

367.80 - 412.00 Pale grey, v.f.g matrix, Qtz- feldspar phyric pumice breccia (fld >> Qtz) & looks Same as CVC

Faulted CTC

412.00 - 460.00m grey, weakly cleaved, weakly Silicified, Qtz - feldspar phyric pumice breccia. (Qtz >> fld)

Fault gauge at 412.00

Alteration

EXPLORATION SKILLS MAPPING CAMP

GRAPHIC LOG

Project Rosebery North | Drill hole No. RJ0032
Location Total depth 460m | Location No.

Coords: 379331.7E/5376180N | RL: -660.49m | Scale: 1:200 | Page 1 of 10
Azim: 278.7 | Incl: -40 | Diam: | Logged by: EYOB Andemeskel | Date 27/04/16

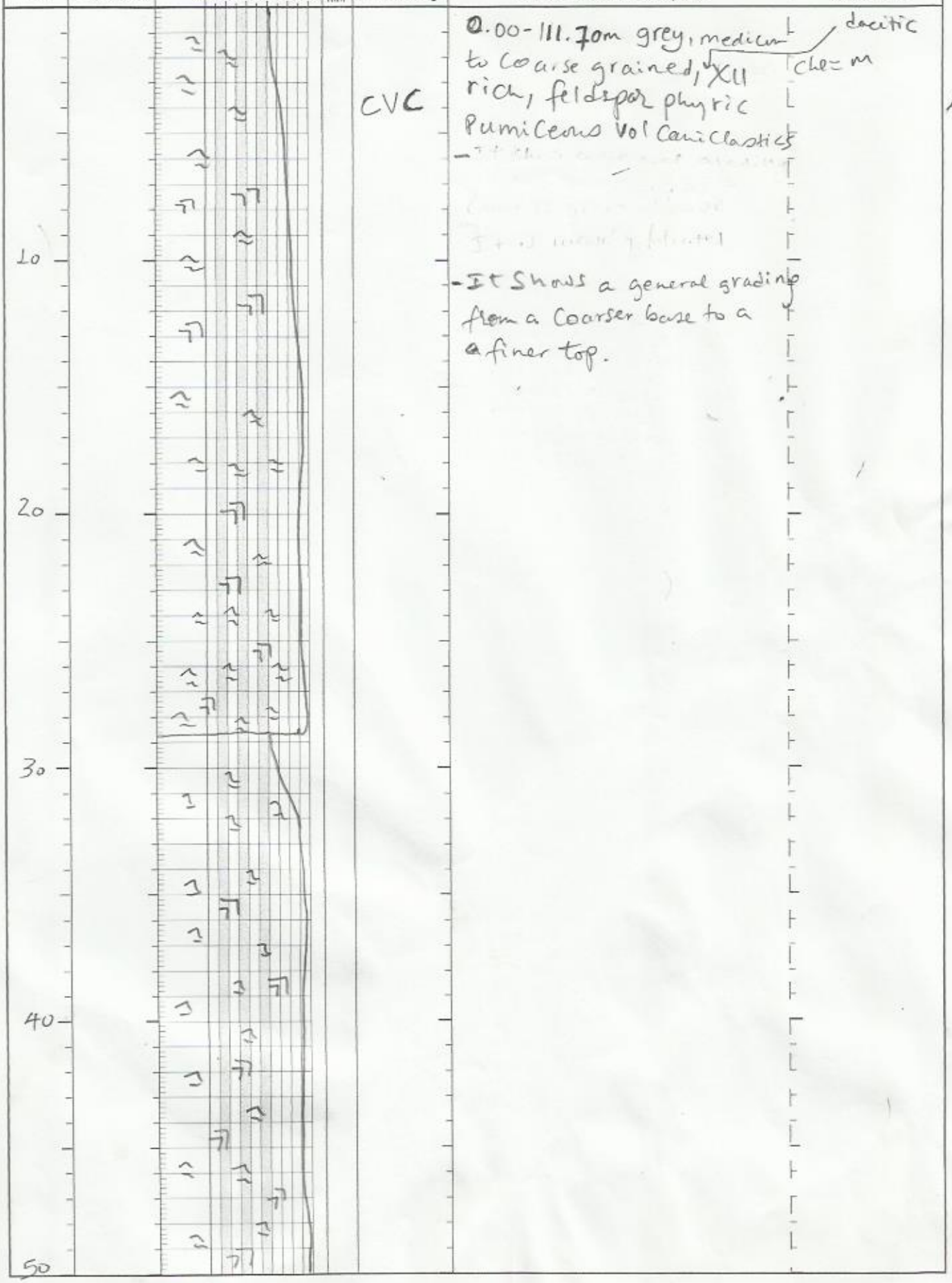

EXPLORATION SKILLS MAPPING CAMP

GRAPHIC LOG

Project Location		Drill hole No. Location No.	R10032
Coords:	RL:	Scale: 1:200	Page 2 of 10
Azim:	Incl: Diam:	Logged by:	Date 27/02/16

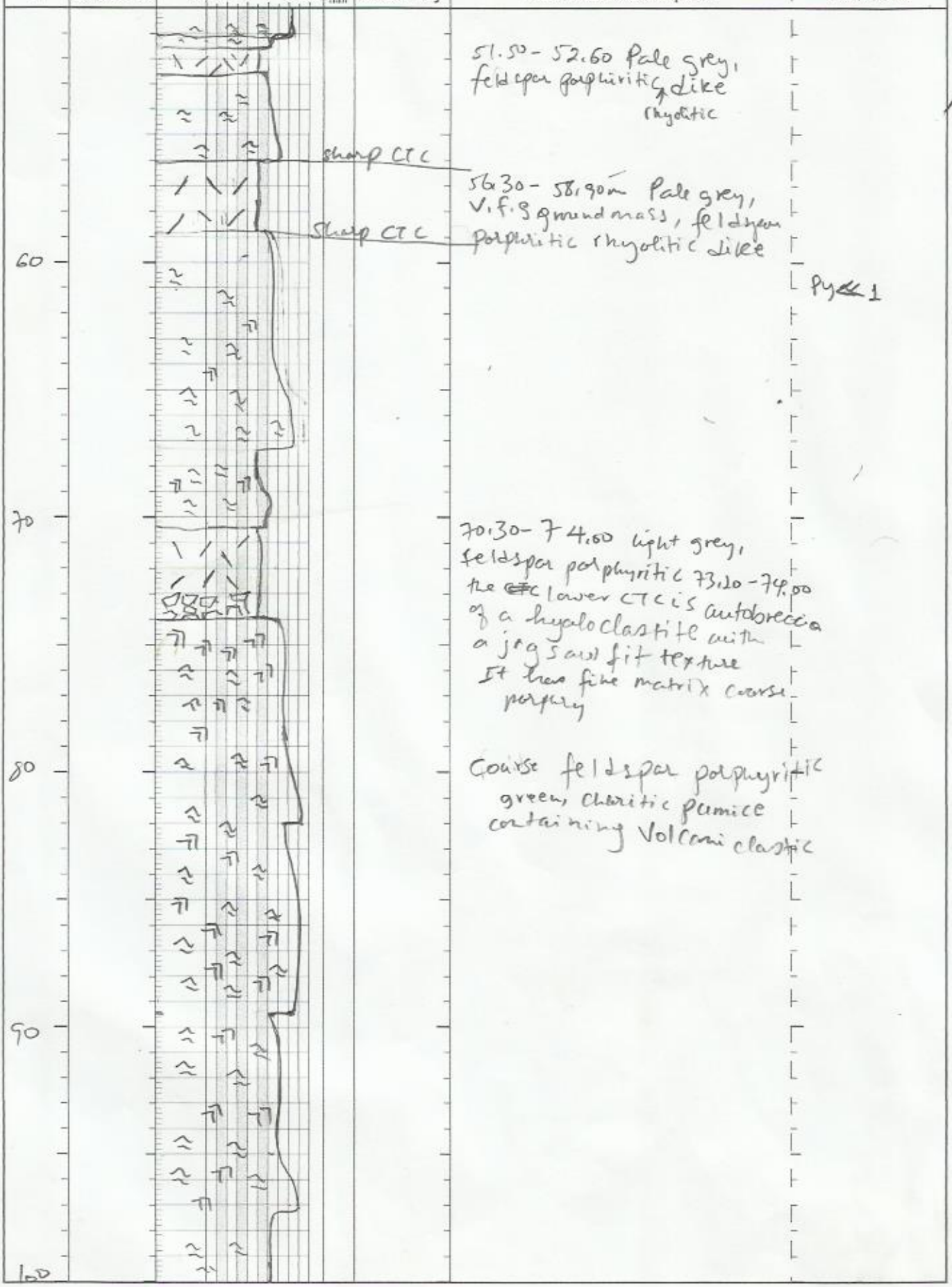

EXPLORATION SKILLS MAPPING CAMP

GRAPHIC LOG

Project Location		Drill hole No.	RD032
		Location No.	
Coords:	RL:	Scale: 1:200	Page 3 of 5
Azim:	Incl: Diam:	Logged by:	Date 27/02/16

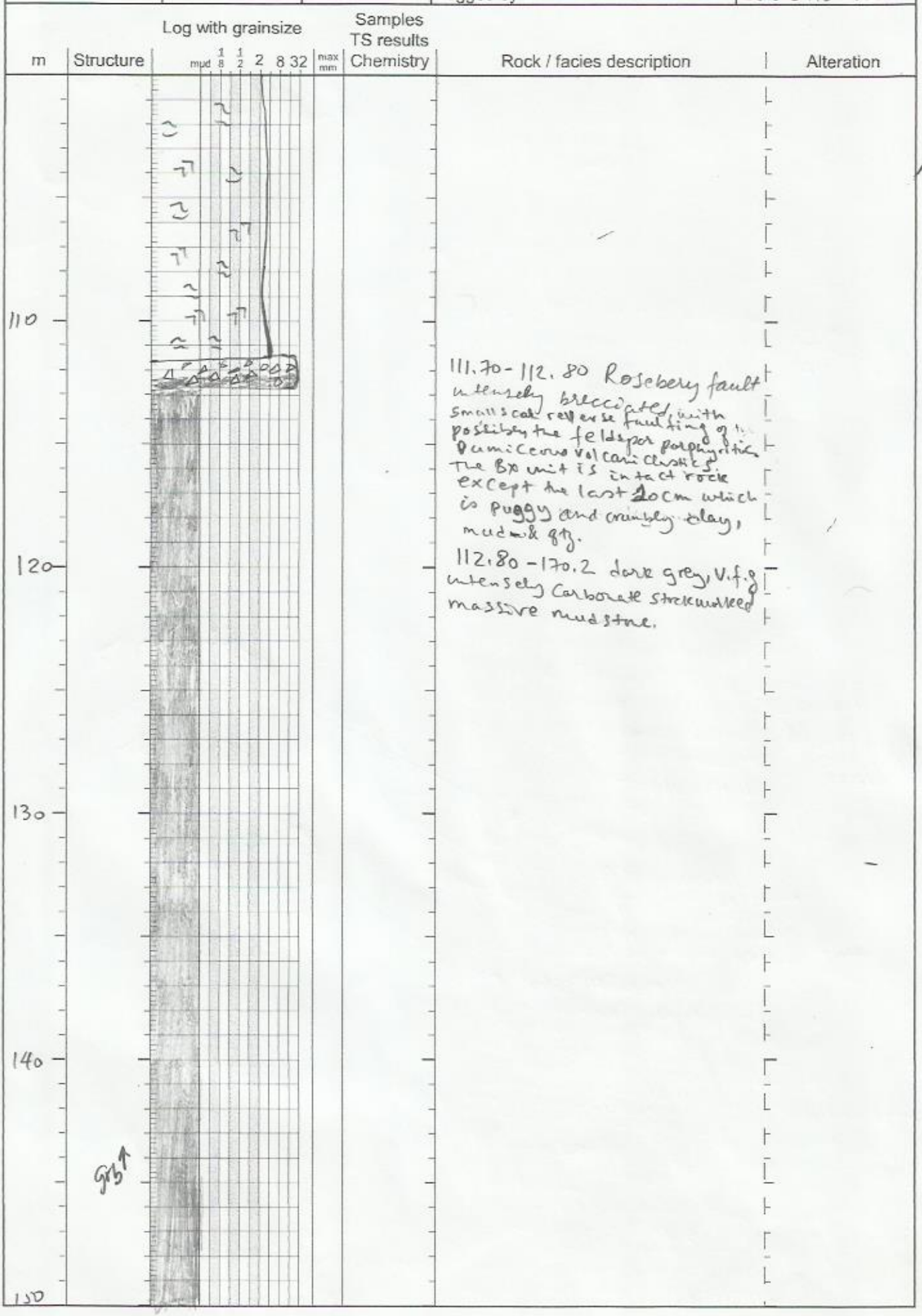

EXPLORATION SKILLS MAPPING CAMP

GRAPHIC LOG

Project
Location

Drill hole No. R10032
Location No.

Page 4 of 10

Coords: | RL: | Scale: 1:200 | Date 27/02/16

Azim: | Incl: | Diam: | Logged by: EYOB ANDEMESKEL

Log with grainsize | Samples TS results Chemistry | Rock / facies description | Alteration

m | Structure | mud 1/8 1/2 2 8 32 max mm

158.50 - 170.20m The mudstone is weakly cleaved, It contains 1-2cm Sulphide (Py, Pyrr) Veins & Patches parallel to the bedding plane — Py ≈ 1%, Pyrr 1%

170.20 - 173.70 grey, weakly cleaved, interbedded mudstone, volcaniclastic siltstone, and very coarse quartz porphritic (>2mm) volcaniclastic Sandstone hosting lenses, massive Sulphides from 171.50 - 171.65 & interbeded veins — 171.5-171.65 >80% Py ≈1% Sp

173.70 - 175.30 mudstone with Pyrite veins

175.30 - 178.50 grey, weakly cleaved, interbedded volcaniclastic siltstone & qtz phyric volcaniclastic sandstone hosting banded semi-massive sulphide Py > 40% from 175.30 - 175.90m — Py > 40

178.50 - 179.90 light grey, weakly cleaved, polymictic, quartz phyric volcaniclastic breccia of mass flow deposit with clasts of quartz-phyric cherty, sandstone, mudstones & feldspar pyric volcanic breccia. clasts are elongated & sub angular. matrix is vsst — clast size ≈ 1-40cm

179.90 - 192.30 mudstone interbeded with quartz-phyric - Pumiceous volcaniclastic sandstone

185.80 - 187.30m banded semi-massive Sulphide 2% Py 15-20% Sp hosted in a siltstone / mudstone interbedded unit — 20% Py 15-20% Sp

irregular CTC; Sharp CTC 75° TCA; Sharp CTC 75° TCA

Same unit noted at 1300 in hole 411R-D1

SE = W; SI = W; SE = M

EXPLORATION SKILLS MAPPING CAMP

GRAPHIC LOG

Project
Location

Drill hole No. R10032
Location No.

Coords:
RL:
Scale: 1:200
Page 5 of 10

Azim:
Incl:
Diam:
Logged by: EYOB ANDEMESKEL
Date 28/02/16

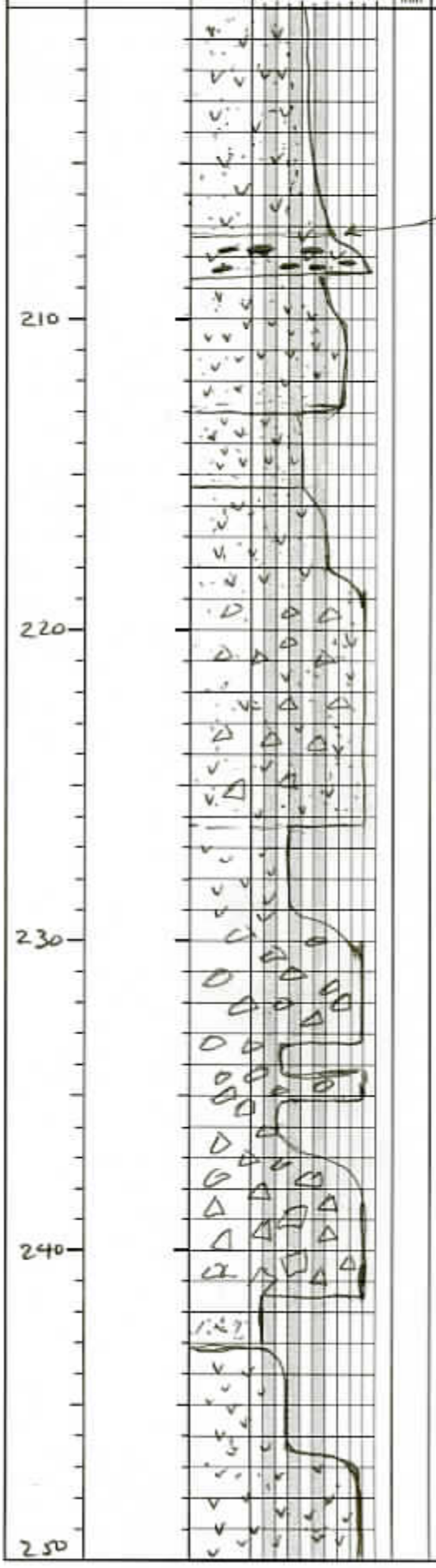

Rock / facies description	Alteration
192.30 - 207.60m Pale grey, graded uphole, medium to coarse grained matrix with qtz-phyric >2mm, volcaniclastic Sandstone	
196.00 - 196.20 massive sulphide	40% Py, 2% sp 2% cpy
207.50 - 207.70 grey, qtz-fsp porphyritic dike intrudes the sequence.	
207.60 - 208.60 Pale grey, polymictic volcaniclastic breccia with clasts of qtz-phyric volcaniclastic Sandstone, clast size ≤ 3cm	
208.60 - 212.70 grey, coarse Grained, qualtz phyric >2cm volcaniclastic sandstone	
212.70 - 215.30 light grey, fine to m.g, XII poor, qtz phyric volcaniclastic Sandstone.	
215.30 - 242.90m Pale grey, v.f.g matrix, XII poor rhyolitic breccia in Sandstone matrix. the lower part from 226.00 - 242.90 shows flow bandings & jigsaw fit texture with intense Silicification.	SE = W SI = W SI = M to S
- It also has stock-work of reddish brown, hematite oxidation after pyrite veining	
242.90 - 250.70m grey, greenish, coarse grained, grading uphole 1-2 cm clast rich polymictic volcaniclastic breccia to volcaniclastic Sandstone	CL = m SE = W

EXPLORATION SKILLS MAPPING CAMP

GRAPHIC LOG

Project Rosebery | Drill hole No. RD032
Location | Location No.

Coords: | RL: | Scale: 1:200 | Page 6 of 10

Azim: | Incl: | Diam: | Logged by: ZYAB | Date 16/05/16

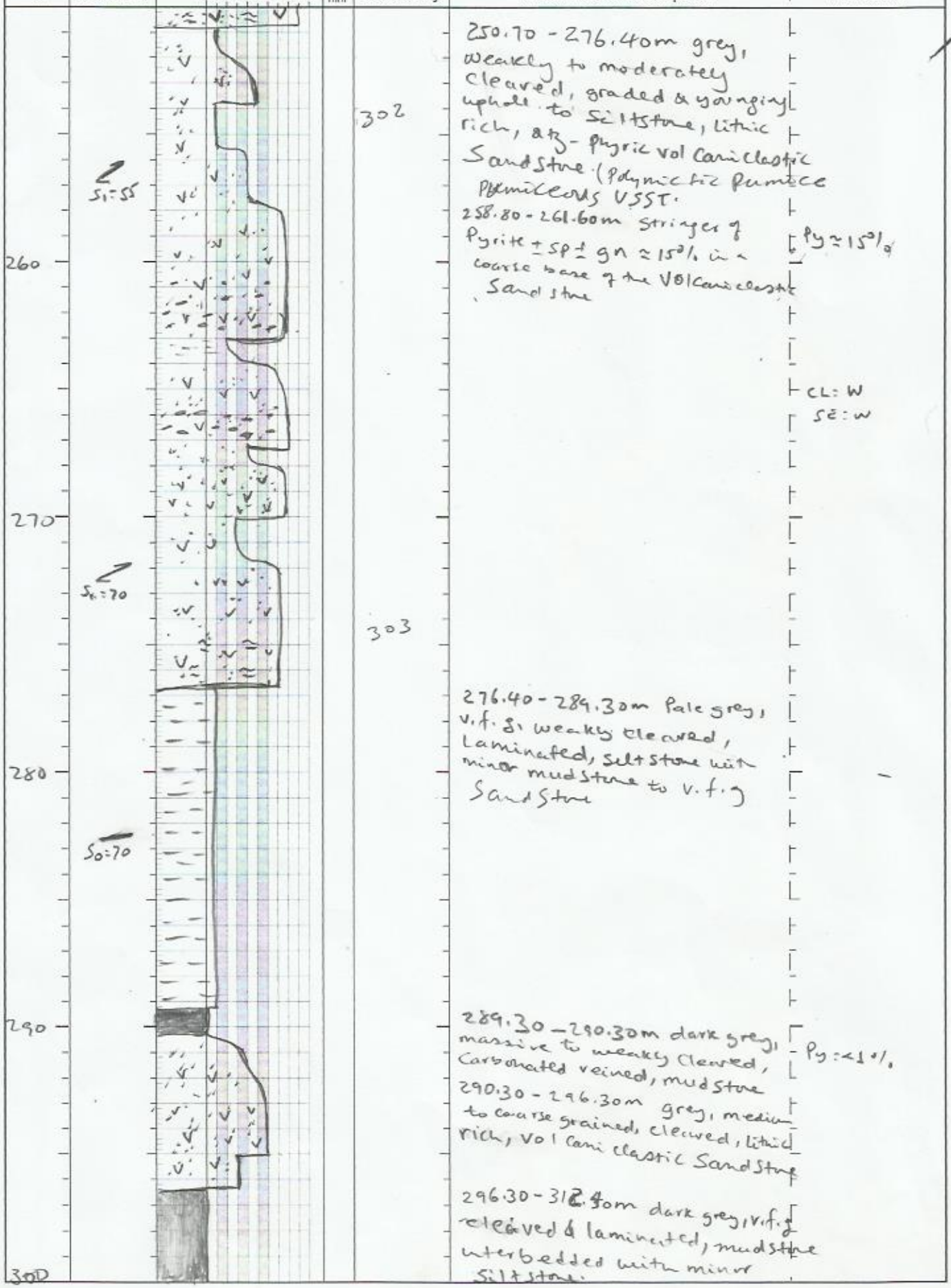

EXPLORATION SKILLS MAPPING CAMP

GRAPHIC LOG

Project Location: Rosebery

Drill hole No. R10032

Location No.

Coords:

RL:

Scale: 1:200

Page 7 of 10

Azim:

Incl:

Diam:

Logged by: E408

Date 16/05/16

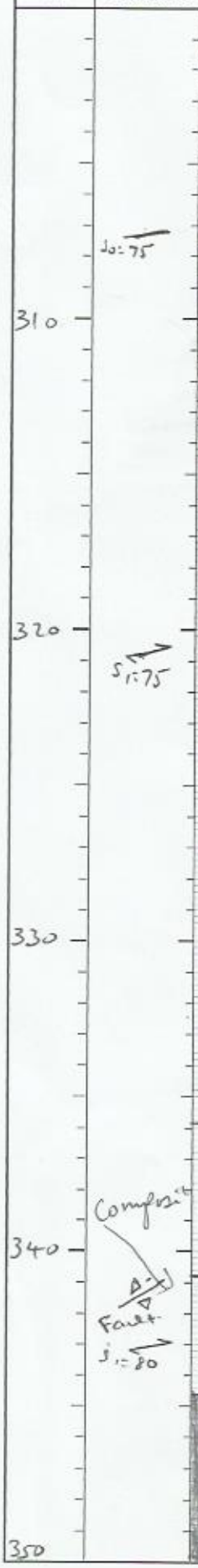

Samples
TS results
Chemistry

304

Rock / facies description

312.40-315.30 grey, v.f.g, cleaved siltstone interbedded with minor mudstone

315.30-335.80m pale grey, weakly cleaved, v.f.g Volcaniclastic Sandstone interbedded with mudstone

335.80-340.90m grey, v.f.g cleaved siltstone interbedded with Volcaniclastic Sandstone

340.70-340.90m intensely broken core Possibly a fault zone.

340.90-344.70m grey, medium grained, quartz Volcaniclastic breccia It has mudstone clasts encorporated.

344.70-351.50m dark grey, v.f.g, mudstone interbedded with siltstone & fine grained Volcaniclastic Sandstone

Alteration

CB = W

Carbonate veining

SE = M

SE = M

EXPLORATION SKILLS MAPPING CAMP

GRAPHIC LOG

Project Location: Rosebery

Drill hole No. R10032

Location No.

Coords:

RL:

Scale: 1:200

Page 8 of 10

Azim:

Incl:

Diam:

Logged by: ETDB

Date 16/05/16

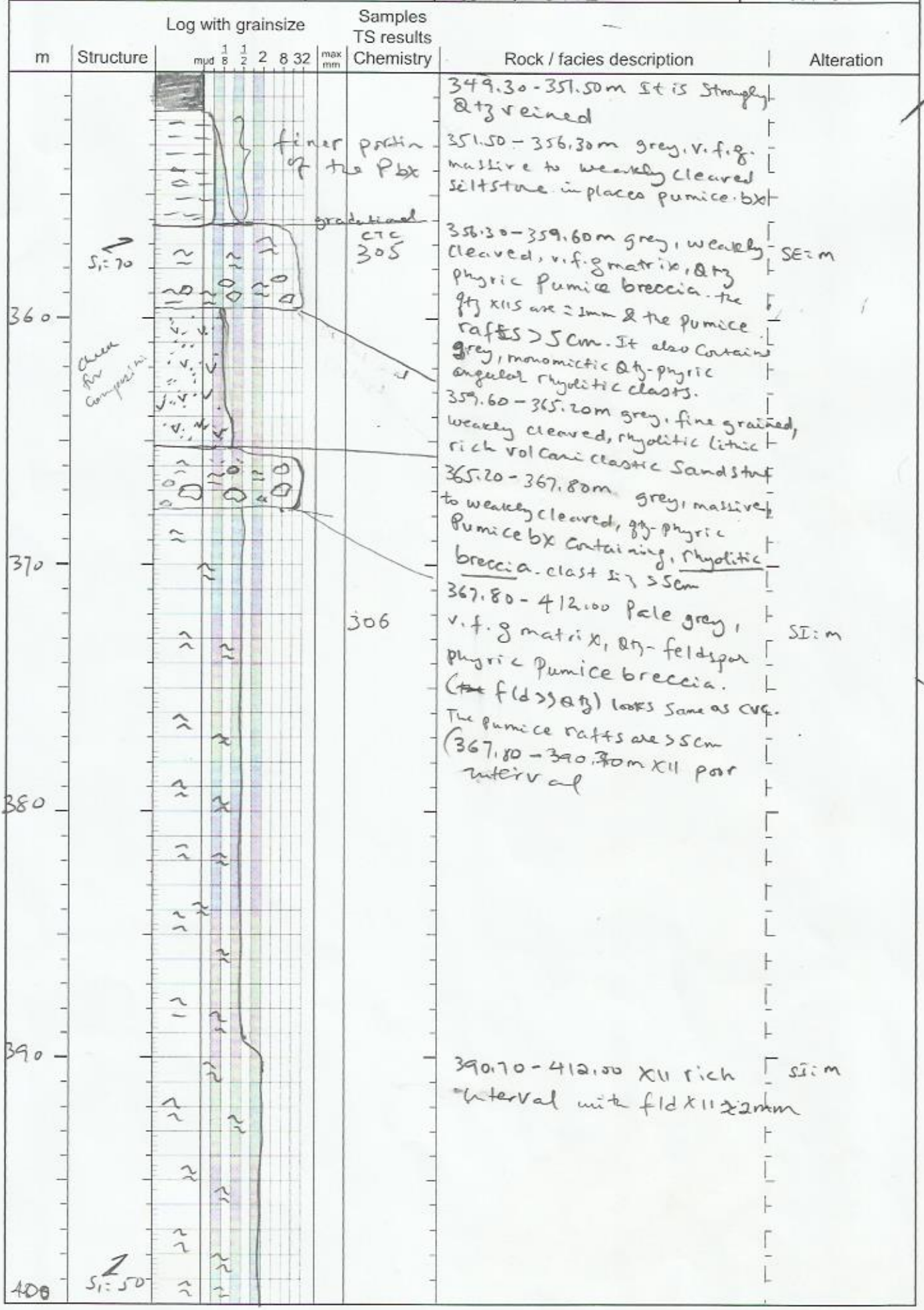

EXPLORATION SKILLS MAPPING CAMP

GRAPHIC LOG

Project Rosebery
Location

Drill hole No. R10032
Location No.

Coords: | RL: | Scale: 1:200 | Page 9 of 10

Azim: | Incl: | Diam: | Logged by: EYOB | Date 16/06/16

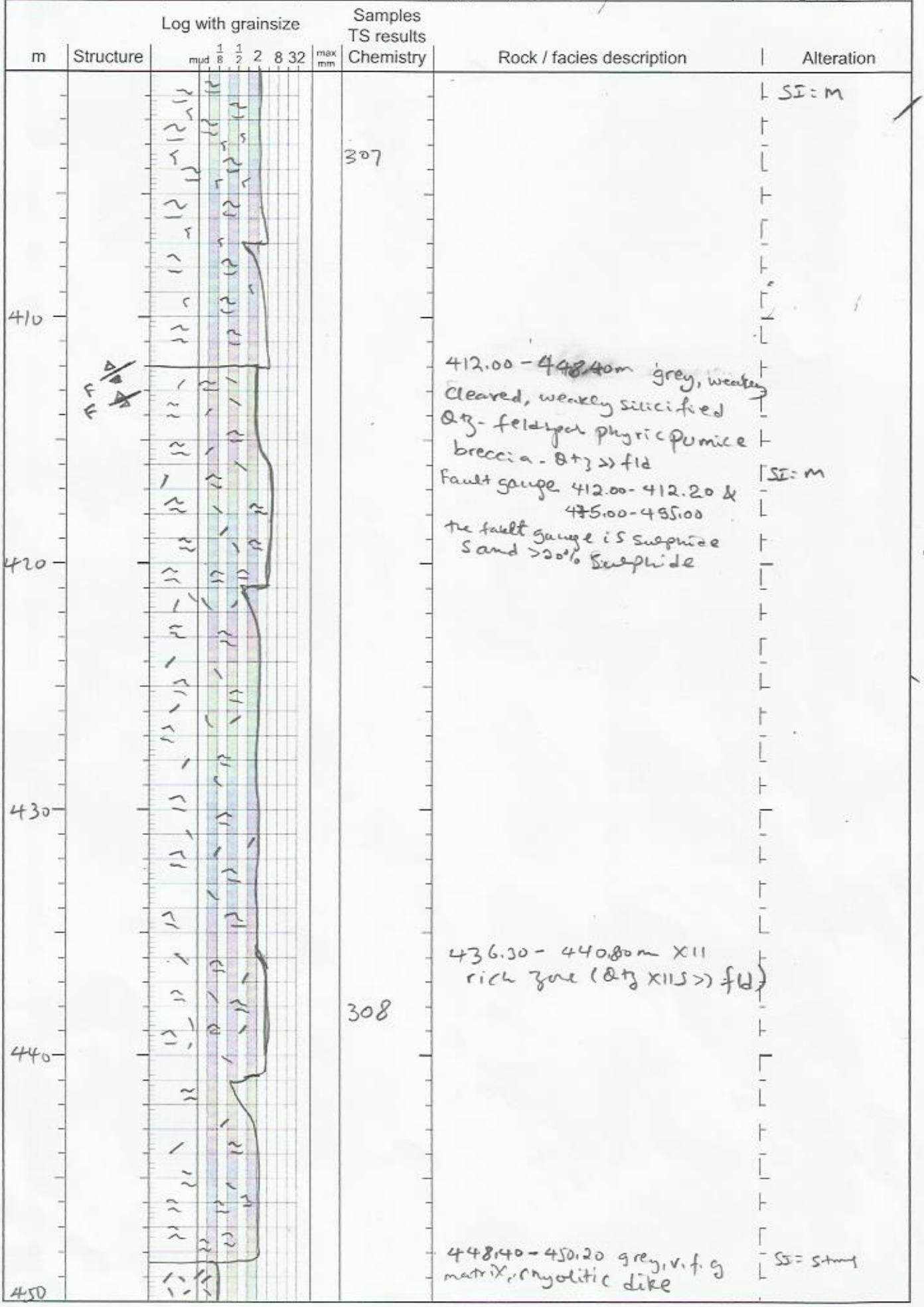

EXPLORATION SKILLS MAPPING CAMP

GRAPHIC LOG

Project Location: Rosebery		Drill hole No.: R10032	Location No.:
Coords:	RL:	Scale: 1:200	Page 10 of 10
Azim:	Incl:	Diam:	Logged by: EYOB / Date: 16/06/16

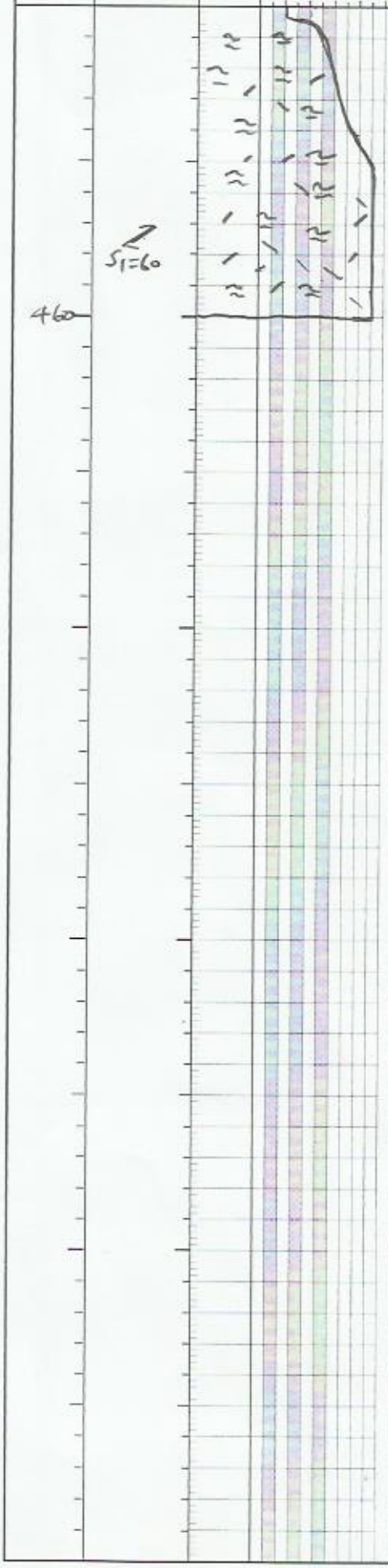

Rock / facies description

450.20 - 460.00 Pale grey, v.f. matrix Qtz-fld phyric Pumice breccia (Qtz » fld)

456.50 - 460.00m the pumice & clasts are strongly flattened & imbricated along weak foliation diagenetically.

Alteration

SI: M

EXPLORATION SKILLS MAPPING CAMP

GRAPHIC LOG

Project ROSEBERY
Location 379429.7 | 5376703N

Drill hole No. R10035
Location No.

Coords:

RL:

Scale: 1:1000

Page 1 of 2

Azim:

Incl:

Diam:

Logged by: EYOB F. ANDEMESKEL

Date 19/04/16

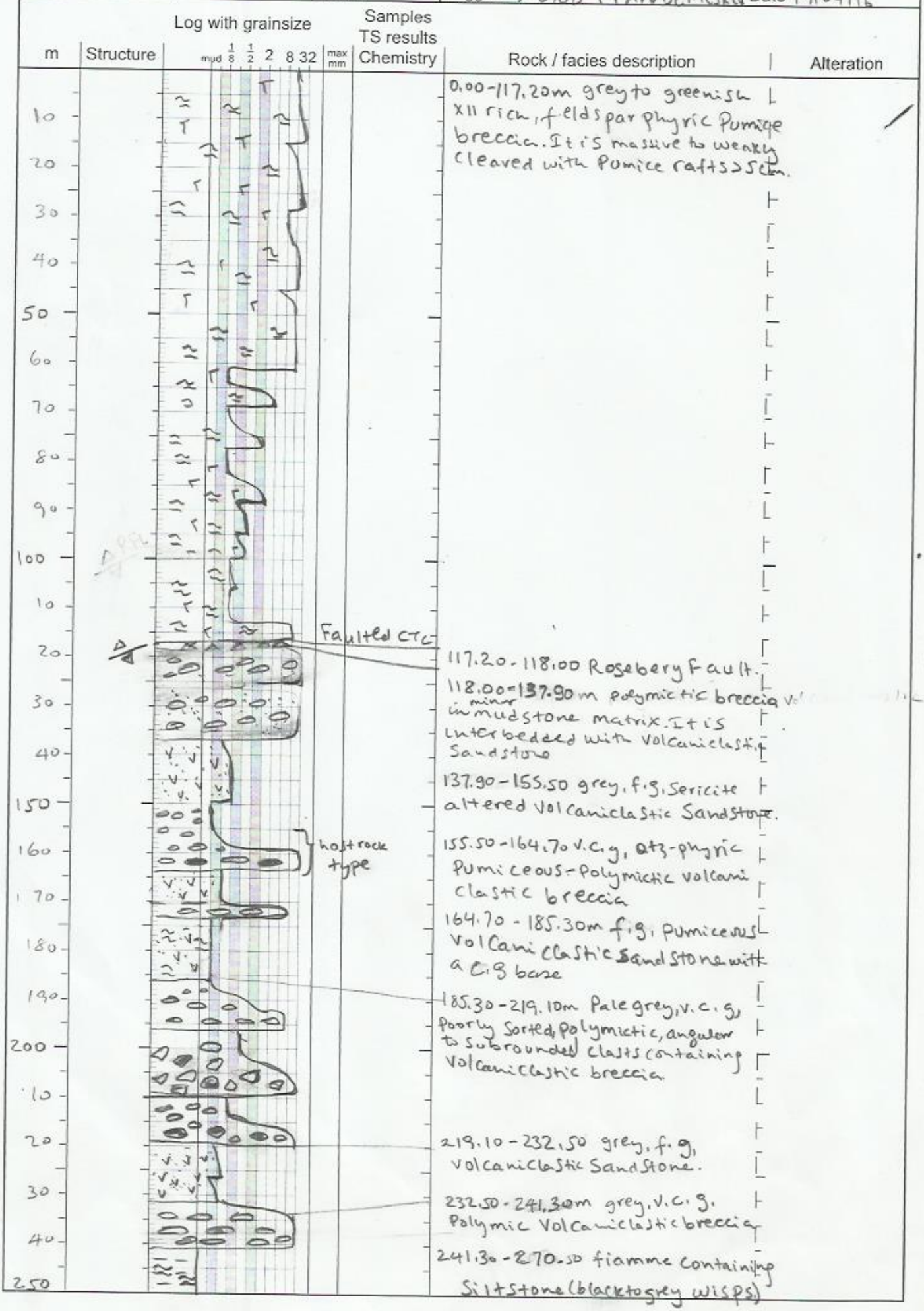

0.00-117.20m grey to greenish X11 rich, feldspar phyric Pumice breccia. It is massive to weakly cleaved with Pumice rafts >5cm.

117.20-118.00 Rosebery Fault.

118.00-137.90 m polymictic breccia with minor mudstone matrix. It is interbedded with Volcaniclastic Sandstone

137.90-155.50 grey, f.g. Sericite altered Volcaniclastic Sandstone.

155.50-164.70 V.C.g, qtz-phyric Pumiceous-Polymictic volcani clastic breccia

164.70-185.30m f.g. Pumiceous Volcani clastic Sandstone with a C.g base

185.30-219.10m Pale grey, V.C.g, poorly sorted, Polymictic, angular to subrounded clasts containing Volcaniclastic breccia

219.10-232.50 grey, f.g, Volcaniclastic Sandstone.

232.50-241.30m grey, V.C.g. Polymic Volcaniclastic breccia

241.30-270.50 fiamme containing Siltstone (black to grey wisps)

EXPLORATION SKILLS MAPPING CAMP

GRAPHIC LOG

Project Rosebery
Location

Drill hole No. R10035
Location No.

Coords: | RL: | Scale: 1:1000 | Page 2 of 2

Azim: | Incl: | Diam: | Logged by: EYOB | Date 19104116

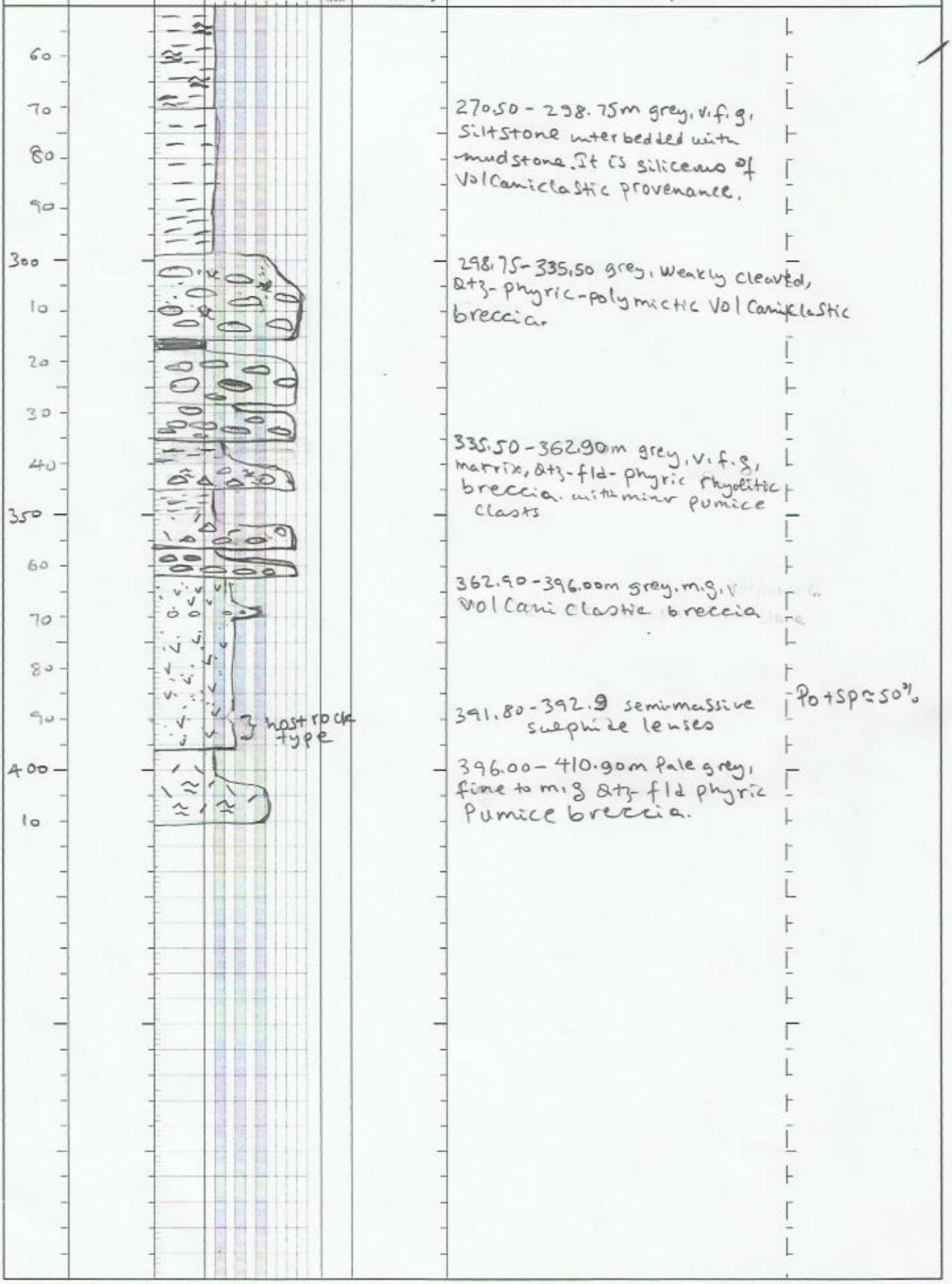

EXPLORATION SKILLS MAPPING CAMP

GRAPHIC LOG

	Project Rosebery Location		Drill hole No. R10035 Location No.
Coords:	RL:	Scale: 1:1000	Page 2 of 2
Azim:	Incl:	Diam:	Logged by: EYOB / Date 19104116

Log with grainsize (mud, 1/8, 1/2, 2, 8, 32, max mm) | Samples, TS results, Chemistry | Structure | m | Rock / facies description | Alteration

60
70
80
90
300
10
20
30
40
350
60
70
80
90
400
10

270.50 - 298.75m grey, v.f.g, siltstone interbedded with mudstone. It is siliceous of volcaniclastic provenance.

298.75 - 335.50 grey, weakly cleaved, Qtz-phyric-polymictic volcaniclastic breccia.

335.50 - 362.90m grey, v.f.g, matrix, Qtz-fld-phyric rhyolitic breccia. with minor pumice clasts

362.90 - 396.00m grey, m.g, volcaniclastic breccia

391.80 - 392.9 semi-massive sulphide lenses — Po+Sp ≈ 50%

396.00 - 410.90m pale grey, fine to m.g Qtz-fld phyric pumice breccia.

host rock type

EXPLORATION SKILLS MAPPING CAMP

GRAPHIC LOG

Project Rosebery		Drill hole No. R10035	
Location 379429.2E/5376703N		Location No.	
Coords: 379429.2E/5376703N	RL: -735.894	Scale: 1:200	Page 1 of 9
Azim: -268.7	Incl: -40	Diam:	Logged by: E40B ANDEMESKEL
			Date 19/04/16

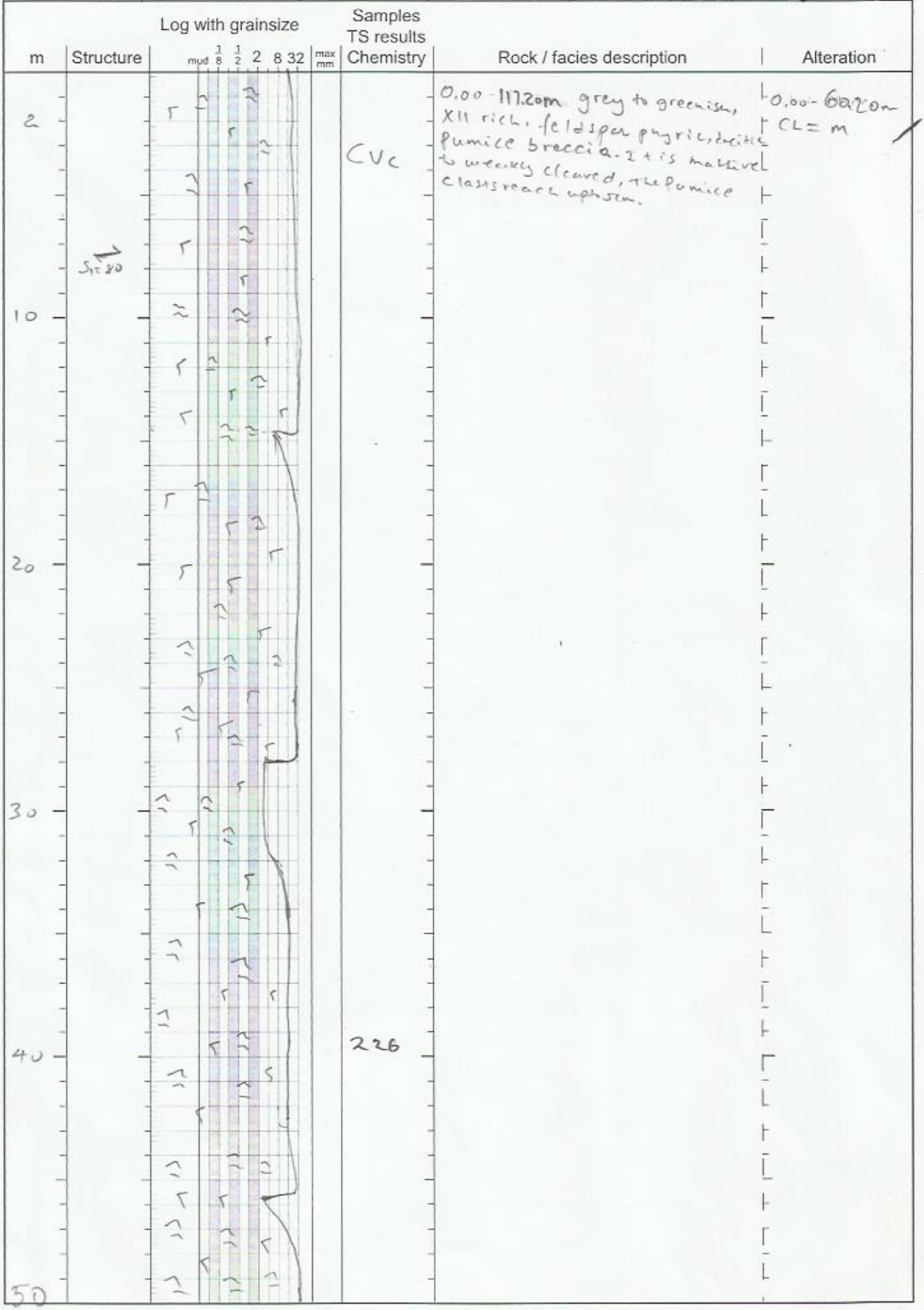

EXPLORATION SKILLS MAPPING CAMP

GRAPHIC LOG

Project Roseberry
Location

Drill hole No. R10035
Location No.

Coords: | RL: | Scale: 1:200 | Page 2 of 9

Azim: | Incl: | Diam: | Logged by: EYOb | Date 19/04/16

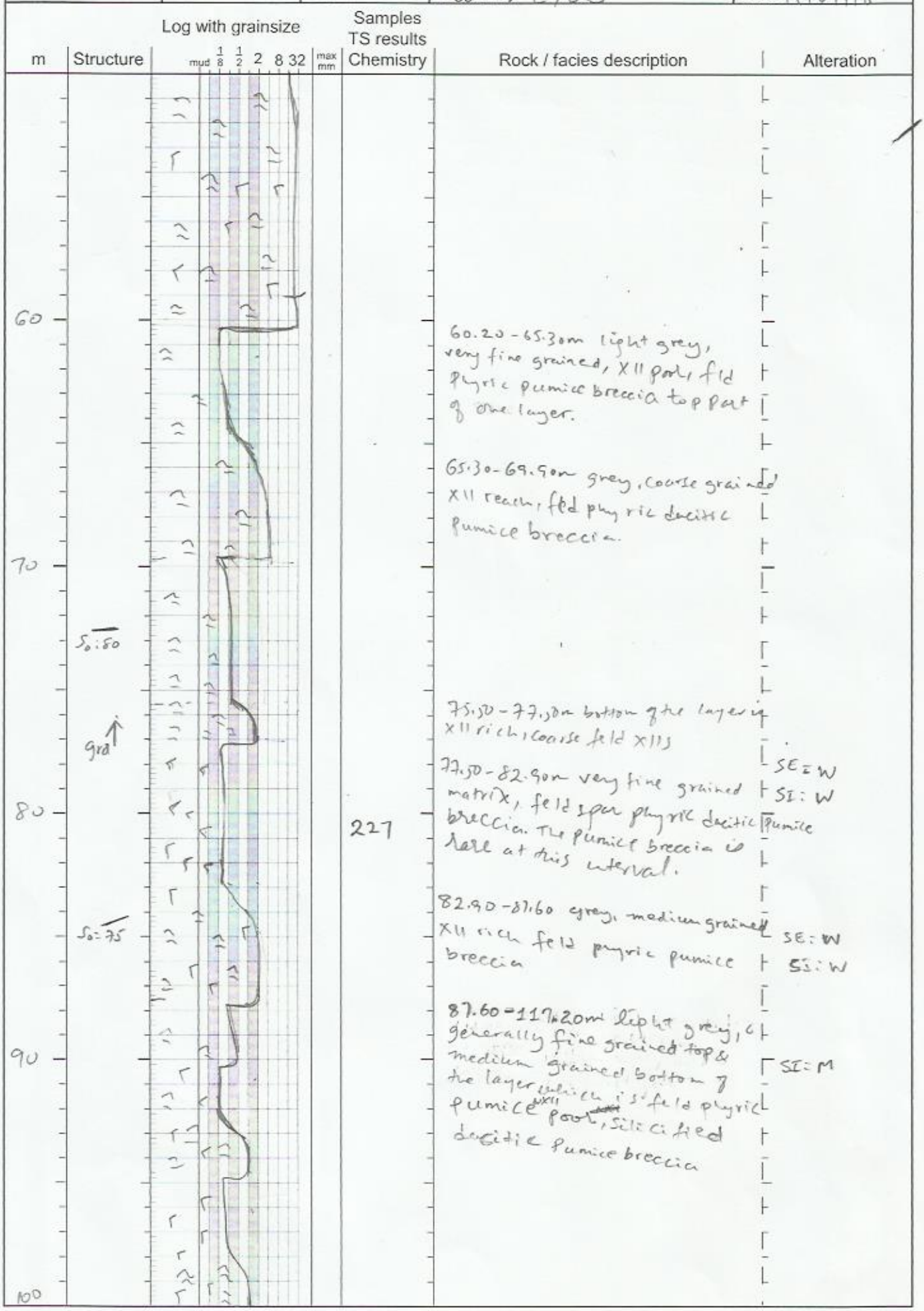

EXPLORATION SKILLS MAPPING CAMP

GRAPHIC LOG

Project		Drill hole No.	R10035
Location		Location No.	
Coords:	RL:	Scale: 1:200	Page 3 of 9
Azim:	Incl:	Diam:	Logged by: Date 19/04/16

Log with grainsize: mud | 1/8 | 1/2 | 2 | 8 | 32 | max mm

Samples: TS results: Chemistry

m	Structure	Rock / facies description	Alteration
			SI = m SE = W
110	S_0=60		
	RF	114.80–117.20 light grey, very coarse grained, feldspar phyric Pumice breccia It contains 2-5cm thick tectnic breccia with jig saw fit texture	
120	Faulted CTC	117.20–118.00m dark grey, intensely brecciated, siliceous unit with minor mud, Rosebery Fault.	CB = m
	S_0=65		
	S_0=60	118.00–125.20 Polymictic Volcani clastic breccia with minor mudstone matrix -It is interbedded with Volcani clastic Sandstone from 121.50–122.90m	CB m
	Slaty CTC		
130	S_0=50	125.20–128.60m. Pale grey, medium grained, moderately foliated, Sericite altered & Py phyric Volcani clastic Sandstone	SE = m CBm
		128.60–137.90m dark grey, Polymictic Volcaniclastic breccia with minor mudstone Clast size ranges from 4–20cm	CB = m
	S_0=55	137.90–151.60m grey, fine to medium grained, moderately Cleaved & Sericite altered Volcaniclastic Sandstone Stringer of Sulphid from 141.8–148.00m	Py from 141.8–148.00 Py ≈ 5% Stringer SE: M
140			
	S_1=60		
150			

229 230 231 232

EXPLORATION SKILLS MAPPING CAMP

GRAPHIC LOG

Project Rosebery		Drill hole No. R10035	
Location		Location No.	
Coords:	RL:	Scale: 1:200	Page 4 of 9
Azim:	Incl:	Diam:	Logged by: EYOB	Date 19

Log with grainsize (mud, 1/8, 1/2, 2, 8, 32, max mm) | Samples / TS results / Chemistry | Structure | m | Rock / facies description | Alteration

160

S₀=60

155.50 - 164.70m grey, very coarse grained, Qtz-phyric polymictic Vol Cani clastic breccia. It is Pumiceous & contains lenticular patches of Sulphide mainly Py-It is host rock to the Rosebery Group clasts are of Qtz-phyric (rhyolitic) vitreous & grey colored.

SE = M

Py = 1-2%

Footwall type

233

164.70 - 170.90m fine to medium grained pumiceous Volcaniclastic Sandstone.

170

170.90 - 172.60m polymictic volcaniclastic breccia

172.60 - 185.30m Pale grey, fine to very fine grained, Pumiceous Vol Cani clastic Sand Stone. It is strongly cleaved & intensely silicified altered from 182.3 - 185.30m

SE: 172.6 - 182.3 Strng

SI = S 182.3 - 185.30

S₁=40

234

180

235

185.30 - 195.50m Pale grey, very coarse grained, poorly sorted polymictic, angular to subrounded clasts containing Vol Caniclastic breccia. Clast size reaches 12cm & grades uphole. It is Qtz-Pyrit

SE = m

190

236

S₀=50

195.50 - 202.00 Pale grey, medium grained, Pumiceous vol Cani clastic Sand Stone. The Pumice raft is coarse feldspar phyric

SE = m

200

223.9 - 229.70

EXPLORATION SKILLS MAPPING CAMP **GRAPHIC LOG**	Project Rosebery Location		Drill hole No. R10035 Location No.
Coords:	RL:	Scale: 1:200	Page 5 of 9
Azim:	Incl:	Diam:	Logged by: EYOB Date 19/04/16

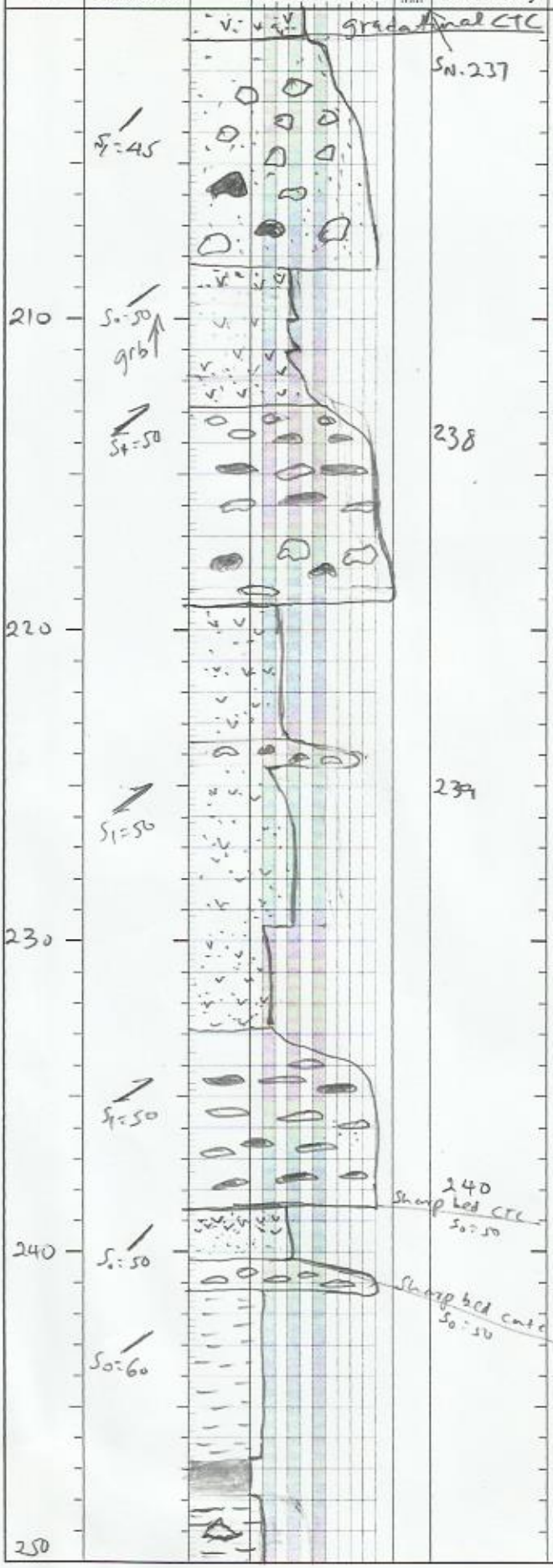

202.00 - 208.20m grey, very coarse grained, moderately cleaved poorly sorted angular to subrounded clasts containing polymict volcaniclastic breccia clast size >5cm at bottom of bed generally imbricated along cleavage — SE = m, CL = w

208.20 - 212.9m grey, m.g, moderately cleaved, volcaniclastic Sandstone (Possibly reworked provenance)

212.90 - 219.10m, grey, coarse grained, poorly sorted at the base, generally grading upholl, strongly sericite altered with Possibly Pumice containing polymict volcanic breccia. — SE = m, CL = w
- clasts are subrounded to angular at the base & lenticular (elongate) upholl imbricated along cleavage
- clasts are mainly Qtz-phyric rhyolitic & glassy.

219.10 - 232.50 grey, fine to medium grained, moderately cleaved, volcaniclastic Sandstone that shows general grading upholl. It contains sparse polymict clasts from 223.9 - 229.70m in a fine to medium grained volcaniclastic sandstone. — SE = m, CL = w

232.50 - 238.60m grey, v.c.g moderately cleaved, subrounded & mainly elongate polymict clasts aligned along the cleavage containing volcaniclastic breccia. dominated by Qtz-phyric rhyolitic clasts >5cm — SE = M, CL = w

238.60 - 240.20 grey, fine to medium grained volcaniclastic sandstone interbedded with grey-wack of basement derived (239.65 - 240.20m)

240.20 - 241.30 polymictic volcanic breccia same as 232.50 - 238.60m — Py = 1%

241.30 - 247.90 grey, f.g, massive to weakly cleaved Sst+Stne interbedded with mud Stone at the base of the interval.

247.50 - 248.00 milky Qtz vein

EXPLORATION SKILLS MAPPING CAMP

GRAPHIC LOG

Project Rosebery		Drill hole No. R10035	
Location		Location No.	
Coords:	RL:	Scale: 1:200	Page 6 of 9
Azim:	Incl:	Diam:	Logged by: Date 22/04/16

Log with grainsize: mud, 1/8, 1/2, 2, 8, 32, max mm

Samples TS results Chemistry

247.90 - 270.50 grey, v.f.g, weakly cleaved, black to grey wispy alteration (mild lithic) containing Siltstone the wispy alteration is possibly Pumice breccia

241

260

S1:55

265.00 - 266.00 dark grey mudstone interbedded with Siltstone

S0:65

270.50 - 273.80m massive, milky Qtz vein cross cutting the Siltstone. dark grey siltstone from 272.50 - 272.90m

270

VQ

VQ

VQ

VQ 82:30

273.80 - 298.75m grey, v.f.g Siltstone interbedded with mudstone - It is very siliceous (volcaniclastic plutholith. (volcaniclastic Siltstone) Sparsely Qtz phyric (colourless Qtz)

280

283.50 - 284.50 stock-work of Qtz veining

S1:60

290

242

S0:70

300

EXPLORATION SKILLS MAPPING CAMP **GRAPHIC LOG**	Project Location		Drill hole No. R10035 Location No.
Coords:	RL:	Scale:	Page 7 of 9
Azim: Incl:	Diam:	Logged by:	Date

m	Structure	Log with grainsize (mud, 1/8, 1/2, 2, 8, 32; max mm)	Samples / TS results / Chemistry	Rock / facies description	Alteration
310	S_0=80			298.75 - 316.50 grey, v.f.g, weakly cleaved, Qtz-phyric Polymictic Vol Caniclastic breccia dominated by dark green wisps which are intensely chlorite + sericite altered Pumice - clasts are sparse & dominated by grey-quartz-phyric, angular to subrounded > 2cm (correlate to 337R 1730-1750)	
			243		
	S_0=70, S_1=80			316.50 - 317.80m dark grey, cleaved & laminated mudstone interbedded with Siltstone.	Py <1%
320	S_1=80			317.80 - 335.50m grey, fine grained matrix, very coarse Polymictic Vol Cani clastic breccia. clast size ranges from cm to greater than 6cm. It contains green Qtz-feldspar phyric rhyolitic & glassy rhyolitic clasts resedimented in a volcaniclastic Sandstone. It shows jigsaw fit texture in a Sandstone matrix. It is glassy as a result of quench fragmentation resulting to hyaloclastite resedimentation	
	Fld phyric				
330			244	- The unit is cross cut by Qtz vein from 330.0m - 333.6m	
	S_1=70		245	335.50 - 338.50m grey, v.f.g matrix, Qtz-fld phyric Pumice breccia (Same as the WSF)	
340				338.50 - 342.70m grey, v.f.g Siltstone	
	S_0=70			342.70 - 351.45m grey, v.f.g massive to weakly cleaved Siltstone	
350					

EXPLORATION SKILLS MAPPING CAMP

GRAPHIC LOG

Project Location: Rosebery		Drill hole No.: R10035	
Coords:	RL:	Scale: 1:200	Page 8 of 9
Azim:	Incl:	Diam:	Logged by: EMG / Date 22/04/16

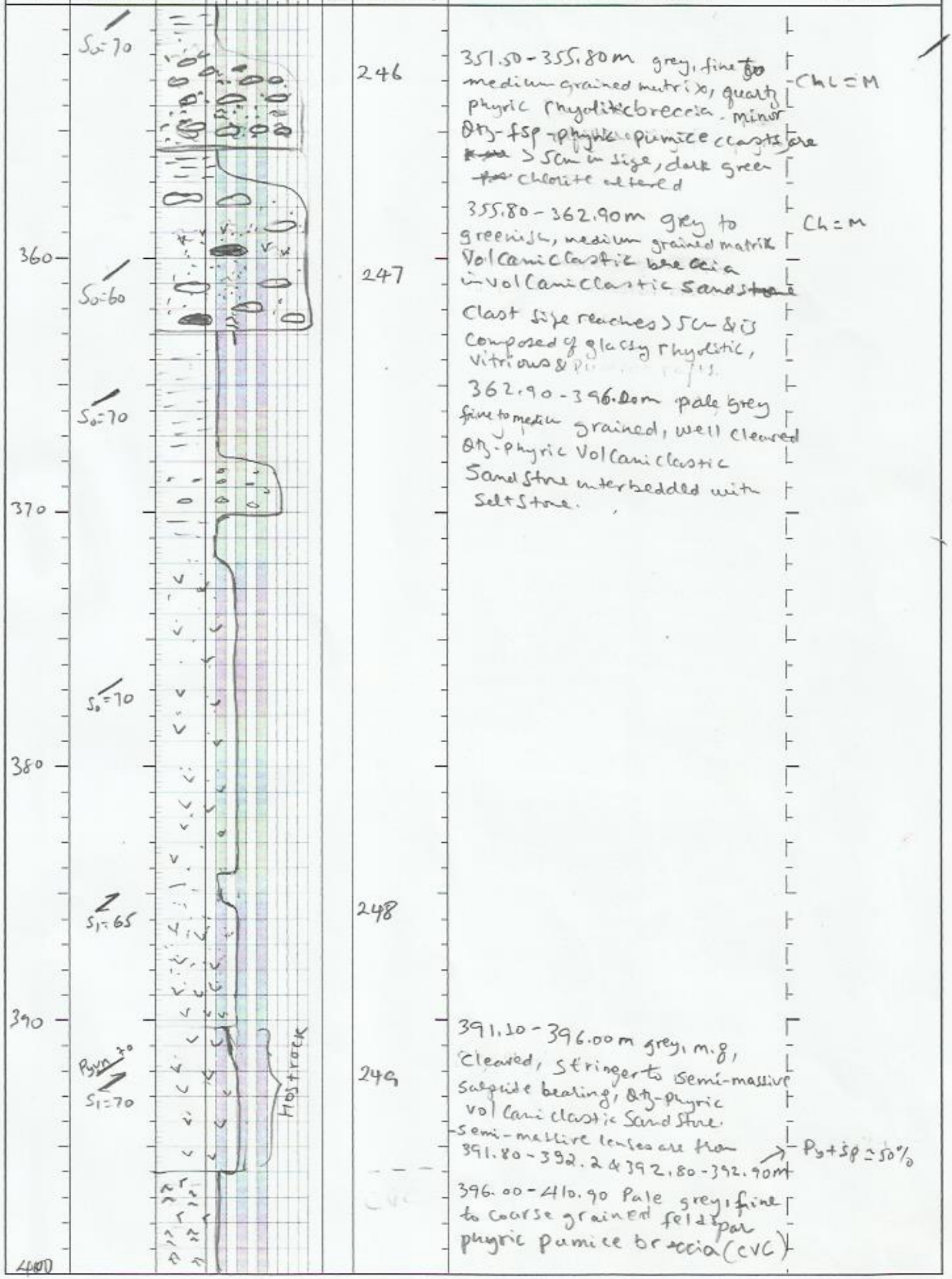

EXPLORATION SKILLS MAPPING CAMP

GRAPHIC LOG

Project Location: Rosebery		Drill hole No.: R10035	Location No.:
Coords:	RL:	Scale: 1:200	Page 9 of 9
Azim:	Incl:	Diam:	Logged by: EYOB	Date: 22/04/16

m	Structure	Log with grainsize (mud, 1/8, 1/2, 2, 8, 32, max mm)	Samples / TS results / Chemistry	Rock / facies description	Alteration
410			250	396.00 - 401.50 is very fine grained XII poor silt part of the feldspar-Qtz phyric Pumice breccia top 401.50 - 410.90 is XII rich Qtz fld phyric Pumice breccia which is massive to weakly bedded.	
420					

Summary log

EXPLORATION SKILLS MAPPING CAMP

GRAPHIC LOG

Project Location: Rosebery

Drill hole No. R10063

Location No.

Coords: 379801.9E 5376323N | RL: | Scale: 1:1000 | Page 1 of 5

Azim: 258.7 | Incl: -40 | Diam: | Logged by: EVOR F. ANDEMESKEL | Date 04/03/16

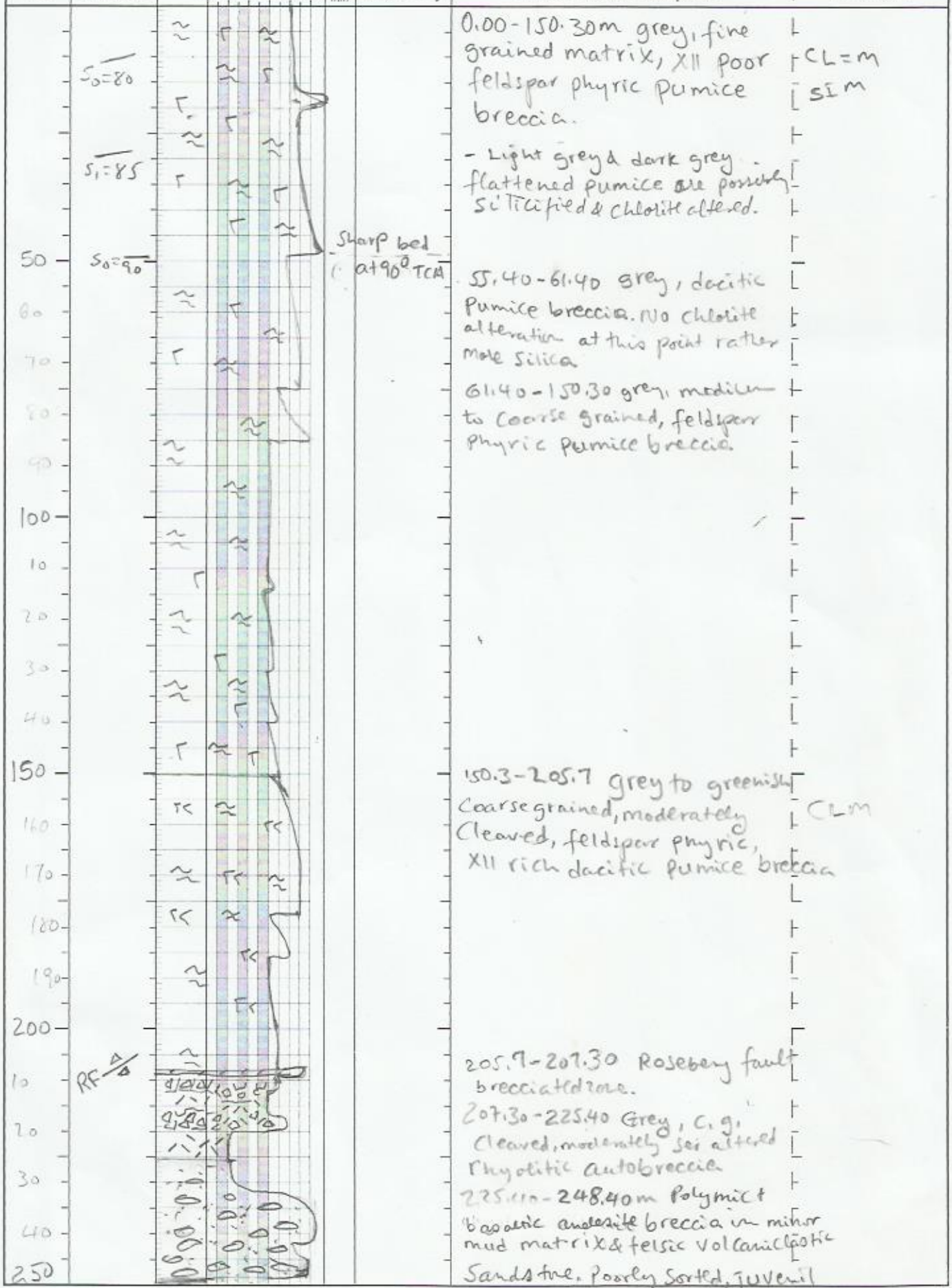

0.00-150.30m grey, fine grained matrix, XII poor feldspar phyric pumice breccia. CL=m SI m

- Light grey & dark grey flattened pumice are possibly silicified & chlorite altered.

55.40-61.40 grey, dacitic pumice breccia. No chlorite alteration at this point rather more silica

61.40-150.30 grey, medium to coarse grained, feldspar phyric pumice breccia.

150.3-205.7 grey to greenish coarse grained, moderately cleaved, feldspar phyric, XII rich dacitic pumice breccia CL-m

205.7-207.30 Rosebery fault brecciated zone.

207.30-225.40 Grey, c.g. cleaved, moderately ser altered rhyolitic autobreccia

225.40-248.40m Polymict basaltic andesite breccia in minor mud matrix & felsic volcaniclastic Sandstone. Poorly sorted, juvenil angular to subrounded clasts

EXPLORATION SKILLS MAPPING CAMP

GRAPHIC LOG

Project Location: Rosebery

Drill hole No. R 10063

Location No.

Coords: | RL: | Scale: 1:1000 | Page 3 of 5

Azim: | Incl: | Diam: | Logged by: EYOB | Date 04/03/15

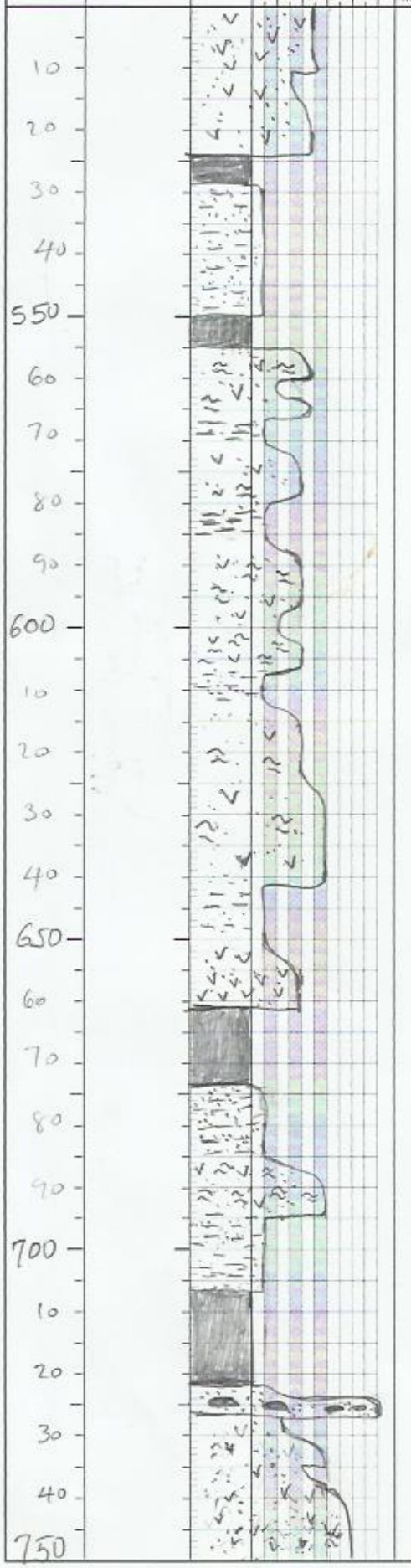

Rock / facies description

524.00 – 555.20 mudstone (shale) / Silt stone

555.20 – 722.50 grey, m.g, alternating pumice rich zone & XII poor, Volcani clastic Sand stone grading uphole to interbedded Silt stone / mudstone.

611.40 –

722. 793.50 medium to coarse grained, weakly cleaved, strongly Sericite & weakly Chlorite altered XII poor N0 / Cani clastic Sand Stone

Alteration

EXPLORATION SKILLS MAPPING CAMP

GRAPHIC LOG

Project Location	Rosebery	Drill hole No. / Location No.	R10063
Coords:		RL:	Scale: 1: 1000
Page 2 of 5			
Azim:	Incl:	Diam:	Logged by: EYOB
Date 04/03/16			

Log with grainsize (mud, 1/8, 1/2, 2, 8, 32, max mm) | Samples | TS results | Chemistry | Structure | m | Rock / facies description | Alteration

248.40 - 256.70 dark grey, weakly cleaved, weakly Qtz-CB veined, mudstone. It contains bands of Sphalerite.

256.70 - 300.70 Pale grey, weakly cleaved, moderately silica & weakly CL + SE altered, XU poor (257.2-281) & Qtz phyric (281.-233) polymict angular clasts, poorly sorted at the base containing Qtz-phyric polymict breccia in volcaniclastic SST
- clasts are aphanitic felsic volcaniclastic
- at 280.-281.80 rhyolitic dike intrudes the volcaniclastic sandstone.

300.70 - 333.0 grey to greenish medium to coarse grained graded, & well sorted, granules to lappilli grey & white andesitic clast containing volcaniclastic sandstone

333.0 - 349.30 siltstone interbedded with mudstone

349.30 - 405.60m medium to coarse grained pumicous volcaniclastic sandstone interbedded with siltstone.

405.00 - 427.80
Polymictic volcaniclastic breccia in volcaniclastic sandstone matrix.
(Same unit hosts mineralization in R10032.
420.30 - 420.80 Semi-massive sulphide lense with Py, Po * Sph Cpy
427.80 - 433.80 mudstone | siltstone
433.80 - 441 Polymict volcaniclastic breccia in volcaniclastic sandstone
441.0 - 478 mudstone | siltstone with disseminated Po + Py veinets

478.30 - 524.40 grey, m.g. Volcaniclastic Sandstone

host rock

$ semi-massive to massive sulphide

EXPLORATION SKILLS MAPPING CAMP

GRAPHIC LOG

Project Location: Rosebery

Drill hole No.: R10063

Location No.:

Coords:

RL:

Scale: 1:1000

Page 4 of 5

Azim:

Incl:

Diam:

Logged by: EYoB

Date 04/03/16

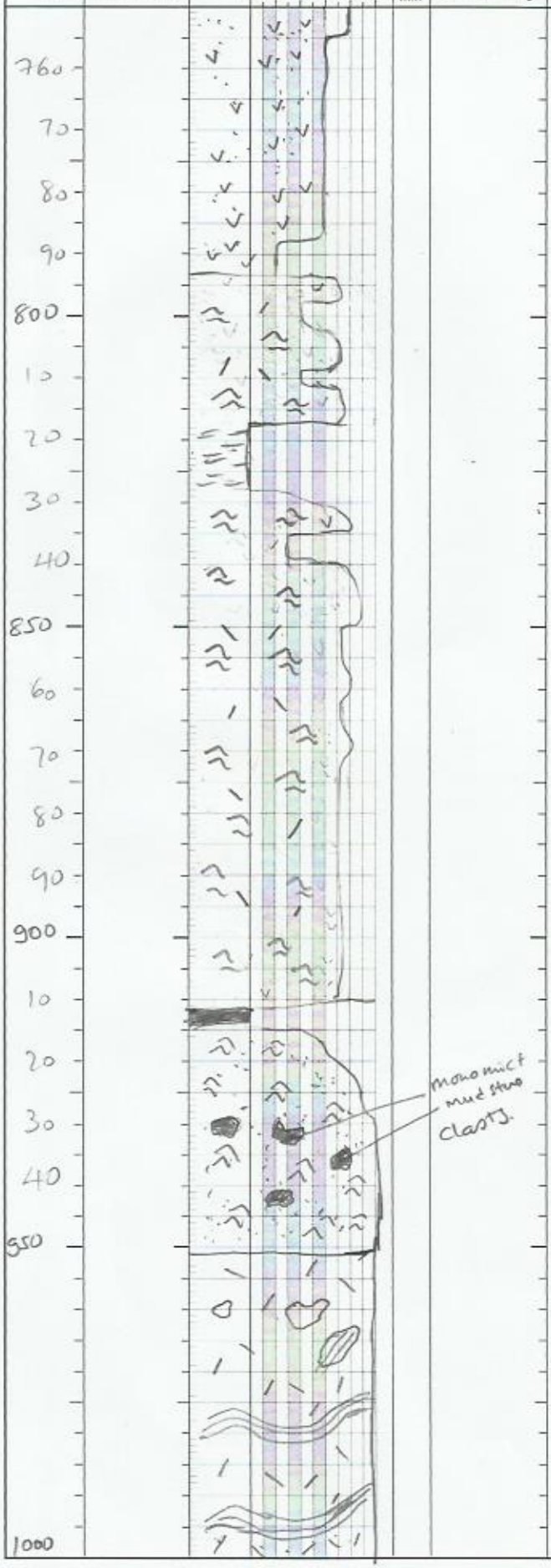

Rock / facies description

793.50 - 854.90 grey, coarse grained, siliceous, massive to weakly cleaved, bedded, coarse Qtz-fsp phyric Pumice breccia

854.90 - 911.80m grey, very coarse grained Qtz-feldspar Phyric Pumice breccia

911.8 - 914.70m Pyritic Shale

914.70 - 951.80m dark grey, fine grained matrix, monomictic clasts of mudstone containing Qtz-fsp phyric Pumice breccia in mudstone

951.8 - 1017.2 grey, fi matrix, Qtz-feld phyric, flow banded rhyolitic breccia.

998.0 - 999.20 monomictic autobreccia of Qtz-phyric rhyolite hyaloclastite with jig saw fit texture

Alteration

EXPLORATION SKILLS MAPPING CAMP

GRAPHIC LOG

Project Location: Rosebery		Drill hole No.: R10063	
Coords:	RL:	Scale: 1:1000	Page 5 of 5
Azim:	Incl: Diam:	Logged by: EYOB	Date 04/03/16

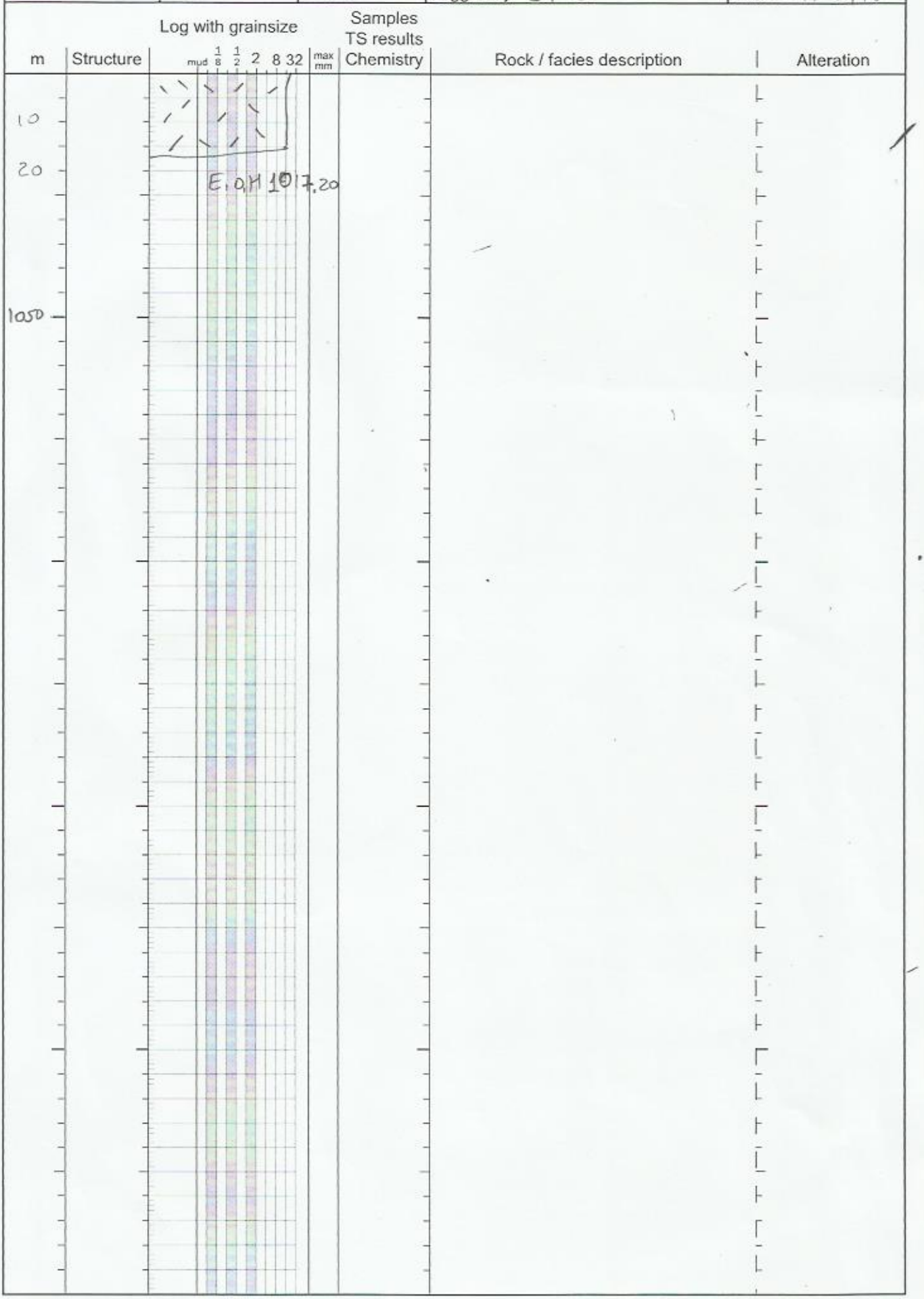

EXPLORATION SKILLS MAPPING CAMP

GRAPHIC LOG

Project Rosebery | Drill hole No. R10063
Location Total depth 1017.20 | Location No.

Coords: 379801.9E/5376323N | RL: 258.7 | Scale: 1:200 | Page 1 of 21
Azim: 258.7 | Incl: -40 | Diam: | Logged by: EYOB F. ANDEMESKEL | Date 1/03/16

Log with grainsize (mud, 1/8, 1/4, 1/2, 2, 8, 32, max mm)

m	Structure	Samples / TS results / Chemistry	Rock / facies description	Alteration
			0.00 - 64.40m grey, fine grained matrix, dacitic, XII poor, fld phyric Pumice breccia.	CL=M
			- light grey & dark grey flattened looking like welded Pumice. The light grey could be silicified while the dark grey is chlorite altered Pumice.	SI=M
		164		
10			- trace of disseminated & veinlets of Pyrrhotite noted @12.8m latches veins of Cpy & Bornite - It is weakly cleaved & the Pumice are flattened along the clevage.	Cpy<1 Bor<1 Py<1 Py<1
20			- The Pumice breccia clasts are dense at the base grading upward to a finer dacitic Pumice breccia - clast size at the base reaches 5cm	CL=M SI=M
30				
40				
		165		
		sharp bed	@48.60 sharp bed CTC @90° TCA	
50				

EXPLORATION SKILLS MAPPING CAMP

GRAPHIC LOG

Project Location		Drill hole No. R 10063 Location No.	
Coords:	RL:	Scale: 1:200	Page 2 of 21
Azim:	Incl: Diam:	Logged by: EYOB	Date 1/03/16

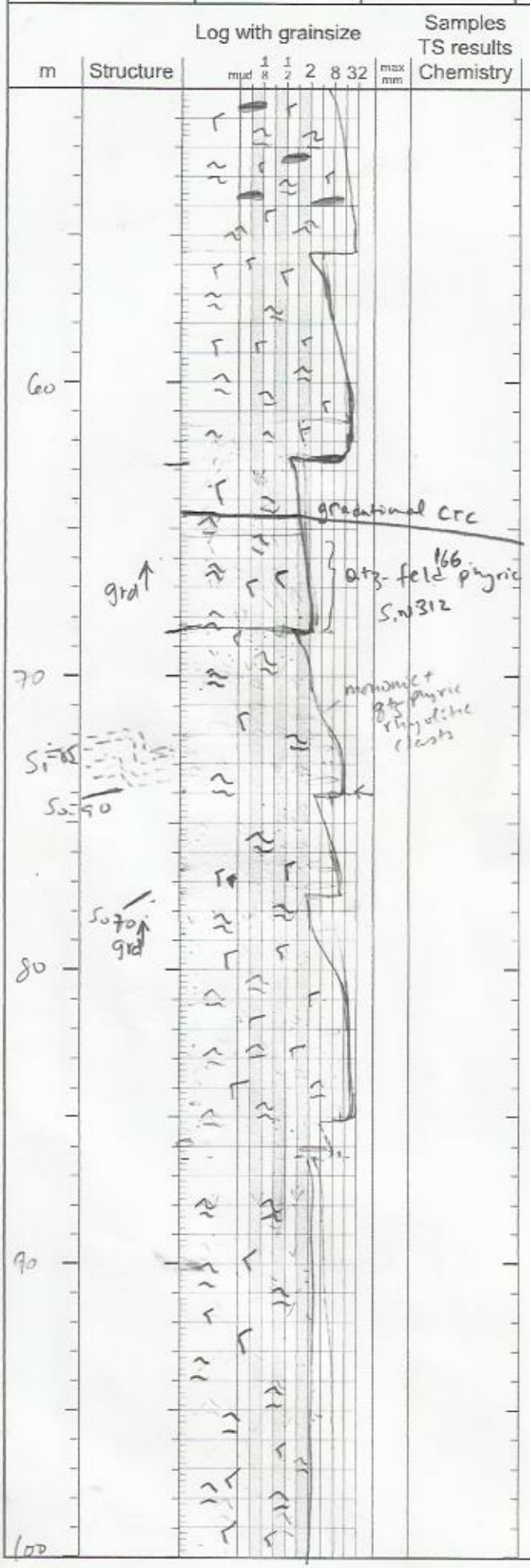

EXPLORATION SKILLS MAPPING CAMP

GRAPHIC LOG

Project Location: Rosebery		Drill hole No.: R10063	
Location No.			
Coords:	RL:	Scale: 1:200	Page 3 of 21
Azim:	Incl:	Diam:	Logged by: EYOB / Date 1/03/16

Log with grainsize (mud, 1/8, 1/2, 2, 8, 32, max mm)

m	Structure	Samples / TS results / Chemistry	Rock / facies description	Alteration
	F		100.80 – 101.40m highly broken core with planar face probably a fault.	
110	Plane			
120			It is weakly cleaved & weakly chl altered with rare pumice	Chl = W
		313		
130				
		314		
140				
150				

EXPLORATION SKILLS MAPPING CAMP

GRAPHIC LOG

Project Rosebery | Drill hole No. R10063
Location | Location No.

Coords: | RL: | Scale: 1:200 | Page 4 of 21

Azim: | Incl: | Diam: | Logged by: EYOB | Date 01/03/16

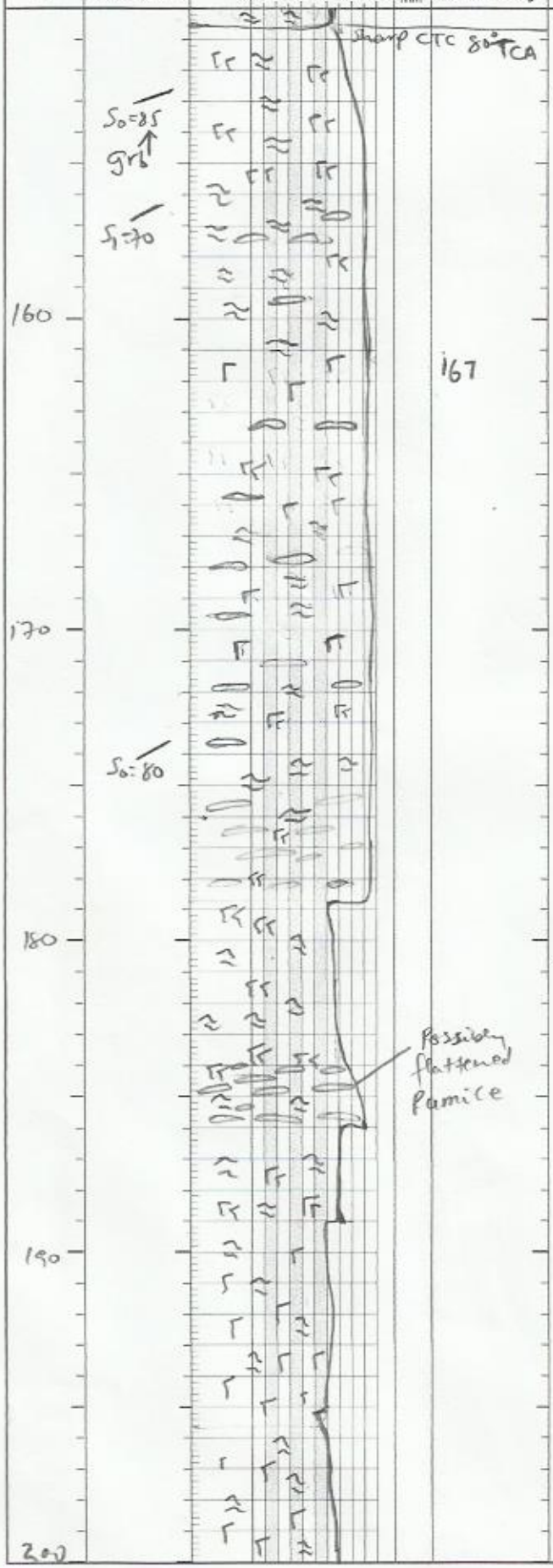

150.30 – 205.7 grey to greenish coarse grained, moderately cleaved, feldspar phyric, XII rich dacitic pumice breccia of EVC. CL=M

Polymict clasts of aphanitic feldsp volcanic (silicified pumice) & grey-greenish (chloritic pumice) are intensely flattened parallel to the cleavage & are X4 cm sized

150.30 – 162.50 is XII rich

162.50 – 171.90 is XII poor

CL=4

171.90 – 178.75 is XII rich

CL=5

178.75 – 189.30 Pale grey, medium grained, feldspar phyric, XII rich, dacitic monomictic Pumice breccia weakly cleaved & clasts aligned along cleavage SE=W SE=W

189.30 – 195.40m XII poor, Pale grey, dacitic Pumice breccia

195.40 – 205.7 Pale grey, XII poor, weakly cleaved dacitic pumice breccia

EXPLORATION SKILLS MAPPING CAMP

GRAPHIC LOG

Project Rosebery | Drill hole No. R10663

Location | Location No.

Coords: | RL: | Scale: 1:200 | Page 5 of 21

Azim: | Incl: | Diam: | Logged by: EYOB | Date 02/03/16

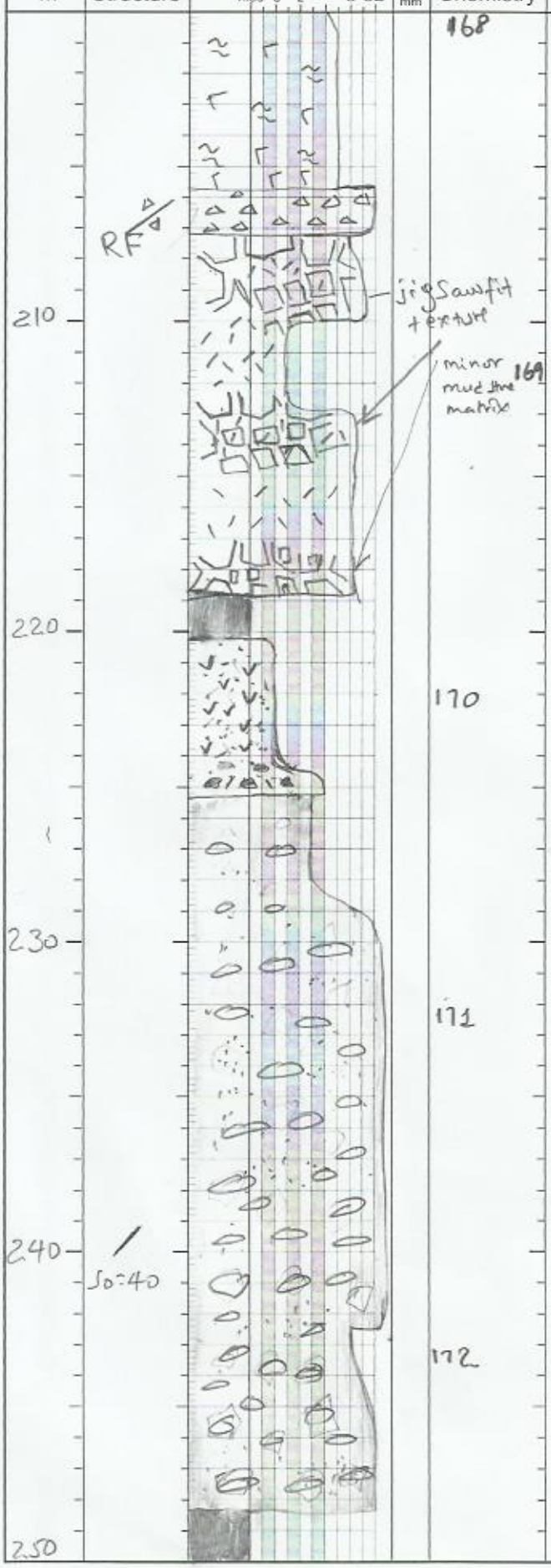

Rock / facies description

205.7 - 207.30 dark grey, intensely brecciated zone, Partly puggy & crumbly, The breccia unit contains quartz, Sulphide (Py) veins & patches (Rosebery Fault.)

207.30 - 218.80m Grey, Coarse grained, cleaved, moderately Sericit altered. rhyolitic breccia with minor mud lithics - It is Possibly a hyaloclastite with jigsaw fit texture. or intensely silicified Pseudo texture.

218.80 - 220.30m - dark grey massive to weakly cleaved mudstone

220.30 - 225.40m grey, fine grained with brownish hematite after Py + Po alteration containing Volcaniclastic Sandstone

225.40 - 248.40m polymictic breccia with minor mud stone matrix clastics. & carbonate veining

- Generally, poorly Sorted, juvenile angular to Sub - rounded clasts are imbricated along cleavage in a mud matrix.

- clasts are aphanitic and quartz - carbonate altered.

Alteration

SE = M
SI = Strong
Py < 1
CPy < 1
Po < 1

EXPLORATION SKILLS MAPPING CAMP

GRAPHIC LOG

Project Roseberry | Drill hole No. R10063
Location | Location No.

Coords: | RL: | Scale: 1:200 | Page 6 of 21
Azim: | Incl: | Diam: | Logged by: EYOB | Date 01/03/16

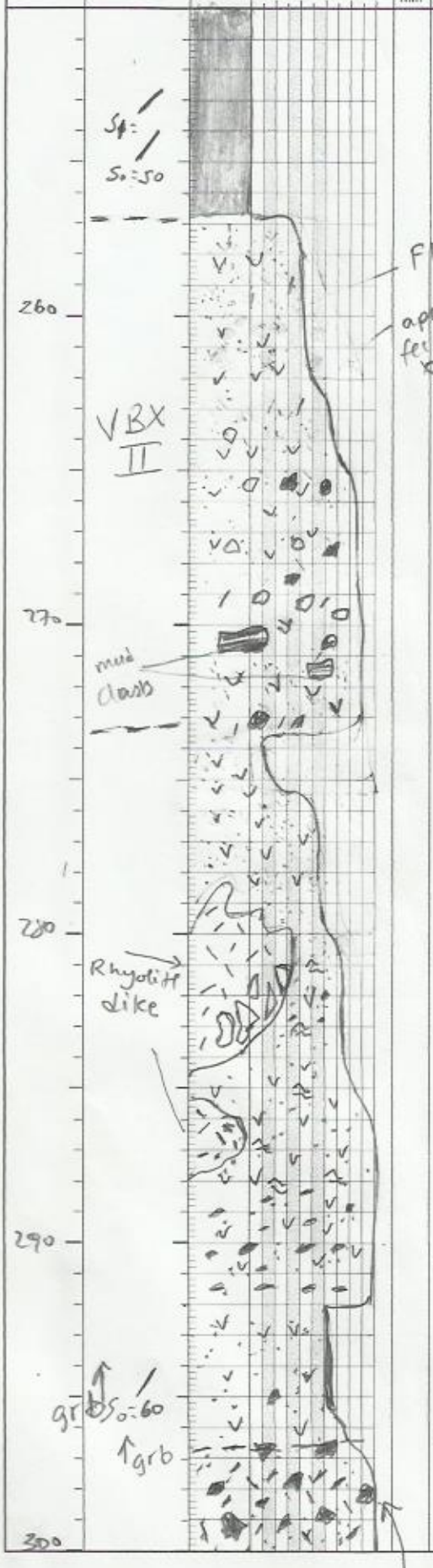

Samples / TS results

Chemistry

173

Fld XII5

aphanitic felsic volcanic clasts (2cm) 174

175

176

177

178

296.9-299.90 basaltic-andesite fiamme of possible pumice groundmass

Rock / facies description

248.40-256.70m dark grey weakly cleaved, weakly Qtz-CB veined, mudstone. It contains bands of Sphalerite It is interbedded with Volcaniclastic Siltstone.

256.70-300.70 Pale grey, weakly cleaved, moderately Silica & weakly Chlorite + Sericite altered, XII poor (257.10-281.8m), Coarse quartz phyric (281.8-233.0)m, Polymictic, poorly sorted, angular clasts at the base Containing Qtz phyric polymictic breccia in Volcaniclastic Sandstone

at 280-281.80 at the contact between the XII poor Volcaniclastic Sandstone & Qtz XII phyric Sandstone is intruded by rhyolite (Stems Qtz XII5) the hot rhyolite was intruded to the sediments & formed a jigsaw fit angular autbreccia of hyaloclastite) & a chilled margine

281.80-292.4m grey, very coarse grained, granular top, Polymictic Volcaniclastic in breccia in Volcaniclastic Sandstone - clast size reaches 3cm, mud clasts and

292.4-296.9 Polymic Volcaniclastic breccia in Volcaniclastic Sandstone with clasts of andesite-basalt (Grey) feldspar phyric dacitic and

Alteration

SP=5%

SI=m
CL=w
SE=w

rhyolitic breccia intruding to VSST

basalt & andesite

EXPLORATION SKILLS MAPPING CAMP

GRAPHIC LOG

Project
Location

Drill hole No. R10063
Location No.

Coords: | RL: | Scale: 1:200 | Page 7 of 21

Azim: | Incl: | Diam: | Logged by: | Date 01/03/16

Log with grainsize (mud, 1/8, 1/4, 2, 8, 32, max mm) | Samples TS results Chemistry | Rock / facies description | Alteration

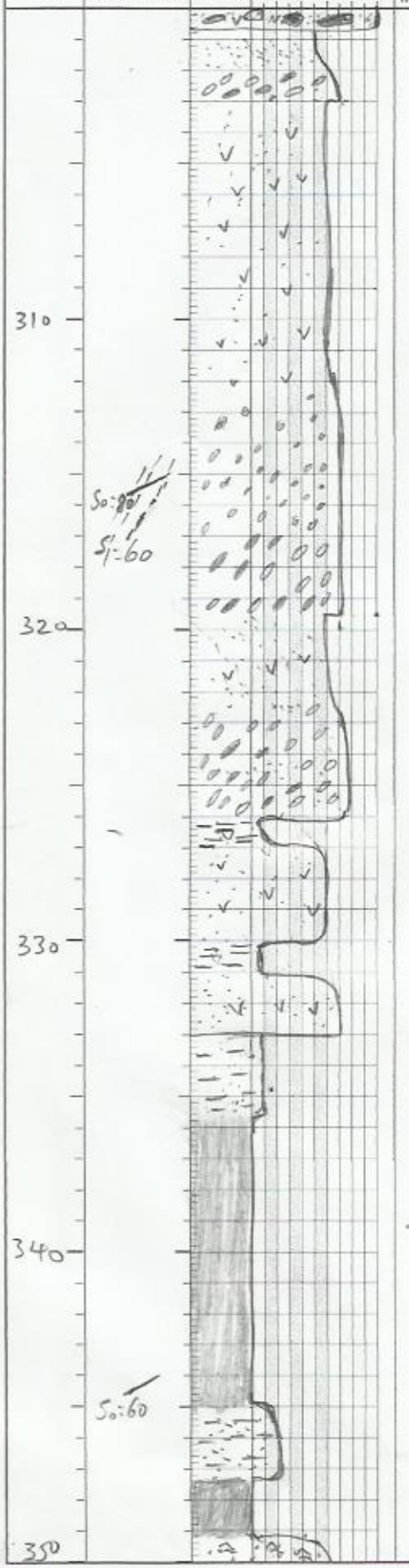

Clasts are poorly sorted, angular to sub-angular fining upward to V.C. grained (granule) Volcaniclastic Sandstone — CL = W, SI = M

300.70-333.00 grey, to greenish grey, medium to coarse grained, graded & well sorted, granules to lappilli andesitic clastic (grey), fiamme & white containing aphanitic rhyolite at the base grading to medium grained XIII poor Volcaniclastic Sandstone — CL = M

179

- It is weakly chlorite altered
- It is thickly bedded.
- clasts are imbricated along the cleavage

330.0-331.20 the Sandstone is interbeded with Siltstone fining upwhole

.180

333.00-349.30m Pale grey to dark grey, massive to weakly cleaved, Siltstone interbedded with mudone & minor fine to medium grained sandstone

349.30-359.00m medium to coarse grained, weakly to moderately chlorite altered

Need to be fixed

EXPLORATION SKILLS MAPPING CAMP

GRAPHIC LOG

Project
Location

Drill hole No. R10063
Location No.

Coords:
RL:
Scale: 1:200
Page 8 of 21

Azim:
Incl:
Diam:
Logged by: E408
Date 02/03/16

Log with grainsize (mud | 1/8 | 1/2 | 2 | 8 | 32 | max mm)

m	Structure	Samples / TS results / Chemistry	Rock / facies description	Alteration
			Volcaniclastic Sandstone with angular to sub-rounded monomictic basaltic-andesite clasts from 352-355.70m	
		181		
360	gr3 So:70		359.00-405.60m, grey, medium- to coarse grained, graded fining up hole with elongated granules to lapilli base volcaniclastic Sandstone grading to Siltstone with Pumice breccia. - Poorly sorted base, thickly bedded moderately sericite & weakly Chlorite altered.	CL=W SE=W ? 360-380 geoch Rhyo dacit
370	So:55	182		SE=M CL=W
			376.20-379.20m dark grey weakly cleaved, Pyritic mudstone/(Shale) interbedded with Siltstone	
380		Pumice rafts RG315	379.20-405.6 coarse grained Volcaniclastic Sandstone (lithic-wacke) interbedded with Siltstone It is moderately Sericite + weakly chlorite altered & is XII poor (rarely 8% phyric It is cleaved parallel to the bedding.	SE=M CL=W
390				
	So=60 So=60	183		
400				

EXPLORATION SKILLS MAPPING CAMP

GRAPHIC LOG

Project Location

Drill hole No. R10063
Location No.

Coords: | RL: | Scale: 1:200 | Page 3 of 21

Azim: | Incl: | Diam: | Logged by: | Date 02/03/16

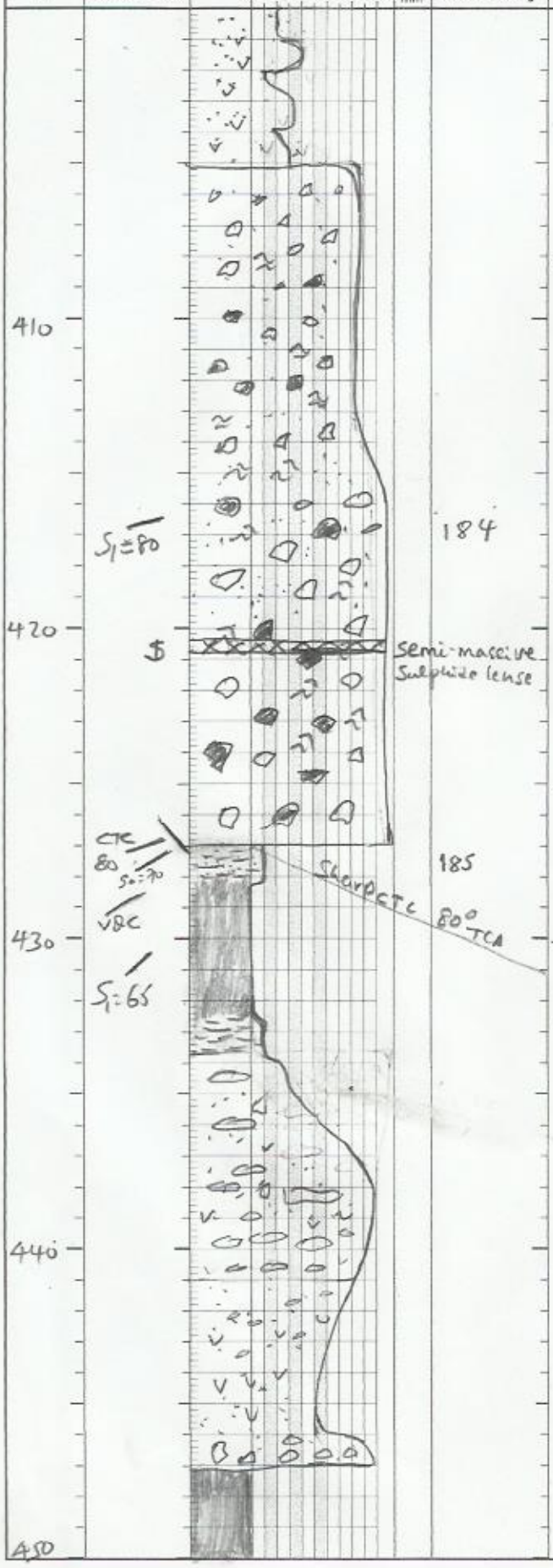

Rock / facies description

405.00 - 427.80m grey, Very Coarse grained, poorly Sorted clasts, matrix Supported, massive to very weakly Cleaved polymictic volcaniclastic breccia in volcaniclastic Sandstone matrix (same unit hosts mineralisation - clasts size >4cm, generally fining upHole (Angular to Subrounded) basaltic - andesite clasts

- weak cleavage developed & clasts are imbricated along the fabric. The dominant clasts are dacitic, andesitic, rhyolitic volcaniclastic sandstone

It is moderately Serice & weakly chlorite altered

- 420.30 - 420.80m Semi-massive Sulphid lense with Py, Pyrr, Sp & Cpy & Py is interbedded. moreover, it continues as Small lenses (<10cm) from 420.80 - 423.60m

- It is not Sampled!

427.80 - 433.80 dark grey weakly cleaved. mudstone interbeded with Siltstone/very fine grained Sandstone. It Contains Pyrrhotite + Pyrite & is the expected host rock (Sampled

433.80 - 441.00 grey, Very coarse grained, Poorly Sorted, matrix Supported, angular to Subround elongate polymict Clasts Containing volcaniclastic breccia in volcaniclastic Sandstone. rare fauna

441.00 - 447.30 grey, Coarse top reverse graded volcaniclastic Sandstone (

447.30 - 459.50 dark grey, Cleaved Carbonate veined mudstone

Alteration

SE = M
CL = W

SI = W in R10032)

420.3 - 420.80
Py ≠ 30
&Pyr : 15
Sp = 5-10%
Cpy = 2%

Pyrr > 5%
Py > 5%

EXPLORATION SKILLS MAPPING CAMP

GRAPHIC LOG

Project Location			Drill hole No. R10063 Location No.
Coords:	RL:	Scale: 1:200	Page 10 of 21
Azim:	Incl:	Diam:	Logged by: Date 02/03/16

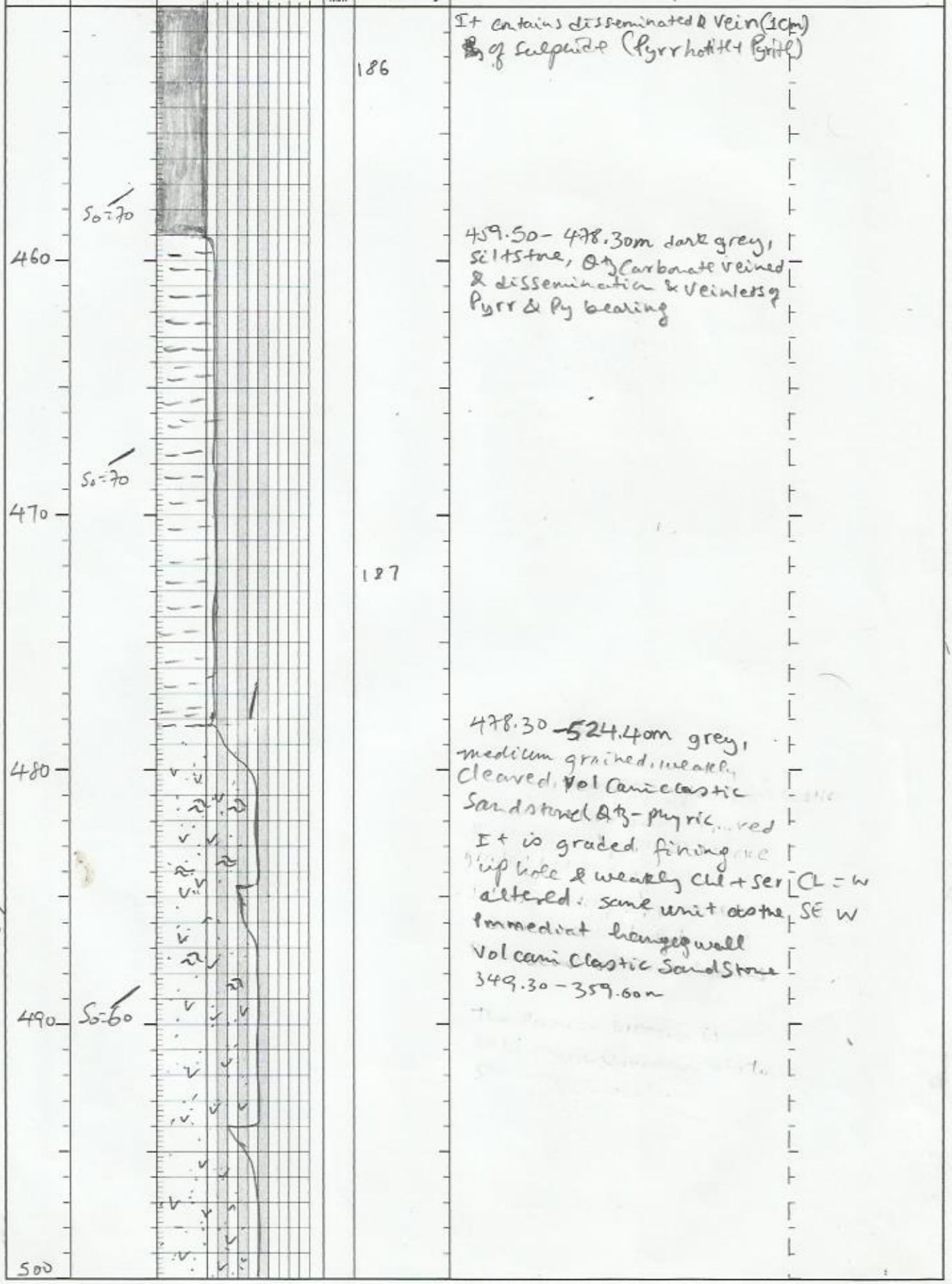

EXPLORATION SKILLS MAPPING CAMP

GRAPHIC LOG

Project / Location		Drill hole No.	R10063
		Location No.	
Coords:	RL:	Scale: 1:200	Page 11 of 21
Azim:	Incl:	Diam:	Logged by: Date 02/03/16

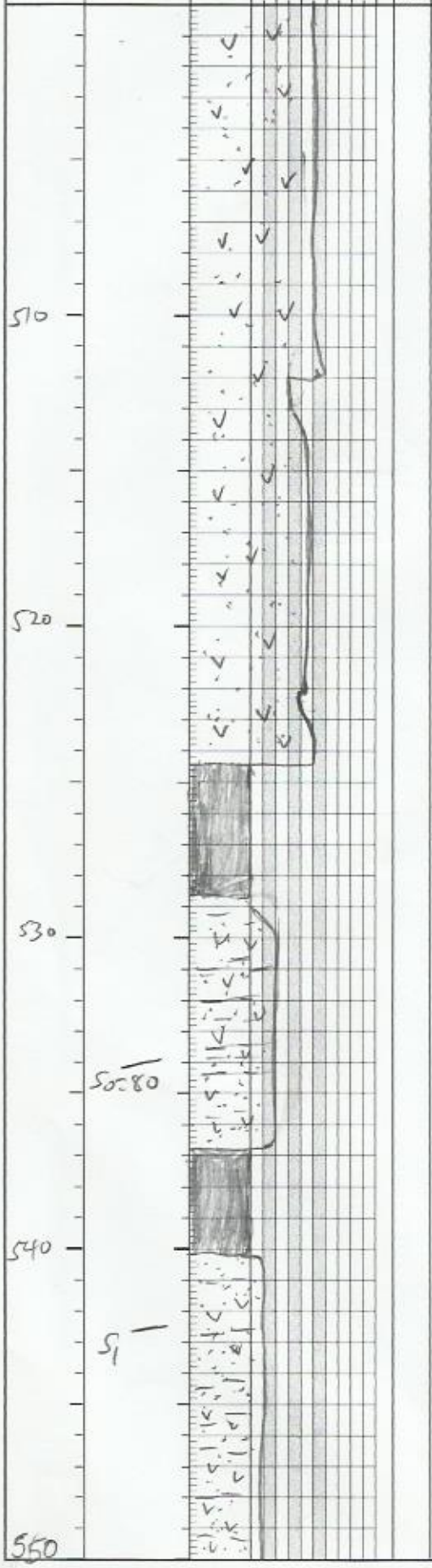

Rock / facies description

524.4–528.60 dark grey, Qtz-Carbonate veined, cleaved disseminated Pyrr hotite containing mudstone / Shale.

528.60–536.85 Pale grey, fine grained Volcani clastic Sandstone / Siltstone as interbeded with mudstone (black Shale)

536.85–540.20 black Shale Qtz-Carbonate veined with Pyrr + Py veining

540.20–552.20m Pale grey fine to medium grained Volcani Clastic Sandstone / Siltstone with disseminated Pyrr + Py

Alteration

Py < 1
Pyrr < 1

Some Sandstone / siltstone as Conglomerate creek

EXPLORATION SKILLS MAPPING CAMP

GRAPHIC LOG

Project Location		Drill hole No. R10063 Location No.	
Coords:	RL:	Scale: 1:200	Page 12 of 21
Azim:	Incl:	Diam:	Logged by: E40B / Date 02/03/16

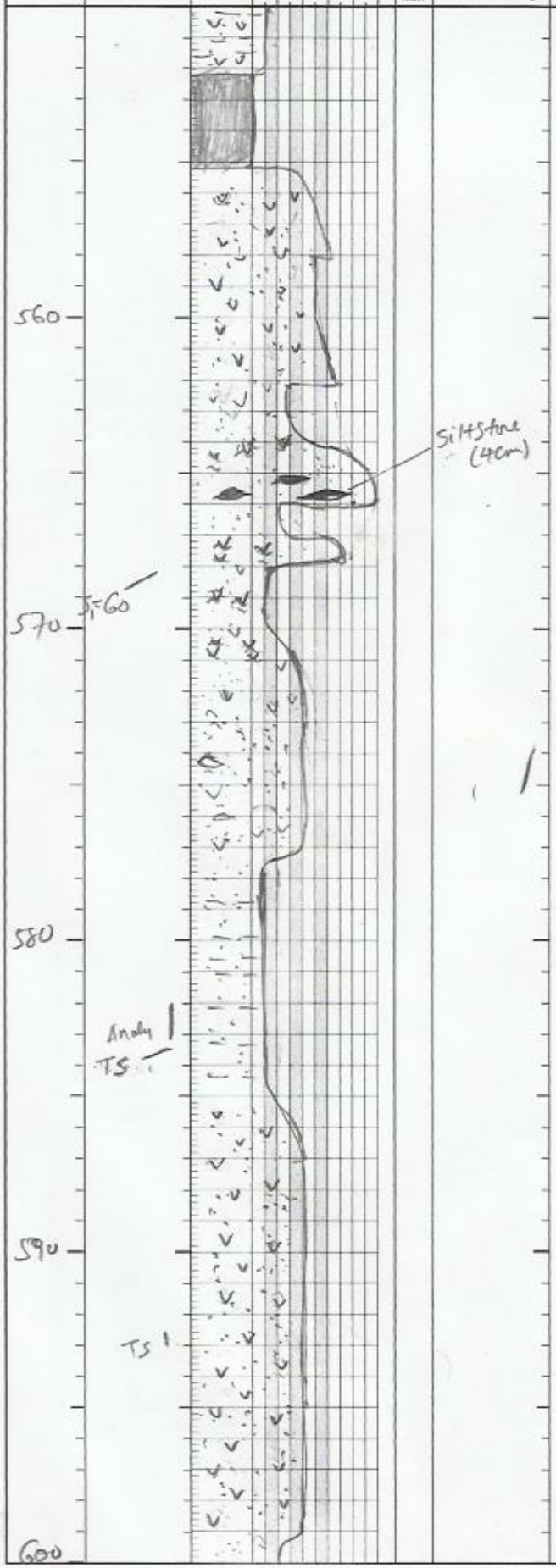

TS = Thin Section Sample

EXPLORATION SKILLS MAPPING CAMP

GRAPHIC LOG

Project / Location		Drill hole No. / Location No.	R10063
Coords:	RL:	Scale: 1:200	Page 13 of 21
Azim:	Incl: / Diam:	Logged by: EVoB	Date 03/03/16

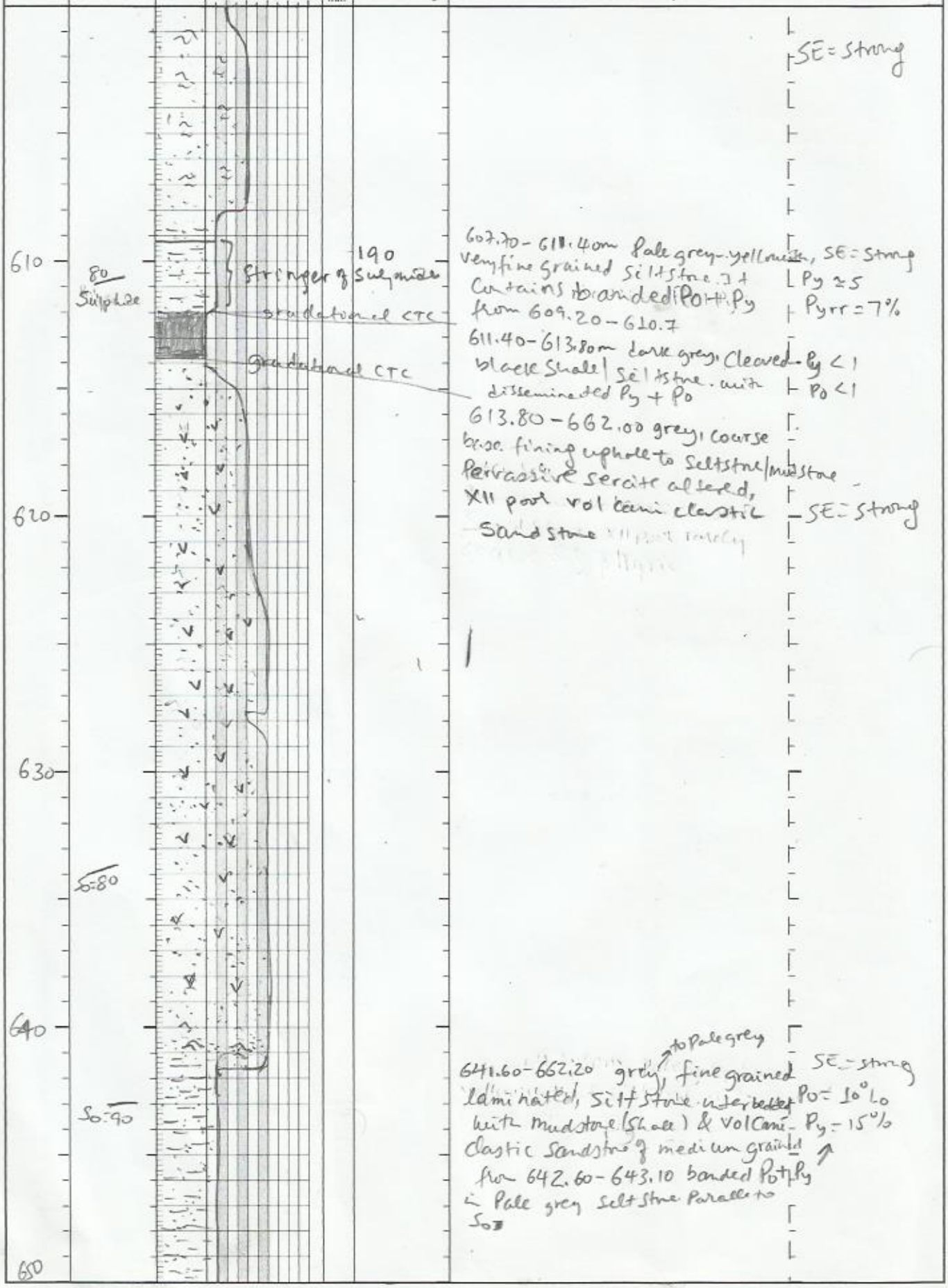

EXPLORATION SKILLS MAPPING CAMP

GRAPHIC LOG

Project
Location

Drill hole No. R10063
Location No.

Coords: | RL: | Scale: 1:200 | Page 14 of 21

Azim: | Incl: | Diam: | Logged by: | Date 03/08/16

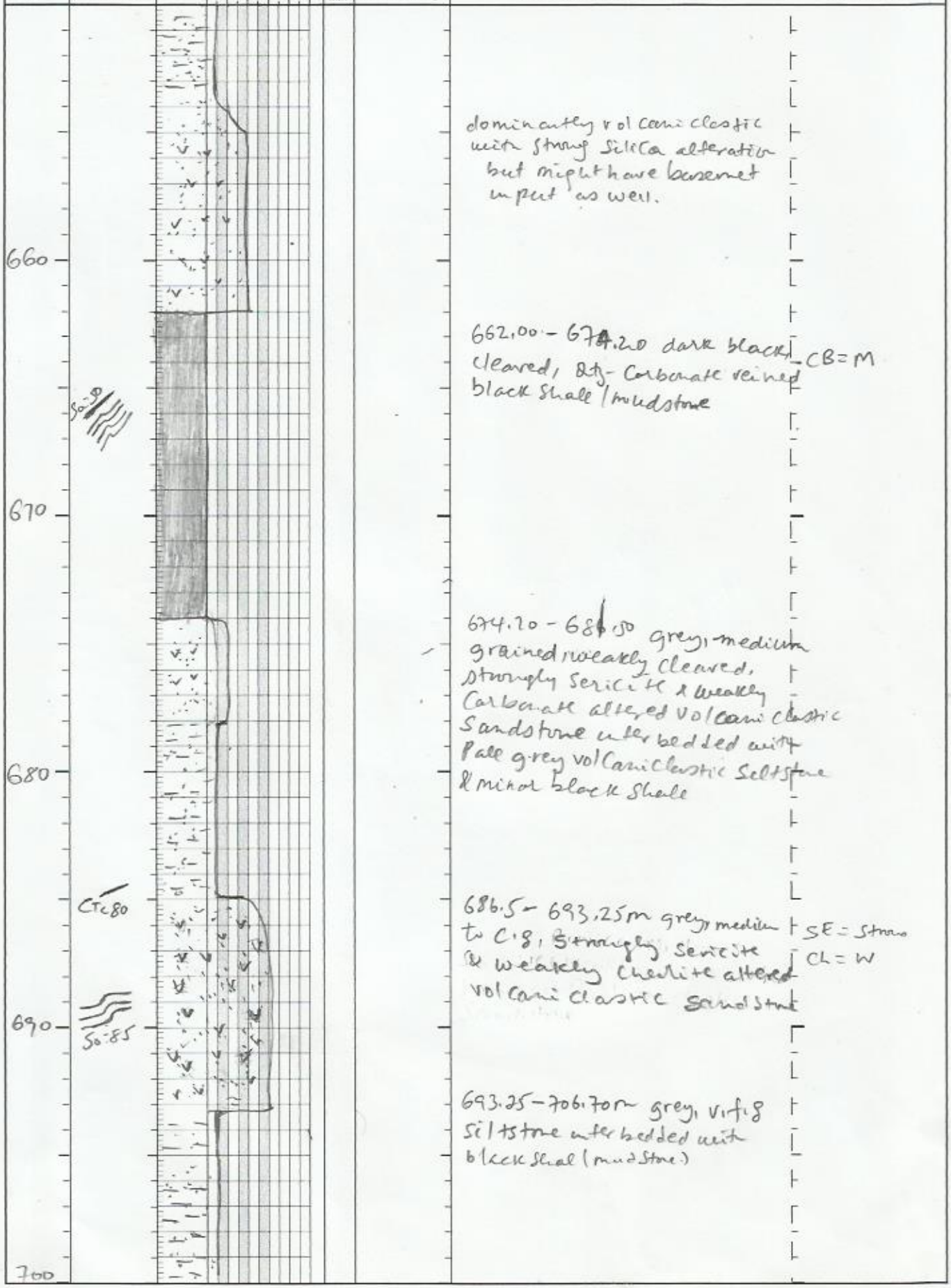

EXPLORATION SKILLS MAPPING CAMP

GRAPHIC LOG

Project Location		Drill hole No. R10063 Location No.	
Coords:	RL:	Scale: 1:200	Page 15 of 21
Azim: Incl:	Diam:	Logged by: EYOB	Date 03/03/16

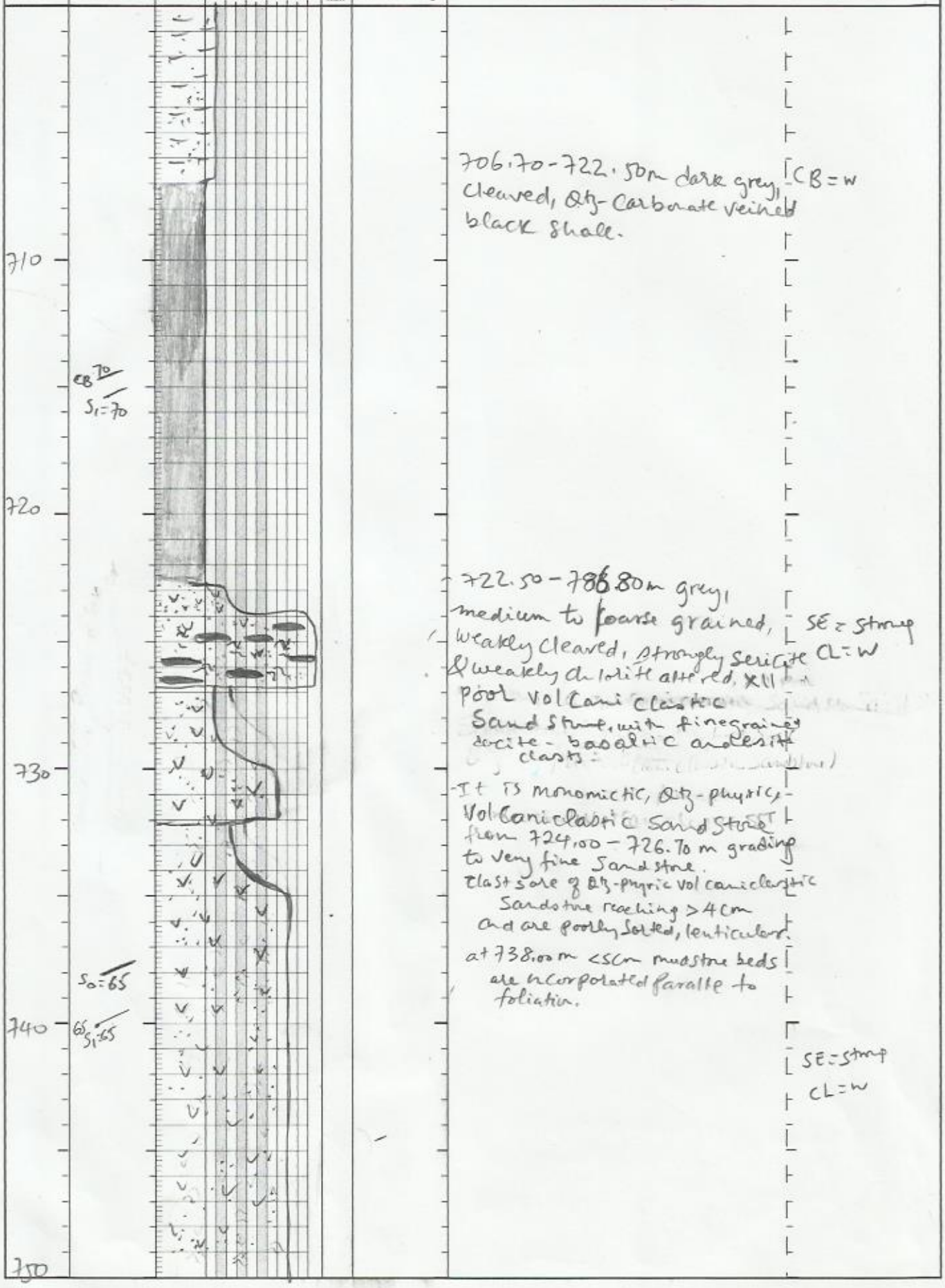

EXPLORATION SKILLS MAPPING CAMP

GRAPHIC LOG

Project Location		Drill hole No. R10063 Location No.	
Coords:	RL:	Scale: 1:200	Page 16 of 21
Azim:	Incl: Diam:	Logged by: E40B	Date 03/03/16

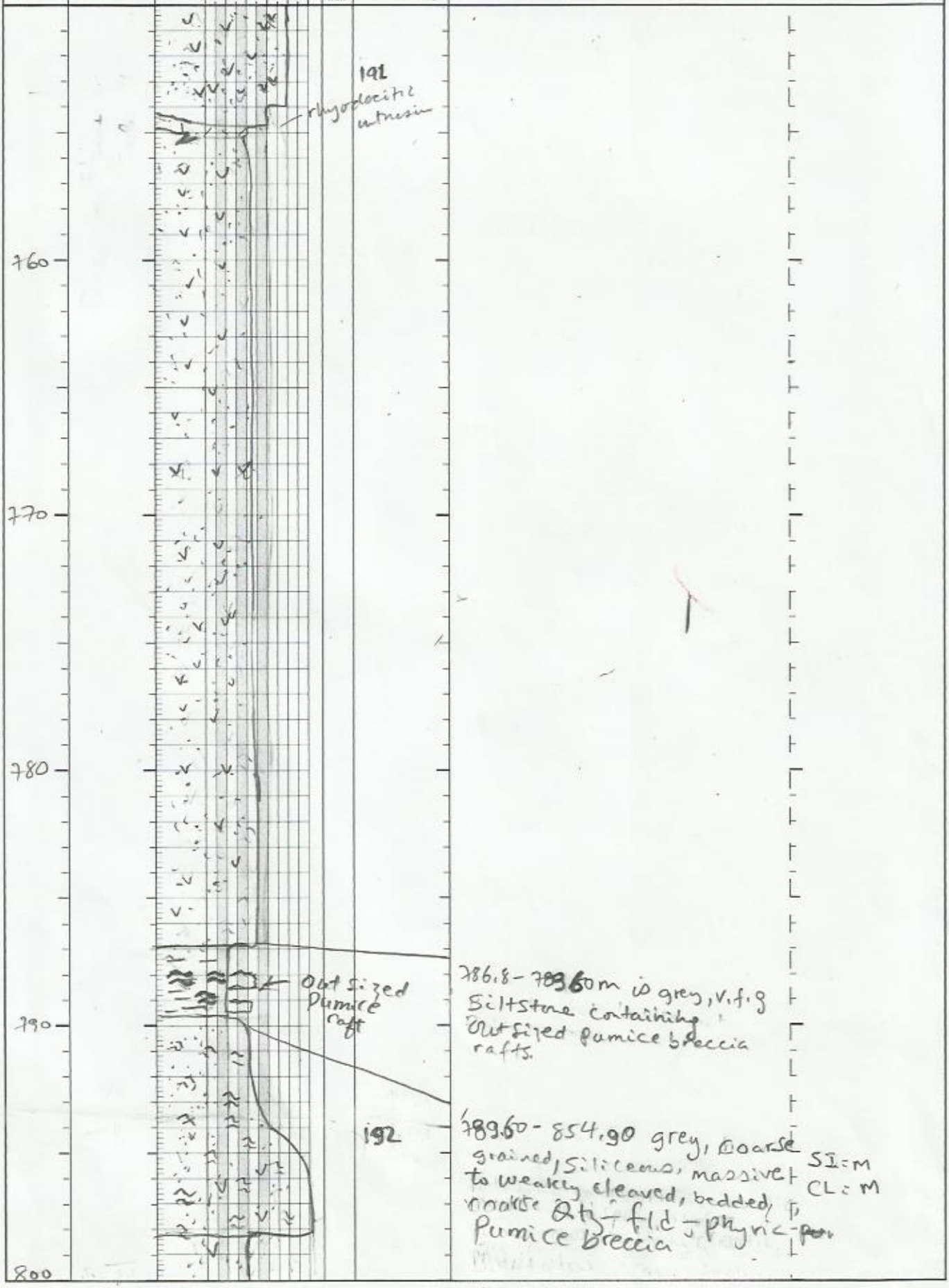

EXPLORATION SKILLS MAPPING CAMP

GRAPHIC LOG

Project Location

Drill hole No. R10063
Location No.

Coords:

RL:

Scale: 1:200

Page 17 of 21

Azim:

Incl:

Diam:

Logged by: EYOB

Date 03/03/16

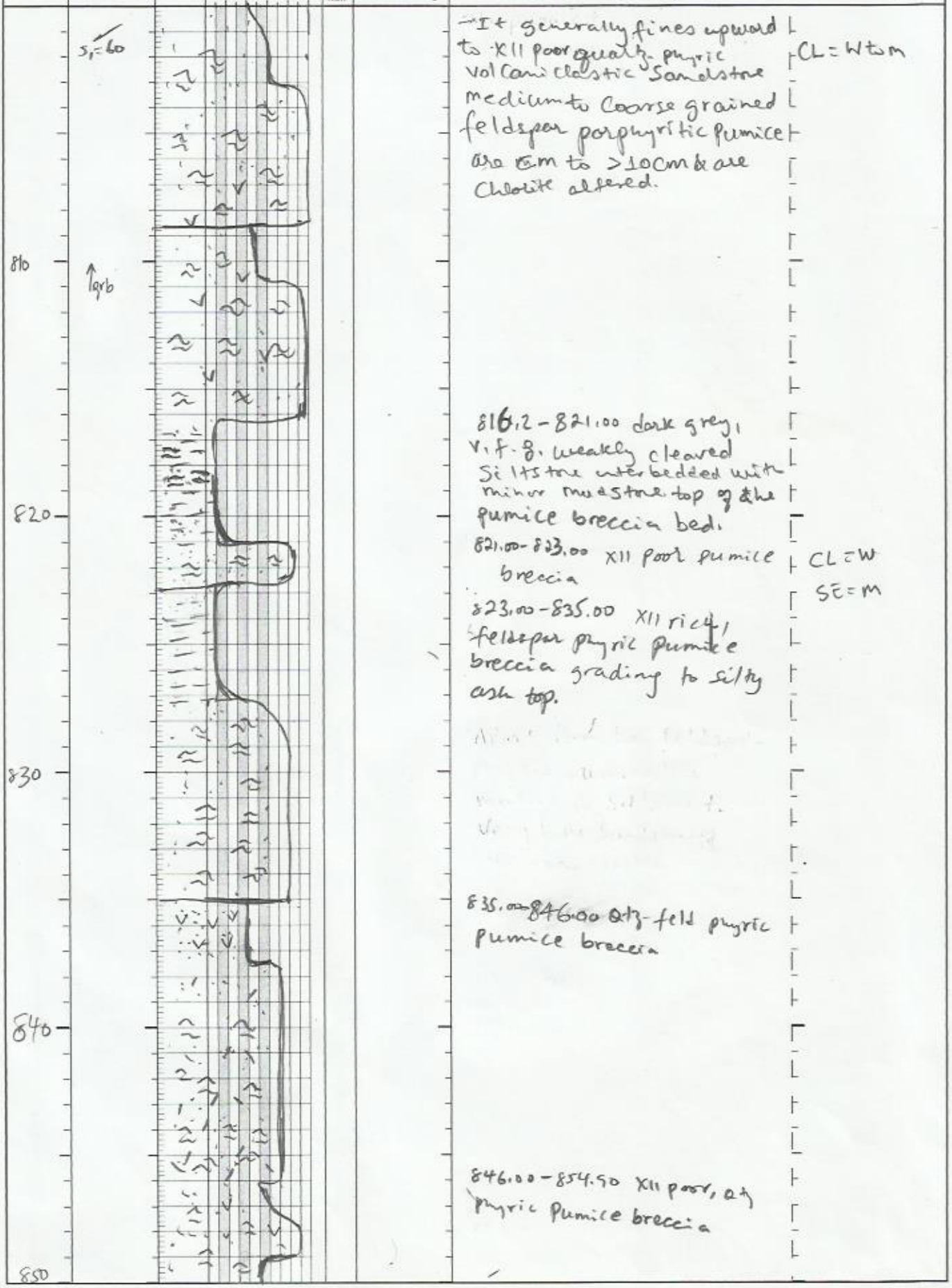

It generally fines upward to XII poor quartz-phyric volcaniclastic Sandstone medium to coarse grained feldspar porphyritic Pumice are 5cm to >10cm & are Chlorite altered.

CL = W to m

816.2 - 821.00 dark grey, v.f.-f. weakly cleaved Siltstone interbedded with minor mudstone top of the pumice breccia bed.

821.00 - 823.00 XII poor pumice breccia

CL = W

SE = m

823.00 - 835.00 XII rich, feldspar phyric pumice breccia grading to silty ash top.

835.00 - 846.00 Qtz-feld phyric Pumice breccia

846.00 - 854.50 XII poor, qtz phyric Pumice breccia

EXPLORATION SKILLS MAPPING CAMP

GRAPHIC LOG

Project
Location

Drill hole No. R10063
Location No.

Coords: | RL: | Scale: 1:200 | Page 18 of 21

Azim: | Incl: | Diam: | Logged by: | Date

Log with grainsize (mud, 1/8, 1/2, 2, 8, 32, max mm) | Samples TS results Chemistry | Rock / facies description | Alteration

849.20 - 854.90 m strong Silica + Sericite alteration — SI = S, SE = S

854.90 - 911.80m grey, Very coarse grained Qtz-feldspar phyric Pumice breccia — SI = S, SE = m

fld >> Qtz, fld averages ≥4mm (megacryst)

861.40 - 871.20m Pumiceous Qtz-phyric Volcaniclastic Sandstone with Qtz XTLS ≥2mm & are Colorless & rounded

193

871.20 - 882.00 grey, Very coarse grained, Qtz-feldspar porphyritic Pumiceous Volcaniclastic Sandstone — SE = m, SI = W

194

880.00 - 881.00 contains angular to sub angular, polymict Pumiceous Volcaniclastic breccia. clasts are of white, grey felsic volcanic & mudstone reaching 3cm in Sandstone

881.10 - 898.20 grey, massive to weakly foliated, XTL poor Qtz-feldspar phyric Pumice breccia

Qtz >> fld

5:70

898.20 - 911.8m

XTL rich & feld >> Qtz

316

EXPLORATION SKILLS MAPPING CAMP

GRAPHIC LOG

Project Location		Drill hole No. R10063 Location No.	
Coords:	RL:	Scale: 1:200	Page 19 of 21
Azim:	Incl: Diam:	Logged by:	Date 03/03/16

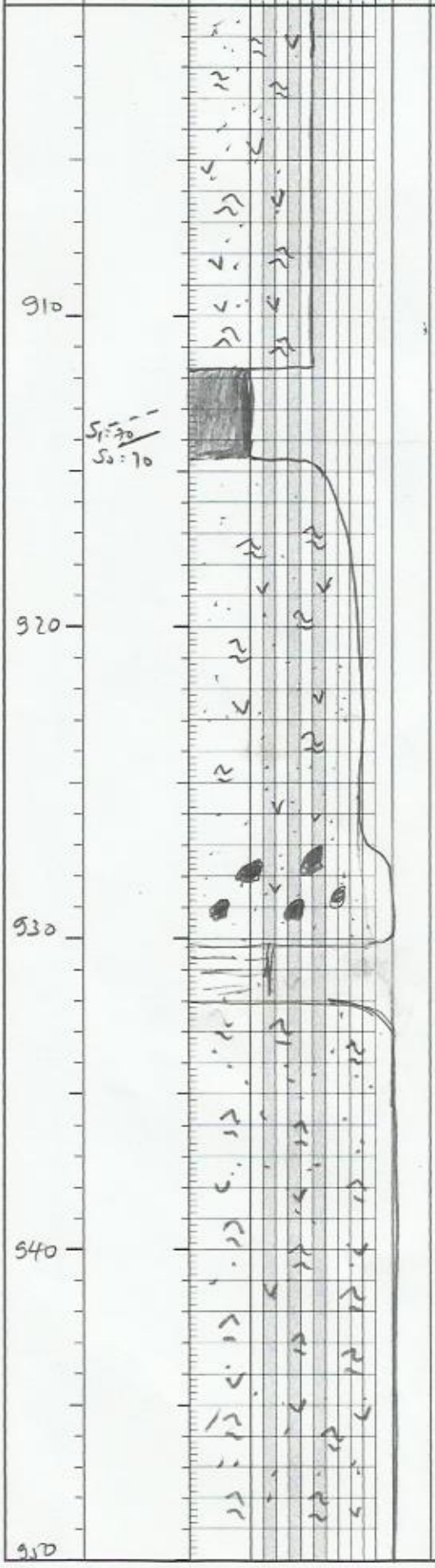

Samples
TS results
Chemistry

195

196

197

903.40- Shows more angular clasts

911.80 - 914.70m dark black cleaved, carbonat altered Pyritic Shale

914.70 - 951.80m dark grey fine grained matrix, monomictic clasts of mudstone, angular to subrounded poorly sorted containing Qtz feldspar, p[illegible] Phyric pumice breccia with significant mud matrix Qtz >> fld It is moderately chl+SE altered

- It is a mass flow deposit with

929.00 - 951 it is XII rich with Qtz & fld ≥ 2mm

Alteration

Py = 5%

CL = m

SE = m

EXPLORATION SKILLS MAPPING CAMP

GRAPHIC LOG

Project
Location

Drill hole No. R10063
Location No.

Coords:
RL:
Scale: 1:200
Page 20 of 21

Azim:
Incl:
Diam:
Logged by: EYOB
Date 03/03/16

Log with grainsize | Samples TS results Chemistry | Rock / facies description | Alteration

m | Structure | mud 1/8 1/2 2 8 32 max mm

951.00 – 1017.2 grey, fine grained matrix, Qtz-fld phyric, flow banded rhyolitic breccia

198

-It is moderately silified & weakly sericite altered
It is possibly intruded by rhyolitic dike that led to autbrecciation & resedimentation

SI = M
SE = W

960

970

980

← Jigsaw fit

990

998.0 – 999.20m shows monomictic autobreccia of Qtz phyric rhyolitic hyaloclastite Jigsaw fit

1000

EXPLORATION SKILLS MAPPING CAMP

GRAPHIC LOG

Project Location		Drill hole No. R10063 Location No.	
Coords:	RL:	Scale: 1:200	Page 21 of 21
Azim:	Incl: Diam:	Logged by: EYOB	Date 03/03/16

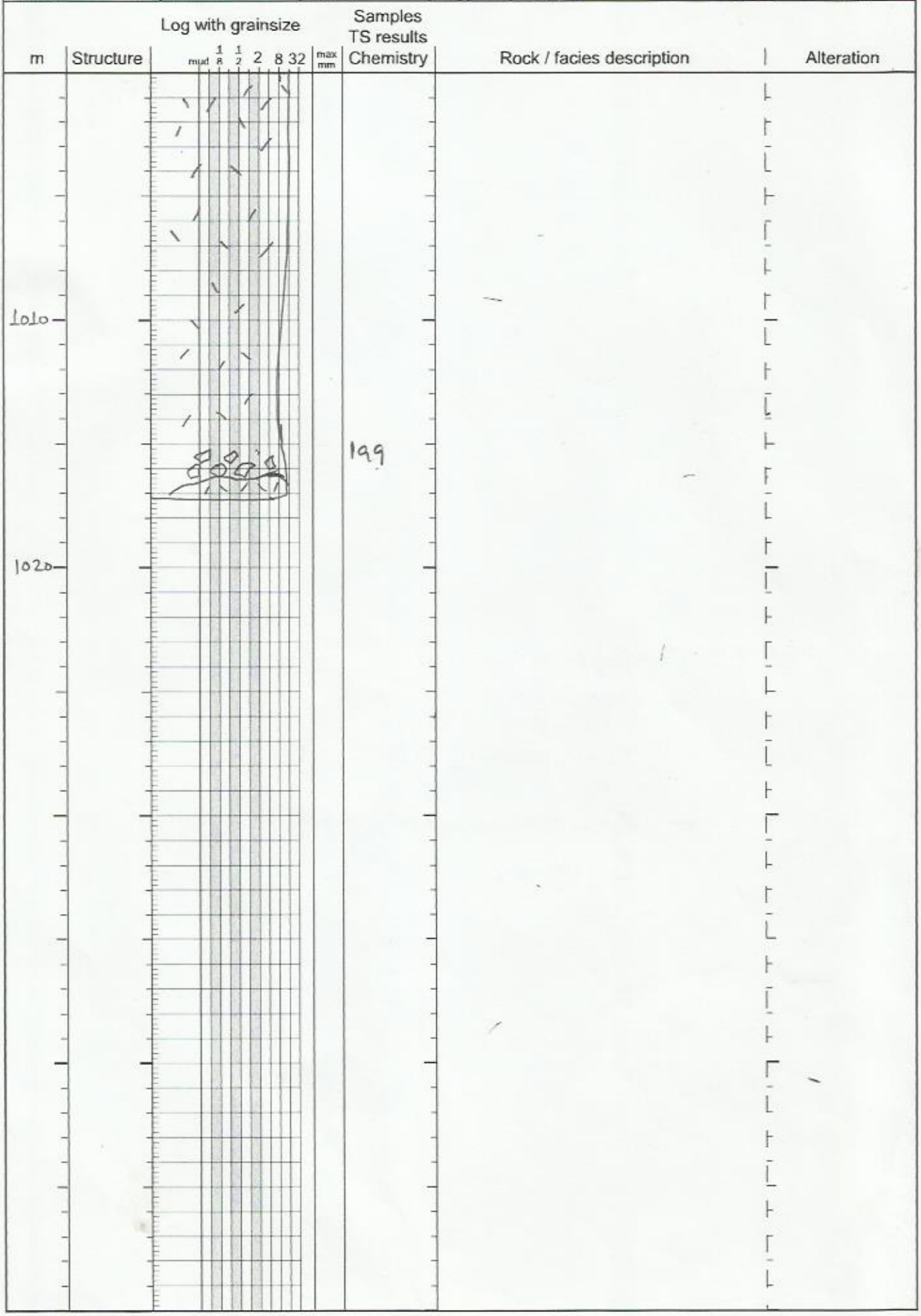

Summary log

EXPLORATION SKILLS MAPPING CAMP

GRAPHIC LOG

Project Nature Creek
Location

Drill hole No. Rosebery BH1
Location No.

Coords: 376538.24E | 5371234.1N | RL: | Scale: 1:1000 | Page 1 of 2

Azim: | Incl: | Diam: | Logged by: EYOB ANDEMESKEL | Date 24/04/15

Log with grainsize (mud, 1/8, 1/2, 2, 8, 32, max mm) | Samples / TS results | Chemistry | Rock / facies description | Alteration (carbonate, chlorite, SiO2)

m	Structure	Chemistry	Rock / facies description
		NR	0.00-4.00 No Recovery.
		QFPT	4.00-7.45 Reddish to Pink colored coarse Qtz XTLS containing highly weathered Possibly ? Quartz-phyric tuff
20	60° RA	ESST	7.45-61.75m Creamy to brown, laminated & bedded dolomitic Sandstone.
30	grd		Conglomerate from 7.45-9.00m
40			15.30-15.90m
50		62	
60		CONG	61.75-73.20 polymictic conglomerate composed of maroon chert & quartz clasts. Fuchsite along foliation plane
70	50:20	SLT	73.20-84.66 creamy, weakly dolomitic sandstone/siltstone
80			
90		CONG	84.66-182.50m Polymictic conglomerate well aligned matrix supported chert, few fuchsitic clasts upto 3cm in sandstone matrix containing. More over, Pyrite veining in places is noted.
100	50:20	63	
	50:20 RA		
150			
160			
170			
180			
190		QFPT	182.50-238.55 light grey, very fine grained, Qtz-fsp phyric pumice breccia - minor Carbonat alteration is also noted.
200			
			Minor Quartz porphry noted
		PQFPT	238.55-273.55 Light grey, fine grained ground mass, Qtz-fsp-phyric pumice breccia
250			

Summary log

EXPLORATION SKILLS MAPPING CAMP

GRAPHIC LOG

Project Location		Drill hole No. Rosebery BH1 Location No.	
Coords:		RL:	Scale: 1:1000
Azim:	Incl:	Diam:	Logged by: E-YDB

Page 2 of 2

Date 24/04/15

m	Structure	Log with grainsize (mud, 1/8, 1/2, 2, 8, 32, max mm)	Samples TS results Chemistry	Rock / facies description	Alteration
250				feldspar phyric, siliceous Qtz-fsp phyric pumice breccia	
260				E.O.H. 290.16	
290					
300					

EXPLORATION SKILLS MAPPING CAMP

GRAPHIC LOG

Project Rosebery Nat one
Location

Drill hole No. Rosebery BH1
Location No.

Coords: 376538.24E / 5371234.1N | RL: | Scale: 1:200 | Page 1 of 6

Azim: 083 | Incl: -45 | Diam: NQ | Logged by: EYOB F.A | Date 27/04/2015

Log with grainsize — Samples — Litho Code — SE — Sidr — Carbonate (FeCo3) — chlorite — HE+LI+Py

m	Structure	mud 1/8 1/2 2 8 32 max mm	Chemistry	Rock / facies description	Alteration
			NR	0.00-4.00 No Recovery of core	SI
			QFPT	4.00-7.45 Reddish to pink colored, medium grained, dispersed coarse quartz crystals containing, highly clay & FeO altered Possibly quartz phyric tuff.	strong clay + FeO
			CONG		
10	grd		ESST	7.45-9.00 light green, medium to coarse matrix supported Sandstone & felspathic & quartz clasts upto 4cm Containing Conglomerate weakly chlorite altered. 7.97-8.07 strongly FeO oxidized with goethite box-work is noted.	
	So:50				
	grd		CONG	9.00-15.30. Creamy to brown with greenish lamination & bedded dolomitic Sandstone. down hole grading in conglomeritic bed from 11.90-12.00m.	weak FeCO3 (Ankerite) alteration
			ESST		
20				15.30-15.90 polymictic Conglomerate containing chert, mafic (doleritic), mud stone & Lithic wacke. The unit graded down hole from 15.70-15.90m. Sandy matrix.	
	grd			15.90-27.30 m. Creamy, dolomitic fine grained Sandstone. bedding 60° LCA. Some beds show down hole grading.	moderate FeCO3 (weak)
			CONG	27.30-31.15 Polymictic Conglomerate of white & maroon to brown Chert, quartz, dolerite & other mafic volcanic clasts 1-3.5cm in a clast Supported Sandstone matrix. Clasts are imbricated along the cleavage @ 55° LCA.	moderate FeCO3 alteration
	55				
	grd		ESST		
				31.15-42.30m Creamy to light green, medium to Coarse grained Sandstone at the base of the beds Containing conglomeritic clasts of Same as the uphole composition. mainly less than 5mm grading down hole	weakly chloritic
40				Epiclastic Sandstone	
			CONG	42.30-42.90m Conglomerate of polymictic Composition with main cherty clasts, quartz Clasts upto 4 Cm imbricated along the cleavage @ 55°.	
			ESST	42.90m-61.75m Creamy & very fine grained 42.90-48.98 & 53.00-61.7m & medium & gray colored 48.98-53.00m very fine	
50					

EXPLORATION SKILLS MAPPING CAMP

GRAPHIC LOG

Project Natone creek | Drill hole No. Roseberry BH1

Location | Location No.

Coords: | RL: | Scale: 1:200 | Page 2 of 6

Azim: | Incl: | Diam: | Logged by: EYOB F.A | Date 27/04/2015

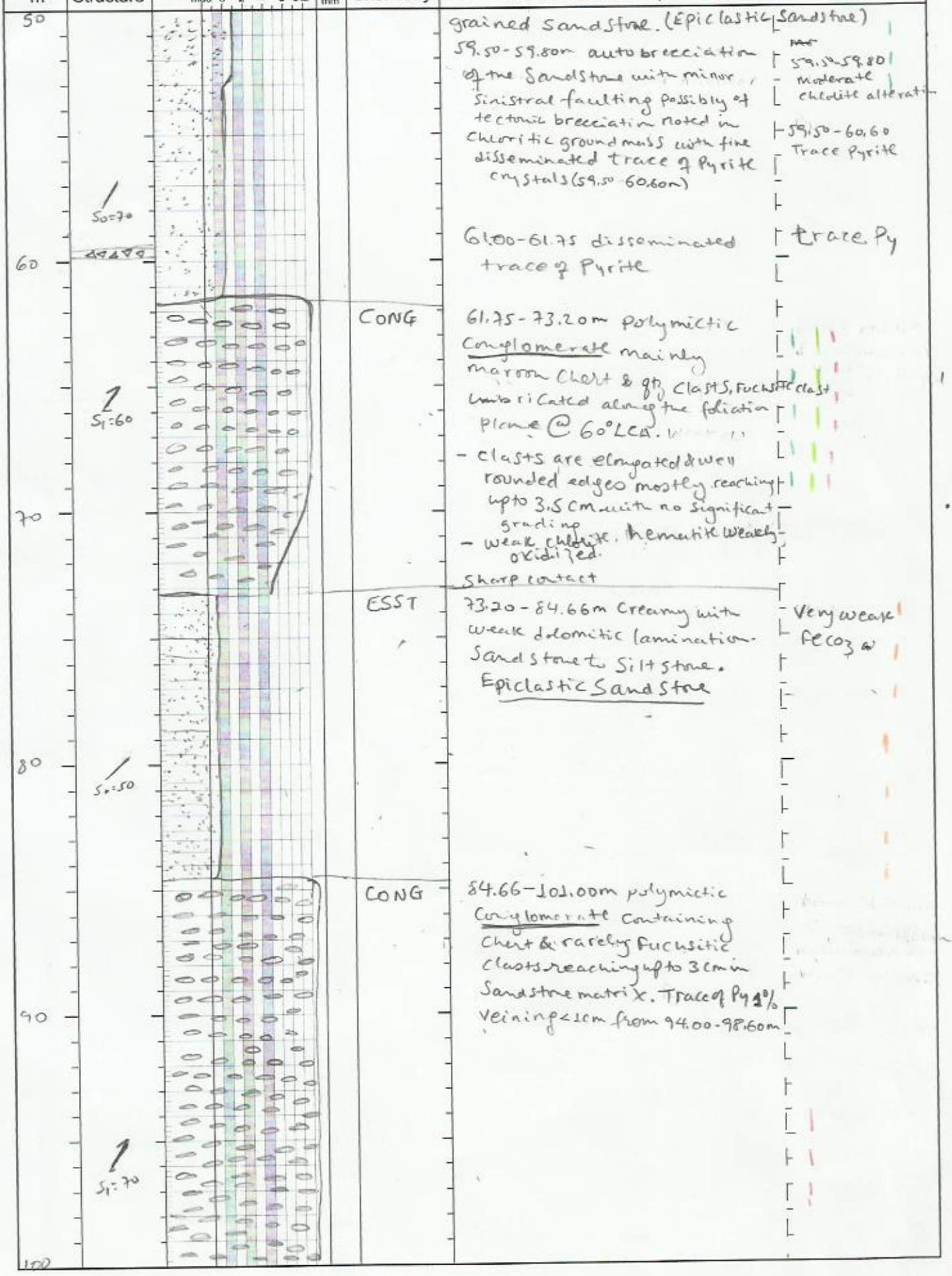

EXPLORATION SKILLS MAPPING CAMP

GRAPHIC LOG

Project Location: Natone creek

Drill hole No. / Location No.: Rosebery BH1

Coords: | RL: | Scale: 1:200 | Page 3 of 6

Azim: | Incl: | Diam: | Logged by: EYOB F. A | Date 27/04/2015

Log with grainsize | Samples TS results Chemistry | Rock / facies description | Alteration

m | Structure | mud 1/8 1/2 2 8 32 max mm

100

E SST

S₁:70

101.00 – 104.90 light grey, vitric tuff, fine to medium grained quartz – feldspar bearing from 101.00 – 102.00 & 102.00 – 104.90 vitric – lithic tuff. Cleaver 70°LCA @ 103.90

Weak sericite, K- & FeCO₃ alteration

OFPT Sandstone with chert, grey sericite Pluto 6615

CONG

104.90 – 152.50m polymictic conglomerate containing clastes aligned along the cleavage, chert, sandstone, mudstone quartz. mostly sub rounded & rarely angular clastes noted.

- Yellow- to light brown FeCO₃ alteration throughout section
- long axis of clasts reach upto 5 cm.

110

120

Weak FeCO₃ + Weak Chlorite

130

S₁:60

140

Locally strong FeCO₃ (Ankerite) alt

150

EXPLORATION SKILLS MAPPING CAMP

GRAPHIC LOG

Project Natone Creek Location		Drill hole No. Rosebery 8 HL Location No.	
Coords:	RL:	Scale: 1:200	Page 4 of 6
Azim:	Incl:	Diam:	Logged by: E 406 F, A	Date 27/04/15

m	Structure	Log with grainsize (mud, 1/8, 1/2, 2, 8, 32, max mm)	Samples / TS results / Chemistry	Rock / facies description	Alteration
160	S_1 = 80 LCA			164.35 - 166.58 hematite + limonite oxidation along fracture with box-work after Pyrite	Weakly HE + LI oxidized
170	S_1 = 85			170.40 - 171.40 moderately HE + LI oxidized Vuggy unit in places with box-works of after pyrite. Cleavage is at high angle to LCA.	Weakly HE + LI oxidized
180			QFPT	182.50 - 238.55 felsic vitric tuff 182.50 - 217.05 light grey, very fine grained vitric tuff with Sericite alteration - minor Carbonate that fizz reacts to HCl.	Weak Carbonat Strong Silicificati
190					
200					

EXPLORATION SKILLS MAPPING CAMP

GRAPHIC LOG

Project
Location

Drill hole No. Rosebery BH1
Location No.

Coords: | RL: | Scale: 1:200 | Page 5 of 6

Azim: | Incl: | Diam: | Logged by: EYOB F.A | Date 27/04/15

Log with grainsize | Samples TS results Chemistry

m	Structure	mud 1/8 1/2 2 8 32 max mm	Rock / facies description	Alteration
210			217.00-220 grey to light green, weakly Chloritic, lithic Qtz-fsp-phyric - Pumice breccia. Pyrite noted within the interval.	weakly Chlorite altered. Py = trace.
220			220-229.00 qtz-feldspar phyric Pumice breccia - Chert & black slate mainly angular and sparsely incorporated within the interval. The schistosity @ 228.40m is 80° LCA	weakly sericite altered.
230	1 S1:80		229.00-238.55 fine, Vitric tuff	
240		gradational CTC PQFPT	238.55-273.55 light grey fine grained groundmass Qtz-fsp-phyric Pumice breccia - fiamme of intense sericite alteration	
250				

S

EXPLORATION SKILLS MAPPING CAMP

GRAPHIC LOG

Project Location: Natne Creek

Drill hole No. Rosebery BH2

Location No.

Coords: 376660E 5372546N | RL: 164 | Scale: 1:200 | Page 1 of 4

Azim: 87 | Incl: -41 | Diam: | Logged by: EYOB F. A- | Date 28/04/15

SE

m	Structure	Log with grainsize (mud, 1/8, 1/2, 2, 8, 32, max mm)	Samples / TS results / Chemistry	Rock / facies description	Alteration
10	S_1:60		QFPT	0.00-18.95m White to creamy quartz- feldspar phyric vitric tuff. Weakly cleaved at 60° LCA. (QFPT) - unit is weakly sericite altered	SE = Weak
20	S_1:60		QFPT	18.95-25.00 Creamy quartz feldspar phyric. Welded clasts up to 4cm containing clastic tuff. Cleaved @ 60° LCA Clasts are felsic monomictic. (QFPT)	weak SE
30			QFPT	25.00-49.75 Creamy to grey with brown weathering, mainly feldspar with minor quartz, phyric vitric tuff. Cleaved @ 60° LCA. (QFPT)	
			64		
				37.25-45.25 Very weak intermittent chlorite alteration	Chlorite => very weak
40	S_1:60			- at 40.30m 1 Stringer Sulphide vein 2cm wide mainly pyrite bearing in quartz vein 60° LCA	Py = trace veinlet 1cm: 15% Py
				44.00-45.25 monomictic clast breccia of felsic vitric tuff Possibly tectonic brecciation	
50			gradational CTE	49.75-147.80m light grey →	

PQFPT

EXPLORATION SKILLS MAPPING CAMP

GRAPHIC LOG

Project Location	Natone Creek	Drill hole No. / Location No.	Rosebery BH2
Coords: 376609E/5372546N	RL: 164	Scale: 1:200	Page 2 of 4
Azim: 87	Incl: -41	Diam:	Logged by: EYOR F.	Date 28/04/15

Log with grainsize (mud, 1/8, 1/2, 2, 8, 32, max mm) | Samples / TS results / Chemistry | Structure | m

Rock / facies description

Qtz-fsp phyric, Vitric ground mass, pumice breccia

Pumice clasts of ~ 4cm & more long axis, strongly Sericitic pumice

Quartz & feldspar phyric crystals.

- Sparse black mud angular clasts are noted throughout the interval same as BH1 volcanics

@72.40 Sulphide Stringer 2cm with mainly Pyrite

@ 88.50m Sulphide Stringer of mainly pyrite @75 LCA

Alteration

SE: weak

Pyrite = stringer

Py = stringer weak

Structure: Z S:60 (70); Z S:60 (90)

Chemistry: 65

m: 60, 70, 80, 90, 100

EXPLORATION SKILLS MAPPING CAMP

GRAPHIC LOG

Project Location	Nature Creek	Drill hole No. Location No.	Rosebery BH 2
Coords:		RL:	Scale: 1:200
Azim:	Incl:	Diam:	Logged by: EYOR E.A

Page 3 of 4

Date 28/04/15

m	Structure	Log with grainsize (mud, 1/8, 1/2, 2, 8, 32, max mm)	Samples / TS results / Chemistry	Rock / facies description	Alteration
				moderate Sericite alteration along pumice is common	SE = weak alteration
110				111–121.00m black muds tone clasts sparsely incorporated	
120	↓ Gradin			at 118.25 the coarse pumaceous clasts decrease in abundance & the groundmass is of vitric grading down hole	
130				131.10 – 140.30 weakly Fe ox spots & veining altered Pumiceous tuff.	
140				138.90 – 140.30, strongly brecciated zone, Clast size ≈ 3cm	
	↓ gradi	intermixed CTC & injection of the SST	SST	146.50 – 147.80m, Pale grey, v.f.g. fsp-phyric ash top of the pumice breccia. (S.N 35941 (Part) 147.80 – 166.15 dark green weakly bedded to massive argillic sandstone.	
150					

EXPLORATION SKILLS MAPPING CAMP

GRAPHIC LOG

Project Natone Creek
Location

Drill hole No. Rosebery BH2
Location No.

Coords: | RL: | Scale: 1:200 | Page 4 of 4

Azim: | Incl: | Diam: | Logged by: EYOB F. A | Date 28/04/15

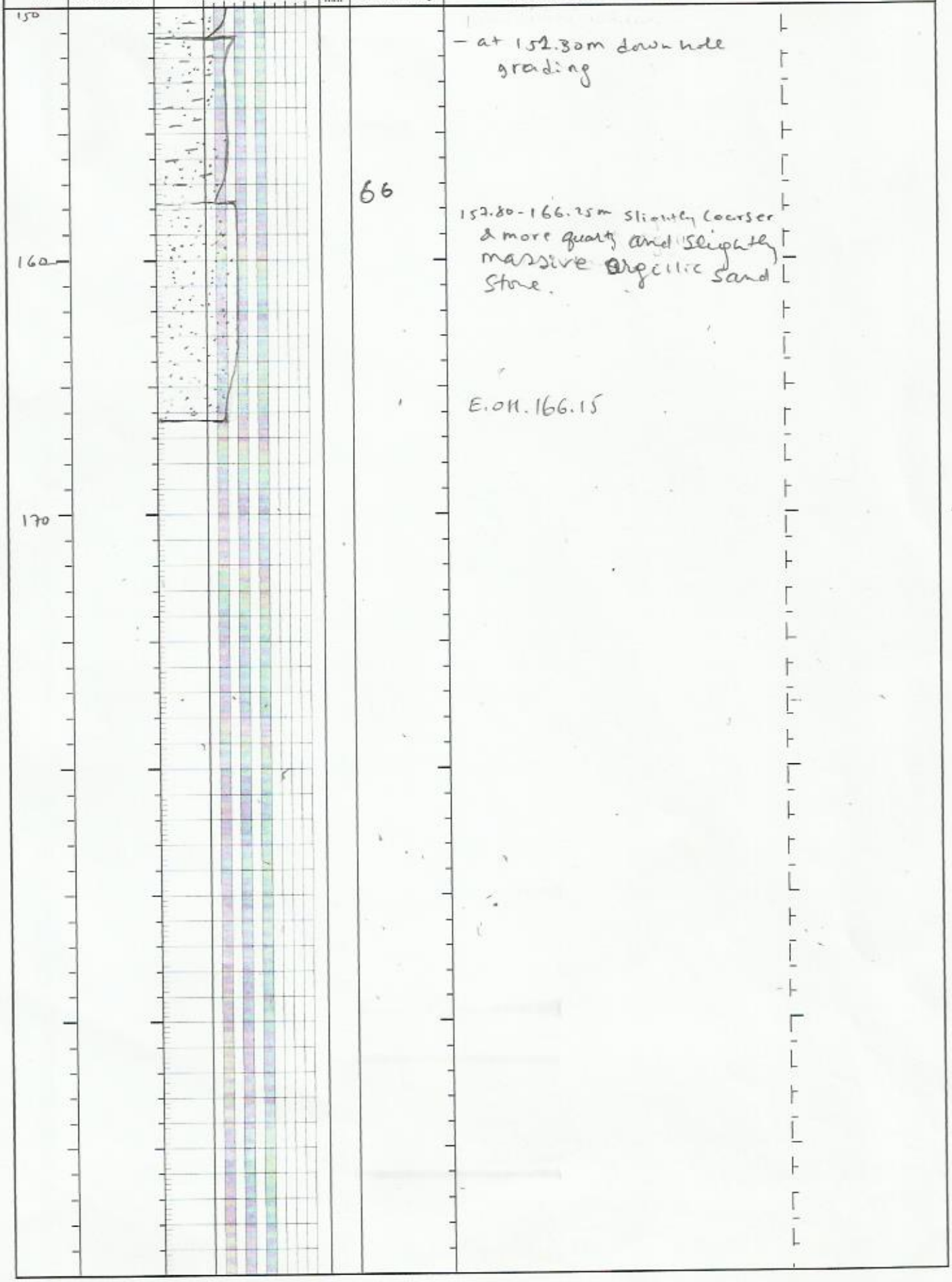

Summary log

EXPLORATION SKILLS MAPPING CAMP

GRAPHIC LOG

Project COMSTAFF		Drill hole No. 18DH2	
Location		Location No.	
Coords: 376697.218 5373385.89 N	RL: 132	Scale: 1:1000	Page 1 of 1
Azim: 270	Incl: -50	Diam:	Logged by: EYOB	Date 24/04/15

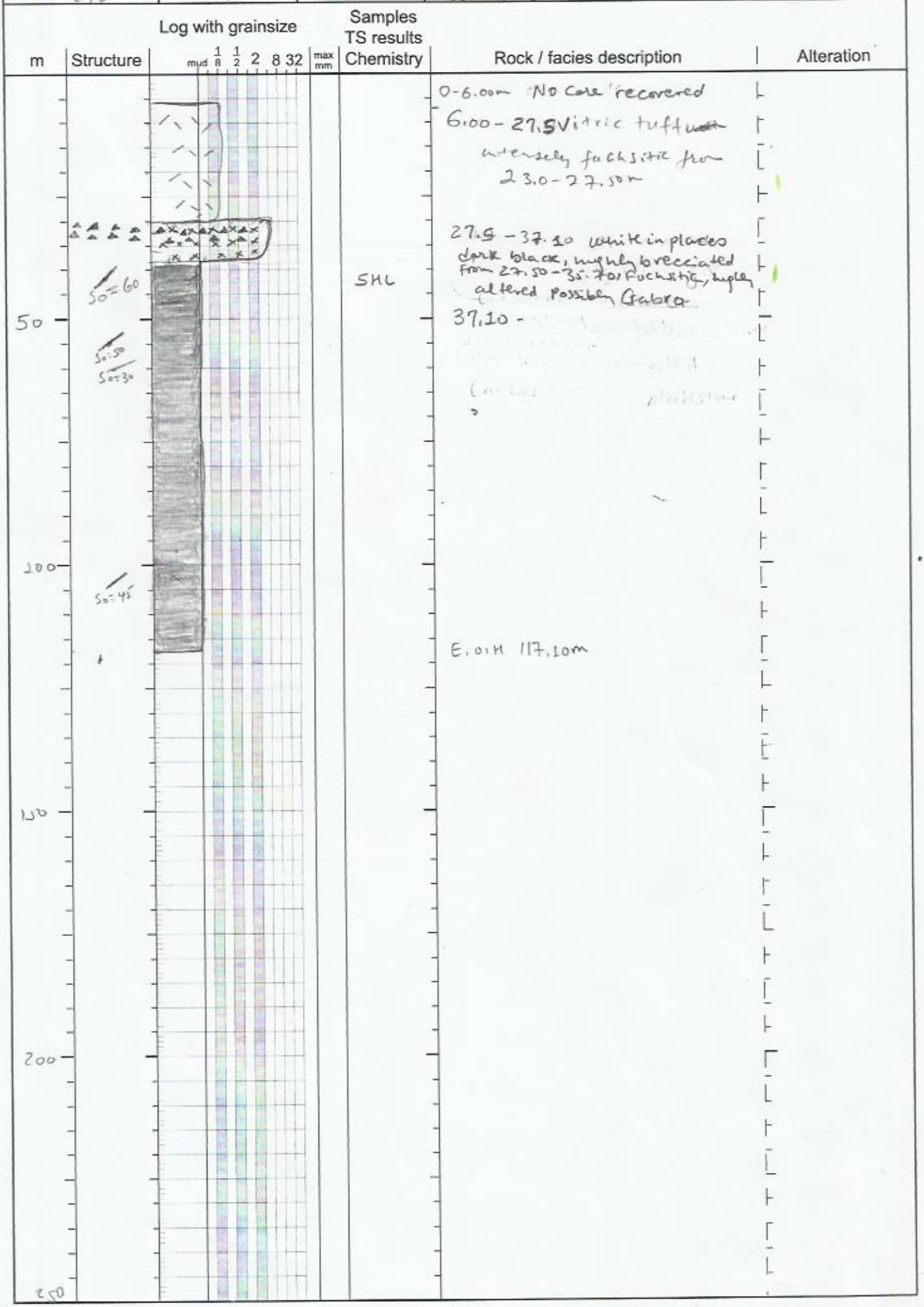

EXPLORATION SKILLS MAPPING CAMP

GRAPHIC LOG

Project COMSTAFF
Location

Drill hole No. 18DH2
Location No.

Coords: 376697.2IE 1537385.89N | RL: 132 | Scale: 1:200 | Page 1 of 3

Azim: 270 | Incl: -50 | Diam: | Logged by: EYOB F.A | Date 28/04/15

Carbonate and Fuchsite

m	Structure	Log with grainsize (mud, 1/8, 1/2, 2, 8, 32, max mm)	Samples / TS results / Chemistry	Litho Code	Rock / facies description	Alteration
			NR		0-6.00m No core recovery except one piece of core possibly of glacial overburde-	
			QFPT		6.00-27.50m strongly broken core of vitric tuff. Greenish from 23.00-27.50m due to strong Chromite in Fuchsite	
10						
20					23.00-27.50m greenish due to strong chromite in Fuchsite.	
			GBR		▲ 27.50-37.10 white in places dark black, highly brecciated from 27.50-35.70m, Fuchsitic from 33.00-35.80m. Gabro. It is more competent from 35.80-37.00 quarz-Carbonate veining in the brecciated section is prominant.	Fuchsite moderate to strong - Clay altered weakly.
30	Z 51°-55°					
			SHL		37.10-114.80 lightgrey to black colored muddy Shale lightfold @ 60° LCA Parallel to the cleavage noted at 41.80-42.80 - Unit is finely laminated	
40	1. 60				42.80-48.00 black, thinly laminated fissile Carbonaceous Shale	
					48.00-53.00 relatively massive with Carbonat veinlets	
50						

▲ breccia

EXPLORATION SKILLS MAPPING CAMP

GRAPHIC LOG

Project Comstaff		Drill hole No. 180H2	
Location		Location No.	
Coords:	RL:	Scale: 1:200	Page 2 of 3
Azim:	Incl:	Diam:	Logged by: EYoB	Date 28/04/15

Log with grainsize

Samples

TS results

Chemistry

m | Structure | mud | 1/8 | 1/2 | 2 | 8 | 32 | max mm | Rock / facies description | Alteration

51.20-51.90 Unit is cut by quartz veining.

57.40-58.60 dolomitic mudstone

58.60-84.80 black, carbonaceous mudstone.

84.80-117.50 thinly laminated pelitic mudstone with intercalation of carbonaceous shale.

S_0:60

S_0:30

S_0:25

S_0:60

S_0:40

60

70

80

90

100

EXPLORATION SKILLS MAPPING CAMP

GRAPHIC LOG

Project Comstaff		Drill hole No. 18DH2	
Location		Location No.	
Coords:	RL:	Scale: 1:200	Page 3 of 3
Azim:	Incl:	Diam:	Logged by: EYoR
			Date 28/04/15

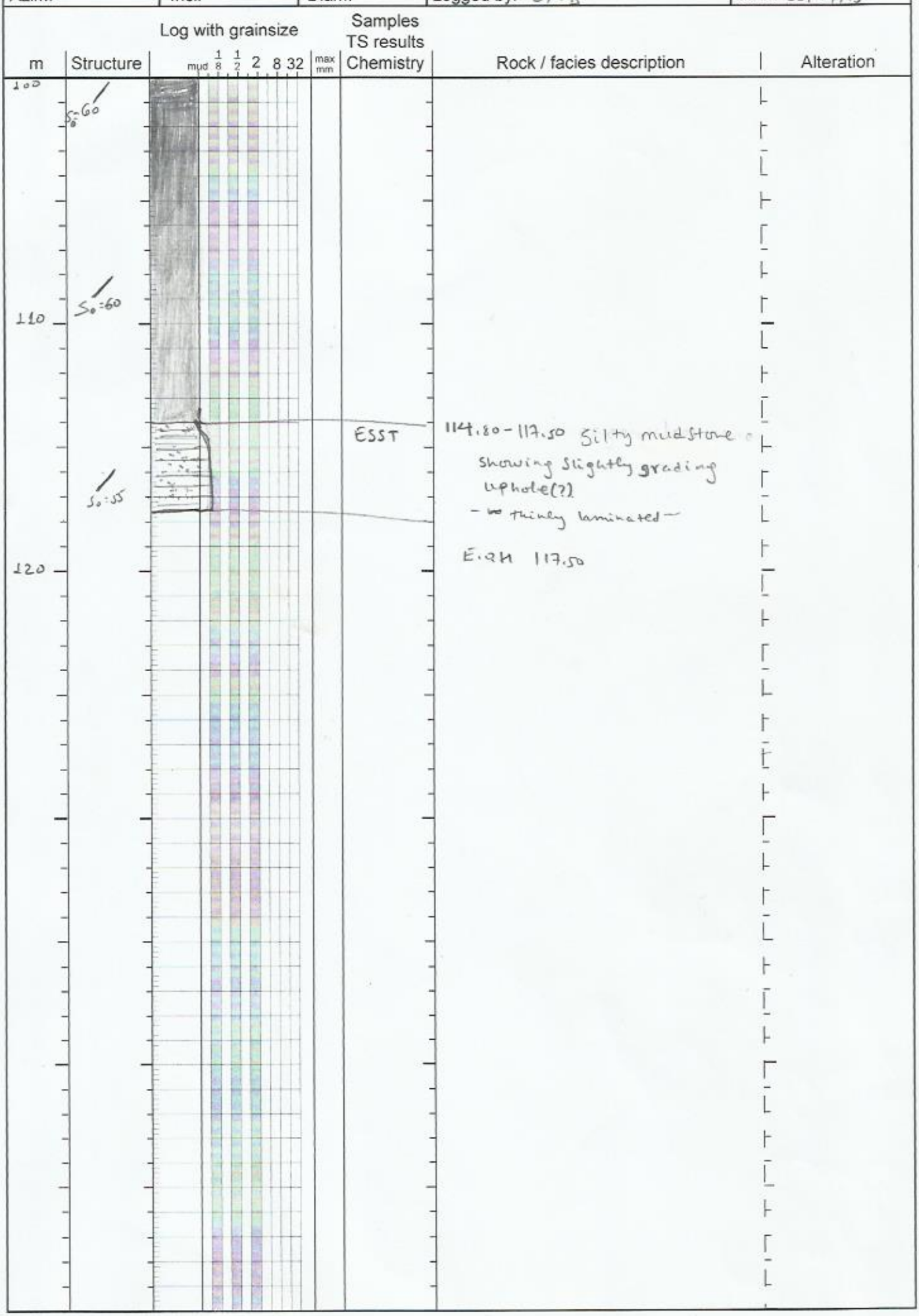

Summary log

EXPLORATION SKILLS MAPPING CAMP **GRAPHIC LOG**	Project Location	Drill hole No. CHP264 Location No.
Coords: 376,443E, 5371806N	RL:	Scale: 1:1000 Page 1 of 1
Azim: 273 Incl: -45	Diam:	Logged by: EYOB Date 24/04/14

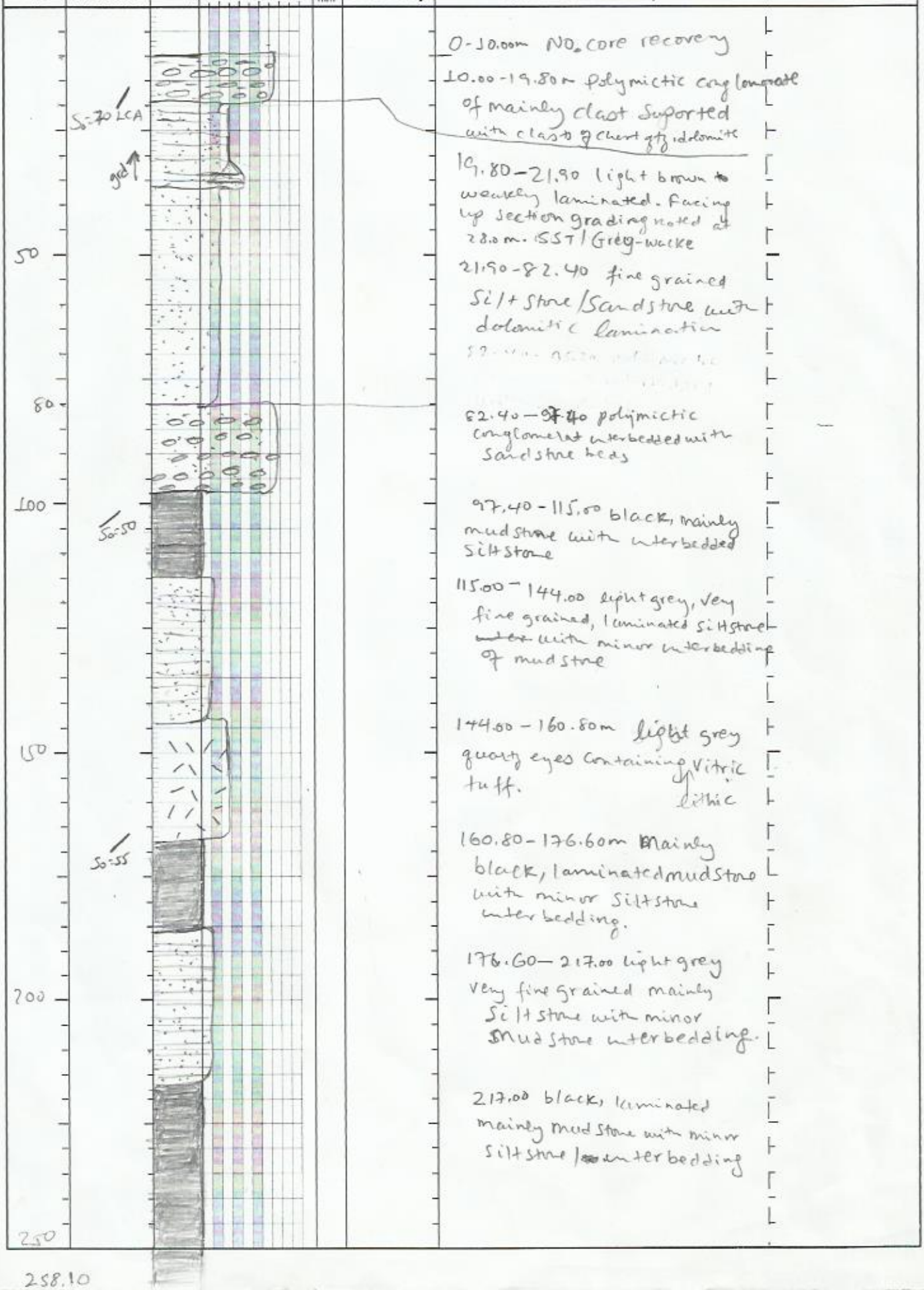

0-10.00m No core recovery

10.00-19.80m polymictic conglomerate of mainly clast suported with clasts of chert qtz idolomite

19.80-21.90 light brown to weakly laminated. Facing up section grading noted at 28.0m. SST / Grey-wacke

21.90-82.40 fine grained Silt stone / Sandstone with dolomitic lamination

82.40-97.40 polymictic conglomelat interbedded with Sandstone beds

97.40-115.00 black, mainly mudstone with interbedded Siltstone

115.00-144.00 light grey, very fine grained, laminated Siltstone with minor interbedding of mudstone

144.00-160.80m light grey quartz eyes containing Vitric tuff. lithic

160.80-176.60m Mainly black, laminated mudstone with minor Siltstone interbedding.

176.60-217.00 light grey very fine grained mainly Siltstone with minor Mudstone interbedding.

217.00 black, laminated mainly mudstone with minor Siltstone interbedding

EXPLORATION SKILLS MAPPING CAMP

GRAPHIC LOG

Project Location	Natone Creek	Drill hole No. / Location No.	CHP264
Coords: 376443E, 5371806N		RL: 273m	Scale: 1:200
Page 1 of 6			
Azim: 273	Incl: -45	Diam:	Logged by: EYOR RA
Date 29/04/05			

Log with grainsize (mud, 1/8, 1/2, 2, 8, 32, max mm) | Samples / TS results | Lith-code / Chemistry | Rock / facies description | Alteration

Alteration: weak CB, moderate, strong

m	Structure	Lith-code / Chemistry	Rock / facies description	Alteration
		NR	0-10.00m No core recovery	
10		CONG	10.00-19.80m dolomitic mainly Sandstone matrix supported Polymictic Conglomerate elongated & imbricated along the cleavage. Main Clasts are Sandstone, maroon to white chert, dolomitic clasts. ranging mm to long axis reaching 4cm.	$FeCO_3$ => Weak
	So:45			
	S1:45		10.00-15.33 more matrix supported where as the lower interval is more of clast supported indicating grading upwards (?) - Possibly cleavage superimposed on bedding (?)	
20	So:45	SLT	19.80-23.30m	
	So:30 grd grd	ESST	light brown, very fine grained, laminated Siltstone / Sandstone laminae Set at 20m to 80 LCA - Conglomerate 20.00-20.15 in Sandstone	
			23.30-29.00 Pale green Pebbly Sandstone. grading upholes indicating facing East @ 26.80m & 28.00m (ESST)	weake $FeCO_3$ + hematite oxidation
30		SLT	29.00-40.60 Creamy to yellow brown, very fine grained Siltstone / Sandstone. weakly laminated. mostly highly broken core.	
	So:36.80			
40		GBR	40.60-46.80 Reddish-brown strongly hematite + limonite oxidized, sheared, acid bleached hence vuggy cleaved 30° LCA, 46.60-46.80 Pyrite intensively altered hence difficult (possibly gabbro (?)	HE + LI => Strong Acid bleached zone.
	S1:50			
	breccia zone	ESST	46.80-61.90 epiclastic Sandstone 46.80-55.06 Creamy to yellow brown fine to medium grained Sandstone / Siltstone. highly brecciated zone	
50				

boundary

EXPLORATION SKILLS MAPPING CAMP

GRAPHIC LOG

Project Location: Natone Creek

Drill hole No. / Location No.: CHP264

Coords: | RL: | Scale: 1:200 | Page 2 of 6

Azim: | Incl: | Diam: | Logged by: EYOB, F. A | Date 29/04/15

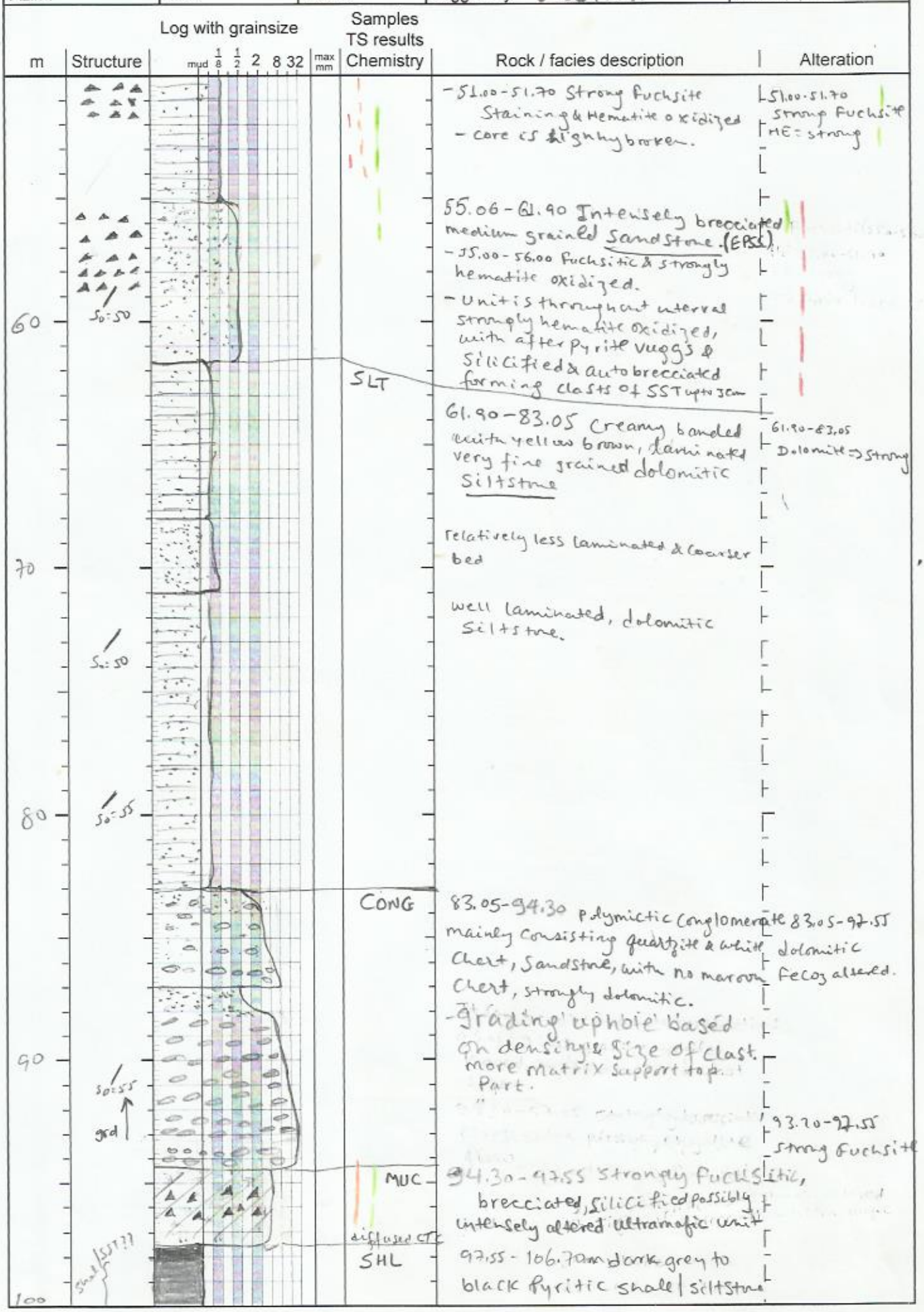

- 51.00-51.70 Strong fuchsite staining & Hematite oxidized
- core is slightly broken.

Alteration: 51.00-51.70 strong fuchsite ME = strong

55.06-61.90 Intensely brecciated medium grained sandstone. (EPSL)

- 55.00-56.00 fuchsitic & strongly hematite oxidized.
- Unit is throughout interval strongly hematite oxidized, with after pyrite vuggs & silicified & autobrecciated forming clasts of SST upto 3cm

61.90-83.05 Creamy banded with yellow brown, laminated very fine grained dolomitic siltstone

Alteration: 61.90-83.05 Dolomite => strong

relatively less laminated & coarser bed

well laminated, dolomitic siltstone.

83.05-94.30 Polymictic conglomerate mainly consisting quartzite & white chert, sandstone, with no maroon chert, strongly dolomitic.

- grading uphole based on densing & size of clast. more matrix support top part.

Alteration: 83.05-97.55 dolomitic FeCo3 altered.

Alteration: 93.20-97.55 strong fuchsite

94.30-97.55 strongly fuchsitic, brecciated, silicified possibly intensely altered ultramafic unit

97.55-106.70 dark grey to black pyritic shale | siltstone

EXPLORATION SKILLS MAPPING CAMP

GRAPHIC LOG

Project Location: Natme creek		Drill hole No.: CHP264	
Coords:	RL:	Scale: 1:200	Page 3 of 6
Azim:	Incl:	Diam:	Logged by: EYOR R.A
			Date 29/04/15

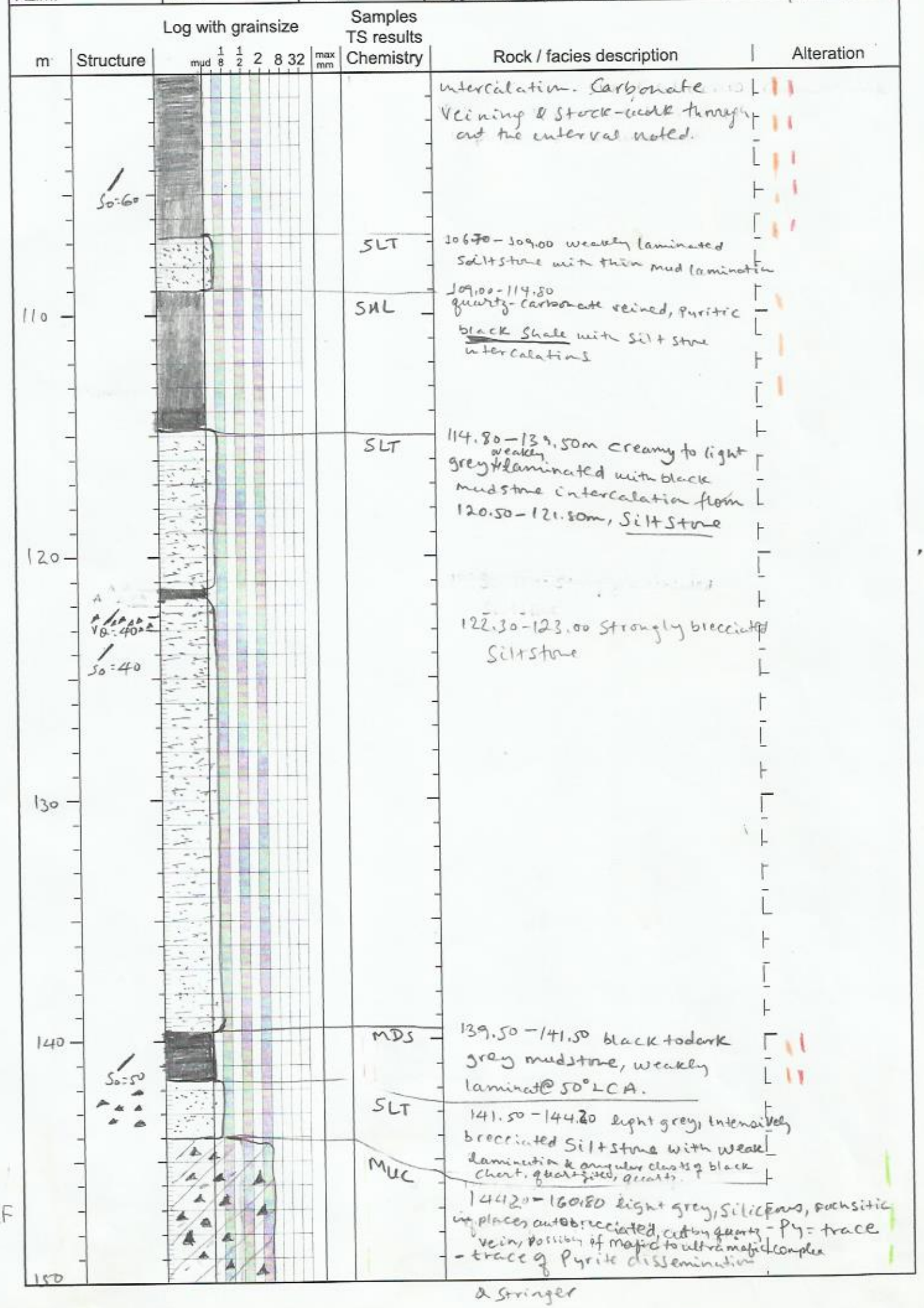

EXPLORATION SKILLS MAPPING CAMP

GRAPHIC LOG

Project / Location: Nature Creek		Drill hole No.: CHP264	
Coords:	RL:	Scale: 1:200	Page 4 of 6
Azim:	Incl: / Diam:	Logged by: EYOB	Date: 29/04/15

Log with grainsize (mud, 1/8, 1/2, 2, 8, 32, max mm) | Samples / TS results / Chemistry | Rock / facies description | Alteration

m

160

170

180

190

200

Structure: S_i 40 / 2

S_o 65 / 1

S_o 60 / 1

S_o 55 / 1

SLT — 160.80 – 173.70m light green to grey, very fine grained thinly black shale laminated Siltstone

SHL — 173.70 – 176.60m dark grey to black Pyritic carbonate altered Shale

SLT — 176.60 – 217.60m light green to grey colored, laminated, mainly Siltstone with grey wacke & mud stone minor intercalation. Trace of oxidized disseminated Pyrite

185.40 – 187.30 dark grey, relatively massive, grey wacke, slightly coarse

Alteration: Weak Carbonate; Weak Chlorite; Trace Py

EXPLORATION SKILLS MAPPING CAMP

GRAPHIC LOG

Project Natou creek
Location

Drill hole No. CHP 264
Location No.

Coords: | RL: | Scale: 1:200 | Page 5 of 6

Azim: | Incl: | Diam: | Logged by: E40B F.A | Date 29/04/15

m	Structure	Log with grainsize (mud, 1/8, 1/2, 2, 8, 32, max mm)	Samples / TS results / Chemistry	Rock / facies description	Alteration
				- unit is greenish down the interval due to weak chlorite alteration	Chlorite → weak
				205.60 - 205.05 dark grey, massive silty grey wacke. Slump CTC @ top 40° LCA lower slump CTC 30 LCA	
210				205.05 - 217.55 light green, laminated & interbedded with black fissile shale. weakly carbonate altered Iron	
				217.55 - 249.65 highly fissile & thinly laminated shale	
			SHL	217.55 - 258.20 dark grey to black shale, which highly fissile up to 245.00 & massive & silty 245.00 to the end of hole.	
220	S_0: 70				
230	S_0: 40			230.30 - 237.30 quartz carbonate veining & stock-worked mudstone with siltstone intercalation	
240	S_0: 60				
				24.9.65 - 250.50 muddy siltstone.	

EXPLORATION SKILLS MAPPING CAMP

GRAPHIC LOG

Project / Location		Drill hole No. / Location No.	CHP 264
Coords:	RL:	Scale: 1:200	Page 6 of 6
Azim:	Incl: / Diam:	Logged by: EYOB F. A	Date 29/04/15

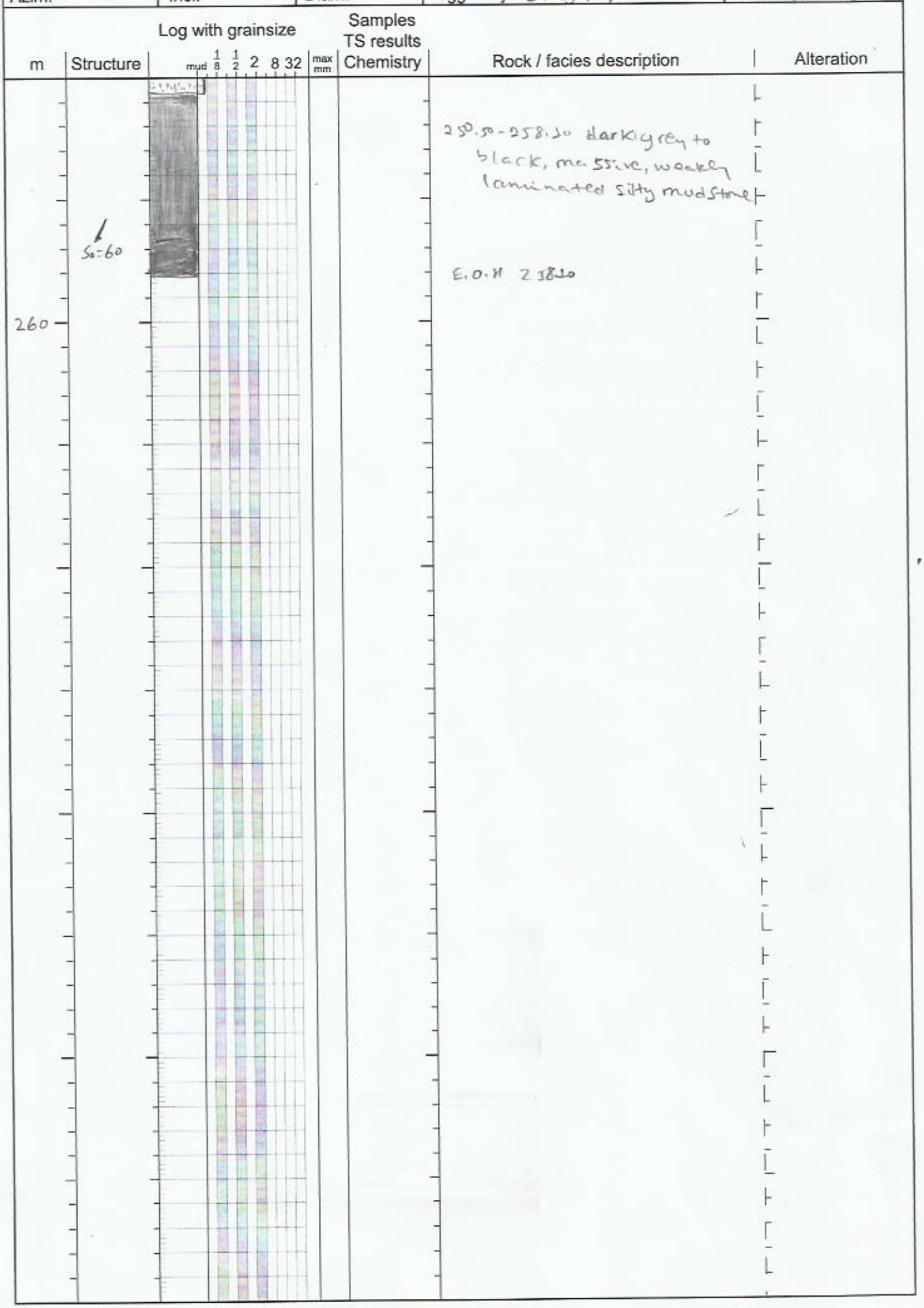

Appendix 3
Representative petrographic descriptions

			Marianoak Formation					Xll= crystals, Qtz= quartz, Fsp= feldspar, brx= breccia	
			Abbreviations: cgr= very coarse grained, mgr= medium grained, fgr= fine grained						
Hole_ID	Sample №	interval	Lithofacies	Chem Units	Characteristics	petrographic and volcanic textures observed features	color	Mode of formation, emplacement process and timing	Qtz : Fsp
R10032	RG158	171.80-172.00	Mudstone		Mudstone interbedded with minor sandstone and siltstone	polycrystalline qtz (1-2%), Carbonate veined, shards 0.5mm (1-2%), Fsp 2-3%	dark black	Prolonged period of pelagic sedimentation (volcanic quiescence)	
R10032	RG162	226.00-226.15	VBX II/VSST	VBX II/VSST	Rhyolitic breccia in volcaniclastic sandstone	angular qtz Xll fragments (2-3 mm, 10%), euhedral Fsp (0.25-0.50mm, 1-2%), qtz phyric rhyolite brx (0.5mm, 5%)	grey	Resedimented rhyolitic breccia	
R10032	RG163	226.90-227.15	VBX II/VSST	VBX II/VSST	Rhyolitic volcaniclastic breccia in volcaniclastic sandstone	Qtz (20-25%), angular to sub-rounded, qtz-phyric rhyolitic clasts (4-6 mm, 5%), Fsp (1-2%)		resedimented rhyolitic breccia partly showing quench fragmentation	
R10063	RG177	290.75-290.80	VBX I/VSST	VBX I/VSST	Bed thickness of 18 m, cgr, granular top polymictic volcaniclastic breccia in volcaniclastic sandstone, clast size reaching ~3cm, mud lithic, basaltic andesite and qtz-phyric juvenile clasts	weakly sericite altered, angular to sub-rounded basaltic andesite clasts (1-2 mm, 10-15%), Fsp 1-2%, clasts are imbricated along foliation plane	grey	reworked from effusive volcanic products of intermediate to mafic composition	
R10063	RG181	356.40-356.6	VBX I/VSST	VBX I/VSST	10 m single bed thickness, stratified top with mudstone and siltstone. Highly flattened andesitic juvenile clasts	Angular to sub rounded, altered, basaltic andesite clasts. No significant quartz or Fsp noted	grey	reworked from effusive volcanic products of intermediate to mafic composition	lithics dominated
R10063	RG182	370.00-370.2	VBX I/VSST	VBX I/VSST	poorly sorted, mgr-cgr, normal graded to stratified top, thickly bedded, moderately sericite and weakly chlorite altered	basaltic andesite (5-10%), rhyolite clasts 1-2%, opaque minerals-magnetite (1-2%)	Grey	Dominated by basaltic andesite clasts with minor rhyolitic clasts. Hence, it is reworked from multiple sources	
R10063	RG184	416.40-416.70	VBX I/VSST	VBX I/VSST	Very cgr, poorly sorted, matrix supported, massive to weakly cleaved,	Angular to sub-rounded clasts, euhedral Fsp xlls (5%), qtz (1-2%), basaltic andesite l (5-10%)	Grey	reworked from effusive volcanic products of intermediate to mafic composition with minor felsic contribution	05:95

Appendix 3
Representative petrographic descriptions

			Marianoak Formation						
Hole_ID	Sample №	interval	Lithofacies	Chem Units	Characteristics	petrographic and volcanic textures observed features	color	Mode of formation, emplacement process and timing	Qtz : Fsp
R10063	RG190	609.3-609.6	VBX I/VSST	VBX I/VSST	Volcaniclastic siltstone	V.fgr, ellipsoidal with rounded edges, polycrystaline qtz (0.1-0.2 mm, 5%) and andesitic basalt (0.5-1mm, 5%)	Grey	significant reworking as the framework is rounded to sub-round. It is interpreted to be deposited from low density turbidity currents deposit below wave base as it is interbedded with thin mudstone beds.	
R10063	RG192	794.00-794.15	Qtz-fsp Phyric pbx	Rhy C	massive to weakly graded Qtz-Fsp phyric PBX	Pumice clasts (1-5cm, 50-60 %), angular to sub-rounded cgr qtz (0.25-0.5 mm, 5%), fgr qtz ~15%, and glass shards	grey	Syn-eruptive pyroclastic deposit of qtz-feldspar phyric pumice breccia	90:10
R10063	RG195	909.3-909.45	qtz-fsp-phyric pbx	Rhy B	massive to weakly graded Qtz-Fsp phyric Pbx	mgr, angular to sub-rounded qtz xll fragments (2%, 0.5-2 mm) and fgr qtz <0.5 mm, 15%), euhedral Fsp (5%, 0.5-2 mm) and pumice clasts (1-5 cm, 50-60 %) and glass shards	grey	Syn-eruptive pyroclastic deposit of qtz-phyric pumice breccia	80:20
R10063	RG197	933.20-933.4	Qtz-phyric pbx	Rhy A	Single bed thickness 18m, very coarse base with clast supported base and stratified top with siltstone and mudstone	Pumice clasts (1-5 cm, 50-60 %), mgr to cgr angular to sub-rounded qtz xll fragments (1-2%, 0.25-2 mm) and V.fgr qtz <0.25 mm, 10%), former glass shards (5-10%), Fsp (1-2%, 0.25-1mm)	Dark grey	Syn-eruptive pyroclastic deposit of qtz-phyric pumice breccia	95:05
R10063	RG199	1115.30-1115.50	Peperite	Peperite	vcgr, monomictic, curviplanar, rhyolitic clasts set in siltstone and mudstone matrix	angular to sub-rounded qtz xlls of 10-15% in siltstone to mudstone matrix	grey to brownish	Syn-eruption felsic lava in contact with unconsolidated mudstone and siltstone	

Appendix 3
Representative petrographic descriptions

Central area							Qtz=quartz, Fsp= feldspar, Xll= crystals, Cgr=coarse grained, fgr=fine grained, mgr=medium grained, CCF=Crimson Creek Formation, MUC=mafic ultra-mafic complex	
Hole №	Sample №	interval	Lithofacies	Characteristics	petrographic and volcanic textures observed features	colour	Mode of formation, emplacement process and timing	Qtz : fsp proportion
RBH1	RG062	52.00-52.12	quartz-wacke	fgr-cgr, thickly bedded, lithic-wacke	Sub-rounded to angular qtz (0.1-0.2 mm, 10-20%, sub-rounded mafic lithics (0.2-0.3, 10-15%), mica grains (1%)	grey	Epiclastic reworking of qtz and mica grains are interpreted to be sourced from the Precambrian basement, CCF and MUC	
RBH1	RG063	106.24-106.40	Salisbury conglomerate	Polymictic conglomerate with chert, quartzite, mudstone and sandstone matrix. Clast size averages to 3.5 cm	Metamorphic qtz (5-7%, 1-2mm, mafic clast 0.5-1mm, 1%, siltstone 2-4 mm in dolomitic (calcite) matrix	Grey	Epiclastic reworking, metamorphic qtz and chert are interpreted to be sourced from the Precambrian basement whereas the mafic, mudstone and siltstone clasts are possibly sourced either from the CCF or MUC deposited from high energy density currents	
RBH2	RG064	34.60-34.75	Qtz-Fsp-phyric PBX (Rhyolitic)	Qtz Fsp phyric Pbx with minor mud lithics and significant pumice clasts	mgr qtz xlls (0.1-0.5mm, 1-2%), pumice clasts (40-60%)	grey	syn eruption, felsic pyroclastic deposited by high density mass-flow currents	
RBH2	RG065	85.35-85.47	Qtz-Fsp-phyric PBX (Rhyolitic)	Qtz Fsp phyric Pbx with minor mud lithics and significant pumice clasts	mgr qtz xlls (0.1-0.5mm, 1%,) the rest is sericite altered groundmass	grey	syn-eruption deposit from high density mass-flow currents	
RBH2	RG355	147.00m	Volcaniclastic Sandstone	Fsp phyric andesitic volcaniclastic sandstone	Euhedral Fsp (0.5-1mm, 15-20%), sub-rounded to angular andesite lithics (0.5-1mm, 10%), angular to sub-rounded qtz crystals (0.25-0.5mm, 2-3%)	Pale grey	reworked from effusive volcanism as it lacks voluminous pumice clasts. Deposited from low to moderate concentration mass-flow currents	05:95
RBH2	RG066	157.95-158.07	Quartz-wacke	mgr sandstone, graded bed, single bed thickness of about 10cm	Sub-rounded to angular, fgr qtz (0.2-0.3mm, 7-10%), mafic lithics (3-5%, 0.3-0.5mm), minor mica grains	grey	Epiclastic, reworked from the extra-basinal basement and deposited from low to moderate density currents	

Appendix 3
Representative petrographic descriptions

				Southern area petrography					
Hole №	Sample №	interval	Litho Group	Characteristics	petrographic and volcanic textures observed features	color	Mode of formation, emplacement process and timing	Facies vertical location	Qtz:fsp proportion
Ring River	R002	375133E/5366679N	Greywacke	light grey to greenish, cgr, massive, 10% Fsp, mafic lithics and trace of pyrite containing SST	euhedral to anhedral, feldspar (0.5-1 mm, 7-10%), basaltic andesite lithics (0.5-1mm, 2-3 %) quartz (1-2%), clay (10-15 %) and minor magnetite	Grey-greenish	epiclastic sediment deposition as low-density turbidity currents from feldspar crystal rich and mafic provenance		15:85
Ring River	RG225	374489E/5367678N	VBX	massive, feldspathic crystal rich VBX	euhedral Fsp (1-2 mm, 10-15), embayed qtz crystal fragments (1-2mm, 2-3%), angular to sub-rounded andesitic lithics (1-2%) and minor opaque minerals (magnetite) in chlorite altered groundmass	grey-greenish	syn-eruption of explosive eruption		05:95

Rosebery Mine sequence

Hole number	Sample №	interval	Litho facies/subfacies	Geochemical subunits	Characteristics	Petrographic and volcanic textures observed features on hand specimen	colour	emplacement timing and process	Location facies	Qtz :fld proportion
339R	RG347	1298.6-1298.75	WSF 2C rhyolitic volcaniclastic breccia	WSF 2C	Grey aphanitic and quartz phyric clasts containing volcaniclastic breccia	Aphanitic clasts (1-3cm, 50-60%), qtz xll frag rich (0.25-0.5mm, 10-15%), Fsp (<0.25mm, 1-2%), lithics (0.5mm, 2%)	grey	Reworked from effusive volcanism as it lacks large volume of pumice clasts	base of subunit 2C	85:15
337R	RG336	1013.00-1013.2	WSF 2B polymictic breccia	WSF 2B	polymicitic volcaniclastic breccia with aphanitic and feldspar phyric basaltic andesite and quartz crystal fragments	Aphanitic and fsp phyric basaltic andesite, amyloidal basalt (2.0-2.50mm, 5-7%), Fsp (3-5%), angular quartz-crystals (0.5 mm, 3-5%), magnetite (1%), sericite altered groundmass	grey	Reworked from effusive volcanism as it lacks large volume of pumice clasts	top of subunit 2B	50:50
337R	RG339	1106.30-1106.5	WSF 2A Basaltic andesite volcaniclastic breccia	WSF 2A	feldspar phyric basaltic andesite volcaniclastic breccia	Feldspar-phyric basaltic andesite (1-10 cm, 40-70) Fsp (0.5-1.00mm, 10%), Qtz (1-2%, 0.25mm), angular to sub-rounded basaltic andesite clasts (0.5-1mm)	grey	Reworked from effusive volcanism as it lacks large volume of pumice clasts	base of subunit WSF 2A	05:95
397R	RG350	1356.80-1357.00	WSF 2A Basaltic andesite volcaniclastic breccia	WSF 2A	feldspar phyric basaltic andesite clast	Feldspar-phyric basaltic andesite (1-10cm, 40-70%), euhedral Fsp (0.5-1.00mm, 10%), angular to sub-rounded often embayed qtz (1-2%, 0.5mm), angular to sub-rounded basaltic andesite clasts (0.5-1mm)	grey to greenish	Reworked from effusive volcanism as it lacks large volume of pumice clasts.	base of subunit WSF 2A	
337R	RG340	1135-1135.10	WSF 1: qtz-fsp phyric pumice breccia	WSF 1B	quartz-feldspar phyric pumice breccia	Pumice-fiamme (1-5 cm, 60-80%), angular qtz crystal frag, fractured and often embayed (0.5 mm, 5-10%), euhedra Fsp xlls (10-15 %), (shards 2-5%), qtz-phyric rhyolite clasts rounded to sub-angular (1-2%) in moderately sericite and weakly chlorite and carbonate altered	Grey	Syn-eruption mass flow deposit	Top of WSF 1B	40:60
337R	RG342	1190.95-1191.10	WSF 1: qtz-fsp-phyric pumice breccia	WSF 1A	quartz-phyric pumice breccia	Pumice-fiamme clasts (1-5 cm, 60-80%), euhedral Fsp Xlls (0.25-0.50mm, 2-3%), angular qtz crystal fragments (0.25-0.50mm, 15-20%), glass shards (2-3%), lithics (1-2%), sericite altered groundmass	Grey	Syn-eruption massflow deposit	middle of WSF 1A	90:10
337R	RG344	1251.5-1251.65	Host rock 2	Host rock 2	quartz-phyric volcaniclastic sandstone (Host rock)	Angular to sub-rounded qtz xll frag (0.5mm, 10-15%), euhedral Fsp (0.50-0.75 mm, 5%), lithics 0.50-1.0mm (1-2%), secondary calcite	grey	post-eruption epiclastic deposit as low concentration turbidity currents from distal rhyolite centre	host rock 2	65:35
337R	RG345	1271.2-1271.40	host rock 1	host rock 1	feldspar phyric volcaniclastic sandstone	Euhedral Fsp xlls rich (0.5-1mm, 30-40%), mafic lithics 2-3%, calcite xlls as matrix	pale grey	post eruption reworked from proximal source possibly the underlying Hercules Pumice Fm as it has similar composition	host rock 1	98:02
337R	RG251	1461.91-1462.05	Hercules Pumice Formation	Hercules Pumice Formation	Feldspar phyric pumice breccia	Euhedral Fsp xll frag (0.5-1.0mm, 5%), Qtz (1-2%), glass shards and minor lithics	grey	Syn-eruptive pyroclastic deposit of Feldspar phyric pumice breccia	CVC	60:40

Appendix 4A

Rosebery Mine host stratigraphy including the Marianoak Formation

Project_Des	Project	Prospect	Hole_ID	Depth_From	Depth_To	SAMPLE_TA	Al_pct	Ca_pct	Cr_ppm	Fe_pct	Ga_ppm	Ge_ppm	Hf_ppm	K_pct	La_ppm	Mg_pct	Mn_pct	Na_ppm	P_ppm	Sc_ppm	Th_ppm	Ti_ppm	U_ppm	V_ppm	Y_ppm	Zr_ppm
Rosebery	ROS	RMN	250R	290	290.1	D1801283	5.6	0.96	4	1.52	11.75	0.2	4.2	1.5	52.9	0.36	0.0658	24000	230	6.4	22.7	1590	5.5	13	21.4	148
Rosebery	ROS	RMN	250R	300	300.1	D1801284	6.79	0.94	5	2.62	15.4	0.2	3.8	1.31	41.5	0.55	0.0526	34000	410	11.8	17.2	2450	4.3	40	17.5	134
Rosebery	ROS	RMN	250R	310	310.1	D1801285	6.39	1.29	5	2.35	17.2	0.22	4.2	2.46	42	0.6	0.0631	19500	410	11	16.3	2750	4.6	43	17.2	150
Rosebery	ROS	RMN	250R	320	320.1	D1801286	7.81	3.02	130	5.36	19.6	0.21	3.2	3.58	31.5	2.29	0.123	2600	970	23.7	13.8	3130	5.2	275	15.8	122
Rosebery	ROS	RMN	250R	330	330.1	D1801287	7.04	2.91	8	3.26	16.85	0.19	2.4	2.84	27.5	0.74	0.112	18800	710	21.3	6.4	5450	1.7	79	21.4	89.1
Rosebery	ROS	RMN	250R	340	340.1	D1801288	7.23	2.3	4	2.2	19	0.18	4.7	3.45	34.6	0.8	0.152	17800	510	12.6	15.1	3590	3.6	41	23.1	169
Rosebery	ROS	RMN	250R	350	350.1	D1801289	6.39	4.83	6	2.86	14.15	0.2	3.2	1.67	45.6	0.74	0.22	26600	420	12.6	12.5	2960	2.9	37	27.6	118
Rosebery	ROS	RMN	250R	360	360.1	D1801290	6.99	2.09	7	3.01	18	0.19	3	2.53	24.7	0.65	0.12	23400	600	17.2	9.2	3770	2.5	54	18.7	112
Rosebery	ROS	RMN	250R	369.9	370	D1801291	6	0.32	6	5.19	13.6	0.32	3.7	2.3	23.1	0.54	0.309	22800	520	10.6	10.8	2400	3.5	35	15.6	133
Rosebery	ROS	RMN	250R	380	380.1	D1801292	5.77	4.39	9	3.98	13.95	0.17	3.2	1.91	42.6	1.11	0.228	20000	400	10.5	14.1	2380	3.6	30	24.4	124
Rosebery	ROS	RMN	250R	390	390.1	D1801293	6.25	2.7	6	2.04	14.75	0.18	3.8	1.86	34.5	0.74	0.144	29400	450	11.6	12	3060	2.8	35	20.2	132.5
Rosebery	ROS	RMN	250R	400	400.1	D1801294	5.82	1.15	8	3.02	15.55	0.28	3.7	1.28	26.4	0.45	0.0786	40000	520	9.6	11	2370	3.6	35	13.6	137
Rosebery	ROS	RMN	250R	410	410.1	D1801295	5.35	4.56	5	1.78	15.1	0.19	4.1	2	35.7	0.38	0.148	25200	200	6.8	13.4	2050	3.6	13	18.8	146.5
Rosebery	ROS	RMN	250R	420	420.1	D1801296	6.13	1.77	9	1.93	13.95	0.2	3.5	1.93	28.5	0.37	0.0822	32600	200	8.3	13.3	1790	3.4	20	21.3	125
Rosebery	ROS	RMN	250R	430	430.1	D1801297	5.94	2.41	26	2.92	18.7	0.33	3.9	2.2	19.7	0.51	0.116	36800	340	10.7	9.4	2600	3.1	42	18.6	138.5
Rosebery	ROS	RMN	250R	440	440.1	D1801298	6.37	0.83	6	1.95	16.85	0.19	4.2	2.14	41.3	0.44	0.0454	29800	230	8.2	16.3	2220	4.3	15	20.2	147.5
Rosebery	ROS	RMN	250R	450	450.1	D1801299	5.93	1.32	4	1.48	12.95	0.19	4.8	1.83	51.9	0.43	0.0813	23600	120	4.9	20.1	1350	4.7	9	23.5	174
Rosebery	ROS	RMN	250R	460	460.1	D1801300	6.39	0.4	5	1.64	14.6	0.16	5	2.65	45	0.28	0.0294	24400	130	5.8	20.1	1410	5	12	26.7	183.5
Rosebery	ROS	RMN	250R	470	470.1	D1801301	6.32	1.24	9	1.74	13.05	0.17	4.6	1.97	44.9	0.27	0.0563	25900	130	5.6	17.9	1470	4.6	11	29.8	167.5
Rosebery	ROS	RMN	250R	480	480.1	D1801302	5.91	0.74	8	2.6	17.8	0.88	4	2.25	343	0.39	0.108	12800	170	5.8	16.5	1270	3.9	16	25	141
Rosebery	ROS	RMN	250R	490	490.1	D1801303	5.17	0.8	6	1.92	9.31	0.2	3.9	0.76	50.4	0.23	0.0683	32400	100	3.6	16	950	4.1	8	21	145.5
Rosebery	ROS	RMN	250R	500	500.1	D1801304	6.37	0.52	5	2.01	15.85	0.27	4.8	2.45	31.9	0.33	0.0507	26300	170	6.2	14	1830	4.5	17	19.6	174.5
Rosebery	ROS	RMN	250R	510	510.1	D1801305	7.78	0.54	7	2.05	16.1	0.13	3.9	2.74	34.8	0.45	0.0612	32100	200	7.8	26.5	1440	7.2	27	20.6	120.5
Rosebery	ROS	RMN	250R	520	520.1	D1801306	6.11	0.24	25	1.51	10.5	0.13	2.8	1.06	35.6	0.24	0.0444	35400	300	5.5	12.8	1880	4.6	34	16.4	93
Rosebery	ROS	RMN	250R	530	530.1	D1801307	3.68	0.82	13	0.95	7.3	0.17	2.3	1.06	65.2	0.32	0.0325	15600	50	2.2	19.5	680	5.8	9	21.4	67.6
Rosebery	ROS	RMN	250R	540	540.1	D1801308	6.88	1.17	2	1.12	14.9	0.18	4	3.91	63.6	0.88	0.0571	800	50	2.6	35.8	920	9.9	3	26.7	111.5
Rosebery	ROS	RMN	250R	550	550.1	D1801309	6.11	1.01	5	1.17	11.95	0.17	3.5	2.32	55.5	0.57	0.0569	18500	50	2.3	30.1	830	6.7	3	22.4	99.3
Rosebery	ROS	RMN	250R	561	561.1	D1801310	8.15	0.65	3	1.05	19.2	0.19	4.8	4.69	79.7	0.8	0.0314	3500	70	3	40.4	1110	9.4	3	25.9	135
Rosebery	ROS	RMN	250R	570	570.1	D1801311	5.76	0.84	7	1.05	13.35	0.19	3.1	2.6	66	0.63	0.0406	13100	70	2.6	29.1	860	8.3	6	23.4	91.8
Rosebery	ROS	RMN	250R	580.2	580.3	D1801312	7.92	0.85	4	1.23	17.25	0.18	4.8	4.94	67.1	1.06	0.0327	800	80	3.2	40.6	1140	12.2	5	26.2	135.5
Rosebery	ROS	RMN	250R	590	590.1	D1801313	6.95	1.27	9	1.73	16.7	0.14	3.8	3.02	28.8	0.49	0.0678	20000	240	7.8	20.4	1490	6.3	31	17	126
Rosebery	ROS	RMN	250R	600	600.1	D1801314	5.92	3.46	1	1.65	13	0.2	4.2	3.6	52.7	0.57	0.166	3100	180	3.5	19.8	1140	5.6	6	21.4	136
Rosebery	ROS	RMN	250R	620	620.1	D1801316	6.82	0.92	9	1.13	14.3	0.16	3.2	1.47	36.9	0.25	0.0596	38000	260	6.6	15.8	1210	4.7	25	15.9	107.5
Rosebery	ROS	RMN	250R	630	630.1	D1801317	8.32	1.18	15	1.68	21.4	0.21	5.2	4.79	72.5	0.75	0.106	700	150	5.4	32.7	1600	8.3	26	21	172.5
Rosebery	ROS	RMN	250R	650	650.1	D1801319	5.51	2.54	5	2.54	10	0.14	2.4	1.59	20.7	0.5	0.13	26700	250	5.8	9.9	1240	2.4	19	16.5	79
Rosebery	ROS	RMN	250R	660	660.1	D1801320	6.63	0.96	3	1.42	17.2	0.19	3.2	3.73	31.6	0.45	0.0705	14900	310	7.1	11.6	1690	4.3	30	12.1	105.5
Rosebery	ROS	RMN	250R	670	670.1	D1801321	5.94	0.52	7	0.9	11.1	0.06	2.5	1.13	3.4	0.16	0.0343	35500	230	4.6	11.2	1030	3.2	20	8.9	82.7
Rosebery	ROS	RMN	250R	680	680.1	D1801322	6.57	0.66	6	1.07	10.3	0.09	2.6	0.34	14.4	0.12	0.116	53500	260	4.3	12	830	3	15	10.7	85.5
Rosebery	ROS	RMN	250R	699	699.1	D1801324	6.89	0.94	5	1.69	17.95	0.21	3.3	3.61	24	0.32	0.094	21100	330	6.7	10.8	1780	4	32	9.6	105.5
Rosebery	ROS	RMN	250R	710	710.1	D1801325	5.45	1.7	21	1.24	10.9	0.12	2.2	1.68	23.2	0.23	0.0957	22500	210	6.3	10.9	1160	2.5	15	11	72.9
Rosebery	ROS	RMN	250R	740	740.1	D1801328	6.88	1.42	4	1.53	14	0.17	4.5	2.06	39.9	0.47	0.0387	26300	180	4	19.9	1870	5.3	8	22.4	161.5
Rosebery	ROS	RMN	250R	750	750.1	D1801329	7.08	0.76	2	3.65	15.3	0.17	4.7	3.83	33	0.57	0.94	3300	200	3.8	19.6	1590	6.1	8	19.3	161
Rosebery	ROS	RMN	250R	760	760.1	D1801330	6.93	0.74	3	1.65	15.25	0.23	4.7	2.53	67.7	0.96	0.0345	16000	180	4	21	1850	5.2	7	22.5	169.5
Rosebery	ROS	RMN	250R	770	770.1	D1801331	7.05	0.35	2	1.97	15.05	0.17	4.4	2.72	44.4	1.21	0.0281	8700	190	4.1	20.1	1740	5.9	7	19.9	155.5
Rosebery	ROS	RMN	250R	780	780.1	D1801332	8	1.36	2	1.56	19.05	0.21	5.7	4.29	39.3	0.86	0.131	9500	210	4.9	22.9	1940	7.4	10	19.1	204
Rosebery	ROS	RMN	250R	790	790.1	D1801333	5.93	1.33	4	1.27	12.5	0.19	3.8	1.71	37.2	0.48	0.0471	26400	180	3.7	18.5	1470	4.3	7	17	138
Rosebery	ROS	RMN	250R	800	800.1	D1801334	6.23	3.73	5	2.47	13.5	0.23	3.9	2.79	49.6	1.15	0.168	11900	170	4.7	18	1500	4.6	8	34.1	142
Rosebery	ROS	RMN	250R	810	810.14	D1801335	6.97	0.48	5	3.55	16.1	0.24	4.5	3.97	56	0.42	0.771	900	190	4.1	19.5	1220	4.7	9	16.8	159.5
Rosebery	ROS	RMN	250R	819.7	819.9	D1801336	5.5	1.6	5	1.38	11.55	0.22	4.1	1.25	27	0.34	0.0963	36800	150	3.4	14.5	1300	4	7	12.9	149
Rosebery	ROS	RMN	250R	830	830.1	D1801337	5.16	6.68	3	1.59	10.15	0.2	3.4	1.37	43.6	0.48	0.214	24000	130	5.7	16	1280	4	6	32.9	134
Rosebery	ROS	RMN	250R	850	850.1	D1394776	5.41	1.57	8	1.57	14.15	0.09	3.4	2.66	20.2	0.52	0.102	900	80	3.2	28.1	630	9.7	18	14.5	86.4
Rosebery	ROS	RMN	250R	860.5	860.6	D1394777	6.6	3.12	16	2.66	18.4	0.11	4.1	3.41	20.1	0.91	0.289	800	220	7	30.4	1390	10.6	48	18.9	103
Rosebery	ROS	RMN	250R	870	870.1	D1394778	6.82	0.77	7	0.82	16.15	0.14	4	3.78	67.1	0.67	0.0295	800	70	2.5	36.9	1030	10.9	5	18.8	120
Rosebery	ROS	RMN	250R	880.8	880.9	D1394779	4.54	1.88	13	2.55	11.6	0.1	2.6	1.89	30.6	0.56	0.108	500	70	2.2	25.4	400	7.5	7	22.9	77.6
Rosebery	ROS	RMN	250R	889.8	889.9	D1394780	3.98	14.55	16	1.9	9.44	0.12	1.8	1.78	26.2	0.5	0.166	1500	480	11	8.6	1770	2.7	35	20.6	66.6
Rosebery	ROS	RMN	250R	899.4	899.5	D1394781	3.92	16.55	14	1.59	9.05	0.1	1.7	1.51	24.6	0.35	0.148	5100	280	12.8	7.5	1770	2.2	31	21.2	62.4
Rosebery	ROS	RMN	250R	910	910.1	D1394782	4.08	5.05	21	3.15	9.46	0.1	2.3	1.7	31.2	0.92	0.0892	700	250	6.1	12.9	1540	3.8	45	18.2	82
Rosebery	ROS	RMN	250R	920	920.1	D1394783	6.92	4.35	81	3.64	17.85	0.12	3.6	3.04	31.9	1.31	0.15	1100	550	14.9	12.9	3170	3.5	110	17.5	132.5

Appendix 4A

Rosebery Mine host stratigraphy including the Marianoak Formation

Project_Des	Project	Prospect	Hole_ID	Depth_From	Depth_To	SAMPLE_TA	Al_pct	Ca_pct	Cr_ppm	Fe_pct	Ga_ppm	Ge_ppm	Hf_ppm	K_pct	La_ppm	Mg_pct	Mn_pct	Na_ppm	P_ppm	Sc_ppm	Th_ppm	Ti_ppm	U_ppm	V_ppm	Y_ppm	Zr_ppm
Rosebery	ROS	RMN	250R	929.8	929.9	D1394784	6.45	3.94	89	4.41	16.4	0.13	3.6	2.86	37	1.28	0.144	900	400	15.6	13.4	4160	3.6	103	20	134
Rosebery	ROS	RMN	250R	940	940.1	D1394785	6.61	2.95	59	4.52	16.35	0.12	3.1	2.94	36.2	1.33	0.19	900	250	13.9	13.5	2780	3.8	81	14.1	116
Rosebery	ROS	RMN	250R	950	950.1	D1394786	7.86	0.93	93	4.65	21.3	0.19	3.9	3.29	28.8	1.43	0.0759	1900	360	18.1	12	2800	3.7	107	12.7	148
Rosebery	ROS	RMN	337R	940	940.1	D1801711	6.18	0.62	2	4.25	18.35	0.26	4.2	3.01	46.7	0.55	0.69	6400	210	4.9	16.6	1530	4.6	28	11.4	155.5
Rosebery	ROS	RMN	337R	950	950.1	D1801712	6.52	1.02	2	3.26	18.3	0.3	5	1.58	74.6	0.48	0.0924	25200	220	5.5	17.4	1430	4.7	17	14.9	186.5
Rosebery	ROS	RMN	337R	960	960.1	D1801713	5.21	4.49	1	1.58	13.1	0.17	4.4	2.81	23.6	0.49	0.19	600	120	3.9	19.5	1050	4.7	3	21.2	149
Rosebery	ROS	RMN	337R	970	970.1	D1801714	5.35	1.87	2	2.24	15.45	0.54	4.9	2.14	130	0.71	0.118	6700	160	5.5	18.5	1400	4.3	7	32.2	186
Rosebery	ROS	RMN	337R	980	980.1	D1801715	5.09	2.9	2	1.6	12.45	0.11	4.1	1.72	12.9	0.5	0.136	12400	180	5.3	16.2	1500	3.2	8	23.7	152.5
Rosebery	ROS	RMN	337R	990	990.1	D1801716	5.82	1.45	3	1.53	14.45	0.19	3.5	1.71	30.2	0.45	0.0813	19300	160	7	15.1	1630	3.3	11	20.1	118
Rosebery	ROS	RMN	337R	1000	1000.1	D1801717	6.03	2.66	5	1.95	13.95	0.19	2.1	1.76	38.1	0.59	0.149	19200	260	7.2	8.9	1680	2	27	12.7	74
Rosebery	ROS	RMN	337R	1010	1010.1	D1801718	6.07	0.71	8	1.27	15.2	0.25	4	1.88	49	0.33	0.0725	28300	240	8.9	13.6	2170	3.8	15	22.6	141.5
Rosebery	ROS	RMN	337R	1020	1020.1	D1801719	7.05	0.68	20	1.91	16.85	0.26	4.6	2.14	53	0.56	0.0666	26000	330	9.8	15.7	2280	4.2	18	27	163
Rosebery	ROS	RMN	337R	1029.4	1029.5	D1801720	7.26	0.84	3	2.5	18.75	0.25	3.8	2.58	38.4	0.71	0.105	22400	210	9	12.7	1950	3.9	15	13	134.5
Rosebery	ROS	RMN	337R	1040	1040.1	D1801721	7.1	0.75	14	2.55	20.5	0.27	5	2.35	46.6	0.8	0.0902	21600	290	9.9	16.9	2210	4.7	18	29.7	179
Rosebery	ROS	RMN	337R	1050	1050.1	D1801722	6.9	0.35	3	1.69	17.9	0.32	6.1	3.75	69.5	0.54	0.0617	9800	100	5.2	26.7	1480	6.7	5	35.9	208
Rosebery	ROS	RMN	337R	1060	1060.2	D1801723	5.73	4.04	89	3.27	16.75	0.2	2.9	2.27	26.9	1.08	0.224	6300	400	18.6	10.6	3180	4.6	152	31.1	111
Rosebery	ROS	RMN	337R	1069.8	1069.9	D1801724	7.35	1	5	3.23	19.8	0.28	4.2	2.74	37.8	1.03	0.112	15100	530	15.1	12.6	3510	3.8	43	35.6	152.5
Rosebery	ROS	RMN	337R	1079.5	1079.7	D1801725	5.84	4.27	102	3.94	16.55	0.21	2.9	2.5	29.2	1.75	0.178	1300	640	17.3	10.5	2890	4.5	161	23.6	107.5
Rosebery	ROS	RMN	337R	1090	1090.1	D1801726	6.7	3.22	4	2.77	17.5	0.25	3.6	1.54	38.1	0.87	0.171	24500	500	14.7	12.1	3330	3.2	41	34.5	125.5
Rosebery	ROS	RMN	337R	1100	1100.1	D1801727	6.78	0.79	3	3.33	22.6	0.25	4.8	1.99	30.4	0.98	0.108	28600	590	14.7	11	3970	3.9	51	29.3	180
Rosebery	ROS	RMN	337R	1110.1	1110.2	D1801728	7.52	1.33	5	2.53	19.15	0.26	4.3	1.36	48	0.63	0.111	34900	510	15.1	15.9	3470	4	38	38.2	161
Rosebery	ROS	RMN	337R	1120.1	1120.2	D1801729	6.37	2.55	5	2.3	17.65	0.23	3.5	1.53	32.6	0.63	0.137	25300	440	13.6	12	3050	3	39	31.4	121.5
Rosebery	ROS	RMN	337R	1130	1130.1	D1801730	6.68	1.18	8	1.82	20.9	0.4	6.2	4.06	96.4	0.55	0.0726	10600	140	7	27.5	1690	6.8	14	44.6	210
Rosebery	ROS	RMN	337R	1141.3	1141.4	D1801731	7.17	0.37	18	1.73	21	0.27	4.6	3.39	34.9	0.4	0.0437	28200	380	11.6	13.5	2420	4.5	31	11.2	168.5
Rosebery	ROS	RMN	337R	1150	1150.1	D1801732	6.44	0.63	3	1.33	14.45	0.23	5.2	1.99	53.7	0.26	0.0512	31000	130	5.7	19.7	1510	5	9	23.3	191
Rosebery	ROS	RMN	337R	1160	1160.1	D1801733	6.49	0.34	3	1.63	15.1	0.16	5.2	1.97	31.9	0.35	0.0435	27000	120	6.4	19.6	1540	5.3	10	22	187
Rosebery	ROS	RMN	337R	1170	1170.1	D1801734	7.83	0.12	3	1.14	19.2	0.25	5.1	4.06	61.7	1.13	0.0325	6900	100	3.7	38.1	1160	10	8	28.1	148
Rosebery	ROS	RMN	337R	1180.7	1180.8	D1801735	4.82	0.27	5	1.36	12	0.23	3.1	1.72	60.4	0.84	0.0393	8600	50	2.6	24.6	710	9.2	5	20	81.1
Rosebery	ROS	RMN	337R	1190	1190.1	D1801736	5.96	0.54	4	1.13	15.85	0.23	4.1	1.58	59.1	0.65	0.0278	24100	80	3.2	29.5	1000	7.5	9	22.2	116.5
Rosebery	ROS	RMN	337R	1200	1200.1	D1801737	6.1	1.24	4	1.11	14.8	0.24	3.7	1.6	63.9	0.62	0.0283	21300	60	3.3	30.5	890	7.4	7	18.1	104.5
Rosebery	ROS	RMN	337R	1210.1	1210.2	D1801738	7.22	1.19	6	1.35	17.85	0.16	4.5	3.23	37.9	0.72	0.0341	8500	190	4.6	34.8	1230	9.8	16	14.2	130
Rosebery	ROS	RMN	337R	1220	1220.1	D1801739	5.3	2.99	92	5.29	16.15	0.2	2.4	1.57	25.8	2.43	0.102	2700	870	16.8	10.6	2160	2.7	102	10.4	92.4
Rosebery	ROS	RMN	337R	1230	1230.1	D1801740	5.86	2.13	116	5.93	17.2	0.22	2.7	1.58	25.5	1.81	0.0477	7200	750	19	10.6	1950	2.6	124	10.3	99.8
Rosebery	ROS	RMN	337R	1240	1240.2	D1801741	6.15	1.47	14	1.34	15.5	0.18	4	2.17	41.7	0.58	0.067	15400	130	4.2	25.6	1190	5.8	23	14.3	138.5
Rosebery	ROS	RMN	337R	1250	1250.2	D1801742	7.33	0.85	38	3.53	20	0.26	5.1	2.42	33	1.62	0.279	7700	590	10.8	15.7	3110	6.5	91	25.1	194
Rosebery	ROS	RMN	337R	1260	1260.2	D1801743	9.25	2.49	14	2.87	23.7	0.23	5.1	2.03	25.6	0.85	0.0867	28700	580	14.6	9.5	2840	8	58	18.6	186
Rosebery	ROS	RMN	337R	1270	1270.2	D1801744	7.65	11.05	5	2.02	16.25	0.19	2.4	0.77	28.8	0.57	0.297	30300	650	13	6.6	2850	14.8	58	23.3	87.9
Rosebery	ROS	RMN	337R	1280	1280.2	D1801745	8.19	1.39	3	2	22.2	0.31	6.6	1.61	51.1	0.92	0.0865	32700	630	13.6	15.8	3100	6.1	45	32.8	250
Rosebery	ROS	RMN	337R	1290	1290.2	D1801746	6.31	1.67	2	1.15	16.55	0.31	4.5	2.39	68.9	0.63	0.244	7300	170	4.5	19.2	1590	5	8	30.8	165.5
Rosebery	ROS	RMN	337R	1300	1300.1	D1801747	6.12	1.41	2	1.03	16.65	0.24	4.5	3.02	46.8	0.26	0.24	2700	150	4	18.4	1470	4.5	6	23.7	159
Rosebery	ROS	RMN	337R	1310	1310.1	D1801748	6.89	0.57	3	0.95	18.8	0.26	5.3	4.02	50.4	0.35	0.0721	2100	200	5	20.7	1920	6.1	9	24.4	193
Rosebery	ROS	RMN	337R	1320	1320.1	D1801749	8.42	0.77	3	1.35	22.7	0.32	6.5	4.71	59.8	0.71	0.0638	10400	220	6.2	26.8	2400	7	11	25.9	230
Rosebery	ROS	RMN	337R	1331.6	1331.7	D1801750	6.71	1.08	4	1.57	17.1	0.27	4.8	3.37	59.3	0.43	0.171	13500	170	4.6	21.7	1700	5.5	8	20	175
Rosebery	ROS	RMN	337R	1340	1340.1	D1801751	5.8	1.45	3	1.39	14.45	0.23	4.1	3.53	40.7	0.34	0.42	8100	170	3.9	17.2	1430	4.2	7	16.2	150.5
Rosebery	ROS	RMN	337R	1350	1350.1	D1801752	6.41	2.28	2	1.45	16.25	0.18	4.9	4.46	36.1	0.42	0.269	3800	160	4.5	19.1	1770	4.8	8	19.8	176.5
Rosebery	ROS	RMN	337R	1359.1	1359.2	D1801753	7.29	1.1	2	1.67	17.8	0.25	5.5	4.84	61.8	0.49	0.089	6700	180	5.1	23.4	1930	6.1	8	19.1	195.5
Rosebery	ROS	RMN	337R	1369.1	1369.2	D1801754	7.12	0.43	3	1.22	15.4	0.21	5.1	2.58	58.7	0.21	0.0388	29900	190	4.6	20.9	1820	5.6	7	20.5	181.5
Rosebery	ROS	RMN	337R	1380.2	1380.3	D1801755	6.25	3.58	1	2.59	15.45	0.2	4.7	2.64	36.7	0.9	0.129	13900	170	4	17.6	1730	5.4	7	20.5	173.5
Rosebery	ROS	RMN	337R	1390	1390.1	D1801756	6.78	1.6	4	1.62	15.6	0.2	5	2.44	42.9	0.44	0.0681	27200	180	4.7	19.7	1790	5	8	23.7	178
Rosebery	ROS	RMN	337R	1400	1400.1	D1801757	7.04	0.34	5	1.35	12.95	0.15	4.6	1.26	41.8	0.26	0.0204	42600	190	4.4	21.6	1740	3.9	7	17.4	166
Rosebery	ROS	RMN	337R	1410	1410.1	D1801758	5.94	0.85	3	1.4	12.85	0.14	4	1.4	39.9	0.31	0.045	33300	180	3.6	17.4	1370	5.3	7	16.9	147.5
Rosebery	ROS	RMN	337R	1420	1420.1	D1801759	5.55	0.11	5	1.22	10.7	0.13	3.4	2.17	29.7	0.21	0.0139	26000	160	3.3	15.9	1290	3.8	6	12.1	114
Rosebery	ROS	RMN	337R	1429.1	1429.2	D1801760	6.22	0.12	6	1.5	14.65	0.17	4	3.3	38.2	0.29	0.0155	21000	180	4.5	19.1	1450	3.6	7	14.7	147.5
Rosebery	ROS	RMN	337R	1440	1440.1	D1801761	5.91	0.22	5	1.19	11.3	0.16	3.9	2.43	36.9	0.23	0.0196	27400	170	3.6	18	1500	4.7	6	14.5	136.5
Rosebery	ROS	RMN	337R	1450	1450.1	D1801762	5.74	1.47	4	1.38	13.15	0.2	3.7	2	41.9	0.31	0.0669	22200	180	3.8	16.2	1350	3.9	8	15.4	133.5
Rosebery	ROS	RMN	337R	1460	1460.1	D1394414	6.49	1.05	7	1.75	16.75	0.17	5.2	2.14	64.2	0.52	0.0805	26700	230	5.2	25.2	1910	5.8	15	20.7	181
Rosebery	ROS	RMN	337R	1470	1470.1	D1394415	7.04	0.77	7	1.92	17.75	0.16	4.7	4.03	49.5	0.51	0.0402	17900	200	4.7	23.4	2100	6	9	21	163
Rosebery	ROS	RMN	337R	1480	1480.1	D1394416	6.42	0.54	11	1.76	14.35	0.14	3.9	1.5	39.6	0.31	0.0321	34200	190	4.2	19.3	1680	4.2	8	15.6	132.5

Appendix 4A

Rosebery Mine host stratigraphy including the Marianoak Formation

Project_Des	Project	Prospect	Hole_ID	Depth_From	Depth_To	SAMPLE_TA	Al_pct	Ca_pct	Cr_ppm	Fe_pct	Ga_ppm	Ge_ppm	Hf_ppm	K_pct	La_ppm	Mg_pct	Mn_pct	Na_ppm	P_ppm	Sc_ppm	Th_ppm	Ti_ppm	U_ppm	V_ppm	Y_ppm	Zr_ppm
Rosebery	ROS	RMN	337R	1490	1490.1	D1394417	5.7	1.77	5	1.41	11.1	0.11	3.7	0.95	22.6	0.21	0.101	34800	160	3.6	16.2	1630	4.2	6	17.3	125.5
Rosebery	ROS	RMN	337R	1500	1500.1	D1394418	5.51	1.16	9	2.28	13.25	0.17	3.2	2.37	62.4	0.49	0.326	3600	70	1.8	25.4	700	6.3	2	15.5	95.2
Rosebery	ROS	RMN	337R	1510	1510.1	D1394419	5.48	2.04	35	2.4	13.7	0.14	3.3	2.14	38	0.71	0.0916	7300	290	12.3	15.3	2020	4.6	69	14.6	115.5
Rosebery	ROS	RMN	337R	1520	1520.1	D1394420	8.32	1.82	16	3.01	21.6	0.17	5.3	3.3	53.2	1.13	0.063	4600	220	8.2	34.8	1850	7.7	45	20.4	171.5
Rosebery	ROS	RMN	337R	1530	1530.1	D1394421	7.77	2.53	26	2.4	21.7	0.16	5.4	3.28	47.6	0.97	0.14	8000	370	10.4	25.2	2720	6.5	70	21.4	186
Rosebery	ROS	RMN	337R	1540	1540.1	D1394422	5.74	5.69	18	3.07	13.65	0.16	4	1.15	41.9	0.72	0.116	13700	380	11.4	16.7	2170	5.2	59	18.6	144.5
Rosebery	ROS	RMN	337R	1550	1550.1	D1394423	7.24	0.84	14	2.5	19.95	0.15	5.7	1.96	42.5	0.66	0.0311	13900	400	9.3	24.6	2630	7.2	69	19.1	193
Rosebery	ROS	RMN	337R	1560	1560.1	D1394424	8.3	0.11	8	2.02	20.5	0.16	5.2	2.8	67.9	0.71	0.0142	7800	130	3.8	38	1380	9.4	14	18.7	170.5
Rosebery	ROS	RMN	337R	1570	1570.1	D1394425	4.49	1.14	95	3.18	12.05	0.13	2.3	0.71	35.6	0.78	0.0342	12100	390	13	9	2250	2.7	81	13.4	87.4
Rosebery	ROS	RMN	337R	1580	1580.1	D1394426	7.97	0.76	23	2.86	23.9	0.17	5.7	1.85	37	1.13	0.0326	15200	300	16.9	32.4	1780	17.6	78	24.8	166
Rosebery	ROS	RMN	337R	1590	1590.2	D1394427	8.46	2.17	154	6.53	20.1	0.21	5.3	1.68	48.3	0.8	0.0323	18500	1240	46.5	16.5	3620	8.4	237	17	194.5
Rosebery	ROS	RMN	337R	1600	1600.1	D1394428	7.83	2.01	85	3.52	19.1	0.16	4.5	1.28	43.2	0.6	0.047	25800	500	21.7	13.2	3190	9.7	112	18.8	161.5
Rosebery	ROS	RMN	337R	1610	1610.1	D1394429	8.07	0.61	114	2.93	22	0.15	4.3	1.48	30.3	0.82	0.0166	27300	750	19.5	12.2	3190	11.4	137	14.3	150.5
Rosebery	ROS	RMN	337R	1620	1620.1	D1394430	8.1	1.05	14	3.33	21.1	0.21	7.1	1.95	57.3	0.93	0.0441	18400	660	25.7	20.1	3980	5.8	149	28.3	271
Rosebery	ROS	RMN	337R	1630	1630.1	D1394431	7.74	2.46	7	4.15	22.3	0.17	7.5	3.26	35.6	0.58	0.45	1800	680	16.1	16.3	4130	4.1	113	31.9	280
Rosebery	ROS	RMN	337R	1640	1640.1	D1394432	7.95	1.56	9	4.16	21.2	0.19	7.6	3.47	46.8	0.33	0.954	9300	600	13.8	18.8	4080	4.8	99	22.5	279
Rosebery	ROS	RMN	337R	1650	1650.1	D1394433	6.93	0.46	6	11.95	19.05	0.24	6.5	3.17	42.4	0.49	0.237	500	430	14.8	15.8	2890	4.3	62	29.3	247
Rosebery	ROS	RMN	337R	1660	1660.1	D1394434	7.1	2.61	56	3.16	18.35	0.14	5.4	3.28	33.6	0.39	0.311	2600	570	14.8	16.1	3670	3.9	120	18.8	196
Rosebery	ROS	RMN	337R	1670	1670.1	D1394435	4.9	3	13	1.92	13.55	0.15	4.9	2.4	34.1	0.31	0.384	500	280	10.2	13.3	1870	3.1	55	23.1	177.5
Rosebery	ROS	RMN	337R	1680	1680.1	D1394436	9.98	0.98	73	4.09	26.7	0.29	8.1	4.94	84.3	0.47	0.139	900	990	31.5	26.1	5070	6.6	208	27.2	292
Rosebery	ROS	RMN	337R	1690	1690.1	D1394437	5.65	1.17	5	1.49	16.2	0.15	3.8	2.81	36.3	0.19	0.303	2200	50	3.6	30.9	440	8.5	11	21.5	93.2
Rosebery	ROS	RMN	337R	1700	1700.1	D1394438	6.68	0.88	13	1.75	18.3	0.19	5.1	3.61	73	0.26	0.201	400	90	4.3	32.4	990	7.4	10	25	168
Rosebery	ROS	RMN	337R	1710	1710.1	D1394439	6.63	1.32	3	1.36	18.25	0.18	4.9	3.61	77	0.23	0.0897	1300	90	3.3	39.4	970	7.7	10	24.5	147
Rosebery	ROS	RMN	337R	1720	1720.1	D1394440	6.28	3.45	69	2.46	16.05	0.21	4.4	2.65	75	0.86	0.15	2000	520	11.4	25.5	2260	5.8	76	19.7	145
Rosebery	ROS	RMN	337R	1730	1730.1	D1394441	5.33	2.1	8	3.58	14.05	0.16	3.5	1.34	58.6	1.19	0.0547	4200	80	4.5	30.8	750	7.8	36	21.6	111.5
Rosebery	ROS	RMN	337R	1740	1740.1	D1394442	6.93	1.7	29	1.72	17.4	0.16	4.4	1.81	51.3	0.82	0.0506	18700	290	5	34.2	1640	8.4	46	21.1	128
Rosebery	ROS	RMN	337R	1750	1750.1	D1394443	7.34	0.37	8	1.47	18.75	0.18	6	1.4	78.2	0.42	0.037	31600	100	4.7	37	1180	9.2	13	25.1	208
Rosebery	ROS	RMN	397R	1100	1100.2	D1395368	6.58	2.39	4	2.8	15	0.23	4.8	2.74	45.4	0.6	0.154	16100	500	9.9	15.4	2580	3.9	63	19.2	182
Rosebery	ROS	RMN	397R	1110	1110.2	D1395369	6.22	1.25	6	2.64	14.75	0.3	4.7	3.35	89.3	0.44	0.418	500	500	5.1	18.3	1700	5	18	14.8	158.5
Rosebery	ROS	RMN	397R	1120	1120.2	D1395370	5.73	1.27	2	3.41	13.3	0.25	3.6	3.1	52	0.53	0.284	900	190	4.1	15	1360	6	8	13.9	115
Rosebery	ROS	RMN	397R	1130	1130.2	D1395371	6.99	1.21	3	2.36	16.7	0.27	4.6	3.65	72.4	0.54	0.281	3400	220	5.9	18.5	1590	6.5	16	18.2	140.5
Rosebery	ROS	RMN	397R	1140	1140.2	D1395372	6.64	1.03	1	4.71	16.95	0.41	4.2	2.04	122.5	0.9	0.063	18100	320	7.9	16.6	1610	5.1	21	27.9	131
Rosebery	ROS	RMN	397R	1150	1150.2	D1395373	7.47	1.02	131	8.71	24.2	0.39	2.1	1.78	18.8	3.49	0.168	20900	310	21.3	3.7	2840	1.8	97	10.4	72.3
Rosebery	ROS	RMN	397R	1160	1160.2	D1395374	8.02	1.01	61	6.89	25.6	0.42	2.4	2.57	91.5	2.49	0.128	19000	380	24.1	8.2	2920	2.1	117	30.7	89.7
Rosebery	ROS	RMN	397R	1170	1170.2	D1395375	7.04	4.01	40	6.11	13.85	0.28	2.2	0.86	22.7	2.7	0.192	21800	320	21.1	6.5	2650	2	149	26.6	76.8
Rosebery	ROS	RMN	397R	1180	1180.2	D1395376	7.34	3.24	39	5.92	13.9	0.24	2.6	0.67	20.2	2.54	0.231	27600	320	21.5	7.7	2710	2.2	136	35.1	92
Rosebery	ROS	RMN	397R	1190	1190.2	D1395377	7.46	1.61	47	9.14	16.75	0.32	2.2	0.27	24.1	2.72	0.241	24200	340	22.1	7.2	2760	2.4	140	31.2	79.1
Rosebery	ROS	RMN	397R	1200	1200.2	D1395378	6.83	2.36	38	7.39	24	0.24	3.3	0.56	13.2	2.01	0.168	26700	290	16.6	7.7	2440	3.5	107	31.2	118
Rosebery	ROS	RMN	397R	1210	1210.2	D1395379	7.34	1.16	20	5.07	20	0.28	5.4	2.21	37.9	1.39	0.091	15700	220	13.2	15.1	1820	4	57	21.8	196.5
Rosebery	ROS	RMN	397R	1220	1220.2	D1395380	6.56	0.35	4	1.74	13.7	0.14	2.5	3.18	4.3	0.35	0.178	4600	100	6.3	20	1890	2.9	13	6.7	76.1
Rosebery	ROS	RMN	397R	1230	1230.2	D1395381	8.94	0.69	15	3.6	21.8	0.2	2.4	4.86	6	0.6	0.138	1300	20	6.9	88.6	5320	9.2	16	20.3	66.3
Rosebery	ROS	RMN	397R	1240	1240.2	D1395382	8.71	1.07	5	6.98	20.4	0.38	1.8	3.18	17.8	1.74	0.152	13400	270	28.3	6.2	3890	1.9	125	12.6	63.7
Rosebery	ROS	RMN	397R	1250	1250.2	D1395383	6.49	3.14	19	2.22	16.15	0.2	3.8	2.17	44.8	0.48	0.176	14700	290	10.5	13.3	2120	3.5	35	17.9	131
Rosebery	ROS	RMN	397R	1260	1260.2	D1395384	5	11.15	1	3.3	11.25	0.15	2.5	0.91	25.6	1.5	0.432	13000	290	6	11.4	1410	2.8	30	15.7	91
Rosebery	ROS	RMN	397R	1270	1270.2	D1395385	7.78	1.85	3	2.54	19.2	0.24	4	1.45	62.6	0.51	0.273	40300	540	14.6	13	3200	3.1	48	23.3	138.5
Rosebery	ROS	RMN	397R	1280	1280.2	D1395386	6.68	1.26	4	2.19	16.25	0.22	4.1	1.96	49.9	0.53	0.191	20100	360	10.4	15.4	2980	3.8	26	21.3	139
Rosebery	ROS	RMN	397R	1290	1290.2	D1395387	6.87	1.89	3	1.41	17.35	0.2	4.7	1.89	50.3	0.47	0.0945	22100	220	8.9	17.1	2220	4.3	13	32.9	150.5
Rosebery	ROS	RMN	397R	1300	1300.2	D1395388	6.97	1.44	3	1.45	15.5	0.2	4.6	1.38	50.8	0.37	0.0702	28900	190	8.2	17.1	1960	4.3	12	33.2	147
Rosebery	ROS	RMN	397R	1310	1310.2	D1395389	5.79	0.79	2	0.94	10.85	0.11	5	1.5	20.1	0.37	0.0592	18600	120	5.1	17.1	1420	4.3	9	19.6	166.5
Rosebery	ROS	RMN	397R	1320	1320.2	D1395390	6.69	0.29	2	2.99	15.85	0.34	4.9	1.64	149.5	1.53	0.117	12500	130	5.6	17.4	1440	4.6	11	39.6	165.5
Rosebery	ROS	RMN	397R	1330	1330.2	D1395391	6.72	0.39	2	1.62	15.45	0.18	5.3	2.04	50.9	0.87	0.0654	14000	140	6.6	18.9	1670	5.6	12	33.8	178.5
Rosebery	ROS	RMN	397R	1340	1340.2	D1395392	7.57	3.06	2	2.01	17.6	0.18	3.4	2.41	36.8	0.47	0.159	17100	300	8.9	13.4	1980	3.1	27	22.8	108.5
Rosebery	ROS	RMN	397R	1350	1350.2	D1395393	7.22	0.86	3	1.19	15.45	0.15	3	2.07	37.1	0.34	0.0424	21600	340	12	13.3	1930	3.3	32	39.8	99.2
Rosebery	ROS	RMN	397R	1360	1360.2	D1395394	8.66	0.92	2	3.1	25.6	0.23	7.5	3.75	41	1.18	0.0983	12900	230	8.1	17.7	1720	10.2	12	35.4	260
Rosebery	ROS	RMN	397R	1370	1370.2	D1395395	7.78	1.57	2	2.17	18.05	0.18	3.7	2.21	28.2	0.62	0.0984	21000	290	9.6	14.6	2230	3.9	28	24.6	120
Rosebery	ROS	RMN	397R	1380	1380.2	D1395396	7.98	1.08	4	3.66	20.5	0.26	5.2	2.28	41.9	1.05	0.115	21100	450	13.3	20.2	3330	5.8	51	27.3	172

Appendix 4A

Rosebery Mine host stratigraphy including the Marianoak Formation

Project_Des	Project	Prospect	Hole_ID	Depth_From	Depth_To	SAMPLE_TA	Al_pct	Ca_pct	Cr_ppm	Fe_pct	Ga_ppm	Ge_ppm	Hf_ppm	K_pct	La_ppm	Mg_pct	Mn_pct	Na_ppm	P_ppm	Sc_ppm	Th_ppm	Ti_ppm	U_ppm	V_ppm	Y_ppm	Zr_ppm
Rosebery	ROS	RMN	397R	1390	1390.2	D1395397	6.62	3.93	128	4.2	17.45	0.2	2.9	2.77	26.6	1.79	0.142	800	800	19.8	10.6	2750	3.4	127	11.2	102
Rosebery	ROS	RMN	397R	1400	1400.2	D1395398	6.94	1.67	3	3.01	19	0.27	4.4	2.52	64.4	0.88	0.103	15600	500	13.3	13.2	3130	3.6	42	20	150
Rosebery	ROS	RMN	397R	1410	1410.2	D1395399	6.97	0.85	4	2.76	17.45	0.25	4.2	1.79	33.9	0.64	0.0779	26900	490	13.4	11.4	3170	3.5	39	18.1	145
Rosebery	ROS	RMN	397R	1420	1420.2	D1395401	6.89	0.86	1	1.52	17.5	0.21	5.5	2.71	68.5	0.44	0.0794	16400	160	7.2	21.8	2000	5.3	8	20.3	175.5
Rosebery	ROS	RMN	397R	1430	1430.2	D1395402	5.59	1.92	77	2.95	15.9	0.18	3	2.64	26.9	0.74	0.214	6400	340	16.4	9.9	2560	3.2	170	10.3	104.5
Rosebery	ROS	RMN	397R	1440	1440.2	D1395403	6.62	0.5	3	1.35	15.3	0.18	5.4	1.91	47.8	0.27	0.0555	27100	130	6.4	18.8	1640	4.8	11	17	184.5
Rosebery	ROS	RMN	397R	1450	1450.2	D1395404	6.67	0.72	3	1.33	15.2	0.17	5.5	2.25	48.5	0.33	0.0686	22600	120	6.2	18.7	1630	4.9	11	18.5	183.5
Rosebery	ROS	RMN	397R	1460	1460.2	D1395405	7.32	0.93	3	1.9	16.6	0.19	3.3	2.3	38.1	0.32	0.0629	22700	280	7.3	13.8	2150	3.6	25	13.7	105
Rosebery	ROS	RMN	397R	1470	1470.2	D1395406	6.77	0.37	3	1.53	15.7	0.18	4	2.63	68.8	0.9	0.0597	10600	80	3	30.4	1020	8.7	8	14.2	112
Rosebery	ROS	RMN	397R	1480	1480.2	D1395407	6.1	1.39	1	1.32	14	0.18	4.9	3.24	48.6	0.74	0.434	700	90	2.8	20.3	1330	5.2	4	16.1	164.5
Rosebery	ROS	RMN	397R	1490	1490.2	D1395408	5.57	1.8	-1	1	13.65	0.16	4.5	2.79	44.2	0.41	1.59	800	70	2.2	19	1150	4.9	2	18.1	149.5
Rosebery	ROS	RMN	397R	1500	1500.2	D1395409	4.16	1	1	1.51	9.52	0.15	3	2.1	30.1	0.3	0.304	500	70	2.1	13	950	3.3	3	13.2	101
Rosebery	ROS	RMN	397R	1510	1510.2	D1395410	6.13	1.94	-1	1.14	14.25	0.2	4.5	3.24	53.3	0.4	0.67	600	130	3.5	18.9	1580	4.7	5	23.2	148.5
Rosebery	ROS	RMN	397R	1520	1520.2	D1395411	6.67	1.92	1	1.38	16.1	0.19	4.8	3.7	49.6	0.46	0.831	500	160	4.2	19.5	1730	5	7	22.3	157
Rosebery	ROS	RMN	397R	1530	1530.2	D1395412	6.48	2.63	1	1.46	15.1	0.16	4.6	3.72	39.2	0.56	0.833	300	160	3.9	18.8	1720	4.9	6	19	151.5
Rosebery	ROS	RMN	397R	1560	1560.2	D1395415	6.66	2.81	2	2.55	14.95	0.22	4.7	3.22	54.3	0.84	0.359	700	170	4	19.5	1600	5.2	7	23.5	158.5
Rosebery	ROS	RMN	397R	1570	1570.2	D1395416	6.72	1.6	2	1.35	15.2	0.14	4.4	2.82	45.1	0.32	0.255	10600	180	3.8	19.2	1700	4.3	8	15.8	148
Rosebery	ROS	RMN	397R	1580	1580.2	D1395417	6.57	2.64	2	1.53	14.95	0.14	4.4	3.29	38.8	0.45	0.256	7000	170	3.7	18.9	1700	4.3	9	16.4	144.5
Rosebery	ROS	RMN	397R	1590	1590.2	D1395418	8.26	0.5	2	2.52	20.4	0.19	5.6	3.74	53	2.19	0.0445	4700	190	4.3	24	1840	6.2	9	23.6	186.5
Rosebery	ROS	RMN	397R	1600	1600.2	D1395419	6.33	1.03	2	1.54	13.9	0.12	4.3	2.08	42.1	0.29	0.0668	21900	150	3	20.2	1520	4.6	5	21.7	146.5
Rosebery	ROS	RMN	397R	1610	1610.2	D1395420	6.64	0.83	7	1.64	16	0.16	4.3	4.96	45.7	0.35	0.077	3300	210	4.2	19.6	1820	4.6	10	21	144
Rosebery	ROS	RMN	397R	1620	1620.2	D1395421	6.1	0.99	3	1.57	12.55	0.1	4.2	1.69	22.7	0.17	0.142	25200	220	3.5	18.6	1600	4.4	7	17.7	138
Rosebery	ROS	RMN	397R	1640	1640.2	D1395423	7.5	2.23	42	2.44	20	0.17	6.1	3.19	48.6	0.53	0.174	8300	760	19.7	15.9	3490	3.5	146	23.3	226
Rosebery	ROS	RMN	397R	1650	1650.2	D1395424	6.68	3.61	57	3.76	17.1	0.18	5.2	2.81	47.1	0.84	0.259	5500	920	26.2	13.6	3330	3	150	21.2	195.5
Rosebery	ROS	RMN	397R	1660	1660.2	D1395425	5.88	4.08	24	4.94	15.6	0.19	5.9	2.29	48.8	0.87	0.347	4800	680	27.5	15.5	2530	3.4	160	24.8	223
Rosebery	ROS	RMN	397R	1670	1670.2	D1395426	6.7	2.18	31	3.1	17.2	0.16	5.5	2.92	45.9	0.53	0.246	2000	830	20.6	14.4	3100	3.1	140	20	206
Rosebery	ROS	RMN	397R	1680	1680.2	D1395427	7.8	2.58	43	2.25	22.3	0.15	6.8	3.16	44.5	0.31	0.12	3300	850	13.8	15.6	4620	3.4	145	23.2	247
Rosebery	ROS	RMN	397R	1690	1690.2	D1395428	6.92	2.03	47	4.03	17.45	0.17	5.3	2.14	49.1	0.72	0.0824	3300	730	21.2	14	3640	3.1	150	20.6	203
Rosebery	ROS	RMN	397R	1700	1700.2	D1395429	6.65	2.24	33	5.84	16.9	0.19	5	1.17	45.4	1.03	0.079	4400	540	18.9	14.2	3300	2.8	134	18.1	177
Rosebery	ROS	RMN	397R	1710	1710.2	D1395430	7.48	1.46	33	3.27	19.65	0.18	6.2	2	51.7	0.61	0.0488	5200	990	19.8	16.6	4470	3.3	151	25.9	221
Rosebery	ROS	RMN	397R	1720	1720.2	D1395431	8.18	2.02	35	2.7	22.3	0.15	6.6	2.49	40.8	0.48	0.0589	6800	1240	21	17	5100	3.2	169	24.8	250
Rosebery	ROS	RMN	397R	1730	1730.2	D1395432	8.32	0.59	12	3.57	23.8	0.19	7.6	2.83	42	0.74	0.0651	4100	790	21.1	16	4280	4.1	129	24.4	244
Rosebery	ROS	RMN	397R	1740	1740.2	D1395433	8.64	0.41	26	2.63	25.7	0.2	8.8	3.85	47.7	0.39	0.0193	2800	1150	17.2	19.6	5130	5	158	26.9	314
Rosebery	ROS	RMN	397R	1750	1750.2	D1395434	4.39	6.19	15	5.37	10.8	0.17	4.1	1.47	37.8	2.39	0.462	900	360	31.4	9.8	2000	2.5	117	16.1	151
Rosebery	ROS	RMN	397R	1760	1760.2	D1395435	4.94	2.65	43	9.81	13.05	0.21	3.1	0.59	40.2	1.46	0.224	300	670	47.5	9.6	2550	1.7	302	16.2	121
Rosebery	ROS	RMN	397R	1770	1770.2	D1395436	6.49	5.17	20	3.1	15.9	0.19	5.6	2.85	52.2	1.88	0.23	1400	830	15	14.6	3950	3.1	116	22.6	215
Rosebery	ROS	RMN	397R	1780	1780.2	D1395437	3.72	10.05	5	5.11	8.93	0.13	3	1.58	27.3	3.97	0.32	800	370	10.2	7.4	1810	1.6	56	16.2	110.5
Rosebery	ROS	RMN	397R	1790	1790.2	D1395438	8.68	1.32	9	1.37	23.2	0.17	7	4.05	61.7	0.56	0.046	1700	800	14.8	20.4	5450	4.5	150	26	252
Rosebery	ROS	RMN	397R	1800	1800.2	D1395439	6.83	3.54	8	4.79	16.55	0.17	5.3	2.62	39.4	1.58	0.14	1000	630	21.4	12.7	4190	2.8	139	20	190.5
Rosebery	ROS	RMN	397R	1810	1810.2	D1395440	5.25	3.81	13	3.7	13.55	0.16	4.7	2.21	36.8	1.4	0.298	800	570	17.3	11.3	2770	2.4	119	20	176
Rosebery	ROS	RMN	397R	1820	1820.2	D1395441	5.27	7.2	21	3.41	13.35	0.14	4.6	1.97	41.8	0.52	0.352	700	610	26.3	11.2	2920	2.4	153	17.5	169.5
Rosebery	ROS	RMN	397R	1830	1830.2	D1395442	7.18	5.93	33	5.7	17.95	0.23	5.2	2.77	57.5	1.42	0.419	1000	1010	17	16	3900	3.1	136	18.7	195
Rosebery	ROS	RMN	397R	1840	1840.2	D1395443	4.12	7.14	34	7.9	9.77	0.2	3	1.16	42.8	2.3	0.487	400	610	50.2	8.3	2270	1.7	190	13.3	124
Rosebery	ROS	RMN	397R	1850	1850.2	D1395444	2.13	13	6	4.92	5.17	0.11	2.2	0.98	20.4	5.54	0.439	400	250	7.1	5.6	1130	1.2	49	11.2	84.6
Lake Rosebe	LRO	SRL	411R-D1	1200	1200.2	D1395111	6.98	0.5	11	11.6	29.2	0.76	1.7	4.23	27	2.69	0.149	13400	530	28.4	4.9	3660	2.3	229	11.4	60.3
Lake Rosebe	LRO	SRL	411R-D1	1210	1210.2	D1395112	5.61	1.47	4	1.49	13.35	0.45	4.3	2.01	44.8	0.31	0.11	18000	130	5	18.1	1390	4.4	10	21.4	138
Lake Rosebe	LRO	SRL	411R-D1	1220	1220.2	D1395113	6.22	0.95	3	3.53	16.1	0.36	2.5	3.32	23.8	0.4	0.475	700	250	8.5	12	1670	3.2	27	14.2	81.2
Lake Rosebe	LRO	SRL	411R-D1	1230	1230.2	D1395114	7.31	1.41	4	1.89	17.25	0.37	4	1.57	47.6	0.51	0.0673	36400	500	13.4	15.3	3000	4	38	19.2	130.5
Lake Rosebe	LRO	SRL	411R-D1	1240	1240.2	D1395115	6.12	0.82	6	1.61	15.25	0.29	4.4	1.69	52.3	0.38	0.0551	28100	190	7.2	19.2	1880	4.9	10	21.6	128
Lake Rosebe	LRO	SRL	411R-D1	1250	1250.2	D1395116	6.74	0.97	5	1.39	19.35	0.31	4.5	2.52	54.2	0.33	0.167	24900	200	8.4	19.8	2080	5.1	14	23.8	138
Lake Rosebe	LRO	SRL	411R-D1	1260	1260.2	D1395117	5.76	1.35	4	1.36	15.15	0.26	4.1	1.95	37.6	0.35	0.0935	19900	150	6.9	19	1560	4.6	11	24	125
Lake Rosebe	LRO	SRL	411R-D1	1270	1270.2	D1395118	6.58	1.25	3	1.49	15.7	0.25	5.2	2.07	32.3	0.35	0.0898	23300	140	6.5	20.6	1660	5.4	12	25.1	163
Lake Rosebe	LRO	SRL	411R-D1	1280	1280.2	D1395119	5.46	1.96	3	1.31	12.65	0.25	4.7	1.83	42.8	0.27	0.136	18900	110	5.5	18.3	1380	4.7	8	24	152
Lake Rosebe	LRO	SRL	411R-D1	1290	1290.2	D1395120	5.69	1.75	2	1.67	14.7	0.29	4.3	1.93	50.3	0.28	0.185	18000	130	6.1	16.2	1290	3.9	12	22.9	136
Lake Rosebe	LRO	SRL	411R-D1	1300	1300.2	D1395121	5.94	1.91	3	1.35	14.85	0.27	2.6	2.13	32	0.26	0.14	20300	380	7.1	11.3	1910	2.9	30	14.9	86.3
Lake Rosebe	LRO	SRL	411R-D1	1310	1310.2	D1395122	5.61	2.47	3	1.5	13.1	0.24	3.3	1.48	34.1	0.18	0.158	24900	160	6.6	14.2	1150	3.2	5	15.9	106
Lake Rosebe	LRO	SRL	411R-D1	1320	1320.2	D1395123	5.27	1.12	2	1	12.45	0.21	3.4	1.79	40.7	0.18	0.0682	19200	170	4	16	1210	3.7	8	14.2	116
Lake Rosebe	LRO	SRL	411R-D1	1330	1330.2	D1395124	7.04	1.32	27	2.92	15.4	0.2	3	2.67	37	0.66	0.136	15400	400	7.9	14.3	1910	5.3	80	12.6	95

Appendix 4A

Rosebery Mine host stratigraphy including the Marianoak Formation

Project_Des	Project	Prospect	Hole_ID	Depth_From	Depth_To	SAMPLE_TA	Al_pct	Ca_pct	Cr_ppm	Fe_pct	Ga_ppm	Ge_ppm	Hf_ppm	K_pct	La_ppm	Mg_pct	Mn_pct	Na_ppm	P_ppm	Sc_ppm	Th_ppm	Ti_ppm	U_ppm	V_ppm	Y_ppm	Zr_ppm
Lake Rosebe	LRO	SRL	411R-D1	1350	1350.2	D1395126	6.24	1.13	5	1.7	14.95	0.24	3.8	2	47.7	0.5	0.0832	21200	230	7.3	19.1	1570	4.8	25	16.8	113
Lake Rosebe	LRO	SRL	411R-D1	1360	1360.2	D1395127	6.33	2.64	4	2.15	18.55	0.29	4.1	1.9	46.1	0.56	0.18	29500	440	11.9	13.2	2950	3.1	36	21.2	126.5
Lake Rosebe	LRO	SRL	411R-D1	1370	1370.2	D1395128	6.78	1.26	15	1.68	18.1	0.33	4.6	2.98	60.6	0.42	0.102	17600	240	8.9	20	2180	5	19	26	140.5
Lake Rosebe	LRO	SRL	411R-D1	1410	1410.2	D1395132	6.28	0.8	2	1.51	15.95	0.28	5.2	2.14	53.6	0.27	0.0416	27100	120	6	20.7	1420	5.5	10	27.5	170.5
Lake Rosebe	LRO	SRL	411R-D1	1420	1420.2	D1395133	5.67	1.12	2	1.38	13.35	0.25	4.7	1.84	48.9	0.35	0.144	20900	110	5.2	19.3	1230	4.8	7	21.7	154.5
Lake Rosebe	LRO	SRL	411R-D1	1440	1440.2	D1395134	7.22	0.45	1	1.09	18.9	0.19	4.5	3.08	52.5	1.47	0.0345	3200	140	1.8	27.9	930	9.1	1	14.8	122.5
Lake Rosebe	LRO	SRL	411R-D1	1450	1450.2	D1395135	7.01	0.7	2	0.99	18.7	0.22	4.9	1.86	59.7	1.02	0.0442	8900	70	2.3	29.1	910	9.5	3	18.9	137.5
South Roseb	SRO	BAK	BP272	9	9.2	D1806668	6	0.23	2	0.95	15.85	0.13	3.9	3.88	27.7	0.21	0.0428	800	30	2.1	31.8	370	8	1	20	97.5
South Roseb	SRO	BAK	BP272	24.5	24.7	D1806669	4.15	0.9	4	1.34	7.28	0.13	2.1	0.86	32	0.24	0.0965	21700	20	1.2	17.4	190	5.5	1	18.5	55.6
South Roseb	SRO	BAK	BP272	35.5	35.7	D1806670	5.82	0.03	3	1.15	10.85	0.14	3.5	2.69	35.5	0.15	0.0728	2300	40	1.4	30.2	320	8.7	1	12.4	88.2
South Roseb	SRO	BAK	BP272	45.5	45.7	D1806671	5.16	0.01	3	5.22	15.25	0.15	3.7	2.59	38.6	0.21	0.313	600	60	2.5	31.8	350	6.9	4	17.2	98.8
South Roseb	SRO	BAK	BP272	56.5	56.7	D1806672	4.33	0.01	2	0.8	10.85	0.1	2.3	2.45	23.5	0.27	0.0157	300	30	1.2	19.2	270	4.3	1	13.4	61.2
South Roseb	SRO	BAK	BP272	66.5	66.7	D1806673	5.08	0.42	4	0.93	11.2	0.11	3.3	1.64	29.6	0.26	0.0357	17900	30	1.6	28.1	310	8.5	1	17	85.6
South Roseb	SRO	BAK	BP272	76.5	76.7	D1806674	6.86	1.8	146	3	19.95	0.15	3.8	3.33	35.7	1.25	0.201	1500	630	19.3	12.2	3220	4.1	187	16.8	123
South Roseb	SRO	BAK	BP272	86.5	86.7	D1806675	4.59	0.09	7	2.44	11.3	0.14	2.6	2.42	45.7	0.4	1.015	400	80	3.1	22.2	450	6.8	8	13.3	66.8
South Roseb	SRO	BAK	BP272	96.5	96.7	D1806676	7.02	0.68	2	0.99	20.3	0.13	5.8	2.04	19	0.35	0.0484	32500	20	1.8	46.5	210	15.5	1	26.9	107.5
South Roseb	SRO	BAK	BP272	106.5	106.7	D1806677	5.75	0.65	2	1.16	14.8	0.16	4.9	2.01	57	0.42	0.0597	18300	60	3.3	27.3	770	6.8	5	21.6	153
South Roseb	SRO	BAK	BP272	116.5	116.7	D1806678	7.38	0.26	2	1.94	22.2	0.16	6.1	2.98	45.7	0.78	0.0317	15900	70	4.4	31	1020	7.5	6	22.2	191
South Roseb	SRO	BAK	BP272	126.5	126.7	D1806679	6.05	0.65	2	1.76	16.5	0.17	5.1	2.01	59.2	0.82	0.059	18300	60	3.6	28	810	6.3	5	22.6	160.5
South Roseb	SRO	BAK	BP272	136.5	136.7	D1806680	5.13	0.43	9	1.58	15	0.17	4.2	2.27	60.9	0.55	0.0416	7700	90	3.9	23.1	940	7.1	13	19.4	133
South Roseb	SRO	BAK	BP272	146.5	146.7	D1806681	4.9	0.95	2	1.08	13.65	0.18	3.4	2.47	45.2	0.61	0.052	5500	50	1.7	27.8	360	7.8	2	19.3	90.2
South Roseb	SRO	BAK	BP272	156.5	156.7	D1806682	6.13	0.53	3	2.55	18.05	0.18	4.2	3.44	76.7	0.77	0.575	400	70	3.8	40.8	710	8.9	11	25.8	128.5
South Roseb	SRO	BAK	BP272	166.5	166.7	D1806683	6.37	2.36	85	4.36	18.4	0.23	5.6	3.4	57.1	1.13	0.483	400	830	15.4	22.5	2820	5.4	111	23.5	198.5
South Roseb	SRO	BAK	BP272	176.5	176.7	D1806684	6.81	2.64	41	3.09	17.1	0.17	5.4	2.21	50.7	0.71	0.0687	11400	800	16.4	14.8	3600	3.3	124	24.8	196
South Roseb	SRO	BAK	BP272	186.5	186.7	D1806685	6.5	0.3	108	5.87	18.7	0.15	3	2.9	30.6	1.15	0.827	1600	750	20.5	12.2	2660	3.4	124	14.4	106.5
South Roseb	SRO	BAK	BP272	196.5	196.7	D1806686	6.35	1.35	77	3.67	17.65	0.2	4.1	2.74	56.8	1.16	0.0639	1600	760	17.4	17.1	2810	4.3	97	15.5	143.5
South Roseb	SRO	BAK	BP272	206.5	206.7	D1806687	4.46	3.53	75	7.21	12.9	0.12	2.2	1.41	21.8	1.72	1.47	2300	480	14	8.6	2010	2.6	93	16.1	78.6
South Roseb	SRO	BAK	BP272	216.5	216.7	D1806688	7.37	1.7	56	3.11	19.25	0.22	6.4	3.35	69.1	1.11	0.0794	1900	680	16.7	26.6	3000	6.4	92	26.8	234
South Roseb	SRO	BAK	BP272	227	227.2	D1806689	6.32	1.43	6	2.85	16.75	0.16	5.7	1.94	40.6	0.95	0.118	13800	620	16	14	3370	3.4	123	19.8	198
South Roseb	SRO	BAK	BP272	237	237.2	D1806690	6.02	0.93	102	4.39	17.7	0.15	3	2.15	29.2	1.58	0.0577	3000	640	20.3	12.1	3090	3.1	178	13.5	106.5
South Roseb	SRO	BAK	BP272	247	247.2	D1806691	6.31	1.25	106	4.37	18.2	0.16	3.2	2.36	34.2	1.46	0.05	3600	660	20.9	12.6	3020	3.2	162	13.2	110.5
South Roseb	SRO	BAK	BP272	257	257.2	D1806692	5.77	1.54	97	4.08	17.6	0.15	2.9	2.22	28.5	1.35	0.0559	4800	630	19.3	11.5	2600	3	142	12.4	103.5
South Roseb	SRO	BAK	BP272	267	267.2	D1806693	6.02	1.26	95	4.29	17.95	0.18	3	2.07	29.6	1.46	0.0277	5300	630	19.8	11.9	2780	3	145	13.1	103
South Roseb	SRO	BAK	BP272	278	278.2	D1806694	5.56	2.57	95	4.26	16.85	0.14	2.9	2.12	29.5	1.51	0.0771	5300	600	18.9	11.8	2770	3.1	131	13.1	104.5
South Roseb	SRO	BAK	BP272	288	288.2	D1806695	5.14	2.22	86	5.33	14.9	0.15	2.5	1.7	32.9	1.5	0.0957	5600	540	17.9	10.8	2660	2.7	120	13.5	93.9
South Roseb	SRO	BAK	BP272	298	298.2	D1806696	8.1	1.17	12	1.63	21.7	0.23	8.8	4	78	0.87	0.0457	9700	700	9.6	30.9	4310	8.5	84	24.8	329
South Roseb	SRO	BAK	BP272	308	308.2	D1806697	6.42	0.77	54	3.47	17.55	0.17	4.8	2.45	54.1	1.02	0.0416	5400	640	14.8	20.7	2940	4.9	112	18.5	174
South Roseb	SRO	BAK	BP272	318	318.2	D1806698	6.99	0.34	28	3.14	17.9	0.2	7.5	2.81	82.7	1.19	0.0227	2100	420	12	32.1	2630	7.3	66	25.1	273
South Roseb	SRO	BAK	BP272	328	328.2	D1806699	5.48	0.79	17	5.08	13.35	0.15	5.8	1.4	61.2	2.02	0.0353	3300	360	8.5	24	2050	5.7	40	21.8	218
South Roseb	SRO	BAK	BP272	338	338.2	D1806700	7.88	2.84	13	3.26	20.4	0.24	8.2	2.55	76.8	1.37	0.052	16400	800	10.3	31.2	3510	7	69	26.2	296
South Roseb	SRO	BAK	BP272	348	348.2	D1806701	4.39	2.24	21	3.27	10.15	0.17	4.3	0.87	50.9	0.93	0.0513	12500	400	7.8	18.2	1870	4.2	43	18.1	166.5
South Roseb	SRO	BAK	BP272	358	358.2	D1806702	6.21	0.71	30	3.99	16.2	0.18	5.7	1.91	64.4	1.3	0.0488	8900	510	13.9	25	2510	6.3	82	20.2	211
South Roseb	SRO	BAK	BP272	368	368.2	D1806703	6.68	0.33	26	3.36	17.1	0.2	7.6	2.58	76.4	1.29	0.0151	4000	550	11.2	31	2870	7.5	62	24.4	272
South Roseb	SRO	BAK	BP272	378	378.2	D1806704	7.36	0.23	129	3.61	20.5	0.18	4.5	2.89	45.3	1.14	0.0116	8800	690	22	18.3	3750	7.6	123	16.3	143
South Roseb	SRO	BAK	BP272	388	388.2	D1806705	6.65	0.18	111	6.77	17.55	0.26	3.6	1.28	40.4	2.19	0.0496	10000	640	22.4	14	2520	3	160	14.1	131.5
South Roseb	SRO	BAK	BP272	398	398.2	D1806706	3.64	4.4	53	3.48	10.25	0.13	2	1.39	20	2.58	0.234	1900	270	9.8	9.9	1960	2.6	105	10.6	67.9
South Roseb	SRO	BAK	BP272	408	408.2	D1806707	7.1	1.01	43	3.37	17.7	0.2	6	3.2	46.1	1.33	0.108	4500	660	17.8	18	3030	4.8	113	18.3	216
South Roseb	SRO	BAK	BP272	418	418.2	D1806708	6.49	4.04	89	4.15	15.7	0.19	4.4	0.75	47.2	2.11	0.098	27000	780	21.7	15.1	2630	4	134	16.2	155
South Roseb	SRO	BAK	BP273	230	230.1	D1806533	6.86	3.18	27	3.16	17.45	0.16	6.1	3.21	42.1	0.82	0.107	3800	850	17.6	14.2	3700	3.5	132	23.6	234
South Roseb	SRO	BAK	BP273	240	240.2	D1806534	5.8	3.66	12	3.12	14.45	0.16	4.7	2.74	34.1	0.51	0.214	1000	570	15.5	12.4	3350	3	124	21.6	180.5
South Roseb	SRO	BAK	BP273	250	250.1	D1806535	7.26	1.73	19	4.26	17.45	0.22	6.4	3.36	71.5	1.19	0.272	1000	620	11.2	27.8	3380	6.8	82	25.6	254
South Roseb	SRO	BAK	BP273	260	260.2	D1806536	6.89	2.57	27	3.41	17.85	0.19	6	2.67	49.9	1.05	0.114	7700	920	17.9	15	3430	3.5	128	28.7	224
South Roseb	SRO	BAK	BP273	270	270.2	D1806537	7.13	1.25	27	5.36	17.7	0.2	6.7	3.27	57.9	0.85	0.774	800	800	25.2	17.5	3540	4.1	147	27.9	249
South Roseb	SRO	BAK	BP273	280	280.1	D1806538	7.23	2.28	9	4	19	0.17	5.7	2.31	38.4	0.98	0.205	11100	560	18.2	12.3	4100	2.9	145	20.9	216
South Roseb	SRO	BAK	BP273	290	290.1	D1806539	8.54	2	37	5.53	24	0.24	8.6	3.11	49.6	1.51	0.0694	6400	1230	20.6	16.9	4410	4.8	189	29	333
South Roseb	SRO	BAK	BP273	300	300.1	D1806540	3.87	14.55	18	4.57	9.87	0.14	3.3	0.35	28.9	1.97	0.214	6300	530	13.1	8.8	2030	2.2	99	19.4	146.5
South Roseb	SRO	BAK	BP273	310	310.1	D1806541	5.48	5.41	13	3.38	14.8	0.13	6.6	1.63	52	1.25	0.106	5700	680	14.4	15.4	2750	3.6	94	22.8	236
South Roseb	SRO	BAK	BP273	320	320.1	D1806542	6.94	2.18	43	4.61	17.75	0.15	5.7	0.87	45.5	1.85	0.0559	24900	860	25.5	12	3360	3.4	150	23.3	203

Appendix 4A

Rosebery Mine host stratigraphy including the Marianoak Formation

Project_Des	Project	Prospect	Hole_ID	Depth_From	Depth_To	SAMPLE_TA	Al_pct	Ca_pct	Cr_ppm	Fe_pct	Ga_ppm	Ge_ppm	Hf_ppm	K_pct	La_ppm	Mg_pct	Mn_pct	Na_ppm	P_ppm	Sc_ppm	Th_ppm	Ti_ppm	U_ppm	V_ppm	Y_ppm	Zr_ppm
South Roseb	SRO	BAK	BP273	330	330.1	D1806543	5.02	6.29	13	2.96	13.7	0.13	5.6	1.56	48.5	1.55	0.0937	5000	430	14.7	14	2600	3.2	87	21.4	196.5
South Roseb	SRO	BAK	BP273	340	340.1	D1806544	5.16	10.7	28	3.24	13	0.11	4.5	1.8	40.6	1.6	0.192	6000	460	13.1	11.3	2570	2.7	82	20	164
South Roseb	SRO	BAK	BP273	350	350.1	D1806545	5.25	0.53	5	2.04	14.05	0.14	3.9	2.1	54.2	1.04	0.128	6000	90	3.9	30.5	770	8.2	15	18	116
South Roseb	SRO	BAK	BP273	360	360.1	D1806546	6.12	0.79	4	1.89	17.15	0.17	4.3	2.2	60.5	1.17	0.0415	9700	70	3.2	34	690	6.3	9	23.9	122.5
South Roseb	SRO	BAK	BP273	370	370.1	D1806547	8.43	0.41	5	2.66	25.3	0.16	6.9	4.08	56.5	0.95	0.658	1500	80	5	51.3	1080	12.6	16	24.8	188
South Roseb	SRO	BAK	BP273	380	380.2	D1806548	4.67	1.78	29	4.93	13.75	0.13	3.7	0.78	42	0.8	0.0762	19900	2500	5.8	19.4	1230	6.3	30	28.2	122.5
South Roseb	SRO	BAK	BP273	390	390.2	D1806549	8.91	1.06	40	3.5	22.9	0.22	8.2	3.19	52.2	1.47	0.076	8700	550	18.2	25.1	3630	6.9	117	31.8	297
South Roseb	SRO	BAK	BP273	400	400.2	D1806550	10.9	0.36	44	4.59	24.7	0.18	7.6	3.01	42.2	1.38	0.0416	22500	690	18.2	22.2	4090	9.8	122	19.9	274
South Roseb	SRO	BAK	BP273	410	410.1	D1806551	13.3	0.61	16	2.69	35.2	0.22	13.6	5.85	56.5	0.98	0.413	2200	710	23.3	23.6	5150	8.3	121	36.9	489
South Roseb	SRO	BAK	BP273	420	420.1	D1806552	8.76	0.28	55	2.13	22.8	0.19	6.4	3.92	62.8	0.9	0.0322	4500	430	11.9	26.8	3500	6.1	55	25.6	214
South Roseb	SRO	BAK	BP273	430	430.1	D1806553	5.93	0.27	65	2.51	14.6	0.13	3.6	1.92	38.1	0.76	0.037	11300	440	12.2	13.9	3200	3.5	67	15.7	119.5
South Roseb	SRO	BAK	BP273	440	440.2	D1806554	5.23	0.55	27	1.71	7.55	0.13	3.3	0.69	44.8	0.12	0.0755	32200	310	3.5	13.8	1350	3.2	15	15.5	111
North Hercu	NHR	JPT	JP357	35.5	35.6	D1808245	5.96	0.04	4	2.55	15.45	0.18	4.1	2.45	38.6	0.24	0.478	1900	140	3.7	19.8	1310	6.7	5	24.5	147
North Hercu	NHR	JPT	JP357	40.1	40.2	D1808246	8.05	1.97	1	1.29	21.6	0.22	5.5	3.03	58.2	0.94	0.623	4700	240	5	27	2100	6.7	9	37.4	204
North Hercu	NHR	JPT	JP357	45.1	45.2	D1808247	6.52	3.14	2	1.64	16.25	0.2	4.3	1.64	42.5	2.5	0.267	5600	230	4.4	20	1570	5.7	6	30.3	155.5
North Hercu	NHR	JPT	JP357	50.1	50.2	D1808248	7.4	0.98	2	1.74	22.2	0.21	6.3	2.33	48.1	1.47	0.164	9400	190	4.3	24.9	1930	7.2	7	31	226
North Hercu	NHR	JPT	JP357	55.1	55.2	D1808249	6.14	5.67	1	1.52	15.45	0.21	4.3	2.51	49.6	2.64	0.929	2600	150	3.6	21.4	1460	6.2	5	34	154.5
North Hercu	NHR	JPT	JP357	60.1	60.2	D1808250	4.5	0.06	5	0.61	11.2	0.15	3.2	1.93	32.3	0.15	0.0115	1600	100	2.3	16.6	1120	6.2	3	18.3	120.5
North Hercu	NHR	JPT	JP357	75.1	75.2	D1808253	6.19	1.05	9	1.42	17.6	0.22	4	2.23	56.3	0.43	0.0874	12700	110	4.3	33.4	930	8.7	12	17.9	121.5
North Hercu	NHR	JPT	JP357	80.2	80.3	D1808254	5.64	1.11	5	1.38	22.8	0.12	3.9	2.27	9.5	0.48	0.0761	12000	20	2.1	41.6	180	16.5	-1	23.9	84.9
North Hercu	NHR	JPT	JP357	85.1	85.2	D1808255	6.3	0.66	3	0.98	23.1	0.11	5.4	2.01	7	0.34	0.0477	24400	20	1.9	50.9	200	12.8	-1	21.1	112.5
North Hercu	NHR	JPT	JP357	90.1	90.2	D1808256	6.46	0.18	4	0.87	32.1	0.1	4.9	3.48	2.7	0.32	0.0203	5700	10	1.7	40	200	17.2	-1	19.5	104.5
North Hercu	NHR	JPT	JP357	95.1	95.2	D1808257	5.36	1.5	28	1.74	17.35	0.22	3.3	2.65	59	0.71	0.0693	700	50	8.2	21.6	1830	10.2	49	20.9	114.5
North Hercu	NHR	JPT	JP357	100.1	100.2	D1808258	3.27	3.59	39	2.44	10.1	0.17	3.5	1.56	25.8	1.34	0.132	400	300	7.7	8.8	1910	2.5	39	15.1	141
Rosebery	ROS	UDG	R10032	90	90.1	D1800158	5.83	1.92	8	1.71	10.65	0.16	3.2	2.35	41.4	0.23	0.0896	25700	190	4	14	1660	2.6	8	12.4	114
Rosebery	ROS	UDG	R10032	100	100.1	D1800159	7.72	0.79	3	1.92	17.55	0.1	4.7	2.84	16.3	0.43	0.046	26600	220	5.2	22.6	2160	6.3	11	15.7	171.5
Rosebery	ROS	UDG	R10032	110	110.1	D1800160	7.18	1.62	4	1.77	15.65	0.09	4	2.77	16	0.41	0.124	21300	250	5.3	17.8	2000	4.5	11	18.6	142
Rosebery	ROS	UDG	R10032	130	130.1	D1800161	6.09	4.94	86	3.17	16.2	0.18	3.3	2.87	41.9	1.61	0.146	1500	590	14	14.8	2720	4.4	100	16.4	117.5
Rosebery	ROS	UDG	R10032	140	140.1	D1800162	6.26	5.29	64	3.34	16.05	0.17	3.4	2.65	38.1	1.69	0.0722	4100	390	12.9	14.7	2750	4.5	92	14.8	122.5
Rosebery	ROS	UDG	R10032	150	150.1	D1800163	6.08	8.73	68	3.14	14.5	0.17	3	1.96	46.7	1.68	0.07	4300	1970	11.3	14.3	2380	4.2	68	17.4	109
Rosebery	ROS	UDG	R10032	160	160.1	D1800164	6.1	2.69	58	3.01	15.85	0.18	3.4	2.28	44	1.6	0.067	3400	2860	11.6	15.7	2340	4.2	86	16.7	121
Rosebery	ROS	UDG	R10032	170	170.1	D1800165	9.18	1.42	12	3.39	23.9	0.22	6.3	4.47	55.9	0.56	0.0438	7800	740	12.5	27.8	3320	6.7	50	20.1	233
Rosebery	ROS	UDG	R10032	180	180.1	D1800166	4.63	1.75	56	2.03	12.65	0.13	2	1.89	31.9	0.59	0.138	6200	920	10.6	8.8	2370	3.2	103	10.6	71.9
Rosebery	ROS	UDG	R10032	190	190.1	D1800167	5.92	4.3	51	3.27	15.6	0.18	3.2	2.82	45.3	1.4	0.225	3100	2430	11.1	15.8	2290	4.7	71	17.9	119
Rosebery	ROS	UDG	R10032	200	200.1	D1800168	7.41	0.47	11	1.56	19.4	0.16	5.1	3.48	52.5	0.6	0.0165	7100	250	7.5	21.7	2280	6.3	21	17.5	170.5
Rosebery	ROS	UDG	R10032	210	210.1	D1800169	7.62	1.49	4	1.29	19.05	0.16	3.9	3.8	71	0.94	0.0589	6500	90	2.9	41.1	970	9.5	8	15.5	107.5
Rosebery	ROS	UDG	R10032	220	220.1	D1800170	5.56	1.15	6	1.31	12.35	0.1	3.1	1.61	42.5	0.33	0.08	21800	60	1.7	30	630	6.6	1	12.9	99
Rosebery	ROS	UDG	R10032	230	230.1	D1800171	6.17	0.72	3	1.64	16.65	0.1	3.3	3.21	36.7	0.31	0.219	2600	40	1.8	30.5	670	7.2	1	14.1	102.5
Rosebery	ROS	UDG	R10032	240	240.1	D1800172	6.31	0.44	3	2.59	16.5	0.14	3.4	3.26	66.7	0.34	0.589	800	70	1.7	31.1	690	7.2	1	12.4	107.5
Rosebery	ROS	UDG	R10032	250	250.1	D1800173	6.63	2.16	64	3.74	15.35	0.15	3.9	1.9	38.5	0.75	0.0686	11400	490	12.8	13.7	2580	3.2	135	13.2	158
Rosebery	ROS	UDG	R10032	260	260.1	D1800174	7.35	1.75	81	9.46	17.55	0.28	4.5	1.71	46	0.76	0.0632	21300	710	20.5	12.3	2130	3.1	139	15.1	182.5
Rosebery	ROS	UDG	R10032	270	270.1	D1800175	6.89	1.69	57	7.07	18.05	0.23	5	1.51	47.6	1.4	0.0855	13000	840	23.2	14.7	3160	3.4	194	19.2	198.5
Rosebery	ROS	UDG	R10032	280	280.1	D1800176	7.36	3.9	45	3.32	18.35	0.21	5.9	1.8	45.5	0.74	0.109	22600	1140	22.1	16.5	4340	3.4	171	22.7	231
Rosebery	ROS	UDG	R10032	290	290.1	D1800177	6.61	0.93	70	4.61	17.8	0.21	4.3	2.17	41.1	1.17	0.0316	3500	640	19.7	14.4	3710	3.9	126	17.4	162
Rosebery	ROS	UDG	R10032	300	300.1	D1800178	4.24	1.85	83	4.06	11.8	0.14	1.9	1.17	20.2	1	0.0798	3400	640	13	7.5	2980	1.9	172	8	69.2
Rosebery	ROS	UDG	R10032	310	310.1	D1800179	9.26	2.92	12	1.92	25.7	0.17	6.9	3.28	40.9	0.51	0.0575	11500	1130	20.8	15.3	6670	2.7	189	25.8	258
Rosebery	ROS	UDG	R10032	320.3	320.4	D1800180	6.36	2.16	21	3.93	16.9	0.2	5.1	1.2	46.1	0.96	0.0421	6400	760	13.6	14.8	3630	3.2	106	18.4	198
Rosebery	ROS	UDG	R10032	330	330.1	D1800181	6.19	2.51	18	5.89	17.15	0.26	4.7	1.37	44	1.34	0.0906	6300	670	33.9	13.5	2510	2.9	160	17.9	183
Rosebery	ROS	UDG	R10032	340	340.1	D1800182	5.49	3.71	18	3.01	13.5	0.17	4.4	1.77	36.1	0.82	0.134	9400	520	15.9	12.3	2520	2.7	104	15.7	172
Rosebery	ROS	UDG	R10032	352.8	352.9	D1800183	6.48	0.4	16	3.21	17.9	0.15	4.6	2.29	41	0.95	0.027	5600	150	5.3	41.5	1030	9.3	28	13.5	132.5
Rosebery	ROS	UDG	R10032	360	360.1	D1800184	6.23	2.23	13	2.55	15.3	0.17	4.8	2.07	40.5	1.08	0.0827	10700	420	13.5	14.2	2720	3	75	18.9	192
Rosebery	ROS	UDG	R10032	370	370.1	D1800185	6.71	0.91	6	1.36	20.5	0.07	4.5	2.91	12.5	0.48	0.0386	10400	30	1.7	45.8	220	15.1	1	24.1	86.5
Rosebery	ROS	UDG	R10032	380	380.1	D1800186	6.38	0.52	5	1.39	17.45	0.08	4.3	4.64	13.2	0.25	0.138	8400	30	1.6	43.7	190	15.1	-1	25.6	83.4
Rosebery	ROS	UDG	R10032	390	390.1	D1800187	5.86	0.47	7	0.79	14.5	0.06	3.8	3.36	14.4	0.15	0.0255	17500	30	1.4	36.6	180	12.7	1	28.8	74.7
Rosebery	ROS	UDG	R10032	399	399.1	D1800188	5.67	0.03	4	0.72	15.45	0.15	3.9	6.14	17.6	0.09	0.0063	1600	50	3	39.3	170	14.8	-1	28.6	73.7
Rosebery	ROS	UDG	R10032	410	410.1	D1800189	6.21	0.85	4	2.81	15.55	0.15	4	2.93	12.6	0.57	0.146	12600	20	1.9	34.8	180	13.4	4	21.6	77.3
Rosebery	ROS	UDG	R10032	420	420.1	D1800190	6.61	0.25	3	1.43	17.75	0.2	4	4	34.5	0.55	0.0258	3300	40	2.1	37.3	410	11	1	18.6	105
Rosebery	ROS	UDG	R10032	430	430.1	D1800191	4.96	0.22	6	0.82	8.62	0.17	2.8	1.52	33.3	0.1	0.0227	26900	40	1.5	27.8	300	8	1	19	75

Appendix 4A

Rosebery Mine host stratigraphy including the Marianoak Formation

Project_Des	Project	Prospect	Hole_ID	Depth_From	Depth_To	SAMPLE_TA	Al_pct	Ca_pct	Cr_ppm	Fe_pct	Ga_ppm	Ge_ppm	Hf_ppm	K_pct	La_ppm	Mg_pct	Mn_pct	Na_ppm	P_ppm	Sc_ppm	Th_ppm	Ti_ppm	U_ppm	V_ppm	Y_ppm	Zr_ppm
Rosebery	ROS	UDG	R10032	439.5	439.6	D1800192	5.76	0.25	4	0.99	11.1	0.2	3.1	2.89	37.4	0.18	0.021	21900	40	1.7	31.3	330	8.8	1	21.9	86.3
Rosebery	ROS	UDG	R10032	450	450.1	D1800193	6.6	0.08	3	2.6	20.3	0.28	3.9	4.42	46.8	0.27	0.0129	1400	50	2.6	36.9	390	12.6	1	33.6	100.5
Rosebery	ROS	UDG	R10032	459	459.1	D1800194	5.61	1.41	3	1.21	14.25	0.24	3.2	3.35	37.3	0.41	0.0668	2200	40	1.9	32	330	8.8	-1	22.2	84.4
Rosebery	ROS	UDG	R10035	100.5	100.6	D1800085	7.35	0.92	2	2.03	18.25	0.2	4.5	3.85	67.1	0.74	0.0441	5700	210	5	21.3	2070	5.4	9	21	162
Rosebery	ROS	UDG	R10035	110.4	110.5	D1800086	5.65	1.87	3	1.09	13.25	0.13	4.1	3.58	34.2	0.25	0.0902	15800	150	3.4	16.6	1520	3.2	6	17.7	151.5
Rosebery	ROS	UDG	R10035	122.6	122.7	D1800087	7.8	0.81	3	2.33	18.3	0.19	4.4	4.19	57.7	0.39	0.971	1800	270	9.2	19.8	1790	5.3	21	16	154
Rosebery	ROS	UDG	R10035	127.9	128	D1800088	7.17	1.7	2	1.51	17.55	0.19	4.3	2.37	55.6	0.46	0.0818	24200	230	8.5	17.9	1860	4.1	15	14.3	153.5
Rosebery	ROS	UDG	R10035	132.7	132.8	D1800089	6.86	3.97	80	2.95	21.4	0.16	4.5	3.88	29.3	1.22	0.146	3000	620	14.4	11	2270	3.4	106	14.7	174.5
Rosebery	ROS	UDG	R10035	139.3	139.4	D1800090	6.1	2.97	27	2.06	15.3	0.15	3.1	1.93	27.7	0.86	0.13	24400	960	13.6	8.4	1630	1.9	97	12.3	122.5
Rosebery	ROS	UDG	R10035	148.9	149	D1800091	5.31	0.85	2	0.68	13.05	0.09	2.9	2.21	43.5	0.4	0.04	8600	50	1.5	26.1	590	5.9	1	11.5	93
Rosebery	ROS	UDG	R10035	161.5	161.6	D1800092	7.26	1.07	7	1.75	20.6	0.15	4.3	2.88	67.1	0.47	0.0505	14400	110	3.5	36.7	1050	8.4	14	18.9	143
Rosebery	ROS	UDG	R10035	164.9	165	D1800093	7.17	0.59	21	0.97	16.15	0.12	4.6	2.03	54.7	0.3	0.0257	29500	220	7.1	32.2	1630	7.8	44	15.8	159
Rosebery	ROS	UDG	R10035	170.4	170.5	D1800094	7.13	0.42	15	0.98	22.8	0.11	4.4	3.21	55.5	0.28	0.0175	9500	170	7.1	30.3	1610	7.8	42	15.8	152.5
Rosebery	ROS	UDG	R10035	179.4	179.5	D1800095	3.73	1.43	4	1.26	7.44	0.07	2.3	1.44	34	0.47	0.0899	7200	40	1.3	18.3	400	4.3	2	12.6	88.5
Rosebery	ROS	UDG	R10035	191	191.1	D1800096	6.63	2.02	18	2.92	18	0.13	4.5	2.65	37.9	0.58	0.688	10500	390	12.2	16.1	2350	4.4	76	18.2	173.5
Rosebery	ROS	UDG	R10035	200	200.1	D1800097	6.78	1.36	21	3.57	17.85	0.16	4.9	1.49	43.4	0.64	0.0652	19700	480	19	14.2	2410	4.3	110	18.5	189
Rosebery	ROS	UDG	R10035	210.6	210.7	D1800098	7.11	2.06	10	2.45	21.3	0.15	5.2	2.02	35.4	0.43	0.0535	17000	750	12.4	11.5	4530	3	152	18.9	205
Rosebery	ROS	UDG	R10035	219.4	219.5	D1800099	6.39	1.34	6	1.65	19.45	0.11	6.3	1.73	27	0.39	0.0328	11300	520	10.1	16.3	2990	3.7	60	22.7	251
Rosebery	ROS	UDG	R10035	230.1	230.2	D1800100	5.64	4.13	9	2.96	15.4	0.16	4.7	1.33	32.8	0.56	0.078	12500	510	13.4	11.7	2860	2.5	85	19	186.5
Rosebery	ROS	UDG	R10035	241.6	241.7	D1800101	6.09	1.35	10	3.46	18.3	0.19	4.7	1.45	60.9	0.81	0.036	10900	130	15	29.9	1040	6.9	70	17.4	161
Rosebery	ROS	UDG	R10035	252.1	252.2	D1800102	5.82	0.36	3	1.88	16.1	0.14	4	1.15	63.8	1.14	0.0163	6700	70	3	36	680	6.5	7	19.6	128.5
Rosebery	ROS	UDG	R10035	262.7	262.8	D1800103	5.96	0.43	7	2.13	17.4	0.14	4.2	1.08	57.4	1.25	0.0184	7900	80	3.1	38.7	630	9.4	8	21.1	123.5
Rosebery	ROS	UDG	R10035	269.3	269.4	D1800104	5.87	0.17	3	1.83	15.7	0.11	4.1	1.69	43.2	0.69	0.0146	4600	90	3.8	37.1	790	7.1	10	16.7	134
Rosebery	ROS	UDG	R10035	279.2	279.3	D1800105	5.49	0.1	5	2.42	14.55	0.13	3.5	1.67	56	0.93	0.0189	2700	80	4.1	33.7	640	6.2	11	17	111
Rosebery	ROS	UDG	R10035	290.6	290.7	D1800106	6.67	0.64	2	1.77	19.85	0.11	4.6	2.43	29.2	0.6	0.0325	11600	40	1.6	36.2	400	8.4	-1	17.7	109
Rosebery	ROS	UDG	R10035	300.7	300.8	D1800107	6.48	0.18	3	1.82	17.2	0.15	4.3	2.08	72.8	1.01	0.0189	4200	100	3	36.9	880	7	9	14.4	131
Rosebery	ROS	UDG	R10035	311.3	311.4	D1800108	6.93	1.31	10	1.67	18.4	0.18	4.7	2.33	74.5	0.93	0.0424	6500	170	4.2	40.1	1200	6.6	21	18.1	148
Rosebery	ROS	UDG	R10035	320.9	321	D1800109	5.69	0.25	3	1.77	15.05	0.12	3.5	1.45	50.7	1.09	0.0207	12400	50	2.7	36.4	570	7.3	6	18.3	98.9
Rosebery	ROS	UDG	R10035	330	330.1	D1800110	6.87	0.79	14	2.75	18.9	0.15	4.6	2.86	54.8	0.9	0.166	2300	190	4.7	40.3	1210	9.9	30	20.2	137
Rosebery	ROS	UDG	R10035	341.2	341.3	D1800111	6.35	0.25	6	1.25	17.4	0.1	4.1	1.84	37.6	0.56	0.0224	19700	40	2.4	35.2	510	7.5	2	20.5	111.5
Rosebery	ROS	UDG	R10035	350.7	350.8	D1800112	6.61	1.06	15	1.58	18.1	0.13	4.6	2.11	43	0.62	0.0326	20500	70	2.3	38.6	490	10.2	2	21.7	121
Rosebery	ROS	UDG	R10035	359.9	360	D1800113	6.91	1.18	49	2.34	18.95	0.13	4.7	1.44	37.6	0.63	0.043	33800	340	10.2	25.9	2120	7.5	88	22.8	153
Rosebery	ROS	UDG	R10035	370.9	371	D1800114	6.46	1.29	5	2.66	17.55	0.15	6.2	1.74	43.6	0.79	0.0713	21600	310	9.3	15.6	2510	3.7	49	22.9	241
Rosebery	ROS	UDG	R10035	381	381.1	D1800115	6.6	1.54	10	2.88	17.4	0.17	6	1.95	41.5	0.93	0.077	11600	410	10.8	16.2	2750	3.6	58	22.7	238
Rosebery	ROS	UDG	R10035	390.2	390.3	D1800116	7.14	0.98	10	2.69	19.05	0.18	5.9	2.18	52.7	0.73	0.0474	13200	480	12.2	16.1	3050	4.3	70	23.2	229
Rosebery	ROS	UDG	R10035	400.4	400.5	D1800117	4.8	2.97	5	2.26	12.8	0.11	3.3	1.85	13	0.81	0.22	8900	30	1.6	31.1	210	11.1	2	21.4	66.2
Rosebery	ROS	UDG	R10035	410.1	410.2	D1800118	5.92	0.57	4	0.95	15.15	0.07	3.7	1.78	15.1	0.23	0.0622	26900	20	1.3	39.6	200	13.8	1	25	77
Rosebery	ROS	UDG	R10063	10.1	10.2	D1800138	8.07	0.52	3	3.42	19.75	0.25	5.1	4.23	66.9	1.42	0.454	2300	250	4.3	22.5	2230	5.7	15	13.9	179.5
Rosebery	ROS	UDG	R10063	20.4	20.5	D1800139	6	0.46	4	2.04	13.8	0.17	3.9	3.2	46.8	0.97	0.505	500	210	3.8	17.7	1840	4.2	11	12.3	133.5
Rosebery	ROS	UDG	R10063	29.7	29.8	D1800140	6.63	0.67	6	2.55	15.55	0.22	3.8	2.68	59.1	0.92	0.16	13800	290	4.5	17.5	1920	4	15	14.2	136
Rosebery	ROS	UDG	R10063	40	40.1	D1800141	6.84	0.68	2	2.64	16.1	0.15	3.9	3.6	39.4	1.15	0.434	800	250	4.9	18	1930	4.5	13	11.6	136.5
Rosebery	ROS	UDG	R10063	50.2	50.3	D1800142	7.18	1.07	46	2.68	18.25	0.19	4	4.08	48.2	1.74	0.132	1800	540	9.8	18.4	2480	4.4	46	14	142
Rosebery	ROS	UDG	R10063	61.5	61.6	D1800143	6.63	1.25	6	1.86	14.25	0.14	2.4	3.19	42.5	0.21	0.058	21800	440	7.4	18.2	2180	4	49	13.4	74.5
Rosebery	ROS	UDG	R10063	71.2	71.3	D1800144	8.11	0.56	2	2.55	20.8	0.19	5.2	5.08	59.6	0.77	0.107	9900	240	5.1	27.3	2240	9.2	10	26	190
Rosebery	ROS	UDG	R10063	77.2	77.3	D1800145	6.67	1.34	16	1.29	15.75	0.16	4.1	4.22	46	0.39	0.0617	8300	200	4	21.3	1780	4.3	8	15.5	143.5
Rosebery	ROS	UDG	R10063	90.2	90.3	D1800146	8.11	0.33	7	1.98	18.25	0.13	2.8	4.63	36	0.23	0.0314	20800	510	9.4	21.8	2560	6.3	68	10.8	86.5
Rosebery	ROS	UDG	R10063	98.8	98.9	D1800147	6.27	1.49	6	1.8	13.05	0.13	2.2	3.47	34.4	0.2	0.0721	16800	420	10.8	17.3	2010	5	43	13.3	69.8
Rosebery	ROS	UDG	R10063	114.6	114.7	D1800148	6.27	0.56	5	1.66	13.9	0.12	2.1	3.7	32	0.28	0.048	500	410	6.6	16.9	2050	4.5	52	8.8	62.4
Rosebery	ROS	UDG	R10063	120	120.1	D1800149	6.79	1.25	5	2.32	14.55	0.15	2.2	3.9	38.2	0.24	0.0884	16500	470	6.8	18.9	2280	4.9	52	12.2	67.4
Rosebery	ROS	UDG	R10063	130.1	130.2	D1800150	5.89	0.93	8	1.9	13.5	0.16	2.4	3.5	33.9	0.13	0.0431	20500	450	7.7	16.3	2220	4.7	46	10.9	69.7
Rosebery	ROS	UDG	R10063	140.8	140.9	D1800151	7.08	0.94	12	2	15.35	0.15	2.4	3.96	38.6	0.18	0.0468	20500	500	6.7	20.5	2390	5.2	50	11.7	74.9
Rosebery	ROS	UDG	R10063	151.7	151.8	D1800152	6.79	2.29	10	2.38	14.85	0.16	2.3	4.9	38.2	0.28	0.0794	11700	460	8	18.9	2300	4.7	50	13.2	71.5
Rosebery	ROS	UDG	R10063	159.8	159.9	D1800153	7.28	1.41	8	1.89	16.5	0.18	4.2	4.15	50.9	0.62	0.0597	10900	260	5	21.7	2080	5.3	15	21.1	145
Rosebery	ROS	UDG	R10063	170.8	170.9	D1800154	8.13	1.43	5	2.2	18.55	0.19	4.3	4.94	49.1	0.65	0.0654	10400	360	6.5	21.3	2460	6.3	20	21.2	155.5
Rosebery	ROS	UDG	R10063	179.8	179.9	D1800155	6.58	2.56	8	2.2	15	0.16	2.3	4.77	36.6	0.29	0.126	13700	470	7.2	16.6	2350	3.7	51	13.6	72.9
Rosebery	ROS	UDG	R10063	190.7	190.8	D1800156	7.08	1.41	5	1.81	17.7	0.17	3.9	2.95	46.5	0.45	0.0719	21500	280	5.6	17.4	2300	4.9	13	17.2	138
Rosebery	ROS	UDG	R10063	200.8	200.9	D1800157	5.86	2.54	4	1.64	14.85	0.11	4.2	4.99	20.1	0.31	0.178	6700	200	3.6	16.9	1610	3.7	8	20.3	147.5
Rosebery	ROS	UDG	R10063	210	210.1	D1800897	4.29	3.85	4	5.32	9.75	0.1	2.9	1.6	24.8	0.77	0.436	600	260	3.9	12.5	1310	3.8	14	21.1	92.6

Appendix 4A

Rosebery Mine host stratigraphy including the Marianoak Formation

Project_Des	Project	Prospect	Hole_ID	Depth_From	Depth_To	SAMPLE_TA	Al_pct	Ca_pct	Cr_ppm	Fe_pct	Ga_ppm	Ge_ppm	Hf_ppm	K_pct	La_ppm	Mg_pct	Mn_pct	Na_ppm	P_ppm	Sc_ppm	Th_ppm	Ti_ppm	U_ppm	V_ppm	Y_ppm	Zr_ppm
Rosebery	ROS	UDG	R10063	220	220.1	D1800898	6.28	4.81	201	3.74	16.2	0.17	3.7	2.82	38.1	1.54	0.268	700	420	14	13.9	2390	3.6	95	16.6	124.5
Rosebery	ROS	UDG	R10063	230	230.1	D1800899	6.75	5.77	32	4.54	15.4	0.12	2.5	2.98	33.6	1.72	0.235	7200	540	18.5	8.8	3160	2.4	145	12.4	83.9
Rosebery	ROS	UDG	R10063	239.8	239.9	D1800900	4.98	4.56	41	3.56	12.4	0.14	3.3	2.31	40.7	1.39	0.182	400	440	9.8	14.6	2440	3.9	80	12.5	109
Rosebery	ROS	UDG	R10063	250	250.1	D1800901	4.8	6.99	42	5.14	11.85	0.12	3	2.05	37.9	1.75	0.235	2800	410	10	12.1	2030	3.7	77	12.7	100
Rosebery	ROS	UDG	R10063	260	260.1	D1800902	4.26	3.1	4	1.87	6.24	0.17	2.7	0.56	45	0.97	0.205	26500	240	2	11.1	1040	3.7	7	14.4	96.2
Rosebery	ROS	UDG	R10063	270.2	270.3	D1800903	5.53	1.36	3	1.83	11.75	0.17	3.2	1.85	40.7	0.79	0.0841	12800	40	1.5	25	560	6.4	2	15.8	96.9
Rosebery	ROS	UDG	R10063	280	280.1	D1800904	5.6	1.57	14	2.16	14	0.21	4	2.15	51	1.17	0.0612	4300	360	6.6	16.3	1930	6.3	48	19.6	140.5
Rosebery	ROS	UDG	R10063	290	290.1	D1800905	5.86	8.6	37	2.19	11.6	0.15	4.4	0.92	45.7	0.97	0.149	25600	2210	16.6	11.4	2630	5.9	104	21.5	159.5
Rosebery	ROS	UDG	R10063	300	300.1	D1800906	7.14	9.65	64	3.54	16.5	0.14	5.9	1.11	41.7	1.24	0.348	39100	930	26.5	15.4	3700	3.7	172	18.8	219
Rosebery	ROS	UDG	R10063	310	310.1	D1800907	6.85	1.33	37	2.17	11.65	0.26	5.1	0.75	59	0.76	0.0591	37200	800	14.6	14.9	3230	3.4	111	18	182
Rosebery	ROS	UDG	R10063	320	320.1	D1800908	6.06	12.7	34	3.7	14.55	0.13	5	1.19	47.7	1.42	0.183	10900	690	16.3	13.2	3230	3.3	131	21.9	179
Rosebery	ROS	UDG	R10063	330	330.1	D1800909	6.03	1.13	16	4.94	17.1	0.21	4.9	1.02	52	1.3	0.0439	11400	700	17.2	14.9	2630	3.4	118	17.8	186.5
Rosebery	ROS	UDG	R10063	340	340.1	D1800910	4.64	2	32	2.7	11.3	0.14	3.8	1.48	35.7	1.41	0.102	3600	210	7.2	17.3	1810	4.2	36	13.2	128
Rosebery	ROS	UDG	R10063	350	350.1	D1800911	7.32	2.31	3	1.61	16.85	0.24	6.2	2.46	42.6	0.65	0.0368	9700	450	10	18	2790	4.8	32	20.5	224
Rosebery	ROS	UDG	R10063	360	360.1	D1800912	9.45	0.33	17	1.8	23.3	0.2	5.5	3.52	66.3	0.67	0.0104	7200	150	5.5	47.9	1010	5.8	34	15.7	154
Rosebery	ROS	UDG	R10063	370	370.1	D1800913	10.25	0.37	16	3.03	26.7	0.26	12.6	4.49	62.7	0.62	0.0193	16700	770	12.8	39.7	4100	18	116	28.5	439
Rosebery	ROS	UDG	R10063	380	380.1	D1800914	9.04	1.27	2	5.13	19.8	0.24	7.7	2.64	50.7	2.68	0.0537	5600	550	11.7	21.4	2500	9.9	41	28.6	280
Rosebery	ROS	UDG	R10063	390	390.1	D1800915	7.21	2.97	36	4	16.2	0.24	5.1	1.5	51	1.23	0.0601	16600	490	12.3	18.2	2540	7.3	92	17.4	192
Rosebery	ROS	UDG	R10063	400	400.1	D1800916	9.52	2.93	7	2.15	22.6	0.25	9.1	3.29	65.8	0.98	0.0513	16700	770	13.8	25.9	3770	9.2	61	31.9	304
Rosebery	ROS	UDG	R10063	410	410.1	D1800917	7.37	3.21	10	3.31	20.4	0.17	6.3	2.22	45.5	1.18	0.0652	8700	560	16.4	15.7	3310	4.1	103	33.5	244
Rosebery	ROS	UDG	R10063	420	420.1	D1800918	8.35	0.9	28	4.61	21.6	0.18	7.1	3.27	40.7	0.36	0.0112	12200	680	20.6	16.6	3980	15.3	144	30.5	258
Rosebery	ROS	UDG	R10063	439.9	440	D1800920	7.81	1.33	11	3.78	21.1	0.15	4.7	1.8	34.2	0.93	0.0584	18300	720	21.3	12.1	3750	3.2	144	25.3	187.5
Rosebery	ROS	UDG	R10063	450	450.1	D1800921	6.86	2.24	22	4.28	18.7	0.16	4	1.22	34.6	0.91	0.0696	23300	570	15.5	11.2	2840	2.9	131	19.2	156.5
Rosebery	ROS	UDG	R10063	460	460.1	D1800922	6.32	1.87	48	2.58	16.6	0.14	3.6	2.61	44.5	1.07	0.0388	3000	360	9.7	21	2490	5.9	71	14.4	124
Rosebery	ROS	UDG	R10063	469.5	469.6	D1800923	5.72	3.27	133	4.25	16.1	0.15	2.9	1.4	38.1	1.6	0.0518	11200	710	18.2	13.2	3530	4.2	102	13.9	105
Rosebery	ROS	UDG	R10063	480	480.1	D1800924	6.71	1.14	17	1.86	18.7	0.15	5.8	2.36	41.9	0.55	0.0588	21700	700	17	13.3	4510	3.8	172	20	223
Rosebery	ROS	UDG	R10063	490	490.1	D1800925	4.3	0.9	7	2.47	11.35	0.17	4.6	1.28	73.4	0.63	0.0372	5500	260	9.4	13	1440	3.1	39	26	181
Rosebery	ROS	UDG	R10063	500	500.1	D1800926	7.01	3.66	80	2.49	19.7	0.17	5.2	2.38	36.7	0.48	0.0707	14100	780	14.1	12	3940	3.2	136	25.8	208
Rosebery	ROS	UDG	R10063	510	510.1	D1800927	6.96	1.71	51	6.19	17.75	0.21	5.3	1.35	54.1	0.85	0.0872	15500	690	19.9	15.3	3250	3.7	148	33.3	208
Rosebery	ROS	UDG	R10063	519.8	519.9	D1800928	6.37	3.12	46	4.14	18.3	0.18	5	1.67	45.5	0.57	0.0839	16000	860	19.7	13.6	3080	3.1	140	23.6	194
Rosebery	ROS	UDG	R10063	526.4	526.5	D1801001	4.3	4.41	62	4.02	12.7	0.17	2.4	1.26	28.5	0.93	0.0632	3600	580	13	9.7	2870	2.6	104	12.9	92.9
Rosebery	ROS	UDG	R10063	530	530.1	D1800929	7.49	2.64	14	4	19.3	0.19	5.5	2.28	43.9	1.18	0.057	7300	640	22.2	15.5	4110	3.8	160	24.5	220
Rosebery	ROS	UDG	R10063	537.7	537.8	D1801002	6.18	4.94	58	3.34	16.85	0.18	4.1	2.01	34.4	1.15	0.077	3400	620	17.7	14.9	3770	4.2	120	19.4	157.5
Rosebery	ROS	UDG	R10063	541.4	541.5	D1800930	7.24	2.3	8	3.84	18.35	0.18	5.1	2.17	38	1.12	0.0584	7100	650	21.3	13.2	3970	3.1	174	23.5	207
Rosebery	ROS	UDG	R10063	550	550.1	D1800931	6.06	4.73	6	3.09	15.9	0.15	4.5	1.55	33.5	0.97	0.0594	10100	610	19.4	10.9	3760	2.4	144	19.1	185
Rosebery	ROS	UDG	R10063	554.7	554.8	D1801003	6.19	1.92	55	4.8	16.2	0.22	4.2	2.09	62.6	1.04	0.0623	2600	710	13.9	19.5	3460	5.7	116	23	169.5
Rosebery	ROS	UDG	R10063	560	560.1	D1800932	7.04	2.34	11	3.32	18.15	0.23	6.6	2.29	73.7	1.07	0.047	5700	580	10.5	26.4	3490	7	73	25	264
Rosebery	ROS	UDG	R10063	570	570.1	D1800933	7.3	4.24	25	3.38	17.8	0.19	4.6	1.91	47	1.08	0.0541	13900	690	12.7	16.2	3270	4.5	102	18.6	185.5
Rosebery	ROS	UDG	R10063	580	580.1	D1800934	5.77	6.85	15	4.02	13.95	0.2	5.7	1.46	59.1	1.76	0.122	5200	560	11	24	2960	6.2	81	22.4	228
Rosebery	ROS	UDG	R10063	589.9	590	D1800935	9.09	3.6	9	2.81	25.5	0.25	11	3.88	72.6	0.85	0.0482	3800	700	11.2	33.4	5550	8.3	87	26.4	415
Rosebery	ROS	UDG	R10063	600	600.1	D1800936	6.74	2.39	3	2.74	16.9	0.21	7.1	2.01	64.6	1.1	0.0472	11300	440	8.9	28	3420	6.5	46	24.3	279
Rosebery	ROS	UDG	R10063	610.6	610.7	D1800937	8.05	6.74	280	4.91	18.2	0.17	2.8	2.75	21.9	0.75	0.178	8100	1160	42.3	7.4	5000	3.3	238	15.5	105.5
Rosebery	ROS	UDG	R10063	620	620.1	D1800938	6.82	4.25	94	4.91	15.4	0.18	3.8	1.68	40.8	1.11	0.13	11100	670	28.2	13.1	3100	3.4	154	15.3	148
Rosebery	ROS	UDG	R10063	630	630.1	D1800939	6.12	5.75	81	4.66	14.05	0.17	3.6	1.39	38.7	1.65	0.104	13800	610	24.1	12.3	2860	3.2	133	16	145
Rosebery	ROS	UDG	R10063	640	640.1	D1800940	7.5	4.06	101	4.42	17.5	0.17	4.9	2.15	38.3	1.14	0.13	12900	810	24.8	17.8	3560	4.6	154	18.5	190
Rosebery	ROS	UDG	R10063	650	650.1	D1800941	6.59	1.88	45	4.16	17.5	0.18	4.7	2.76	47.2	0.79	0.0726	1800	730	17.1	16.1	2610	5	138	16.8	186
Rosebery	ROS	UDG	R10063	660	660.1	D1800942	6.63	1.66	12	2.83	16	0.18	5.5	2.62	53.3	0.78	0.0491	2700	530	11.1	19.4	2770	5.1	71	20.5	217
Rosebery	ROS	UDG	R10063	669.6	669.7	D1800943	6.57	2.91	142	4.63	19.15	0.19	3	2.18	35.4	1.77	0.0662	4900	760	21.9	12.4	4120	3	138	13.4	111
Rosebery	ROS	UDG	R10063	680.3	680.4	D1800944	6.28	2.43	7	3.41	14.25	0.26	5.4	2.21	63.4	0.89	0.0757	6700	660	11.8	18.7	2540	4.7	63	21.7	206
Rosebery	ROS	UDG	R10063	683.9	684	D1801004	6.53	1.57	94	4.41	17.6	0.18	3.8	2.39	37.1	0.76	0.0617	4100	850	17	13.8	2760	3.8	116	14.2	144
Rosebery	ROS	UDG	R10063	690	690.1	D1800945	6.9	5.24	29	4.99	17.4	0.19	4.3	2.37	50.3	1.48	0.144	7700	690	19.5	14.4	3070	3.5	117	21.4	171
Rosebery	ROS	UDG	R10063	700	700.1	D1800946	4.17	7.33	55	4.64	9.72	0.12	2.6	1.82	22.8	2.81	0.118	3000	420	18	9.5	1760	2.7	90	15.3	106
Rosebery	ROS	UDG	R10063	710.7	710.8	D1800947	7.51	0.67	70	4.22	21	0.2	4.5	3.12	54.3	1.12	0.0364	1800	920	19.4	19.4	3210	5.2	118	16.1	169
Rosebery	ROS	UDG	R10063	718	718.1	D1800948	3.95	4.91	63	4.59	11.05	0.13	2.2	1.17	24.4	2.95	0.12	1000	410	12	9	2230	2.6	75	12.8	94.9
Rosebery	ROS	UDG	R10063	729.9	730	D1800949	5.51	0.45	3	0.94	13.9	0.15	3.8	3.01	52.1	0.31	0.0312	15300	50	2.3	30.1	460	7	3	21.8	109.5
Rosebery	ROS	UDG	R10063	750	750.1	D1800951	6.65	0.83	12	2.93	17.45	0.21	5.7	1.85	52.8	0.55	0.0551	21300	430	12.6	15.1	3100	4	75	17.9	218
Rosebery	ROS	UDG	R10063	760	760.1	D1800952	6.3	0.2	4	3.03	17.4	0.19	5.7	2.03	62	0.77	0.04	12500	390	11.8	14.9	2380	3.6	50	19.4	240
Rosebery	ROS	UDG	R10063	770	770.1	D1800953	6.59	0.56	9	2.59	17.9	0.17	6.1	1.53	34.4	0.52	0.0395	28600	470	11.1	15.1	2880	4.1	58	21.3	243

Appendix 4A

Rosebery Mine host stratigraphy including the Marianoak Formation

Project_Des	Project	Prospect	Hole_ID	Depth_From	Depth_To	SAMPLE_TA	Al_pct	Ca_pct	Cr_ppm	Fe_pct	Ga_ppm	Ge_ppm	Hf_ppm	K_pct	La_ppm	Mg_pct	Mn_pct	Na_ppm	P_ppm	Sc_ppm	Th_ppm	Ti_ppm	U_ppm	V_ppm	Y_ppm	Zr_ppm
Rosebery	ROS	UDG	R10063	780	780.1	D1800954	7.41	0.54	8	2.74	23.4	0.17	7.7	3.27	39.6	0.83	0.0506	13300	410	14.7	17.6	3330	4.9	68	22.3	290
Rosebery	ROS	UDG	R10063	789.9	790	D1800955	7.13	0.38	64	2.98	17.35	0.14	5.8	1.83	24	0.83	0.0402	29300	600	29.8	14.8	3150	5.9	153	15.2	217
Rosebery	ROS	UDG	R10063	800	800.1	D1800956	5.13	2.37	4	1.39	14.45	0.18	3.2	2.33	38.6	0.49	0.13	18000	40	2.3	23.4	340	7.6	3	20.2	89.3
Rosebery	ROS	UDG	R10063	810.1	810.2	D1800957	5.39	0.58	4	1.4	15.25	0.15	3.5	2.5	41.6	0.45	0.06	18300	40	2.1	26.8	380	7.2	2	16.6	98.8
Rosebery	ROS	UDG	R10063	820	820.1	D1800958	4.48	0.22	4	1.65	11.65	0.12	3.3	1.86	27.4	0.54	0.022	12900	30	2.3	25	460	7.3	4	12.4	101
Rosebery	ROS	UDG	R10063	830	830.1	D1800959	5.97	0.43	3	1.01	19.4	0.13	4.1	4.49	14	0.48	0.0258	7400	30	1.3	32.1	210	14.9	1	41.1	93.1
Rosebery	ROS	UDG	R10063	840	840.1	D1800960	4.55	0.33	5	0.6	6.9	0.13	3	0.43	17.2	0.09	0.0151	36100	20	0.93	24.5	160	8.6	1	17.5	64.2
Rosebery	ROS	UDG	R10063	850.1	850.2	D1800961	7.29	0.53	25	2.59	20.7	0.16	4.1	2.36	28.5	0.8	0.0356	26500	620	13.9	10	3120	3.1	122	14.1	167
Rosebery	ROS	UDG	R10063	860	860.1	D1800962	6.41	0.59	3	1.22	21.2	0.19	3.8	3.7	66.2	0.55	0.0487	8800	120	3.6	33.9	1040	7.3	11	15	120
Rosebery	ROS	UDG	R10063	870	870.1	D1800963	5.52	1.03	4	1.46	16.3	0.18	3.6	2.08	56.1	0.58	0.0525	22500	110	3.3	29.8	850	6.2	9	15.2	109
Rosebery	ROS	UDG	R10063	879.9	880	D1800964	4.17	1.1	4	0.96	11.8	0.16	2.6	2.42	44.3	0.3	0.0522	12300	100	2.3	22.3	680	7.8	8	13.6	86.7
Rosebery	ROS	UDG	R10063	890	890.1	D1800965	5.68	1.47	3	1.41	16.15	0.2	3.5	3.67	59.8	0.5	0.118	11100	100	3.5	33.1	670	7	7	15	107
Rosebery	ROS	UDG	R10063	900	900.1	D1800966	6.04	1.34	3	1.55	16.55	0.2	3.5	3.87	54.7	0.5	0.14	18900	120	3.6	29.3	870	5.6	10	13.8	112
Rosebery	ROS	UDG	R10063	910	910.1	D1800967	4.79	1.3	5	1.36	10.75	0.19	2.6	2.74	56.9	0.37	0.134	19000	100	2.5	23.9	670	4.6	7	11.7	83.4
Rosebery	ROS	UDG	R10063	920	920.1	D1800968	5.85	0.37	3	1.24	15.25	0.14	3.3	2.91	37.1	0.31	0.0254	14200	40	2.1	31.2	360	11	1	18.4	94.3
Rosebery	ROS	UDG	R10063	930	930.1	D1800969	5.69	0.29	5	1.93	14.15	0.15	3.1	3	35.9	0.59	0.0278	10400	30	1.8	29.9	330	9.5	1	15.8	87.9
Rosebery	ROS	UDG	R10063	939.1	939.2	D1800970	7.63	0.34	2	1.52	18.25	0.1	4.1	4.18	3.5	0.51	0.0248	18100	10	2.5	38.9	460	12.3	1	12.1	115.5
Rosebery	ROS	UDG	R10063	950	950.1	D1800971	6.53	0.26	3	1.26	16.7	0.15	3.5	3.44	33.7	0.41	0.022	13800	30	2.1	33.4	370	10.2	2	18.6	104
Rosebery	ROS	UDG	R10063	960.1	960.2	D1800972	5.88	0.39	3	1.2	15.65	0.14	3.5	4.85	32.9	0.47	0.0357	1500	30	1.7	30.9	330	11.2	1	20.7	101
Rosebery	ROS	UDG	R10063	970	970.1	D1800973	5.66	0.55	3	1.17	13.35	0.15	3.3	2.95	32.4	0.36	0.0478	17400	30	1.7	30.5	310	10.1	-1	24.7	95
Rosebery	ROS	UDG	R10063	980	980.1	D1800974	6.36	0.22	3	1.24	17.3	0.17	3.7	4.87	36.8	0.35	0.0324	5800	40	1.8	34.7	340	10.8	1	27.6	103
Rosebery	ROS	UDG	R10063	990	990.1	D1800975	6.24	0.3	2	2.55	16.1	0.18	3.7	5.2	43.8	0.77	0.0405	1300	50	3.4	34.1	510	10.4	2	17.3	115
Rosebery	ROS	UDG	R10063	1000	1000.1	D1800976	6.54	0.25	2	1.57	18.55	0.17	4.3	4.39	45.7	0.47	0.035	6800	40	4	36.8	530	11.7	2	22.7	130.5
Rosebery	ROS	UDG	R10063	1010	1010.1	D1800977	6.74	0.14	2	1.25	20.1	0.18	4.5	4.82	44.8	0.56	0.0203	600	50	4.1	38.2	550	11.8	1	23.6	139
Rosebery	ROS	UDG	R10063	1017.1	1017.2	D1800978	5.19	0.15	3	1.08	12.25	0.16	3.2	4.11	40.4	0.32	0.0194	4600	40	2.9	28.5	400	8.5	1	17.3	96.7

Appendix 5
Rock catalogue

Utas#	Field #	Drill Hole	Depth (m)	AMG UTMN/UTME	Rock Name	Location	Age	Supergroup	Group	Formation	Hand specimen	Thin Section
180540	RG002			5366679N/375133E	greywacke	Conliffe Creek, Tas, Australia	Middle Cambrian	WVSS	Rosebery Group		R	1TS
180541	RG004			5366669N/375130E	siltstone	Conliffe Creek, Tas, Australia	Middle Cambrian	WVSS	Rosebery Group		R	1TS
180542	RG006			5366703N/375153E	siltstone	Conliffe Creek, Tas, Australia	Middle Cambrian	WVSS	Rosebery Group		R	1TS
180543	RG0017			5366497N375232E	Mudstone	Bather Creek, Tas, Australia	Middle Cambrian	WVSS	Rosebery Group		R	1TS
180544	RG020			5366390N/75217E	Quartz-wacke	Bather Creek, Tas, Australia	Late Cambrian	WVSS	Rosebery Group	Stitt Quartzite	R	1TS
180545	RG022			5366761N/375093E	Quartz-wacke	Ring River, Tas, Australia	Late Cambrian	WVSS	Rosebery Group	Stitt Quartzite	R	1TS
180546	RG024			5367761N/375431E	shale	Bakere Creek, Tas, Australia	Late Cambrian	WVSS	Rosebery Group	Stitt Quartzite	R	1TS
180547	RG031			5367645N/375641E	Quartz-wacke	Bakere Creek, Tas, Australia	Late Cambrian	WVSS	Rosebery Group	Stitt Quartzite	R	1TS
180548	RG036			536740N8/375740E	Quartz-wacke	Bakere Creek, Tas, Australia	Late Cambrian	WVSS	Rosebery Group	Stitt Quartzite	R	1TS
180549	RG036B			5367394N/5367394E	volcaniclastic sandstone	Bakere Creek, Tas, Australia	Middle Cambrian	WVSS	Rosebery Group		R	1TS
180550	RG039			5366997N/375015E	Siltstone	Ring River, Tas, Australia	Middle Cambrian	WVSS	Rosebery Group		R	1TS
180551	RG040			5366997N/375027E	Quartz-wacke	Ring River, Tas, Australia	Late Cambrian	WVSS	Rosebery Group		R	1TS
180552	RG044			5367623E/375376N	Mudstone		Late Cambrian	WVSS	Rosebery Group	Stitt Quartzite	R	1TS
180553	RG059			5372425E/377855E	volcaniclastic sandstone	Chamberlain, Tas, Australia	Middle Cambrian	WVSS	Rosebery Group		R	1TS
180554	RG62	RBH1	52	5371234N/376538E	dolomitic sandstone	Natone Creek, Tas, Australia	Middle Cambrian	WVSS	Rosebery Group	Westcott Argilitlite	R	1TS
180555	RG63	RBH1	106.24	5371234N/376539E	polymictic conglomerate	Natone Creek, Tas, Australia	Middle Cambrian	WVSS	Rosebery Group	Salibury Conglomer	R	1TS
180556	RG64	RBH2	34.6	5372546N/376660E	Quartz-feldspar-phyric pumice breccia	Natone Creek, Tas, Australia	Middle Cambrian	WVSS	Rosebery Group	NV	R	1TS
180557	RG65	RBH2	85.35	5372546N/376660E	Quartz-feldspar-phyric pumice breccia	Natone Creek, Tas, Australia	Middle Cambrian	WVSS	Rosebery Group	NV	R	1TS
180558	RG66	RBH2	157.95	5372546N/376660E	Sandstone	Natone Creek, Tas, Australia	Middle Cambrian	WVSS	Rosebery Group	Stitt Quartizite	R	1TS
180559	RG67	CHP264	151.3	5371806N/376443E	Fuchsitic mafic ultramafic complex	Natone Creek, Tas, Australia	Middle Cambrian	basement	Mufic ultra mafic	basement (MUC)	R	1TS
180560	RG68	CHP264	199.25	5371806N/376443E	siltstone	Natone Creek, Tas, Australia	Middle Cambrian	WVSS	Rosebery Group	Westcott Argilitlite	R	1TS
180561	RG69	CHP264	221.15	5371806N/376443E	mudstone	Natone Creek, Tas, Australia	Middle Cambrian	WVSS	Rosebery Group	Westcott Argilitlite	R	1TS
180562	RG70	MPBH1	40.8	5364110N/374655E	greywacke	Moore's Pimple, Tas,Australia		Middle Camb	WVSS	WSF	R	1TS
180563	RG71	MPBH1	73.85	5364110N/374655E	volcaniclastic sandstone	Moore's Pimple, Tas,Australia		Middle Camb	WVSS	WSF	R	1TS
180564	RG72	MPBH1	125.2	5364110N/374655E	volcaniclastic sandstone	Moore's Pimple, Tas,Australia		Middle Camb	WVSS	WSF	R	1TS

Appendix 5
Rock catalogue

Utas#	Field #	Drill Hole	Depth (m)	AMG UTMN/UTME	Rock Name	Location	Age	Supergroup	Group	Formation	Hand specimen	Thin Section
180565	RG73	MPBH1	130.45	5364110N/374655E	volcaniclastic sandstone	Moore's Pimple, Tas,Australia		Middle Camb	WVSS	Rosebery Group	R	1TS
180566	RG74	MPBH1	137.9	5364110N/374655E	Rhyolitic breccia	Moore's Pimple, Tas,Australia		Middle Camb	WVSS	Rosebery Group	R	1TS
180567	RG75	MPBH1	157.1	5364110N/374655E	Rhyolitic breccia	Moore's Pimple, Tas,Australia		Middle Camb	WVSS	Rosebery Group	R	1TS
180568	RG76	MPBH1	200.25	5364110N/374655E	Rhyolitic breccia	Moore's Pimple, Tas,Australia		Middle Camb	WVSS	Rosebery Group	R	1TS
180569	RG77	RRD001	195.65	5365235N/375240E	Volcaniclastic sandstone	Moore's Pimple, Tas,Australia		Middle Camb	WVSS	Rosebery Group	R	1TS
180570	RG78	RRD001	227.8	5365235N/375240E	epiclastic sandstone	Moore's Pimple, Tas,Australia		Middle Camb	WVSS	Rosebery Group	R	1TS
180571	RG137			5375512N/377234E	Quartz-wacke	Flume Road, Tas, Australia	Late Cambrian	Owen Group	Rosebery Group		R	1TS
180572	RG139			5374954N/377399E	Quartz-wacke	Flume Road, Tas, Australia	Late Cambrian	Owen Group	Rosebery Group		R	1TS
180573	RG141			5374728N/377922E	volcaniclastic sandstone	Flume Road, Tas, Australia	Late Cambrian	Owen Group	Rosebery Group		R	1TS
180574	RG147	411R-D1	1320	537839N/379742E	Quartz-phyric pumice breccia	Rosebery, Tas, Australia	Middle Cambrian	WVSS		WSF	R	1TS
180575	RG148	411R-D1	1312.7	5378392N/379741E	Quartz-phyric pumice breccia	Rosebery, Tas, Australia	Middle Cambrian	WVSS		WSF	R	
180576	RG149	411R-D1	1364.3	5378392N/379741E	siltstone/mudstone	Rosebery, Tas, Australia	Middle Cambrian	WVSS		WSF	R	1TS
180577	RG150	411R-D1	1371.2	5378392N/379741E	Quartz-phyric pumice breccia	Rosebery, Tas, Australia	Middle Cambrian	WVSS		WSF	R	
180578	RG151	411R-D1	1400.2	5378392N/379741E	Quartz-phyric pumice breccia	Rosebery, Tas, Australia	Middle Cambrian	WVSS		WSF	R	
180579	RG152	411R-D1	1437.15	5378392N/379741E	volcaniclastic sandstone	Rosebery, Tas, Australia	Middle Cambrian	WVSS	Rosebery Group	MRF	R	1TS
180580	RG153	411R-D1	1446.9	5378392N/379741E	volcaniclastic sandstone	Rosebery, Tas, Australia	Middle Cambrian	WVSS	Rosebery Group	MRF	R	1TS
180581	RG154	R10032	11.8	5376180N/379332E	Feldspar-phyric pbx	Rosebery, Tas, Australia	Middle Cambrian	WVSS	CVC	HPF	R	1TS
180582	RG155	R10032	47.5	5376180N/379332E	Feldspar-phyric pbx	Rosebery, Tas, Australia	Middle Cambrian	WVSS	CVC	HPF	R	
180583	RG156	R10032	56.3	5376180N/379332E	Fsp-phyric pbx	Rosebery, Tas, Australia	Middle Cambrian	WVSS	CVC	HPF	R	1TS
180584	RG157	R10032	119.9	5376180N/379332E	mudstone	Rosebery, Tas, Australia	Middle Cambrian	WVSS	Rosebery Group	MRF	R	
180585	RG158	R10032	171.8	5376180N/379332E	siltstone/mudstone	Rosebery, Tas, Australia	Middle Cambrian	WVSS	Rosebery Group	MRF	R	1TS
180586	RG159	R10032	179	5376180N/379332E	polymictic volcaniclastic breccia	Rosebery, Tas, Australia	Middle Cambrian	WVSS	Rosebery Group	MRF	R	1TS
180587	RG160	R10032	188	5376180N/379332E	volcaniclastic sandstone	Rosebery, Tas, Australia	Middle Cambrian	WVSS	Rosebery Group	MRF	R	1TS
180588	RG161	R10032	192.2	5376180N/379332E	black mudstone	Rosebery, Tas, Australia	Middle Cambrian	WVSS	Rosebery Group	MRF	R	
180589	RG162	R10032	226	5376180N/379332E	rhyolitic breccia in volcaniclastic sandstone	Rosebery, Tas, Australia	Middle Cambrian	WVSS	Rosebery Group	MRF	R	1TS

Appendix 5
Rock catalogue

Utas#	Field #	Drill Hole	Depth (m)	AMG UTMN/UTME	Rock Name	Location	Age	Supergroup	Group	Formation	Hand specimen	Thin Section
180590	RG163	R10032	266.9	5376180N/379332E	Rhyolitic breccia	Rosebery, Tas, Australia	Middle Cambrian	WVSS	Rosebery Group	MRF	R	1TS
180591	RG164	R10063	8.8	5376323N/379802E	Fsp-phyric pbx	Rosebery, Tas, Australia	Middle Cambrian	MRV	CVC	HPF	R	
180592	RG165	R10063	47.8	5376323N/379802E	Fsp-phyric pbx	Rosebery, Tas, Australia	Middle Cambrian	MRV	CVC	HPF	R	
180593	RG166	R10063	66.5	5376323N/379802E	Fsp-phyric pbx	Rosebery, Tas, Australia	Middle Cambrian	MRV	CVC	HPF	R	
180594	RG167	R10063	161.25	5376323N/379802E	Fsp-phyric pbx	Rosebery, Tas, Australia	Middle Cambrian	MRV	CVC	HPF	R	1TS
180595	RG168	R10063	202.2	5376323N/379802E	Fsp-phyric pbx	Rosebery, Tas, Australia	Middle Cambrian	MRV	CVC	HPF	R	
180596	RG169	R10063	212.2	5376323N/379802E	polymictic volcaniclastic breccia	Rosebery, Tas, Australia	Middle Cambrian	WVSS	Rosebery Group	MRF	R	1TS
180597	RG170	R10063	223.1	5376323N/379802E	Rhyolitic intrusion	Rosebery, Tas, Australia	Middle Cambrian	WVSS	Rosebery Group	MRF	R	1TS
180598	RG171	R10063	233.5	5376323N/379802E	Polymictic breccia	Rosebery, Tas, Australia	Middle Cambrian	WVSS	Rosebery Group	MRF	R	
180599	RG172	R10063	243.5	5376323N/379802E	polymictic volcaniclastic breccia	Rosebery, Tas, Australia	Middle Cambrian	WVSS	Rosebery Group	MRF	R	
180600	RG173	R10063	252.8	5376323N/379802E	black mudstone	Rosebery, Tas, Australia	Middle Cambrian	WVSS	Rosebery Group	MRF	R	
180601	RG174	R10063	261.3	5376323N/379802E	volcaniclastic sandstone	Rosebery, Tas, Australia	Middle Cambrian	WVSS	Rosebery Group	MRF	R	1TS
180602	RG175	R10063	271.4	5376323N/379802E	Polymictic breccia	Rosebery, Tas, Australia	Middle Cambrian	WVSS	Rosebery Group	MRF	R	1TS
180603	RG176	R10063	280.1	5376323N/379802E	volcaniclastic sandstone	Rosebery, Tas, Australia	Middle Cambrian	WVSS	Rosebery Group	MRF	R	
180604	RG177	R10063	290.75	5376323N/379802E	Polymictic volcaniclastic breccia	Rosebery, Tas, Australia	Middle Cambrian	WVSS	Rosebery Group	MRF	R	1TS
180605	RG178	R10063	296.9	5376323N/379802E	Polymictic volcaniclastic breccia	Rosebery, Tas, Australia	Middle Cambrian	WVSS	Rosebery Group	MRF	R	1TS
180606	RG179	R10063	309.5	5376323N/379802E	volcaniclastic sandstone	Rosebery, Tas, Australia	Middle Cambrian	WVSS	Rosebery Group	MRF	R	
180607	RG180	R10063	330.9	5376323N/379802E	volcaniclastic siltstone	Rosebery, Tas, Australia	Middle Cambrian	WVSS	Rosebery Group	MRF	R	
180608	RG181	R10063	356.4	5376323N/379802E	volcaniclastic sandstone	Rosebery, Tas, Australia	Middle Cambrian	WVSS	Rosebery Group	MRF	R	1TS
180609	RG182	R10063	370	5376323N/379802E	volcaniclastic sandstone	Rosebery, Tas, Australia	Middle Cambrian	WVSS	Rosebery Group	MRF	R	1TS
180610	RG183	R10063	397.5	5376323N/379802E	volcaniclastic sandstone	Rosebery, Tas, Australia	Middle Cambrian	WVSS	Rosebery Group	MRF	R	1TS
180611	RG184	R10063	416.4	5376323N/379802E	polymictic volcaniclastic breccia	Rosebery, Tas, Australia	Middle Cambrian	WVSS	Rosebery Group	MRF	R	1TS
180612	RG185	R10063	427.75	5376323N/379802E	polymictic volcaniclastic breccia	Rosebery, Tas, Australia	Middle Cambrian	WVSS	Rosebery Group	MRF	R	1TS
180613	RG186	R10063	452.3	5376323N/379802E	volcaniclastic sandstone	Rosebery, Tas, Australia	Middle Cambrian	WVSS	Rosebery Group	MRF	R	1TS
180614	RG187	R10063	472.4	5376323N/379802E	black mudstone	Rosebery, Tas, Australia	Middle Cambrian	WVSS	Rosebery Group	MRF	R	

Appendix 5
Rock catalogue

Utas#	Field #	Drill Hole	Depth (m)	AMG UTMN/UTME	Rock Name	Location	Age	Supergroup	Group	Formation	Hand specimen	Thin Section
180615	RG188	R10063	521.25	5376323N/379802E	volcaniclastic sandstone	Rosebery, Tas, Australia	Middle Cambrian	WVSS	Rosebery Group	MRF	R	
180616	RG189	R10063	526.85	5376323N/379802E	mudstone	Rosebery, Tas, Australia	Middle Cambrian	WVSS	Rosebery Group	MRF	R	1TS
180617	RG190	R10063	609.3	5376323N/379802E	volcaniclastic siltstone	Rosebery, Tas, Australia	Middle Cambrian	WVSS	Rosebery Group	MRF	R	1TS
180618	RG191	R10063	752.5	5376323N/379802E	volcaniclastic sandstone	Rosebery, Tas, Australia	Middle Cambrian	WVSS	Rosebery Group	MRF	R	
180619	RG192	R10063	794	5376323N/379802E	Qtz-Fsp-phyric Pbx	Rosebery, Tas, Australia	Middle Cambrian	WVSS	Rosebery Group	MRF	R	1TS
180620	RG193	R10063	869.5	5376323N/379802E	Qtz-Fsp-phyric Pbx	Rosebery, Tas, Australia	Middle Cambrian	WVSS	Rosebery Group	MRF	R	
180621	RG194	R10063	874	5376323N/379802E	Qtz-Fsp-phyric Pbx	Rosebery, Tas, Australia	Middle Cambrian	WVSS	Rosebery Group	MRF	R	1TS
180622	RG195	R10063	909.3	5376323N/379802E	Qtz-Fsp-phyric Pbx	Rosebery, Tas, Australia	Middle Cambrian	WVSS	Rosebery Group	MRF	R	1TS
180623	RG196	R10063	914.7	5376323N/379802E	mudstone	Rosebery, Tas, Australia	Middle Cambrian	WVSS	Rosebery Group	MRF	R	
180624	RG197	R10063	933.2	5376323N/379802E	mudstone	Rosebery, Tas, Australia	Middle Cambrian	WVSS	Rosebery Group	MRF	R	1TS
180625	RG198	R10063	955.7	5376323N/379802E	rhyolitic brx	Rosebery, Tas, Australia	Middle Cambrian	WVSS	Rosebery Group	MRF	R	
180626	RG199	R10063	1115.3	5376323N/379802E	rhyolitic brx silica altered volcaniclastic	Rosebery, Tas, Australia	Middle Cambrian	WVSS	Rosebery Group	MRF	R	1TS
180627	RG200	JP357	34.5	376847N/5369973E	siltstone	Rosebery, Tas, Australia	Middle Cambrian	WVSS	CVC	HPF	R	1TS
180628	RG201	JP357	37.3	376847N/5369973E	crystal poor pumice breccia	Rosebery, Tas, Australia	Middle Cambrian	MRV	CVC	HPF	R	1TS
180629	RG202	JP357	53.3	376847N/5369973E	Sericite altered, feldspar phyric pumice breccia	Rosebery, Tas, Australia	Middle Cambrian	MRV	CVC	HPF	R	
180630	RG203	JP357	58.5	376847N/5369973E	Sericite altered, feldspar phyric pumice breccia	Rosebery, Tas, Australia	Middle Cambrian	MRV	CVC	HPF	R	
180631	RG204	JP357	64.5	376847N/5369973E	crystal poor pumice breccia	Rosebery, Tas, Australia	Middle Cambrian	MRV	CVC	HPF	R	1TS
180632	RG205	JP357	66.5	376847N/5369973E	crystal poor pumice breccia	Rosebery, Tas, Australia	Middle Cambrian	MRV	CVC	HPF	R	
180633	RG206	JP357	69.5	376847N/5369973E	Pumiceous siltstone	Rosebery, Tas, Australia	Middle Cambrian	MRV	CVC	HPF	R	1TS
180634	RG207	JP357	79.75	376847N/5369973E	Quartz feldspar phyric pumice breccia	Rosebery, Tas, Australia	Middle Cambrian	WVSS	Rosebery Group	MRF	R	1TS
180635	RG208	JP357	88	376847N/5369973E	Quartz feldspar phyric pumice breccia	Rosebery, Tas, Australia	Middle Cambrian	WVSS	Rosebery Group	MRF	R	
180636	RG225			5367678N/374489E	volcaniclastic breccia/sandstone	Rosebery, Tas, Australia	Middle Cambrian	WVSS	Rosebery Group		R	
180637	RG226	R10035	39.35	5376702N/379429.E	Felspar phyric pumice breccia	Rosebery, Tas, Australia	Middle Cambrian	MRV	CVC	HPF	R	
180638	RG227	R10035	81.45	5376702N/379429.E	Feldspar-phyric pumice breccia, stratified top	Rosebery, Tas, Australia	Middle Cambrian	MRV	CVC	HPF	R	
180639	RG228	R10035	115	5376702N/379429.E	Feldspar-phyric pumice breccia	Rosebery, Tas, Australia	Middle Cambrian	MRV	Rosebery Group	MRF	R	

Appendix 5
Rock catalogue

Utas#	Field #	Drill Hole	Depth (m)	AMG UTMN/UTME	Rock Name	Location	Age	Supergroup	Group	Formation	Hand specimen	Thin Section
180640	RG229	R10035	119.4	5376702N/379429.E	volcaniclastic sandstone breccia in mudstone matrix	Rosebery, Tas, Australia	Middle Cambrian	MRV	Rosebery Group	MRF	R	
180641	RG230	R10035	128.25	5376702N/379429.E	volcaniclastic sandstone	Rosebery, Tas, Australia	Middle Cambrian	MRV	Rosebery Group	MRF	R	
180642	RG231	R10035	133.6	5376702N/379429.E	volcaniclastic breccia in minor mudstone matrix	Rosebery, Tas, Australia	Middle Cambrian	MRV	Rosebery Group	MRF	R	
180643	RG232	R10035	146.4	5376702N/379429.E	volcaniclastic sandstone	Rosebery, Tas, Australia	Middle Cambrian	MRV	Rosebery Group	MRF	R	
180644	RG233	R10035	163.7	5376702N/379429.E	quartz-phyric rhyolitic volcaniclastic breccia	Rosebery, Tas, Australia	Middle Cambrian	MRV	Rosebery Group	MRF	R	
180645	RG234	R10035	178.65	5376702N/379429.E	quartz phyric volcaniclastic breccia	Rosebery, Tas, Australia	Middle Cambrian	MRV	Rosebery Group	MRF	R	
180646	RG235	R10035	185	5376702N/379429.E	polymictic volcaniclastic breccia	Rosebery, Tas, Australia	Middle Cambrian	MRV	Rosebery Group	MRF	R	
180647	RG236	R10035	193.9	5376702N/379429.E	polymictic volcaniclastic breccia	Rosebery, Tas, Australia	Middle Cambrian	MRV	Rosebery Group	MRF	R	
180648	RG237	R10035	200.8	5376702N/379429.E	volcaniclastic sandstone	Rosebery, Tas, Australia	Middle Cambrian	MRV	Rosebery Group	MRF	R	
180649	RG238	R10035	231.7	5376702N/379429.E	polymictic volcaniclastic breccia	Rosebery, Tas, Australia	Middle Cambrian	MRV	Rosebery Group	MRF	R	
180650	RG239	R10035	225.5	5376702N/379429.E	volcaniclastic sandstone	Rosebery, Tas, Australia	Middle Cambrian	MRV	Rosebery Group	MRF	R	
180651	RG240	R10035	238.3	5376702N/379429.E	polymictic volcaniclastic breccia	Rosebery, Tas, Australia	Middle Cambrian	MRV	Rosebery Group	MRF	R	
180652	RG241	R10035	256.6	5376702N/379429.E	siltstone	Rosebery, Tas, Australia	Middle Cambrian	MRV	Rosebery Group	MRF	R	
180653	RG242	R10035	291.6	5376702N/379429.E	siltstone	Rosebery, Tas, Australia	Middle Cambrian	MRV	Rosebery Group	MRF	R	
180654	RG243	R10035	313	5376702N/379429.E	rhyotlic volcaniclastic breccia	Rosebery, Tas, Australia	Middle Cambrian	MRV	Rosebery Group	MRF	R	
180655	RG244	R10035	332.7	5376702N/379429.E	rhyotlic volcaniclastic breccia	Rosebery, Tas, Australia	Middle Cambrian	MRV	Rosebery Group	MRF	R	
180656	RG245	R10035	337.2	5376702N/379429.E	Quartz feldspar phyric volcaniclastic breccia	Rosebery, Tas, Australia	Middle Cambrian	MRV	Rosebery Group	MRF	R	
180657	RG246	R10035	352.8	5376702N/379429.E	Quartz-phyric rhyolitic breccia	Rosebery, Tas, Australia	Middle Cambrian	MRV	Rosebery Group	MRF	R	
180658	RG247	R10035	361.3	5376702N/379429.E	Quartz-phyric rhyolitic breccia	Rosebery, Tas, Australia	Middle Cambrian	MRV	Rosebery Group	MRF	R	
180659	RG248	R10035	385.7	5376702N/379429.E	volcaniclastic sandstone	Rosebery, Tas, Australia	Middle Cambrian	MRV	Rosebery Group	MRF	R	
180660	RG249	R10035	392.1	5376702N/379429.E	volcaniclastic sandstone with semi-massive sulphide	Rosebery, Tas, Australia	Middle Cambrian	MRV	Rosebery Group	MRF	R	
180661	RG250	R10035	404.9	5376702N/379429.E	Qtz-Fsp-phyric pumice breccia	Rosebery, Tas, Australia	Middle Cambrian	MRV	Rosebery Group	MRF	R	
180662	RG251	337R	1461.9	5377212N/379968E	Fsp-phyric pumice breccia of	Rosebery, Tas, Australia	Middle Cambrian	MRV	CVC	MRF	R	1TS
180663	RG252	337R	1508	5377212N/379968E	volcaniclastic sandstone	Rosebery, Tas, Australia	Middle Cambrian	MRV	Rosebery Group	MRF	R	
180664	RG253	337R	1510.2	5377212N/379968E	polymictic volcaniclastic breccia	Rosebery, Tas, Australia	Middle Cambrian	MRV	Rosebery Group	MRF	R	

Appendix 5
Rock catalogue

Utas#	Field #	Drill Hole	Depth (m)	AMG UTMN/UTME	Rock Name	Location	Age	Supergroup	Group	Formation	Hand specimen	Thin Section
180665	RG254A	337R	1519.5	5377212N/379968E	volcaniclastic sandstone	Rosebery, Tas, Australia	Middle Cambrian	MRV	Rosebery Group	MRF	R	
180666	RG254B	337R	1548.7	5377212N/379968E	polymictic volcaniclastic breccia	Rosebery, Tas, Australia	Middle Cambrian	MRV	Rosebery Group	MRF	R	
180667	RG255	337R	1560.9	5377212N/379968E	polymictic volcaniclastic breccia	Rosebery, Tas, Australia	Middle Cambrian	MRV	Rosebery Group	MRF	R	
180668	256	337R	1572.5	5377212N/379968E	epiclastic sandstone	Rosebery, Tas, Australia	Middle Cambrian	MRV	Rosebery Group	MRF	R	
180669	257A	337R	1579.8	5377212N/379968E	polymictic volcaniclastic breccia	Rosebery, Tas, Australia	Middle Cambrian	MRV	Rosebery Group	MRF	R	
180670	257B	337R	1586	5377212N/379968E	volcaniclastic sandstone	Rosebery, Tas, Australia	Middle Cambrian	MRV	Rosebery Group	MRF	R	
180671	RG258	337R	1595.6	5377212N/379968E	stringer to semi-massive sulphide	Rosebery, Tas, Australia	Middle Cambrian	MRV	Rosebery Group	MRF	R	
180672	RG259	337R	1601.2	5377212N/379968E	volacaniclastic sandstone bearing stringer to semi-	Rosebery, Tas, Australia	Middle Cambrian	MRV	Rosebery Group	MRF	R	
180673	RG260	337R	1608.4	5377212N/379968E	Qtz-phyric volcaniclastic sandstone	Rosebery, Tas, Australia	Middle Cambrian	MRV	Rosebery Group	MRF	R	
180674	RG261	337R	1618.3	5377212N/379968E	interbeddd with siltstone with stringer of sulphide	Rosebery, Tas, Australia	Middle Cambrian	MRV	Rosebery Group	MRF	R	
180675	RG262	337R	1622.3	5377212N/379968E	polymictic volcaniclastic breccia with andesite, basaltic clasts	Rosebery, Tas, Australia	Middle Cambrian	MRV	Rosebery Group	MRF	R	
180676	RG263	337R	1638.1	5377212N/379968E	Very fine grained, volcaniclastic siltstone	Rosebery, Tas, Australia	Middle Cambrian	MRV	Rosebery Group	MRF	R	
180677	RG264	337R	1646.2	5377212N/379968E	Very fine grained, volcaniclastic siltstone	Rosebery, Tas, Australia	Middle Cambrian	MRV	Rosebery Group	MRF	R	
180678	RG265	337R	1654.9	5377212N/379968E	Very fine grained, volcaniclastic siltstone	Rosebery, Tas, Australia	Middle Cambrian	MRV	Rosebery Group	MRF	R	
180679	RG266	337R	1673	5377212N/379968E	Siltstone	Rosebery, Tas, Australia	Middle Cambrian	MRV	Rosebery Group	MRF	R	
180680	RG267	337R	1683.9	5377212N/379968E	greywacke	Rosebery, Tas, Australia	Middle Cambrian	MRV	Rosebery Group	MRF	R	
180681	RG268	337R	1696	5377212N/379968E	Qtz-phyric pumice breccia	Rosebery, Tas, Australia	Middle Cambrian	MRV	Rosebery Group	MRF	R	
180682	RG269	337R	1720.5	5377212N/379968E	Qtz- phyric pumice breccia	Rosebery, Tas, Australia	Middle Cambrian	MRV	Rosebery Group	MRF	R	
180683	RG270	337R	1740.8	5377212N/379968E	Qtz-phyric rhyolitic breccia	Rosebery, Tas, Australia	Middle Cambrian	MRV	Rosebery Group	MRF	R	
180684	RG271	337R	1745.3	5377212N/379968E	Qtz-Fsp-phyric pumice breccia	Rosebery, Tas, Australia	Middle Cambrian	MRV	Rosebery Group	MRF	R	
180685	RG272	337R	1754	5377212N/379968E	Qtz-Fsp-phyric pumice breccia	Rosebery, Tas, Australia	Middle Cambrian	MRV	Rosebery Group	MRF	R	
180686	RG273	337R	1757.2	5377212N/379968E	Qtz-Fsp-phyric pumice breccia	Rosebery, Tas, Australia	Middle Cambrian	MRV	Rosebery Group	MRF	R	
180687	RG274	BP272	5.4	5372988N/378059E	volcaniclastic sandstone	Rosebery, Tas, Australia	Middle Cambrian	MRV	Rosebery Group	MRF	R	
180688	RG275	BP272	29.8	5372988N/378059E	volcaniclastic sandstone	Rosebery, Tas, Australia	Middle Cambrian	MRV	Rosebery Group	MRF	R	
180689	RG276	BP272	42.4	5372988N/378059E	mudstone with some breccia	Rosebery, Tas, Australia	Middle Cambrian	MRV	Rosebery Group	MRF	R	

Appendix 5
Rock catalogue

Utas#	Field #	Drill Hole	Depth (m)	AMG UTMN/UTME	Rock Name	Location	Age	Supergroup	Group	Formation	Hand specimen	Thin Section
180690	RG277	BP272	65.35	5372988N/378059E	Qtz-phyric volcaniclastic sandstone/pumice breccia	Rosebery, Tas, Australia	Middle Cambrian	MRV	Rosebery Group	MRF	R	
180691	RG278	BP272	89.9	5372988N/378059E	volcaniclastic sandstone with pumice	Rosebery, Tas, Australia	Middle Cambrian	MRV	Rosebery Group	MRF	R	
180692	RG279	BP272	108.4	5372988N/378059E	intensely silica altered volcaniclastic sandstone	Rosebery, Tas, Australia	Middle Cambrian	MRV	Rosebery Group	MRF	R	
180693	RG280	BP272	128	5372988N/378059E	volcaniclastic sandstone	Rosebery, Tas, Australia	Middle Cambrian	MRV	Rosebery Group	MRF	R	
180694	RG281	BP272	137.4	5372988N/378059E	volcaniclastic sandstone	Rosebery, Tas, Australia	Middle Cambrian	MRV	Rosebery Group	MRF	R	
180695	RG282	BP272	176.9	5372988N/378059E	volcaniclastic sandstone	Rosebery, Tas, Australia	Middle Cambrian	MRV	Rosebery Group	MRF	R	
180696	RG283	BP272	285.15	5372988N/378059E	Qtz-phyric volcaniclastic sandstone	Rosebery, Tas, Australia	Middle Cambrian	MRV	Rosebery Group	MRF	R	
180697	RG284	BP272	300.7	5372988N/378059E	Siltstone	Rosebery, Tas, Australia	Middle Cambrian	MRV	Rosebery Group	MRF	R	
180698	RG285	BP272	208.35	5372988N/378059E	mudstone	Rosebery, Tas, Australia	Middle Cambrian	MRV	Rosebery Group	MRF	R	
180699	RG286A	BP272	325.6	5372988N/378059E	Siltstone	Rosebery, Tas, Australia	Middle Cambrian	MRV	Rosebery Group	MRF	R	
180700	RG286B	BP272	355.3	5372988N/378059E	Qtz-phyric volcaniclastic sandstone	Rosebery, Tas, Australia	Middle Cambrian	MRV	Rosebery Group	MRF	R	
180701	RG287	BP272	398.6	5372988N/378059E	Siltstone	Rosebery, Tas, Australia	Middle Cambrian	MRV	Rosebery Group	MRF	R	
180702	RG288	BP272	416	5372988N/378059E	volcaniclastic sandstone	Rosebery, Tas, Australia	Middle Cambrian	MRV	Rosebery Group	MRF	R	
180703	RG289	BP273	214.4	5373287N/378236E	Qtz-Fsp-phyric pumice breccia	Rosebery, Tas, Australia	Middle Cambrian	MRV	Rosebery Group	MRF	R	
180704	RG290	BP273	222	5373287N/378236E	Qtz-Fsp-phyric pumice breccia	Rosebery, Tas, Australia	Middle Cambrian	MRV	Rosebery Group	MRF	R	
180705	RG291	BP273	243.6	5373287N/378236E	Siltstone	Rosebery, Tas, Australia	Middle Cambrian	MRV	Rosebery Group	MRF	R	
180706	RG292	BP273	254.2	5373287N/378236E	volcaniclastic sandstone	Rosebery, Tas, Australia	Middle Cambrian	MRV	Rosebery Group	MRF	R	
180707	RG293	BP273	278.2	5373287N/378236E	volcaniclastic sandstone with wispy clasts	Rosebery, Tas, Australia	Middle Cambrian	MRV	Rosebery Group	MRF	R	
180708	RG294	BP273	289.6	5373287N/378236E	volcaniclastic sandstone with wispy clasts	Rosebery, Tas, Australia	Middle Cambrian	MRV	Rosebery Group	MRF	R	
180709	RG295	BP273	324	5373287N/378236E	Volcaniclastic sandstone	Rosebery, Tas, Australia	Middle Cambrian	MRV	Rosebery Group	MRF	R	
180710	RG296A	BP273	352.35	5373287N/378236E	rhyolitic breccia in volcaniclastic sandstone	Rosebery, Tas, Australia	Middle Cambrian	MRV	Rosebery Group	MRF	R	
180711	RG296B	BP273	367.85	5373287N/378236E	rhyolitic breccia in volcaniclastic sandstone	Rosebery, Tas, Australia	Middle Cambrian	MRV	Rosebery Group	MRF	R	
180712	RG297	BP273	378.6	5373287N/378236E	mudstone with some breccia	Rosebery, Tas, Australia	Middle Cambrian	MRV	Rosebery Group	MRF	R	
180713	RG298	BP273	403.3	5373287N/378236E	polymictic volcaniclastic breccia with andesite, basaltic clasts	Rosebery, Tas, Australia	Middle Cambrian	MRV	Rosebery Group	MRF	R	
180714	RG299	BP273	442.7	5373287N/378236E	Volcaniclastic sandstone with sparse pumice	Rosebery, Tas, Australia	Middle Cambrian	MRV	Rosebery Group	MRF	R	

Appendix 5
Rock catalogue

Utas#	Field #	Drill Hole	Depth (m)	AMG UTMN/UTME	Rock Name	Location	Age	Supergroup	Group	Formation	Hand specimen	Thin Section
180715	RG300	R10032	238	5376179N/379331E	rhyolitic breccia	Rosebery, Tas, Australia	Middle Cambrian	MRV	Rosebery Group	MRF	R	
180716	RG301	R10032	247.2	5376179N/379331E	Polymict, volcaniclastic sandstone	Rosebery, Tas, Australia	Middle Cambrian	MRV	Rosebery Group	MRF	R	
180717	RG302	R10032	254.8	5376179N/379331E	siltstone/mudstone	Rosebery, Tas, Australia	Middle Cambrian	MRV	Rosebery Group	MRF	R	
180718	RG303	R10032	274.7	5376179N/379331E	volcaniclastic sandstone	Rosebery, Tas, Australia	Middle Cambrian	MRV	Rosebery Group	MRF	R	
180719	RG304	R10032	335.3	5376179N/379331E	volcaniclastic sandstone	Rosebery, Tas, Australia	Middle Cambrian	MRV	Rosebery Group	MRF	R	
180720	RG305	R10032	357.1	5376179N/379331E	Qtz-Fsp-phyric-pumice breccia	Rosebery, Tas, Australia	Middle Cambrian	MRV	Rosebery Group	MRF	R	
180721	RG306	R10032	372.2	5376179N/379331E	Qtz-Fsp-phyric pumice breccia with minor quartz	Rosebery, Tas, Australia	Middle Cambrian	MRV	Rosebery Group	MRF	R	
180722	RG307	R10032	403.4	5376179N/379331E	Qtz-Fsp-phyric pumice breccia with minor quartz	Rosebery, Tas, Australia	Middle Cambrian	MRV	Rosebery Group	MRF	R	
180723	RG308	R10032	438.1	5376179N/379331E	Qtz-phyric pumice breccia	Rosebery, Tas, Australia	Middle Cambrian	MRV	Rosebery Group	MRF	R	
180724	RG309	R10032	173.4	5376179N/379331E	Qtz-phyric volcaniclastic sandstone	Rosebery, Tas, Australia	Middle Cambrian	MRV	Rosebery Group	MRF	R	
180725	RG310	R10032	175.6	5376179N/379331E	semi-massive sulphide	Rosebery, Tas, Australia	Middle Cambrian	MRV	Rosebery Group	MRF	R	
180726	RG311	R10032	182.7	5376179N/379331E	Qtz-phyric VSST (Pumice) in siltstone	Rosebery, Tas, Australia	Middle Cambrian	MRV	Rosebery Group	MRF	R	
180727	RG315	R10063	378.3	5376323N/79802E	mudstone	Rosebery, Tas, Australia	Middle Cambrian	MRV	Rosebery Group	MRF	R	
180728	RG316	R10063	899.6	5376323N/79802E	Qtz-Fsp-phyric pumice breccia	Rosebery, Tas, Australia	Middle Cambrian	MRV	Rosebery Group	MRF	R	
180729	RG317	R10063	560	5376323N/79802E	volcaniclastic sandstone	Rosebery, Tas, Australia	Middle Cambrian	MRV	Rosebery Group	MRF	R	
180730	RG318	R10063	590	5376323N/79802E	volcaniclastic sandstone	Rosebery, Tas, Australia	Middle Cambrian	MRV	Rosebery Group	MRF	R	
180731	RG319	R10063	630	5376323N/79802E	volcaniclastic sandstone	Rosebery, Tas, Australia	Middle Cambrian	MRV	Rosebery Group	MRF	R	
180732	RG320	R10063	690	5376323N/79802E	volcaniclastic sandstone	Rosebery, Tas, Australia	Middle Cambrian	MRV	Rosebery Group	MRF	R	
180733	RG321	411R-D1	669.7	5378393N/379742	pumice breccia	Rosebery, Tas, Australia	Middle Cambrian	MRV	CVC	MBF	R	
180734	RG322	411R-D1	759.8	5378393N/379743	polymictic volcaniclastic breccia	Rosebery, Tas, Australia	Middle Cambrian	MRV	CVC	MBF	R	
180735	RG323	411R-D1	830.3	5378393N/379744	dacite	Rosebery, Tas, Australia	Middle Cambrian	MRV	CVC	MBF	R	
180736	RG324	411R-D1	981.4	5378393N/379745	polymictic volcaniclastic breccia	Rosebery, Tas, Australia	Middle Cambrian	MRV	CVC	MBF	R	
180737	RG325	411R-D1	1104.9	5378393N/379746	andesite	Rosebery, Tas, Australia	Middle Cambrian	MRV	CVC	MBF	R	
180738	RG326	411R-D1	1138.6	5378393N/379747	polymictic volcaniclastic breccia	Rosebery, Tas, Australia	Middle Cambrian	MRV	CVC	MBF	R	
180739	RG327	411R-D1	1182.7	5378393N/379748	mudstone	Rosebery, Tas, Australia	Middle Cambrian	MRV	CVC	MBF	R	

Appendix 5
Rock catalogue

Utas#	Field Nu	Drill Hole	Depth (m)	AMG UTMN/UTME	Rock Name	Location	Age	Supergroup	Group	Formation	Hand specimen	Thin Section
180740	RG328	411R-D1	1124.9	5378393N/379749	xll poor pumice breccia	Rosebery, Tas, Australia	Middle Cambrian	MRV	CVC	MBF	R	
180741	RG329	397R	1434.7	5377807N/379927E	Qtz-phyric pumice breccia	Rosebery, Tas, Australia	Middle Cambrian	MRV		WSF	R	
180742	RG330	397R	1449.5	5377807N/379927E	Qtz-phyric pumice breccia	Rosebery, Tas, Australia	Middle Cambrian	MRV		WSF	R	
180743	RG331	397R	1579.1	5377807N/379927E	Fsp-phyric pumice breccia	Rosebery, Tas, Australia	Middle Cambrian	MRV	HPF	HPF	R	
180744	RG332	397R	1592	5377807N/379927E	volcaniclastic sandstone	Rosebery, Tas, Australia	Middle Cambrian	MRV	HPF	HPF	R	
180745	RG333	397R	1611.3	5377807N/379927E	Fsp-phyric pumice breccia	Rosebery, Tas, Australia	Middle Cambrian	MRV	HPF	HPF	R	
180746	RG334	397R	1692.6	5377807N/379927E	basaltic andesite polymictic volcaniclastic breccia	Rosebery, Tas, Australia	Middle Cambrian	MRV	Rosebery Group	MRF	R	
180747	RG335	397R	1760.7	5377807N/379927E	basaltic andesite polymictic volcaniclastic breccia	Rosebery, Tas, Australia	Middle Cambrian	MRV	Rosebery Group	MRF	R	
180748	RG336	337R	1013	5377212N/379967E	crystal rich volcaniclastic breccia	Rosebery, Tas, Australia	Middle Cambrian	MRV		WSF	R	1TS
180749	RG337	337R	1029.2	5377212N/379967E	polymictic volcaniclastic breccia	Rosebery, Tas, Australia	Middle Cambrian	MRV		WSF	R	
180750	RG338	337R	1067.5	5377212N/379967E	Volcaniclastic sandstone/Breccia	Rosebery, Tas, Australia	Middle Cambrian	MRV		WSF	R	
180751	RG339	337R	1106.3	5377212N/379967E	Fsp-phyric basaltic andesite volcaniclastic breccia	Rosebery, Tas, Australia	Middle Cambrian	MRV		WSF	R	1TS
180752	RG340	337R	1135	5377212N/379967E	Qtz-Fsp-phyric pumice breccia	Rosebery, Tas, Australia	Middle Cambrian	MRV		WSF	R	1TS
180753	RG341	337R	1171.4	5377212N/379967E	Qtz-Fsp-phyric pumice breccia	Rosebery, Tas, Australia	Middle Cambrian	MRV		WSF	R	
180754	RG342	337R	1190.95	5377212N/379967E	Qtz-Fsp-phyric pumice breccia	Rosebery, Tas, Australia	Middle Cambrian	MRV		WSF	R	1TS
180755	RG343	337R	1211.8	5377212N/379967E	Qtz-Fsp-phyric pumice breccia	Rosebery, Tas, Australia	Middle Cambrian	MRV		WSF	R	
180756	RG344	337R	1251.5	5377212N/379967E	Qtz-phyric volcaniclastic sandstone	Rosebery, Tas, Australia	Middle Cambrian	MRV	Host rock	HPF	R	1TS
180757	RG345	337R	1271.2	5377212N/379967E	Fsp-phyric volcaniclastic sandstone	Rosebery, Tas, Australia	Middle Cambrian	MRV	Host rock	HPF	R	1TS
180758	RG346	397R	1253.5	5377808N/379927E	Polymictic volcaniclastic brecia	Rosebery, Tas, Australia	Middle Cambrian	MRV		WFS	R	
180759	RG347	397R	1298.6	5377808N/379927E	Polymictic volcaniclastic brecia	Rosebery, Tas, Australia	Middle Cambrian	MRV		WFS	R	1TS
180760	RG348	397R	1323.8	5377808N/379927E	crystal rich volcaniclastic breccia	Rosebery, Tas, Australia	Middle Cambrian	MRV		WFS	R	
180761	RG349	397R	1347.1	5377808N/379927E	andesite clasts containnig volcaniclastic breccia	Rosebery, Tas, Australia	Middle Cambrian	MRV		WFS	R	
180762	RG350	397R	1356.8	5377808N/379927E	andesite clasts containnig volcaniclastic breccia	Rosebery, Tas, Australia	Middle Cambrian	MRV		WFS	R	1TS
180763	RG351	397R	1384.2	5377808N/379927E	mudstone/siltstone containnig volcaniclastic breccia	Rosebery, Tas, Australia	Middle Cambrian	MRV		WFS	R	
180764	RG352	397R	1422.5	5377808N/379927E	mudstone/siltstone containnig volcaniclastic breccia	Rosebery, Tas, Australia	Middle Cambrian	MRV		WFS	R	

Appendix 5
Rock catalogue

Utas#	Field Nu	Drill Hole	Depth (m)	AMG UTMN/UTME	Rock Name	Location	Age	Supergroup	Group	Formation	Hand specimen	Thin Section
180765	RG353	397R	1467.2	5377808N/379927E	Qtz-phyric pumice breccia	Rosebery, Tas, Australia	Middle Cambrian	MRV		WFS	R	
180766	RG354	397R	1492.65	5377808N/379927E	crystal poor pumice breccia	Rosebery, Tas, Australia	Middle Cambrian	MRV		WFS	R	
180767	RG355	RBH2	147	5372546N/376660N	volcaniclastic sandstone	Rosebery, Tas, Australia	Middle Cambrian	MRV	Rosebery Group	NV	R	1TS